Aide à la décision pour le remplacement valvulaire aortique percutané

Vincent Auffret

THESE DE DOCTORAT DE

L'UNIVERSITE DE RENNES 1
COMUE UNIVERSITE BRETAGNE LOIRE

ECOLE DOCTORALE N° 605
Biologie Santé
Spécialité : Analyse et traitement de l'information et des images médicales

Par
« Vincent AUFFRET»

« Aide à la décision pour le remplacement valvulaire aortique percutané »

Thèse présentée et soutenue à Rennes, le 07 Octobre 2019
Unité de recherche : Inserm U1099 – LTSI

Rapporteurs avant soutenance :

Céline Fouard MCU-HDR - Université de Grenoble Alpes
Anne Bernard PU-PH - Université de Tours

Composition du Jury :

Président :	Martine Gilard	PU-PH - Université de Bretagne Occidentale
Examinateurs :	Hélène Eltchninoff	PU-PH - Université de Rouen Normandie
	Céline Fouard	MCU-HDR - Université de Grenoble Alpes
	Michel Rochette	Directeur technique – ANSYS France
Dir. de thèse :	Pascal Haigron	PU - Université de Rennes 1
Co-dir. de thèse :	Hervé Le Breton	PU-PH - Université de Rennes 1

Remerciements

Ce projet de Thèse n'aurait pu aboutir sans le soutien et la contribution de nombreuses personnes que je tenais à remercier.

Tout d'abord, je remercie le Docteur Céline Fouard et le Professeur Anne Bernard d'avoir accepté d'être rapporteurs de ce travail. Vous me faites l'honneur de juger ce travail, recevez ici l'expression de ma profonde gratitude pour l'intérêt que vous y porterez.

Je remercie le Professeur Héléne Eltchaninoff, véritable pionnière du remplacement valvulaire aortique percutané, de me faire l'honneur de participer à ce jury et de juger ce travail. Soyez assurée de mon profond respect.

Mes remerciements vont également au Professeur Martine Gilard qui a elle aussi largement contribué au rayonnement de la cardiologie interventionnelle structurelle française. C'est un privilège de vous compter parmi les membres de ce jury. Recevez ici l'expression de ma sincère reconnaissance.

Je remercie chaleureusement Michel Rochette, pour son dynamisme dans les collaborations que nous avons pu mener avec ANSYS dans le cadre de cette Thèse, ainsi que pour sa disponibilité « au pied levé » pour prendre part à ce jury.

Je remercie le Professeur Hervé Le Breton, co-directeur de ce travail, pour sa confiance et son soutien, qui furent indispensables au cours de la longue et parfois difficile aventure qu'a représentée cette Thèse. Nul doute que ces éléments seront également nécessaires dans les prochaines étapes de mon cursus universitaire. Merci également de m'avoir ouvert les portes de la cardiologie interventionnelle, il y a quelques années maintenant, et de me permettre de pratiquer cette spécialité passionnante, dans toute sa diversité, au sein d'une unité où règne une ambiance cordiale et bienveillante sous votre impulsion.

A tout seigneur, tout honneur, je tiens également à exprimer ma gratitude et mon profond respect à mon directeur de Thèse, le Professeur Pascal Haigron. Je suis sincèrement reconnaissant pour ta patience, ton enseignement, ta rigueur scientifique et ta minutie tout au long de ce travail. Notre collaboration a débuté lors de mon Master II et je ne doute pas qu'elle se poursuivra au-delà de cette Thèse dans la dynamique de recherche que le LTSI, et toi en particulier, avez su crée en médecine cardiovasculaire.

Je n’oublie pas ici les personnes sans lesquelles je n’aurais jamais pu accomplir ce travail, je pense notamment à l’aide inestimable que m’ont apporté Miguel Castro et Phuoc Vy dans les aspects de traitement de l’image et de simulation numérique, respectivement. Je remercie également l’équipe de Therenva avec qui je prends un réel plaisir à échanger et collaborer au quotidien. J’exprime également toute ma gratitude et mon amitié au Dr Josep Rodés-Cabau, à sa formidable équipe de recherche et à tous mes co-fellows de l’Institut Universitaire de Cardiologie et de Pneumologie de Québec pour leur accueil, leur soutien et les bons moments passés ensemble au cours d’une année riche tant sur le plan professionnel que personnel.

Je remercie mes maîtres et collègues rennais pour leurs enseignements et encouragements tout au long de mon parcours.

Merci à mes amis, dont je ne ferai pas la liste ici au risque d’en oublier, qui m’ont apporté leur soutien au quotidien et permis de sortir, de manière salutaire, la tête de mon travail.

Je remercie ma famille au sens large, mon frère et ma sœur, ma grand-mère et bien entendu mes parents pour leur intérêt et leur soutien indéfectible depuis le début de mon parcours. J’ai beaucoup de chance de vous avoir.

Enfin, je remercie Carine pour sa compréhension et son soutien dans un parcours parfois compliqué pour une jeune famille. Paul, Adrien et toi êtes ce que j’ai de plus cher. Merci pour tout.

Table des matières

Table des Figures

Résumé

La sténose aortique serrée constitue la valvulopathie acquise de l'adulte la plus fréquente affectant jusqu'à 10% des octogénaires. Sa prise en charge percutanée est en plein essor et confronte les cliniciens à des problématiques nouvelles constituant à ce titre un champ de recherche important. Notre travail s'inscrit dans le cadre des gestes médico-chirurgicaux assistés par ordinateur et vise à proposer des solutions d'aide à la décision basées sur l'assistance informatique. Cette Thèse est ainsi composée de 4 parties.

Une première partie porte sur la problématique médicale dans laquelle s'inscrit le remplacement valvulaire aortique percutané (TAVI) ainsi que le contexte actuel du TAVI en France et s'appuie sur un article évaluant l'évolution des caractéristiques des patients et des procédures à l'échelle nationale entre 2010 et 2015 dans les registres nationaux FRANCE 2 et FRANCE TAVI. Ce premier chapitre identifie des problématiques médicales auxquelles les opérateurs restent confrontés au quotidien notamment la sélection optimale des candidats et la minimisation des complications de la procédure dans le contexte d'une réduction du profil de risque des patients traités.

La seconde partie s'intéresse à l'étude de population, par des méthodes statistiques classiques, pour établir des facteurs prédictifs de résultats du TAVI ou de survenue d'une complication donnée afin d'aider le clinicien dans sa planification de la procédure. Cette partie est articulée autour de 3 articles portant sur les facteurs prédictifs d'accidents vasculaires cérébraux post-TAVI, les troubles conductifs post-TAVI et les facteurs prédictifs de « mauvais résultats » après TAVI. Nous démontrons l'intérêt de ce type d'analyse qui resteront nécessaires à l'avenir mais abordons également leurs limites qui expliquent pourquoi d'autres pistes doivent être explorées pour stocker, trier, restituer les informations pertinentes à l'opérateur voire les augmenter pour faciliter ses décisions notamment en préopératoire.

L'objet de la 3ème partie est d'aborder un système d'aide à la décision par ordinateur de type « case-based reasoning » (CBR) qui pourrait tirer bénéfice de l'identification de ces facteurs pronostiques et à terme les intégrer dans une interface globale et ergonomique d'aide à la décision. Nous avons ainsi travaillé dans le cadre du projet européen H2020 EurValve sur l'élaboration d'un CBR dont la problématique se concentre pour l'instant sur le choix optimal de la voie d'abord, du type et de la taille de prothèse. Notre travail s'est concentré sur une étape analytique de la conception de ce type de système portant sur l'étude et l'amélioration de la mesure de similarité utilisée pour rapprocher le cas à traiter (problème) de ses plus proches voisins (cas déjà traités et leur « solution » thérapeutique).

Enfin, une dernière partie porte sur l'augmentation des informations disponibles pour l'aide à la décision en préopératoire par la simulation numérique spécifique patient. Après un état de l'art des méthodes utilisées dans le domaine du TAVI, nous avons travaillé à l'élaboration et le paramétrage d'un modèle de simulation de l'insertion du guide rigide dans le ventricule gauche (une des premières étapes de la procédure qui peut conditionner le positionnement de la prothèse et donc le résultat final). Afin de réaliser une première validation de cette simulation spécifique patient exploitant l'imagerie tomodensitométrique 3D préopératoire, l'approche proposée repose sur l'extraction de la région d'intérêt dans le volume 3D (segmentation) et sa mise en correspondance avec l'imagerie fluoroscopique 2D peropératoire par le biais d'un recalage 3D/2D. Nos travaux sur ces méthodes de traitement de l'image nécessaires à la mise en œuvre et la validation de notre stratégie de simulation sont également discutés dans cette partie. Enfin nous présentons une application clinique potentielle du modèle de simulation portant sur l'influence de la forme du guide et de ses conditions d'insertion sur sa stabilité et les forces de pression s'exerçant sur le ventricule gauche.

Mots clés: Sténose aortique; Remplacement valvulaire aortique; Transcatheter Aortic Valve Implantation; Aide à la décision; Simulation numérique

Introduction

La sténose aortique serrée constitue la pathologie valvulaire cardiaque acquise la plus fréquente chez l'adulte. Pendant plusieurs décennies, son seul traitement curatif était représenté par la chirurgie cardiaque de remplacement valvulaire aortique, geste dont la lourdeur ne permettait pas le traitement d'un grand nombre de patients âgés, comorbides et fragiles qui se retrouvaient dès lors dans une impasse thérapeutique. A l'instar de l'angioplastie coronaire, apparue à la fin des années 70 comme une alternative au pontage aorto-coronarien chirurgical, le remplacement valvulaire aortique percutané, désigné sous son acronyme anglo-saxon TAVI (pour Transcatheter Aortic Valve Implantation), s'inscrit dans cette optique de réduction du caractère invasif des traitements afin d'offrir une solution thérapeutique pérenne au plus grand nombre. Développée et réalisée pour la première fois en 2002 par l'équipe du CHU de Rouen, cette technique était initialement dévolue à des patients récusés chirurgicalement ou à très haut risque chirurgical. Fort de ses bons résultats chez ces patients, la technique a démontré, en un peu plus de quinze ans d'existence, son efficacité dans le traitement des patients porteurs d'une sténose aortique serrée, quel que soit leur risque chirurgical, constituant une véritable révolution dans la prise en charge de cette pathologie.

Ce changement de paradigme, extrêmement rapide dans le contexte médical, soulève bien entendu de nombreuses interrogations, sources d'une recherche biomédicale intense. A l'étape préopératoire, l'évolution du profil de risque des patients implique des problèmes de sélection des candidats à une procédure TAVI afin d'éviter les gestes « futiles ». Elle impose également une individualisation toujours plus grande dans la planification et la réalisation du geste, afin de se confronter avantageusement à l'étalon chirurgical dont les résultats sont excellents et largement éprouvés, notamment chez les patients à risque chirurgical faible. Lors des phases opératoires et post-opératoires, les cliniciens restent confrontés à plusieurs problématiques. Les difficultés de prédiction du positionnement final de la prothèse après largage selon son positionnement initial et donc la problématique de la sélection de la position de départ optimale, la prédiction du résultat en terme de risque de fuite périprothétique, ou encore l'identification des patients à risque de complications de la procédure afin de mettre en œuvre les mesures préventives ou la prise en charge les plus adaptées restent des questions du quotidien pour les opérateurs.

L'avènement de cette prise en charge endovasculaire s'est largement appuyé sur l'imagerie médicale, élément indispensable dans la sélection des patients et la planification du geste. A ce titre, les procédures TAVI confrontent en routine les cliniciens à la discordance entre la richesse des informations anatomiques obtenues grâce à l'imagerie tridimensionnelle préopératoire et les limites de l'imagerie fluoroscopique utilisée en peropératoire dans ce contexte mini-invasif ne permettant qu'une perception imparfaite de la configuration anatomique et des dispositifs endovasculaires.

Pour répondre aux problématiques soulevées par ces procédures, l'usage actuel des données cliniques et d'imagerie par les praticiens, largement basé sur l'empirisme et des approches statistiques, ne permet pas l'exploitation pleine et entière des informations recueillies en préopératoire non seulement à propos d'un cas particulier mais également issues des expériences passées. Ainsi, le TAVI pourrait bénéficier, quelle que soit la phase de la procédure considérée, mais notamment pour les problématiques d'aide à la décision, de méthodes novatrices comme l'assistance au geste par l'informatique s'inscrivant dans le concept global de gestes médico-chirurgicaux assistés par ordinateur (GMCAO ou Computer Assisted Medical Intervention – CAMI). L'ambition des GMCAO est de faciliter l'exploitation par le clinicien de données acquises, définies ou calculées avant l'intervention et de permettre la restitution des informations pertinentes lors de toutes les phases de l'intervention, y compris sur le lieu de l'intervention. Les objectifs scientifiques qui en découlent sont la conception, le développement et l'évaluation de modèles des organes et des procédures cliniques, de méthodes de reconstruction, traitement et fusion de l'image et des données, de simulateurs destinés à apprendre le geste, à le monitorer, ou à en anticiper les conséquences, et enfin l'élaboration de systèmes de guidage robotisés ou non. Afin d'élaborer des solutions d'aide à la décision ou à l'action compatibles avec la routine clinique et de restituer l'information pertinente au travers d'interfaces ergonomiques, les moyens mis en œuvre reposent sur différentes sources d'informations et technologies: données d'imagerie, simulation et réalité augmentée, micro-technologies et robotique médicale. Classiquement, les GMCAO sont structurés autour d'un cycle *Perception-Raisonnement-Action* (1,2), relativement comparable à celui suivi par le clinicien lors de la planification et de la réalisation d'un geste thérapeutique. La phase de *Perception* consiste notamment en l'acquisition de toutes les données (imageries, expérience de l'opérateur, divers capteurs…) permettant une modélisation générique ou spécifique-patient d'une structure anatomique ou d'un geste particulier. Il s'agit donc d'identifier tous les attributs anatomiques, physiologiques ou mécaniques nécessaires puis de faire intervenir des fonctions

d'analyse d'image, de caractérisation et de reconstruction/description des structures anatomiques, mais aussi de recalage/fusion de données et de suivi des structures et/ou dispositifs. La phase de *Raisonnement* vise à fournir au clinicien les éléments d'aide à la décision (sélection des patients, choix des options thérapeutiques, planification préopératoire, planification et adaptation peropératoire, analyse post-opératoire). Les moyens mis en œuvre pour ainsi définir la stratégie et le mode opératoire s'appuient sur des méthodes algorithmiques visant à modéliser et/ou prédire les conséquences d'un acte interventionnel aux stades pré- per- et post-opératoires. Différentes approches, plus ou moins individualisées, sont envisageables (analyse et modélisation statistique à partir d'une cohorte de patients, modélisation biomécanique et simulation spécifique patient des interactions outils/tissus, etc…). Enfin, la phase *d'Action* consiste essentiellement en la réalisation de l'acte en lui-même et fait intervenir les problématiques de navigation, de robotique médicale et d'interfaçage homme/machine. Malgré ses attraits potentiels, la diffusion de cette approche dans le domaine médical reste inégale selon les spécialités considérées, bien souvent car les questions concernant ses bénéfices clinique, logistique et médico-économiques restent en suspens. Dans le contexte médical et du TAVI, la simulation numérique en est un exemple puisque si plusieurs études ont évalué son intérêt potentiel pour la prédiction de différents éléments de la procédure, son usage n'est pas encore solidement ancré dans la pratique courante. En effet, si elle offre la possibilité théorique d'explorer diverses configurations anatomiques, de considérer différents outils et de simuler de multiples conditions opératoires, elle se heurte également, dans le milieu médical, à des obstacles à son utilisation courante comme le caractère unique à chaque individu de l'anatomie et des propriétés mécaniques des tissus biologiques complexifiant la mise au point de modèle de simulation spécifique patient.

Dans ce contexte, l'objectif de cette Thèse est d'aborder de façon non exhaustive, la problématique de l'aide à la décision dans le domaine du TAVI, l'apport et les limites des méthodes d'analyse statistique classiquement employées dans le domaine médical et enfin l'intérêt potentiel pour les compléter d'approches d'assistance par ordinateur à l'aide à la décision. Cette Thèse, articulée autour de ses contributions originales, présentées à travers dix articles, se compose ainsi de quatre chapitres. Le premier chapitre vise à rappeler les éléments médicaux essentiels à la compréhension des problématiques liées au TAVI. Il rappelle, dans un article original, le contexte actuel du TAVI en France en présentant le profil des patients traités, les complications hospitalières et les résultats à court terme des procédures par une analyse du registre national FRANCE TAVI. Le deuxième chapitre aborde l'apport et les limites des

approches statistiques habituellement employées dans le domaine médical pour mettre en évidence des facteurs de risque de complications de la procédure afin de permettre une meilleure sélection des candidats au TAVI et une individualisation plus grande de la planification et de la réalisation du geste visant à prévenir et prendre en charge de manière optimale les complications chez les patients à haut risque. Pour compléter ces approches « classiques », le troisième chapitre introduit l'intérêt de l'assistance par ordinateur à la décision en présentant notre travail sur un système d'aide à la décision basé sur le « case-based reasoning » adapté aux questions de choix de la voie d'abord et de la prothèse dans le cadre d'une procédure TAVI. Cet aspect d'assistance informatique à l'aide à la décision lors de la phase pré-opératoire est ensuite développé dans le chapitre 4 en se positionnant sous le prisme de la simulation numérique. Ce chapitre propose une revue de la littérature concernant les méthodes de simulation évaluées dans le contexte du TAVI permettant d'exposer le rationnel, les résultats et applications potentielles de nos travaux sur un modèle numérique de simulation du positionnement initial du guide rigide, utilisé lors des procédures, au niveau de l'aorte ascendante et du ventricule gauche. Les méthodes de traitement de l'image (segmentation automatique de structures anatomiques, recalage d'image) mises en œuvre pour produire ce modèle de simulation et les travaux en découlant sont également présentés dans ce chapitre.

Ce travail faisant intervenir plusieurs disciplines impliquées dans les technologies de santé, nous avons tenté de tenir un discours intelligible pour les différents acteurs en rappelant dans chaque chapitre certaines notions théoriques ou concepts méthodologiques dans les limites de notre champ de compétences.

Chapitre 1

Contexte clinique et état des lieux du TAVI en France

L'objectif de ce chapitre est de préciser les éléments cliniques nécessaires à la compréhension des problématiques entourant le TAVI. Dans un premier temps, nous rappelons la cadre pathologique dans lequel s'inscrit le TAVI puis nous détaillons les éléments nécessaires au bilan préopératoire, notamment les éléments d'imagerie. Les grandes étapes et le matériel utilisé lors de la procédure sont ensuite abordés. Enfin, à travers un article original, un état des lieux récent des indications, conditions techniques de réalisation, complications hospitalières et résultats à court terme du TAVI en France, est présenté.

1.1 Sténose aortique

Le TAVI est dans la grande majorité des cas pratiqué pour traiter une sténose aortique serrée symptomatique. Dans cette section, nous rappelons brièvement des éléments d'anatomie, de physiologie et d'épidémiologie concernant la valve aortique et la sténose aortique serrée.

1.1.1 Rappels anatomiques

La valve aortique est l'une des quatre principales valves du cœur. Elle se situe à l'extrémité de la voie d'éjection du ventricule gauche, séparant ce dernier de l'aorte (**Figure 1**). Elle est constituée de 3 feuillets semi-lunaires, appelés cusps, correspondants à de petits replis d'endocarde sur une lame fibreuse attachée à la paroi du ventricule gauche et de l'aorte. Ces cusps soutiennent les trois sinus de Valsalva, renflements de la partie initiale de l'aorte ascendante, d'où naissent les 2 artères coronaires. Les cusps sont donc logiquement désignées sous les noms de cusp coronaire gauche, cusp coronaire droite et cusp non coronaire. Plus rarement, la valve aortique peut n'être formé que de deux feuillets (bicuspidie aortique) et exceptionnellement d'un (unicuspidie) ou de quatre feuillets (quadricuspidie aortique).

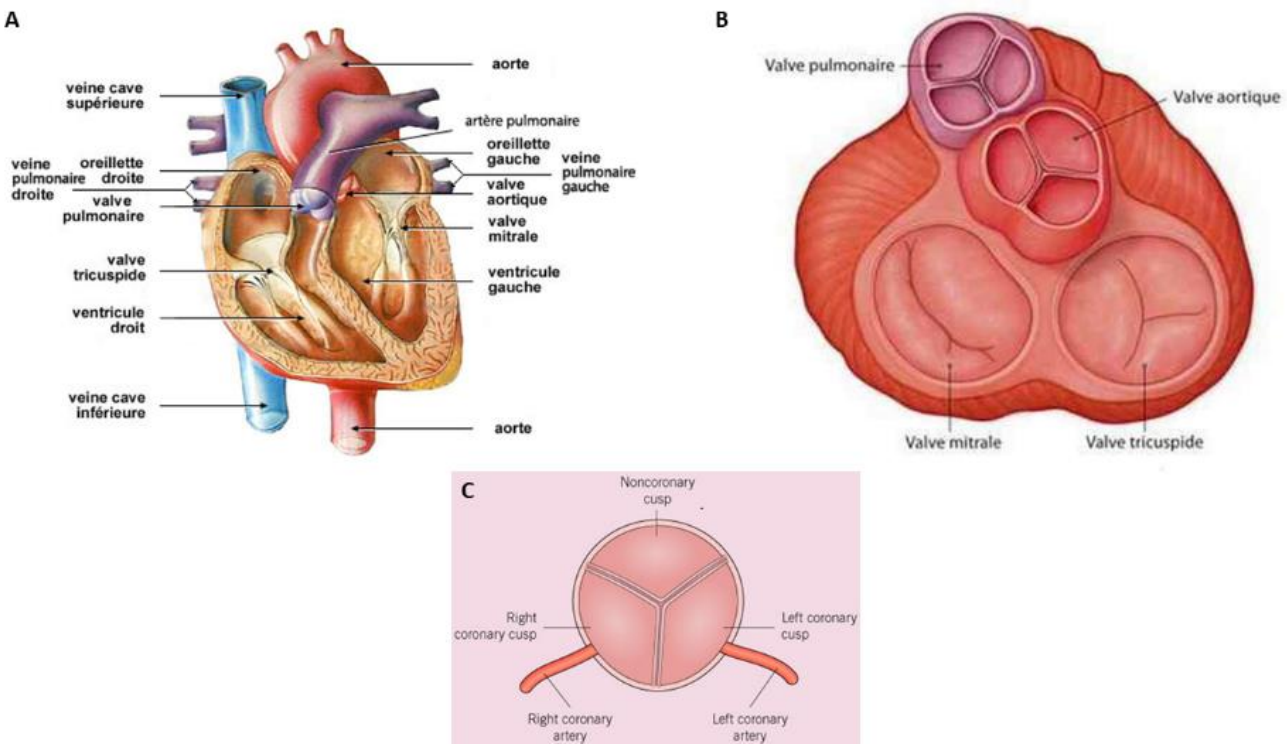

Figure 1 – Anatomie de la valve aortique. A) Rapports anatomiques avec les structures cardiaques environnantes. B) Vue de la base du cœur, oreillettes réséquées et rapports avec les autres valves cardiaques. C) Coupe transversale de la valve aortique présentant la dénomination des cusps et le rapport aux artères coronaires.

1.1.2 Fonctionnement physiologique de la valve aortique

Au cours du cycle cardiaque, la valve aortique contrôle le passage du flux d'éjection sanguin du ventricule gauche vers l'aorte. Lors de la phase de relaxation et de remplissage ventriculaire, appelée diastole, la valve reste fermée pour éviter un reflux de sang de l'aorte vers la cavité ventriculaire. Lors de la phase de contraction ventriculaire, appelée systole, la valve s'ouvre pour permettre l'éjection du flux sanguin du ventricule gauche vers l'aorte. La surface d'ouverture normale de la valve aortique est généralement comprise entre 2.5 et 3.5 cm^2. Ces mouvements d'ouverture et de fermeture de la valve aortique sont des phénomènes passifs, sous la dépendance du régime de pression ventriculaire et aortique au cours du cycle cardiaque. La valve s'ouvre lorsque la pression intra-ventriculaire gauche dépasse la pression aortique en début de systole et vice versa en fin de systole (**Figure 2**).

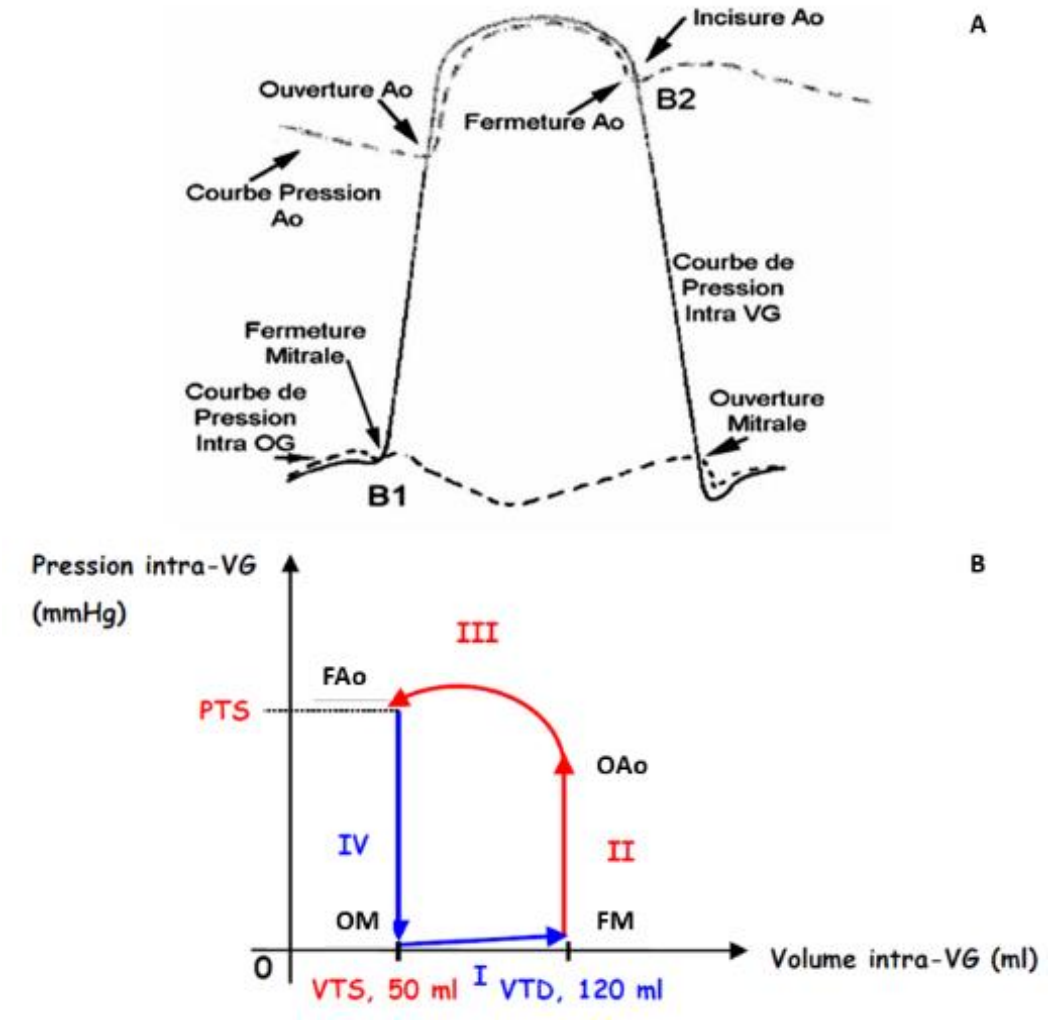

Figure 2 – Cycle cardiaque et mouvement de la valve aortique. A) Courbes de pression aortique (Ao), ventriculaire gauche (VG) et de l'oreillette gauche (OG) au cours du cycle cardiaque et leur relation avec les mouvements des valves aortiques et mitrales. B1 et B2 correspondent respectivement au premier bruit cardiaque (fermeture des valves atrio-ventriculaires) et au deuxième bruit cardiaque (fermeture des valves ventriculo-artérielles) à l'auscultation cardiaque. B) Courbe pression volume ventriculaire gauche. En bleu la diastole avec la phase de remplissage ventriculaire (I) et la phase de relaxation iso-volumique (IV) et en rouge la systole avec la phase de contraction iso-volumique (II) et la phase d'éjection ventriculaire (III). Fao : Fermeture de la valve aortique ; FM : Fermeture de la valve mitrale ; OAo : Ouverture de la valve aortique, OM : Ouverture de la valve mitrale, PTS : Pression télé-systolique ; VTD : Volume télé-diastolique ; VTS : Volume télé-systolique.

1.1.3 Mécanismes et conséquences physiopathologiques de la sténose aortique serrée.

De nombreux facteurs de risque anatomiques, génétiques et cliniques interviennent dans la genèse d'une sténose aortique serrée (**Figure 3**) (3). Ces différents mécanismes agissent au niveau cellulaire et moléculaire conduisant au dépôt de calcifications sur les feuillets valvulaires aortiques. Le phénomène est lentement aggravatif conduisant à une diminution progressive de la surface d'ouverture aortique par limitation du jeu des feuillets valvulaires. Lorsque la surface devient $\leq 1 cm^2$, on parle de sténose aortique serrée. Cette surface d'ouverture aortique réduite réalise un obstacle à l'éjection du volume sanguin par le ventricule gauche et réalise physiopathologiquement pour ce dernier une surcharge en pression pure qui est responsable des adaptations anatomiques observées dans la sténose aortique serrée (**Figure 4**). L'élévation de la pression intra-ventriculaire gauche conduit à une augmentation de la tension pariétale à laquelle le ventricule gauche répond par une hypertrophie précoce, selon la loi de Laplace. Cette hypertrophie entraîne une altération de la fonction de relaxation (diastolique) du muscle cardiaque, contribuant à entretenir une pression intra-ventriculaire gauche élevée. L'élévation chronique du régime de pression contribue en amont du ventricule gauche à une dilatation de l'oreillette gauche puis à un stade avancé à une élévation des pressions dans l'artère pulmonaire. Par ailleurs, l'hypertrophie peut être délétère pour la perfusion coronaire, notamment par des phénomènes de compression de la microcirculation, entraînant de la fibrose intra-myocardique qui favorise l'apparition généralement tardive d'une diminution de la fonction contractile du ventricule gauche (dysfonction systolique).

L'ensemble de ces éléments physiopathologiques expliquent les symptômes d'insuffisance cardiaque gauche qui peuvent être observés en cas de sténose aortique serrée avec notamment une dyspnée et une asthénie d'effort progressivement aggravative, conduisant les patients à réduire progressivement leurs activités. Par ailleurs, des douleurs thoraciques d'angor d'effort liées à l'hypoperfusion coronaire et des syncopes d'effort sont également rencontrées chez les patients.

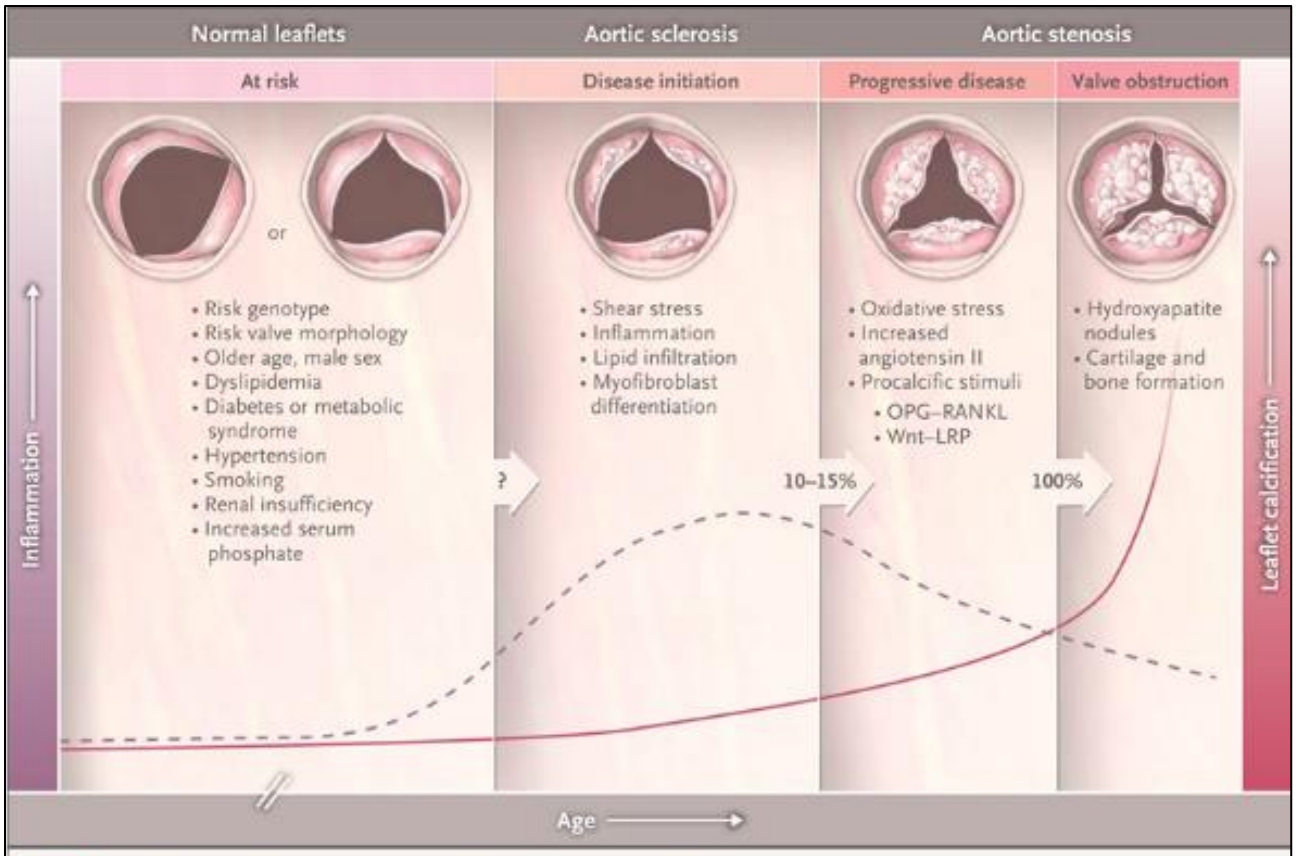

Figure 2. **Disease Mechanisms and Time Course of Calcific Aortic Stenosis.**

Shown is the relationship among disease stage, valve anatomy, clinical risk factors, mechanisms of disease, and the age of the patient. Endothelial disruption with inflammation (dashed line) and lipid infiltration are key elements in the initiation of disease. There are few data on the prevalence of disease initiation in at-risk patients, and progressive disease develops in only a subgroup of these patients. Progressive leaflet disease, which is associated with several disease pathways, develops in approximately 10 to 15% of patients with aortic sclerosis. Once these disease mechanisms are activated, leaflet calcification results in severe aortic stenosis in nearly all patients. With end-stage disease, tissue calcification (red line) is the predominant tissue change, resulting in valve obstruction. Current imaging approaches are reliable only when substantial leaflet changes are present (in patients with progressive disease or valve obstruction), which limits clinical studies of interventions to prevent or slow the progression of early disease. LRP denotes lipoprotein receptor–related protein complex, OPG osteoprotegerin, and RANKL receptor activator of nuclear factor κB ligand.

Figure 3 – Mécanismes impliqués dans le développement des calcifications valvulaires aortiques. Reproduite d'après Otto C et al (3).

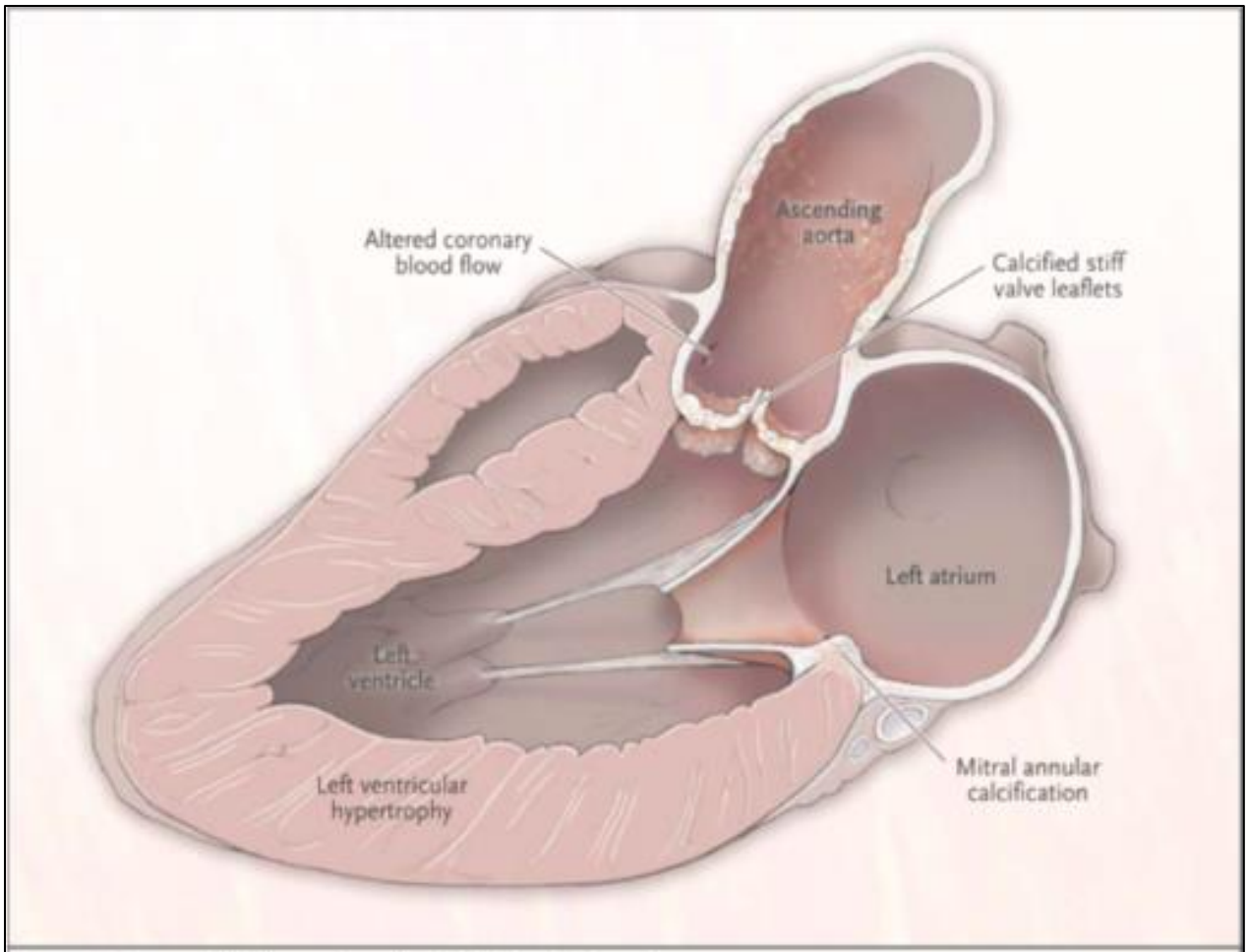

Figure 3. **Anatomical Changes Associated with Aortic Stenosis.**
Aortic-valve stenosis is associated with left ventricular hypertrophy, diastolic dysfunction, and decreased longitudinal shortening, although the ejection fraction remains normal in most patients. Left atrial enlargement is common owing to elevated left ventricular filling pressures. Calcification is often seen in the ascending aorta and mitral annulus, as well as on the valve leaflets. Mitral annular calcification is often accompanied by mild-to-moderate mitral regurgitation and can extend onto the leaflets, causing obstruction to left ventricular inflow. Patients with a severely calcified, rigid, and fragile ("porcelain") ascending aorta have better outcomes with transcatheter aortic-valve replacement than with surgical replacement. Coronary blood-flow patterns are abnormal owing to an increased left ventricular mass and a reduced diastolic pressure gradient.

Figure 4- Modifications anatomiques et fonctionnelles induites par une sténose aortique. Reproduite d'après Otto C et al (3).

1.1.4 Epidémiologie de la sténose aortique

La sténose aortique est la valvulopathie acquise de l'adulte la plus fréquente, représentant un tiers des patients inclus dans le registre européen Euro Heart Survey (4). Sa prévalence augmente avec l'âge, puisque si elle n'est que de 0.2% des adultes de 50 à 59 ans, elle atteint 9.8% des octogénaires pour une prévalence globale de 2.8% chez les plus de 75 ans

(3). En France, en 2015, 14 992 actes de remplacement valvulaire aortique isolé ont été réalisé en raison d'une sténose aortique serrée dont 45% par voie percutanée (5). Le nombre d'actes connait une augmentation graduelle depuis environ 2010, en rapport avec l'augmentation de l'activité de TAVI **(Figure 5)**.

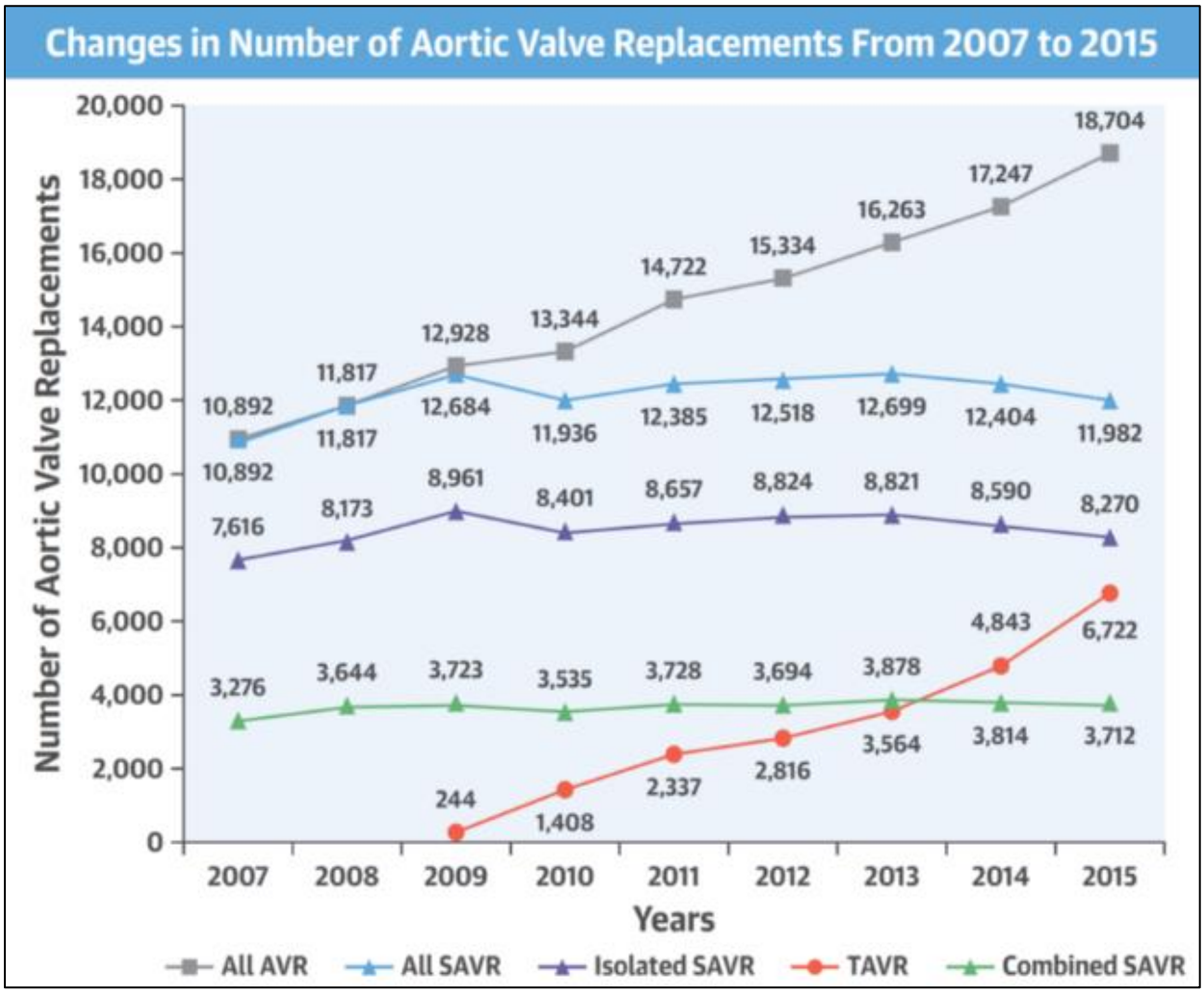

Figure 5- Evolution du nombre de gestes de remplacement valvulaire aortique chirurgicaux (isolés ou combinés à une autre chirurgie) et percutanés en France entre 2007 et 2015. Reproduite d'après Nguyen V et al (5).

En l'absence de traitement, la mortalité des formes symptomatiques de sténose aortique serrée avoisine les 70% à 2 ans chez des patients comorbides à haut risque chirurgical (6) ; un chiffre quasiment réduit de moitié par le traitement chirurgical ou percutané (6,7). En France, en 2015, la mortalité hospitalière d'un geste de remplacement valvulaire aortique isolé était inférieure à 2% et 3% pour la chirurgie et le TAVI, respectivement (5).

1.1.5 Traitement de la sténose aortique serrée

Il n'existe à ce jour aucun traitement pharmacologique validé permettant de prévenir le développement des calcifications valvulaires aortiques, de limiter leur évolution voire de les faire régresser une fois installées.

Le traitement de référence historique de la sténose aortique serrée est la chirurgie de remplacement valvulaire aortique. Cette chirurgie est réalisée à cœur arrêté et nécessite donc l'usage d'une circulation extracorporelle sous anesthésie générale **(Figure 6)**. Cette procédure est le plus souvent réalisée par sternotomie médiane afin d'accéder au médiastin. Le chirurgien procède alors à une aortotomie transversale lui permettant d'exposer la valve aortique pathologique qui sera excisée et remplacée par une prothèse solidarisée à l'anneau aortique par des points de suture **(Figure 7)**. Cette prothèse peut être mécanique ou biologique, formée alors de péricarde bovin ou porcin **(Figure 8)**.

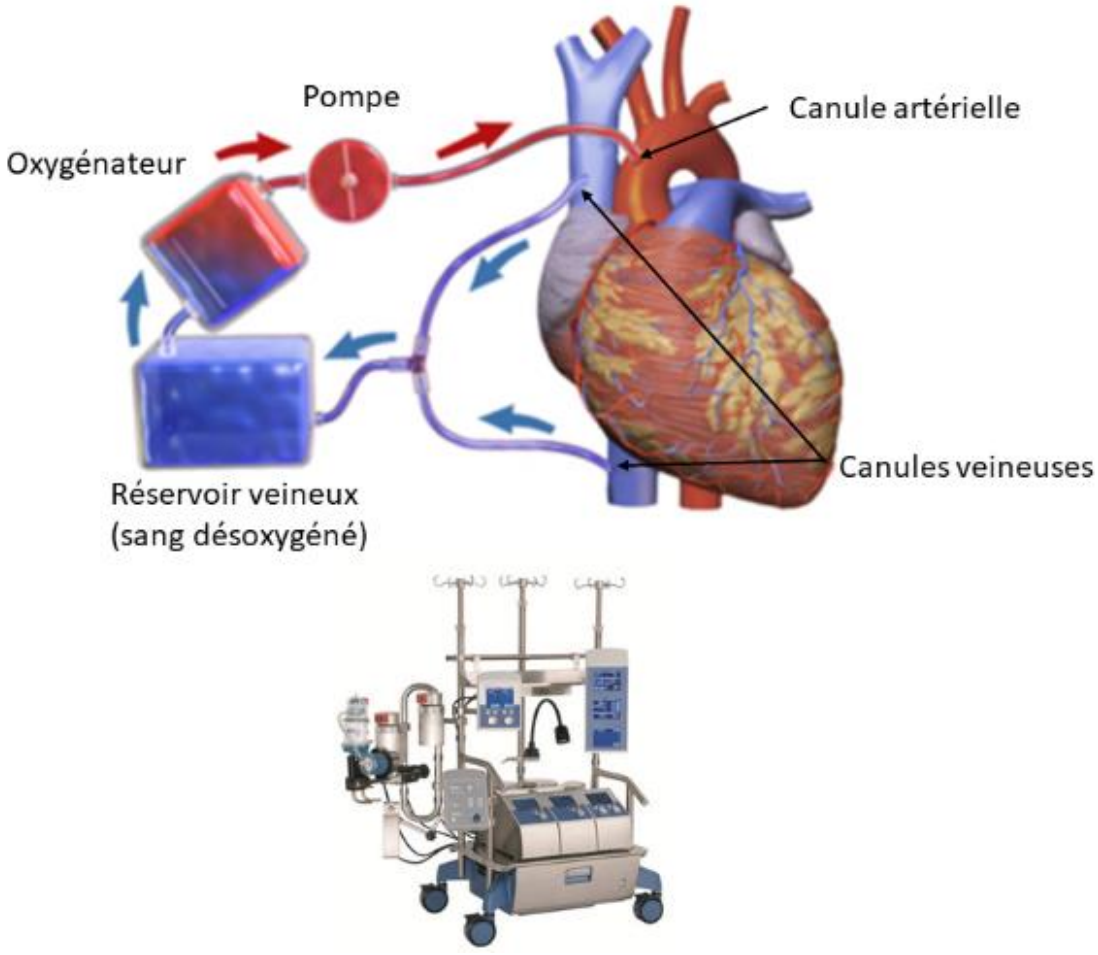

Figure 6 – Principe de fonctionnement d'une circulation extracorporelle et dispositif de circulation extracorporelle.

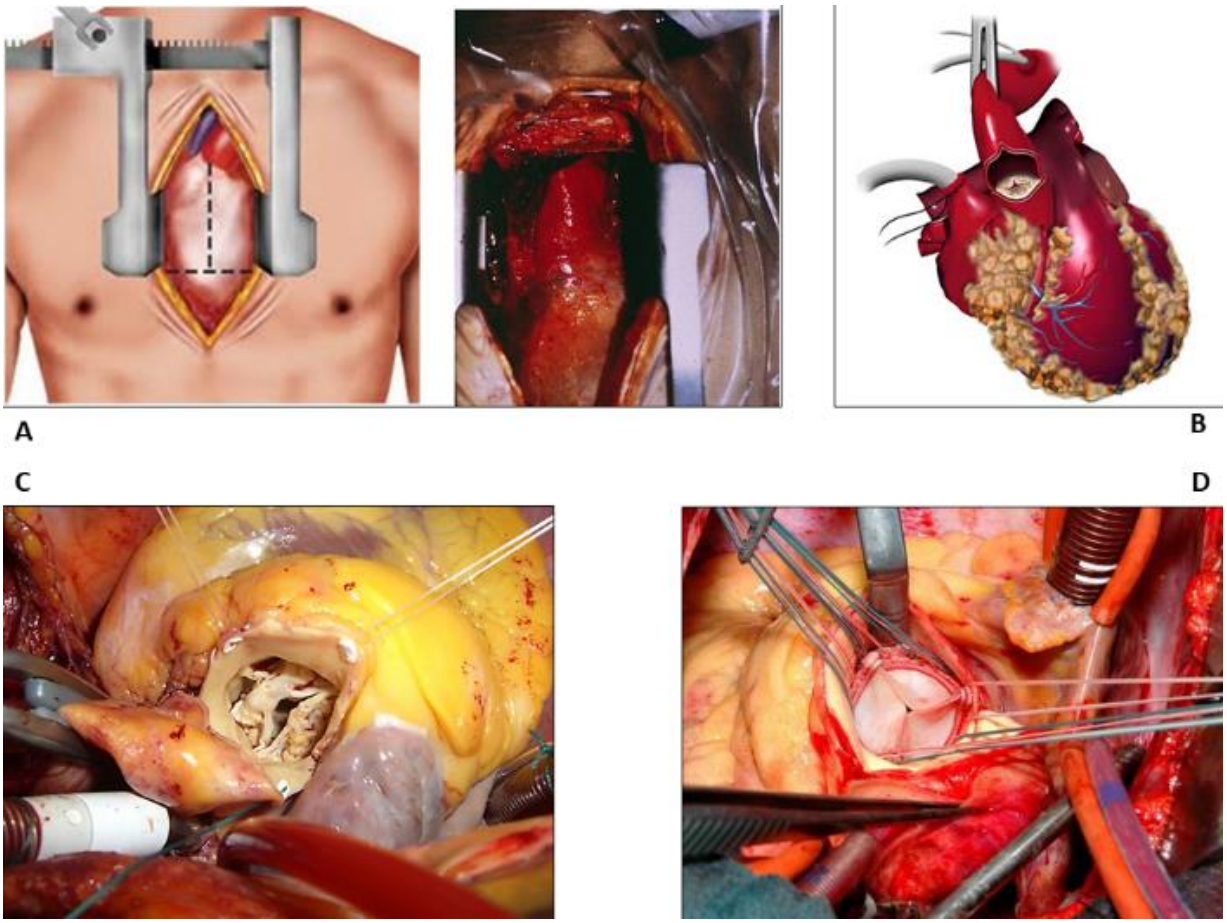

Figure 7 – Chirurgie de remplacement valvulaire aortique. A) Schéma et vue opératoire d'une sternotomie médiane. B) Principe de l'aortotomie transversale. C) Vue opératoire d'une sténose aortique serrée. D) Mise en place d'une prothèse valvulaire biologique en remplacement de la valve pathologique.

Figure 8 – Prothèses valvulaires. Valve mécanique à gauche et biologique (bioprothèse) à droite.

La chirurgie de remplacement valvulaire aortique est donc une chirurgie « lourde », nécessitant un séjour d'environ 48h en réanimation, une hospitalisation d'une durée totale de 7 à 10j en règle générale et une période de convalescence de durée variable mais s'étendant le plus souvent sur plusieurs semaines. S'agissant d'une chirurgie destinée principalement à des sujets âgés; l'âge moyen des patients traités pour une sténose aortique serrée en France en 2015 était de 72 ans (5) alors que 70% des 65 000 remplacements valvulaires aortiques effectués aux Etats-Unis en 2010 l'ont été chez des plus de 65 ans (3); elle peut se grever d'une importante morbi-mortalité notamment chez les patients comorbides. Ainsi, un tiers des patients présentant une valvulopathie sévère dans le registre Euro Heart Survey n'ont pas bénéficié d'une intervention chirurgicale en raison, pour 55% d'entre eux, de la présence d'au moins une comorbidité extracardiaque contre-indiquant la chirurgie (4). C'est afin d'offrir un traitement pérenne à ces patients contre-indiqués à la chirurgie qu'a initialement été développé le TAVI.

1.2 Remplacement valvulaire aortique percutané (TAVI)

1.2.1 Rappel historique

C'est grâce à leurs travaux autopsiques et sur l'animal initiés dans les années 90, qu'a finalement pu être implantée le 16 Avril 2002, la première valve aortique percutanée, par le Pr Cribier et son équipe au CHU de Rouen (8). Cette première a généré un important enthousiasme de la communauté médicale et un intérêt croissant des partenaires industriels. La société Edwards Lifesciences a acquis la start-up du Pr Cribier, pour développer la valve expandable à ballonnet Edwards SAPIEN alors que la société Medtronic a racheté la société CoreValve qui développait depuis 2004 une valve auto-expandable dans un stent en nitinol. Ces deux prothèses ont obtenu le marquage CE en 2007 et ont été évaluées dans de nombreux travaux multicentriques internationaux confirmant la faisabilité de la technique, la qualité hémodynamique des prothèses et du résultat fonctionnel de la procédure mais identifiant également des complications parfois plus spécifiques d'un type de prothèse ou d'une voie d'abord potentielle (9–11). Le registre FRANCE, incluant 244 patients dans 16 centres français entre Février et Juin 2009, a montré un taux de succès de la procédure de 98.3% avec une

mortalité à 30 jours de 12.7% chez des patients présentant une mortalité prédite à 30 jours selon l'EuroSCORE[1] (score de risque chirurgical usuel en chirurgie cardiaque) de 25.6±11.4% (12).

En 2010, la publication des résultats de la cohorte B de l'essai randomisé PARTNER (Placement of Aortic Transcatheter Valves Trial) marque un tournant évolutif majeur pour le TAVI (13). Trois cent cinquante-huit patients inopérables ont été inclus et randomisés pour bénéficier d'un TAVI avec une valve expandable à ballonnet ou du traitement médical optimal. A 1 an, la mortalité était réduite de 20% dans le groupe TAVI (49.7% vs. 30.7%), un résultat statistiquement significatif faisant ainsi du TAVI le traitement de référence des patients inopérables. La cohorte A, publiée l'année suivante, a quant à elle démontré la non-infériorité du TAVI à la chirurgie de remplacement valvulaire aortique chez les patients à haut risque chirurgical, en comparant 348 patients traités par TAVI, là encore avec une valve Edwards SAPIEN, à 351 patients traités chirurgicalement (14). La mortalité à 1 an du groupe chirurgical était de 26.8% contre 24.2% dans le bras TAVI (hazard ratio : 0.93 ; intervalle de confiance à 95% : 0.71-1.22 ; p=0.62). On notait, néanmoins, un taux d'accidents vasculaires cérébraux (AVC) plus important à 30 jours et 1 an dans le bras TAVI, générant des inquiétudes légitimes sur les complications neuro-vasculaires potentielles du TAVI à ce stade.

Le registre FRANCE 2, publié en 2012, témoigne de la rapidité d'implémentation de la technique dans la pratique courante, ayant inclus pas moins de 3195 patients à haut risque (Logistic EuroSCORE moyen : 21.9 ± 14.3%), traités dans les 33 centres français ouverts à l'époque (plus le centre de Monaco), entre Janvier 2010 et Octobre 2011(15). Ce registre a confirmé les excellents résultats de la technique malgré l'expansion rapide à des centres qui pour certains réalisaient leurs premières procédures dans le cadre du registre avec un taux de succès de procédure de 96.9%, une mortalité à 30 jours de 9.7% et à 1 an de 24.0%. Les taux de complications majeures étaient acceptables au regard de la population étudiée avec des taux d'AVC majeurs, d'infarctus du myocarde, de saignements majeurs, d'implantation de stimulateur cardiaque définitif (pacemaker) et de migration valvulaire respectivement de 2.3%, 1.2%, 1.2%, 15.6% et 1.3%. Enfin avec des valves et des dispositifs d'introduction de première génération, les taux de fuites para prothétiques au moins modérées et de complications vasculaires majeures étaient de 16.5% et 4.7%, respectivement.

En 2014, l'étude randomisée U.S CoreValve High Risk Study démontre, pour la première fois, la supériorité du TAVI avec implantation d'une prothèse auto-expandable sur la

[1] http://www.euroscore.org/

chirurgie chez des patients jugés à haut risque chirurgical (Logistic EuroSCORE : 17.6±13.0%), avec une mortalité à 1 an de 14.2% dans le groupe TAVI et 19.1% dans le groupe chirurgical (p=0.04 pour la supériorité) (16). Les taux d'AVC étaient identiques entre les 2 groupes.

Fort de ces succès chez les patients à haut risque chirurgical, le TAVI a alors été évalué chez des patients à risque intermédiaire dans les études PARTNER 2A (Valve Edwards SAPIEN XT) et SURTAVI (Valves CoreValve pour 84% des cas et EVOLUT R pour 16%), publiées respectivement en 2016 et 2017 (17,18). Ces 2 études randomisées au design similaire, incluant respectivement 2032 et 1660 patients, ont démontré la non-infériorité du TAVI à la chirurgie sur le critère composite des décès toutes causes et des AVC majeurs à 2 ans. Là aussi, les taux d'accidents neuro-vasculaires n'étaient pas significativement différents entre les 2 bras d'étude apportant des éléments rassurants par rapport aux résultats des premières études randomisées. Ces études ont contribué à un élargissement des indications du TAVI dans les dernières recommandations européennes et à une augmentation exponentielle du nombre de procédures en routine clinique. Ainsi, en Allemagne, dès 2012, le nombre de TAVI réalisés toutes voies d'abord confondues dépassait déjà le nombre de remplacements valvulaires aortiques chirurgicaux, et deux ans plus tard, le TAVI transvasculaire (transfémoral, transaortique ou sous-clavier) représentait la première option de traitement du rétrecissement aortique serré (19,20).

En mars 2019, les résultats de grandes études randomisées évaluant le TAVI chez des patients à bas risque chirurgical ont été publiés (21,22). L'étude PARTNER 3 a inclus 1000 patients dans 71 centres démontrant, au bout d'un suivi d'un an, non seulement la non-infériorité, mais également la supériorité du TAVI transfémoral avec implantation d'une valve Edwards Sapien de 3ème génération par rapport à la chirurgie sur un critère composite incluant les décès, les AVC et les réhospitalisations liées à la procédure, la valve ou une insuffisance cardiaque (8.5% vs. 15.1%) (21). L'étude EVOLUT Low Risk, comparant le TAVI quasi-exclusivement par voie transfémorale (99.0%) avec implantation d'une prothèse auto-expandable (EVOLUT R : 74.1% ; EVOLUT PRO : 22.3%) à la chirurgie chez 1468 patients, a démontré la non-infériorité du TAVI à la chirurgie sur un critère primaire composité associant le décès et les AVC majeurs à 2 ans (5.3% vs. 6.7%) (22). Ces 2 études sont également les premières études randomisées à démontrer une diminution du taux d'AVC à 30j dans le groupe de traitement percutané. Plusieurs critères secondaires de ces 2 études étaient également en faveur du TAVI (taux de nouvelle arythmie cardiaque post-opératoire, saignements majeurs, insuffisance rénale, durée d'hospitalisation). A contrario, les taux de fuite para prothétiques

modérée à sévère et d'implantation d'un stimulateur cardiaque définitif, numériquement plus élevés dans le bras TAVI de l'étude PARTNER 3, étaient significativement plus importants dans le bras TAVI, comparativement à la chirurgie, dans l'étude EVOLUT Low Risk. Au total, ces études devraient conduire à un nouvel élargissement des indications de traitement percutané dans les années à venir, faisant du TAVI la référence dans le traitement de la sténose aortique serrée symptomatique quel que soit le risque chirurgical. Enfin, le TAVI est désormais évalué dans de nouvelles indications comme le traitement des sténoses aortiques modérées chez des patients avec insuffisance cardiaque (Transcatheter Aortic Valve Replacement to UNload the Left Ventricle in Patients With ADvanced Heart Failure - TAVR UNLOAD ; NCT02661451) ou le traitement précoce des patients asymptomatiques (Evaluation of Transcatheter Aortic Valve Replacement Compared to SurveilLance for Patients With AsYmptomatic Severe Aortic Stenosis - EARLY TAVR, NCT03042104), traduisant la rapidité d'évolution quasiment sans équivalent dans le domaine médical d'une technique apparue il y a moins de 20 ans.

1.2.2 Indications actuelles du TAVI

Les indications de remplacement valvulaires aortiques sont actuellement définies par les recommandations 2017 de la société européenne de cardiologie (**Figures 9**)(23).

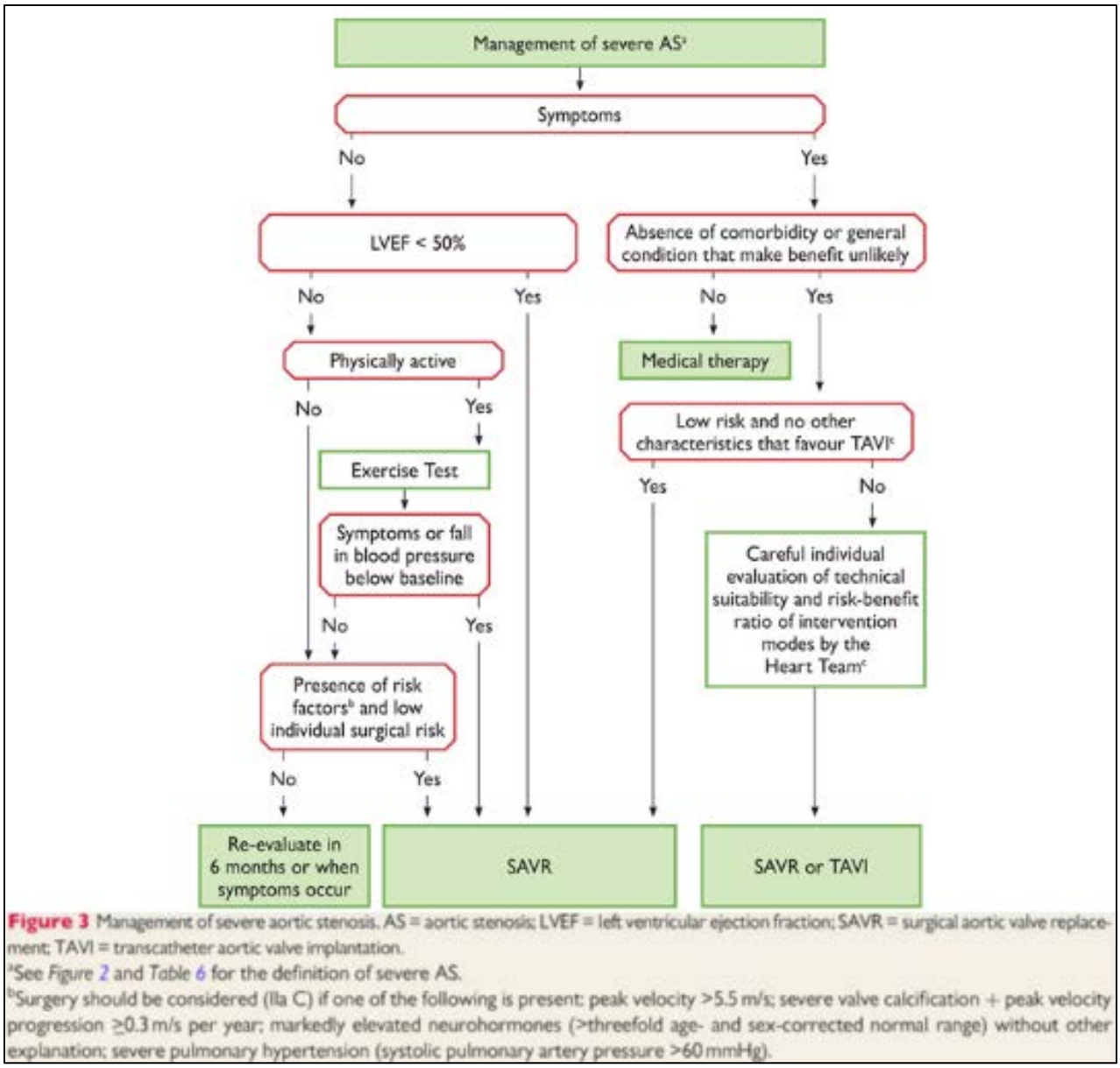

Figure 3 Management of severe aortic stenosis. AS = aortic stenosis; LVEF = left ventricular ejection fraction; SAVR = surgical aortic valve replacement; TAVI = transcatheter aortic valve implantation.
[a]See *Figure 2* and *Table 6* for the definition of severe AS.
[b]Surgery should be considered (IIa C) if one of the following is present: peak velocity >5.5 m/s; severe valve calcification + peak velocity progression ≥0.3 m/s per year; markedly elevated neurohormones (>threefold age- and sex-corrected normal range) without other explanation; severe pulmonary hypertension (systolic pulmonary artery pressure >60 mmHg).

Figure 9 – Algorithme décisionnel devant une sténose aortique serrée. Reproduite d'après Baumgartner H et al (23).

Dans ces recommandations, le TAVI est recommandé en première intention chez les patients symptomatiques inopérables (recommandation de grade I). Chez les patients symptomatiques opérables, à risque chirurgical intermédiaire ou haut, il est recommandé que le choix de l'intervention entre chirurgie et TAVI soit réalisé au cours de réunions multidisciplinaires comprenant cardiologues interventionnels et non-interventionnels, chirurgiens, gériatres et anesthésistes notamment (concept de « Heart Team »). Ce choix est individualisé selon les caractéristiques de chaque patient. Les recommandations précisent les

éléments cliniques et paracliniques, en faveur ou en défaveur de l'une ou l'autre technique, qui doivent guider la Heart Team dans sa décision **(Figure 10)**. Il faut toutefois noter que le TAVI n'a pour l'instant pas de place dans ces recommandations chez les patients asymptomatiques et les patients à bas risque chirurgical.

Table 7 Aspects to be considered by the Heart Team for the decision between SAVR and TAVI in patients at increased surgical risk (see Table of Recommendations in section 5.2.)

	Favours TAVI	Favours SAVR
Clinical characteristics		
STS/EuroSCORE II <4% (logistic EuroSCORE I <10%)[a]		+
STS/EuroSCORE II ≥4% (logistic EuroSCORE I ≥10%)[a]	+	
Presence of severe comorbidity (not adequately reflected by scores)	+	
Age <75 years		+
Age ≥75 years	+	
Previous cardiac surgery	+	
Frailty[b]	+	
Restricted mobility and conditions that may affect the rehabilitation process after the procedure	+	
Suspicion of endocarditis		+
Anatomical and technical aspects		
Favourable access for transfemoral TAVI	+	
Unfavourable access (any) for TAVI		+
Sequelae of chest radiation	+	
Porcelain aorta	+	
Presence of intact coronary bypass grafts at risk when sternotomy is performed	+	
Expected patient–prosthesis mismatch	+	
Severe chest deformation or scoliosis	+	
Short distance between coronary ostia and aortic valve annulus		+
Size of aortic valve annulus out of range for TAVI		+
Aortic root morphology unfavourable for TAVI		+
Valve morphology (bicuspid, degree of calcification, calcification pattern) unfavourable for TAVI		+
Presence of thrombi in aorta or LV		+
Cardiac conditions in addition to aortic stenosis that require consideration for concomitant intervention		
Severe CAD requiring revascularization by CABG		+
Severe primary mitral valve disease, which could be treated surgically		+
Severe tricuspid valve disease		+
Aneurysm of the ascending aorta		+
Septal hypertrophy requiring myectomy		+

CABG = coronary artery bypass grafting; CAD = coronary artery disease; EuroSCORE = European System for Cardiac Operative Risk Evaluation; LV = left ventricle; SAVR = surgical aortic valve replacement; STS = Society of Thoracic Surgeons; TAVI = transcatheter aortic valve implantation.

[a]STS score (calculator: http://riskcalc.sts.org/stswebriskcalc/#/calculate); EuroSCORE II (calculator: http://www.euroscore.org/calc.html); logistic EuroSCORE I (calculator: http://www.euroscore.org/calcge.html); scores have major limitations for practical use in this setting by insufficiently considering disease severity and not including major risk factors such as frailty, porcelain aorta, chest radiation etc.[103] EuroSCORE I markedly overestimates 30-day mortality and should therefore be replaced by the better performing EuroSCORE II with this regard; it is nevertheless provided here for comparison as it has been used in many TAVI studies/registries and may still be useful to identify the subgroups of patients for decision between intervention modalities and to predict 1-year mortality.

Figure 10 – Eléments permettant de guider le choix de l'intervention de remplacement valvulaire aortique chez les patients à risque chirurgical intermédiaire à haut.
Reproduite d'après Baumgartner H et al (23)

1.2.3 Principes du TAVI

Le TAVI consiste en l'implantation, à cœur battant, sans sternotomie ni circulation extracorporelle, d'une prothèse valvulaire biologique dans la valve native pathologique du patient, dont les calcifications permettent « d'ancrer » la prothèse.

A) Voies d'abord potentielles

Le TAVI est réalisé dans environ 85% des cas par ponction, le plus souvent percutanée (un abord chirurgical par une courte incision inguinale est possible dans de rares cas), d'une artère fémorale commune (24). La voie fémorale, étant la plus simple à mettre en œuvre et celle donnant les meilleurs résultats, est aujourd'hui considérée comme la voie de première intention par les centres pratiquant le TAVI (17,25,26). En cas d'impossibilité de réaliser le TAVI par voie fémorale, en raison d'un calibre artériel insuffisant et/ou d'importantes tortuosités ou calcifications, plusieurs autres voies sont décrites dans la littérature et utilisées couramment en clinique (**Figure 11**) (27). Ces voies alternatives, utilisées en routine, peuvent être divisées en voies transartérielles, transaxillaire/sous-clavière ou transcarotide, et en voies transthoraciques, transaortique ou transapicale. Elles nécessitent toutes un abord mini-chirurgical (en dehors de très rares cas d'abord sous-clavier percutané). La voie d'abord trans-cavale reste aujourd'hui anecdotique (28). Le choix entre ces différentes voies est réalisé par la Heart Team local selon des critères anatomiques et cliniques spécifiques de chaque patient et selon l'expérience locale des opérateurs. L'immense majorité des TAVI fémoraux est réalisé sous anesthésie locale, éventuellement associé à une sédation légère du patient. L'anesthésie locale avec sédation est également possible pour les voies transartérielles mais l'anesthésie générale reste la règle en cas de voie alternative à l'abord fémoral.

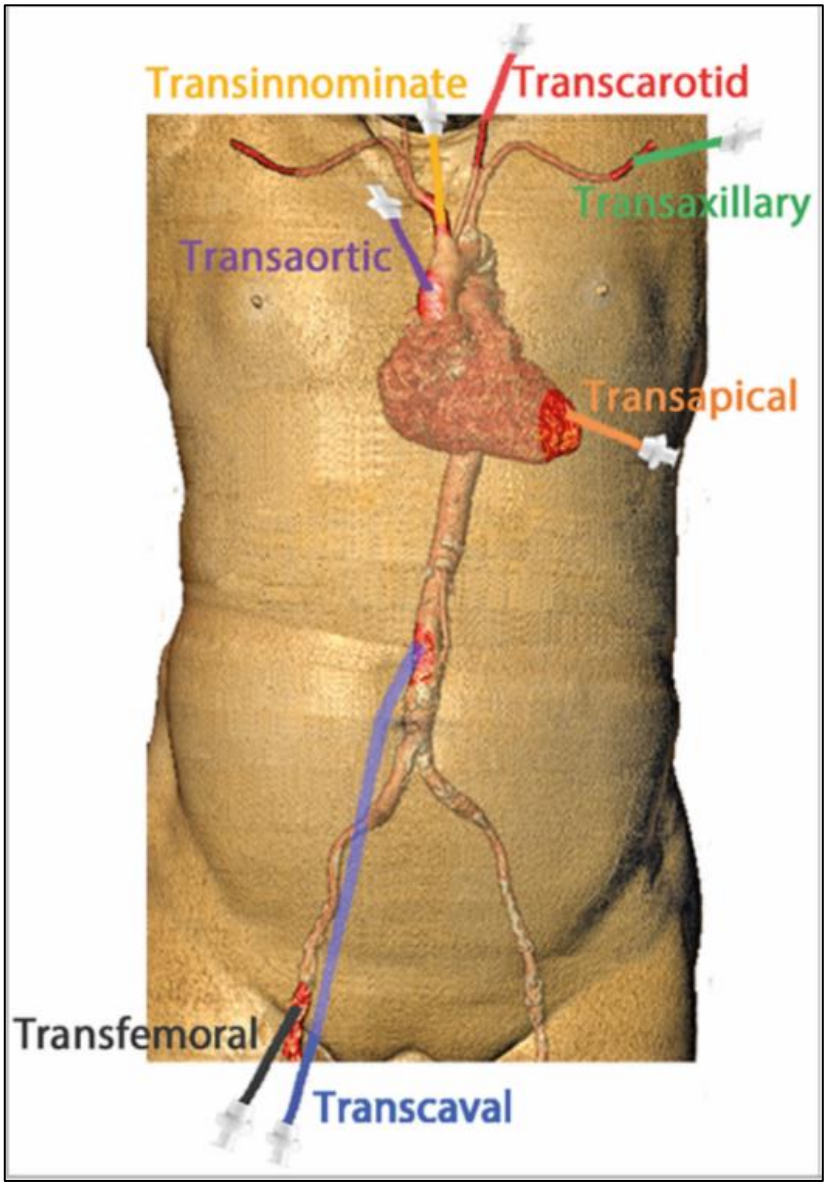

Figure 11 – Voies d'abord potentielles du TAVI. Reproduite d'après Lanz J et al (27)

B) Prothèses implantées

Deux types de prothèses sont actuellement implantés de manière courante en France. La SAPIEN 3, 3ème génération de la prothèse à expansion par ballonnet de la société Edwards Lifescience se compose d'un stent radio-opaque en alliage chrome-cobalt, d'une valve à 3 feuillets en péricarde bovin et d'un manchon en tissu de polyéthylène téréphtalate (**Figure 12**). La valve est traitée pour empêcher la formation de calcification et est stérilisée dans une solution de glutaraldéhyde. Cette valve dispose d'une jupe externe sur la partie inférieure du stent destinée à réduire les fuites paravalvulaires. Cette bioprothèse est produite en 4 diamètres: 20

mm, 23 mm, 26 mm et 29 mm. Les 3 premières sont compatibles avec un système d'introduction (désilet) de 14F de diamètre externe initial (1F=1 French= 0.33mm), la dernière nécessitant un introducteur de 16F.

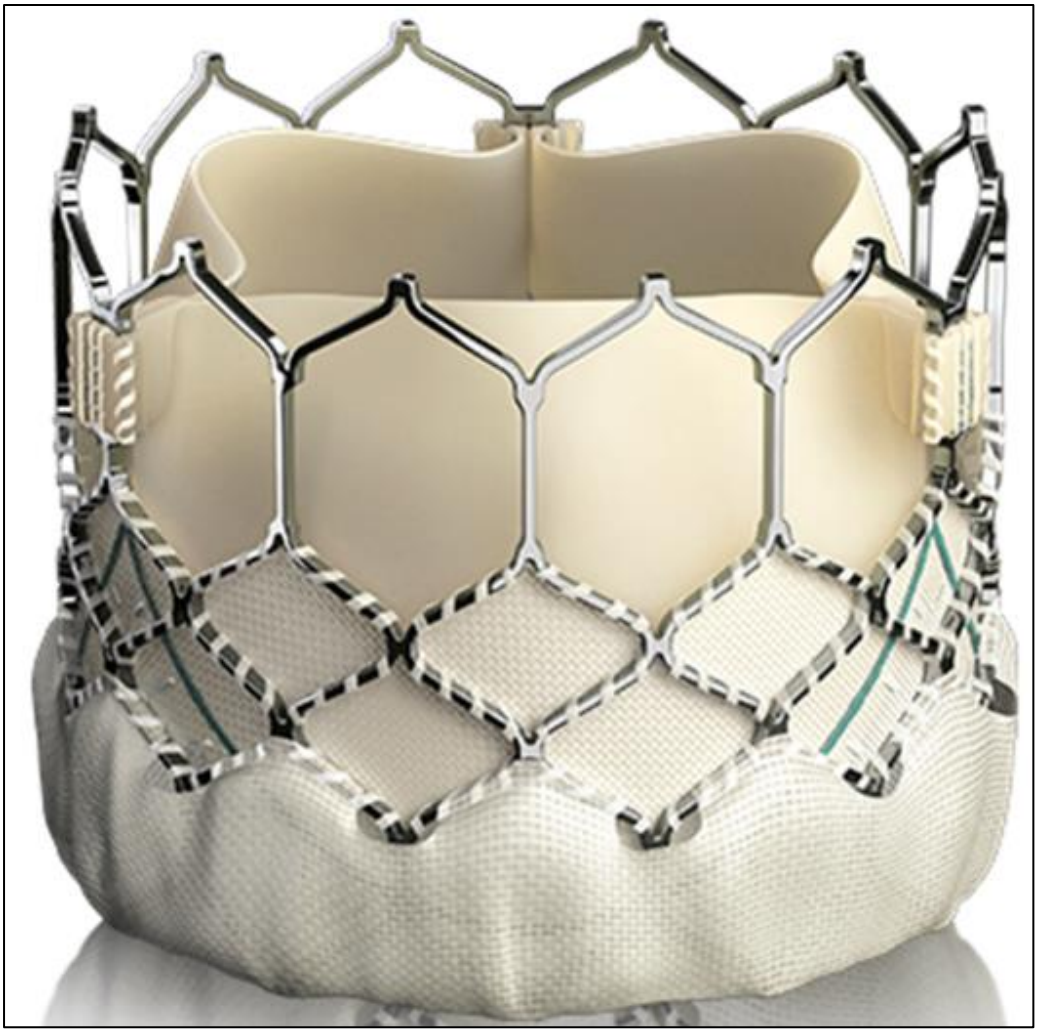

Figure 12- Prothèse Edwards SAPIEN 3

La bioprothèse COREVALVE EVOLUT PRO, de la société Medtronic, est une valve biologique en péricarde porcin montée sur une armature radio-opaque auto-expansible en Nitinol (**Figure 13**). Elle est composée de 3 feuillets fixés sur une jupe interne par des sutures de polyéthylène de très haut poids moléculaire et traités par acide alpha-amino oléique afin de prévenir le développement de calcifications. La bioprothèse possède également une membrane extérieure en tissu péricardique porcin. La prothèse est disponible en 3 diamètres : 23mm, 26mm et 29 mm (une taille de 34mm est disponible avec la précédente génération de cette prothèse l'EVOLUT R). La prothèse EVOLUT PRO est le plus souvent implantée sans système

d'introduction séparé via son cathéter d'introduction 16F disposant d'un désilet pré-monté (« In line sheath ») mais peut également être délivrée via un désilet 20F.

Figure 13- Prothèse Medtronic COREVALVE EVOLUT PRO

De nombreuses autres prothèses, auto-expansibles ou à déploiement mécanique, sont actuellement à des stades avancés de développement voire de mise sur le marché et seront peut-être utilisées en routine dans les années à venir (**Figure 14**). Ces prothèses ne seront pas détaillées ici.

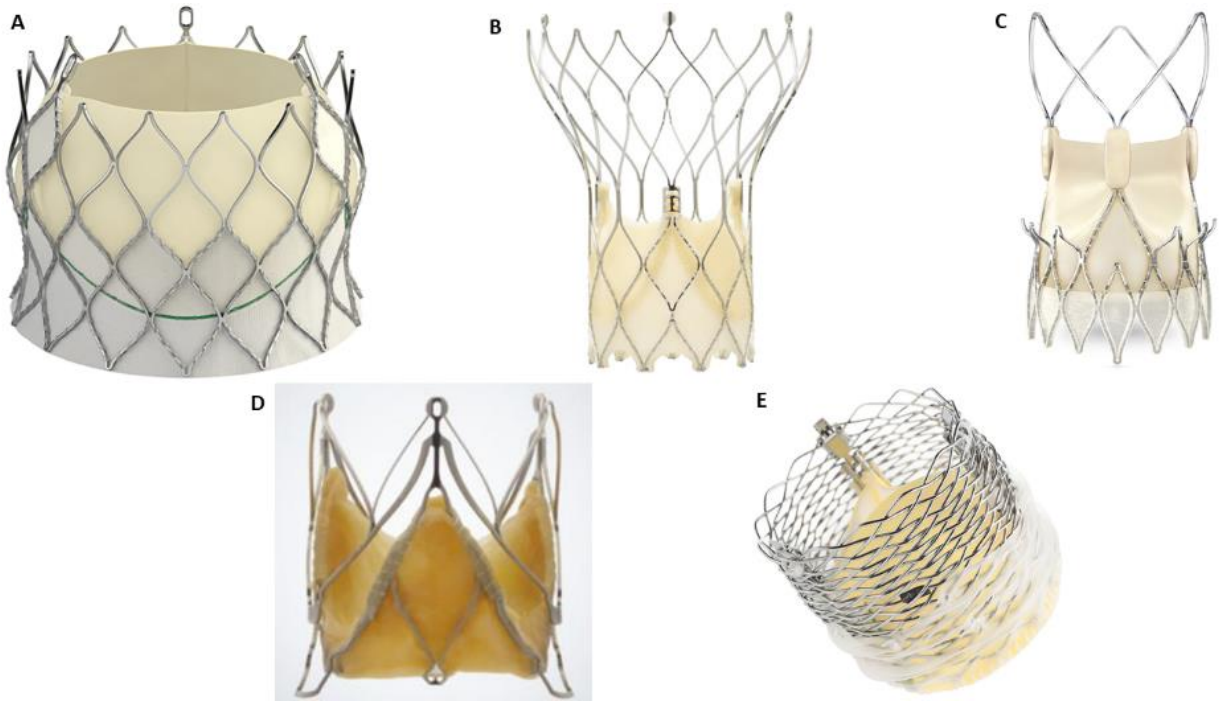

Figure 14 – Exemples de prothèses aortiques percutanées évaluées chez l'Homme. A- Prothèse CENTERA de la société Edwards Lifesciences. B- Prothèse PORTICO de la société Abbott. C- Prothèse ACCURATE NEO de la société Boston Scientific. D- Prothèse JENAVALVE de la société du même nom. E- Prothèse LOTUS EDGE de la société Boston Scientific.

C) Bilan pré-opératoire

Le premier examen clé du bilan pré-opératoire est l'échocardiographie qui va permettre d'établir le diagnostic (**Figure 15**). Plusieurs modes d'imagerie (2D, couleur) et de doppler (pulsé, continu) sont utilisés pour confirmer l'existence d'une sténose aortique serrée (classiquement définie par l'association d'une surface valvulaire < 1 cm^2 ou <0.6cm^2/m^2 de surface corporelle, d'un gradient de pression moyen transvalvulaire > 40 mmHg et d'une vitesse maximale transvalvulaire > 4 m/s), rechercher une autre atteinte valvulaire, évaluer le retentissement de la sténose aortique sur le ventricule gauche et les pressions intra-cardiaques et rechercher une dilatation aortique associée.

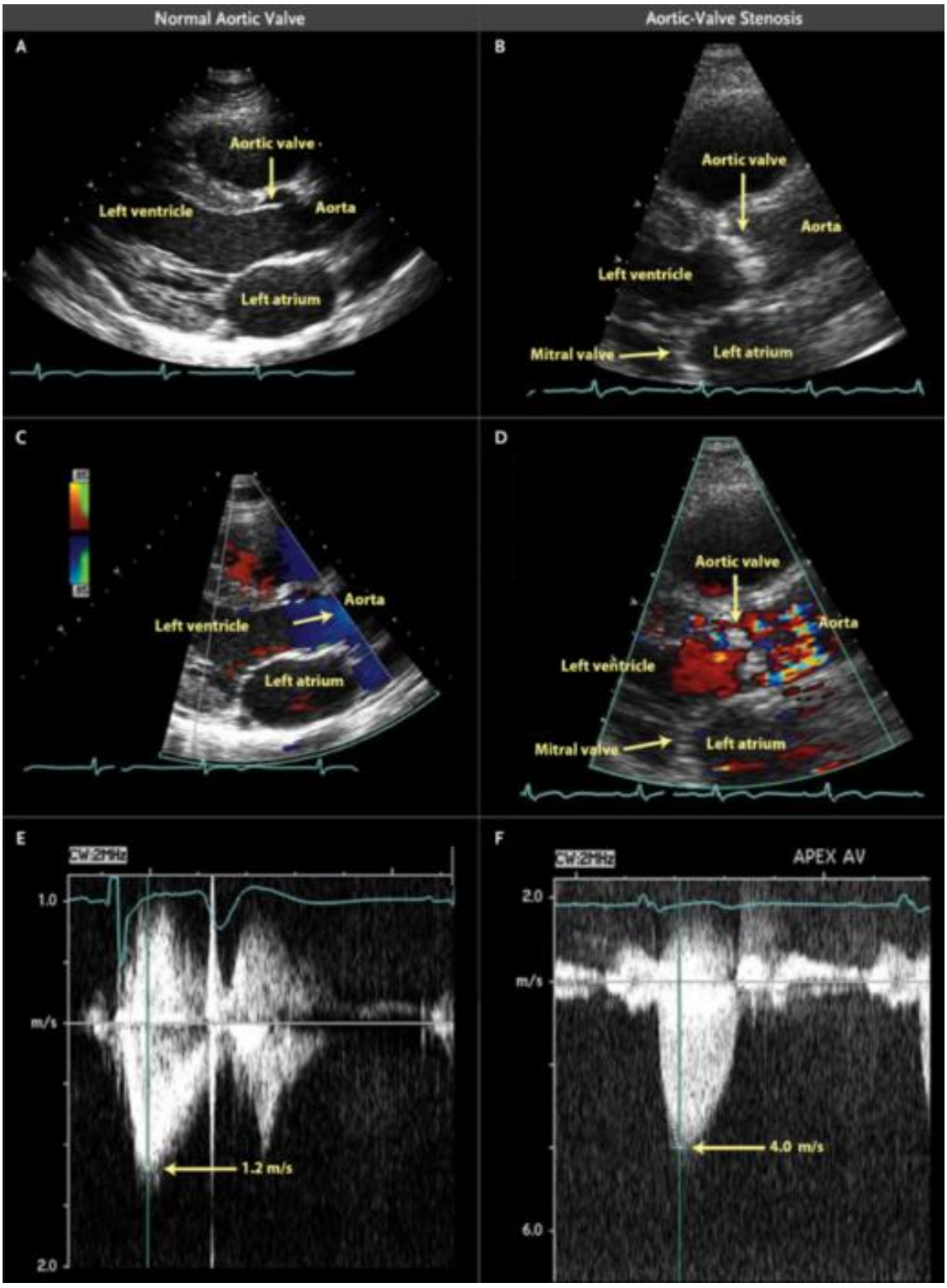

Figure 15 – Evaluation échocardiographique d'une sténose aortique serrée. Reproduite d'après Otto C et al (3). A- Coupe parasternale grand axe en 2D montrant une valve aortique normale avec des feuillets fins vu en position ouverte en systole (flèche jaune). Le ventricule gauche est de dimension normale sans hypertrophie pariétale notable, l'oreillette gauche n'est pas dilatée. B- Coupe correspondante d'une sténose aortique serrée avec des

feuillets épaissis et calcifiés, apparaissant sous la forme d'une bande blanche relativement immobile en systole. Le ventricule gauche est hypertrophique et l'oreillette gauche dilatée. C- Coupe parasternale grand axe en doppler couleur d'une valve aortique normale avec un flux antérograde normal à travers la valve en systole (en bleu). D- Coupe correspondante d'une sténose aortique serrée avec un flux normal (en rouge) sous la valve dans la chambre de chasse du ventricule gauche et un aspect d'aliasing (mélange de flux bleu et rouge) au niveau de la valve traduisant l'accélération de flux et la chute de pression occasionnée par la sténose aortique. E- Enregistrement en doppler continu du flux antérograde à travers une valve aortique normale obtenu en coupe apicale 5 cavités. L'échelle verticale montre la vitesse transvalvulaire, orientée vers le bas car le flux « fuit » la sonde d'échocardiographie dans cette vue. L'électrocardiogramme est visible en haut de l'image en bleu avec des marqueurs de temps standard (0.2ms pour les petites graduations, 1s pour les grandes graduations). La forme du flux est normale avec un aspect triangulaire à pic précoce en systole et une vitesse maximale basse de 1.2 m/s. F- Image correspondante dans le cas d'une sténose aortique serrée. La forme du flux apparait plus arrondie avec un pic retardé en milieu de systole. La vitesse transvalvulaire est nettement augmentée à 4.0 m/s.

Le bilan pré-opératoire réalisé dans le cadre d'un TAVI comprend par ailleurs les examens habituellement pratiqués dans ce contexte en cas de valvulopathie sévère :

- Coronarographie pour la recherche d'une atteinte artérielle coronaire associée
- Echo-doppler des troncs supra-aortiques à la recherche d'une sténose notamment carotidienne qui pourrait nécessiter une prise en charge
- Explorations fonctionnelles respiratoires à la recherche d'une atteinte pulmonaire associée
- Recherche de foyers infectieux dentaires par un panoramique dentaire et une consultation spécialisée.
- Parfois évaluation gériatrique.

Le deuxième examen fondamental, spécifiquement réalisé pour le bilan pré-TAVI, est l'angioscanner (tomodensitométrie à rayons X)(29). Son principe repose sur la projection et l'atténuation de rayons X par les tissus qu'ils traversent. La reconstruction 3D par tomographie à partir des images 2D recueillies nécessite d'acquérir une multitude de projections radiographiques sous différentes incidences autour du patient. Ainsi, les sources et détecteurs à

rayon X tournent autour du patient dans un arceau en réalisant une succession d'acquisitions. Simultanément, une translation longitudinale de la table d'examen sur laquelle est située le patient permet d'obtenir un balayage cranio-caudal de son anatomie complète par une multitude de coupes axiales (généralement environ 1000 coupes axiales sont nécessaires à l'exploration de toute l'aorte thoracoabdominale). L'acquisition est réalisée avec injection d'un produit de contraste iodé, atténuant fortement les rayons X et permettant de visualiser la lumière vasculaire.

Cet examen a pour buts l'évaluation des voies d'abord potentielles, la recherche d'une éventuelle contre-indication extra-cardiaque (néoplasie), de préciser les mesures de l'anneau aortique, des sinus de Valsalva (renflement de la partie initiale de l'aorte ascendante), de l'aorte ascendante, la distance entre l'anneau et les ostia coronaires (pour évaluer le risque d'occlusion coronaire périprocédural), de guider la procédure en déterminant à l'avance l'incidence d'implantation perpendiculaire au plan de l'anneau aortique (**Figures 16 à 19**). La faisabilité de la procédure, ainsi que le type et la taille de prothèse à implanter seront donc déterminés par l'analyse de l'angioscanner. En général, une acquisition synchronisée à l'électrocardiogramme (ECG) et centrée sur le massif cardiaque et l'aorte ascendante est d'abord obtenu après l'injection de produit de contraste permettant de réaliser des reconstructions du volume tous les 10% du cycle cardiaque (temps séparant 2 systoles). Ces reconstructions permettent notamment la mesure de l'anneau aortique en télé-systole au moment où ses dimensions sont les plus grandes. La synchronisation de l'acquisition à l'ECG est nécessaire à l'obtention de reconstructions fiables à chaque phase du cycle cardiaque. En effet, le cœur étant perpétuellement en mouvement, sa position change au cours de la rotation de l'arceau du scanner autour du patient, ne permettant donc pas l'obtention de l'information suffisante à la reconstruction 3D du volume acquis en un seul cycle cardiaque. Ainsi, l'information nécessaire est obtenue sur plusieurs cycles cardiaques, le temps que l'arceau effectue des rotations complètes autour de l'ensemble du volume à acquérir qui sera ensuite reconstruit en « synchronisant » les données obtenues selon les phases de l'ECG auxquelles elles ont été acquises. Deux modes de synchronisation sont possibles : prospective consistant à déclencher l'acquisition seulement aux phases cardiaques souhaitées (le plus souvent télé-diastolique lorsque les mouvements cardiaques sont limités) et rétrospective consistant à enregistrer en totalité plusieurs battements cardiaques puis à trier les projections selon leur phase cardiaque. Ce dernier mode est classiquement utilisé dans le cadre du bilan pré-TAVI afin de disposer des phases télé-systoliques. La durée d'acquisition élevée de la synchronisation rétrospective

entraine une exposition plus forte du patient aux rayons X ce qui explique qu'on limite cette acquisition à un champ de vue restreint. Une seconde acquisition non synchronisée à l'ECG, ne nécessitant pas de nouvelle injection de produit de contraste (le produit injecté se trouvant généralement toujours dans le secteur artériel du patient), est réalisée, immédiatement à la suite de la première acquisition, sur un large champ de vue s'étendant des bifurcations carotidiennes jusque sous les bifurcations des artères fémorales et servira notamment à l'évaluation des axes vasculaires.

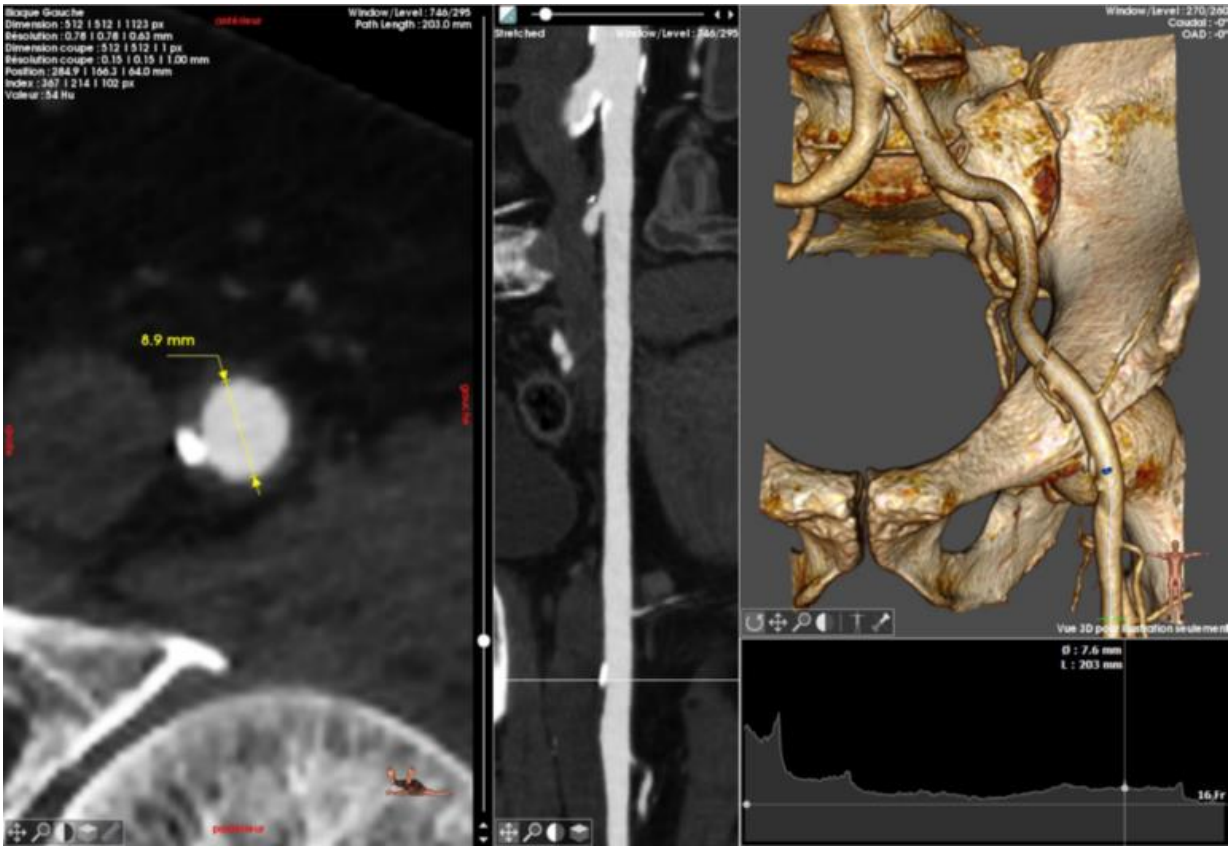

Figure 16 – Evaluation des axes ilio-fémoraux au scanner. Interface du module de mesure « TAVI » du logiciel Endosize de la société Therenva. A gauche, vue en coupe perpendiculaire à la ligne centrale de l'axe ilio-fémoral gauche. Au centre, vue étirée (« streched ») du vaisseau permettant une rotation à 360° autour de l'axe du vaisseau. En haut à droite, vue 3D en volume rendering permettant de visualiser les rapports aux structures osseuses du bassin. En bas à droite, vue du profil du diamètre minimum du vaisseau permettant d'évaluer la compatibilité avec différentes tailles d'introducteurs.

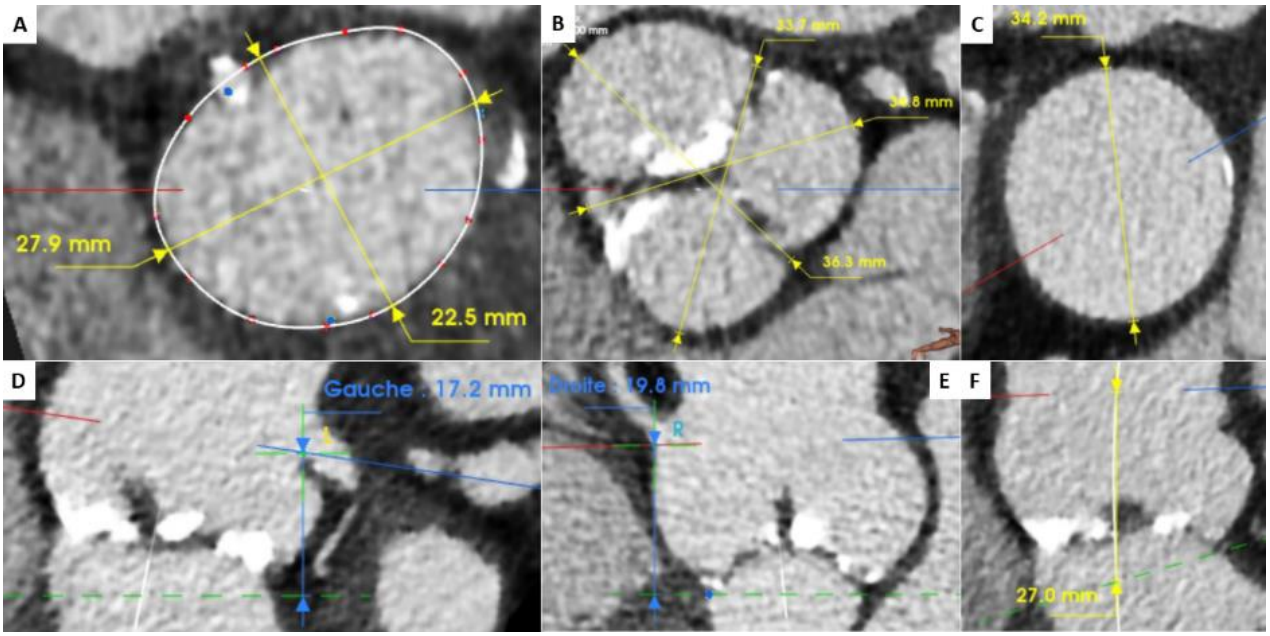

Figure 17 – Evaluation de la racine aortique au scanner. Interface du module de mesure « TAVI » du logiciel Endosize de la société Therenva. A- Mesures de l'anneau aortique. B- Mesures des sinus de Valsalva. C- Mesure de l'aorte ascendante à 30 mm de l'anneau aortique. D- Distance entre l'anneau aortique (ligne pointillée verte) et l'ostium du tronc commun de la coronaire gauche. E- Distance entre l'anneau aortique (ligne pointillée verte) et l'ostium de la coronaire droite. F- Distance entre l'anneau aortique (ligne pointillée verte) et la jonction sino-tubulaire.

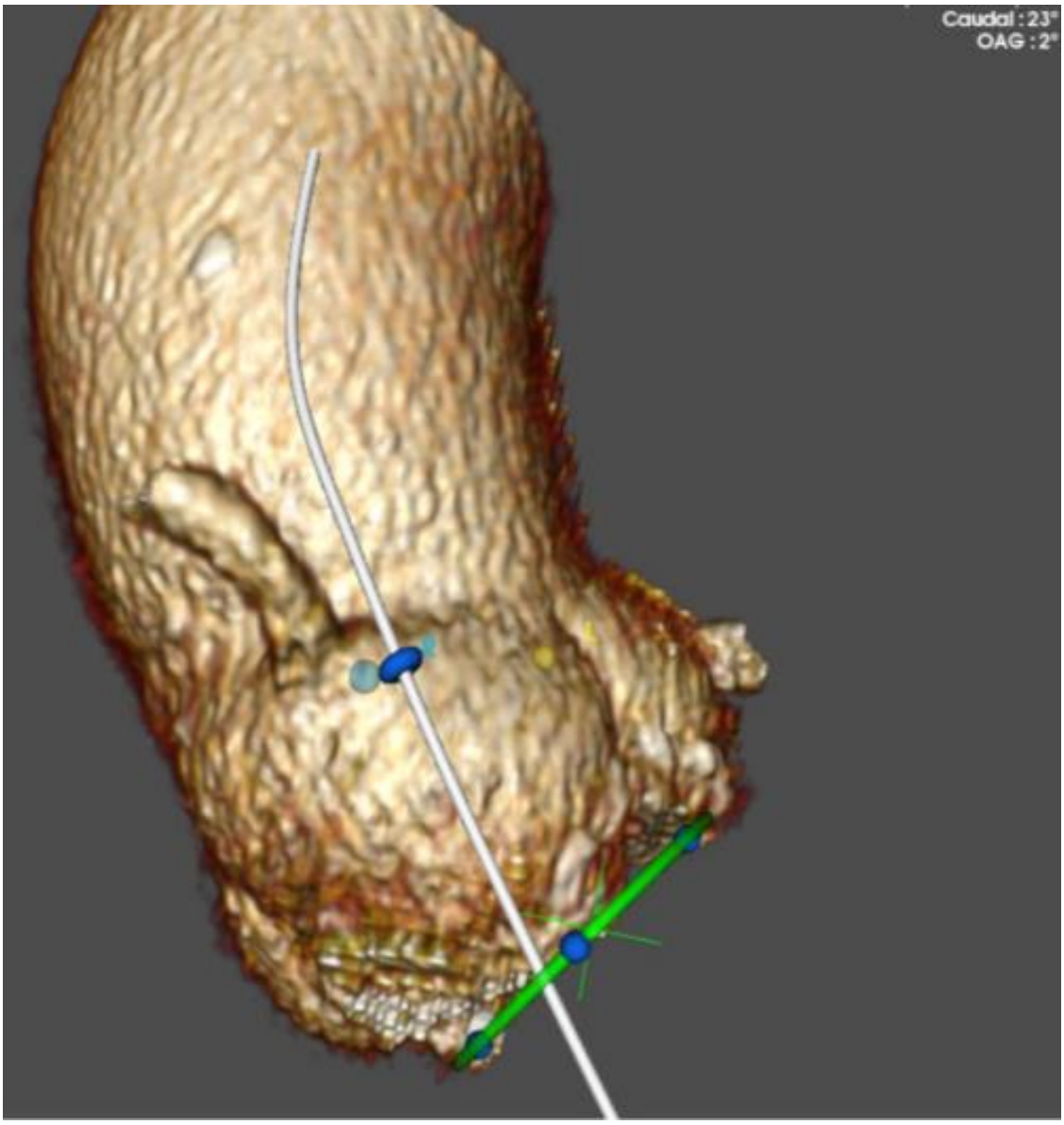

Figure 18 – Evaluation de l'incidence d'implantation au scanner. Interface du module de mesure « TAVI » du logiciel Endosize de la société Therenva. Vue 3D en volume rendering de la racine aortique, perpendiculaire à l'anneau aortique qui apparait comme une ligne verte (alors qu'il apparait circulaire ou ovalaire dans les incidences non perpendiculaires) avec alignement des points les plus bas de chacune des trois cusps aortiques (ronds bleus).

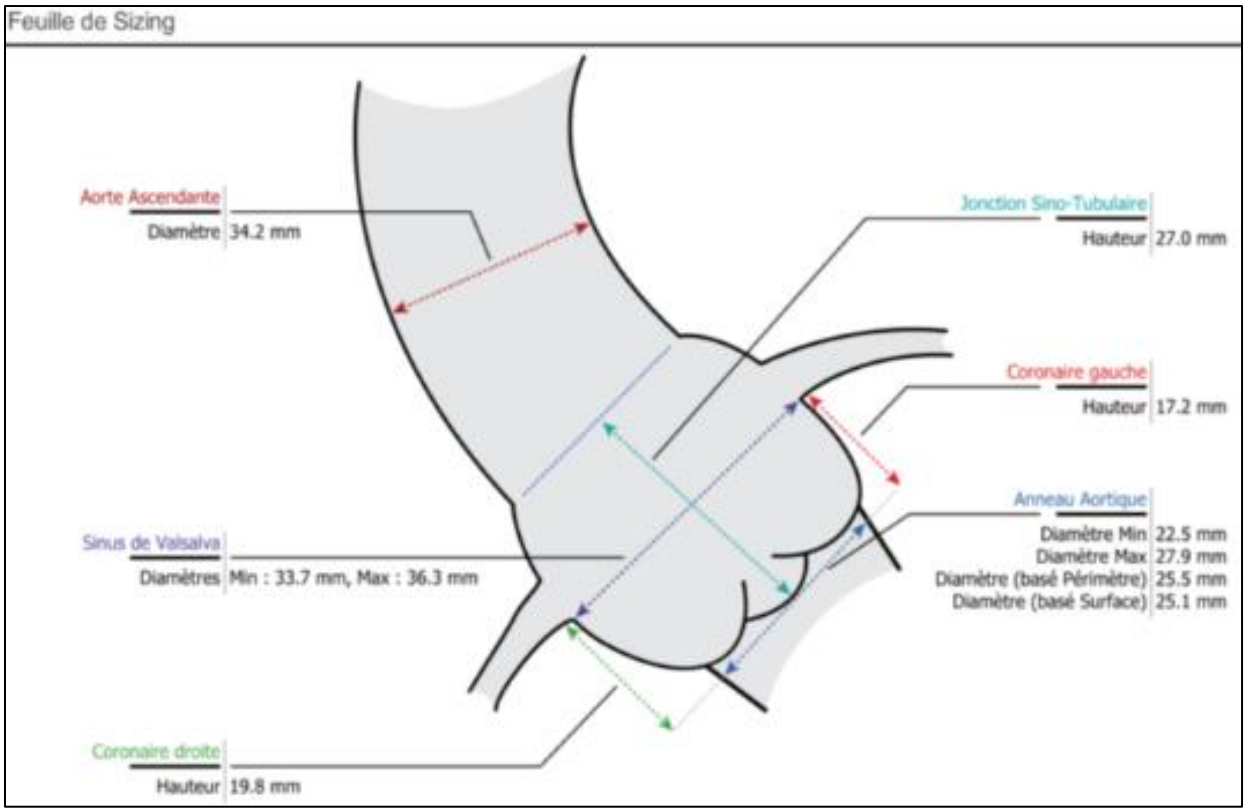

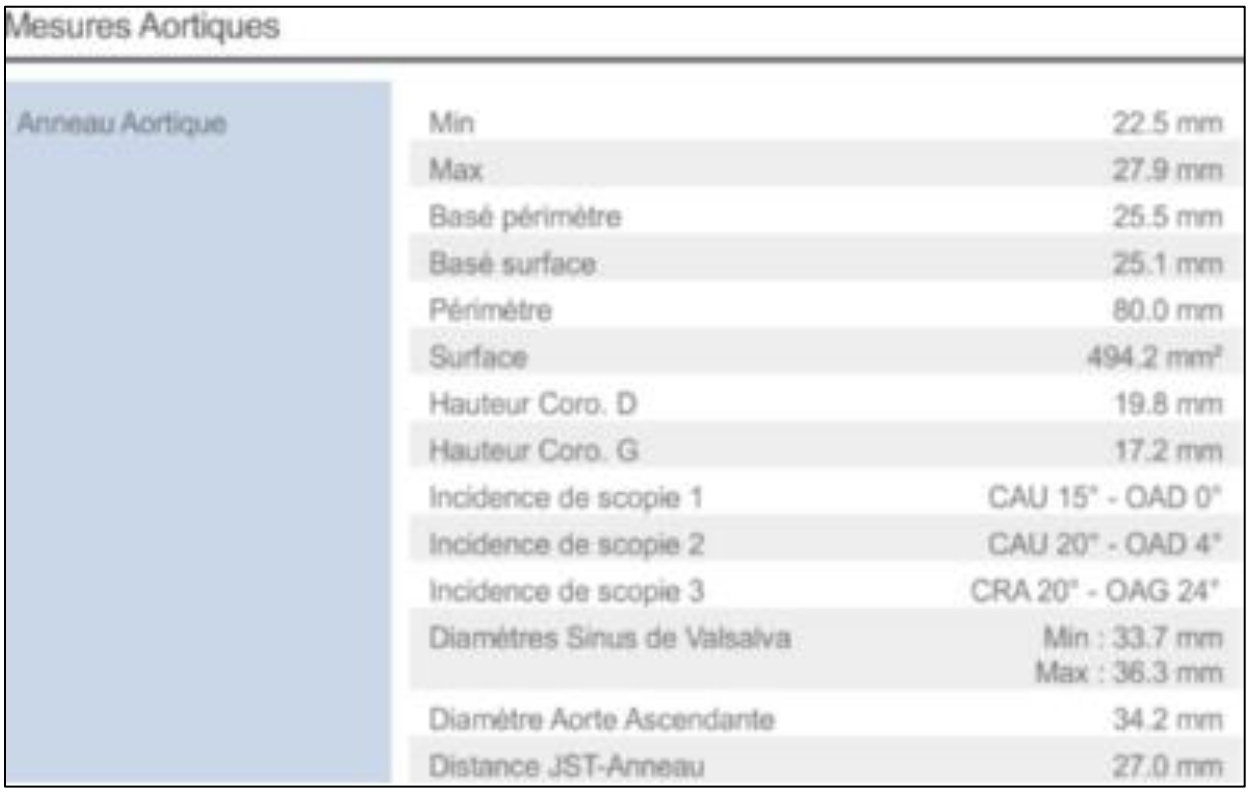

Mesures Aortiques

Anneau Aortique	
Min	22.5 mm
Max	27.9 mm
Basé périmètre	25.5 mm
Basé surface	25.1 mm
Périmètre	80.0 mm
Surface	494.2 mm²
Hauteur Coro. D	19.8 mm
Hauteur Coro. G	17.2 mm
Incidence de scopie 1	CAU 15° - OAD 0°
Incidence de scopie 2	CAU 20° - OAD 4°
Incidence de scopie 3	CRA 20° - OAG 24°
Diamètres Sinus de Valsalva	Min : 33.7 mm Max : 36.3 mm
Diamètre Aorte Ascendante	34.2 mm
Distance JST-Anneau	27.0 mm

Figure 19 – Rapport de mesure de la racine aortique généré par le logiciel Endosize

D) Déroulement d'une procédure TAVI

Les procédures de remplacement valvulaire aortique percutané sont réalisées dans un environnement stérile, en salle de cathétérisme (coronarographie), en salle hybride ou au bloc opératoire. Le patient peut être placé sous anesthésie générale ou sédation vigile avant le démarrage de la procédure selon les habitudes de chaque centre. Nous décrirons ici le déroulement d'une procédure transfémorale.

* Dispositif d'imagerie per-opératoire

Les procédures TAVI sont réalisées sous contrôle fluoroscopique (ou radioscopique) via un dispositif appelé C-arm, en référence à son arceau en forme de C, nécessaire pour visualiser l'avancement des outils (**Figure 20**). Le principe de ce système est similaire à la radiographie à la différence qu'il produit une séquence d'images en temps réel plutôt qu'un cliché unique.

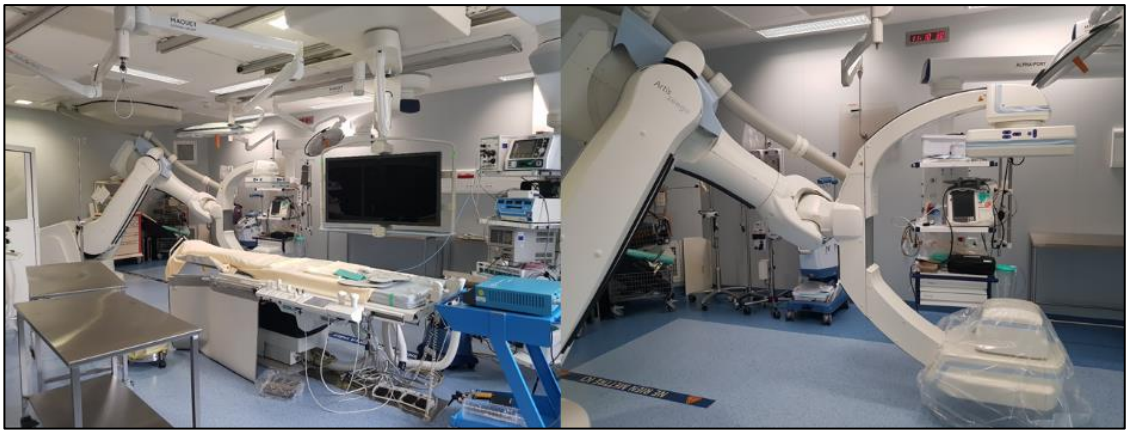

Figure 20 – Salle d'intervention hybride Système DynaCT (Siemens Medical Solutions, Forchheim, Allemagne) et son C-arm de fluoroscopie Artis Zeego

Plus précisément, son principe repose sur la projection de rayons X d'une source à un récepteur. Lorsque le rayon X traverse un corps, son intensité est atténuée selon la nature et l'épaisseur des tissus traversés, avant d'impacter le récepteur. Le récepteur restitue alors une image en niveau de gris qui rend compte de l'atténuation des rayons. En particulier, les os atténuent fortement les rayons X et sont dits radio-opaques (au niveau d'énergie utilisés en

pratique clinique). Cependant, les tissus mous, comme l'aorte, ne le sont pas. Ainsi, l'injection d'agents de contraste est nécessaire pour visualiser la lumière des vaisseaux. Une acquisition des structures vasculaires avec injection de produit contraste est alors appelé angiographie. L'utilisation de cet appareil est soumise à deux contraintes : la minimisation de l'exposition du patient au rayon X et la minimisation d'injection de produit de contraste. En effet, les agents de contraste iodés utilisés ont un effet néphrotoxique dose-dépendant.

En plus d'une radioscopie 2D en temps réel, certains appareils proposent la reconstruction du volume 3D per-opératoire dite Cone Beam Computed Tomography (CBCT). Cette acquisition 3D nécessite que le C-arm soit fixé et intégré dans la salle d'opération et que l'asservissement de la motorisation du bras robotisé permette à la fois la rotation rapide de l'arceau et la connaissance précise des positions de la source et du capteur à rayons X. Les salles d'intervention dites « hybrides » sont équipées de ces dernières générations de C-arm. Le CBCT présente quelques inconvénients liés à l'irradiation, l'injection de produit de contraste et l'utilisation de la stimulation cardiaque pour atténuer les mouvements cardiaques pendant l'acquisition. Dans le cadre du TAVI, il est encore très peu commun d'effectuer un CBCT. Le principe de la reconstruction du volume 3D est similaire à celui de la tomodensitométrie à rayons X (scanner).

Dans certains cas, lorsqu'elle est réalisée sous anesthésie générale, l'intervention peut éventuellement être guidée par contrôle échocardiographique trans-oesophagien afin de recueillir des données supplémentaires et limiter l'usage des rayons X et des agents de contraste.

*** Mise en place des voies d'abord**

La procédure débute par l'abord le plus souvent percutané (rarement chirurgical) de l'artère fémorale commune sélectionnée comme abord principal (celui permettant l'intriduction de la prothèse). Le niveau de ponction, au-dessus de la bifurcation fémorale, peut être repéré par rapport aux repères osseux en s'aidant du scanner préopératoire (**cf Figure 16**), par guidage échographique ou encore angiographique en réalisant une injection de produit de contraste par voie fémorale controlatérale (**Figure 21**).

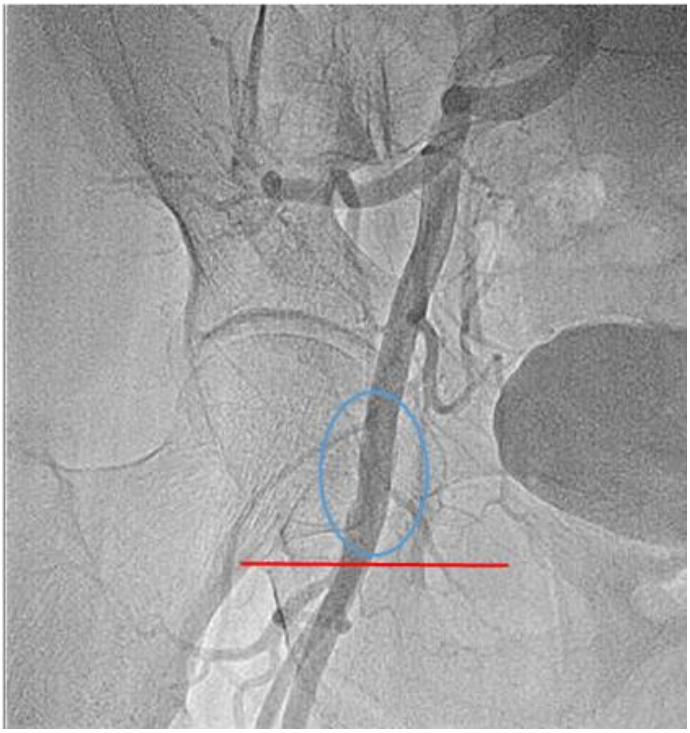

Figure 21 – Angiographie de l'axe ilio-fémoral droit. La ligne rouge représente le niveau de la bifurcation fémorale, l'ellipse bleue la zone de ponction souhaitée au niveau de la terminaison de l'artère fémorale commune.

La technique de ponction utilisée est l'approche rétrograde décrite par Seldinger. Une ponction de l'artère à l'aiguille est effectuée. Une fois un retour de sang pulsatile obtenu, un guide souple et court à bout en « J » est introduit dans l'aiguille qui est alors retirée en assurant une compression manuelle de l'artère fémorale. Sur le guide inséré dans l'artère fémorale est mis en place un introducteur (désilet) de petit diamètre externe (5 ou 6F) à valve anti-retour permettant l'accès à l'artère (**Figure 22**).

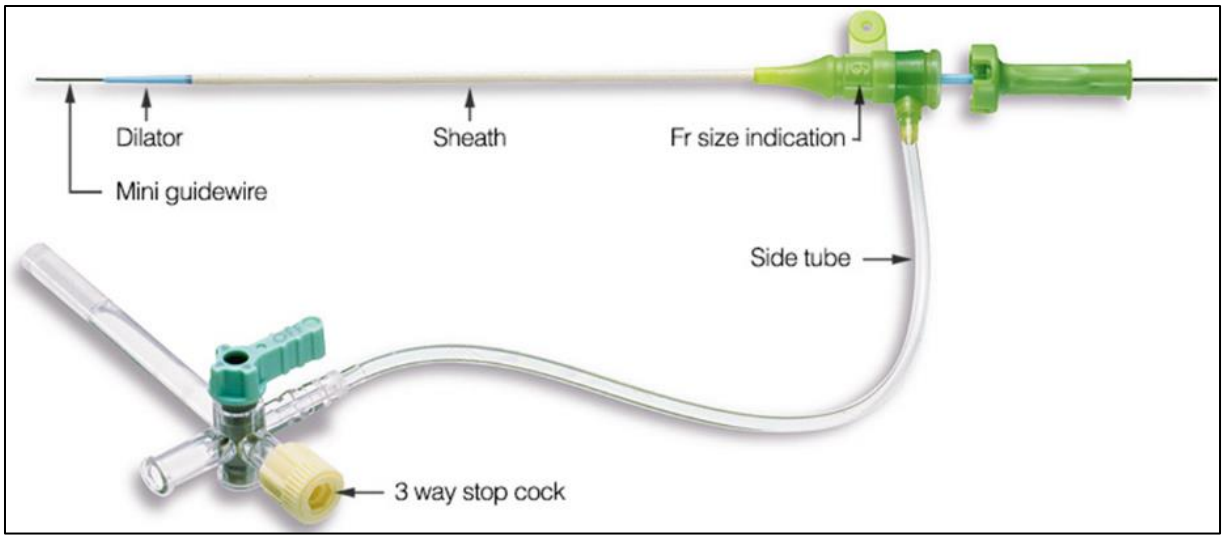

Figure 22- Désilet 6F de la société Terumo.

Via cet introducteur, un guide métallique souple à bout en « J » de 0.89mm de diamètre et 150cm de long est acheminé jusque dans l'aorte thoracique et permet dans un premier temps la mise en place d'un système de fermeture artérielle percutané qui permettra d'obtenir l'hémostase en fin de procédure. Une fois ce système en place, un introducteur de diamètre intermédiaire (10 ou 11F) est inséré dans l'artère fémorale. Une sonde d'angiographie préformée de type Amplatz left (AL) ou Judkins Right (JR) (**Figure 23**) est ensuite montée sur le guide souple permettant son échange pour un guide rigide.

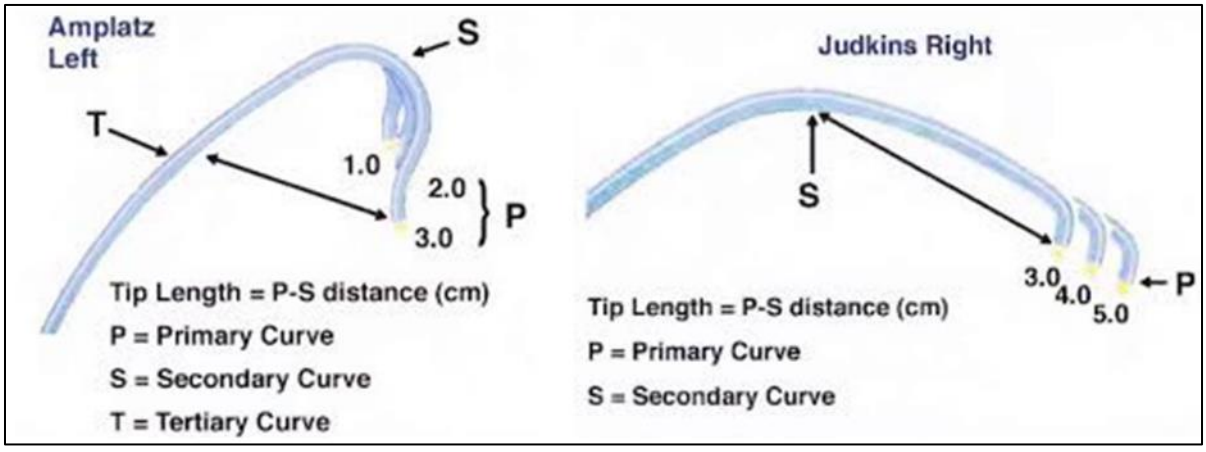

Figure 23 – Sondes préformées Amplatz Left (AL) et Judkins Right (JR).

Le guide rigide est composé d'un corps métallique recouvert d'un revêtement polymère pour diminuer le frottement avec la paroi et les outils glissant dessus ainsi qu'éviter la

coagulation du sang à son contact. Son diamètre nominal est de 0.89 mm pour une longueur de 275cm et il est généralement composé d'un corps de rigidité élevée dans sa partie proximale et d'une extrémité flexible dans sa partie distale[2]. Ce guide a une fonction fondamentale pendant la procédure. Dans un premier temps, il permet de redresser les tortuosités ilio-fémorales et d'apporter le support nécessaire à la mise en place de l'introducteur dédié. Dans un second temps, il est positionné dans le ventricule gauche et fournit le support suffisant à la montée du cathéter porteur puis au positionnement fin et au déploiement de la prothèse. L'un des guides rigides les plus utilisé est le guide SAFARI de la société Boston Scientific qui a la particularité d'avoir une extrémité distale préformée en « queue de cochon », de dimensions variables, qui permet de parfaitement épouser la forme de l'apex du ventricule gauche en limitant les risques de perforation ventriculaire (**Figure 24**).

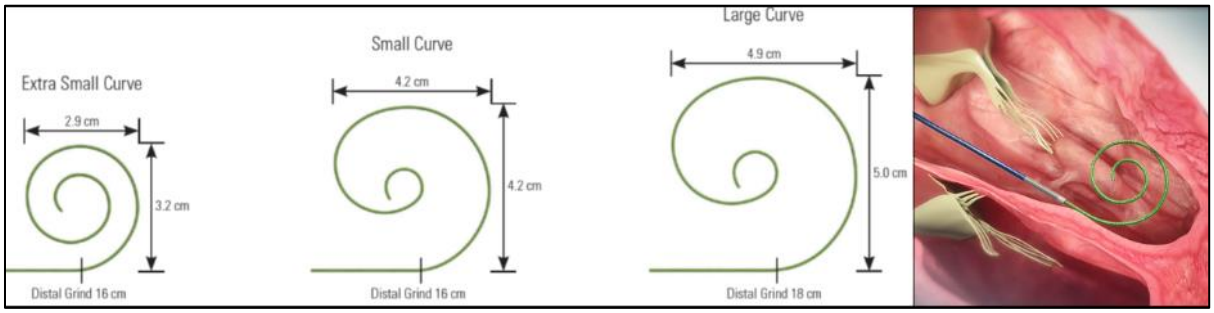

Figure 24 – Guide rigide SAFARI (société Boston Scientific). Le guide, présenté dans ses différentes dimensions permettant de s'adapter aux différentes anatomies, est préformé à son extrémité distale afin d'offrir l'appui le plus important et atraumatique possible au niveau de l'apex ventriculaire gauche.

Une fois le guide rigide positionné dans l'aorte thoracique, l'introducteur dédié au passage de la prothèse, de gros diamètre externe (≥ 14F), est mis en place (**Figure 25**). Dans le cadre de l'implantation d'une prothèse auto-expandable Medtronic EVOLUT R ou PRO, la mise en place d'un désilet dédié n'est pas absolument nécessaire, l'implantation pouvant être réalisée en utilisant seulement le cathéter porteur.

[2] Les termes « proximal » et « distal » sont définis en référence à la position de l'opérateur.

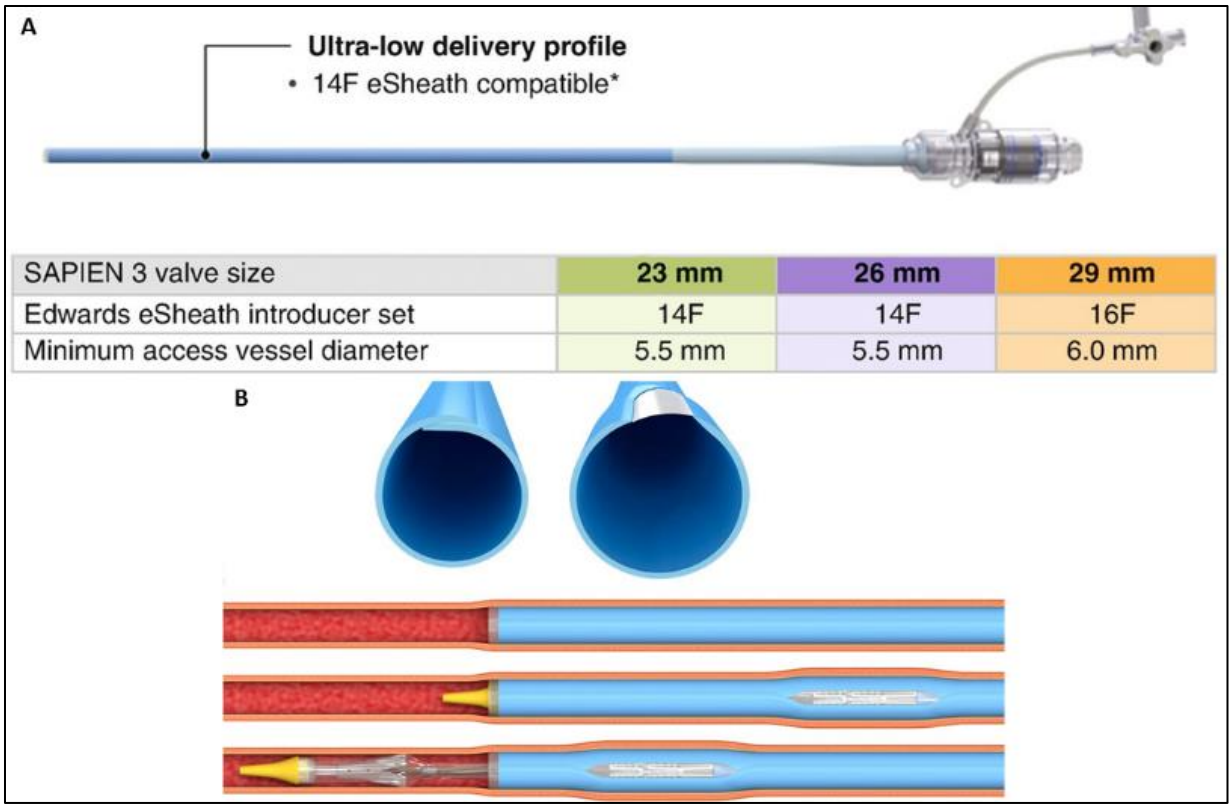

SAPIEN 3 valve size	23 mm	26 mm	29 mm
Edwards eSheath introducer set	14F	14F	16F
Minimum access vessel diameter	5.5 mm	5.5 mm	6.0 mm

Figure 25- Introducteur (désilet ou « sheath ») dédié au TAVI transfémoral de la société Edwards. A- Introducteur dans ses différentes dimensions et recommandations constructeur sur le diamètre minimal de l'axe ilio-fémoral compatible avec son utilisation. B- Cet introducteur à la particularité de « s'ouvrir » lors du passage du cathéter porteur de la prothèse permettant une introduction à un calibre réduit et une dilatation uniforme par la lumière du vaisseau limitant les risques de traumatisme vasculaire.

En dehors de cet abord principal, des abords secondaires par des introducteurs de calibre usuel (5 ou 6F) sont nécessaires. Un abord artériel fémoral controlatéral ou radial est effectué pour mettre en place au niveau de l'aorte ascendante une sonde, multiperforée, « queue de cochon » (ou « pigtail ») qui servira à réaliser les injections de produit de contraste au niveau de l'aorte ascendante (aortographies) permettant ainsi de valider l'incidence d'implantation pré déterminée au scanner, de positionner la prothèse et de contrôler le résultat en fin de procédure (**Figure 26**). Un abord veineux fémoral controlatéral à l'abord principal est également réalisé afin de mettre en place une sonde de stimulation cardiaque temporaire dans le ventricule droit (**Figure 26**). Cette sonde permet de réaliser des stimulations cardiaques rapides (180-200 battements/min) qui ont pour effet d'entrainer une chute brutale du débit cardiaque par réduction drastique du volume d'éjection systolique et donc une stabilisation du matériel au

niveau valvulaire aortique lors de certaines phases de la procédure. Cette sonde permet également une stimulation cardiaque temporaire en cas de complication de la procédure par l'apparition de troubles de la conduction cardiaque de haut degré (principalement bloc atrioventriculaire complet).

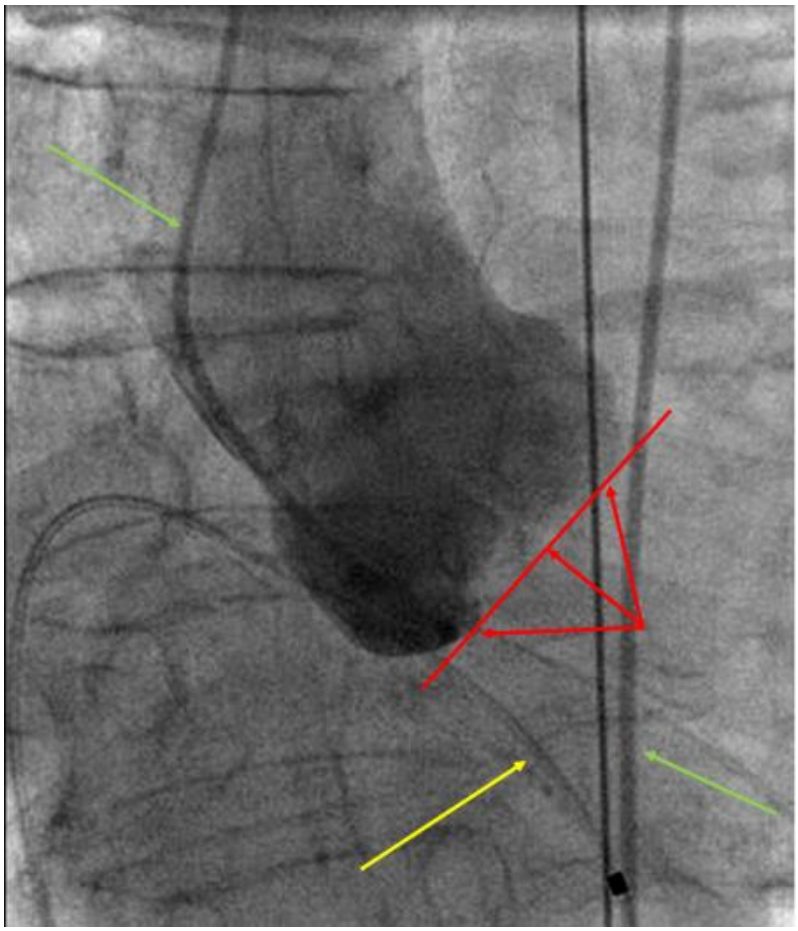

Figure 26 – Aortographie dans l'incidence de pose au cours d'une procédure TAVI.

Ligne et flèches rouges représentant le plan de l'anneau aortique avec alignement des 3 cusps aortiques. Flèche jaune désignant la sonde de stimulation cardiaque temporaire dans le ventricule droit. Flèches vertes désignant la sonde « pigtail » au niveau de l'aorte thoracique ascendante et descendante (insertion par voie fémorale).

*** Franchissement de la valve aortique et valvuloplastie au ballon**

Une fois les abords obtenus, l'incidence de pose validée et la sonde de stimulation vérifiée, une sonde AL ou JR est de nouveau montée sur le guide rigide via l'abord principal et

positionnée dans l'aorte ascendante. Le guide rigide est retiré et à l'aide de la sonde, orientée vers la valve aortique, l'orifice aortique est franchi par un guide souple à bout droit de 0.89mm de diamètre. Une fois ce guide dans le ventricule gauche, la sonde y est avancée et le guide souple est alors de nouveau échangé pour le guide rigide, positionné à l'apex du ventricule gauche (**Figure 24**).

Une valvuloplastie aortique peut alors être réalisée (étape facultative réalisée à la discrétion de l'opérateur). Son principe est d'effectuer, sous stimulation cardiaque rapide, l'inflation manuelle d'un ballon, de calibre adapté à la mesure de l'anneau aortique du patient, au niveau de la valve aortique. Cette manœuvre, appelée pré-dilatation, favorise le franchissement ultérieur de la valve aortique par la prothèse qui présente un encombrement spatial plus important (**Figure 27**).

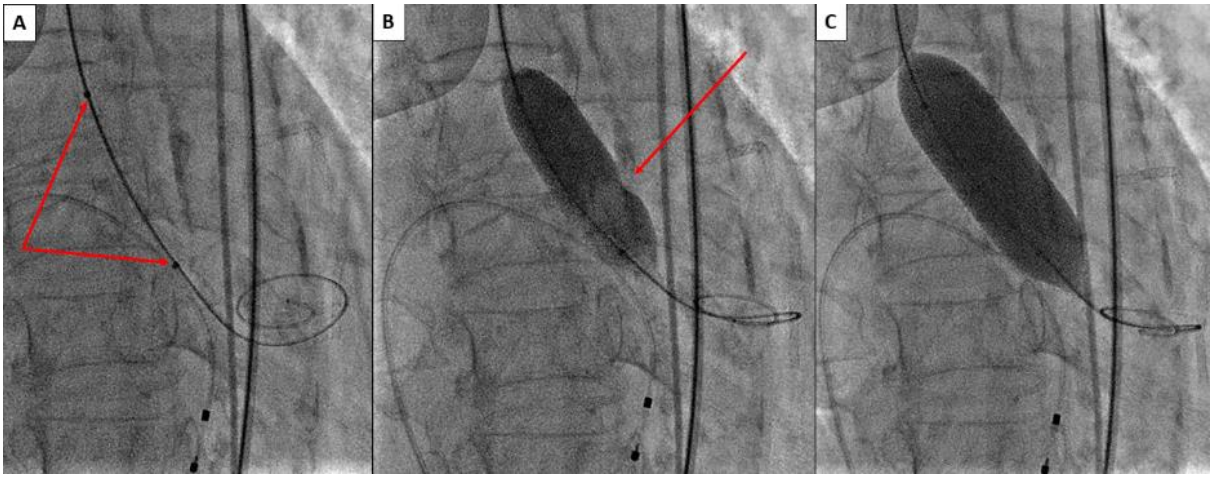

Figure 27 – Valvuloplastie aortique au ballon. A- Ballon de valvuloplastie, situé entre les 2 marqueurs radio-opaques (flèches rouges), positionné sur le guide rigide, au niveau de la valve aortique. B- Inflation manuelle progressive du ballon permettant de constater la persistance d'une « empreinte » liée à une calcification de la valve aortique (flèche rouge). C- Inflation complète du ballon permettant de faire céder l'empreinte. Valvuloplastie efficace.

*** Acheminement, positionnement et déploiement de la prothèse**

Les prothèses implantées en pratique courante ont été décrites à la *section 1.2.3 b)*. Afin de permettre leur insertion dans l'artère fémorale, elles doivent être comprimées radialement (« serties » de l'anglais *to crimp*) et positionnées sur un ballon (prothèse SAPIEN 3) ou insérées dans une gaine rétractable (prothèse EVOLUT R et PRO). Cette manœuvre est réalisée sur un cathéter porteur présentant une lumière interne qui permet le positionnement du cathéter sur le

guide rigide et ainsi l'acheminement de la prothèse jusqu'à la valve aortique. Le cathéter porteur de la prothèse EVOLUT est l'EnveoPRO et celui de la prothèse SAPIEN 3 est le Commander (**Figure 28**). Ce dernier a la particularité d'avoir un mécanisme pour modifier l'incurvation du cathéter grâce aux commandes sur le manche afin de faciliter la navigation dans la crosse de l'aorte et le positionnement coaxial au grand axe de l'aorte, de la prothèse au niveau de la valve aortique.

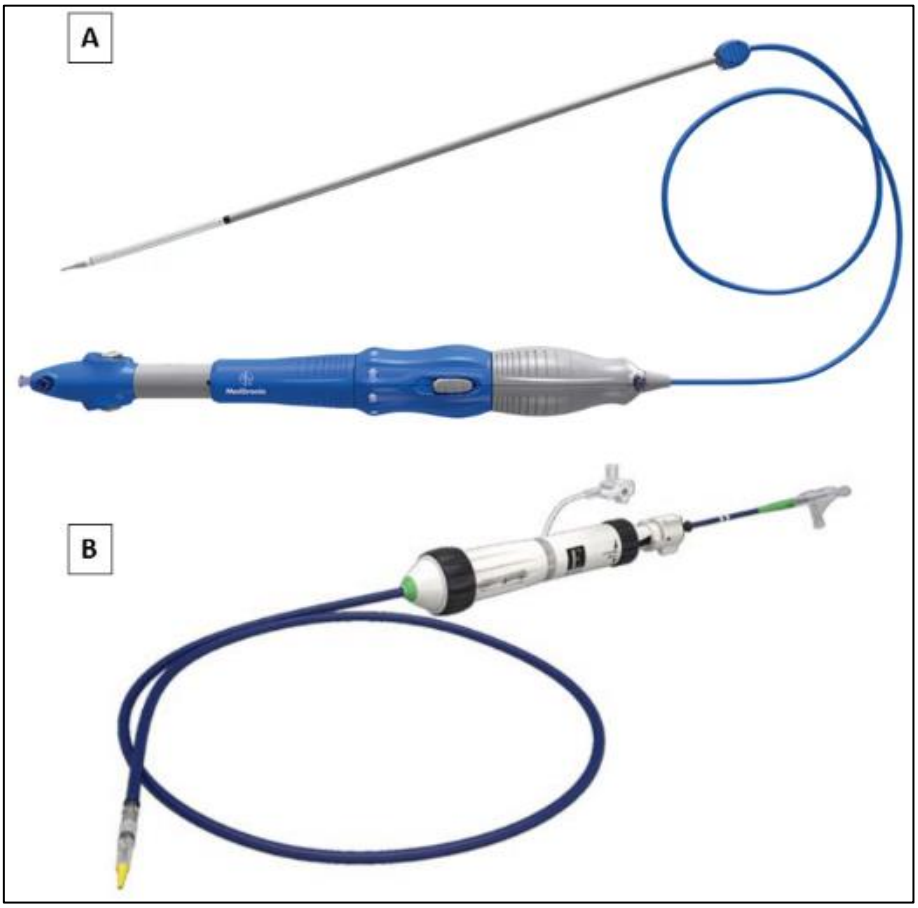

Figure 28 – Cathéters porteurs utilisés lors des procédures TAVI. A- Cathéter Enveo PRO de la prothèse EVOLUT. B- Cathéter Commander de la prothèse SAPIEN 3.

Une fois que la prothèse a été positionnée en regard de la valve aortique native à l'aide du cathéter porteur, son positionnement fin est assuré, sous contrôle angiographique avec injection de faibles quantités de produit de contraste, par des mouvements de poussée/traction sur le cathéter porteur et/ou le guide rigide, ainsi qu'à l'aide d'une molette dédiée, située sur le manche du cathéter de pose pour la valve SAPIEN 3. Pour cette dernière, un marqueur central situé sur le ballon aide au bon positionnement, qui est généralement vérifié par une courte

séquence d'aortographie sous stimulation cardiaque rapide, juste avant le déploiement de la prothèse par inflation du ballon. Pour la prothèse auto-expansible EVOLUT, le déploiement est plus progressif et nécessite le plus souvent de petites injections répétées pour vérifier la stabilité de la position de largage choisie. La prothèse étant recapturable jusqu'à environ 85% de son déploiement, une angiographie est effectuée à ce stade pour s'assurer de sa bonne position. (**Figure 29**). En cas de positionnement satisfaisant, la prothèse peut être déployée/larguée. La prothèse SAPIEN 3 est déployée sous stimulation cardiaque rapide par inflation progressive de son ballon, qui est maintenu à inflation maximale pendant 5 à 6 secondes avant déflation puis l'arrêt de la stimulation cardiaque. La prothèse EVOLUT ne nécessite pas de stimulation cardiaque rapide mais son largage peut, dans certains cas, être facilité par une stimulation cardiaque à environ 120/min qui stabilise le matériel.

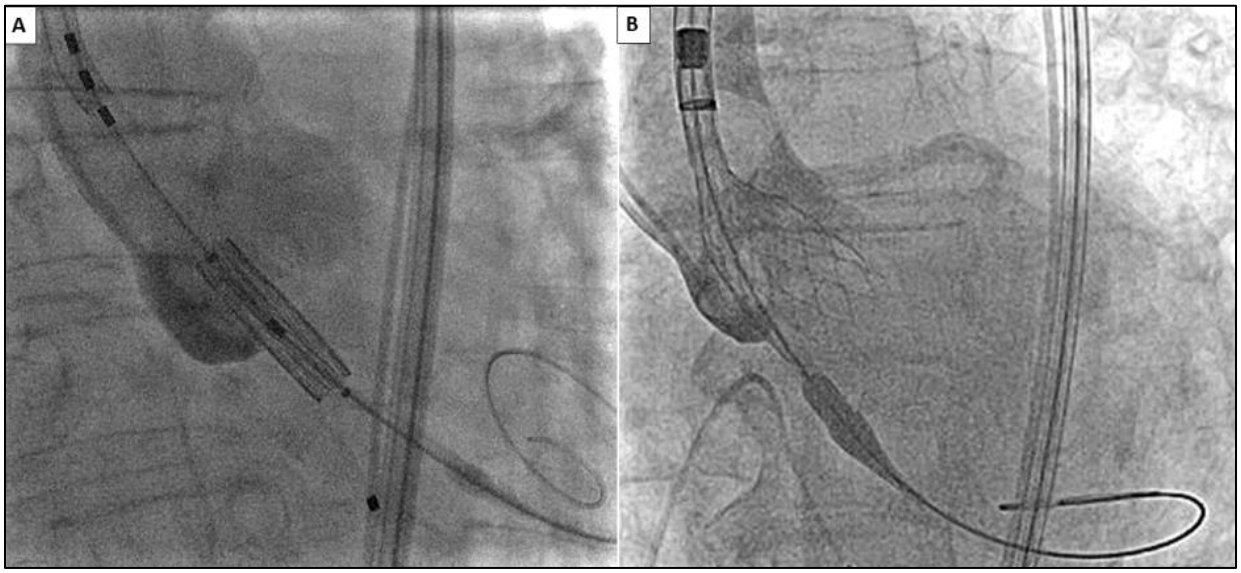

Figure 29 – Positionnement de la prothèse. A- Aortographie avant déploiement d'une prothèse SAPIEN 3. B- Aortographie avant largage complet de la prothèse EVOLUT. A ce stade du déploiement, cette dernière fonctionne normalement, permettant la stabilité hémodynamique du patient, et peut être recapturée en cas de mauvaise position.

*** Evaluation angiographique du résultat et éventuelles actions correctrices**

Une fois la prothèse déployée, une aortographie avec une quantité plus importante de produit de contraste (environ 30ml) est réalisée afin d'évaluer le résultat de l'implantation : évaluation de la présence et du degré (minime, modéré ou sévère) d'une fuite aortique para

prothétique résiduelle, recherche de complications rares (occlusion coronaire, rupture d'anneau, dissection aortique,…) (**Figure 30).**

En cas de fuite résiduelle modérée à sévère, des mesures correctrices peuvent être prises: post-dilatation de la prothèse au ballon, implantation d'une seconde prothèse dans la première, selon le mécanisme en cause dans la fuite.

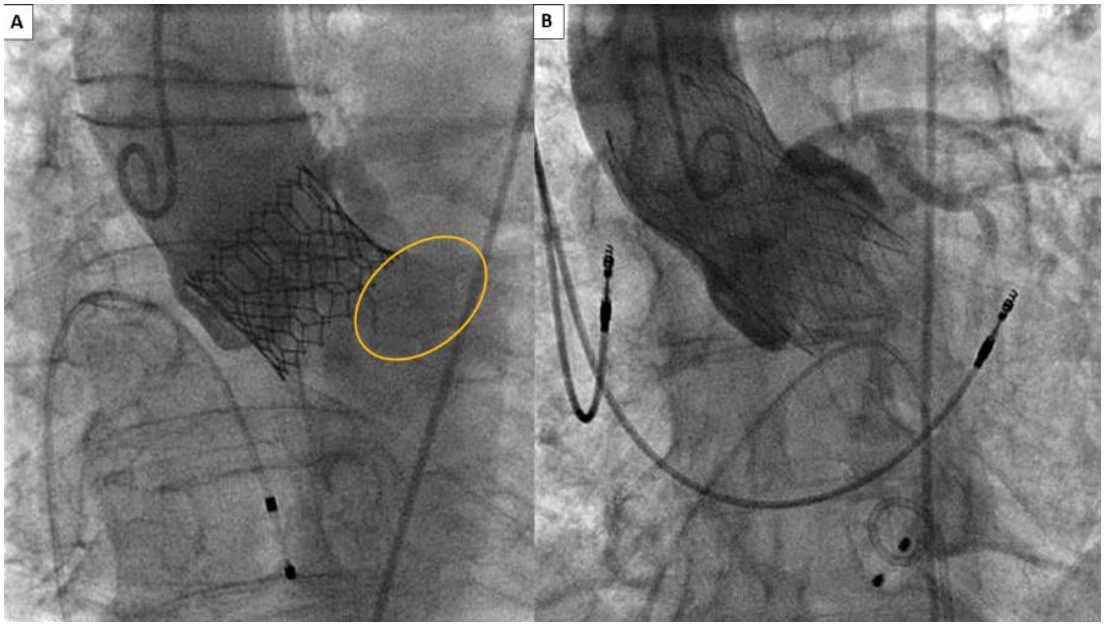

Figure 30 – Evaluation angiographique post-déploiement de la prothèse. A- Evaluation après implantation d'une prothèse SAPIEN 3. Sur cette séquence, une fuite para prothétique minime était visualisée sous la forme d'un reflux, excentrée par rapport à la prothèse, du produit de contraste au niveau de la chambre de chasse ventriculaire gauche (ellipse jaune). B- Evaluation après implantation d'une prothèse EVOLUT PRO.

*** Retrait du dispositif d'implantation et fermeture des abords vasculaires**

En cas de résultat satisfaisant, la procédure se termine par le retrait du dispositif d'implantation puis par la fermeture de l'abord vasculaire principal à l'aide du dispositif de suture artérielle percutanée mis en place en début de procédure. Dans environ 5% des cas, un échec de fermeture artérielle par ce dispositif nécessite le recours à un stent couvert ou à une fermeture chirurgicale afin d'obtenir l'hémostase (24).

Enfin, les accès secondaires sont retirés et l'hémostase obtenue soit par compression manuelle soit par un dispositif de fermeture spécifique pour ces accès de calibre usuel. Il faut

néanmoins noter que la sonde de stimulation cardiaque temporaire mise en place par voie veineuse peut être laissée en place en cas d'apparition d'un trouble conductif per-procédure (bloc de branche gauche et à fortiori bloc auriculoventriculaire de haut degré) ou en cas de situation à plus haut risque de développement d'un trouble conductif dans les 24-48 heures suivant la procédure (patient avec bloc de branche droite pré-existant, implantation d'une valve auto expansible,…).

1.3 Positionnement du TAVI en France

Cette section présente, à travers un premier article original, issu de l'analyse conjointe des registres nationaux FRANCE 2 et FRANCE TAVI et publié dans le *Journal of the American College of Cardiology* en 2017, un état des lieux récent de l'évolution des indications, conditions techniques de réalisation, complications hospitalières et résultats à court terme du TAVI en France entre 2010 et 2015.

JOURNAL OF THE AMERICAN COLLEGE OF CARDIOLOGY
© 2017 BY THE AMERICAN COLLEGE OF CARDIOLOGY FOUNDATION
PUBLISHED BY ELSEVIER

VOL. 70, NO. 1, 2017
ISSN 0735-1097/$36.00
http://dx.doi.org/10.1016/j.jacc.2017.04.053

Temporal Trends in Transcatheter Aortic Valve Replacement in France

FRANCE 2 to FRANCE TAVI

Vincent Auffret, MD, MSc,[a] Thierry Lefevre, MD,[b] Eric Van Belle, MD, PhD,[c] Hélène Eltchaninoff, MD, PhD,[d] Bernard Iung, MD, PhD,[e] René Koning, MD,[f] Pascal Motreff, MD, PhD,[g] Pascal Leprince, MD, PhD,[h] Jean Philippe Verhoye, MD, PHD,[i] Thibaut Manigold, MD,[j] Geraud Souteyrand, MD,[g] Dominique Boulmier, MD,[a] Patrick Joly, MD,[k] Frédéric Pinaud, MD, PhD,[l] Dominique Himbert, MD,[e] Jean Philippe Collet, MD, PhD,[m] Gilles Rioufol, MD, PhD,[n] Said Ghostine, MD,[o] Olivier Bar, MD,[p] Alain Dibie, MD,[q] Didier Champagnac, MD,[r] Lionel Leroux, MD, PhD,[s] Frédéric Collet, MD, PhD,[t] Emmanuel Teiger, MD, PhD,[u] Olivier Darremont, MD,[v] Thierry Folliguet, MD, PhD,[w] Florence Leclercq, MD, PhD,[x] Thibault Lhermusier, MD, PhD,[y] Patrick Olhmann, MD, PhD,[z] Bruno Huret, MD,[aa] Luc Lorgis, MD, PhD,[bb] Laurent Drogoul, MD,[cc] Bernard Bertrand, MD,[dd] Christian Spaulding, MD,[ee] Laurent Quilliet, MD,[ff] Thomas Cuisset, MD, PhD,[gg] Maxence Delomez, MD,[hh] Farzin Beygui, MD, PhD,[ii] Jean-Philippe Claudel, MD,[jj] Alain Hepp, MD,[kk] Arnaud Jegou, MD,[ll] Antoine Gommeaux, MD,[mm] Anfani Mirode, MD,[nn] Luc Christiaens, MD, PhD,[oo] Charles Christophe, MD,[pp] Claude Cassat, MD,[qq] Damien Metz, MD, PhD,[rr] Lionel Mangin, MD,[ss] Karl Isaaz, MD, PhD,[tt] Laurent Jacquemin, MD,[uu] Philippe Guyon, MD,[vv] Christophe Pouillot, MD,[ww] Serge Makowski, MD,[xx] Vincent Bataille, PhD,[yy] Josep Rodés-Cabau, MD,[zz] Martine Gilard, MD, PhD,[aaa] Hervé Le Breton, MD,[a] for the FRANCE TAVI Investigators*

ABSTRACT

BACKGROUND Transcatheter aortic valve replacement (TAVR) is standard therapy for patients with severe aortic stenosis who are at high surgical risk. However, national data regarding procedural characteristics and clinical outcomes over time are limited.

OBJECTIVES The aim of this study was to assess nationwide performance trends and clinical outcomes of TAVR during a 6-year period.

METHODS TAVRs performed in 48 centers across France between January 2013 and December 2015 were prospectively included in the FRANCE TAVI (French Transcatheter Aortic Valve Implantation) registry. Findings were further compared with those reported from the FRANCE 2 (French Aortic National CoreValve and Edwards 2) registry, which captured all TAVRs performed from January 2010 to January 2012 across 34 centers.

RESULTS A total of 12,804 patients from FRANCE TAVI and 4,165 patients from FRANCE 2 were included in this analysis. The median age of patients was 84.6 years, and 49.7% were men. FRANCE TAVI participants were older but at lower surgical risk (median logistic European System for Cardiac Operative Risk Evaluation [EuroSCORE]: 15.0% vs. 18.4%; $p < 0.001$). More than 80% of patients in FRANCE TAVI underwent transfemoral TAVR. Transesophageal echocardiography guidance decreased from 60.7% to 32.3% of cases, whereas more recent procedures were increasingly performed in hybrid operating rooms (15.8% vs. 35.7%). Rates of Valve Academic Research Consortium–defined device success increased from 95.3% in FRANCE 2 to 96.8% in FRANCE TAVI ($p < 0.001$). In-hospital and 30-day mortality rates were 4.4% and 5.4%, respectively, in FRANCE TAVI compared with 8.2% and 10.1%, respectively, in FRANCE 2 ($p < 0.001$ for both). Stroke and potentially life-threatening complications, such as annulus rupture or aortic dissection, remained stable over time, whereas rates of cardiac tamponade and pacemaker implantation significantly increased.

CONCLUSIONS The FRANCE TAVI registry provided reassuring data regarding trends in TAVR performance in an all-comers population on a national scale. Nonetheless, given that TAVR indications are likely to expand to patients at lower surgical risk, concerns remain regarding potentially life-threatening complications and pacemaker implantation. (Registry of Aortic Valve Bioprostheses Established by Catheter [FRANCE TAVI]; NCT01777828) (J Am Coll Cardiol 2017;70:42–55)

Listen to this manuscript's audio summary by *JACC* Editor-in-Chief Dr. Valentin Fuster.

Over the past decade, transcatheter aortic valve replacement (TAVR) has evolved from an emerging technique to mainstream therapy for patients with severe aortic stenosis who are deemed to have a prohibitive (1,2) or high (2–4) surgical risk. Growing experience and refined transcatheter devices allowed a shift toward simplified procedures as well as the performance of TAVR in lower-surgical risk patients (5,6). The publication of the PARTNER 2 (Placement of Aortic Transcatheter Valves 2) randomized trial (7) will likely accentuate this trend and result in an exponential increase in TAVR performance. Several registries provided valuable insights into the dissemination and outcomes of TAVR on a national basis (8–13). However, data relating to the evolution of patients and procedural characteristics, and outcomes over time on a nationwide scale, remain scarce (13–15). Moreover, most of these registries did not include data reflecting contemporary practice trends.

Following the end of the inclusion period of the FRANCE 2 (French Aortic National CoreValve and Edwards 2) registry (8) in January 2012, another national TAVR monitoring program, the FRANCE TAVI (French Transcatheter Aortic Valve Implantation) registry, was designed and launched in January 2013. In the present study, we report the characteristics and short-term outcomes of patients included in this registry. Furthermore, we provide a comparison with the FRANCE 2 registry patients to ascertain national patterns of changing procedural characteristics and clinical outcomes of TAVR recipients in France during a 6-year period.

SEE PAGE 56

METHODS

Launched in January 2013, FRANCE TAVI is an initiative of GACI, the French Society of Cardiology's

ABBREVIATIONS AND ACRONYMS

ACC = American College of Cardiology

ESV = Edwards SAPIEN valve

EuroSCORE = European System for Cardiac Operative Risk Evaluation

FRANCE 2 = French Aortic National CoreValve and Edwards 2 registry

MCV = Medtronic CoreValve

PPI = permanent pacemaker implantation

STS = The Society of Thoracic Surgeons

TAVR = transcatheter aortic valve replacement

TVT = transcatheter valve therapy

From the [a]Cardiology and Vascular Diseases Service, Pontchaillou University Hospital Center, Center for Clinical Investigation 804, University of Rennes 1, Signal and Image Treatment Laboratory (LTSI), National Institute of Health and Medical Research U1099, Rennes, France; [b]Paris South Cardiovascular Institute, Jacques-Cartier Private Hospital, Massy, France; [c]Department of Cardiology, University of Lille 2, Regional University Hospital Center of Lille, National Institute of Health and Medical Research U1011, University Hospital Federation Integra, Lille, France; [d]Cardiology Service, Rouen-Charles-Nicolle University Hospital Center, National Institute of Health and Medical Research U644, Rouen, France; [e]Department of Cardiology, University Hospital Department Fire and Paris-Diderot University, Public Assistance Hospitals of Paris, Bichat Hospital, Paris, France; [f]Cardiology Service, Saint Hilaire Clinic, Rouen, France; [g]Department of Cardiology, Gabriel Montpied University Hospital Center, Image Science for Interventional Techniques, Cardiovascular Interventional Therapy and Imaging, National Scientific Research Center Unité Mixte de Recherche (UMR) 6284, University of the Auvergne, Clermont-Ferrand, France; [h]Sorbonne-Pierre-et-Marie-Curie University, Public Assistance Hospitals of Paris, Groupe Hospitalier de la Pitié Salpêtrière (GHPS), Cardiac Surgery, Paris, France; [i]Thoracic and Cardiovascular Surgery Service, Pontchaillou University Hospital Center, University of Rennes 1, Signal and Image Treatment Laboratory (LTSI), National Institute of Health and Medical Research U1099, Rennes, France; [j]Cardiology Service, Thoracic Institute, Guillaume et René Laennec University Hospital Center, Nantes, France; [k]Cardiology Federation, Saint Joseph Hospital, Marseille, France; [l]Cardiac Surgery Service, University Hospital Center of Angers, National Scientific Research Center UMR 6214, National Institute of Health and Medical Research 1083, University of Angers, Angers, France; [m]Cardiology Service, La Pitié-Salpêtrière University Hospital Center, Public Assistance Hospitals of Paris, Paris, France; [n]Division of Cardiology, Center for Clinical Investigation of Lyon, Louis Pradel University Hospital Center, Bron, France; [o]Department of Cardiology, Marie Lannelongue Center, Le Plessis Robinson, France; [p]Cardiology Service, Saint Gatien Clinic, Tours, France; [q]Department of Cardiology, Montsouris Mutualist Institute, Paris, France; [r]Cardiology Service, Clinic of the Tonkin, Villeurbanne, France; [s]Department of Interventional Cardiology, Cardiology Hospital of the Haut-Lévêque, University of Bordeaux, Pessac, France; [t]Cardiology Service, Clairval Private Hospital, Marseille, France; [u]Department of Cardiology, Henri-Mondor Hospital, Public Assistance Hospitals of Paris, Créteil, France; [v]Cardiology Service, Saint Augustin Clinic, Bordeaux, France; [w]Cardiovascular Surgery Service, University Hospital Center of Nancy, Vandœuvre-lès-Nancy, France; [x]Cardiology Service, Arnaud de Villeneuve University Hospital Center, Montpellier, France; [y]Department of Cardiology, University Hospital Center of Toulouse, National Institute of Health and Medical Research U1048, University of Toulouse 3, Toulouse, France; [z]Department of Cardiology, University Hospital Center of Strasbourg, New Civil Hospital, University of Strasbourg, Strasbourg, France; [aa]Cardiology Service, Saint Martin Private Hospital, Caen, France; [bb]Department of Cardiology, Pharmacology and Cardiometabolic Physiopathology Laboratory, University Hospital Center of Dijon, National Institute of Health and Medical Research U866, University of Burgundy, Dijon, France; [cc]Cardiology Service, Arnaud Tzanck Institute, Saint Laurent du Var, France; [dd]University Cardiology Clinics, University Hospital Center of Grenoble, Grenoble, France; [ee]Department of Cardiology, Georges Pompidou European Hospital, Public Assistance Hospitals of Paris, Center for Expertise on Sudden Death, National Institute of Health and Medical Research U970, Paris Descartes University, Paris, France; [ff]Cardiology Service, Heart, Thorax, and Vascular Center, Trousseau University Hospital Center, François Rabelais University, Tours, France; [gg]Department of Cardiology, La Timone University Hospital Center, Public Assistance Hospitals of Marseille, National Institute of Health and Medical Research UMR1062, French National Institute for Agricultural Research UMR 1260, University of Aix-Marseille, Marseille, France; [hh]Cardiology Service, Polyclinic du Bois, Lille, France; [ii]Cardiology Service, Côte de Nacre University Hospital Center, Caen, France; [jj]Cardiology Service, Protestant Infirmary of Lyon, Caluire et Cuire, France; [kk]Cardiovascular Surgery Service, Clinic of the Sauvegarde, Lyon, France; [ll]Cardiology Service, Parly 2 Private Hospital, Le Chesnay, France; [mm]Cardiology Service, Bois Bernard Private Hospital, Bois-Bernard, France; [nn]Department of Cardiology, University Hospital Center of Amiens, Amiens, France; [oo]Department of Cardiology,

working group of interventional cardiology, with the participation of the French Society of Thoracic and Cardiovascular Surgery. Device manufacturers partly funded the registry but had no role in data collection or analysis or in manuscript preparation.

Designed as an all-comers registry, it prospectively includes data on all patients who underwent TAVR for severe aortic stenosis in 48 of 50 active TAVR centers in France and who volunteered to participate. FRANCE TAVI was designed in continuity with the FRANCE 2 registry (8) to provide further data on baseline characteristics of patients as well as procedural aspects and clinical outcomes of TAVR recipients on a national scale. A shortened version of the case report form from FRANCE 2 was used for FRANCE TAVI, but definitions remained identical between the 2 registries except for major bleeding and vascular complications (Online Appendix).

The decision to perform TAVR and the choices of approach and device used were made on the basis of assessment by a multidisciplinary heart team at each participating center, as previously described (8). Procedures and post-procedural management were performed in accordance with each site's routine protocol. A 30-day follow-up was recommended in the case report form and was performed either on site or by telephone contact with the patient and the patient's physician depending on each site's protocol. Patients included in the registry provided written informed consent for the procedure and for anonymous processing of their data. The registry was approved by the Institutional Review Board of the French Ministry of Higher Education and Research and by the National Commission for Data Protection and Liberties. FRANCE TAVI is supported by the French Society of Cardiology.

The FRANCE TAVI dataset was collected using a dedicated web-based interface from the French Society of Cardiology. All data, including in-hospital complications and follow-up, were site reported according to the definitions within the national dataset (Online Appendix). The database was managed by the French Society of Cardiology, which implemented regular data quality checks, including range checks and assessments of internal consistency. In cases of missing, extreme, or inconsistent values, centers were contacted and asked to verify and modify records as appropriate.

STUDY GROUP AND ENDPOINTS. For the purposes of this analysis, a FRANCE TAVI database encompassing all patients included from January 2, 2013, to

La Miletrie University Hospital Center, Poitiers, France; [pp]Cardiology Service, Claude Bernard Hospital Clinic, Metz, France; [qq]Cardiology Service, Dupuytren University Hospital Center, Limoges, France; [rr]Cardiology and Vascular Pathology Service, Robert Debré University Hospital Center, Reims, France; [ss]Cardiology Service, Hospital Center of Annecy-Genevois, Metz-Tessy, France; [tt]Department of Cardiology, University Hospital Center of Saint-Etienne, Saint-Etienne, France; [uu]Cardiology Service, Emile Müller Hospital, Hospital Group of the Mulhouse and South Alsace Region, Mulhouse, France; [vv]Department of Interventional Cardiology, Cardiology Center of the North, Saint-Denis, France; [ww]Cardiology Service, Saint Clotilde Clinic, Saint Denis de La Réunion, La Réunion, France; [xx]Cardiac Surgery Service, Ambroise Paré Clinic, Neuilly-sur-Seine, France; [yy]Department of Epidemiology and Public Health, University of Toulouse 3, National Institute of Health and Medical Research UMR 1027, University Hospital Center of Toulouse, Toulouse, France; [zz]University Institute of Cardiology and Pulmonology, Laval University, Québec City, Québec, Canada; and the [aaa]Department of Cardiology, La Cavale Blanche University Hospital Center, Optimization of Physiological Regulations, Science and Technical Training and Research Unit, University of Western Brittany, Brest, France. Edwards Lifesciences and Medtronic partly funded the FRANCE TAVR registry. Edwards Lifesciences and Medtronic had no role in data management, data analysis, or writing of the manuscript. Dr. Auffret has received fellowship support from the French Cardiology Federation (Fédération Française de Cardiologie); and has received research grants from Abbott, Edwards Lifesciences, Medtronic, Biosensors, Terumo, and Boston Scientific. Dr. Le Breton has received speaker fees from Edwards Lifesciences and Medtronic. Dr. Rodés-Cabau has received research grants from Edwards Lifesciences, Medtronic, and St. Jude Medical. Dr. Eltchaninoff has served as a proctor for and received lecture fees from Edwards Lifesciences. Dr. Lefevre has served as a proctor for Edwards Lifesciences and Abbott. Dr. Koning has clinical research relationships with Boehringer Ingelheim, Boston scientific, Abbott, Biosensor, and Biotronik. Dr. Leprince has served as a proctor for Medtronic. Dr. Jean Philippe Collet has received research grants from Bristol-Myers Squibb and Medtronic; and lecture fees from Bristol-Myers Squibb, Bayer, Daichii-Sankyo, AstraZeneca, and Medtronic. Dr. Himbert has served as a proctor and consultant for Edwards Lifesciences; and has served as a proctor for Medtronic. Dr. Souteyrand has served as a consultant to Medtronic, St. Jude Medical, Abbott, and Terumo. Dr. Teiger has served as a proctor for Medtronic. Dr. Iung has received consulting fees from Boehringer Ingelheim; and has received a speaker fee from Edwards Lifesciences. Dr. Spaulding has received research grants from the French Ministry of Health; has received consulting fees from Abiomed, Zoll, Medtronic, and Medpass; has received speaker fees from AstraZeneca, Cordis, Servier, Lead-Up, Bayer, The Medicines Company, Eli Lilly, and WebMD; and is a member of the advisory board of Xeltis. Dr. Beygui has received institutional research grants from AstraZeneca, Medtronic, Biosensor, St. Jude Medical, ACIST, and Daichii-Sankyo; and has received consulting and presentation honoraria from AstraZeneca, Medtronic, and Bristol-Myers Squibb. All other authors have reported that they have no relationships relevant to the contents of this paper to disclose.

*The key personnel, institutions, and organizations participating in the FRANCE TAVI Registry are listed in the Online Appendix.

Deepak L. Bhatt, MD, MPH, served as Guest Editor for this paper.

Manuscript received January 8, 2017; revised manuscript received April 5, 2017, accepted April 24, 2017.

FIGURE 1 Study Flow Chart

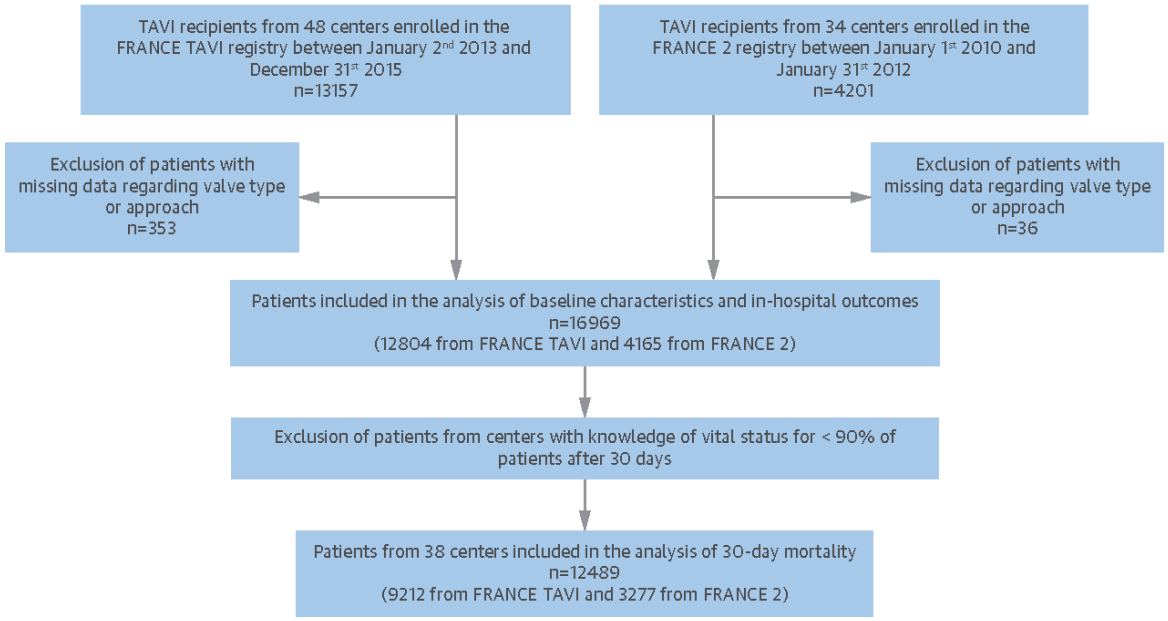

Few patients in the FRANCE 2 (French Aortic National CoreValve and Edwards 2) and FRANCE TAVI (French Transcatheter Aortic Valve Implantation) registries were excluded for the initial analysis of baseline characteristics and hospital outcomes. TAVI = transcatheter aortic valve implantation.

December 31, 2015, was locked. To evaluate longitudinal changes in patients' characteristics, TAVR performance, and clinical outcomes over time, we used the data from FRANCE 2, which consecutively included all patients who underwent TAVR in France from January 2010 to January 31, 2012. Detailed methodology and definitions used in this registry have been published elsewhere (8). In both databases, patients with missing data on valve type or approach (n = 389) were excluded from the analysis (**Figure 1**). Baseline characteristics and in-hospital outcomes for these patients are documented in Online Table 1.

The primary endpoint of the study was in-hospital all-cause mortality reported in the full cohort. Secondary endpoints were in-hospital complications in the full cohort and 30-day all-cause mortality reported among centers in which vital status after 30 days was known for at least 90% of patients, to ensure the comparability of follow-up completeness between registries. Baseline characteristics and in-hospital outcomes of patients with versus without reported 30-day follow-up are presented in Online Table 2.

In cases of discrepancies in definitions of patients' characteristics or outcomes between the 2 registries, no formal statistical comparison was made between the 2 groups of patients, and data of the FRANCE TAVI group were reported separately.

STATISTICAL ANALYSIS. Because data came from multiple recruitment centers, 2-level analyses were used to assess whether patients' characteristics, procedural data, and outcomes were different according to registry (FRANCE 2 or FRANCE TAVI) or year of inclusion, by taking into account the effects of potential common context of patients (first level) recruited in different centers (second level). For these 2 levels of analyses, patients' characteristics or outcomes were used as predicted variables, and registry or year of inclusion was an explanatory variable. Depending on the predicted variable's type, different models were used: a 2-level linear model for continuous data; a 2-level logistic model for dichotomous data; and a 2-level multinomial logit model for polytomous data. Analyses according to year of inclusion were limited to centers that participated in both registries, and the ordinal effect of year of inclusion was tested by inserting the variable in its continuous form in the relevant model. Statistical analyses were performed using Stata Statistical Software release 10 (StataCorp, LLC, College Station, Texas). Given that

TABLE 1 Baseline Characteristics

	FRANCE 2 (n = 4,165)	FRANCE TAVI (n = 12,804)	p Value
Clinical characteristics			
Age, yrs	82.8 ± 7.1	83.4 ± 7.2	0.001
Median	84.3 (79.3-87.8)	84.7 (80.4-88.1)	
Male	2,111/4,165 (50.7)	6,314/12,804 (49.3)	0.065
Body mass index, kg/m²	26.0 ± 5.0 4,156	26.5 ± 5.3 12,623	<0.001
Logistic EuroSCORE, %	21.7 ± 14.2 4,045	17.9 ± 12.3 12,341	<0.001*
Median	18.4 (11.4-28.5)	15.0 (9.5-23.0)	
<10	797 (19.7)	3,244 (26.3)	
10-19	1,415 (35.0)	4,894 (39.7)	
20-39	1,400 (34.6)	3,469 (28.1)	
≥40	433 (10.7)	734 (5.9)	
NYHA functional class III or IV	3,124/4,157 (75.2)	8,269/12,241 (67.6)	<0.001
≥2 APE within previous year	484/4,142 (11.7)	1,715/1,2038 (14.3)	<0.001
Clinical history			
Coronary artery disease†	1,851/4,149 (44.6)	5,093/11,961 (42.6)	0.117
Previous myocardial infarction <90 days	51/4,158 (1.2)	238/12,622 (1.9)	0.018
Previous CABG	730/4,149 (17.6)	1,441/12,684 (11.4)	<0.001
Previous SAVR	69/4,149 (1.7)	559/12,659 (4.4)	<0.001
Previous permanent pacemaker	597/4,145 (14.4)	1,807/12,655 (14.3)	0.769
Atrial fibrillation	1,070/4,108 (26.1)	2,763/11,119 (24.9)	<0.001
Previous stroke/TIA	411/4,149 (9.9)	1,395/12,631 (11.0)	0.074
Diabetes mellitus	1,045/4,149 (25.2)	3,271/12,617 (25.9)	0.314
Peripheral vascular disease	1,139/4,158 (27.4)	2,853/12,629 (22.6)	<0.001
Chronic pulmonary disease	1,009/4,149 (24.3)	2,551/12,641 (20.2)	<0.001
Serum creatinine ≥200 μmol/l	354/4,158 (8.5)	635/12,178 (5.2)	<0.001
Renal dialysis	104/4,149 (2.5)	235/12,443 (1.9)	0.025
Life expectancy <1 yr	96/4,149 (2.3)	356/12,261 (2.9)	<0.001
Echocardiographic findings			
Ejection fraction, %	53.2 ± 14.2 4,104	55.2 ± 13.6 12,378	<0.001
Median	55 (45-65)	60 (45-65)	
<50%	1,382 (33.7)	3,400/12,378 (27.5)	<0.001
Aortic valve area, cm²	0.67 ± 0.18 3,911	0.69 ± 0.26 11,569	<0.001
Aortic annulus, mm	22.2 ± 2.2 3,828	23.6 ± 2.7 11,340	<0.001
Aortic mean gradient, mm Hg	48.1 ± 16.5 4,047	47.2 ± 15.9 12,340	0.001
Moderate or severe AR	735/3,931 (18.7)	2,118/10,118 (20.9)	0.065
Moderate or severe MR	850/3,940 (21.6)	2,369/10,498 (22.6)	0.792
Severe PH (sPAP >60 mm Hg)	419/3,221 (13.0)	1,280/9,715 (13.2)	0.924

Values are mean ± SD, median (IQR), n/N (%), n, or n (%). *Test performed using log-transformed variable. †Presence of at least 1 significant lesion (≥50%) on the pre-procedural coronary angiogram.

APE = acute pulmonary edema; AR = aortic regurgitation; CABG = coronary artery bypass graft; EuroSCORE = European System for Cardiac Operative Risk Evaluation; FRANCE 2 = French Aortic National CoreValve and Edwards 2 registry; FRANCE TAVI = French Transcatheter Aortic Valve Implantation registry; IQR = interquartile range; MR = mitral regurgitation; NYHA = New York Heart Association; PH = pulmonary hypertension; SAVR = surgical aortic valve replacement; sPAP = systolic pulmonary artery pressure; TIA = transient ischemic attack.

few patients were included in the FRANCE 2 registry during January 2012 (n = 221), TAVR cases performed in 2011 and 2012 within this registry were grouped together for the purpose of descriptive analysis. All tests were 2-sided at the 0.05 significance level.

RESULTS

This analysis included a total of 12,804 patients entered into FRANCE TAVI from January 2013 to December 2015 and 4,165 patients enrolled in the FRANCE 2 registry from January 2010 to January 2012 (Figure 1). Baseline characteristics of the study group are summarized in Table 1.

The median age of these patients was 84.6 years (interquartile range [IQR]: 80.1 to 88.0 years), and 49.7% were men. Overall, FRANCE TAVI participants were older, had lower surgical risk as estimated by the logistic European System for Cardiac Operative Risk Evaluation (EuroSCORE 1), and were less likely to present with coexisting conditions or severe symptoms. The rate of patients with a previous surgical aortic valve replacement markedly increased from 1.7% in FRANCE 2 to 4.4% in FRANCE TAVI (p < 0.001). Regarding echocardiographic findings, FRANCE TAVI participants had a larger aortic annulus and lower rates of impaired left ventricular function.

Table 2 shows linear trends in baseline characteristics over time among centers that participated in both registries (31 centers; n = 13,745). The percentage of octogenarians increased from 69.8% in 2010 to 76.9% in 2014 to 2015, whereas the logistic EuroSCORE gradually decreased over time, with only 28.8% of patients with a score ≥20% in 2015 compared with 51.1% in 2010. The median logistic EuroSCORE decreased from 20.3% (IQR: 12.1% to 30.8%) to 13.6% (IQR: 9.0% to 21.0%) over the study period. This trend was consistently observed whether the valve used was the Edwards SAPIEN valve (ESV; Edwards Lifesciences, Irvine, California) or the Medtronic CoreValve (MCV; Medtronic, Minneapolis, Minnesota) or whether the valve was delivered transfemorally; increasing age was observed only within transfemoral TAVR and MCV recipients (Online Tables 3 to 5). Interestingly, "valve-in-valve" procedures accounted for almost 10% of MCV recipients in 2015.

Within FRANCE TAVI, clinical characteristics of ESV and MCV recipients were mainly comparable (Online Table 6). In contrast, patients who underwent transfemoral and nontransfemoral procedures had major differences in baseline characteristics (Online Table 7).

PROCEDURAL CHARACTERISTICS. Although ESV and MCV were used exclusively in FRANCE 2, other devices (Lotus, Boston Scientific, Natick, Massachusetts; Direct Flow Medical, Santa Rosa, California; Centera, Edwards Lifesciences; Portico, St. Jude Medical, St. Paul, Minnesota; and JenaValve, Irvine,

TABLE 2 Baseline Characteristics per Year of Inclusion Within Centers Involved in Both Registries

	FRANCE 2		FRANCE TAVI			
	2010 (n = 1,378)	2011/2012 (n = 2,385)	2013 (n = 2,512)	2014 (n = 3,177)	2015 (n = 4,293)	p Value for Trend
Clinical characteristics						
Age, yrs	82.4 ± 7.3 1,378	82.9 ± 7.2 2,385	83.1 ± 7.5 2,512	83.2 ± 7.3 3,177	83.0 ± 7.3 4,293	0.01
Median	83.8 (78.6-87.6)	84.4 (79.7-87.8)	84.5 (80.2-87.9)	84.5 (80.1-88.2)	84.3 (80.2-87.8)	
Male	705/1,378 (51.2)	1,207/2,385 (50.6)	1,226/2,512 (48.8)	1,551/3,177 (48.8)	2,122/4,293 (49.4)	0.126
Body mass index, kg/m^2	26.0 ± 5.1 1,372	26.1 ± 5.0 2,382	26.5 ± 5.2 2,483	26.5 ± 5.3 3,151	26.6 ± 5.2 4,194	<0.001
Logistic EuroSCORE, %	23.2 ± 14.7 1,325	20.5 ± 14.0 2,318	18.7 ± 12.5 2,410	17.7 ± 12.1 3,059	16.7 ± 11.6 4,131	<0.001*
Median	20.3 (12.1-30.8)	16.7 (10.4-27.1)	15.3 (10.0-24.0)	15.0 (9.5-23.0)	13.6 (9.0-21.0)	
<10	232 (17.5)	527 (22.7)	564 (23.4)	804 (26.3)	1,234 (29.9)	
10-19	416 (31.4)	862 (37.2)	949 (39.4)	1,221 (39.9)	1,709 (41.4)	
20-39	505 (38.1)	705 (30.4)	718 (29.8)	869 (28.4)	1,005 (24.3)	
≥40	172 (13.0)	224 (9.7)	179 (7.4)	165 (5.4)	183 (4.4)	
NYHA functional class III or IV	1,040/1,378 (75.6)	1,750/2,381 (73.5)	1,706/2,460 (69.4)	2,047/3,074 (66.6)	2,546/4,041 (63.0)	<0.001
≥2 APE within previous year	191/1,374 (13.9)	261/2,367 (11.0)	322/2,424 (13.3)	386/3,025 (12.8)	516/4,066 (12.7)	0.137
Clinical history						
Coronary artery disease†	593/1,375 (43.1)	1,078/2,372 (45.5)	976/2,340 (41.7)	1,281/3,006 (42.6)	1,646/3,858 (42.7)	0.338
Previous myocardial infarction <90 days	17/1,377 (1.2)	32/2,379 (1.4)	54/2,476 (2.2)	46/3,145 (1.5)	62/4,207 (1.5)	0.555
Previous CABG	275/1,375 (20.0)	374/2,372 (15.8)	314/2,499 (12.6)	345/3,164 (10.9)	416/4,211 (9.9)	<0.001
Previous SAVR	22/1,375 (1.6)	41/2,372 (1.7)	78/2,498 (3.1)	146/3,158 (4.6)	214/4,199 (5.1)	<0.001
Previous permanent pacemaker	205/1,371 (15.0)	342/2,372 (14.4)	382/2,487 (15.4)	452/3,157 (14.3)	554/4,212 (13.2)	0.076
Atrial fibrillation	378/1,356 (27.9)	605/2,352 (25.7)	583/2,273 (25.7)	676/2,865 (23.6)	771/3,406 (22.6)	<0.001
Previous stroke/TIA	139/1,375 (10.1)	231/2,372 (9.7)	276/2,490 (11.1)	371/3,151 (11.8)	428/4,211 (10.2)	0.590
Diabetes mellitus	375/1,375 (27.3)	588/2,372 (24.8)	640/2,487 (25.7)	798/3,144 (25.4)	1,097/4,208 (26.1)	0.949
Peripheral vascular disease	436/1,377 (31.7)	580/2,379 (24.4)	531/2,495 (21.3)	655/3,161 (20.7)	887/4,212 (21.1)	<0.001
Chronic pulmonary disease	359/1,375 (26.1)	572/2,372 (24.1)	561/2,499 (22.5)	618/3,156 (19.6)	631/4,210 (15.0)	<0.001
Serum creatinine ≥200 μmol/l	148/1,377 (10.8)	161/2,379 (6.8)	131/2,443 (5.4)	180/3,054 (5.9)	188/4,014 (4.7)	<0.001
Renal dialysis	44/1,375 (3.2)	51/2,372 (2.2)	56/2,481 (2.3)	67/3,127 (2.1)	61/4,072 (1.5)	<0.001
Life expectancy <1 yr	50/1,375 (3.6)	44/2,372 (1.9)	104/2,409 (4.3)	80/3,043 (2.6)	144/4,036 (3.6)	0.146
Echocardiographic findings						
Ejection fraction, %	52.4 ± 14.5 1,359	53.5 ± 14.1 2,347	54.3 ± 13.8 2,439	54.6 ± 13.5 3,099	55.6 ± 13.2 4,109	<0.001
Median	55 (40-64)	55 (45-65)	57 (45-65)	59 (45-65)	60 (49-65)	
<50%	490 (36.1)	773 (32.9)	755 (31.0)	857 (27.7)	1,046 (25.5)	<0.001
Aortic valve area, cm^2	0.66 ± 0.18 1,300	0.67 ± 0.18 2,221	0.68 ± 0.24 2,319	0.69 ± 0.23 2,877	0.71 ± 0.25 3,766	<0.001
Aortic annulus, mm	22.0 ± 2.1 1,268	22.3 ± 2.2 2,177	23.4 ± 2.7 2,230	23.4 ± 2.6 2,797	23.7 ± 2.7 3,726	<0.001
Aortic mean gradient, mm Hg	47.8 ± 16.6 1,348	48.2 ± 16.4 2,305	47.3 ± 15.9 2,444	47.1 ± 15.6 3,078	47.1 ± 15.9 4,059	0.003
Moderate or severe AR	234/1,289 (18.2)	446/2,247 (19.9)	401/1,867 (21.5)	572/2,725 (21.0)	734/3,227 (22.8)	0.051
Moderate or severe MR	300/1,296 (23.1)	497/2,253 (22.1)	468/2,139 (21.9)	594/2,757 (21.6)	773/3,264 (23.7)	0.992
Severe PH (sPAP >60 mm Hg)	157/1,079 (14.5)	223/1,818 (12.3)	268/1,964 (13.7)	319/2,485 (12.8)	360/3,015 (11.9)	0.109

Values are mean ± SD, n, median (IQR), n/N (%), or n (%). *Test performed using log-transformed variable. †Presence of at least 1 significant lesion (≥50%) on the pre-procedural coronary angiogram.
Abbreviations as in Table 1.

California) were available but seldom used in FRANCE TAVI (Table 3). There was a slight but significant decrease in ESV implantations, which nevertheless represented ~65% of TAVR procedures overall.

Transfemoral access increased in FRANCE TAVI compared with FRANCE 2, whereas there was a dramatic decrease in the use of transapical access in ESV recipients, from 27.9% in 2010 to 4.7% in 2015 among centers that participated in both registries ($p < 0.001$). However, nonfemoral approaches were still used in 17.2% of cases in FRANCE TAVI because of an increase in alternative approaches, especially direct aortic access in 698 patients (5.5%) and transcarotid access in 435 patients (3.4%).

TABLE 3 Procedural Characteristics

	FRANCE 2 (n = 4,165)	FRANCE TAVI (n = 12,804)	p Value
Location			
Catheterization laboratory	3,006/4,164 (72.2)	7,573/12,746 (59.4)	ref
Operating room	460/4,164 (11.0)	625/12,746 (4.9)	<0.001
Hybrid room	698/4,164 (15.8)	4,548/12,746 (35.7)	<0.001
General anesthesia	2,862/4,164 (68.7)	6,531/12,645 (51.7)	<0.001
TEE guidance	2,527/4,164 (60.7)	3,672/11,373 (32.3)	<0.001
Approach			
Transfemoral	3,058 (73.4)	10,602 (82.8)	ref
Transapical	732 (17.6)	541 (4.2)	<0.001
Subclavian	241 (5.8)	385 (3.0)	<0.001
Others	134 (3.2)	1,276 (10.0)	<0.001
Valve type			
Edwards SAPIEN*	2,759 (66.2)	8,232 (64.3)	ref
Medtronic CoreValve	1,406 (33.8)	4,465 (34.9)	<0.001
Others	0 (0.0)	107 (0.8)	–
Need for a second valve	94 (2.3)	236 (1.8)	0.155
Conversion to surgery	49 (1.2)	65/12,557 (0.5)	<0.001
Device success	3,970 (95.3)	12,139/12,544 (96.8)	<0.001

Values are n/N (%) or n (%). *Including all iterations (SAPIEN, SAPIEN XT, SAPIEN 3).
TEE = transesophageal echocardiography; other abbreviations as in Table 1.

Most procedures were performed in catheterization laboratories, although there was a significant decrease in their usage rate in favor of hybrid operating rooms from FRANCE 2 to FRANCE TAVI (Table 3). During the study period, a gradual shift toward simplified procedures was observed. In centers participating in both registries, general anesthesia and transesophageal guidance decreased from 70.3% to 47.2% and from 64.1% to 26.7%, respectively (Table 4).

Although there was no significant change in the need for a second valve in FRANCE TAVI (1.8 vs. 2.3%; p = 0.16) (Tables 3 and 4), device success significantly increased (96.8 vs. 95.3%; p < 0.001). Within FRANCE TAVI, the use of MCV, compared with ESV implantation, was associated with a lower rate of transfemoral approach use (80.7 vs. 83.8%; p < 0.001), a higher risk of need for a second valve (3.6% vs. 0.9%; p < 0.001), and a lower rate of procedural success (94.4% vs. 98.1%; p < 0.001). Procedural success was comparable between transfemoral and nontransfemoral approaches (96.7% vs. 97.1%; p = 0.20).

IN-HOSPITAL AND 30-DAY OUTCOMES. In-hospital deaths primarily had cardiovascular causes; the in-hospital mortality rate decreased gradually over time and was significantly lower in FRANCE TAVI than in FRANCE 2 (4.4% vs. 8.1%; p < 0.001) (Tables 5 and 6). By 2015, in-hospital mortality rates of 2.4%, 3.4%, 2.4%, and 4.2% were achieved in ESV, MCV, transfemoral, and nontransfemoral TAVR recipients, respectively, who were treated in centers participating in both registries, thus resulting in an overall in-hospital mortality rate of 2.7%. In-hospital outcomes according to valve type and approach within the FRANCE TAVI group are summarized in Online Tables 8 and 9.

The rate of patients discharged by day 5 post-TAVR increased from 11.9% to 24.7% from FRANCE 2 to FRANCE TAVI (p < 0.001). Infrequent complications (annulus rupture, aortic dissection, valve migration) did not significantly decrease over time, and rates of cardiac tamponade significantly increased (Table 5). Stroke rates were low and comparable (2.0% in FRANCE 2 and 2.0% in FRANCE TAVI; p = 0.82). Importantly, permanent pacemaker implantation (PPI) increased from 12.6% in FRANCE 2 to 17.5% in FRANCE TAVI (p < 0.001) because of a marked increase in ESV recipients (from 8.4% in 2010 to 15.1% in 2015 among centers participating in both registries). Within FRANCE TAVI, the rates of major bleeding and vascular complications requiring surgical or percutaneous interventions were 8.9% and 7.7%, respectively.

Among patients with an immediate pre-discharge echocardiogram, the rate of moderate or severe aortic regurgitation was significantly lower in FRANCE TAVI compared with FRANCE 2 (10.2% vs. 15.7%; p < 0.001), mainly because of ESV recipients, who had a 7.4% rate of moderate to severe aortic regurgitation compared with 15.1% among MCV recipients (p < 0.001) (Online Table 8).

A total of 12,489 patients from 38 centers that documented vital status for ≥90% of their TAVR patients were included in the 30-day mortality analysis (Table 5). Among these patients, 99.5% of the 3,277 patients from FRANCE 2 and 97.4% of the 9,212 patients from FRANCE TAVI had a known 30-day vital status. Mortality rates were 10.1% versus 5.4% among patients from FRANCE 2 and FRANCE TAVI, respectively (p < 0.001).

IMPACT OF TAVR ADOPTION. To evaluate the impact of centers starting their TAVR program following the inclusion period of FRANCE 2, we compared, within the FRANCE TAVI group, patients enrolled at centers that participated in both registries with patients enrolled at centers that participated in the FRANCE TAVI registry only (Online Tables 10 to 12). The latter patients were older, with a nonsignificantly higher surgical risk. These patients treated at centers that participated only in the FRANCE TAVI registry also were more likely to have undergone transfemoral access (89.6% vs. 80.9%; p < 0.001), with a

TABLE 4 Procedural Characteristics per Year of Inclusion Within Centers Involved in Both Registries

	FRANCE 2		FRANCE TAVI			
	2010 (n = 1,378)	2011/2012 (n = 2,385)	2013 (n = 2,512)	2014 (n = 3,177)	2015 (n = 4,293)	p Value for Trend
Location						
Catheterization laboratory	993 (72.1)	1,692 (70.9)	1,641/2,511 (65.4)	1,998/3,172 (63.0)	2,339/4,267 (54.8)	ref
Operating room	154 (11.2)	302 (12.7)	141/2,511 (5.6)	1,16/3,172 (3.7)	307/4,267 (7.2)	0.026
Hybrid room	231 (16.8)	391 (16.4)	729/2,511 (29.0)	1,058/3,172 (33.3)	1,621/4,267 (38.0)	<0.001
General anesthesia	968 (70.3)	1,497/2,384 (62.8)	1,364/2,504 (54.5)	1,839/3,162 (58.2)	1,991/4,222 (47.2)	<0.001
TEE guidance	883 (64.1)	1,281/2,384 (53.7)	866/2,322 (37.3)	1,041/2,937 (35.4)	964/3,616 (26.7)	<0.001
Approach						
Transfemoral	1,036 (75.2)	1,712 (71.8)	1,976 (78.7)	2,534 (79.8)	3,563 (83.0)	ref
Transapical	265 (19.2)	390 (16.3)	178 (7.1)	144 (4.5)	166 (3.9)	<0.001
Subclavian	70 (5.1)	164 (6.9)	120 (4.8)	101 (3.2)	114 (2.7)	<0.001
Others	7 (0.5)	119 (5.0)	238 (9.5)	398 (12.5)	450 (10.5)	<0.001
Valve type						
Edwards SAPIEN*	958 (69.5)	1,533 (64.3)	1,466 (58.4)	1,868 (58.8)	3,015 (70.2)	ref
Medtronic CoreValve	420 (30.5)	852 (35.7)	1,027 (40.9)	1,270 (40.0)	1,230 (28.7)	0.004
Others	0 (0.0)	0/2,376 (0.0)	19 (0.7)	39 (1.2)	48 (1.1)	–
Need for a second valve	28 (2.0)	55 (2.3)	58 (2.3)	72 (2.3)	56 (1.3)	0.012
Conversion to surgery	18 (1.3)	26 (1.1)	21/2,501 (0.8)	19/3,151 (0.6)	15/4,162 (0.4)	<0.001
Device success	1,315 (95.4)	2,275 (95.4)	2,332/2,441 (95.5)	2,995/3,106 (96.4)	4,158/4,248 (97.9)	<0.001

Values are n (%) or n/N (%). *Including all iterations (SAPIEN, SAPIEN XT, SAPIEN 3).
Abbreviations as in Tables 1 and 3.

numerically higher use of ESVs (66.7% vs. 63.6%; p = 0.77) and conscious sedation (51.5% vs. 47.5%; p = 0.33). Procedural success, however, was comparable between groups (96.5% vs. 96.8%; p = 0.55), and there was no difference in in-hospital mortality rates (5.0% vs. 4.2%; p = 0.14).

DISCUSSION

The present analysis is the first report of the second national French TAVR monitoring program, with a systematic comparison with its predecessor for evaluating TAVR performance trends across France during a 6-year period (**Central Illustration**). The chief findings of our analysis are as follows: 1) significant changes in baseline characteristics of patients occurred with an important decrease in estimated surgical risk over time, thus reflecting lower rates of comorbidities within FRANCE TAVI despite the inclusion of older patients; 2) >80% of patients benefited from the "transfemoral first" policy adopted by centers, whereas transapical access declined significantly in favor of alternative procedural access; 3) approximately 50% and 70% of procedures were performed using conscious sedation and without transesophageal guidance, respectively, with sustained procedural success; 4) in-hospital and 30-day mortality rates were significantly lower in FRANCE TAVI (4.4% and 5.4%, respectively); 5) infrequent but life-threatening complications did not decline over time, with a significant increase in cardiac tamponade rates; and 6) PPI rates markedly increased, especially within ESV recipients.

Unlike previous reports of large multicenter registries (13,14), we demonstrated highly significant changes in baseline characteristics and risk profile of TAVR recipients across France. The improved patient risk profile at baseline (evidenced by a steep decrease in the logistic EuroSCORE) was perhaps the most striking change. Several reasons could explain this trend. First, the favorable outcomes and sustained midterm hemodynamic performances demonstrated in high-risk patients with both ESV and MCV (16,17) could have encouraged the performance of TAVR in lower-risk patients. Second, operators may have been influenced by the current trends in published reports that highlight predictors of early and late death post-TAVR, as well as factors associated with procedural futility (14,16–19). Indeed, rates of coexisting conditions, such as chronic pulmonary disease, peripheral vascular disease, chronic kidney disease, or left ventricular dysfunction that have been independently linked to an increased mortality rate (12,14,16,18–20), were all lower in FRANCE TAVI. Despite a lack of specificity in the TAVR setting, a logistic EuroSCORE ≥40% is a well-known predictor of higher early and late death (14), and it was uncommon (6%) in FRANCE TAVI. The logistic EuroSCORE, albeit less

TABLE 5 Outcomes

	FRANCE 2 (n = 4,165)	FRANCE TAVI (n = 12,804)	p Value
In-hospital outcomes			
Time from implantation to discharge			<0.001*
Median, days	9 (7-13)	8 (6-11)	
	4,086	12,672	
1-5	484 (11.9)	3,132 (24.7)	
6-9	1,758 (43.0)	5,744 (45.3)	
≥10	1,844 (45.1)	3,796 (30.0)	
Complications			
Death			<0.001
From all-cause	339 (8.1)	562 (4.4)	
Cause of death			
CV death	210/339 (62.0)	370/562 (66.0)	ref
Non-CV death	112/339 (33.0)	160/562 (28.3)	0.205
Unknown	17/339 (5.0)	32/562 (5.7)	0.798
Annulus rupture	14 (0.3)	52/12,557 (0.4)	0.643
Aortic dissection	10 (0.2)	46/12,557 (0.4)	0.234
Valve migration	56 (1.3)	139/12,557 (1.1)	0.202
Tamponade	56 (1.3)	256/12,557 (2.0)	0.004
Stroke	83 (2.0)	249/12,557 (2.0)	0.824
STEMI	34 (0.8)	27/12,557 (0.2)	<0.001
Permanent pacemaker implantation†	446/3,548 (12.6)	1,870/10,681 (17.5)	<0.001
Pulmonary embolism	5 (0.1)	18/12,557 (0.1)	0.669
Renal failure	195 (4.7)	480/12,557 (3.8)	0.049
Renal dialysis	54 (1.3)	86/12,557 (0.7)	<0.001
Echocardiographic findings			
Aortic valve area, cm^2	1.81 ± 0.50	1.76 ± 0.56	<0.001
	2,175	4,724	
Aortic mean gradient, mm Hg	10.6 ± 5.4	10.3 ± 6.3	0.224
	3,481	10,684	
Moderate or severe AR	565/3,611 (15.7)	1,119/11,007 (10.2)	<0.001
Moderate or severe MR	550/3,426 (15.8)	1,519/9,544 (15.9)	0.379
Vital status after 30 days‡			
Dead	330/3,277 (10.1)	493/9,212 (5.4)	<0.001
Alive	2,932/3,277 (89.4)	8,480/9,212 (92.1)	ref
Unknown	15/3,277 (0.5)	2,39/9,212 (2.6)	<0.001
Cause of death			
CV death	193/330 (58.5)	310/493 (62.9)	ref
Non-CV death	108/330 (32.7)	147/493 (29.8)	0.396
Unknown	29/304 (8.8)	36/493 (7.3)	0.393

Values are median (IQR), n, n (%), n/N (%), or mean ± SD. *Test performed using log-transformed variable. †Numbers are given for patients without prior permanent pacemaker. ‡In a subgroup of 12,489 subjects from 38 centers with sufficient follow-up data (centers in which vital status after 30 days was known for at least 90% of the patients). Among these centers, vital status follow-up was complete for 99.5% of the FRANCE 2 patients and 97.4% of the FRANCE TAVI patients, thus leading to rates of 0.5% and 2.6% of unknown 30-day vital status, respectively.

CV = cardiovascular; STEMI = ST-segment elevation myocardial infarction; other abbreviations as in Table 1.

accurate than the Society of Thoracic Surgeons (STS) scoring system among TAVR recipients, is the most established score in Europe for evaluating operative risk (21). This score is calculated on the basis of death from all cardiac surgical procedures; however, its development cohort mainly included patients undergoing coronary artery bypass grafting. It consists of an online EuroSCORE calculator that includes 17 baseline and procedural variables, which provide a 30-day predicted mortality rate with a cutoff of >20% representing high-risk patients. Similar to the STS score, it imperfectly captures some comorbidities, such as frailty, cirrhosis, porcelain aorta, or hostile chest. Interestingly, the STS score and the logistic EuroSCORE provide similar estimated mortality rates for low-risk patients, whereas the logistic EuroSCORE tends consistently to overestimate the operative risk among high-risk patients (21). Third, early nonrandomized reports demonstrating TAVR results comparable to those of surgical aortic valve replacement and superior to those observed in high-risk patients among lower-surgical risk groups also likely contributed to these patterns in procedural evolution (22,23). Finally, the aging of TAVR recipients could reflect the reluctance of some heart teams to perform operations in octogenarians, even patients with minimal comorbidities; thus the teams adopted a TAVR policy for these patients. Although differing commissioning structures may play a significant role in differences in the evolution of baseline characteristics observed over time from 1 national registry to another (13,14), the inclusion of patients treated in 2015 whose changes were even more pronounced likely accentuated discrepancies between the present report and previous reports from other national registries.

The evolution toward a more simplified TAVR procedure is another major finding of the present report. Although the contribution of approach per se has been debated, transfemoral access seems to have mortality and morbidity benefits that justify its use as a first-line strategy (24). The increasing availability of smaller delivery systems enabled this approach to be used increasingly over time, ultimately in >80% of FRANCE TAVI patients overall. Conversely, we observed a dramatic decline in transapical access, with rates much lower than the ~25% to 30% reported in previous registries (9,10,14). However, such a trend was also reported by the STS/American College of Cardiology (ACC) transcatheter valve therapy (TVT) registry for procedures performed in 2014 within the United States (13). Future reports should focus on outcomes of newer alternative approaches (e.g., direct aortic, transcarotid).

Local anesthesia provided good clinical outcomes compared with general anesthesia in a propensity-matched analysis of the FRANCE 2 registry (25). Concerns also emerged regarding a higher rate of significant paravalvular leak associated with this technique, which does not allow periprocedural transesophageal guidance. However, despite the widespread use of local anesthesia in FRANCE TAVI, device success was greater, and moderate or severe

TABLE 6 Outcomes per Year of Inclusion Within Centers Involved in Both Registries

	FRANCE 2		FRANCE TAVI			
	2010 (n = 1,378)	2011/2012 (n = 2,385)	2013 (n = 2,512)	2014 (n = 3,177)	2015 (n = 4,293)	p Value for Trend
In-hospital outcomes						
Time from implantation to discharge						<0.001*
Median, days	9 (7-13) 1,358	9 (7-13) 2,328	8 (6-12) 2,502	8 (6-11) 3,166	7 (5-10) 4,245	
1-5	135 (9.9)	298 (12.8)	553 (22.1)	684 (21.6)	1,193 (28.1)	
6-9	556 (41.0)	998 (42.9)	1,056 (42.2)	1,416 (44.7)	1,927 (45.4)	
≥10	667 (49.1)	1,032 (44.3)	893 (35.7)	1,066 (33.7)	1,125 (26.5)	
Complications						
Death						
From all-cause	119 (8.6)	186 (7.8)	150 (6.0)	156 (4.9)	115 (2.7)	<0.001
Cause of death						
CV death	68/119 (57.1)	119/186 (64.0)	102/150 (68.0)	96/156 (61.5)	71/115 (61.7)	ref
Non-CV death	41/119 (34.5)	61/186 (32.8)	40/150 (26.7)	57/156 (36.5)	28/115 (24.4)	0.413
Unknown	10/119 (8.4)	6/186 (3.2)	8/150 (5.3)	3/156 (1.9)	16/115 (13.9)	0.236
Annulus rupture	4 (0.3)	9 (0.4)	13/2,501 (0.5)	14/3,151 (0.4)	9/4,162 (0.2)	0.404
Aortic dissection	3 (0.2)	6 (0.3)	15/2,501 (0.6)	11/3,151 (0.4)	7/4,162 (0.2)	0.437
Valve migration	19 (1.4)	31 (1.3)	34/2,501 (1.4)	36/3,151 (1.1)	44/4,162 (1.1)	0.204
Tamponade	22 (1.6)	23 (1.0)	51/2,501 (2.0)	60/3,151 (1.9)	79/4,162 (1.9)	0.027
Stroke	24 (1.7)	57 (2.4)	57/2,501 (2.3)	66/3,151 (2.1)	66/4,162 (1.6)	0.149
STEMI	8 (0.6)	24 (1.0)	12/2,501 (0.5)	5/3,151 (0.2)	5/4,162 (0.1)	<0.001
Permanent pacemaker implantation†	158/1,166 (13.6)	268/2,030 (13.2)	342/2,096 (16.3)	505/2,684 (18.8)	659/3,587 (18.4)	<0.001
Pulmonary embolism	2 (0.2)	2 (0.1)	2/2,501 (0.1)	4/3,151 (0.1)	8/4,162 (0.2)	0.336
Renal failure	74 (5.4)	102 (4.3)	142/2,501 (5.7)	129/3,151 (4.1)	141/4,162 (3.4)	<0.001
Renal dialysis	23 (1.7)	26 (1.1)	21/2,501 (0.8)	32/3,151 (1.0)	17/4,162 (0.4)	<0.001
Echocardiographic findings						
Aortic valve area, cm^2	1.76 ± 0.50 697	1.82 ± 0.52 1,270	1.73 ± 0.55 1,014	1.74 ± 0.57 1,187	1.67 ± 0.50 1,409	<0.001
Aortic mean gradient, mm Hg	10.9 ± 5.8 1,169	10.5 ± 5.3 2,002	9.7 ± 6.9 2,188	9.8 ± 5.7 2,649	11.5 ± 6.7 3,426	<0.001
Moderate or severe AR	203/1,202 (16.9)	330/2,071 (15.9)	301/2,259 (13.3)	333/2,749 (12.1)	306/3,505 (8.7)	<0.001
Moderate or severe MR	190/1,154 (16.5)	323/1,990 (16.2)	324/1,975 (16.4)	382/2,451 (15.6)	480/2,931 (16.4)	0.392
Vital status after 30 days‡						
Dead	105/1,021 (10.3)	182/1,854 (9.8)	148/2,043 (7.2)	143/2,462 (6.0)	114/3,411 (3.3)	<0.001
Alive	912/1,021 (89.3)	1663/1,854 (89.7)	1,877/2,043 (91.9)	2,283/2,462 (92.7)	3,130/3,411 (91.8)	ref
Unknown	4/1,021 (0.4)	9/1,854 (0.5)	18/2,043 (0.9)	36/2,462 (1.5)	167/3,411 (4.9)	<0.001
Cause of death						
CV death	58/105 (55.2)	107/182 (58.8)	97/148 (65.6)	82/143 (57.3)	68/114 (59.7)	ref
Non-CV death	36/105 (34.3)	58/182 (31.9)	40/148 (27.0)	53/143 (37.1)	33/114 (28.9)	0.868
Unknown	11/105 (10.5)	17/182 (9.3)	11/148 (7.4)	8/143 (5.6)	13/114 (11.4)	0.777

Values are median (IQR), n, n (%), n/N (%), or mean ± SD. *Test performed using log-transformed variable. †Number are given for patients without prior permanent pacemaker. ‡In a subgroup of 10,791 subjects from 24 centers with sufficient follow-up data (centers in which vital status after 30 days was known for at least 90% of the patients). Among these centers, vital status follow-up was complete for 99.5% of the FRANCE 2 patients and 97.2% of the FRANCE TAVI patients, thus leading to rates of 0.5% and 2.8% of unknown 30-day vital status, respectively.

Abbreviations as in Tables 1 and 5.

paravalvular leaks were less frequent than in FRANCE 2. These findings are likely the result of growing experience of operators, refined annulus sizing using 3-dimensional imaging techniques, and the availability of devices with a dedicated sealing skirt. Interestingly, unlike with baseline characteristics, changes in procedural aspects were more pronounced among centers that did not participate in FRANCE 2. As previously demonstrated (26), these centers probably benefited from the global knowledge and shared experience of trained operators at the start of their TAVR program and therefore promptly achieved favorable technical and clinical outcomes.

The reported 4.4% and 5.4% in-hospital and 30-day mortality rates, respectively, in the present study were within the range of recent publications. Reporting outcomes of patients treated between 2011

CENTRAL ILLUSTRATION **Temporal Trends in TAVR in France**

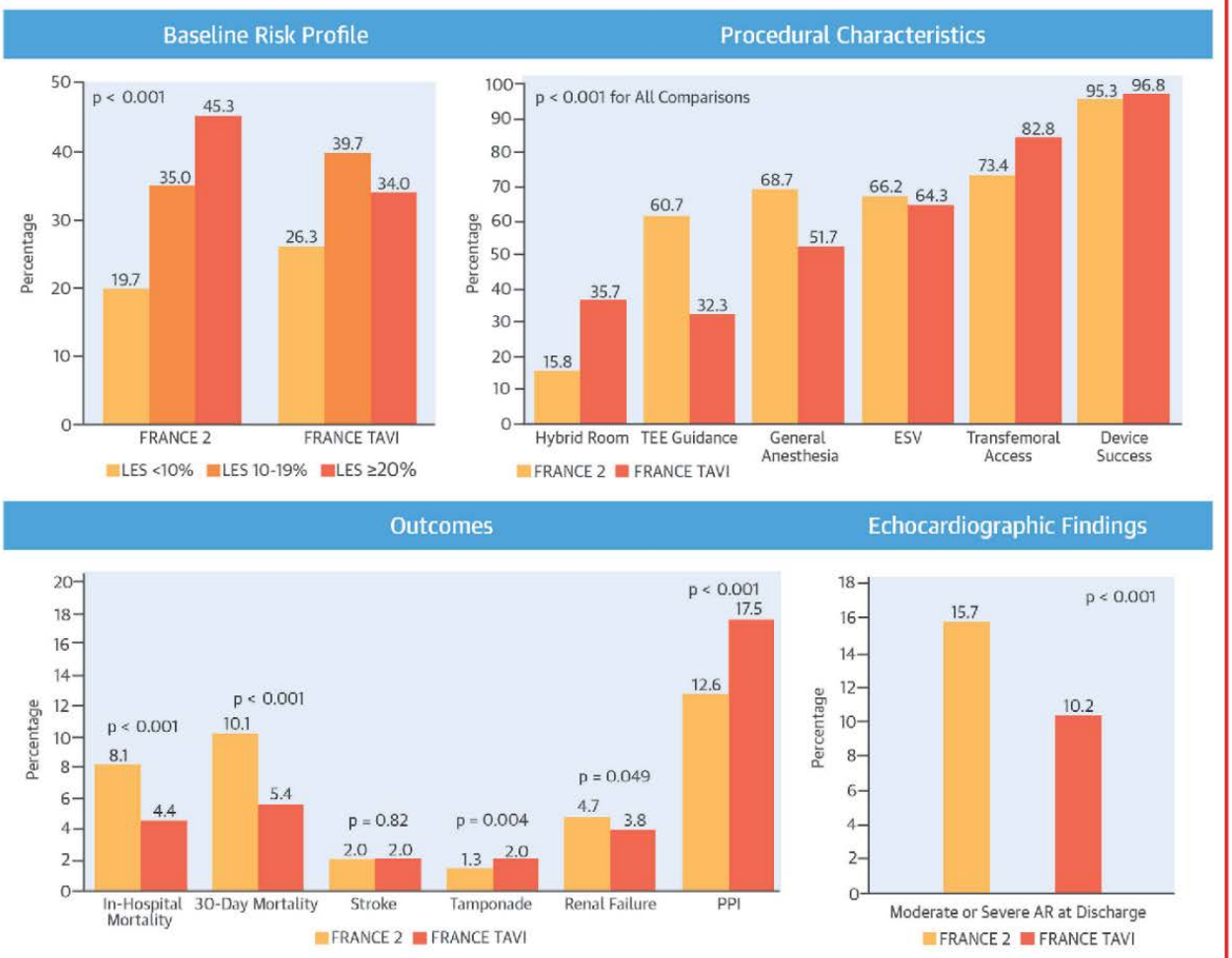

Auffret, V. et al. J Am Coll Cardiol. 2017;70(1):42-55.

In this comparison of patients from the FRANCE 2 (French Aortic National CoreValve and Edwards 2) (2010 to 2012) and FRANCE TAVI (French Transcatheter Aortic Valve Implantation) (2013 to 2015) registries who underwent transcatheter aortic valve replacement (TAVR), patients in FRANCE TAVI had a lower risk profile and significantly lower mortality rates but significantly higher rates of tamponade and pacemaker implantation. AR — aortic regurgitation; ESV — Edwards SAPIEN valve (Edwards Lifesciences, Irvine, California); LES — logistic European System for Cardiac Operative Risk Evaluation (EuroSCORE); PPI — permanent pacemaker implantation; TEE — transesophageal echocardiography.

and 2013, the German Aortic Valve Registry (GARY) (10) and STS/ACC TVT (9) registries demonstrated in-hospital mortality rates of 5.2% and 5.5%, respectively, whereas the 30-day mortality rate was 7.6% in the STS/ACC TVT registry. The gradual decrease in mortality rates demonstrated in the present study also was highlighted in the U.K. TAVR registry during the period from 2007 to 2012 (14). This trend was even more pronounced in 2015 in FRANCE TAVI because the 3.3% 30-day mortality rate achieved during this single year among experienced centers in an all-comers population compared favorably with the 3.9% mortality rate of the selected PARTNER 2 group of patients (7). Stroke rates were low (2.0%), stable over time, and comparable to those reported by the STS/ACC TVT registry, which provided central adjudication of these neurological events (13). The stability of infrequent but potentially life-threatening

complications (annular rupture, aortic dissection) and the unexpected increase of cardiac tamponade should, however, be emphasized. Given the rapid expansion of TAVR indications, German centers without on-site cardiac surgery have been allowed to perform transfemoral procedures, provided they have documented cooperation with an external surgical center. An analysis of the German AQUA (Aortic Valve Replacement Quality Assurance) registry (27) demonstrated similar rates of complications likely to benefit from emergency cardiac operations, with comparable mortality rates related to these complications, among centers with and without on-site cardiac surgery. However, in the background setting of treating lower-risk patients, the findings of the present study suggest caution regarding the dispersion of TAVR in centers without on-site cardiac surgery, at least until a dedicated series confirms the results of the AQUA registry.

Although debate remains regarding the clinical impact of PPI post-TAVR (28), given that TAVR is set to expand to lower-surgical risk and potentially younger patients, the deleterious consequences of long-term pacing requires careful attention. Moreover, PPI prolongs hospitalization and may jeopardize the cost-effectiveness of TAVR (29). Therefore, the significant increase of PPI observed from FRANCE 2 to FRANCE TAVI is a notable and important finding. Because this trend was exclusively observed in ESV recipients, this is likely to reflect the availability of the latest iteration of ESV (the SAPIEN 3 valve) that was associated with higher rates of PPI during its early use (30,31). Implantation depth is a consistent predictor of PPI, and an implantation technique aiming at a 70% aortic valve position produced rates of PPI comparable to those observed with previous ESV iterations (31). Whether the implementation of this recommendation yields similar results in large multicenter settings requires careful evaluation in future studies.

STUDY LIMITATIONS. Data completeness in this national registry was acceptable. However, data were site reported and not subject to external validation or adjudication. Therefore, data on numbers of procedures and survival were likely extremely accurate, yet data on procedural morbidity and complications could be less so. Although registries are the only way to capture all-comers data on a national scale, specific details could be lacking, thus allowing a description of trends and associations without providing firm evidence of causality. For 2012, only procedures performed in January were included in the present analysis according to the inclusion period of the FRANCE 2 registry. We excluded patients with missing data on valve type or approach, which we regarded as crucial information to analyze the results of a TAVR procedure. Similarly, 30-day mortality was reported for a subgroup of patients and centers. These exclusion criteria could raise concerns regarding selective reporting, especially underreporting of poor outcomes. However, comparisons of excluded versus included patients and of patients with versus without reported 30-day follow-up demonstrated that excluded patients had a lower risk profile as assessed by the logistic EuroSCORE and that patients without reported 30-day mortality had a lower in-hospital mortality rate (Online Tables 1 and 2). Therefore, underreporting of poor outcomes in the present analysis is unlikely.

CONCLUSIONS

In this first report of the French national TAVR monitoring program (FRANCE TAVI) during the period from 2013 to 2015, device success was achieved in 96.8% of patients, whereas in-hospital and 30-day mortality rates were 4.4% and 5.4%, respectively. These rates compared favorably with those of FRANCE 2 and probably reflected a more refined selection of lower-surgical risk patients, improved procedural planning and execution, newer iterations of transcatheter devices, and enhanced post-procedural care. Nonetheless, given that TAVR indications are likely to expand officially to lower-surgical risk patients, concerns remain regarding rare but potentially life-threatening complications and PPI that should be addressed in future studies.

ACKNOWLEDGMENTS The authors thank Geneviève Mulak, Sandrine Feing, Elodie Drouet, and Nicole Naccache from the Registry Department of the French Society of Cardiology and the Clinical Research Unit-East of the Public Assistance Hospitals of Paris for their assistance in the France TAVR registry supervision. The authors are also grateful to Rishi Puri, MBBS, PhD, and Jean Ferrières, MD, PhD, for their assistance and advice.

ADDRESS FOR CORRESPONDENCE: Dr. Hervé Le Breton, CHU Pontchaillou, Service de Cardiologie et maladies vasculaires, 2 Rue Henri Le Guilloux, 35000 Rennes, France. E-mail: herve.le.breton@chu-rennes.fr.

PERSPECTIVES

COMPETENCY IN PATIENT CARE AND PROCEDURAL SKILLS: Patients undergoing TAVR in France increasingly have a low to intermediate surgical risk. In-hospital and 30-day mortality rates were in the range of those observed in recent randomized trials among intermediate-risk patients. However, conduction disturbances requiring pacemaker implantation remain a concern.

TRANSLATIONAL OUTLOOK: Ongoing randomized trials will shed light on the exact role of TAVR among low-surgical risk patients. Meanwhile, strategies to reduce the incidence of pacemaker implantation should be evaluated. Given the exponential increase in TAVR procedures, the feasibility of TAVR without on-site cardiac surgery may also be elucidated.

REFERENCES

1. Leon MB, Smith CR, Mack M, et al. Transcatheter aortic-valve implantation for aortic stenosis in patients who cannot undergo surgery. N Engl J Med 2010;363:1597–607.

2. Vahanian A, Alfieri O, Andreotti F, et al. Guidelines on the management of valvular heart disease. Eur Heart J 2012;33:2451–96.

3. Smith CR, Leon MB, Mack MJ, et al. Transcatheter versus surgical aortic-valve replacement in high-risk patients. N Engl J Med 2011;364:2187–98.

4. Adams DH, Popma JJ, Reardon MJ, et al. Transcatheter aortic-valve replacement with a self-expanding prosthesis. N Engl J Med 2014;370:1790–8.

5. Tamburino C, Barbanti M, D'Errigo P, et al. 1-year outcomes after transfemoral transcatheter or surgical aortic valve replacement: results from the Italian OBSERVANT study. J Am Coll Cardiol 2015;66:804–12.

6. Thyregod HG, Steinbruchel DA, Ihlemann N, et al. Transcatheter versus surgical aortic valve replacement in patients with severe aortic valve stenosis: 1-year results from the all-comers NOTION randomized clinical trial. J Am Coll Cardiol 2015;65:2184–94.

7. Leon MB, Smith CR, Mack MJ, et al. Transcatheter or surgical aortic-valve replacement in intermediate-risk patients. N Engl J Med 2016;374:1609–20.

8. Gilard M, Eltchaninoff H, Iung B, et al. Registry of transcatheter aortic-valve implantation in high-risk patients. N Engl J Med 2012;366:1705–15.

9. Mack MJ, Brennan JM, Brindis R, et al. Outcomes following transcatheter aortic valve replacement in the United States. JAMA 2013;310:2069–77.

10. Walther T, Hamm CW, Schuler G, et al. Perioperative results and complications in 15,964 transcatheter aortic valve replacements: prospective data from the GARY registry. J Am Coll Cardiol 2015;65:2173–80.

11. Sabate M, Canovas S, Garcia E, et al. In-hospital and mid-term predictors of mortality after transcatheter aortic valve implantation: data from the TAVR national registry 2010–2011. Rev Esp Cardiol 2013;66:949–58.

12. Tamburino C, Capodanno D, Ramondo A, et al. Incidence and predictors of early and late mortality after transcatheter aortic valve implantation in 663 patients with severe aortic stenosis. Circulation 2011;123:299–308.

13. Holmes DR Jr., Nishimura RA, Grover FL, et al. Annual outcomes with transcatheter valve therapy: from the STS/ACC TVT registry. J Am Coll Cardiol 2015;66:2813–23.

14. Ludman PF, Moat N, de Belder MA, et al. Transcatheter aortic valve implantation in the United Kingdom: temporal trends, predictors of outcome, and 6-year follow-up: a report from the UK Transcatheter Aortic Valve Implantation (TAVR) registry, 2007 to 2012. Circulation 2015;131:1181–90.

15. Reinohl J, Kaier K, Reinecke H, et al. Effect of availability of transcatheter aortic-valve replacement on clinical practice. N Engl J Med 2015;373:2438–47.

16. Barbanti M, Petronio AS, Ettori F, et al. 5-year outcomes after transcatheter aortic valve implantation with CoreValve prosthesis. J Am Coll Cardiol Intv 2015;8:1084–91.

17. Mack MJ, Leon MB, Smith CR, et al. 5-year outcomes of transcatheter aortic valve replacement or surgical aortic valve replacement for high surgical risk patients with aortic stenosis (PARTNER 1): a randomised controlled trial. Lancet 2015;385:2477–84.

18. Duncan A, Ludman P, Banya W, et al. Long-term outcomes after transcatheter aortic valve replacement in high-risk patients with severe aortic stenosis: the U.K. Transcatheter Aortic Valve Implantation Registry. J Am Coll Cardiol Intv 2015;8:645–53.

19. Puri R, Iung B, Cohen DJ, Rodes-Cabau J. TAVR or no TAVR: identifying patients unlikely to benefit from transcatheter aortic valve implantation. Eur Heart J 2016;37:2217–25.

20. Rodes-Cabau J, Webb JG, Cheung A, et al. Long-term outcomes after transcatheter aortic valve implantation: insights on prognostic factors and valve durability from the Canadian multicenter experience. J Am Coll Cardiol 2012;60:1864–75.

21. Ben-Dor I, Gaglia MA, Barbash IM, et al. Comparison between Society of Thoracic Surgeons Score and logistic EuroSCORE for predicting mortality in patients referred for transcatheter aortic valve implantation. Cardiovasc Revasc Med 2011;12:345–9.

22. Piazza N, Kalesan B, van Mieghem N, et al. A 3-center comparison of 1-year mortality outcomes between transcatheter aortic valve implantation and surgical aortic valve replacement on the basis of propensity score matching among intermediate-risk surgical patients. J Am Coll Cardiol Intv 2013;6:443–51.

23. Wenaweser P, Stortecky S, Schwander S, et al. Clinical outcomes of patients with estimated low or intermediate surgical risk undergoing transcatheter aortic valve implantation. Eur Heart J 2013;34:1894–905.

24. Blackstone EH, Suri RM, Rajeswaran J, et al. Propensity-matched comparisons of clinical outcomes after transapical or transfemoral transcatheter aortic valve replacement: a Placement of Aortic Transcatheter Valves (PARTNER)-I trial substudy. Circulation 2015;131:1989–2000.

25. Oguri A, Yamamoto M, Mouillet G, et al. Clinical outcomes and safety of transfemoral aortic valve implantation under general versus local anesthesia: subanalysis of the French Aortic National CoreValve and Edwards 2 registry. Circ Cardiovasc Interv 2014;7:602–10.

26. Alli O, Rihal CS, Suri RM, et al. Learning curves for transfemoral transcatheter aortic valve replacement in the PARTNER-I trial: technical performance. Catheter Cardiovasc Interv 2016;87:154–62.

27. Eggebrecht H, Bestehorn M, Haude M, et al. Outcomes of transfemoral transcatheter aortic valve implantation at hospitals with and without on-site cardiac surgery department: insights from the prospective German aortic valve replacement

quality assurance registry (AQUA) in 17 919 patients. Eur Heart J 2016;37:2240–8.

28. Regueiro A, Abdul-Jawad Altisent O, Del Trigo M, et al. Impact of new-onset left bundle branch block and periprocedural permanent pacemaker implantation on clinical outcomes in patients undergoing transcatheter aortic valve replacement: a systematic review and meta-analysis. Circ Cardiovasc Interv 2016;9:e003635.

29. Nazif TM, Dizon JM, Hahn RT, et al. Predictors and clinical outcomes of permanent pacemaker implantation after transcatheter aortic valve replacement: the PARTNER (Placement of AoRtic TraNscathetER Valves) trial and registry. J Am Coll Cardiol Intv 2015;8:60–9.

30. Husser O, Pellegrini C, Kessler T, et al. Predictors of permanent pacemaker implantations and new-onset conduction abnormalities with the SAPIEN 3 balloon-expandable transcatheter heart valve. J Am Coll Cardiol Intv 2016;9:244–54.

31. De Torres-Alba F, Kaleschke G, Diller GP, et al. Changes in the pacemaker rate after transition from Edwards SAPIEN XT to SAPIEN 3 transcatheter aortic valve implantation: the critical role of valve implantation height. J Am Coll Cardiol Intv 2016;9:805–13.

KEY WORDS national registry, outcomes, pacemaker, transfemoral

APPENDIX For key personnel, institutions, and organizations participating in the FRANCE TAVI registry, definitions used in the registry, and supplemental tables, please see the online version of this article.

1.4 Synthèse

Dans ce premier chapitre, nous avons rappelé les bases médicales nécessaires à la compréhension des problématiques entourant le TAVI. La sténose aortique serrée étant la valvulopathie acquise de l'adulte la plus fréquente, sa prise en charge représente, compte-tenu du vieillissement de la population, un véritable enjeu de santé publique. A ce titre, le TAVI a initialement permis d'offrir un traitement pérenne aux patients non-éligibles à une chirurgie de remplacement valvulaire aortique. Néanmoins, la technique a connu, depuis la première implantation chez l'homme en 2002, un essor considérable illustré par la rapidité avec laquelle les études randomisées ont évalué et démontré son intérêt dans des populations à risque chirurgical toujours plus faible. Dans la pratique courante, le nombre de TAVI réalisés annuellement dépasse aujourd'hui le nombre de remplacements valvulaires aortique chirurgicaux isolés (19,30). Cette augmentation de l'activité va de pair, tel qu'illustré par le premier article de cette Thèse, avec une diminution graduelle du profil de risque des patients (24). Même si cela n'est pas encore évident en pratique courante puisque l'âge moyen des patients traités reste nettement supérieur à 80 ans, l'évolution vers le traitement d'une population à risque chirurgical bas à intermédiaire conduira invariablement au traitement de patients plus jeunes (l'âge moyen dans les études randomisées ayant inclus des patients à bas risque était de 74 ans), présentant une espérance de vie plus importante. Ces constatations posent plusieurs problématiques pour l'avenir proche de la technique. L'expansion rapide déjà observée, et à venir, des indications et du nombre de procédures d'une technique initialement dévolue à des patients inopérables, nous impose, en terme de coûts de santé, d'éviter de la proposer dans des indications futiles, qu'il convient dès lors d'identifier. Par ailleurs, nous l'avons vu, certaines complications de la procédure, susceptibles de limiter son bénéfice (AVC, troubles conductifs conduisant à l'implantation d'un stimulateur cardiaque définitif, fuites para prothétiques sévères notamment) restent des problèmes quotidiens dont les taux doivent encore être réduits.

Parmi les axes permettant de s'attaquer à ces problématiques, on peut citer l'identification de facteurs prédictifs d'événements per- ou post-opératoire afin de mieux individualiser la prise en charge thérapeutique. La connaissance de facteurs de risque spécifiques d'une complication donnée offre en effet la possibilité d'identifier les patients à risque et ainsi d'appliquer des méthodes préventives. On peut également par ce biais identifier des « mauvais » candidats à une technique précise. Dans le deuxième chapitre, nous aborderons donc l'apport des études de populations via des méthodes de modélisation statistique usuelles

pour l'aide à la décision et l'identification de patients à haut risque de complications dans le contexte du TAVI.

Chapitre 2

Identification de facteurs prédictifs de complications par l'étude de cohortes de patients.

Le TAVI étant une technique d'émergence récente, l'identification de facteurs de risque est une problématique prépondérante. L'élaboration de facteurs de risque d'événements per- ou post-opératoires a pour finalité d'améliorer les résultats des procédures TAVI par différentes approches: amélioration de la sélection des patients, choix des techniques procédurales (voie d'abord, type et taille de prothèse, pré ou post-dilatation de la prothèse…) les plus adaptées, ou encore meilleure individualisation des soins post-opératoires que ce soit en terme de surveillance médicale ou en terme de traitement médicamenteux. L'objectif de ce deuxième chapitre est d'identifier et de proposer des facteurs de risque pertinents pour la prise en charge des patients au travers de l'étude statistique de cohortes.

Plusieurs facteurs de risque obtenus par des méthodes d'analyse de populations sont présentés dans ce chapitre. Tout d'abord, nous focalisons notre propos sur deux des principales complications de la procédure qui restent des challenges cliniques quotidiens. Dans un premier article original, une méta-analyse de la littérature, nous identifions des facteurs prédictifs d'accident vasculaire cérébral précoce post-TAVI (31). Dans une seconde contribution, à l'aide d'une large revue de la littérature, nous analysons les mécanismes, facteurs prédictifs et implications cliniques des troubles conductifs post-TAVI et proposons des stratégies de prise en charge basés sur cette revue de la littérature (32). Enfin, dans une troisième et dernière partie de ce chapitre, nous nous intéressons à l'identification de « mauvais candidats » à une procédure TAVI. Cet objectif rejoint le concept global de « futilité » de la procédure qui est l'objet de nombreux travaux de recherche (33–40) et implique généralement l'utilisation de critères de jugement composites faisant intervenir à la fois le statut vital du patient mais également son statut fonctionnel afin de mieux refléter le bénéfice global de la procédure. Dans ce cadre, nous présentons un article original visant à travers l'étude de notre cohorte locale à identifier des facteurs prédictifs d'un tel critère composite par des méthodes de modélisation statistique usuelles (régression logistique) (41).

2.1 Accidents vasculaires cérébraux post-TAVI

2.1.1 Problématique

Depuis l'introduction de la technique dans la pratique courante, les AVC ont toujours été l'une des complications les plus scrutées et étudiées. En effet, les premières études randomisées PARTNER 1 A et B chez des patients inopérables ou à haut risque chirurgical suggéraient un risque majoré d'AVC, notamment majeurs, à 30 jours ou 1 an après TAVI en comparaison de la chirurgie (13,14). Néanmoins, les comparaisons randomisées ultérieures, que ce soit avec la première génération de valve auto-expansible chez des patients à haut risque chirurgical (16) ou avec les deux types de prothèses chez des patients à risque intermédiaire (17,18), n'ont pas retrouvé ce sur-risque d'événements cérébrovasculaires précoces ou à moyen terme, rapportant plutôt des taux numériquement inférieurs dans le bras de traitement percutané. Outre la réduction du profil de risque des patients, il est probable que l'expérience accrue des opérateurs, avec des procédures plus courtes, nécessitant moins de manipulation du matériel endovasculaire, associé à la miniaturisation progressive de ce dernier, aient contribué à cette différence de résultats. Des analyses secondaires de ces deux dernières études randomisées, spécifiquement dédiées à l'étude des événements neurovasculaires, ont même récemment suggéré que le TAVI pouvait être associé à un taux significativement plus faible d'AVC précoces (à 30 jours) que la chirurgie (42,43). Ces résultats sont désormais supportés par la publication des essais randomisés chez les patients à bas risque chirurgical qui démontrent une réduction des taux d'AVC à 30 jours après TAVI en comparaison de la chirurgie (21,22).

Bien que le TAVI semble donc associé à un risque neurovasculaire moins important que la chirurgie, les AVC compliquent malgré tout encore 2 à 4% des procédures (24,44). Ces événements restent probablement la complication la plus redoutée, tant par le clinicien que par le patient, compte-tenu de son impact maintes fois démontré sur la mortalité à court et moyen terme (42,43,45,46) mais également sur la qualité de vie en raison des possibles séquelles fonctionnelles (42,43,47). Environ 50% de ces AVC (pour la plupart ischémiques) surviennent dans les 48 premières heures suivant la procédure mais il semble exister une phase précoce de risque accru se prolongeant pendant les 2 à 4 premières semaines post-opératoires suivi d'une phase chronique pendant laquelle l'incidence des AVC décroit graduellement pour rejoindre celle des patients porteurs de sténoses aortiques serrées traités médicalement (45,48,49). Ainsi, ce sur-risque requiert la mise en œuvre de stratégies péri-opératoires de réduction du taux d'AVC. Les mécanismes en lien avec ces AVC sont multiples, soit directement liés à la procédure (embolie de calcifications artérielles ou valvulaires, embolie de tissu artériel ou valvulaire, formation et embolie de thrombus depuis les cathéters, arythmie cardiaque induite

par la procédure…), soit en lien avec un profil de risque accru du patient lui-même (44). L'identification des facteurs de risque d'AVC est donc fondamentale afin de proposer des stratégies individualisées de prévention, notamment pour la sélection d'éventuels candidats aux dispositifs de protection embolique (**Figure 31**). Ces derniers permettent via divers mécanismes de réduire le risque d'embolie cérébrale de débris au cours de la procédure. Ils ont été associés à une réduction des nouvelles lésions ischémiques cérébrales en imagerie par résonance magnétique (50) et pourraient également réduire les déficits neurologiques ou cognitifs cliniques à court terme après TAVI (51–53). Toutefois, leur coût et morbidité propre n'autorisent pas leur utilisation chez tous les patients bénéficiant d'une procédure TAVI.

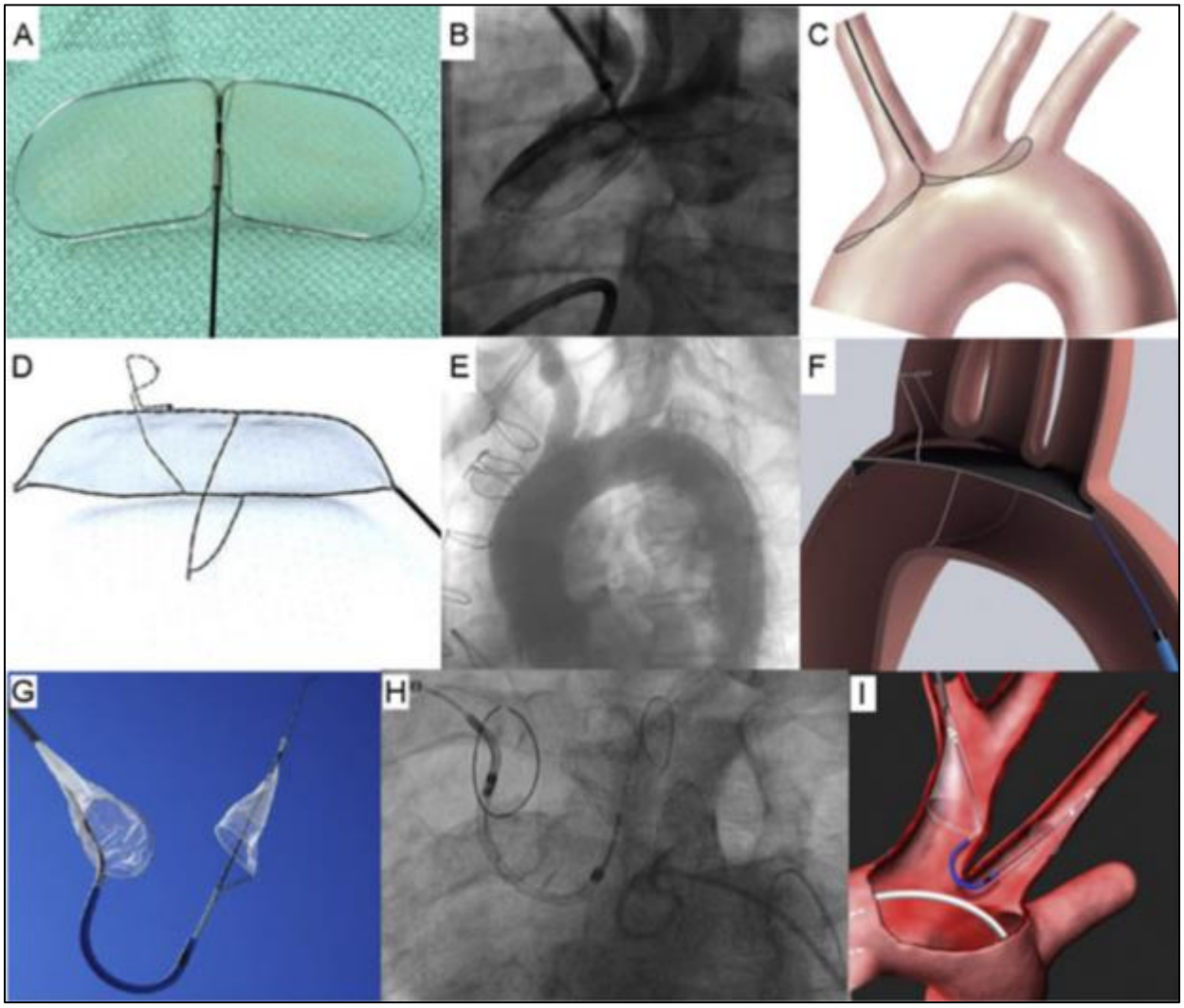

Figure 31- Dispositifs de protection embolique utilisables lors des procédures TAVI. Reproduite d'après Patel PA et al (44). A, D et G représentent respectivement les dispositifs Embrella (Edwards Lifesciences), Triguard (Keystone Heart) et Sentinel (Claret Medical). Les images B et C, E et F et H et I montrent des vues fluoroscopiques et des extraits d'animations

de ces dispositifs respectifs une fois déployés. Les systèmes Embrella et Triguard sont des systèmes de « déflection » des embols positionnés dans la crosse aortique devant les troncs artériels supra-aortiques vascularisant le cerveau alors que le système Sentinel est un système de filtre sous la forme de 2 « paniers » situés dans le tronc artériel brachio-céphalique et la carotide commune gauche.

De nombreuses études se sont attachées à définir des facteurs prédictifs d'AVC après TAVI (45,46,54–57). Récemment, en utilisant les données de plus de 90 000 patients inclus dans le registre américain STS/TVT, Thourani et al. ont proposé un score de risque de prédiction de survenue d'AVC à la phase hospitalière après TAVI reposant sur 13 facteurs prédictifs (58). Malgré l'utilisation de cette large base de données, la validation interne du score de risque n'a montré qu'une capacité très modeste de discrimination (C-statistic=0.62) illustrant la difficulté de stratifier le risque d'événements cérébrovasculaires précoces post-TAVI.

2.1.2 Article original

Dans ce contexte, notre contribution à la littérature repose sur une large méta-analyse de 64 études, incluant un total de 72 318 patients, dont l'objectif est de déterminer les facteurs prédictifs d'accident vasculaire cérébral précoce (≤ 30 jours) après TAVI.

JOURNAL OF THE AMERICAN COLLEGE OF CARDIOLOGY
© 2016 BY THE AMERICAN COLLEGE OF CARDIOLOGY FOUNDATION
PUBLISHED BY ELSEVIER

VOL. 68, NO. 7, 2016
ISSN 0735-1097/$36.00
http://dx.doi.org/10.1016/j.jacc.2016.05.065

ORIGINAL INVESTIGATIONS

Predictors of Early Cerebrovascular Events in Patients With Aortic Stenosis Undergoing Transcatheter Aortic Valve Replacement

Vincent Auffret, MD, MSc,[a,b] Ander Regueiro, MD,[a] María Del Trigo, MD,[a] Omar Abdul-Jawad Altisent, MD,[a] Francisco Campelo-Parada, MD,[a] Olivier Chiche, MD,[a] Rishi Puri, MBBS, PhD,[a] Josep Rodés-Cabau, MD[a]

ABSTRACT

BACKGROUND Identifying transcatheter aortic valve replacement (TAVR) patients at high risk for cerebrovascular events (CVE) is of major clinical relevance. However, predictors have varied across studies.

OBJECTIVES The purpose of this study was to analyze the predictors of 30-day CVE post-TAVR.

METHODS A systematic review of studies that reported the incidence of CVE post-TAVR while providing raw data for predictors of interest was performed. Data on study, patient, and procedural characteristics were extracted. Crude risk ratios (RRs) and 95% confidence intervals for each predictor were calculated.

RESULTS Sixty-four studies involving 72,318 patients (2,385 patients with a CVE within 30 days post-TAVR) were analyzed. Incidence of CVE ranged from 1% to 11% (median 4%) without significant differences between single and multicenter studies, or according to CVE adjudication availability. The summary RRs indicated lower risk for men (RR: 0.82; p = 0.02) and higher risk for patients with chronic kidney disease (RR: 1.29; p = 0.03) and with new-onset atrial fibrillation post-TAVR (RR: 1.85; p = 0.005), and for procedures performed within the first half of center experience (RR: 1.55; p = 0.003). The use of balloon post-dilation tended to be associated with a higher risk of CVE (RR: 1.43; p = 0.07). Valve type (balloon-expandable vs. self-expandable, p = 0.26) and approach (transfemoral vs. nontransfemoral, p = 0.81) did not predict CVE.

CONCLUSIONS Female sex, chronic kidney disease, enrollment date, and new-onset atrial fibrillation were predictors of CVE post-TAVR. This study provides effect estimates to identify high-risk TAVR patients for early CVE, providing possible guidance for tailored preventive strategies. (J Am Coll Cardiol 2016;68:673–84)

Transcatheter aortic valve replacement (TAVR) has expanded considerably in the past decade and now is standard of care for patients with aortic stenosis (AS) deemed at prohibitive surgical risk, while posing a reasonable alternative in high-operative risk patients (1). The recently published PARTNER-2 (Placement of AoRTic TraNscathetER-2) trial (2) confirmed the results of prior studies (3,4),

Listen to this manuscript's audio summary by *JACC* Editor-in-Chief Dr. Valentin Fuster.

From the [a]Quebec Heart & Lung Institute, Laval University, Quebec City, Quebec, Canada; and the [b]Rennes 1 University, Signal and Image Processing Laboratory, Rennes, France. Dr. Auffret received fellowship support from the Fédération Française de Cardiologie; and has received research grants from Abbott, Edwards Lifesciences, Medtronic, Biosensors, Terumo, and Boston Scientific. Dr. Rodés-Cabau has received research grants from Edwards Lifesciences, Keystone, Medtronic, and St. Jude Medical. Drs. Regueiro, Del Trigo, and Abdul-Jawad Altisent have received fellowship support from the Fundacion Alfonso Martin Escudero (Spain). All other authors have reported that they have no relationships relevant to the contents of this paper to disclose. Deepak L. Bhatt, MD, MPH, served as Guest Editor for this paper. Anthony Bavry, MD, served as Assistant Guest Editor for this paper.

Manuscript received April 22, 2016; accepted May 14, 2016.

ABBREVIATIONS AND ACRONYMS

AF = atrial fibrillation
AS = aortic stenosis
BPD = balloon post-dilation
CAD = coronary artery disease
CI = confidence interval
CKD = chronic kidney disease
CVE = cerebrovascular events
DAPT = dual antiplatelet therapy
ESV = Edwards-Sapien valve
MSV = Medtronic CoreValve
NOAF = new-onset atrial fibrillation
PAD = peripheral artery disease
RR = risk ratio
SAPT = single antiplatelet therapy
TAVR = transcatheter aortic valve replacement
TF = transfemoral
TIA = transient ischemic attack
TV-in-TV = transcatheter valve within a transcatheter valve
TVE/M = transcatheter valve embolization or migration

paving the way for a shift toward treating lower surgical-risk patients. Nonetheless, ongoing concerns about periprocedural complications could still compromise such an expansion.

Compared with earlier TAVR appraisals (5,6), recent studies (2,7–11) suggested a decrease in cerebrovascular events (CVE) over time, down to rates of 2.5% to 3%. However, CVE still represents 1 of the most dreadful complications of TAVR. Numerous potential risk factors for CVE have been highlighted by reviews (12–15), and a few dedicated studies (16–21) identified independent predictors that appear to differ from one study to another. Given that the exact place of embolic protection devices in the TAVR therapeutic armamentarium and the optimal antithrombotic regimen post-TAVR remain debated, it is nonetheless of paramount importance to have reliable predictors of CVE in order to offer the possibility of tailored peri- and post-procedural management to patients undergoing TAVR. Therefore, this study sought to provide effect estimates for clinically relevant predictors of CVE within 30 days post-TAVR.

SEE PAGE 685

METHODS

SEARCH STRATEGY. A systematic review of published data on CVE in patients undergoing TAVR was conducted in accordance to the guidance and reporting items specified in the Preferred Reported Items for Systematic Reviews and Meta-Analysis (PRISMA) statement (22). A broad computerized search was performed to identify all relevant studies from PubMed and EMBASE databases. The following key word terms were used: *transcatheter aortic valve*, *TAVI*, *TAVR*, *transcutaneous aortic valve*, and *percutaneous aortic valve*. The MeSH term *Transcatheter Aortic Valve Replacement* was also used. The search strategy is outlined in the Online Appendix. We limited our search to studies published after January 1, 2003, and databases were last accessed on December 9, 2015.

ELIGIBILITY CRITERIA AND STUDY SELECTION. We included any study of original design including at least 50 patients that assessed the incidence of CVE post-TAVR between 2 groups of patients dichotomized according to the presence/absence of a potential predictor. We included studies in which quantitative raw data were available that enabled the calculation of risk ratios (RRs) for the incidence of CVE for the predictors of interest. When potential overlapping study populations were detected (based on participating institutions and inclusion periods), the most recent publication or the publication with the most information of interest was included in the analysis. This process was conducted for each predictor separately. Case reports or studies published in a non-English language were excluded.

Two investigators (V.A. and A.R.) independently conducted the literature searches, study eligibility assessment, and data extraction in duplicate. Any discrepancies were resolved by consensus by a third investigator (J.R.-C.).

DATA EXTRACTION. We extracted data of patients and studies using a standardized data abstraction sheet. The following study-, patient-, and procedure-related data were extracted from the main paper and accompanying supplemental appendix: study design, number of participating centers, region, and period of enrollment, number of patients, length of follow-up, number of CVE post-TAVR, age, sex, baseline procedural risk assessment (by logistic European System for Cardiac Operative Risk Evaluation [EuroSCORE] or Society of Thoracic Surgeons Predicted Risk of Mortality [STS-PROM] score), number of patients with prior stroke and atrial fibrillation (AF) at baseline, access site, valve type, number of patients requiring balloon post-dilation (BPD) or acute valve-in-valve (TV-in-TV), and in-hospital or 30-day all-cause mortality as reported by the authors.

ENDPOINT. Given the important heterogeneity in reporting CVE across TAVR studies, we used the following pre-specified hierarchical order to define the single outcome used for each study: 30-day stroke/transient ischemic attack (TIA); 30-day all stroke; 30-day major stroke; in-hospital stroke/TIA; in-hospital all stroke, and in-hospital major stroke. The selected outcomes were then pooled to provide summary RRs of short-term CVE after TAVR.

PREDICTORS OF INTEREST. On the basis of recently published studies and review (5,12–21), we focused on 16 previously proposed predictors of CVE that could be separated as patient- and procedural-related. The following patient-related factors were studied: age (≥90 years); sex (male); obesity (i.e., body mass index ≥30 kg/m^2); diabetes mellitus; prior AF; known coronary artery disease (CAD); chronic kidney disease (CKD) defined by an estimated glomerular filtration rate <60 ml/min·1.73 m^2; and peripheral artery disease (PAD). The procedure-related predictors included in the present study were as follows: nontransfemoral (TF) approach versus TF approach; the self-expandable valve (CoreValve, Medtronic, Dublin, Ireland) (MCV) versus balloon-expandable valve

FIGURE 1 Flow Chart of Selected Studies

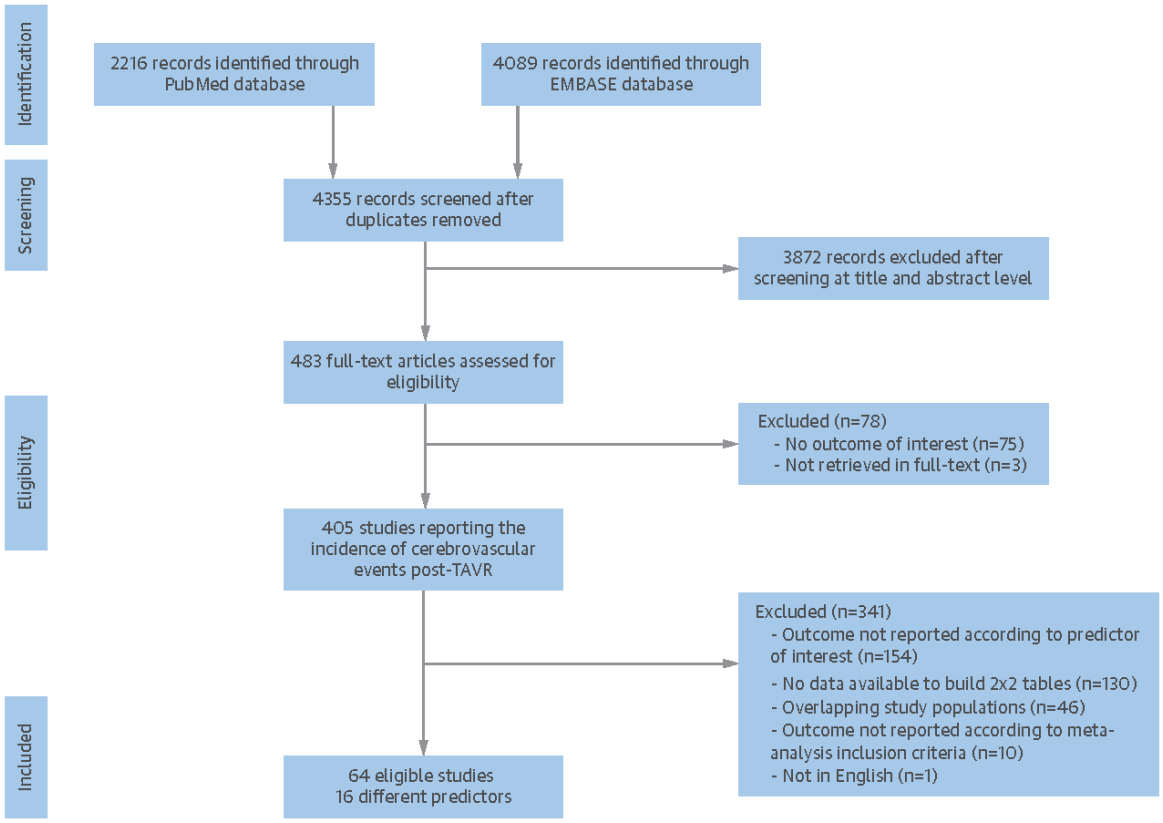

Flow diagram based on the PRISMA statement of studies selected for evaluating predictors of cerebrovascular events after TAVR. TAVR = transcatheter aortic valve replacement.

(Sapien, Edwards Lifesciences, Irvine, California) (ESV); enrollment date, that is, first half versus second half of each center's enrollment period; need for a second valve (TV-in-TV); transcatheter valve embolization or migration (TVE/M); BPD; single antiplatelet therapy (SAPT) versus dual antiplatelet therapy (DAPT); and new-onset atrial fibrillation (NOAF).

STATISTICAL ANALYSIS. Crude RR was the principal summary measure. RRs were retrieved or calculated with the corresponding 95% confidence interval (CI) for each endpoint and entered in the primary analysis. Data across studies were combined using DerSimonian and Laird (23) random effects models. Consistency across studies was assessed with the I^2 index, which takes values between 0% and 100%, with values of 25% typically suggesting low, 50% moderate, and 75% large heterogeneity (24). To assess the potential effect of publication bias, we inspected funnel plots for asymmetry and used the Harbord test (25) as a formal statistical test. Sensitivity analyses were performed after exclusion of studies with fewer than 200 patients and by deriving pooled estimates with Mantel-Haenszel fixed effects models for variables with low heterogeneity. Each predictor was evaluated separately. Descriptive characteristics are presented as mean ± SD or median (interquartile range) as appropriate for continuous variables, and frequencies and percentages for categorical variables. Continuous variables were compared using the Mann-Whitney *U* test after normality was ruled out with the use of the Shapiro-Wilk test. All reported p values are 2-sided. Statistical analyses were performed with the STATA software (version 13.0, STATA Corp., College Station, Texas) and RevMan (Version 5.3.5, The Nordic Cochrane Centre, The Cochrane Collaboration, Copenhagen, Denmark).

RESULTS

INCLUSION OF STUDIES. Figure 1 shows the PRISMA flow diagram. A total of 4,355 records were screened

TABLE 1 Characteristics of Studies Included for the Evaluation of Baseline Predictors

First Author (Ref. #)	Year	Design	Centers	Region	Inclusion Period	Sample Size	Follow-Up (months)*	In-Hospital or 30-Day CVE	Studied Predictors
Leker et al. (26)	2013	Obs.	1	Israel	September 2008–April 2011	72	ND	8 (11)	Male, Diabetes, CAD
Stortecky et al. (19)	2012	Obs.	1	Switzerland	August 2007–October 2011	389	1	14 (4)	Male, AF, CKD, Diabetes, PAD
Stangl et al. (27)	2012	Obs.	1	Germany	July 2009–July 2011	100	3	2 (2)	Male
O'Connor et al. (28)	2015	Obs.	109	International	March 2005–December 2012	11,310	13	453 (4)	Male
Sherif et al. (29)	2014	Obs.	27	Germany	January 2009–June 2010	1,432	12	58 (4)	Male
Nuis et al. (21)	2012	Obs.	1	the Netherlands	November 2005–September 2011	214	13	19 (9)	Male, PAD
Abramowitz et al. (30)	2015	Obs.	1	USA	April 2012–December 2014	734	24	20 (3)	Age ≥90 yrs
Yamamoto et al. (31)	2012	Obs.	1	France	December 2007–June 2011	136	13	9 (7)	Age ≥90 yrs
Konigstein et al. (32)	2015	Obs.	1	Israel	March 2009–October 2013	409	18	22 (5)	BMI ≥30 kg/m^2
Yamamoto et al. (33)	2013	Obs.	34	France	January 2010–October 2011	3,072	4	109 (4)	BMI ≥30 kg/m^2
Nombela-Franco et al. (20)	2012	Obs.	5	International	January 2005–September 2011	1,061	12	54 (5)	Diabetes, AF, CAD
Conrotto et al. (34)	2014	Obs.	4	Italy	June 2007- December 2011	511	13	12 (2)	Diabetes
Minha et al. (35)	2015	Obs.	1	USA	May 2007–April 2013	496	12	25 (5)	Diabetes
Barbash et al. (36)	2015	Obs.	1	USA	2007–2013	371	1	22 (6)	AF
Chopard et al. (37)	2015	Obs.	34	France	January 2010–December 2011	3,875	10	124 (3)	AF
Maan et al. (38)	2015	Obs.	1	USA	June 2008–October 2012	137	1	7 (5)	AF
Yankelson et al. (39)	2014	Obs.	1	Israel	September 2008–April 2013	380	18	6 (2)	AF
Abdel-Wahab et al. (40)	2012	Obs.	27	Germany	January 2009–June 2010	1,382	1	42 (3)	CAD
Abramowitz et al. (41)	2014	Obs.	1	Israel	March 2009–April 2012	249	17	5 (2)	CAD
Gautier et al. (42)	2011	Obs.	1	France	October 2006–October 2009	145	8	6 (4)	CAD
Mancio et al. (43)	2015	Obs.	1	Portugal	August 2007–October 2012	91	16	8 (9)	CAD
Snow et al. (44)	2015	Obs.	31	UK	January 2007–December 2011	2,584	48	79 (3)	CAD
Stefanini et al. (45)	2014	Obs.	1	Switzerland	August 2007–April 2012	445	9	14 (3)	CAD
Allende et al. (46)	2014	Obs.	9	International	January 2005–June 2012	2,075	15	83 (4)	CKD
Ferro et al. (47)	2015	Obs.	33	UK	January 2007–December 2012	3,696	18	96 (2)	CKD
Nguyen et al. (48)	2013	Obs.	1	USA	2007–2012	321	ND	5 (2)	CKD
Oguri et al. (49)	2015	Obs.	34	France	January 2010–October 2011	2,929	ND	103 (4)	CKD
Sinning et al. (50)	2012	Obs.	27	Germany	January 2009–June 2010	1,315	1	42 (3)	PAD

Values are n or n (%). *Follow-up is reported as mean or median as given by the authors.

AF = atrial fibrillation; CAD = coronary artery disease; CKD = chronic kidney disease; CVE = cerebrovascular events; ND = no data; Obs. = observational study; PAD = peripheral artery disease.

at the title and abstract level, of which 483 were retrieved in full text and examined for eligibility. Finally, 64 studies fulfilled the inclusion criteria and were deemed eligible for the analysis (Tables 1 and 2).

CHARACTERISTICS OF THE STUDIES. Twenty-eight studies (19–21,26–50) were used for the analysis of baseline predictors (Table 1), whereas 41 studies (11,19–21,36,37,51–85) were included in the analysis of procedural factors (Table 2). Three studies (64,84,85) were randomized controlled trials, whereas the others were observational registries equally divided between single-center and multicenter design. Patients' enrollment took place between January 2005 and December 2014, and studies were published between 2010 and 2015. Sample sizes varied from 72 to 11,310 patients, whereas follow-up ranged from 1 to 48 months.

CVE definitions followed the Valve Academic Research Consortium (VARC) definitions (86,87) in 42 studies (66%) and were according to the PARTNER trial (88) protocol in 2 studies. Adjudication of CVE was undertaken in 17 studies (27%), only 3 of which used an independent neurologist. Median rate of CVE was 4% (2% to 5%) across publications without adjudication, and 4% (3% to 4%) across publications with adjudication (p = 0.83). Stroke/TIA at 30 days was reported by 20 studies, 30-day all stroke by 27, 30-day major stroke by 14, in-hospital stroke/TIA by 13, in-hospital all stroke by 24, and in-hospital major stroke by 4 (Online Table 1).

CLINICAL AND PROCEDURAL CHARACTERISTICS. Overall, 72,318 patients were evaluated in 64 studies, and 2,385 patients (3.3%) experienced a CVE post-TAVR. The incidence of CVE post-TAVR ranged from 1% to 11% in individual studies with a median of 4% (2% to 6%) across single-center publications and a median of 3% (3% to 4%) in multicenter studies (p = 0.08). The mean age ranged between 78.6 and 84.5 years with a mean percentage of male of

TABLE 2 Characteristics of Studies Included for the Evaluation of Procedural Predictors

First Author (Ref. #)	Year	Design	Centers	Region	Inclusion Period	Sample Size	Follow-Up (months)*	In-hospital or 30-Day CVE	Studied Predictors
Bosmans et al. (51)	2011	Obs.	15	Belgium	ND-April 2010	181	ND	9 (5)	TF access vs. others
Eltchaninoff et al. (52)	2011	Obs.	16	France	February 2009-July 2009	244	1	9 (4)	TF access vs. others
Ewe et al. (53)	2011	Obs.	1	Netherlands	ND	104	12	4 (4)	TF access vs. others
Frohlich et al. (54)	2015	Obs.	33	UK	January 2007-December 2012	3,962	18	111 (3)	TF access vs. others
Imnadze et al. (55)	2015	Obs.	1	Germany	April 2008-April 2013	575	ND	11 (2)	TF access vs. others
Lotfi et al. (56)	2014	Obs.	1	Germany	January 2008-October 2012	345	24	9 (3)	TF access vs. others
Mack et al. (57)	2013	Obs.	224	USA	November 2011-May 2013	7,710	ND	164 (2)	TF access vs. others
Muensterer et al. (58)	2013	Obs.	1	Germany	June 2007-February 2011	341	ND	17 (5)	TF access vs. others
Nombela-Franco et al. (20)	2012	Obs.	5	International	January 2005-September 2011	1,061	12	54 (5)	TF access vs. others, Enrollment date, Pre-procedural SAPT vs. DAPT, NOAF
Petronio et al. (59)	2010	Obs.	13	Italy	June 2007-July 2009	514	7	9 (2)	TF access vs. others
Schymik et al. (60)	2015	Obs.	1	Germany	April 2008-April2012	1,000	47	20 (2)	TF access vs. others
Seiffert et al. (61)	2013	Obs.	1	Germany	March 2008-September 2011	326	9	20 (6)	TF access vs. others, MCV vs. ESV
Stortecky et al. (19)	2012	Obs.	1	Switzerland	August 2007-October 2011	389	1	14 (4)	TF access vs others, TV-in-TV, BPD
Walters et al. (62)	2014	Obs.	8	Australia, New-Zealand	December 2008-December 2010	129	ND	5 (4)	TF access vs. others
Webb et al. (63)	2014	Obs.	16	International	2013-ND	150	ND	6 (4)	TF access vs. others
Abdel-Wahab et al. (64)	2014	RCT	5	Germany	March 2012-December 2013	241	1	10 (4)	MCV vs. ESV
Swedish report (65)	2013	Obs.	7	Sweden	January 2011-December 2011	209	ND	3 (1)	MCV vs. ESV
Chieffo et al. (66)	2013	Obs.	4	Europe	ND-July 2011	408	ND	8 (2)	MCV vs. ESV
Collas et al. (67)	2015	Obs.	23	Belgium	December 2007-March 2012	861	24	44 (5)	MCV vs. ESV
Kasel et al. (68)	2014	Obs.	1	Germany	December 2007-August 2011	100	1	9 (9)	MCV vs. ESV
Ludman et al. (11)	2015	Obs.	33	UK	January 2007-December 2012	3,980	36	104 (3)	MCV vs. ESV, Enrollment date
Sabaté et al. (69)	2013	Obs.	ND	Spain	January 2010-December 2011	1416	8	37 (3)	MCV vs. ESV
Watanabe et al. (70)	2013	Obs.	2	France	October 2008-April 2012	320	11	5 (2)	MCV vs. ESV
Wenaweser et al. (71)	2011	Obs.	1	Switzerland	August 2007-March 2010	200	6	9 (5)	MCV vs. ESV
Wenaweser et al. (72)	2014	Obs.	8	Switzerland	February 2011-March 2013	556	ND	18 (3)	MCV vs. ESV
Lange et al. (73)	2012	Obs.	1	Germany	June 2007-June 2010	420	ND	19 (5)	Enrollment date
Makkar et al. (74)	2013	Obs.	27	USA, Canada, Germany	2007-2012	2,554	ND	96 (4)	TV-in-TV, TVE/M
Nuis et al. (21)	2012	Obs.	1	Netherlands	November 2005-September 2011	214	13	19 (9)	TV-in-TV, TVE/M, BPD
Geisbusch et al. (75)	2010	Obs.	1	Germany	June 2007-September 2009	212	3	16 (8)	TVE/M
Barbanti et al. (76)	2014	Obs.	7	Italy	June 2007-ND	1,376	12	35 (3)	BPD
Hahn et al. (77)	2014	Obs.	27	USA, Canada, Germany	2007-2012	2,135	ND	76 (4)	BPD
Lasa et al. (78)	2014	Obs.	1	Spain	March 2008-March 2012	157	ND	6 (4)	BPD
Stundl et al. (79)	2015	Obs.	1	Germany	June 2011-December 2013	226	ND	5 (2)	BPD
Watanabe et al. (80)	2015	Obs.	1	France	October 2006-July 2012	470	ND	10 (2)	BPD
Durand et al. (81)	2014	Obs.	3	France	January 2010-December 2011	292	1	8 (3)	Pre-procedural SAPT vs. DAPT
Huczek et al. (82)	2015	Obs.	3	Poland	March 2010-February 2014	303	ND	14 (5)	Pre-procedural SAPT vs. DAPT
Poliacikova et al. (83)	2013	Obs.	1	UK	December 2007-June 2012	171	6	4 (2)	Pre-procedural SAPT vs. DAPT
Stabile et al. (84)	2014	RCT	1	Italy	April 2010-April 2011	120	6	3 (3)	Pre-procedural SAPT vs. DAPT
Ussia et al. (85)	2011	RCT	1	Italy	May 2009-August 2010	79	6	5 (6)	Pre-procedural SAPT vs. DAPT
Barbash et al. (36)	2014	Obs.	1	USA	2007-2013	228	1	12 (5)	NOAF
Chopard et al. (37)	2015	Obs.	34	France	January 2010-December 2011	2,622	10	82 (3)	NOAF
Yankelson et al. (39)	2014	Obs.	1	Israel	September 2008-April 2013	380	18	6 (2)	NOAF

Values are n or n (%). *Follow-up is reported as mean or median as given by the authors.

BPD = balloon post-dilation; DAPT = dual antiplatelet therapy; ESV = Edwards-Sapien valve; MCV = Medtronic CoreValve; NOAF = new-onset atrial fibrillation; RCT = randomized controlled trial; SAPT = single antiplatelet therapy; TF = transfemoral; TVE/M = transcatheter valve embolization or migration; TV-in-TV = transcatheter valve within a transcatheter valve; other abbreviations as in Table 1.

47.6 ± 5.4% (range 33.0% to 60.5%). Previous stroke and history of AF were reported in 44 and 38 studies, respectively, and ranged from 7.3% to 23.0% and between 5.4% and 50.6%, respectively.

Only 5 studies did not report any data about the approach used for TAVR. The femoral artery was by far the most common approach, as it was the exclusive access in 7 studies and was used in 77% of cases.

The mean percentages of other approaches were as follows: 18% for transapical, 3% for subclavian, and 1.5% for transaortic, whereas transcarotid access was only mentioned in 1 study (n = 1) (Online Tables 2 and 3). Among 63 studies reporting the type of implanted valve, ESV was used exclusively in 11 (n = 14,400) and MCV in 10 (n = 3,454), whereas both prostheses were available in 42 (n = 54,143). Other devices were marginally implanted. BPD and TV-in-TV were reported by 25% and 41% of studies, respectively, and were used in a mean of 15.5 ± 10.3% and 2.8 ± 1.3% of cases, respectively. The mean short-term mortality was 7.1 ± 2.8%.

DATA SYNTHESIS. At least 2 nonoverlapping datasets were available for each of the 16 predictors of interest (**Tables 1 and 2**).

Among baseline predictors, on the basis of data derived from 6 studies (N = 13,342), male sex was associated with a lower aggregate risk of short-term CVE (RR: 0.82; 95% CI: 0.70 to 0.97; p = 0.02) (**Figure 2**, Online Figure 1). CKD was also significantly associated with CVE (RR: 1.29; 95% CI: 1.03 to 1.63; p = 0.03; 5 studies, N = 9,410). By contrast, no association was found between other baseline risk factors, although a trend toward a lower risk for obese patients was noted (RR: 0.66; 95% CI: 0.40 to -1.07; p = 0.09; 2 studies, N = 3,481). Statistical heterogeneity was low to moderate across baseline predictors, with I^2 estimates ranging between 0% and 45%. No publication bias was demonstrated either by funnel plot inspection or with the use of the Harbord test. In a sensitivity analysis, pooled estimates were derived with Mantel-Haenszel fixed effects models for predictors with a low heterogeneity across studies ($I^2 < 25\%$), yielding comparable results. On the other hand, when restricting the analysis to large studies with ≥200 patients, on the basis of data from 4 studies (N = 13,170) with the use of a random effects model, male sex did not significantly associate with CVE (RR: 0.82; 95% CI: 0.63 to 1.06; p = 0.14), whereas statistical heterogeneity demonstrated a mild increase (from I^2 = 0% to I^2 = 18%). However, when the pooled risk of these 4 studies was derived from a fixed effects model, the result was consistent with the main finding (Online Figure 2).

Among procedural variables, valve type (MCV vs. ESV; 11 studies, N = 8,561) and approach (non-TF vs. TF; 15 studies, N = 17,031) exhibited no association with short-term CVE. Enrollment date was significantly associated with CVE (RR: 1.55; 95% CI: 1.16 to 2.08; p = 0.003; 3 studies, N = 5,454), whereas on the basis of data from 4 studies (N = 4,173), NOAF was the strongest predictor of the occurrence of CVE within 30 days post-TAVR (RR: 1.85; 95% CI: 1.20 to 2.84; p = 0.005). Furthermore, a statistically nonsignificant trend toward a higher risk of CVE (RR: 1.43; 95% CI: 0.97 to 2.10; p = 0.07) was observed for BPD in a pooled analysis of 7 studies (N = 4,967) (**Figure 3**, Online Figure 3). Statistical heterogeneity was low (I^2 = 0 to 26%) without evidence of publication bias. Results were consistent in sensitivity analyses when excluding small studies and when deriving pooled estimates by the use of fixed effects models when statistical heterogeneity was low.

DISCUSSION

The present study is, to the best of our knowledge, the first to provide effect estimates for clinically relevant risk factors for CVE post-TAVR. Our results suggest that female sex, CKD, performance of TAVR during the first half of centers' experience, and post-procedural NOAF are associated with an increased risk of short-term CVE after TAVR (**Central Illustration**). Importantly, transcatheter valve type and approach do not seem to influence the incidence of CVE.

BASELINE PREDICTORS OF CVE. It has been shown that among AS patients, women demonstrated a 50% lower risk of stroke over a follow-up of 4 years (89) despite a more severe valvular disease phenotype at baseline. Our data could indirectly suggest a specific TAVR-related risk in women. Several studies have shown an association between aortic root dimensions and sex irrespective of body surface area and age, with men exhibiting larger aortic annuli and left ventricular outflow tract dimensions than women despite comparable ascending aortic measurements (90,91). This may increase the mechanical interaction between the native and transcatheter aortic valves during valve positioning and implantation, the 2 maneuvers associated with the highest risk of cerebral emboli during the TAVR procedure, as demonstrated by transcranial Doppler studies (5,14). Also, tissue-derived debris originating from the aortic valve or wall were found in two-thirds of the patients with the use of carotid filter devices (92). The hypothesis of CVE being associated with a higher mechanical interaction between native and aortic valve prosthesis is supported by the findings from the PARTNER trial showing a higher rate of stroke (6.3% vs. 2.8%) in patients with small aortic annuli and smaller aortic valve area (93), which are more frequent among women.

CKD was the only additional pre-procedural factor associated with an increased risk of CVE in our analysis. CKD patients within the TAVR population could be considered as advanced atherosclerotic disease equivalents, given the overlapping and synergistic

FIGURE 2 Summary RRs for Each Baseline Predictor of CVE After TAVR

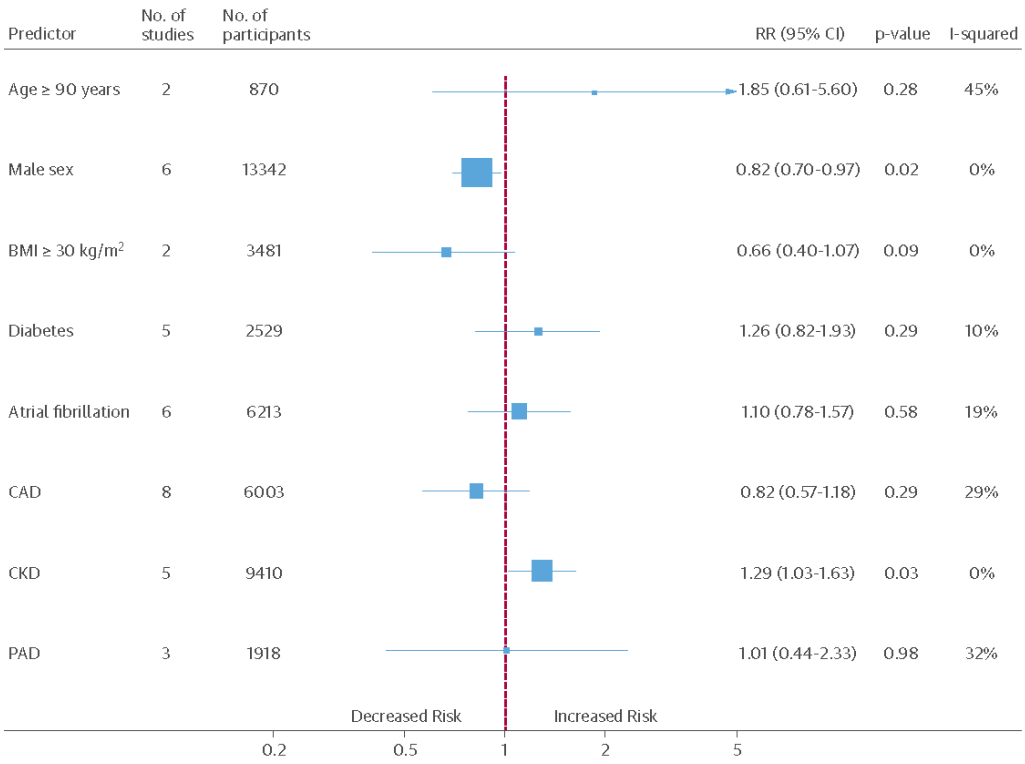

Forest plot of summary crude RRs of each assessed baseline predictor. BMI = body-mass index; CAD = coronary artery disease; CI = confidence interval; CKD = chronic kidney disease; CVE = cerebrovascular events; PAD = peripheral artery disease; RR = risk ratio; TAVR = transcatheter aortic valve replacement.

biological effects of uremia and traditional cardiovascular risk factors within the arterial wall and aortic valve. However, no other factors associated with an increased atherosclerotic burden such as diabetes, peripheral vascular disease, or CAD, were found to associate with CVE post-TAVR in our analysis. Also, it has been shown that CKD patients have a 40% to 45% excess risk of stroke despite adjusting for age, sex, and traditional atherosclerotic risk factors (94). It is therefore increasingly recognized that CKD is not just an "innocent witness" in the atherosclerotic process, but rather promotes it via chronic inflammation, oxidative stress, sympathetic nerve overactivity, thrombogenic factors, and during advanced stages, decreased Klotho protein expression, with perturbed calcium and phosphorus metabolism further promoting vascular calcification and endothelial dysfunction (95). Importantly, this detrimental effect might be even more pronounced in patients with previous cardiovascular diseases (95), inherently common in TAVR recipients. Eventually, the absence of firm guidance about anticoagulation therapy for stroke prevention in patients with severe CKD, as reflected in current therapeutic guidelines, may be another explanation to this increased risk of CVE (95). Despite a high prevalence of AF and NOAF in these patients, physicians may indeed be reluctant to introduce anticoagulants, given their well-demonstrated high bleeding risk in CKD patients.

PROCEDURAL PREDICTORS OF CVE. An important finding of this meta-analysis is the similar risk of CVE according to approach (TF vs. non-TF) and valve type. In a previous meta-analysis of 7,541 patients, Eggebrecht et al. (6) found a lower risk of stroke associated with the transapical approach, and this was partially explained by the absence of manipulation of large-bore catheters throughout the aortic arch. However, further reports, and especially a large meta-analysis by Athappan et al. (5), did not support this hypothesis. Future studies will need to evaluate the potential influence of newer approaches (e.g., transcarotid) and transcatheter valve types on the risk of CVE.

FIGURE 3 Summary RRs for Each Procedural Predictor of CVE After TAVR

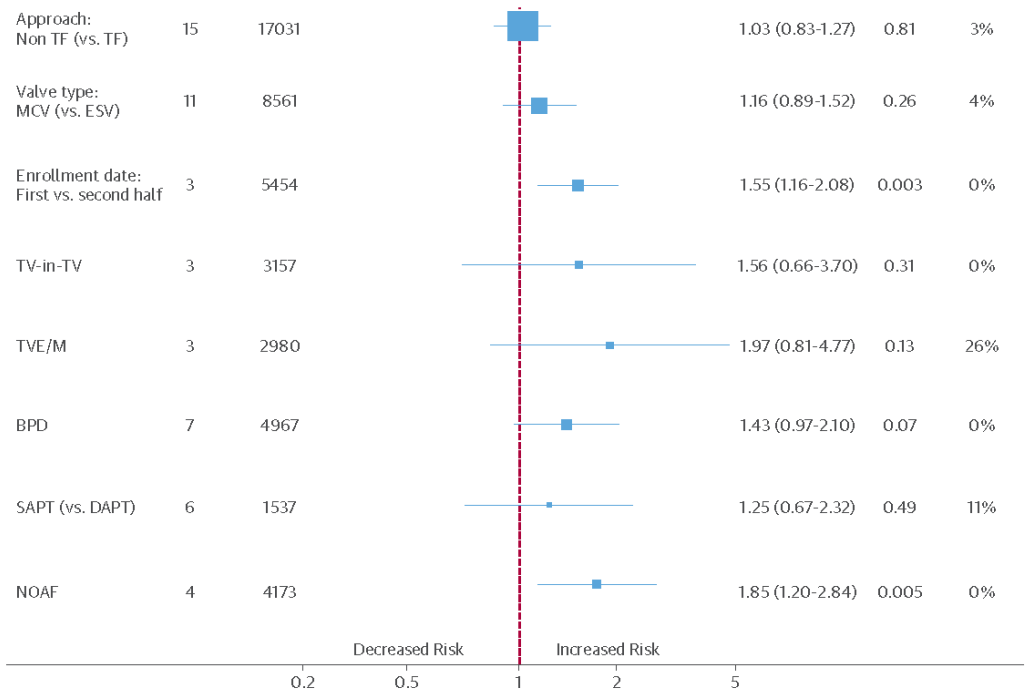

Forest plot of summary crude RRs of each assessed procedural predictor. BPD = balloon post-dilation; DAPT = dual antiplatelet therapy; ESV = Edwards-Sapien valve; MCV = Medtronic CoreValve; NOAF = new-onset atrial fibrillation; SAPT = single antiplatelet therapy; TF = transfemoral; TVE/M = transcatheter valve embolization or migration; TV-in-TV = transcatheter valve within a transcatheter valve; other abbreviations as in Figure 2.

We found a significant association between enrollment date and the risk of CVE post-TAVR. This has already been suggested by Athappan et al. (5) who found a 1.5% drop in stroke risk when comparing early versus late experience within high-volume centers. Nevertheless, precisely identifying the true effect of operator/center experience per se is challenging because numerous factors may influence stroke rates over time, namely refined patient selection, device iterations, and overall procedural improvements. Most early reports alluded to better results with growing experience, but without controlling for potential confounders (74). In an analysis of the PARTNER program, Minha et al. (96) recently demonstrated the influence of a learning curve effect on several outcomes post-TF-TAVR. However, stroke was not related to this effect. After adjustment for procedure- and patient-related factors, no significant association emerged between a learning curve effect and major adverse events. This suggests that post-TAVR outcomes, especially CVE, might be less influenced by operator experience than by other confounders in analyses based on chronology.

BPD is a common practice to reduce moderate or severe paravalvular regurgitation, a consistent predictor of late mortality (97). There has been an ongoing debate about the influence of BPD on stroke rates post-TAVR. In our analysis, we showed a nonsignificant trend toward a higher risk of CVE with BPD. Nonetheless, it should be noted that in previous studies, an increased risk of stroke post-BPD was exclusively demonstrated for early (≤7 days) stroke, and especially for stroke occurring within 24 h post-procedure, which is consistent with an acute embolic mechanism related to BPD (77,98). The analysis of events up to 30 days post-TAVR in the present study may have mitigated this relationship, but the trend we showed supports further research about the exact role of BPD in CVE occurrence. Meanwhile, proper sizing of the aortic annulus using

CENTRAL ILLUSTRATION **Predictors of Cerebrovascular Events Post-TAVR**

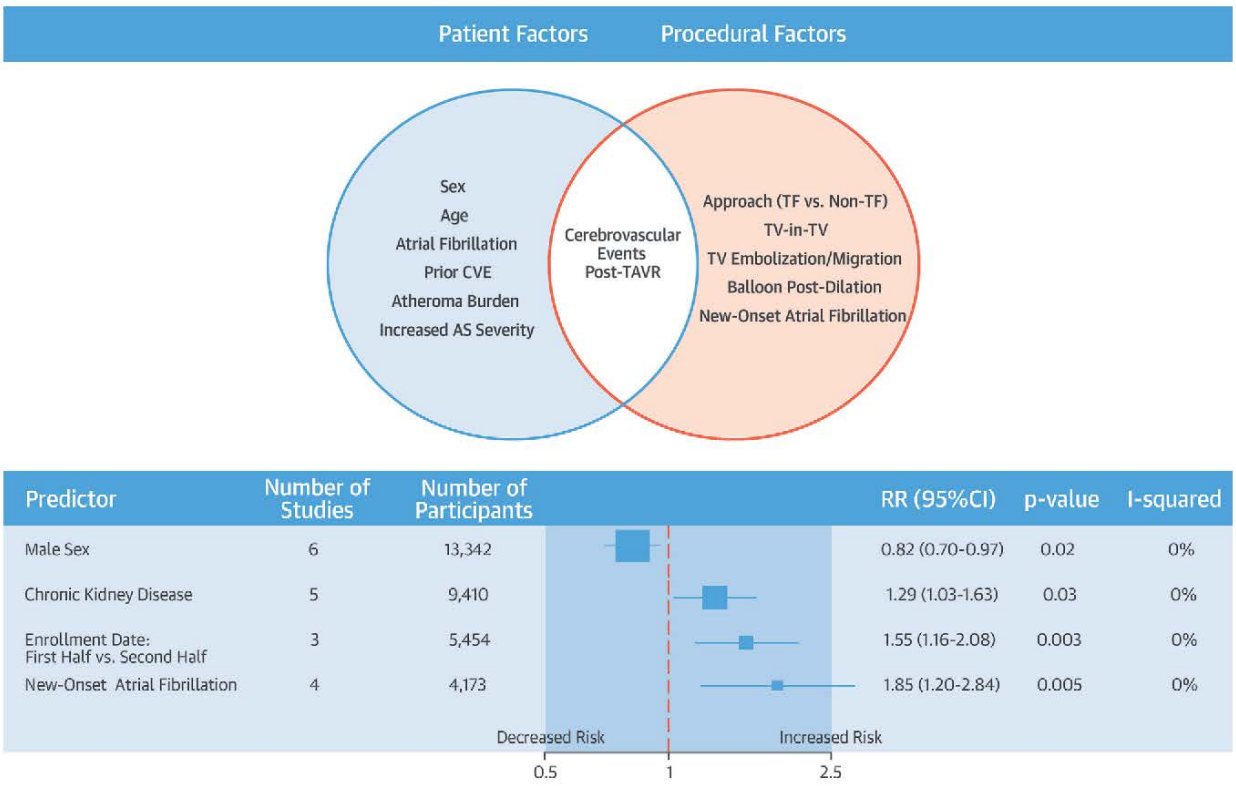

Predictor	Number of Studies	Number of Participants	RR (95%CI)	p-value	I-squared
Male Sex	6	13,342	0.82 (0.70-0.97)	0.02	0%
Chronic Kidney Disease	5	9,410	1.29 (1.03-1.63)	0.03	0%
Enrollment Date: First Half vs. Second Half	3	5,454	1.55 (1.16-2.08)	0.003	0%
New-Onset Atrial Fibrillation	4	4,173	1.85 (1.20-2.84)	0.005	0%

Auffret, V. et al. J Am Coll Cardiol. 2016;68(7):673-84.

Baseline/patient- and periprocedural-related factors associated with a higher risk of stroke post-TAVR. AS — aortic stenosis; CI — confidence interval; CVE — cerebrovascular events; RR — risk ratio; TF — transfemoral; TV — transcatheter valve; TV-in-TV — transcatheter valve within a transcatheter valve; TAVR — transcatheter aortic valve replacement.

3-dimensional imaging techniques, device design iterations aiming at minimizing paravalvular leak (external skirt of the Sapien 3 valve) (99), repositionable prostheses (100), and thorough evaluations of embolic protection devices in patients requiring BPD are warranted.

The strongest predictor of short-term CVE in the present analysis was NOAF, which occurs in ≈5% to 30% of TAVR recipients, mainly after transapical access (37,101). Moreover, it has been shown that NOAF was chiefly associated with CVE occurring 1 to 30 days post-TAVR (20). Our findings support the need for continuous rhythm monitoring during hospitalization post-TAVR to detect otherwise silent episodes of NOAF. Because no clear guidelines exist regarding anticoagulation therapy post-TAVR, the present study along with others (20,21,101) urges the consideration of prompt anticoagulation in these patients after diagnosing AF regardless of the episode duration. Indeed, Amat-Santos et al. (101) demonstrated that even short (<12 h) episodes of AF carried a risk of CVE.

STUDY LIMITATIONS. Despite VARC definition availability, stroke reporting was highly variable across studies, forcing us to pool different outcomes. Moreover, numerous clinically relevant predictors recently emerged (12–18), although our aim was not to evaluate all of them. Nevertheless, even among the selected predictors, actual numbers of events/individuals remained somewhat limited. Despite our methodology, the present analysis lacks statistical power in certain areas, and the possibility of type II error should be kept in mind when interpreting these results. Indeed, an absence of evidence for an effect does not necessarily mean true absence of effect. Finally, we used crude RRs, yet the low number of

studies included in individual meta-analyses did not allow us to adjust for relevant study-level covariates in a meta-regression to increase the robustness of our findings. It was therefore not possible to identify the independent impact of each predictor. However, our overall results should be regarded as hypothesis-generating, supporting the need for uniform and exhaustive reporting of events in the field of TAVR.

CONCLUSIONS

The present meta-analysis provides effect estimates for numerous clinically relevant variables that were considered potential predictors of CVE post-TAVR. A mixed of pre-procedural (female sex, CKD) and procedural (enrollment date, NOAF) factors determined a higher risk of CVE post-TAVR. This represents a first step to help us implement further preventive measures (e.g., use of embolic protection devices, optimizing antithrombotic therapy post-TAVR) in those patients at highest risk. Because TAVR is set to expand its indication to lower surgical-risk patients, CVE remain an ongoing problem, and future efforts should aim at identifying patients who would benefit from tailored therapies.

REPRINT REQUESTS AND CORRESPONDENCE: Dr. Josep Rodés-Cabau, Quebec Heart & Lung Institute, Laval University, 2725 Chemin Ste-Foy, G1V 4GS, Quebec City, Quebec, Canada. E-mail: josep.rodes@criucpq.ulaval.ca.

PERSPECTIVES

COMPETENCY IN PATIENT CARE AND PROCEDURAL SKILLS: Female sex, chronic kidney disease, new-onset atrial fibrillation, and the early phase of implementation at a clinical site predict cerebrovascular ischemic events shortly after TAVR, whereas valve type (balloon-expandable vs. self-expandable) and vascular access route (transfemoral vs. nontransfemoral) did not.

TRANSLATIONAL OUTLOOK: Further studies are needed to define the impact of reducing balloon post-dilation, embolism protection devices, and anticoagulant therapy as measures that might influence the risk of stroke in patients undergoing TAVR.

REFERENCES

1. Nishimura RA, Otto CM, Bonow RO, et al. 2014 AHA/ACC guideline for the management of patients with valvular heart disease: a report of the American College of Cardiology/American Heart Association Task Force on Practice Guidelines. J Am Coll Cardiol 2014;63:e57–185.

2. Leon MB, Smith CR, Mack MJ, et al. Transcatheter or surgical aortic-valve replacement in intermediate-risk patients. N Engl J Med 2016;374:1609–20.

3. Tamburino C, Barbanti M, D'Errigo P, et al. 1-Year outcomes after transfemoral transcatheter or surgical aortic valve replacement: results from the Italian OBSERVANT study. J Am Coll Cardiol 2015;66:804–12.

4. Thyregod HG, Steinbruchel DA, Ihlemann N, et al. Transcatheter versus surgical aortic valve replacement in patients with severe aortic valve stenosis: 1-year results from the all-comers NOTION randomized clinical trial. J Am Coll Cardiol 2015;65:2184–94.

5. Athappan G, Gajulapalli RD, Sengodan P, et al. Influence of transcatheter aortic valve replacement strategy and valve design on stroke after transcatheter aortic valve replacement: a meta-analysis and systematic review of literature. J Am Coll Cardiol 2014;63:2101–10.

6. Eggebrecht H, Schmermund A, Voigtlander T, Kahlert P, Erbel R, Mehta RH. Risk of stroke after transcatheter aortic valve implantation (TAVI): a meta-analysis of 10,037 published patients. EuroIntervention 2012;8:129–38.

7. Holmes DR, Brennan JM, Rumsfeld JS, et al. Clinical outcomes at 1 year following transcatheter aortic valve replacement. JAMA 2015;313:1019–28.

8. Adams DH, Popma JJ, Reardon MJ, et al. Transcatheter aortic-valve replacement with a self-expanding prosthesis. N Engl J Med 2014;370:1790–8.

9. Walther T, Hamm CW, Schuler G, et al. Perioperative results and complications in 15,964 transcatheter aortic valve replacements: prospective data from the GARY registry. J Am Coll Cardiol 2015;65:2173–80.

10. Reinohl J, Kaier K, Reinecke H, et al. Effect of availability of transcatheter aortic-valve replacement on clinical practice. N Engl J Med 2015;373:2438–47.

11. Ludman PF, Moat N, de Belder MA, et al. Transcatheter aortic valve implantation in the United Kingdom: Temporal trends, predictors of outcome, and 6-year follow-up: a report from the UK Transcatheter Aortic Valve Implantation (TAVI) Registry, 2007 to 2012. Circulation 2015;131:1181–90.

12. Freeman M, Barbanti M, Wood DA, et al. Cerebral events and protection during transcatheter aortic valve replacement. Catheter Cardiovasc Interv 2014;84:885–96.

13. Hynes BG, Rodes-Cabau J. Transcatheter aortic valve implantation and cerebrovascular events: the current state of the art. Ann N Y Acad Sci 2012;1254:151–63.

14. Fanning JP, Walters DL, Platts DG, Eeles E, Bellapart J, Fraser JF. Characterization of neurological injury in transcatheter aortic valve implantation: how clear is the picture? Circulation 2014;129:504–15.

15. Mastoris I, Schoos MM, Dangas GD, Mehran R. Stroke after transcatheter aortic valve replacement: incidence, risk factors, prognosis, and preventive strategies. Clin Cardiol 2014;37:756–64.

16. Bosmans J, Bleiziffer S, Gerckens U, et al. The incidence and predictors of early- and mid-term clinically relevant neurological events after transcatheter aortic valve replacement in real-world patients. J Am Coll Cardiol 2015;66:209–17.

17. Tchetche D, Farah B, Misuraca L, et al. Cerebrovascular events post-transcatheter aortic valve replacement in a large cohort of patients: a FRANCE-2 registry substudy. J Am Coll Cardiol Intv 2014;7:1138–45.

18. Miller DC, Blackstone EH, Mack MJ, et al. Transcatheter (TAVR) versus surgical (AVR) aortic valve replacement: occurrence, hazard, risk factors, and consequences of neurologic events in the PARTNER trial. J Thorac Cardiovasc Surg 2012;143:832–43.e13.

19. Stortecky S, Windecker S, Pilgrim T, et al. Cerebrovascular accidents complicating transcatheter aortic valve implantation: frequency, timing and impact on outcomes. EuroIntervention 2012;8:62–70.

20. Nombela-Franco L, Webb JG, de Jaegere PP, et al. Timing, predictive factors, and prognostic

value of cerebrovascular events in a large cohort of patients undergoing transcatheter aortic valve implantation. Circulation 2012;126:3041–53.

21. Nuis RJ, Van Mieghem NM, Schultz CJ, et al. Frequency and causes of stroke during or after transcatheter aortic valve implantation. Am J Cardiol 2012;109:1637–43.

22. Moher D, Liberati A, Tetzlaff J, Altman DG. Preferred reporting items for systematic reviews and meta-analyses: the PRISMA Statement. Open Med 2009;3:e123–30.

23. DerSimonian R, Laird N. Meta-analysis in clinical trials. Control Clin Trials 1986;7:177–88.

24. Higgins JP, Thompson SG. Quantifying heterogeneity in a meta-analysis. Stat Med 2002;21:1539–58.

25. Harbord RM, Egger M, Sterne JA. A modified test for small-study effects in meta-analyses of controlled trials with binary endpoints. Stat Med 2006;25:3443–57.

26. Leker RR, Eichel R, Verber A, Cohen JE, Lotan C, Danenberg HD. Stroke complicating transcatheter aortic valve implantation: incidence, risk factors and outcome. Int J Stroke 2013;8:235–9.

27. Stangl V, Baldenhofer G, Knebel F, et al. Impact of gender on three-month outcome and left ventricular remodeling after transfemoral transcatheter aortic valve implantation. Am J Cardiol 2012;110:884–90.

28. O'Connor SA, Morice MC, Gilard M, et al. Revisiting sex equality with transcatheter aortic valve replacement outcomes: a collaborative, patient-level meta-analysis of 11,310 patients. J Am Coll Cardiol 2015;66:221–8.

29. Sherif MA, Zahn R, Gerckens U, et al. Effect of gender differences on 1-year mortality after transcatheter aortic valve implantation for severe aortic stenosis: results from a multicenter real-world registry. Clin Res Cardiol 2014;103:613–20.

30. Abramowitz Y, Chakravarty T, Jilaihawi H, et al. Comparison of outcomes of transcatheter aortic valve implantation in patients ≥90 years versus <90 years. Am J Cardiol 2015;116:1110–5.

31. Yamamoto M, Meguro K, Mouillet G, et al. Comparison of effectiveness and safety of transcatheter aortic valve implantation in patients aged ≥90 years versus <90 years. Am J Cardiol 2012;110:1156–63.

32. Konigstein M, Havakuk O, Arbel Y, et al. The obesity paradox in patients undergoing transcatheter aortic valve implantation. Clin Cardiol 2015;38:76–81.

33. Yamamoto M, Mouillet G, Oguri A, et al. Effect of body mass index on 30- and 365-day complication and survival rates of transcatheter aortic valve implantation (from the FRench Aortic National CoreValve and Edwards 2 [FRANCE 2] registry). Am J Cardiol 2013;112:1932–7.

34. Conrotto F, D'Ascenzo F, Giordana F, et al. Impact of diabetes mellitus on early and midterm outcomes after transcatheter aortic valve implantation (from a multicenter registry). Am J Cardiol 2014;113:529–34.

35. Minha S, Magalhaes MA, Barbash IM, et al. The impact of diabetes mellitus on outcome of patients undergoing transcatheter aortic valve replacement. IJC Metabolic and Endocrine 2015;9:54–60.

36. Barbash IM, Minha S, Ben-Dor I, et al. Predictors and clinical implications of atrial fibrillation in patients with severe aortic stenosis undergoing transcatheter aortic valve implantation. Catheter Cardiovasc Interv 2015;85:468–77.

37. Chopard R, Teiger E, Meneveau N, et al. Baseline characteristics and prognostic implications of pre-existing and new-onset atrial fibrillation after transcatheter aortic valve implantation: results from the FRANCE-2 registry. J Am Coll Cardiol Intv 2015;8:1346–55.

38. Maan A, Heist EK, Passeri J, et al. Impact of atrial fibrillation on outcomes in patients who underwent transcatheter aortic valve replacement. Am J Cardiol 2015;115:220–6.

39. Yankelson L, Steinvil A, Gershovitz L, et al. Atrial fibrillation, stroke, and mortality rates after transcatheter aortic valve implantation. Am J Cardiol 2014;114:1861–6.

40. Abdel-Wahab M, Zahn R, Horack M, et al. Transcatheter aortic valve implantation in patients with and without concomitant coronary artery disease: comparison of characteristics and early outcome in the German multicenter TAVI registry. Clin Res Cardiol 2012;101:973–81.

41. Abramowitz Y, Banai S, Katz G, et al. Comparison of early and late outcomes of TAVI alone compared to TAVI plus PCI in aortic stenosis patients with and without coronary artery disease. Catheter Cardiovasc Interv 2014;83:649–54.

42. Gautier M, Pepin M, Himbert D, et al. Impact of coronary artery disease on indications for transcatheter aortic valve implantation and on procedural outcomes. EuroIntervention 2011;7:549–55.

43. Mancio J, Fontes-Carvalho R, Oliveira M, et al. Coronary artery disease and symptomatic severe aortic valve stenosis: clinical outcomes after transcatheter aortic valve implantation. Front Cardiovasc Med 2015;2:18.

44. Snow TM, Ludman P, Banya W, et al. Management of concomitant coronary artery disease in patients undergoing transcatheter aortic valve implantation: the United Kingdom TAVI Registry. Int J Cardiol 2015;199:253–60.

45. Stefanini GG, Stortecky S, Cao D, et al. Coronary artery disease severity and aortic stenosis: clinical outcomes according to SYNTAX score in patients undergoing transcatheter aortic valve implantation. Eur Heart J 2014;35:2530–40.

46. Allende R, Webb JG, Munoz-Garcia AJ, et al. Advanced chronic kidney disease in patients undergoing transcatheter aortic valve implantation: insights on clinical outcomes and prognostic markers from a large cohort of patients. Eur Heart J 2014;35:2685–96.

47. Ferro CJ, Chue CD, De Belder MA, et al. Impact of renal function on survival after transcatheter aortic valve implantation (TAVI): an analysis of the UK TAVI registry. Heart 2015;101:546–52.

48. Nguyen TC, Babaliaros VC, Razavi SA, et al. Impact of varying degrees of renal dysfunction on transcatheter and surgical aortic valve replacement. J Thorac Cardiovasc Surg 2013;146:1399–406.

49. Oguri A, Yamamoto M, Mouillet G, et al. Impact of chronic kidney disease on the outcomes of transcatheter aortic valve implantation: results from the FRANCE 2 registry. EuroIntervention 2015;10:e1–9.

50. Sinning JM, Horack M, Grube E, et al. The impact of peripheral arterial disease on early outcome after transcatheter aortic valve implantation: results from the German Transcatheter Aortic Valve Interventions Registry. Am Heart J 2012;164:102–10.e1.

51. Bosmans JM, Kefer J, De Bruyne B, et al. Procedural, 30-day and one year outcome following CoreValve or Edwards transcatheter aortic valve implantation: results of the Belgian National Registry. Interact Cardiovasc Thorac Surg 2011;12:762–7.

52. Eltchaninoff H, Prat A, Gilard M, et al. Transcatheter aortic valve implantation: early results of the FRANCE (FRench Aortic National CoreValve and Edwards) registry. Eur Heart J 2011;32:191–7.

53. Ewe SH, Delgado V, Ng AC, et al. Outcomes after transcatheter aortic valve implantation: transfemoral versus transapical approach. Ann Thorac Surg 2011;92:1244–51.

54. Fröhlich GM, Baxter PD, Malkin CJ, et al. Comparative survival after transapical, direct aortic, and subclavian transcatheter aortic valve implantation (Data from the UK TAVI Registry). Am J Cardiol 2015;116:1555–9.

55. Imnadze G, Franz N, Hofmann S, et al. Benefits of best for groin strategy leading to a transapical TAVI dominance. Thorac Cardiovasc Surg 2015;63:487–92.

56. Lotfi S, Dohmen G, Gotzenich A, et al. Midterm outcomes after transcatheter aortic valve implantation. Innovations (Phila) 2014;9:343–7.

57. Mack MJ, Brennan JM, Brindis R, et al. Outcomes following transcatheter aortic valve replacement in the United States. JAMA 2013;310:2069–77.

58. Muensterer A, Mazzitelli D, Ruge H, et al. Safety and efficacy of the subclavian access route for TAVI in cases of missing transfemoral access. Clin Res Cardiol 2013;102:627–36.

59. Petronio AS, De Carlo M, Bedogni F, et al. Safety and efficacy of the subclavian approach for transcatheter aortic valve implantation with the CoreValve revalving system. Circ Cardiovasc Interv 2010;3:359–66.

60. Schymik G, Wurth A, Bramlage P, et al. Long-term results of transapical versus transfemoral TAVI in a real world population of 1000 patients with severe symptomatic aortic stenosis. Circ Cardiovasc Interv 2015;8.

61. Seiffert M, Schnabel R, Conradi L, et al. Predictors and outcomes after transcatheter aortic valve implantation using different approaches according to the valve academic research consortium definitions. Catheter Cardiovasc Interv 2013;82:640–52.

62. Walters DL, Sinhal A, Baron D, et al. Initial experience with the balloon expandable Edwards-SAPIEN Transcatheter Heart Valve in Australia and New Zealand: The SOURCE ANZ registry: outcomes at 30 days and one year. Int J Cardiol 2014;170:406–12.

63. Webb J, Gerosa G, Lefevre T, et al. Multicenter evaluation of a next-generation balloon-expandable transcatheter aortic valve. J Am Coll Cardiol 2014;64:2235–43.

64. Abdel-Wahab M, Mehilli J, Frerker C, et al. Comparison of balloon-expandable vs. self-expandable valves in patients undergoing transcatheter aortic valve replacement: the CHOICE randomized clinical trial. JAMA 2014;311:1503–14.

65. TAVI annual report 2011. Scand Cardiovas J 2013;47:95–102.

66. Chieffo A, Buchanan GL, Van Mieghem NM, et al. Transcatheter aortic valve implantation with the Edwards SAPIEN versus the Medtronic CoreValve Revalving system devices: a multicenter collaborative study: the PRAGMATIC Plus Initiative (Pooled-RotterdAm-Milano-Toulouse In Collaboration). J Am Coll Cardiol 2013;61:830–6.

67. Collas VM, Dubois C, Legrand V, et al. Midterm clinical outcome following Edwards SAPIEN or Medtronic Corevalve transcatheter aortic valve implantation (TAVI): results of the Belgian TAVI registry. Catheter Cardiovasc Interv 2015;86:528–35.

68. Kasel AM, Cassese S, Ischinger T, et al. A prospective, non-randomized comparison of SAPIEN XT and CoreValve implantation in two sequential cohorts of patients with severe aortic stenosis. Am J Cardiovasc Dis 2014;4:87–99.

69. Sabaté M, Cánovas S, García E, et al. In-hospital and mid-term predictors of mortality after transcatheter aortic valve implantation: data from the TAVI National Registry 2010–2011. Rev Esp Cardiol 2013;66:949–58.

70. Watanabe Y, Hayashida K, Yamamoto M, et al. Transfemoral aortic valve implantation in patients with an annulus dimension suitable for either the Edwards valve or the CoreValve. Am J Cardiol 2013;112:707–13.

71. Wenaweser P, Pilgrim T, Roth N, et al. Clinical outcome and predictors for adverse events after transcatheter aortic valve implantation with the use of different devices and access routes. Am Heart J 2011;161:1114–24.

72. Wenaweser P, Stortecky S, Heg D, et al. Short-term clinical outcomes among patients undergoing transcatheter aortic valve implantation in Switzerland: the Swiss TAVI registry. EuroIntervention 2014;10:982–9.

73. Lange R, Bleiziffer S, Mazzitelli D, et al. Improvements in transcatheter aortic valve implantation outcomes in lower surgical risk patients: a glimpse into the future. J Am Coll Cardiol 2012;59:280–7.

74. Makkar RR, Jilaihawi H, Chakravarty T, et al. Determinants and outcomes of acute transcatheter valve-in-valve therapy or embolization: a study of multiple valve implants in the U.S. PARTNER trial (Placement of AoRTic TraNscathetER Valve Trial Edwards SAPIEN Transcatheter Heart Valve). J Am Coll Cardiol 2013;62:418–30.

75. Geisbusch S, Bleiziffer S, Mazzitelli D, Ruge H, Bauernschmitt R, Lange R. Incidence and management of CoreValve dislocation during transcatheter aortic valve implantation. Circ Cardiovasc Interv 2010;3:531–6.

76. Barbanti M, Petronio AS, Capodanno D, et al. Impact of balloon post-dilation on clinical outcomes after transcatheter aortic valve replacement with the self-expanding CoreValve prosthesis. J Am Coll Cardiol Intv 2014;7:1014–21.

77. Hahn RT, Pibarot P, Webb J, et al. Outcomes with post-dilation following transcatheter aortic valve replacement: the PARTNER I trial (placement of aortic transcatheter valve). J Am Coll Cardiol Intv 2014;7:781–9.

78. Lasa G, Gaviria K, Sanmartin JC, Telleria M, Larman M. Postdilatation for treatment of perivalvular aortic regurgitation after transcatheter aortic valve implantation. Catheter Cardiovasc Interv 2014;83:E112–8.

79. Stundl A, Rademacher MC, Descoups C, et al. Balloon post-dilation and valve-in-valve implantation for the reduction of paravalvular leakage with use of the self-expanding CoreValve prosthesis. EuroIntervention 2016;11:1140–7.

80. Watanabe Y, Hayashida K, Lefèvre T, et al. Is post-dilation useful after implantation of the Edwards valve? Catheter Cardiovasc Interv 2015;85:667–76.

81. Durand E, Blanchard D, Chassaing S, et al. Comparison of two antiplatelet therapy strategies in patients undergoing transcatheter aortic valve implantation. Am J Cardiol 2014;113:355–60.

82. Huczek Z, Kochman J, Grygier M, et al. Preprocedural dual antiplatelet therapy and bleeding events following transcatheter aortic valve implantation (TAVI). Thromb Res 2015;136:112–7.

83. Poliacikova P, Cockburn J, De Belder A, Trivedi U, Hildick-Smith D. Antiplatelet and antithrombotic treatment after transcatheter aortic valve implantation: comparison of regimes. J Invasive Cardiol 2013;25:544–8.

84. Stabile E, Pucciarelli A, Cota L, et al. SAT-TAVI (single antiplatelet therapy for TAVI) study: a pilot randomized study comparing double to single antiplatelet therapy for transcatheter aortic valve implantation. Int J Cardiol 2014;174:624–7.

85. Ussia GP, Scarabelli M, Mul M, et al. Dual antiplatelet therapy versus aspirin alone in patients undergoing transcatheter aortic valve implantation. Am J Cardiol 2011;108:1772–6.

86. Leon MB, Piazza N, Nikolsky E, et al. Standardized endpoint definitions for transcatheter aortic valve implantation clinical trials: a consensus report from the Valve Academic Research Consortium. J Am Coll Cardiol 2011;57:253–69.

87. Kappetein AP, Head SJ, Généreux P, et al. Updated standardized endpoint definitions for transcatheter aortic valve implantation: the Valve Academic Research Consortium-2 consensus document. J Am Coll Cardiol 2012;60:1438–54.

88. Smith CR, Leon MB, Mack MJ, et al. Transcatheter versus surgical aortic-valve replacement in high-risk patients. N Engl J Med 2011;364:2187–98.

89. Cramariuc D, Rogge BP, Lonnebakken MT, et al. Sex differences in cardiovascular outcome during progression of aortic valve stenosis. Heart 2015;101:209–14.

90. Devereux RB, de Simone G, Arnett DK, et al. Normal limits in relation to age, body size and gender of two-dimensional echocardiographic aortic root dimensions in persons >/=15 years of age. Am J Cardiol 2012;110:1189–94.

91. Buellesfeld L, Stortecky S, Kalesan B, et al. Aortic root dimensions among patients with severe aortic stenosis undergoing transcatheter aortic valve replacement. J Am Coll Cardiol Intv 2013;6:72–83.

92. Van Mieghem NM, El Faquir N, Rahhab Z, et al. Incidence and predictors of debris embolizing to the brain during transcatheter aortic valve implantation. J Am Coll Cardiol Intv 2015;8:718–24.

93. Rodés-Cabau J, Pibarot P, Suri RM, et al. Impact of aortic annulus size on valve hemodynamics and clinical outcomes after transcatheter and surgical aortic valve replacement: insights from the PARTNER trial. Circ Cardiovasc Interv 2014;7:701–11.

94. Toyoda K, Ninomiya T. Stroke and cerebrovascular diseases in patients with chronic kidney disease. Lancet Neurol 2014;13:823–33.

95. Vellanki K, Bansal VK. Neurologic complications of chronic kidney disease. Curr Neurol Neurosc Rep 2015;15:50.

96. Minha S, Waksman R, Satler LP, et al. Learning curves for transfemoral transcatheter aortic valve replacement in the PARTNER-I trial: success and safety. Catheter Cardiovasc Interv 2016;87:165–75.

97. Athappan G, Patvardhan E, Tuzcu EM, et al. Incidence, predictors, and outcomes of aortic regurgitation after transcatheter aortic valve replacement: meta-analysis and systematic review of literature. J Am Coll Cardiol 2013;61:1585–95.

98. Nombela-Franco L, Rodés-Cabau J, DeLarochelliere R, et al. Predictive factors, efficacy, and safety of balloon post-dilation after transcatheter aortic valve implantation with a balloon-expandable valve. J Am Coll Cardiol Intv 2012;5:499–512.

99. Binder RK, Stortecky S, Heg D, et al. Procedural results and clinical outcomes of transcatheter aortic valve implantation in Switzerland: an observational cohort study of Sapien 3 Versus Sapien XT transcatheter heart valves. Circ Cardiovasc Interv 2015;8:pii:e002653.

100. Meredith Am IT, Walters DL, Dumonteil N, et al. Transcatheter aortic valve replacement for severe symptomatic aortic stenosis using a repositionable valve system: 30-day primary endpoint results from the REPRISE II study. J Am Coll Cardiol 2014;64:1339–48.

101. Amat-Santos IJ, Rodes-Cabau J, Urena M, et al. Incidence, predictive factors, and prognostic value of new-onset atrial fibrillation following transcatheter aortic valve implantation. J Am Coll Cardiol 2012;59:178–88.

KEY WORDS aortic stenosis, cerebrovascular events, predictors, stroke, transcatheter aortic valve implantation

APPENDIX For supplemental figures and tables, please see the online version of this article.

2.1.3 Synthèse

Dans la première contribution de ce deuxième chapitre, nous proposons des facteurs prédictifs d'AVC précoces après TAVI. Cette étude a potentiellement plusieurs implications cliniques susceptibles d'améliorer la prise en charge des patients en démontrant :

1- Que des facteurs liés au profil du patient comme le sexe féminin ou l'insuffisance rénale (déjà identifiée dans de précédentes études) augmentent le risque d'AVC. Ces facteurs peuvent contribuer, avec d'autres identifiés par de précédents travaux, à la stratification du risque des patients candidats à l'utilisation d'un dispositif de protection embolique.

2- Qu'une faible expérience des centres majore le risque d'AVC précoce ce qui suggère un lien avec la durée des procédures et les manipulations des outils endovasculaires. Cette constatation doit nous pousser à réduire, autant que faire se peut, la durée des procédures de TAVI, sans toutefois que cela n'impacte sur la qualité du geste, et à porter une attention toute particulière sur la nature, la qualité du traitement médicamenteux anti-thrombotique per-procédure ainsi que la surveillance de son efficacité en cas de procédure longue.

3- Qu'une post-dilatation au ballon de la prothèse en cas de résultat non satisfaisant après déploiement tend à augmenter le risque d'événement cérébrovasculaire précoce. Cet élément nous appelle à la plus grande vigilance dans la sélection des patients pour lesquels une technique d'implantation directe (sans pré-dilatation par valvuloplastie aortique au ballon) est effectuée. Ainsi, dans l'attente des résultats d'études prospectives randomisées (The preDIlatation in tRanscathEter aortiC Valve implanTation Trial [DIRECT], NCT02448927; TAVI Without Balloon Predilatation of the Aortic Valve SAPIEN 3 [DIRECTAVI], NCT02729519), il semble préférable de réaliser une prédilatation en cas de sténose aortique très serrée, de volumineuses calcifications valvulaires au scanner ou d'implantation d'une valve auto-expansible dont la force de déploiement radial est plus limitée, dans la mesure où l'usage de la pré-dilatation ne semble pas associé avec un sur-risque d'AVC précoce (59).

4- Que la survenue d'une arythmie cardiaque par fibrillation atriale post-opératoire est un facteur prédictif majeur d'AVC précoce et doit ainsi faire envisager une modification du traitement anti-thrombotique post-procédure avec l'introduction

d'un traitement anticoagulant préventif afin de limiter les risques d'AVC de cause cardioembolique.

2.2 Troubles conductifs post TAVI

2.2.1 Problématique

L'apparition ou l'aggravation de troubles conductifs, principalement le bloc de la branche gauche du faisceau de His et les troubles de conduction atrioventriculaires de haut degré conduisant à l'implantation d'un stimulateur cardiaque définitif, constituent la complication la plus fréquente des procédures TAVI. Il existe une abondante littérature sur ce sujet, bien souvent issue de travaux monocentriques et rétrospectifs. Malgré l'intérêt qu'il suscite, le sujet souffre, à l'heure actuelle, d'un manque de données randomisées et donc d'un faible niveau de preuves scientifiques permettant de guider le clinicien dans la gestion de ces complications.

2.2.2 Article original

Dans la deuxième contribution originale de ce chapitre, nous réalisons une large revue de la littérature afin de résumer les mécanismes, l'incidence, les facteurs prédictifs et l'impact clinique des troubles conductifs post TAVI. Nous proposons à la lumière des données disponibles, en tenant compte de leurs nombreuses limitations, des arbres décisionnels de prise en charge des troubles conductifs les plus communément rencontrés.

Conduction Disturbances After Transcatheter Aortic Valve Replacement

Current Status and Future Perspectives

ABSTRACT: Transcatheter aortic valve replacement (TAVR) has become a well-accepted option for treating patients with aortic stenosis at intermediate to high or prohibitive surgical risk. TAVR-related conduction disturbances, mainly new-onset left bundle-branch block and advanced atrioventricular block requiring permanent pacemaker implantation, remain the most common complication of this procedure. Furthermore, improvements in TAVR technology, akin to the increasing experience of operators/centers, have translated to a major reduction in periprocedural complications, yet the incidence of conduction disturbances has remained relatively high, with perhaps an increasing trend over time. Several factors have been associated with a heightened risk of conduction disturbances and permanent pacemaker implantation after TAVR, with prior right bundle-branch block and transcatheter valve type and implantation depth being the most commonly reported. New-onset left bundle-branch block and the need for permanent pacemaker implantation may have a significant detrimental association with patients' prognosis. Consequently, strategies intended to reduce the risk and to improve the management of such complications are of paramount importance, particularly in an era when TAVR expansion toward treating lower-risk patients is considered inevitable. In this article, we review the available evidence on the incidence, predictive factors, and clinical association of conduction disturbances after TAVR and propose a strategy for the management of these complications.

Vincent Auffret, MD, MSc
Rishi Puri, MBBS, PhD
Marina Urena, MD, PhD
Chekrallah Chamandi, MD
Tania Rodriguez-Gabella, MD
François Philippon, MD
Josep Rodés-Cabau, MD

Correspondence to: Josep Rodés-Cabau, MD, Quebec Heart and Lung Institute, Laval University, 2725 Chemin Ste-Foy, G1V 4GS, Quebec City, QC, Canada. E-mail josep.rodes@criucpq.ulaval.ca

Key Words: arrhythmias, cardiac ■ bundle-branch block ■ pacemaker, artificial ■ transcatheter aortic valve replacement

The advent of transcatheter aortic valve replacement (TAVR) represents a paradigm shift for treating patients with severe symptomatic aortic stenosis who are at high or prohibitive surgical risk.[1–3] The rate of periprocedural complications has decreased over time,[4,5] and TAVR has been increasingly performed with a minimalist approach,[6] evolving into a safe and "routine practice" procedure with predictable outcomes. This provided the rationale for an extension of TAVR indications to treating individuals at lower surgical risk.[7,8] However, unlike other procedural complications, the incidence of conduction disturbances (ie, high-degree atrioventricular block [HAVB] requiring permanent pacemaker implantation [PPM] and new-onset left bundle-branch block [LBBB]) has failed to decrease in recent times, with reports suggesting an increased risk associated with the use of some newer-generation transcatheter valves.[9–14] Although the clinical consequences of new-onset LBBB and PPM after TAVR remain the subject of ongoing debate, the deleterious effects of conduction disturbances and a decrease in left ventricular function induced by a right ventricle–based paced rhythm are supported by solid evidence in other clinical settings.[15–18] These findings highlight the paramount importance of limiting such TAVR-related complications because TAVR is set to expand to patients at intermediate and low surgical risk among whom the detrimental consequences of conduction disturbances and long-term right ventricular pacing may be even more pronounced.[19] This review aims to summarize the current evidence for the incidence, mechanisms, predictors, clinical associations, and management of conduction disturbances after TAVR.

THE CONDUCTION SYSTEM: UNDERSTANDING THE MECHANISMS OF CONDUCTION DISTURBANCES IN TAVR

The close proximity between the aortic valve and the conduction system explains the genesis of periprocedural conduction disturbances during TAVR (Figure I in the online-only Data Supplement). Within the right atrium, the atrioventricular node lies within the triangle of Koch, which is delineated by the tendon of Todaro, the orifice of the coronary sinus, and the insertion point of the tricuspid valve septal leaflet.[20–22] The convergence of the tendon of Todaro and the septal attachment of the tricuspid valve on the atrioventricular component of the membranous septum forms the apex of the triangle, with the coronary sinus ostium forming its base. The atrioventricular node is located just inferior to the apex. The atrioventricular node continues as the bundle of His, piercing the membranous septum and penetrating to the left through the central fibrous body. On the left side, the conduction system exits immediately beneath the membranous septum and is positioned superficially on the crest of the interventricular septum, where it gives rise to the left bundle branch. The left bundle branch is intimately related to the base of the interleaflet triangle separating the noncoronary and right coronary leaflets of the aortic valve. This close relationship is the key to understanding conduction disturbances after TAVR. In the setting of TAVR, conduction disturbances result primarily from a direct mechanical insult to the conduction system associated with various degrees of edema, hematoma, and ischemia, as demonstrated by necropsy studies.[23] Of particular importance, however, is the great interindividual variability of the anteroposterior relationship of the atrioventricular node with respect to the apex of the triangle of Koch, as well as the length of the nonpenetrating (the most proximal part traversing the membranous septum) portion of the His bundle. These anatomic variations have been exquisitely demonstrated by Kawashima and Sato[24] in an autopsy series of 115 elderly patients. They described 3 major variants, with 50% of individuals exhibiting a relatively right-sided atrioventricular bundle and 30% with a left-sided atrioventricular bundle, whereas in ≈20% of patients, the bundle coursed under the membranous septum just below the endocardium. The last 2 above-described variants may expose patients to a higher risk of TAVR-induced conduction disturbances, especially patients with a short membranous septum.[25]

Apart from the mechanical interaction between the transcatheter valve and the conduction system, there is evidence supporting the association between aortic stenosis and conduction disturbances. Several mechanisms have been proposed to explain this association:

calcium deposition on the conduction system as a result of its proximity to the aortic valve complex[26] and the development of left ventricular dysfunction, both of which have been associated with the occurrence of LBBB and advanced AVB in patients with aortic stenosis.[27] Urena et al[28] showed, in a study including 435 consecutive TAVR candidates who had 24-hour electrocardiographic monitoring the day before the procedure, that 3.5% of patients had episodes of advanced AVB or LBBB.

NEW-ONSET LBBB

Incidence

New-onset LBBB after TAVR has been reported with a varying incidence across studies. This may reflect the inclusion of transient LBBB in some studies, discrepancies in the timing of measurement (ie, at hospital discharge or at 30-day follow-up), and differences in the type of transcatheter valve from 1 study to another. New-onset LBBB has been reported in about one fourth (4%–65%) of TAVR procedures with first-generation valves (Figure 1A).[9,22,29–57] The occurrence

Circulation. 2017;136:1049–1069. DOI: 10.1161/CIRCULATIONAHA.117.028352

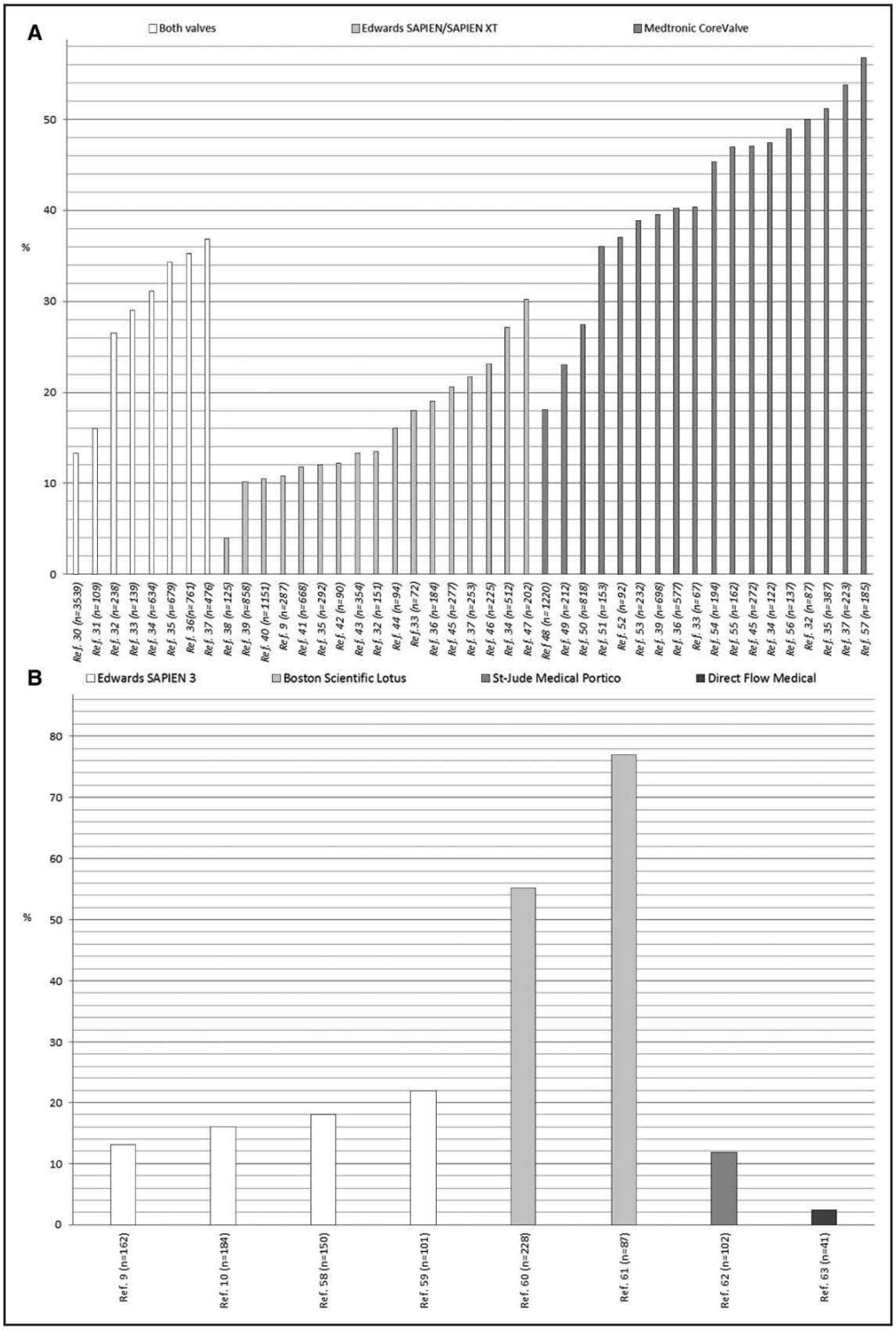

Figure 1. Incidence of new-onset left bundle-branch block (LBBB) after transcatheter aortic valve replacement. **A**, Rates of new-onset LBBB associated with the use of first-generation transcatheter valves. **B**, Rates of new-onset LBBB associated with the use of newer-generation transcatheter valve devices.

of new-onset LBBB has been more frequent when the self-expandable CoreValve system (Medtronic Inc, Minneapolis, MN) is used, with rates ranging from 18% to 65% compared with 4% to 30% reported with the use of the balloon-expandable Edwards SAPIEN/SAPIEN XT valve (Edwards Lifesciences LLC, Irvine, CA)[22] (Figure 1A). Data on the occurrence of new-onset LBBB after TAVR with newer-generation devices remain scarce (Figure 1B).[9,10,58–63] LBBB rates of 12% to 22% have been reported after implantation of the Edwards SAPIEN 3 valve.[9,10,58,59] Similar findings were reported with the self-expandable Portico TAVR system (St. Jude Medical, St. Paul, MN), which does not have a flared inflow and has the theoretical advantage of being partially resheathable and repositionable.[62] However, these rates were considerably higher (55% and 77%) in 2 studies reporting outcomes with the mechanically expanded Lotus valve (Boston Scientific, Natick, MA), which also allows subtle changes in valve position after a suboptimal initial deployment.[60,61]

Timing and Evolution of LBBB After TAVR

In the TAVR setting, most conduction disturbances occur in the acute period (periprocedural or within 24 hours of the procedure).[64,65] Although most events occur during valve expansion, new-onset LBBB may actually occur before valve implantation, mainly during guidewire insertion and balloon predilation.[66]

New-onset LBBB appears in the periprocedural period in 85% to 94% of cases and persists at discharge or 30 days in ≈55% of cases (range, 44% to 65%).[37,40,41,47,50,67] A small proportion of patients (2%–8.6% of cases, representing 6.6%–17.8% of new-onset LBBB) develop subacute LBBB (ie, from >24 hours after TAVR to discharge).[37,47,50] Late resolution of new-onset LBBB beyond discharge or at 30 days seems unlikely,[40,50] considering that the reported rates of persistent new-onset LBBB at 1-year follow-up have been on the order of 60%.[37,40] Likewise, late appearance of LBBB, from discharge to 1 year after TAVR, is a rare phenomenon, described in 0% to 2.9% of patients.[37,40,47,50] Before hospital discharge, persistency of LBBB seems more likely among self-expandable CoreValve recipients (47.5%–72.5%) compared with their balloon-expandable Edwards counterparts (27.1%–43.6%).[34,37] PPM rates of 5% to 14% have been reported at follow-up among patients with new-onset LBBB,[32,37,40,41,50] with the progression toward HAVB being the most frequent indication for PPM across studies. However, Nazif et al[40] reported an equal 47% rate of HAVB and sick sinus syndrome as the primary indications for PPM in balloon-expandable valve recipients with new-onset LBBB after the procedure.

Predictors

The main patient and procedural factors associated with new-onset LBBB after TAVR are summarized in Table 1 and presented more exhaustively in Table I in the online-only Data Supplement. Clinical risk factors of new-onset LBBB after TAVR include the presence of preprocedural conduction abnormalities,[46] especially prolonged QRS duration,[47] female sex, previous coronary artery bypass graft,[34] diabetes mellitus,[35] and the amount of calcification of the aortic valve.[46] Considering procedural characteristics associated with the occurrence of LBBB, the most consistently reported is the prosthesis implantation depth within the left ventricular outflow tract (LVOT).[33,44,45,47,68] The CoreValve prosthesis, which is progressively deployed from its ventricular side exerting high radial forces in the LVOT (often deeper than balloon-expandable valves), has been frequently identified as a predictor of new-onset LBBB.[32,34–36] Besides, several studies suggest that maneuvers associated with an overstretching/overexpansion of the LVOT such as balloon predilation or implantation of large prosthesis in a smaller LVOT increase the risk of TAVR-induced LBBB.[41,42,44,46,68] The role of balloon predilation has been described as a first injury inflicted to the conduction system that is insufficient to generate a persistent and complete AVB but promotes its occurrence after a second injury represented by the valve implantation.[69] Patients' characteristics underlying the appearance of conduction disturbances may differ according to valve type. Indeed, it has been demonstrated that the degree of radial forces exerted on the LVOT, and consequently the conduction system, depends primarily on LVOT diameter for the self-expandable CoreValve, whereas it is associated with the geometry and stiffness (calcifications) of the host tissue for the balloon-expandable Edwards valves.[70]

Table 1. Main Predictors of Left Bundle-Branch Block After Transcatheter Aortic Valve Replacement

Variable	Multivariable Odds Ratio*	References
Implantation of a Medtronic CoreValve (vs Edwards SAPIEN valves)	2.5–8.5	32, 34–36
Depth of implantation, per 1 mm	1.15–1.4	33, 44, 45, 47, 68
Overexpansion of native aortic annulus	1.8/1%; 5.3 if >15%	44, 46
Larger valve size		
Medtronic CoreValve 26 vs 23 mm	4.1	68
Edwards SAPIEN valves: 29 vs 20-23 mm	3.12	41

*Ranges of odds ratio are from published studies with a multivariable analysis.

Circulation. 2017;136:1049–1069. DOI: 10.1161/CIRCULATIONAHA.117.028352

Clinical Association of New-Onset LBBB With Mortality and Need for PPM

Table II in the online-only Data Supplement summarizes the association of new-onset LBBB with all-cause mortality after TAVR in adjusted analyses. So far, results from individual studies[32,34,35,40,41,50,52] have provided inconsistent results. This may reflect the inclusion of patients undergoing PPM within 48 hours or 30 days of TAVR, thus decreasing the risk of progression toward HAVB, in some of these studies. In the largest meta-analysis to date, Regueiro et al[71] pooled data from 8 studies (4756 patients) and failed to show a significant association between the occurrence of TAVR-induced LBBB and 1-year all-cause mortality (risk ratio, 1.21; 95% confidence interval [CI], 0.98–1.50; P=0.07, I^2=50%). In contrast, LBBB was associated with a greater risk of 1-year cardiac mortality, with a pooled estimate of 1.39 (95% CI, 1.04–1.86; P=0.03, I^2=32%) when data from 5 studies (3554 patients) were combined. This relationship may be explained by a specific association between new-onset LBBB, especially when the QRS duration is >160 milliseconds, and the risk of sudden cardiac death during follow-up, as demonstrated by Urena et al.[30,39] This suggests that constant compression of the conduction system by the transcatheter valve may induce the progression of LBBB to HAVB (Figure 2). Other pathophysiological mechanisms underlying this increased cardiac mortality risk include the risk of ventricular arrhythmias in patients with reduced ejection fraction and ventricular dyssynchrony and the evolution toward systolic dysfunction and terminal heart failure,[71] given that new-onset LBBB has been associated with a decreased recovery of left ventricular ejection fraction and a less favorable left ventricular remodeling after TAVR.[40,41,52] QRS duration at discharge may influence the clinical outcomes of new-onset LBBB, as evidenced by Meguro et al,[72] who demonstrated a higher all-cause mortality and rehospitalization for heart failure among patients with a QRS duration >150 milliseconds at discharge.

Few studies evaluated the association of new-onset LBBB with the risk of HAVB or PPM at follow-up after TAVR (Table III in the online-only Data Supplement). Approximately 13% of patients with new-onset LBBB developed HAVB in a study including 45% self-expandable valves recipients,[73] whereas 8% of patients implanted with a balloon-expandable valve presenting LBBB after TAVR eventually required PPM during the index hospitalization in the PARTNER program (Placement of Aortic Transcatheter Valves).[40] In univariable analyses, LBBB has consistently been associated with a higher 30-day risk of PPM, whereas its effect from 30 days to 1 year after TAVR has varied from 1 study to another.[34,40,41,50,51] However, 2 studies of similar sample size had conflicting conclusions about the independent association of LBBB with the risk of PPM (Table III in the online-only Data Supplement).[34,41] This observation may reflect a lower threshold for treating patients with new-onset LBBB because HAVB was the indication for PPM in 47% to 95% of patients across studies.[40,50] However, data from 2 recent meta-analyses suggest an ≈2-fold higher risk of PPM among patients with new-onset LBBB.[71,74]

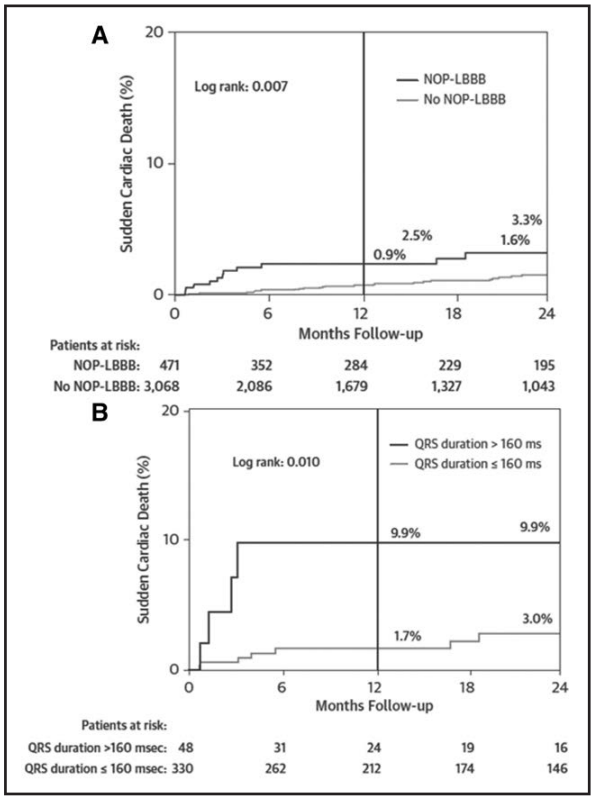

Figure 2. Association of new-onset left bundle-branch block (LBBB) with sudden cardiac death after transcatheter aortic valve replacement.
Kaplan-Meier curves at the 2-year follow-up for sudden cardiac death according to the occurrence of new-onset persistent (NOP) LBBB (**A**) and according to QRS duration (≤160 or >160 milliseconds) among patients with NOP-LBBB (**B**). Reproduced from Urena et al[30] with permission from the publisher. Copyright © 2015, American College of Cardiology Foundation.

PPM AFTER TAVR

Incidence

Figure 3A[1,2,7,39,48,75–102] summarizes the incidence of PPM associated with TAVR using first-generation devices, including the main national or multicenter registries and randomized clinical trials. The rates of PPM after TAVR varied from 2% to 51% in 41 studies included in a recent meta-analysis,[103] and PPM was the most common TAVR complication, with a pooled rate of 13% in an analysis summarizing 49 studies encompassing 16 063

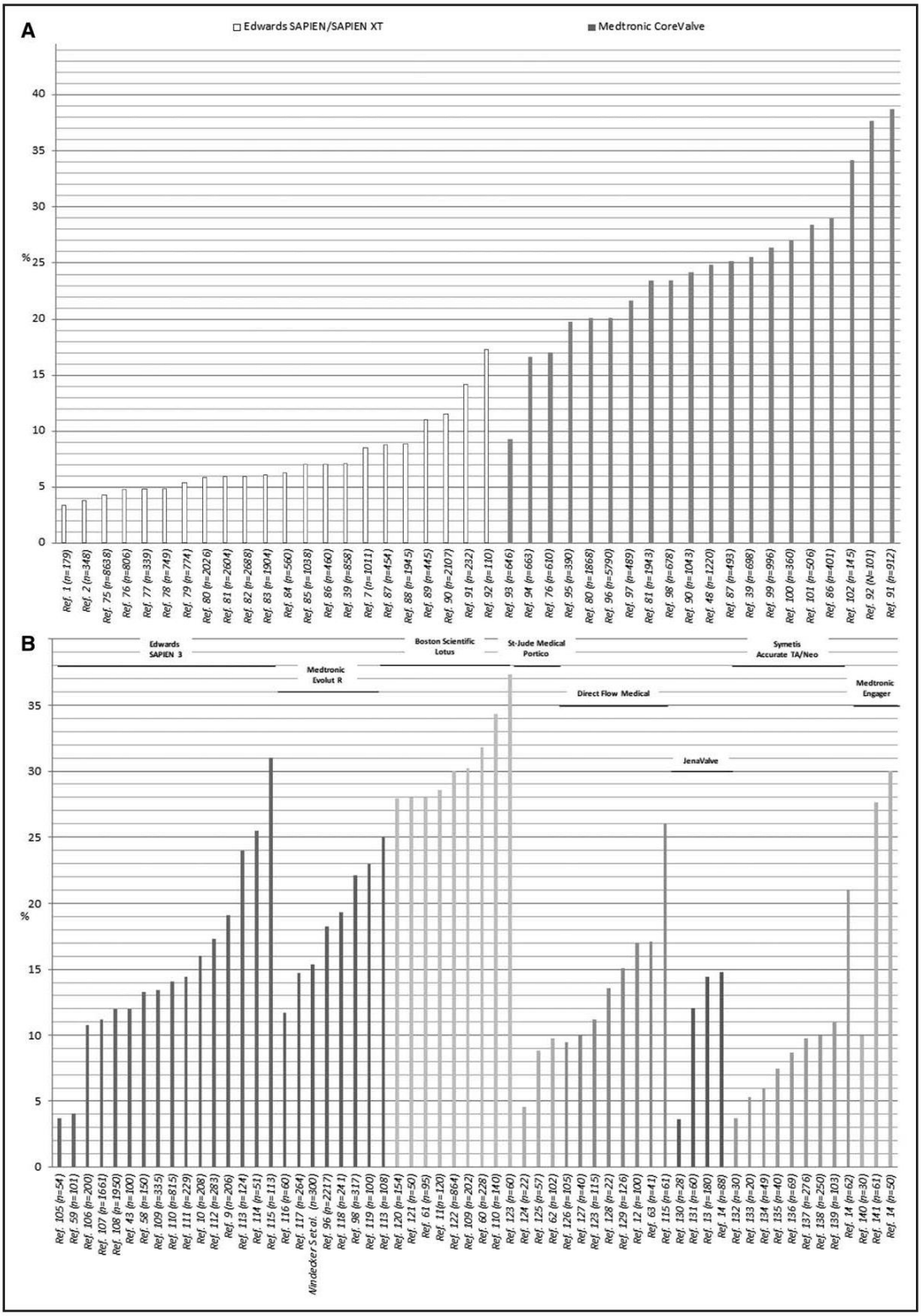

Figure 3. Incidence of permanent pacemaker implantation (PPM) after transcatheter aortic valve replacement. **A**, Rates of PPM associated with the use of prior-generation devices in the main multicenter registries and randomized clinical trials. **B**, Rates of PPM associated with the use of newer-generation devices.

patients.[104] Similar to LBBB, PPM was 5 times more frequent among self-expandable CoreValve recipients (25%–28%) compared with patients who received a balloon-expandable Edwards SAPIEN/SAPIEN XT valve (5%–7%).[65,103,104] This increased risk of PPM with the CoreValve system was confirmed in the CHOICE randomized trial (Comparison of Transcatheter Heart Valves in High Risk Patients With Severe Aortic Stenosis; 37.6% versus 17.3%; $P<0.001$).[92]

The recent adoption of newer iterations of transcatheter aortic valves and delivery systems has led to a major decrease in major periprocedural complications. Nonetheless, the available evidence to date does not support a reduction in PPM rates since the arrival of newer-generation devices (Figure 3B)[9–14,43,58–63,96,98,105–141] (CoreValve Evolut R FORWARD Study, S. Windecker, MD, PhD, unpublished data, 2016), suggesting that the improved repositioning/retrievability capabilities and antiparavalvular leak properties of the majority of these newer valves have little or no influence on the occurrence of conduction disturbances after TAVR. PPM rates >10% (11%–14%) have been reported in multicenter registries using the Edwards SAPIEN 3 valve,[107,108,110] which is as much as twice the PPM rate observed with the prior-generation balloon-expandable Edwards valves. Some groups have suggested that the increased risk of PPM with the SAPIEN 3 valve relates to a device-specific implantation technique and could be mitigated by a higher valve positioning (<25% of ventricular portion).[9,111] Whether the adoption of such a technique in routine clinical practice can achieve PPM rates comparable to those of the SAPIEN/SAPIEN XT valves without compromising safety (valve migration/embolization, periprosthetic aortic regurgitation) remains to be proven. Of note, except for the Portico system with a nonflared annular section and a low valve placement within the stent that allow sealing without deep implantation in the LVOT,[62] no additional features have been specifically designed to address the risk of conduction disturbances. Significant reductions in such complications after TAVR are therefore unlikely in the foreseeable future.

Two additional points should be considered with respect to the incidence of PPM after TAVR. First, patients with a prior pacemaker, although not being exposed to the risk of a new PPM after TAVR, were included in the denominator (ie, as patients without new PPM) in the calculation of PPM rates in most studies, resulting in a systematic underestimation of the real incidence of PPM after TAVR.[142] Second, the indications for PPM may have varied according to operator/center criteria, not always following current guidelines. As an example, some teams undertook prophylactic PPM in patients with new-onset LBBB after TAVR, which in turn resulted in an increased rate of PPM after TAVR. Moreover, the ongoing quest for shorter postprocedural hospital stay[143] is another factor that may have incited teams to proceed earlier with PPM, thus shortening the guideline-recommended period of clinical observation after TAVR for evaluating the permanent versus transient behavior of conduction disturbances.[144] A reduction in PPM rates has been observed with a strict adherence to Class I and II indications as recommended by clinical guidelines.[67,144]

Timing and Evolution of HAVB After TAVR

Like new-onset LBBB, TAVR-induced HAVB occurs mainly in the periprocedural setting; 60% to 96% of these events were recorded within 24 hours of TAVR with both balloon- and self-expandable valves.[73,145,146] Delayed HAVB has been inconsistently defined as occurring after the procedure or >24 hours after valve implantation. Approximately 2% to 7% of patients (representing up to 30% of all patients with HAVB) experienced delayed HAVB ≥48 hours after TAVR[73,147] (A. Kagase, MD, unpublished data, 2016). Of note, in an analysis of 1064 patients undergoing TAVR, the implantation of a self-expandable prosthesis was not an independent predictor of delayed (ie, nonprocedural) HAVB.[73] Consistent with the timing of HAVB, PPM is mainly performed within 7 days of the procedure (85%–90% of cases),[65,148] with a median time from TAVR to PPM of 3 days in the recent report from the Society of Thoracic Surgeons Transcatheter Valve Therapy registry.[75] Data on very late development of HAVB among patients without conduction disturbances at hospital discharge are scarce; however, this seems to be an uncommon phenomenon. Indeed, Toggweiler et al[73] demonstrated that patients with a normal ECG after TAVR (ie, sinus rhythm, no first-degree AVB, and no LBBB) did not experience delayed HAVB up to 8 days after TAVR, which suggests an exceedingly low risk of very late conduction disturbances among this subgroup. Similarly, Urena et al[41] reported a 99.6% 1-year survival free from PPM for HAVB among patients without new-onset LBBB at hospital discharge compared with 89.1% among their new-onset LBBB counterparts.

Like LBBB, TAVR-induced HAVB may resolve over time. Defining recovered HAVB as a transient block without the need for PPM or as a ventricular pacing rate <1% at 30 days, Kagase et al demonstrated an overall recovery rate of 48% in a registry including Edwards SAPIEN XT recipients, including 5 of 30 patients (17%) with PPM with a ventricular pacing rate <1% (A. Kagase, MD, unpublished data, 2016). This recovery rate was 59% for acute HAVB compared with 25% for delayed HAVB ($P=0.025$). The recovery pattern also differed between acute and delayed HAVB, with a more rapid recovery in those patients presenting with acute HAVB (within 24 hours versus ≥6 days). Several studies have provided insights into the fate of these conduction disturbances

by performing systematic interrogations of the implanted pacemakers.[67,68,149–155] Although heterogeneity in defining pacemaker dependency and in the timing of pacemaker interrogation must be acknowledged, these studies provide further evidence that a significant proportion of conduction disturbances resolve during the follow-up period. Thus, overall pacemaker dependency rates after TAVR ranged from 27% to 68%,[150,151] and rates of intrinsic atrioventricular conduction increased from 25.9% at 7 days to 59.3% at 30 days even among patients with a guideline Class I/II indication for PPM after TAVR.[67] However, some patients not classified as pacemaker dependent had high (>10%–20%) ventricular pacing rates in these studies.[151,154,155] Interestingly, Ramazzina et al[153] showed that pacemaker dependency may depend on the initial indication for the pacemaker because at the 12-month follow-up none of the 17 patients who received a prophylactic PPM for new-onset LBBB with or without first-degree AVB had a pacing rate >1% compared with 83% of pacemaker-dependent patients among those who underwent PPM for HAVB. These observations may have important clinical implications in the management of conduction disturbances after TAVR. However, it should be emphasized that the definition of pacemaker dependency needs to be consistent and may currently be inappropriate because even a <1% ventricular pacing rate may be due to paroxysmal HAVB and would therefore be enough to avoid sudden cardiac death. Only pacemakers allowing the detection of HAVB episodes, which should be carefully programmed to preserve native conduction, may identify true pacemaker dependency after TAVR.

Predictors of Need for PPM After TAVR

Several studies have evaluated factors predicting the need for PPM after TAVR (Table 2 and Table IV in the online-only Data Supplement).[10,34,42,44,45,51,55,61,68,69,75,87,91,111,122,145,146,148,153,156–175] In a recent meta-analysis of 41 studies including 11 210 TAVR recipients, Siontis et al[103] identified male sex, first-degree AVB, left anterior hemiblock, and right bundle-branch block (RBBB) as preprocedural predictors of PPM, whereas the presence of intraoperative heart block and the use of a self-expandable prosthesis were the procedural predictors. In that study, the implantation of a CoreValve system was associated with a 2.5-fold higher risk of PPM, which was confirmed in another systematic review[65] and in the recent report of the Society of Thoracic Surgeons Transcatheter Valve Therapy registry.[75] Baseline RBBB is probably the strongest, most consistent clinical predictor of PPM; it has been identified in more than half of the studies evaluating multivariable predictors of PPM (Table 2 and Table IV in the online-only Data Supplement). Similar to new-onset LBBB, calcifications of the aortic valve,[176] LVOT, and mitral annulus[68,111,156] and the depth of prosthesis implantation[9,111,146,157,158] have been associated with PPM after TAVR. Proposed cutoff values for valve implantation depth predicting new-onset LBBB or PPM were 6.3 mm with the Edwards SAPIEN XT[159] and 7 mm or 25% of the stent frame in the LVOT with the Edwards SAPIEN 3[9,111,159] and ranged from 6 to 7.8 mm with the Corevalve system[146,171] and from 5 to 6.7 mm with the Lotus valve.[61,159] Values of 10% to 15% of valve oversizing have been associated with an increased risk of PPM with first-generation devices.[44,46,159,171]

Table 2. Main Predictors of Permanent Pacemaker Implantation After Transcatheter Aortic Valve Replacement

Variable	Multivariable Odds Ratio*	References
Baseline right bundle-branch block	2.8–46.7	10, 34, 45, 51, 55, 61, 68, 69, 111, 122, 145, 146, 148, 156–170
Implantation of a Medtronic CoreValve (vs Edwards SAPIEN/ SAPIEN XT valves)	2.6–25.7	34, 75, 87, 91, 153, 156, 160, 161, 163, 165
Depth of implantation	1.1–1.5/1 mm	10, 44, 51, 61, 111, 146, 157–159, 169, 171–173
Oversizing/stretching of the aortic annulus/ left ventricular outflow tract	1.02–1.5/1%	42, 44, 87, 122, 148, 159, 166, 171, 174
First-degree atrioventricular block	4.0–11.4	157, 164, 175

*Ranges of odds ratio are from published studies with a multivariable analysis.

Of particular interest concerning the postprocedural management of TAVR recipients are the predictors of delayed HAVB and HAVB recovery. The former was studied by Kagase et al in a series of 696 SAPIEN XT recipients including 48 patients with HAVB after TAVR. A total of 16 patients developed delayed HAVB (>24 hours after TAVR). In univariable analyses, the authors failed to identify meaningful associations between electrocardiographic, imaging, or procedural characteristics and the occurrence of delayed HAVB (A. Kagase, MD, unpublished data, 2016). In a larger series of 1064 patients (45% with self-expandable valves), of whom 71 (6.7%) presented with delayed HAVB (defined as nonperiprocedural), Toggweiler et al[73] identified male sex and the presence of LBBB or RBBB after TAVR as independent predictors of delayed HAVB. Mouillet et al[177] also proposed a post-TAVR QRS duration cutoff of >128 milliseconds as a predictor of the evolution to delayed HAVB. Predictors of persistent HAVB ≥30 days after TAVR have also been studied by Kagase et al, who identified baseline RBBB as an independent risk factor (A. Kagase, MD, unpublished data, 2016), whereas baseline RBBB, PR interval duration before and after TAVR, PR interval change (>28 milliseconds) within 3 days of TAVR, and porcelain aorta have been highlighted as independent predictors of pacemaker dependency at 1 year after TAVR.[150,151] Finally, Rivard et al[178] performed

Circulation. 2017;136:1049–1069. DOI: 10.1161/CIRCULATIONAHA.117.028352

pre and post-TAVR electrophysiological studies in a series of 75 consecutive pacemaker-free TAVR recipients. A total of 30 patients developed new-onset LBBB, whereas 14 patients presented HAVB. The δ-HV interval (ie, HV interval after TAVR minus the HV interval before TAVR) was the only independent predictor of HAVB in the study population and the subgroup of patients with new LBBB, with an optimal cutoff of ≥13 milliseconds. When results of the pre-TAVR electrophysiological study were excluded from the analysis, the only predictor of HAVB was the delta QRS duration (ie, QRS duration after TAVR minus QRS duration before TAVR) with an optimal cutoff of 38 milliseconds. In the subgroup of patients with new-onset LBBB, when data from the pre-TAVR electrophysiological study were excluded, the only predictor of HAVB was the HV interval after TAVR, with an optimal cutoff of ≥65 milliseconds (sensitivity and specificity of 80.0% and 77.8%, respectively).[178]

Clinical Association of PPM With Midterm Mortality After TAVR

Table V in the online-only Data Supplement summarizes the studies reporting adjusted analyses of the possible association between PPM and midterm mortality after TAVR. A meta-analysis including 11 studies and 7032 patients showed no significant association between PPM and 1-year all-cause mortality (risk ratio, 1.03; 95% CI, 0.90–1.18; P=0.64, I^2=0%).[71] However, PPM was associated with a trend toward lower 1-year cardiac mortality (risk ratio, 0.77, 95% CI, 0.58–1.01; P=0.06), which may be explained by a reduction in sudden cardiac/unknown death, as previously suggested by Urena et al[39] in a multicenter registry of 1556 patients. Nonetheless, this meta-analysis did not include the latest report from the Society of Thoracic Surgeons Transcatheter Valve Therapy registry encompassing 9785 TAVR recipients that demonstrated an increased risk in 1-year overall mortality among patients who had PPM after TAVR (adjusted hazard-ratio, 1.31; 95% CI, 1.09–1.58; P=0.003; Figure 4).[75] The poorer evolution of left ventricular ejection fraction among TAVR recipients receiving PPM may also explain such an observation.[39,49,52] Therefore, similar to LBBB, the association of PPM with midterm mortality remains controversial, which may reflect differences in PPM indications, pacemaker dependency, and ventricular pacing rates across studies. Moreover, current TAVR recipients are usually elderly patients with numerous noncardiac comorbidities influencing life expectancy. Therefore, the deleterious effects of long-term right ventricular pacing demonstrated in other settings,[179] may not be readily apparent in the sicker TAVR population with a reduced life expectancy that may limit the appearance of right ventricular pacing–induced left ventricular dysfunction with subsequent clinically apparent heart failure. Indeed, Watanabe et al[78] recently demonstrated an increased midterm mortality (>1 year post-TAVR) among patients with baseline RBBB undergoing PPM, a subset of patients likely to exhibit high rates of ventricular pacing[68,149] (A. Kagase, MD, unpublished data, 2016), supporting the hypothesis that, among TAVR recipients, long-term pacing has detrimental effects, which are expressed at primarily midterm to long-term follow-up.[78] Further studies with longer follow-up and data on ventricular pacing rates are needed to confirm the negative association of PPM with mortality and to elucidate its underlying mechanisms.

MANAGEMENT OF CONDUCTION DISTURBANCES AFTER TAVR

Based on the available evidence, Figure 5 summarizes our proposal for the management of post-TAVR conduction disturbances. The proposed recommendations are based on observational studies, most of them retrospective in nature. To date, no randomized data are available in this field yet. Therefore, any recommendation for the management of conduction disturbances after TAVR should be seen as a suggestion and interpreted with caution. In addition to the cutoffs suggested in Figure 5, particular attention should be paid to the evolution of ECG after TAVR for clinical decision making among TAVR recipients. Thus, a stable ECG for at least 48 hours demonstrates good negative predictive value for delayed HAVB.[73]

Preprocedural Electrocardiographic Monitoring

Up to 30% of patients who will eventually require PPM after TAVR exhibit episodes of HAVB or severe bradycardia diagnosed by 24-hour continuous electrocardiographic monitoring before TAVR, suggesting that the inclusion of a preprocedural period of electrocardiographic monitoring in the TAVR workflow may help to identify patients with conduction abnormalities that are not expected to resolve and could lead to an overall reduction in length of hospital stay.[28] Moreover, the presence of preexisting conduction disturbances, particularly RBBB, should probably drive the decision about transcatheter valve type. Considering the very high rate of HAVB after TAVR in those patients with RBBB receiving some types of transcatheter heart valves,[180] the use of valves with a lower risk of HAVB (eg, balloon-expandable valve or a self-expandable valve with a low risk of conduction disturbances) should probably be prioritized in these patients.

Electrocardiographic Monitoring After TAVR

Regardless of the occurrence of conduction disturbances, maintaining continuous telemetry during the hospi-

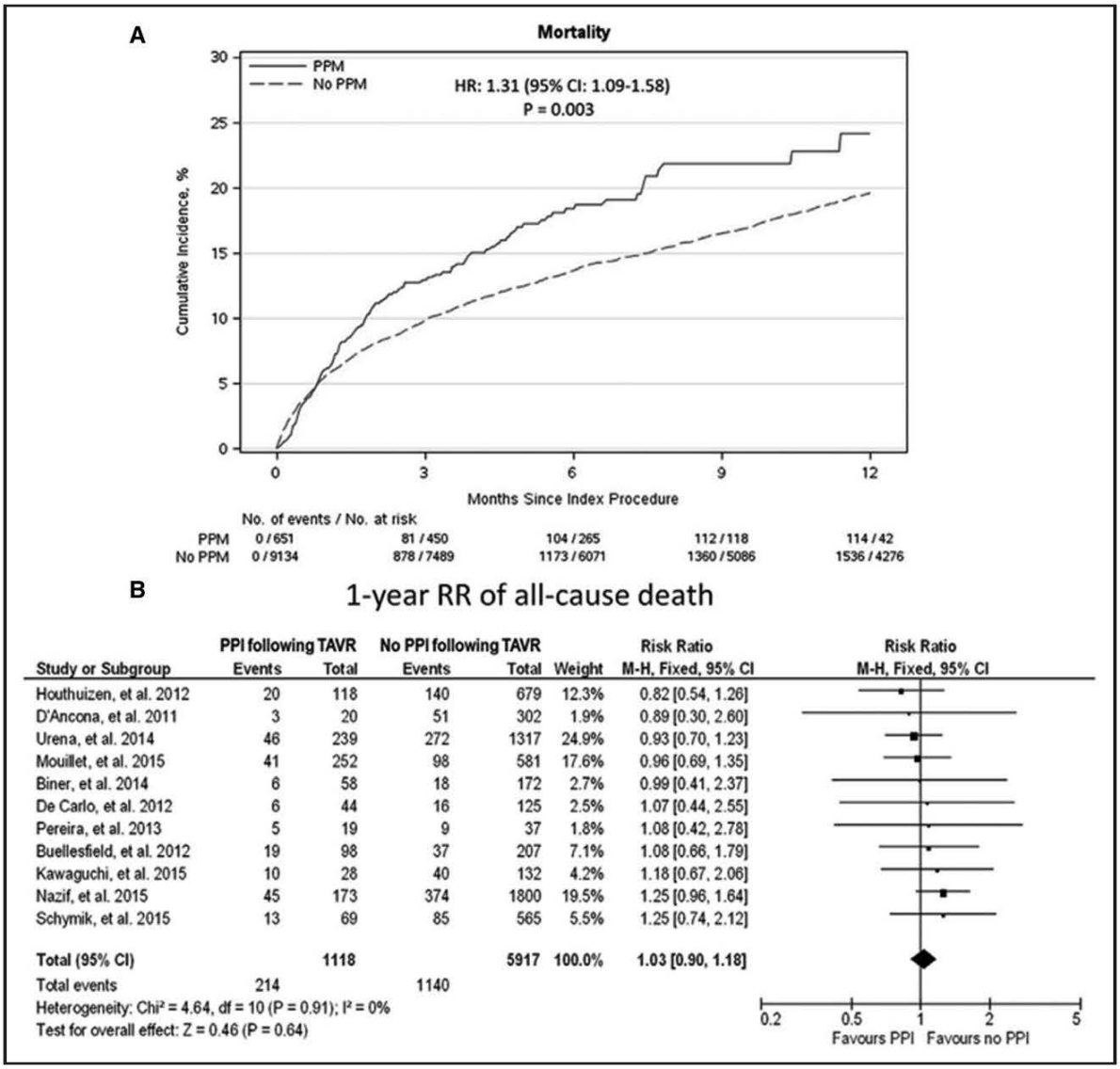

Study or Subgroup	PPI following TAVR Events	Total	No PPI following TAVR Events	Total	Weight	Risk Ratio M-H, Fixed, 95% CI
Houthuizen, et al. 2012	20	118	140	679	12.3%	0.82 [0.54, 1.26]
D'Ancona, et al. 2011	3	20	51	302	1.9%	0.89 [0.30, 2.60]
Urena, et al. 2014	46	239	272	1317	24.9%	0.93 [0.70, 1.23]
Mouillet, et al. 2015	41	252	98	581	17.6%	0.96 [0.69, 1.35]
Biner, et al. 2014	6	58	18	172	2.7%	0.99 [0.41, 2.37]
De Carlo, et al. 2012	6	44	16	125	2.5%	1.07 [0.44, 2.55]
Pereira, et al. 2013	5	19	9	37	1.8%	1.08 [0.42, 2.78]
Buellesfield, et al. 2012	19	98	37	207	7.1%	1.08 [0.66, 1.79]
Kawaguchi, et al. 2015	10	28	40	132	4.2%	1.18 [0.67, 2.06]
Nazif, et al. 2015	45	173	374	1800	19.5%	1.25 [0.96, 1.64]
Schymik, et al. 2015	13	69	85	565	5.5%	1.25 [0.74, 2.12]
Total (95% CI)		**1118**		**5917**	**100.0%**	**1.03 [0.90, 1.18]**
Total events	214		1140			

Heterogeneity: Chi² = 4.64, df = 10 (P = 0.91); I² = 0%
Test for overall effect: Z = 0.46 (P = 0.64)

Figure 4. Association of permanent pacemaker implantation (PPM) with 1-year all-cause mortality after transcatheter aortic valve replacement (TAVR).
Controversies about the association of PPM and midterm all-cause mortality after TAVR. **A**, Kaplan-Meier curve at 1 year and adjusted hazard ratio (HR) associated with PPM for all-cause mortality in the most recent report of the Society of Thoracic Surgeons Transcatheter Valve Therapy registry encompassing 9785 patients, suggesting an increased mortality rate after PPM. **B**, Results of a recent meta-analysis of 11 prior studies including a total of 7032 patients that demonstrated no significant difference in 1-year all-cause mortality between patients who underwent PPM for a clinical indication and patients who did not required PPM after TAVR. CI indicates confidence interval; PPI, permanent pacemaker implantationr; and RR, risk ratio. Reproduced from Fadahunsi et al[75] with permission from the publisher. Copyright © 2016, American College of Cardiology Foundation. Also reproduced from Regueiro et al[71] with permission from the publisher. Copyright © 2016 American Heart Association.

talization period appears to be a simple and inexpensive measure for detecting bradyarrythmias and tachyarrythmias such as new-onset atrial fibrillation, which may increase the risk of potentially preventable thromboembolic events.[181,182] The telemetry can be carried out in a conventional ward unless hospitalization in an intensive care unit is clinically indicated for other reasons.

Management of New-Onset LBBB

The management of new-onset LBBB after TAVR remains highly controversial considering the current lack of specific guidelines (Figure 5A).[144] The presence of new-onset persistent LBBB should prevent early discharge (within 24–48 hours after TAVR), and continuous electrocardiographic monitoring for at

Circulation. 2017;136:1049–1069. DOI: 10.1161/CIRCULATIONAHA.117.028352

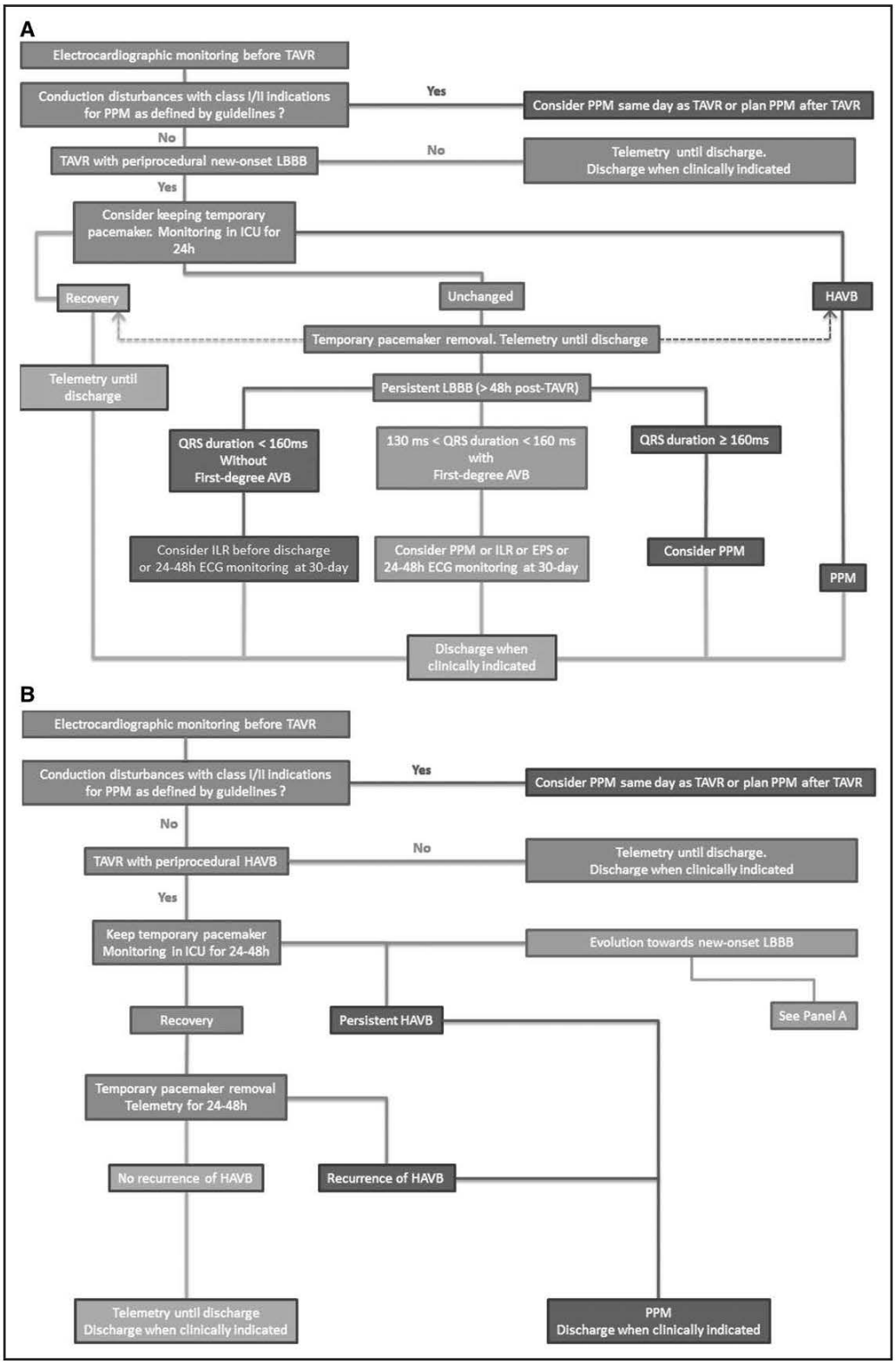

Figure 5. Strategies for the management of conduction disturbances after transcatheter aortic valve replacement (TAVR).

Proposal based on current literature for the management of new-onset left bundle-branch block (LBBB; **A**) and high-degree atrioventricular block (HABV; **B**) during TAVR. Telemetry should be carried out in a conventional ward unless (*Continued*)

least 48 to 72 hours seems appropiate in these cases because of the increased risk of early progression to HAVB.[40,47,73,75,145,148] For these reasons, keeping the temporary pacemaker with intensive care monitoring for 24 hours seems reasonable in these cases.

The progression of LBBB to HAVB should trigger the indication for PPM. However, LBBB will persist in most patients with no further changes (progression or regression) during the hospitalization period.[40,41,47,50] In these cases, we suggest a careful evaluation of the ECG before hospital discharge. No specific measures have been proven effective for the management of these patients. Among others, the exact role of electrophysiological studies and implantable loop recorders in such cases remains unclear. The ongoing MARE study (Ambulatory Electrocardiographic Monitoring for the Detection of High-Degree Atrio-Ventricular Block in Patients With New-Onset Persistent Left Bundle-Branch Block After Transcatheter Aortic Valve Implantation; NCT02153307) and the Assessment of the Prognosis of Persistent Left Bundle-Branch Block (LBBB) After Transcatheter Aortic Valve Implantation (TAVI) by an Electrophysiological and Remote Monitoring Risk Adapted Algorithm study (NCT02482844), among other awaited studies (Table VI in the online-only Data Supplement), will likely shed more light on the natural history of conduction disturbances after TAVR. Meanwhile, and considering the higher risk of HAVB within the months after the procedure in patients with new-onset persistent LBBB,[40,41,71,74] some remote monitoring (implantable loop recorder or 24- to 48-hour electrocardiographic monitoring at 30-day follow-up) may be advisable. This would also apply to those patients with LBBB and first-degree AVB, for whom an electrophysiological study or even PPM may be an option.[178,183] However, the level of evidence for any of these measures remains low.

Particular attention should be paid to those patients with new-onset LBBB and a prolonged QRS duration (particularly >160 milliseconds), which has been associated with an increased risk of overall mortality and sudden cardiac death.[30,35,40,41,50] Thus, we think that this subgroup may have a reasonable indication for PPM. Other prophylactic indications for PPM in the context of new-onset LBBB lack evidence and may lead to an excessive and inappropriate number of PPM. However, further studies are warranted.

Management of HAVB

Similar to the cardiac surgery field, the latest European Society of Cardiology guidelines[144] recommend a period of clinical observation and electrocardiographic monitoring for up to 7 days before PPM in patients with HAVB to determine whether rhythm disturbances after TAVR are transient or permanent (Class I, Level of Evidence C). This watchful period may be shortened only in cases of complete AVB with slow escape rhythm and in cases of HAVB occurring within 24 hours of TAVR and persisting for 48 hours.[144] This contrasts with the observation that ≈50% of patients requiring PPM after TAVR receive this therapy within the 3 days after the procedure.[75] As previously discussed, such a conservative strategy is supported by observations from studies showing the transiency of HAVB in a sizeable proportion of patients and the increased risk of impaired left ventricular remodeling, repeat hospitalization for heart failure, and perhaps ultimately an increased risk of late mortality in pacemaker recipients.[75,184] Nonetheless, a prolonged observation period often implies bedrest with the use of a temporary pacemaker and its inherent risks (thromboembolism, cardiac perforation). Thus, the safety, efficacy, and cost-effectiveness and the impact on functional recovery among aging patients after such a strategy remain largely unknown. Furthermore, it should be highlighted that this watchful period competes with the current trends toward shortened length of stay and even sometimes pacemaker reimbursement patterns. Indeed, some teams recently demonstrated that performing TAVR without intensive care unit admission and adopting a strategy of early discharge was feasible and did not result in an increased risk of rehospitalization or sudden cardiac death,[143,185] suggesting that 24 hours of electrocardiographic monitoring may be sufficient in selected patients. Moreover, performing PPM the same day as TAVR may be a safe option, allowing rapid patient mobilization.[186] Therefore, we think that an observation period of 24 to 48 hours after the HAVB episode appears to be a reasonable compromise, especially in case of intraprocedural HAVB, which is less likely to recover >24 hours after its onset (Figure 5B). A more aggressive strategy of very early PPM (eg, at the time of the procedure), which may be appealing to reduce costs at the short term, would probably be futile in a significant proportion of patients with conduction disturbances that would eventually recover, further jeopardizing the midterm to long-term cost-effectiveness of TAVR.[187] The potential complications associated with PPM should also be taken into account. A recent prospective study demonstrated rates of 12.4% and 9.2% of short- and long-term complications after

Figure 5 Continued. hospitalization in the intensive care unit (ICU) is clinically indicated for other reasons. The recommendation of continuous monitoring until discharge is for detecting not only bradyarrythmias but also tachyarrythmias such as new-onset atrial fibrillation, which may increase the risk of potentially preventable thromboembolic events. AVB indicates atrioventricular block; EPS, electrophysiological study; ILR, implantable loop recorder; and PPM, permanent pacemaker implantation.

Circulation. 2017;136:1049–1069. DOI: 10.1161/CIRCULATIONAHA.117.028352

PPM, respectively.[188] Lead-related complications occurred in 5.5% of patients, whereas 2.2% of patients had pneumothorax within 2 months of PPM. After lead complications, pocket hematoma was the most frequent complication, affecting 2.9% of patients overall. Indeed, dual antiplatelet therapy, a common antithrombotic strategy after TAVR, is associated with a 4-fold hazard of bleeding during the perioperative period,[189] suggesting that TAVR recipients might be at higher risk of complications after PPM. Therefore, conduction disturbances should be considered when antithrombotic therapies are prescribed after TAVR. Whenever possible, introduction of clopidogrel or oral anticoagulation should be postponed until PPM has been performed or deemed unnecessary.

Last, patients with transient HAVB regressing toward new-onset persistent LBBB should be managed as previously discussed (Figure 5A).

Choice of Pacemaker

Algorithms allowing the preservation of spontaneous atrioventricular conduction should be used in patients with paroxysmal HAVB to minimize long-term right ventricular pacing. In addition, resynchronization therapy should be considered in patients with HAVB, a sufficient life expectancy, a high (predictable >40%) percentage of ventricular pacing, and reduced left ventricular ejection fraction (<50%).[179,190] Finally, some reports have shown the beneficial effects of resynchronization therapy in patients with a low left ventricular ejection fraction and persistent LBBB after TAVR.[191,192] Resynchronization therapy may be reasonable among patients with preexisting left ventricular dysfunction and new-onset LBBB persisting at 30 days after TAVR, which might put these patients at higher mortality and morbidity risk. Currently, there are no data on the potential benefits of leadless pacemaker among TAVR recipients. Future studies should aim at defining predictors of low pacing burden, which might help delineate the optimal indication of these devices after TAVR.

CONCLUSIONS

A summary of what is known and what we need to know about conduction disturbances post-TAVR is shown in Table 3.

Conduction disturbances remain a common complication of TAVR that may impair patients' prognosis. This complication is associated with left ventricular dyssynchrony, resulting in a poorer left ventricular function recovery and a higher rate of repeat hospitalization. New-onset LBBB after TAVR is associated with an increased risk of HAVB and sudden cardiac death that may be mitigated by PPM within 30 days after TAVR. However, PPM may also have a deleterious effect on left ventricular ejection fraction and increase the risk of heart failure at the midterm to long-term follow-up. The main risk factors of conduction disturbances include the presence of baseline RBBB, the use of some self-expanding valve systems, and the depth of prosthesis implantation within the LVOT. The use of newer-generation transcatheter valve devices does not seem to reduce the risk of conduction disturbances. Although the selection of the most appropriate device is influenced by numerous factors, including the degree

Table 3. Summary of Evidence From the Literature and Unmet Needs in the Field of Post–Transcatheter Aortic Valve Replacement Conduction Disturbances

What Is Known	What We Need to Know
Conduction disturbances (LBBB and HAVB requiring pacemaker implantation) are the most frequent complication of TAVR.	The optimal timing for temporary pacing and PPM (eg, minimal watchful period) in the presence of HAVB after TAVR.
The main factors determining the occurrence of conduction disturbances after TAVR are a low (more ventricular) transcatheter valve placement, the use of some self-expandable and mechanically expanded valves, and the presence of RBBB before the procedure. Most newer-generation transcatheter valves failed to reduce the incidence of conduction disturbances after TAVR.	The factors determining early and late progression/regression of conduction disturbances after TAVR.
Most conduction disturbances occur during the TAVR procedure or within hours after the procedure. A significant proportion of conduction disturbances (especially LBBB) will be transient, particularly with the use of balloon-expandable valves.	The midterm and long-term clinical impact of transient HAVB according to its timing of occurrence (during the procedure vs after the procedure).
Persistent LBBB at hospital discharge is associated with a negative effect on left ventricular function and a higher risk of HAVB requiring PPM at follow-up.	The clinical impact (mortality, heart failure) of LBBB after TAVR on midterm and long-term clinical outcomes (controversial results to date).
PPM after TAVR is not associated with an increased cardiac mortality rate at 1-y follow-up.	The long-term clinical impact of PPM after TAVR.
	Role of "prophylactic" PPM in some cases of LBBB after TAVR (eg, those with larger QRS, first-degree AVB).
	Role of resynchronization therapy in patients with reduced ventricular function and new persistent LBBB after TAVR.

AVB indicates atrioventricular block; HAVB, high-degree atrioventricular block; LBBB, left bundle-branch block; PPM, permanent pacemaker implantation; RBBB, right bundle-branch block; and TAVR, transcatheter aortic valve replacement.

of native valve calcification or the risk of coronary obstruction, current data suggest that the use of a balloon-expandable valve or a self-expandable valve with a lower risk of conduction disturbances should be considered in patients at high risk of PPM (eg, those with RBBB at baseline). Limiting the indications of PPM to those strictly recommended in guidelines also reduces the need for PPM, and the risks and benefits of implementing a more prolonged period of electrocardiographic monitoring in the TAVR workflow need to be adequately assessed in prospective studies. Moreover, further studies are needed to better elucidate the factors associated with the development and recovery of conduction disturbances after TAVR, the optimal timing of PPM, and the management of the challenging group of patients with new-onset LBBB.

DISCLOSURES

Dr Rodés-Cabau has received research grants from Edwards Lifesciences and Medtronic and holds the Canadian Research Chair "Fondation Famille Jacques Larivière" for the Development of Structural Heart Disease Interventions. Dr Auffret received fellowship support from the Fédération Française de Cardiologie and research grants from Abbott, Edwards Lifescience, Medtronic, Biosensors, Terumo, and Boston Scientific. The other authors report no conflicts.

AFFILIATIONS

From University Hospital Pontchaillou, Cardiology and Vascular Disease Department, CIC-IT 804, Rennes 1 University, Signal and Image Processing Laboratory (LTSI), INSERM U1099, France (V.A.); Quebec Heart and Lung Institute, Laval University, Quebec City, Canada (V.A., R.P., C.C., T.R.-G., F.P., J.R.,-C.); and Bichat-Claude Bernard University Hospital, Paris, France (M.U.).

FOOTNOTES

The online-only Data Supplement is available with this article at http://circ.ahajournals.org/lookup/suppl/doi:10.1161/CIRCULATIONAHA.117.028352/-/DC1.

Circulation is available at http://circ.ahajournals.org.

REFERENCES

1. Leon MB, Smith CR, Mack M, Miller DC, Moses JW, Svensson LG, Tuzcu EM, Webb JG, Fontana GP, Makkar RR, Brown DL, Block PC, Guyton RA, Pichard AD, Bavaria JE, Herrmann HC, Douglas PS, Petersen JL, Akin JJ, Anderson WN, Wang D, Pocock S; PARTNER Trial Investigators. Transcatheter aortic-valve implantation for aortic stenosis in patients who cannot undergo surgery. *N Engl J Med*. 2010;363:1597–1607. doi: 10.1056/NEJMoa1008232.
2. Smith CR, Leon MB, Mack MJ, Miller DC, Moses JW, Svensson LG, Tuzcu EM, Webb JG, Fontana GP, Makkar RR, Williams M, Dewey T, Kapadia S, Babaliaros V, Thourani VH, Corso P, Pichard AD, Bavaria JE, Herrmann HC, Akin JJ, Anderson WN, Wang D, Pocock SJ; PARTNER Trial Investigators. Transcatheter versus surgical aortic-valve replacement in high-risk patients. *N Engl J Med*. 2011;364:2187–2198. doi: 10.1056/NEJMoa1103510.
3. Nishimura RA, Otto CM, Bonow RO, Carabello BA, Erwin JP 3rd, Guyton RA, O'Gara PT, Ruiz CE, Skubas NJ, Sorajja P, Sundt TM 3rd, Thomas JD, American College of Cardiology/American Heart Association Task Force on Practice Guidelines. 2014 AHA/ACC guideline for the management of patients with valvular heart disease: executive summary: a report of the American College of Cardiology/American Heart Association Task Force on Practice Guidelines. *J Am Coll Cardiol*. 2014;63:2438–2488. doi: 10.1016/j.jacc.2014.02.537.
4. Reinöhl J, Kaier K, Reinecke H, Schmoor C, Frankenstein L, Vach W, Cribier A, Beyersdorf F, Bode C, Zehender M. Effect of availability of transcatheter aortic-valve replacement on clinical practice. *N Engl J Med*. 2015;373:2438–2447. doi: 10.1056/NEJMoa1500893.
5. Vahl TP, Kodali SK, Leon MB. Transcatheter aortic valve replacement 2016: a modern-day "through the looking-glass" adventure. *J Am Coll Cardiol*. 2016;67:1472–1487. doi: 10.1016/j.jacc.2015.12.059.
6. Babaliaros V, Devireddy C, Lerakis S, Leonardi R, Iturra SA, Mavromatis K, Leshnower BG, Guyton RA, Kanitkar M, Keegan P, Simone A, Stewart JP, Ghasemzadeh N, Block P, Thourani VH. Comparison of transfemoral transcatheter aortic valve replacement performed in the catheterization laboratory (minimalist approach) versus hybrid operating room (standard approach): outcomes and cost analysis. *JACC Cardiovasc Interv*. 2014;7:898–904. doi: 10.1016/j.jcin.2014.04.005.
7. Leon MB, Smith CR, Mack MJ, Makkar RR, Svensson LG, Kodali SK, Thourani VH, Tuzcu EM, Miller DC, Herrmann HC, Doshi D, Cohen DJ, Pichard AD, Kapadia S, Dewey T, Babaliaros V, Szeto WY, Williams MR, Kereiakes D, Zajarias A, Greason KL, Whisenant BK, Hodson RW, Moses JW, Trento A, Brown DL, Fearon WF, Pibarot P, Hahn RT, Jaber WA, Anderson WN, Alu MC, Webb JG; PARTNER 2 Investigators. Transcatheter or surgical aortic-valve replacement in intermediate-risk patients. *N Engl J Med*. 2016;374:1609–1620. doi: 10.1056/NEJMoa1514616.
8. Thourani VH, Kodali S, Makkar RR, Herrmann HC, Williams M, Babaliaros V, Smalling R, Lim S, Malaisrie SC, Kapadia S, Szeto WY, Greason KL, Kereiakes D, Ailawadi G, Whisenant BK, Devireddy C, Leipsic J, Hahn RT, Pibarot P, Weissman NJ, Jaber WA, Cohen DJ, Suri R, Tuzcu EM, Svensson LG, Webb JG, Moses JW, Mack MJ, Miller DC, Smith CR, Alu MC, Parvataneni R, D'Agostino RB Jr, Leon MB. Transcatheter aortic valve replacement versus surgical valve replacement in intermediate-risk patients: a propensity score analysis. *Lancet*. 2016;387:2218–2225. doi: 10.1016/S0140-6736(16)30073-3.
9. De Torres-Alba F, Kaleschke G, Diller GP, Vormbrock J, Orwat S, Radke R, Reinke F, Fischer D, Reinecke H, Baumgartner H. Changes in the pacemaker rate after transition from Edwards SAPIEN XT to SAPIEN 3 transcatheter aortic valve implantation: the critical role of valve implantation height. *JACC Cardiovasc Interv*. 2016;9:805–813. doi: 10.1016/j.jcin.2015.12.023.
10. Husser O, Pellegrini C, Kessler T, Burgdorf C, Thaller H, Mayr NP, Kasel AM, Kastrati A, Schunkert H, Hengstenberg C. Predictors of permanent pacemaker implantations and new-onset conduction abnormalities with the SAPIEN 3 balloon-expandable transcatheter heart valve. *JACC Cardiovasc Interv*. 2016;9:244–254. doi: 10.1016/j.jcin.2015.09.036.
11. Meredith Am IT, Walters DL, Dumonteil N, Worthley SG, Tchétché D, Manoharan G, Blackman DJ, Rioufol G, Hildick-Smith D, Whitbourn RJ, Lefèvre T, Lange R, Müller R, Redwood S, Allocco DJ, Dawkins KD. Transcatheter aortic valve replacement for severe symptomatic aortic stenosis using a repositionable valve system: 30-day primary endpoint results from the REPRISE II study. *J Am Coll Cardiol*. 2014;64:1339–1348. doi: 10.1016/j.jacc.2014.05.067.
12. Schofer J, Colombo A, Klugmann S, Fajadet J, DeMarco F, Tchétché D, Maisano F, Bruschi G, Latib A, Bijuklic K, Weissman N, Low R, Thomas M, Young C, Redwood S, Mullen M, Yap J, Grube E, Nickenig G, Sinning JM, Hauptmann KE, Friedrich I, Lauterbach M, Schmoeckel M, Davidson C, Lefevre T. Prospective multicenter evaluation of the Direct Flow Medical transcatheter aortic valve. *J Am Coll Cardiol*. 2014;63:763–768. doi: 10.1016/j.jacc.2013.10.013.
13. Silaschi M, Treede H, Rastan AJ, Baumbach H, Beyersdorf F, Kappert U, Eichinger W, Rüter F, de Kroon TL, Lange R, Ensminger S, Wendler O. The JUPITER registry: 1-year results of transapical aortic valve implantation using a second-generation transcatheter heart valve in patients with aortic stenosis. *Eur J Cardiothorac Surg*. 2016;50:874–881. doi: 10.1093/ejcts/ezw170.
14. Seiffert M, Conradi L, Kloth B, Koschyk D, Schirmer J, Schnabel RB, Blankenberg S, Reichenspurner H, Diemert P, Treede H. Single-centre experience with next-generation devices for transapical aortic valve implantation. *Eur J Cardiothorac Surg*. 2015;47:39–45. doi: 10.1093/ejcts/ezu041.

15. Elder DH, Lang CC, Choy AM. Pacing-induced heart disease: understanding the pathophysiology and improving outcomes. *Expert Rev Cardiovasc Ther*. 2011;9:877–886. doi: 10.1586/erc.11.82.
16. Zhang ZM, Rautaharju PM, Soliman EZ, Manson JE, Cain ME, Martin LW, Bavry AA, Mehta L, Vitolins M, Prineas RJ. Mortality risk associated with bundle branch blocks and related repolarization abnormalities (from the Women's Health Initiative [WHI]). *Am J Cardiol*. 2012;110:1489–1495. doi: 10.1016/j.amjcard.2012.06.060.
17. Zannad F, Huvelle E, Dickstein K, van Veldhuisen DJ, Stellbrink C, Køber L, Cazeau S, Ritter P, Maggioni AP, Ferrari R, Lechat P. Left bundle branch block as a risk factor for progression to heart failure. *Eur J Heart Fail*. 2007;9:7–14. doi: 10.1016/j.ejheart.2006.04.011.
18. Zhou Q, Henein M, Coats A, Gibson D. Different effects of abnormal activation and myocardial disease on left ventricular ejection and filling times. *Heart*. 2000;84:272–276.
19. Urena M, Rodés-Cabau J. Conduction abnormalities: the true Achilles' heel of transcatheter aortic valve replacement? *JACC Cardiovasc Interv*. 2016;9:2217–2219. doi: 10.1016/j.jcin.2016.09.040.
20. Young Lee M, Chilakamarri Yeshwant S, Chava S, Lawrence Lustgarten D. Mechanisms of heart block after transcatheter aortic valve replacement: cardiac anatomy, clinical predictors and mechanical factors that contribute to permanent pacemaker implantation. *Arrhythm Electrophysiol Rev*. 2015;4:81–85. doi: 10.15420/aer.2015.04.02.81.
21. Piazza N, de Jaegere P, Schultz C, Becker AE, Serruys PW, Anderson RH. Anatomy of the aortic valvar complex and its implications for transcatheter implantation of the aortic valve. *Circ Cardiovasc Interv*. 2008;1:74–81. doi: 10.1161/CIRCINTERVENTIONS.108.780858.
22. van der Boon RM, Nuis RJ, Van Mieghem NM, Jordaens L, Rodés-Cabau J, van Domburg RT, Serruys PW, Anderson RH, de Jaegere PP. New conduction abnormalities after TAVI–frequency and causes. *Nat Rev Cardiol*. 2012;9:454–463. doi: 10.1038/nrcardio.2012.58.
23. Moreno R, Dobarro D, López de Sá E, Prieto M, Morales C, Calvo Orbe L, Moreno-Gomez I, Filgueiras D, Sanchez-Recalde A, Galeote G, Jiménez-Valero S, Lopez-Sendon JL. Cause of complete atrioventricular block after percutaneous aortic valve implantation: insights from a necropsy study. *Circulation*. 2009;120:e29–e30. doi: 10.1161/CIRCULATIONAHA.109.849281.
24. Kawashima T, Sato F. Visualizing anatomical evidences on atrioventricular conduction system for TAVI. *Int J Cardiol*. 2014;174:1–6. doi: 10.1016/j.ijcard.2014.04.003.
25. Hamdan A, Guetta V, Klempfner R, Konen E, Raanani E, Glikson M, Goitein O, Segev A, Barbash I, Fefer P, Spiegelstein D, Goldenberg I, Schwammenthal E. Inverse relationship between membranous septal length and the risk of atrioventricular block in patients undergoing transcatheter aortic valve implantation. *JACC Cardiovasc Interv*. 2015;8:1218–1228. doi: 10.1016/j.jcin.2015.05.010.
26. Yater WM, Cornell VH. Heart block due to calcareous lesions of the bundle of His: review and report of a case with detailed histopathologic study. *Ann Intern Med*. 1935;8:777–789.
27. MacMillan RM, Demorizi NM, Gessman LJ, Maranhao V. Correlates of prolonged HV conduction in aortic stenosis. *Am Heart J*. 1985;110(pt 1):56–60.
28. Urena M, Hayek S, Cheema AN, Serra V, Amat-Santos IJ, Nombela-Franco L, Ribeiro HB, Allende R, Paradis JM, Dumont E, Thourani VH, Babaliaros V, Francisco Pascual J, Cortés C, Del Blanco BG, Philippon F, Lerakis S, Rodés-Cabau J. Arrhythmia burden in elderly patients with severe aortic stenosis as determined by continuous electrocardiographic recording: toward a better understanding of arrhythmic events after transcatheter aortic valve replacement. *Circulation*. 2015;131:469–477. doi: 10.1161/CIRCULATIONAHA.114.011929.
29. Bax JJ, Delgado V, Bapat V, Baumgartner H, Collet JP, Erbel R, Hamm C, Kappetein AP, Leipsic J, Leon MB, MacCarthy P, Piazza N, Pibarot P, Roberts WC, Rodés-Cabau J, Serruys PW, Thomas M, Vahanian A, Webb J, Zamorano JL, Windecker S. Open issues in transcatheter aortic valve implantation, part 2: procedural issues and outcomes after transcatheter aortic valve implantation. *Eur Heart J*. 2014;35:2639–2654. doi: 10.1093/eurheartj/ehu257.
30. Urena M, Webb JG, Eltchaninoff H, Muñoz-García AJ, Bouleti C, Tamburino C, Nombela-Franco L, Nietlispach F, Moris C, Ruel M, Dager AE, Serra V, Cheema AN, Amat-Santos IJ, de Brito FS, Lemos PA, Abizaid A, Sarmento-Leite R, Ribeiro HB, Dumont E, Barbanti M, Durand E, Alonso Briales JH, Himbert D, Vahanian A, Immè S, Garcia E, Maisano F, del Valle R, Benitez LM, García del Blanco B, Gutiérrez H, Perin MA, Siqueira D, Bernardi G, Philippon F, Rodés-Cabau J. Late cardiac death in patients undergoing transcatheter aortic valve replacement: incidence and predictors of advanced heart failure and sudden cardiac death. *J Am Coll Cardiol*. 2015;65:437–448. doi: 10.1016/j.jacc.2014.11.027.
31. Regeer MV, Merkestein LR, de Weger A, Kamperidis V, van der Kley F, van Rosendael PJ, Marsan NA, Klautz RJ, Schalij MJ, Bax JJ, Delgado V. Left bundle branch block after sutureless, transcatheter, and stented biological aortic valve replacement for aortic stenosis. *EuroIntervention*. 2017;12:1660–1666. doi: 10.4244/EIJ-D-15-00256.
32. Franzoni I, Latib A, Maisano F, Costopoulos C, Testa L, Figini F, Giannini F, Basavarajaiah S, Mussardo M, Slavich M, Taramasso M, Cioni M, Longoni M, Ferrarello S, Radinovic A, Sala S, Ajello S, Sticchi A, Giglio M, Agricola E, Chieffo A, Montorfano M, Alfieri O, Colombo A. Comparison of incidence and predictors of left bundle branch block after transcatheter aortic valve implantation using the CoreValve versus the Edwards valve. *Am J Cardiol*. 2013;112:554–559. doi: 10.1016/j.amjcard.2013.04.026.
33. Aktug Ö, Dohmen G, Brehmer K, Koos R, Altiok E, Deserno V, Herpertz R, Autschbach R, Marx N, Hoffmann R. Incidence and predictors of left bundle branch block after transcatheter aortic valve implantation. *Int J Cardiol*. 2012;160:26–30. doi: 10.1016/j.ijcard.2011.03.004.
34. Schymik G, Tzamalis P, Bramlage P, Heimeshoff M, Würth A, Wondraschek R, Gonska BD, Posival H, Schmitt C, Schröfel H, Luik A. Clinical impact of a new left bundle branch block following TAVI implantation: 1-year results of the TAVIK cohort. *Clin Res Cardiol*. 2015;104:351–362. doi: 10.1007/s00392-014-0791-2.
35. Houthuizen P, Van Garsse LA, Poels TT, de Jaegere P, van der Boon RM, Swinkels BM, Ten Berg JM, van der Kley F, Schalij MJ, Baan J Jr, Cocchieri R, Brueren GR, van Straten AH, den Heijer P, Bentala M, van Ommen V, Kluin J, Stella PR, Prins MH, Maessen JG, Prinzen FW. Left bundle-branch block induced by transcatheter aortic valve implantation increases risk of death. *Circulation*. 2012;126:720–728. doi: 10.1161/CIRCULATIONAHA.112.101055.
36. Bernardi FL, Ribeiro HB, Carvalho LA, Sarmento-Leite R, Mangione JA, Lemos PA, Abizaid A, Grube E, Rodes Cabau J, De Brito FS Jr. Direct transcatheter heart valve implantation versus implantation with balloon predilatation: insights from the Brazilian TAVR Registry. *Circ Cardiovasc Interv*. 2016;9:e003605. doi: 10.1161/CIRCINTERVENTIONS.116.003605.
37. Houthuizen P, van der Boon RM, Urena M, Van Mieghem N, Brueren GB, Poels TT, Van Garsse LA, Rodés-Cabau J, Prinzen FW, de Jaegere P. Occurrence, fate and consequences of ventricular conduction abnormalities after transcatheter aortic valve implantation. *EuroIntervention*. 2014;9:1142–1150. doi: 10.4244/EIJV9I10A194.
38. Laynez A, Ben-Dor I, Barbash IM, Hauville C, Sardi G, Maluenda G, Xue Z, Satler LF, Pichard AD, Lindsay J, Waksman R. Frequency of conduction disturbances after Edwards SAPIEN percutaneous valve implantation. *Am J Cardiol*. 2012;110:1164–1168. doi: 10.1016/j.amjcard.2012.05.057.
39. Urena M, Webb JG, Tamburino C, Muñoz-García AJ, Cheema A, Dager AE, Serra V, Amat-Santos IJ, Barbanti M, Immè S, Briales JH, Benitez LM, Al Lawati H, Cucalon AM, García Del Blanco B, López J, Dumont E, Delarochellière R, Ribeiro HB, Nombela-Franco L, Philippon F, Rodés-Cabau J. Permanent pacemaker implantation after transcatheter aortic valve implantation: impact on late clinical outcomes and left ventricular function. *Circulation*. 2014;129:1233–1243. doi: 10.1161/CIRCULATIONAHA.113.005479.
40. Nazif TM, Williams MR, Hahn RT, Kapadia S, Babaliaros V, Rodés-Cabau J, Szeto WY, Jilaihawi H, Fearon WF, Dvir D, Dewey TM, Makkar RR, Xu K, Dizon JM, Smith CR, Leon MB, Kodali SK. Clinical implications of new-onset left bundle branch block after transcatheter aortic valve replacement: analysis of the PARTNER experience. *Eur Heart J*. 2014;35:1599–1607. doi: 10.1093/eurheartj/eht376.
41. Urena M, Webb JG, Cheema A, Serra V, Toggweiler S, Barbanti M, Cheung A, Ye J, Dumont E, DeLarochellière R, Doyle D, Al Lawati HA, Peterson M, Chisholm R, Igual A, Ribeiro HB, Nombela-Franco L, Philippon F, Garcia del Blanco B, Rodés-Cabau J. Impact of new-onset persistent left bundle branch block on late clinical outcomes in patients undergoing transcatheter aortic valve implantation with a balloon-expandable valve. *JACC Cardiovasc Interv*. 2014;7:128–136. doi: 10.1016/j.jcin.2013.08.015.
42. Nishiyama T, Tanosaki S, Tanaka M, Yanagisawa R, Yashima F, Kimura T, Arai T, Tsuruta H, Murata M, Aizawa Y, Kohno T, Maekawa Y, Hayashida K, Takatsuki S, Fukuda K. Predictive factor and clinical consequence of left bundle-branch block after a transcatheter aortic valve implantation. *Int J Cardiol*. 2017;227:25–29. doi: 10.1016/j.ijcard.2016.11.063.
43. Jochheim D, Zadrozny M, Theiss H, Baquet M, Maimer-Rodrigues F, Bauer A, Lange P, Greif M, Kupatt C, Hausleiter J, Hagl C, Massberg S, Mehilli J. Aortic regurgitation with second versus third-generation balloon-expandable prostheses in patients undergoing transcatheter aortic valve implantation. *EuroIntervention*. 2015;11:214–220. doi: 10.4244/EIJV11I2A40.

44. Katsanos S, van Rosendael P, Kamperidis V, van der Kley F, Joyce E, Debonnaire P, Karalis I, Bax JJ, Marsan NA, Delgado V. Insights into new-onset rhythm conduction disorders detected by multi-detector row computed tomography after transcatheter aortic valve implantation. *Am J Cardiol*. 2014;114:1556–1561. doi: 10.1016/j.amjcard.2014.08.020.
45. van der Boon RM, Houthuizen P, Urena M, Poels TT, van Mieghem NM, Brueren GR, Altintas S, Nuis RJ, Serruys PW, van Garsse LA, van Domburg RT, Cabau JR, de Jaegere PP, Prinzen FW. Trends in the occurrence of new conduction abnormalities after transcatheter aortic valve implantation. *Catheter Cardiovasc Interv*. 2015;85:E144–E152. doi: 10.1002/ccd.25765.
46. Hein-Rothweiler R, Jochheim D, Rizas K, Egger A, Theiss H, Bauer A, Massberg S, Mehilli J. Aortic annulus to left coronary distance as a predictor for persistent left bundle branch block after TAVI. *Catheter Cardiovasc Interv*. 2017;89:E162–E168. doi: 10.1002/ccd.26503.
47. Urena M, Mok M, Serra V, Dumont E, Nombela-Franco L, DeLarochellière R, Doyle D, Igual A, Larose E, Amat-Santos I, Côté M, Cuéllar H, Pibarot P, de Jaegere P, Philippon F, Garcia del Blanco B, Rodés-Cabau J. Predictive factors and long-term clinical consequences of persistent left bundle branch block following transcatheter aortic valve implantation with a balloon-expandable valve. *J Am Coll Cardiol*. 2012;60:1743–1752. doi: 10.1016/j.jacc.2012.07.035.
48. Muñoz-García AJ, del Valle R, Trillo-Nouche R, Elízaga J, Gimeno F, Hernández-Antolín R, Teles R, de Gama Ribeiro V, Molina E, Cequier A, Urbano-Carrillo C, Cruz-González I, Payaslian M, Patricio L, Sztejfman M, Iñiguez A, Rodríguez V, Scuteri A, Caorsi C, López-Otero D, Avanzas P, Alonso-Briales JH, Hernández-García JM, Morís C; Ibero-American Registry Investigators. The Ibero-American transcatheter aortic valve implantation registry with the CoreValve prosthesis: early and long-term results. *Int J Cardiol*. 2013;169:359–365. doi: 10.1016/j.ijcard.2013.09.006.
49. Weber M, Brüggemann E, Schueler R, Momcilovic D, Sinning JM, Ghanem A, Werner N, Grube E, Schiller W, Mellert F, Welz A, Nickenig G, Hammerstingl C. Impact of left ventricular conduction defect with or without need for permanent right ventricular pacing on functional and clinical recovery after TAVR. *Clin Res Cardiol*. 2015;104:964–974. doi: 10.1007/s00392-015-0865-9.
50. Testa L, Latib A, De Marco F, De Carlo M, Agnifili M, Latini RA, Petronio AS, Ettori F, Poli A, De Servi S, Ramondo A, Napodano M, Klugmann S, Ussia GP, Tamburino C, Brambilla N, Colombo A, Bedogni F. Clinical impact of persistent left bundle-branch block after transcatheter aortic valve implantation with CoreValve Revalving System. *Circulation*. 2013;127:1300–1307. doi: 10.1161/CIRCULATIONAHA.112.001099.
51. López-Aguilera J, Segura Saint-Gerons JM, Mazuelos Bellido F, Suárez de Lezo Herreros de Tejada J, Pineda SO, Pan Álvarez-Ossorio M, Romero Moreno MÁ, Pavlovic D, Suárez de Lezo Cruz Conde J. Effect of new-onset left bundle branch block after transcatheter aortic valve implantation (CoreValve) on mortality, frequency of re-hospitalization, and need for pacemaker. *Am J Cardiol*. 2016;118:1380–1385. doi: 10.1016/j.amjcard.2016.07.057.
52. Carrabba N, Valenti R, Migliorini A, Marrani M, Cantini G, Parodi G, Dovellini EV, Antoniucci D. Impact on left ventricular function and remodeling and on 1-year outcome in patients with left bundle branch block after transcatheter aortic valve implantation. *Am J Cardiol*. 2015;116:125–131. doi: 10.1016/j.amjcard.2015.03.054.
53. Lenders GD, Collas V, Hernandez JM, Legrand V, Danenberg HD, den Heijer P, Rodrigus IE, Paelinck BP, Vrints CJ, Bosmans JM. Depth of valve implantation, conduction disturbances and pacemaker implantation with CoreValve and CoreValve Accutrak system for Transcatheter Aortic Valve Implantation, a multi-center study. *Int J Cardiol*. 2014;176:771–775. doi: 10.1016/j.ijcard.2014.07.092.
54. Sinning JM, Petronio AS, Van Mieghem N, Zucchelli G, Nickenig G, Bekeredjian R, Bosmans J, Bedogni F, Branny M, Stangl K, Kovac J, Nordell A, Schiltgen M, Piazza N, de Jaegere P. Relation between clinical best practices and 6-month outcomes after transcatheter aortic valve implantation with CoreValve (from the ADVANCE II Study). *Am J Cardiol*. 2017;119:84–90. doi: 10.1016/j.amjcard.2016.09.016.
55. Calvi V, Conti S, Pruiti GP, Capodanno D, Puzzangara E, Tempio D, Di Grazia A, Ussia GP, Tamburino C. Incidence rate and predictors of permanent pacemaker implantation after transcatheter aortic valve implantation with self-expanding CoreValve prosthesis. *J Interv Card Electrophysiol*. 2012;34:189–195. doi: 10.1007/s10840-011-9634-5.
56. López-Aguilera J, Segura Saint-Gerons JM, Mazuelos Bellido F, Suárez de Lezo J, Ojeda Pineda S, Pan Álvarez-Ossorio M, Romero Moreno MÁ, Pavlovic D, Espejo Pérez S, Suárez de Lezo J. Atrioventricular conduction changes after CoreValve transcatheter aortic valve implantation. *Rev Esp Cardiol (Engl Ed)*. 2016;69:28–36. doi: 10.1016/j.rec.2015.02.026.
57. Khawaja MZ, Rajani R, Cook A, Khavandi A, Moynagh A, Chowdhary S, Spence MS, Brown S, Khan SQ, Walker N, Trivedi U, Hutchinson N, De Belder AJ, Moat N, Blackman DJ, Levy RD, Manoharan G, Roberts D, Khogali SS, Crean P, Brecker SJ, Baumbach A, Mullen M, Laborde JC, Hildick-Smith D. Permanent pacemaker insertion after CoreValve transcatheter aortic valve implantation: incidence and contributing factors (the UK CoreValve Collaborative). *Circulation*. 2011;123:951–960. doi: 10.1161/CIRCULATIONAHA.109.927152.
58. Webb J, Gerosa G, Lefèvre T, Leipsic J, Spence M, Thomas M, Thielmann M, Treede H, Wendler O, Walther T. Multicenter evaluation of a next-generation balloon-expandable transcatheter aortic valve. *J Am Coll Cardiol*. 2014;64:2235–2243. doi: 10.1016/j.jacc.2014.09.026.
59. Vahanian A, Urena M, Walther T, Treede H, Wendler O, Lefèvre T, Spence MS, Redwood S, Kahlert P, Rodes-Cabau J, Leipsic J, Webb J. Thirty-day outcomes in patients at intermediate risk for surgery from the SAPIEN 3 European approval trial. *EuroIntervention*. 2016;12:e235–e243. doi: 10.4244/EIJV12I2A37.
60. Rampat R, Khawaja MZ, Byrne J, MacCarthy P, Blackman DJ, Krishnamurthy A, Gunarathne A, Kovac J, Banning A, Kharbanda R, Firoozi S, Brecker S, Redwood S, Bapat V, Mullen M, Aggarwal S, Manoharan G, Spence MS, Khogali S, Dooley M, Cockburn J, de Belder A, Trivedi U, Hildick-Smith D. Transcatheter aortic valve replacement using the repositionable LOTUS valve: United Kingdom experience. *JACC Cardiovasc Interv*. 2016;9:367–372. doi: 10.1016/j.jcin.2015.12.012.
61. Zaman S, McCormick L, Gooley R, Rashid H, Ramkumar S, Jackson D, Hui S, Meredith IT. Incidence and predictors of permanent pacemaker implantation following treatment with the repositionable Lotus™ transcatheter aortic valve. *Catheter Cardiovasc Interv*. 2017;90:147–154. doi: 10.1002/ccd.26857.
62. Manoharan G, Linke A, Moellmann H, Redwood S, Frerker C, Kovac J, Walther T. Multicentre clinical study evaluating a novel resheathable annular functioning self-expanding transcatheter aortic valve system: safety and performance results at 30 days with the Portico system. *EuroIntervention*. 2016;12:768–774. doi: 10.4244/EIJV12I6A125.
63. Giustino G, Latib A, Panoulas VF, Montorfano M, Chieffo A, Taramasso M, Sato K, Agricola E, Alfieri O, Colombo A. Early outcomes with Direct Flow Medical versus first-generation transcatheter aortic valve devices: a single-center propensity-matched analysis. *J Interv Cardiol*. 2015;28:583–593. doi: 10.1111/joic.12248.
64. Massoullié G, Bordachar P, Ellenbogen KA, Souteyrand G, Jean F, Combaret N, Vorilhon C, Clerfond G, Farhat M, Ritter P, Citron B, Lusson JR, Motreff P, Ploux S, Eschalier R. New-onset left bundle branch block induced by transcutaneous aortic valve implantation. *Am J Cardiol*. 2016;117:867–873. doi: 10.1016/j.amjcard.2015.12.009.
65. Erkapic D, De Rosa S, Kelava A, Lehmann R, Fichtlscherer S, Hohnloser SH. Risk for permanent pacemaker after transcatheter aortic valve implantation: a comprehensive analysis of the literature. *J Cardiovasc Electrophysiol*. 2012;23:391–397. doi: 10.1111/j.1540-8167.2011.02211.x.
66. Nuis RJ, Van Mieghem NM, Schultz CJ, Tzikas A, Van der Boon RM, Maugenest AM, Cheng J, Piazza N, van Domburg RT, Serruys PW, de Jaegere PP. Timing and potential mechanisms of new conduction abnormalities during the implantation of the Medtronic CoreValve System in patients with aortic stenosis. *Eur Heart J*. 2011;32:2067–2074. doi: 10.1093/eurheartj/ehr110.
67. Petronio AS, Sinning JM, Van Mieghem N, Zucchelli G, Nickenig G, Bekeredjian R, Bosmans J, Bedogni F, Branny M, Stangl K, Kovac J, Schiltgen M, Kraus S, de Jaegere P. Optimal implantation depth and adherence to guidelines on permanent pacing to improve the results of transcatheter aortic valve replacement with the Medtronic CoreValve System: the CoreValve prospective, international, post-market ADVANCE-II study. *JACC Cardiovasc Interv*. 2015;8:837–846. doi: 10.1016/j.jcin.2015.02.005.
68. Boerlage-Van Dijk K, Kooiman KM, Yong ZY, Wiegerinck EM, Damman P, Bouma BJ, Tijssen JG, Piek JJ, Knops RE, Baan J Jr. Predictors and permanency of cardiac conduction disorders and necessity of pacing after transcatheter aortic valve implantation. *Pacing Clin Electrophysiol*. 2014;37:1520–1529. doi: 10.1111/pace.12460.
69. Lange P, Greif M, Vogel A, Thaumann A, Helbig S, Schwarz F, Schmitz C, Becker C, D'Anastasi M, Boekstegers P, Pohl T, Laubender RP, Steinbeck G, Kupatt C. Reduction of pacemaker implantation rates after CoreValve® implantation by moderate predilatation. *EuroIntervention*. 2014;9:1151–1157. doi: 10.4244/EIJV9I10A195.
70. Tzamtzis S, Viquerat J, Yap J, Mullen MJ, Burriesci G. Numerical analysis of the radial force produced by the Medtronic-CoreValve and Edwards-

SAPIEN after transcatheter aortic valve implantation (TAVI). *Med Eng Phys*. 2013;35:125–130. doi: 10.1016/j.medengphy.2012.04.009.
71. Regueiro A, Abdul-Jawad Altisent O, Del Trigo M, Campelo-Parada F, Puri R, Urena M, Philippon F, Rodés-Cabau J. Impact of new-onset left bundle branch block and periprocedural permanent pacemaker implantation on clinical outcomes in patients undergoing transcatheter aortic valve replacement: a systematic review and meta-analysis. *Circ Cardiovasc Interv*. 2016;9:e003635. doi: 10.1161/CIRCINTERVENTIONS.115.003635.
72. Meguro K, Lellouche N, Yamamoto M, Fougeres E, Monin JL, Lim P, Mouillet G, Dubois-Rande JL, Teiger E. Prognostic value of QRS duration after transcatheter aortic valve implantation for aortic stenosis using the CoreValve. *Am J Cardiol*. 2013;111:1778–1783. doi: 10.1016/j.amjcard.2013.02.032.
73. Toggweiler S, Stortecky S, Holy E, Zuk K, Cuculi F, Nietlispach F, Sabti Z, Suciu R, Maier W, Jamshidi P, Maisano F, Windecker S, Kobza R, Wenaweser P, Lüscher TF, Binder RK. The electrocardiogram after transcatheter aortic valve replacement determines the risk for post-procedural high-degree AV block and the need for telemetry monitoring. *JACC Cardiovasc Interv*. 2016;9:1269–1276. doi: 10.1016/j.jcin.2016.03.024.
74. Ando T, Takagi H; ALICE (All-Literature Investigation of Cardiovascular Evidence) Group. The prognostic impact of new-onset persistent left bundle branch block following transcatheter aortic valve implantation: a meta-analysis. *Clin Cardiol*. 2016;39:544–550. doi: 10.1002/clc.22567.
75. Fadahunsi OO, Olowoyeye A, Ukaigwe A, Li Z, Vora AN, Vemulapalli S, Elgin E, Donato A. Incidence, predictors, and outcomes of permanent pacemaker implantation following transcatheter aortic valve replacement: analysis from the U.S. Society of Thoracic Surgeons/American College of Cardiology TVT Registry. *JACC Cardiovasc Interv*. 2016;9:2189–2199. doi: 10.1016/j.jcin.2016.07.026.
76. Sabaté M, Cánovas S, García E, Hernández Antolín R, Maroto L, Hernández JM, Alonso Briales JH, Muñoz García AJ, Gutiérrez-Ibañes E, Rodríguez-Roda J; Collaborators of the TAVI National Group. In-hospital and mid-term predictors of mortality after transcatheter aortic valve implantation: data from the TAVI National Registry 2010-2011. *Rev Esp Cardiol (Engl Ed)*. 2013;66:949–958. doi: 10.1016/j.rec.2013.07.003.
77. Rodés-Cabau J, Webb JG, Cheung A, Ye J, Dumont E, Osten M, Feindel CM, Natarajan MK, Velianou JL, Martucci G, DeVarennes B, Chisholm R, Peterson M, Thompson CR, Wood D, Toggweiler S, Gurvitch R, Lichtenstein SV, Doyle D, DeLarochellière R, Teoh K, Chu V, Bainey K, Lachapelle K, Cheema A, Latter D, Dumesnil JG, Pibarot P, Horlick E. Long-term outcomes after transcatheter aortic valve implantation: insights on prognostic factors and valve durability from the Canadian multicenter experience. *J Am Coll Cardiol*. 2012;60:1864–1875. doi: 10.1016/j.jacc.2012.08.960.
78. Watanabe Y, Kozuma K, Hioki H, Kawashima H, Nara Y, Kataoka A, Nagura F, Nakashima M, Shirai S, Tada N, Araki M, Takagi K, Yamanaka F, Yamamoto M, Hayashida K. Pre-existing right bundle branch block increases risk for death after transcatheter aortic valve replacement with a balloon-expandable valve. *JACC Cardiovasc Interv*. 2016;9:2210–2216. doi: 10.1016/j.jcin.2016.08.035.
79. D'Onofrio A, Salizzoni S, Agrifoglio M, Cota L, Luzi G, Tartara PM, Cresce GD, Aiello M, Savini C, Cassese M, Cerillo A, Punta G, Cioni M, Gabbieri D, Zanchettin C, Agostinelli A, Mazzaro E, Di Gregorio O, Gatti G, Faggian G, Filippini C, Rinaldi M, Gerosa G. Medium term outcomes of transapical aortic valve implantation: results from the Italian Registry of Trans-Apical Aortic Valve Implantation. *Ann Thorac Surg*. 2013;96:830–835. doi: 10.1016/j.athoracsur.2013.04.094.
80. Ludman PF, Moat N, de Belder MA, Blackman DJ, Duncan A, Banya W, MacCarthy PA, Cunningham D, Wendler O, Marlee D, Hildick-Smith D, Young CP, Kovac J, Uren NG, Spyt T, Trivedi U, Howell J, Gray H; UK TAVI Steering Committee and the National Institute for Cardiovascular Outcomes Research. Transcatheter aortic valve implantation in the United Kingdom: temporal trends, predictors of outcome, and 6-year follow-up: a report from the UK Transcatheter Aortic Valve Implantation (TAVI) Registry, 2007 to 2012. *Circulation*. 2015;131:1181–1190. doi: 10.1161/CIRCULATIONAHA.114.013947.
81. Di Mario C, Eltchaninoff H, Moat N, Goicolea J, Ussia GP, Kala P, Wenaweser P, Zembala M, Nickenig G, Alegria Barrero E, Snow T, Iung B, Zamorano P, Schuler G, Corti R, Alfieri O, Prendergast B, Ludman P, Windecker S, Sabate M, Gilard M, Witowski A, Danenberg H, Schroeder E, Romeo F, Macaya C, Derumeaux G, Maggioni A, Tavazzi L; Transcatheter Valve Treatment Sentinel Registry (TCVT) Investigators of the EURObservational Research Programme (EORP) of the European Society of Cardiology. The 2011-12 pilot European Sentinel Registry of Transcatheter Aortic Valve Implantation: in-hospital results in 4,571 patients. *EuroIntervention*. 2013;8:1362–1371. doi: 10.4244/EIJV8I12A209.
82. Schymik G, Lefèvre T, Bartorelli AL, Rubino P, Treede H, Walther T, Baumgartner H, Windecker S, Wendler O, Urban P, Mandinov L, Thomas M, Vahanian A. European experience with the second-generation Edwards SAPIEN XT transcatheter heart valve in patients with severe aortic stenosis: 1-year outcomes from the SOURCE XT Registry. *JACC Cardiovasc Interv*. 2015;8:657–669. doi: 10.1016/j.jcin.2014.10.026.
83. Salizzoni S, D'Onofrio A, Agrifoglio M, Colombo A, Chieffo A, Cioni M, Besola L, Regesta T, Rapetto F, Tarantini G, Napodano M, Gabbieri D, Saia F, Tamburino C, Ribichini F, Cugola D, Aiello M, Sanna F, Iadanza A, Pompei E, Stefàno P, Cappai A, Minati A, Cassese M, Martinelli GL, Agostinelli A, Fiorilli R, Casilli F, Reale M, Bedogni F, Petronio AS, Mozzillo RA, Bonmassari R, Briguori C, Liso A, Sardella G, Bruschi G, Fiorina C, Filippini C, Moretti C, D'Amico M, La Torre M, Conrotto F, Di Bartolomeo R, Gerosa G, Rinaldi M; TAVI Team. Early and mid-term outcomes of 1904 patients undergoing transcatheter balloon-expandable valve implantation in Italy: results from the Italian Transcatheter Balloon-Expandable Valve Implantation Registry (ITER). *Eur J Cardiothorac Surg*. 2016;50:1139–1148. doi: 10.1093/ejcts/ezw218.
84. Webb JG, Doshi D, Mack MJ, Makkar R, Smith CR, Pichard AD, Kodali S, Kapadia S, Miller DC, Babaliaros V, Thourani V, Herrmann HC, Bodenhamer M, Whisenant BK, Ramee S, Maniar H Jr, Kereiakes D, Xu K, Jaber WA, Menon V, Tuzcu EM, Wood D, Svensson LG, Leon MB. A randomized evaluation of the SAPIEN XT transcatheter heart valve system in patients with aortic stenosis who are not candidates for surgery. *JACC Cardiovasc Interv*. 2015;8:1797–1806. doi: 10.1016/j.jcin.2015.08.017.
85. Thomas M, Schymik G, Walther T, Himbert D, Lefèvre T, Treede H, Eggebrecht H, Rubino P, Michev I, Lange R, Anderson WN, Wendler O. Thirty-day results of the SAPIEN Aortic Bioprosthesis European Outcome (SOURCE) Registry: a European registry of transcatheter aortic valve implantation using the Edwards SAPIEN valve. *Circulation*. 2010;122:62–69. doi: 10.1161/CIRCULATIONAHA.109.907402.
86. Collas VM, Dubois C, Legrand V, Kefer J, De Bruyne B, Dens J, Rodrigus IE, Herijgers P, Bosmans JM; Belgian TAVI Registry Participants. Midterm clinical outcome following Edwards SAPIEN or Medtronic Corevalve transcatheter aortic valve implantation (TAVI): results of the Belgian TAVI registry. *Catheter Cardiovasc Interv*. 2015;86:528–535. doi: 10.1002/ccd.25999.
87. Giustino G, Van der Boon RM, Molina-Martin de Nicolas J, Dumonteil N, Chieffo A, de Jaegere PP, Tchetche D, Marcheix B, Millischer D, Cassagneau R, Carrié D, Van Mieghem NM, Colombo A. Impact of permanent pacemaker on mortality after transcatheter aortic valve implantation: the PRAGMATIC (Pooled Rotterdam-Milan-Toulouse in Collaboration) Pacemaker substudy. *EuroIntervention*. 2016;12:1185–1193. doi: 10.4244/EIJV12I9A192.
88. Dizon JM, Nazif TM, Hess PL, Biviano A, Garan H, Douglas PS, Kapadia S, Babaliaros V, Herrmann HC, Szeto WY, Jilaihawi H, Fearon WF, Tuzcu EM, Pichard AD, Makkar R, Williams M, Hahn RT, Xu K, Smith CR, Leon MB, Kodali SK; PARTNER Publications Office. Chronic pacing and adverse outcomes after transcatheter aortic valve implantation. *Heart*. 2015;101:1665–1671. doi: 10.1136/heartjnl-2015-307666.
89. Binder RK, Stortecky S, Heg D, Tueller D, Jeger R, Toggweiler S, Pedrazzini G, Amann FW, Ferrari E, Noble S, Nietlispach F, Maisano F, Raber L, Roffi M, Grunenfelder J, Juni P, Huber C, Windecker S, Wenaweser P. Procedural results and clinical outcomes of transcatheter aortic valve implantation in Switzerland: an observational cohort study of Sapien 3 versus Sapien XT transcatheter heart valves. *Circ Cardiovasc Interv*. 2015;8:e002653. doi: 10.1161/CIRCINTERVENTIONS.115.002653.
90. Gilard M, Eltchaninoff H, Iung B, Donzeau-Gouge P, Chevreul K, Fajadet J, Leprince P, Leguerrier A, Lievre M, Prat A, Teiger E, Lefevre T, Himbert D, Tchetche D, Carrié D, Albat B, Cribier A, Rioufol G, Sudre A, Blanchard D, Collet F, Dos Santos P, Meneveau N, Tirouvanziam A, Caussin C, Guyon P, Boschat J, Le Breton H, Collart F, Houel R, Delpine S, Souteyrand G, Favereau X, Ohlmann P, Doisy V, Grollier G, Gommeaux A, Claudel JP, Bourlon F, Bertrand B, Van Belle E, Laskar M; FRANCE 2 Investigators. Registry of transcatheter aortic-valve implantation in high-risk patients. *N Engl J Med*. 2012;366:1705–1715. doi: 10.1056/NEJMoa1114705.
91. Ledwoch J, Franke J, Gerckens U, Kuck KH, Linke A, Nickenig G, Krülls-Münch J, Vöhringer M, Hambrecht R, Erbel R, Richardt G, Horack M, Zahn R, Senges J, Sievert H, German Transcatheter Aortic Valve Interventions Registry Investigators. Incidence and predictors of permanent pacemaker implantation following transcatheter aortic valve implantation: analysis from the German transcatheter aortic valve interventions registry. *Catheter Cardiovasc Interv*. 2013;82:E569–E577. doi: 10.1002/ccd.24915.
92. Abdel-Wahab M, Mehilli J, Frerker C, Neumann FJ, Kurz T, Tölg R, Zachow D, Guerra E, Massberg S, Schäfer U, El-Mawardy M, Richardt G; CHOICE

Investigators. Comparison of balloon-expandable vs self-expandable valves in patients undergoing transcatheter aortic valve replacement: the CHOICE randomized clinical trial. *JAMA*. 2014;311:1503–1514. doi: 10.1001/jama.2014.3316.
93. Piazza N, Grube E, Gerckens U, den Heijer P, Linke A, Luha O, Ramondo A, Ussia G, Wenaweser P, Windecker S, Laborde JC, de Jaegere P, Serruys PW. Procedural and 30-day outcomes following transcatheter aortic valve implantation using the third generation (18 Fr) CoreValve Revalving System: results from the multicentre, expanded evaluation registry 1-year following CE mark approval. *EuroIntervention*. 2008;4:242–249.
94. Tamburino C, Capodanno D, Ramondo A, Petronio AS, Ettori F, Santoro G, Klugmann S, Bedogni F, Maisano F, Marzocchi A, Poli A, Antoniucci D, Napodano M, De Carlo M, Fiorina C, Ussia GP. Incidence and predictors of early and late mortality after transcatheter aortic valve implantation in 663 patients with severe aortic stenosis. *Circulation*. 2011;123:299–308. doi: 10.1161/CIRCULATIONAHA.110.946533.
95. Adams DH, Popma JJ, Reardon MJ, Yakubov SJ, Coselli JS, Deeb GM, Gleason TG, Buchbinder M, Hermiller J Jr, Kleiman NS, Chetcuti S, Heiser J, Merhi W, Zorn G, Tadros P, Robinson N, Petrossian G, Hughes GC, Harrison JK, Conte J, Maini B, Mumtaz M, Chenoweth S, Oh JK; U.S. CoreValve Clinical Investigators. Transcatheter aortic-valve replacement with a self-expanding prosthesis. *N Engl J Med*. 2014;370:1790–1798. doi: 10.1056/NEJMoa1400590.
96. Sorajja P, Kodali S, Reardon M, Szeto W, Chetcuti S, Hermiller J Jr, Adams D, Popma J. Tct-672 outcomes in the commercial use of self-expanding prostheses in transcatheter aortic valve replacement: a comparison of the Medtronic CoreValve and Evolut R platforms in the Society of Thoracic Surgeons/American College of Cardiology Transcatheter Valve Therapy Registry™. *J Am Coll Cardiol*. 2016;68:B271–B272.
97. Popma JJ, Adams DH, Reardon MJ, Yakubov SJ, Kleiman NS, Heimansohn D, Hermiller J Jr, Hughes GC, Harrison JK, Coselli J, Diez J, Kafi A, Schreiber T, Gleason TG, Conte J, Buchbinder M, Deeb GM, Carabello B, Serruys PW, Chenoweth S, Oh JK; CoreValve United States Clinical Investigators. Transcatheter aortic valve replacement using a self-expanding bioprosthesis in patients with severe aortic stenosis at extreme risk for surgery. *J Am Coll Cardiol*. 2014;63:1972–1981. doi: 10.1016/j.jacc.2014.02.556.
98. Noble S, Stortecky S, Heg D, Tueller D, Jeger R, Toggweiler S, Ferrari E, Nietlispach F, Taramasso M, Maisano F, Grünenfelder J, Jüni P, Huber C, Carrel T, Windecker S, Wenaweser P, Roffi M. Comparison of procedural and clinical outcomes with Evolut R versus Medtronic CoreValve: a Swiss TAVI registry analysis. *EuroIntervention*. 2017;12:e2170–e2176. doi: 10.4244/EIJ-D-16-00677.
99. Linke A, Wenaweser P, Gerckens U, Tamburino C, Bosmans J, Bleiziffer S, Blackman D, Schäfer U, Müller R, Sievert H, Søndergaard L, Klugmann S, Hoffmann R, Tchétché D, Colombo A, Legrand VM, Bedogni F, lePrince P, Schuler G, Mazzitelli D, Eftychiou C, Frerker C, Boekstegers P, Windecker S, Mohr FW, Woitek F, Lange R, Bauernschmitt R, Brecker S; ADVANCE Study Investigators. Treatment of aortic stenosis with a self-expanding transcatheter valve: the international multi-centre ADVANCE Study. *Eur Heart J*. 2014;35:2672–2684. doi: 10.1093/eurheartj/ehu162.
100. de Brito FS Jr, Carvalho LA, Sarmento-Leite R, Mangione JA, Lemos P, Siciliano A, Caramori P, São Thiago L, Grube E, Abizaid A; Brazilian TAVI Registry Investigators. Outcomes and predictors of mortality after transcatheter aortic valve implantation: results of the Brazilian registry. *Catheter Cardiovasc Interv*. 2015;85:E153–E162. doi: 10.1002/ccd.25778.
101. Meredith IT, Walton A, Walters DL, Pasupati S, Muller DW, Worthley SG, Yong G, Whitbourn R, Duffy SJ, Ormiston J. Mid-term outcomes in patients following transcatheter aortic valve implantation in the CoreValve Australia and New Zealand Study. *Heart Lung Circ*. 2015;24:281–290. doi: 10.1016/j.hlc.2014.09.023.
102. Thyregod HG, Steinbrüchel DA, Ihlemann N, Nissen H, Kjeldsen BJ, Petursson P, Chang Y, Franzen OW, Engstrøm T, Clemmensen P, Hansen PB, Andersen LW, Olsen PS, Søndergaard L. Transcatheter versus surgical aortic valve replacement in patients with severe aortic valve stenosis: 1-year results from the All-Comers NOTION randomized clinical trial. *J Am Coll Cardiol*. 2015;65:2184–2194. doi: 10.1016/j.jacc.2015.03.014.
103. Siontis GC, Jüni P, Pilgrim T, Stortecky S, Büllesfeld L, Meier B, Wenaweser P, Windecker S. Predictors of permanent pacemaker implantation in patients with severe aortic stenosis undergoing TAVR: a meta-analysis. *J Am Coll Cardiol*. 2014;64:129–140. doi: 10.1016/j.jacc.2014.04.033.
104. Khatri PJ, Webb JG, Rodés-Cabau J, Fremes SE, Ruel M, Lau K, Guo H, Wijeysundera HC, Ko DT. Adverse effects associated with transcatheter aortic valve implantation: a meta-analysis of contemporary studies. *Ann Intern Med*. 2013;158:35–46. doi: 10.7326/0003-4819-158-1-201301010-00007.
105. Wendt D, Al-Rashid F, Kahlert P, Eissmann M, El-Chilali K, Janosi RA, Pasa S, Tsagakis K, Liakopoulos O, Erbel R, Jakob H, Thielmann M. Low incidence of paravalvular leakage with the balloon-expandable Sapien 3 transcatheter heart valve. *Ann Thorac Surg*. 2015;100:819–825.
106. Deimling R, Frey N, Frank D. Comparison of the new balloon-expandable Edwards Sapien-3 vs Sapien XT valve: a large-scale single-center experience. *J Am Coll Cardiol*. 2015;66:B282.
107. Kodali S, Thourani VH, White J, Malaisrie SC, Lim S, Greason KL, Williams M, Guerrero M, Eisenhauer AC, Kapadia S, Kereiakes DJ, Herrmann HC, Babaliaros V, Szeto WY, Hahn RT, Pibarot P, Weissman NJ, Leipsic J, Blanke P, Whisenant BK, Suri RM, Makkar RR, Ayele GM, Svensson LG, Webb JG, Mack MJ, Smith CR, Leon MB. Early clinical and echocardiographic outcomes after SAPIEN 3 transcatheter aortic valve replacement in inoperable, high-risk and intermediate-risk patients with aortic stenosis. *Eur Heart J*. 2016;37:2252–2262. doi: 10.1093/eurheartj/ehw112.
108. Wendler O, Schymik G, Treede H, Baumgartner H, Dumonteil N, Ihlberg L, Neumann FJ, Tarantini G, Zamarano JL, Vahanian A. SOURCE 3 Registry: design and 30-day results of the European Postapproval registry of the latest generation of the SAPIEN 3 transcatheter heart valve. *Circulation*. 2017;135:1123–1132. doi: 10.1161/CIRCULATIONAHA.116.025103.
109. Seeger J, Gonska B, Rottbauer W, Wohrle J. Outcome with the repositionable and retrievable Boston Scientific Lotus valve compared with the balloon-expandable Edwards Sapien 3 valve in patients undergoing transfemoral aortic valve replacement [published online ahead of print June 10, 2017]. *Circ Cardiovasc Interv*. doi: 10.1161/CIRCINTERVENTIONS.116.004670. http://circinterventions.ahajournals.org/content/10/6/e004670.long.
110. Pilgrim T, Stortecky S, Nietlispach F, Heg D, Tueller D, Toggweiler S, Ferrari E, Noble S, Maisano F, Jeger R, Roffi M, Grunenfelder J, Huber C, Wenaweser P, Windecker S. Repositionable versus balloon-expandable devices for transcatheter aortic valve implantation in patients with aortic stenosis. *J Am Heart Assoc*. 2016;5:e004088.
111. Mauri V, Reimann A, Stern D, Scherner M, Kuhn E, Rudolph V, Rosenkranz S, Eghbalzadeh K, Friedrichs K, Wahlers T, Baldus S, Madershahian N, Rudolph TK. Predictors of permanent pacemaker implantation after transcatheter aortic valve replacement with the SAPIEN 3. *JACC Cardiovasc Interv*. 2016;9:2200–2209. doi: 10.1016/j.jcin.2016.08.034.
112. Sawaya FJ, Spaziano M, Lefèvre T, Roy A, Garot P, Hovasse T, Neylon A, Benamer H, Romano M, Unterseeh T, Morice MC, Chevalier B. Comparison between the SAPIEN S3 and the SAPIEN XT transcatheter heart valves: a single-center experience. *World J Cardiol*. 2016;8:735–745. doi: 10.4330/wjc.v8.i12.735.
113. Ben-Shoshan J, Konigstein M, Zahler D, Margolis G, Chorin E, Steinvil A, Arbel Y, Aviram G, Granot Y, Barkagan M, Keren G, Halkin A, Banai S, Finkelstein A. Comparison of the Edwards SAPIEN S3 versus Medtronic Evolut-R devices for transcatheter aortic valve implantation. *Am J Cardiol*. 2017;119:302–307. doi: 10.1016/j.amjcard.2016.09.030.
114. Murray MI, Geis N, Pleger ST, Kallenbach K, Katus HA, Bekeredjian R, Chorianopoulos E. First experience with the new generation Edwards Sapien 3 aortic bioprosthesis: procedural results and short term outcome. *J Interv Cardiol*. 2015;28:109–116. doi: 10.1111/joic.12182.
115. Schulz E, Jabs A, Tamm A, Herz P, Schulz A, Gori T, von Bardeleben S, Kasper-König W, Hink U, Vahl CF, Münzel T. Comparison of transcatheter aortic valve implantation with the newest-generation Sapien 3 vs. Direct Flow Medical valve in a single center cohort. *Int J Cardiol*. 2017;232:186–191. doi: 10.1016/j.ijcard.2017.01.032.
116. Manoharan G, Walton AS, Brecker SJ, Pasupati S, Blackman DJ, Qiao H, Meredith IT. Treatment of symptomatic severe aortic stenosis with a novel resheathable supra-annular self-expanding transcatheter aortic valve system. *JACC Cardiovasc Interv*. 2015;8:1359–1367. doi: 10.1016/j.jcin.2015.05.015.
117. Kalra SS, Firoozi S, Yeh J, Blackman DJ, Rashid S, Davies S, Moat N, Dalby M, Kabir T, Khogali SS, Anderson RA, Groves PH, Mylotte D, Hildick-Smith D, Rampat R, Kovac J, Gunarathne A, Laborde JC, Brecker SJ. Initial experience of a second-generation self-expanding transcatheter aortic valve: the UK & Ireland Evolut R Implanters' Registry. *JACC Cardiovasc Interv*. 2017;10:276–282. doi: 10.1016/j.jcin.2016.11.025.
118. Popma JJ, Reardon MJ, Khabbaz K, Harrison JK, Hughes GC, Kodali S, George I, Deeb GM, Chetcuti S, Kipperman R, Brown J, Qiao H, Slater J, Williams MR. Early clinical outcomes after transcatheter aortic valve replacement using a novel self-expanding bioprosthesis in patients with severe aortic stenosis who are suboptimal for surgery: results of the Evolut

R U.S. Study. *JACC Cardiovasc Interv*. 2017;10:268–275. doi: 10.1016/j.jcin.2016.08.050.
119. Gomes B, Geis NA, Chorianopoulos E, Meder B, Leuschner F, Katus HA, Bekeredjian R. Improvements of procedural results with a new-generation self-expanding transfemoral aortic valve prosthesis in comparison to the old-generation device. *J Interv Cardiol*. 2017;30:72–78. doi: 10.1111/joic.12356.
120. De Backer O, Götberg M, Ihlberg L, Packer E, Savontaus M, Nielsen NE, Jørgensen TH, Nykänen A, Baranowski J, Niemelä M, Eskola M, Bjursten H, Søndergaard L. Efficacy and safety of the Lotus Valve System for treatment of patients with severe aortic valve stenosis and intermediate surgical risk: results from the Nordic Lotus-TAVR registry. *Int J Cardiol*. 2016;219:92–97. doi: 10.1016/j.ijcard.2016.05.072.
121. Gooley RP, Talman AH, Cameron JD, Lockwood SM, Meredith IT. Comparison of self-expanding and mechanically expanded transcatheter aortic valve prostheses. *JACC Cardiovasc Interv*. 2015;8:962–971. doi: 10.1016/j.jcin.2015.03.014.
122. Van Mieghem N, van Gils L, Wöhrle J, Hildick-Smith D, Bleiziffer S, Blackman D, Abdel-Wahab M, Linke A, Ince H, Wenaweser P, Werner N, Allocco DJ, Dawkins KD, Falk V. Tct-733 predictors of permanent pacemaker implantation in patients treated in routine clinical practice with the repositionable and fully retrievable lotus valve. *J Am Coll Cardiol*. 2016;68:B296.
123. Giannini F, Latib A, Montorfano M, Ruparelia N, Longoni M, Aurelio A, Jabbour R, Regazzoli D, Ferri LA, Mangieri A, Ancona M, Tanaka A, Agricola E, Chieffo A, Alfieri O, Colombo A. Tct-698 comparison of the fully repositionable and retrievable Lotus valve and Direct Flow Medical valve for the treatment of severe aortic stenosis: a high-volume single center experience. *J Am Coll Cardiol*. 2016;68:B282.
124. Del Trigo M, Dahou A, Webb JG, Dvir D, Puri R, Abdul-Jawad Altisent O, Campelo-Parada F, Thompson C, Leipsic J, Stub D, DeLarochellière R, Paradis JM, Dumont E, Doyle D, Mohammadi S, Pasian S, Côté M, Pibarot P, Rodés-Cabau J. Self-expanding Portico valve versus balloon-expandable SAPIEN XT valve in patients with small aortic annuli: comparison of hemodynamic performance. *Rev Esp Cardiol (Engl Ed)*. 2016;69:501–508. doi: 10.1016/j.rec.2015.08.019.
125. Perlman GY, Cheung A, Dumont E, Stub D, Dvir D, Del Trigo M, Pelletier M, Alnasser S, Ye J, Wood D, Thompson C, Blanke P, Leipsic J, Seidman MA, LeBlanc H, Buller CE, Rodés-Cabau J, Webb JG. Transcatheter aortic valve replacement with the Portico valve: one-year results of the early Canadian experience. *EuroIntervention*. 2017;12:1653–1659. doi: 10.4244/EIJ-D-16-00299.
126. Naber CK, Pyxaras SA, Ince H, Latib A, Frambach P, den Heijer P, Wagner D, Butter C, Colombo A, Kische S. Real-world multicentre experience with the Direct Flow Medical repositionable and retrievable transcatheter aortic valve implantation system for the treatment of high-risk patients with severe aortic stenosis. *EuroIntervention*. 2016;11:e1314–e1320. doi: 10.4244/EIJV11I11A254.
127. Zhang Y, Pyxaras SA, Wolf A, Schmitz T, Naber CK. Propensity-matched comparison between Direct Flow Medical, Medtronic Corevalve, and Edwards Sapien XT prostheses: device success, thirty-day safety, and mortality. *Catheter Cardiovasc Interv*. 2015;85:1217–1225. doi: 10.1002/ccd.25831.
128. Treede H, Tübler T, Reichenspurner H, Grube E, Pascotto A, Franzen O, Mueller R, Low R, Bolling SF, Meinertz T, Schofer J. Six-month results of a repositionable and retrievable pericardial valve for transcatheter aortic valve replacement: the Direct Flow Medical aortic valve. *J Thorac Cardiovasc Surg*. 2010;140:897–903. doi: 10.1016/j.jtcvs.2010.01.017.
129. Kische S, D'Ancona G, Agma HU, El-Achkar G, Dißmann M, Ortak J, Ince H. Trans-catheter aortic valve implantation with the Direct Flow Medical prosthesis: single center short-term clinical and echocardiographic outcomes. *Catheter Cardiovasc Interv*. 2017;89:420–428. doi: 10.1002/ccd.26528.
130. Reuthebuch O, Koechlin L, Kaufmann BA, Kessel-Schaefer A, Gahl B, Eckstein FS. Transapical transcatheter aortic valve implantation using the JenaValve: a one-year follow-up. *Thorac Cardiovasc Surg*. 2015;63:493–500. doi: 10.1055/s-0035-1552980.
131. Treede H, Mohr FW, Baldus S, Rastan A, Ensminger S, Arnold M, Kempfert J, Figulla HR. Transapical transcatheter aortic valve implantation using the JenaValve™ system: acute and 30-day results of the multicentre CE-mark study. *Eur J Cardiothorac Surg*. 2012;41:e131–e138. doi: 10.1093/ejcts/ezs129.
132. Chu MW, Bagur R, Losenno KL, Jones PM, Diamantouros P, Teefy P, Gelinas JJ, Kiaii B. Early clinical outcomes of a novel self-expanding transapical transcatheter aortic valve bioprosthesis. *J Thorac Cardiovasc Surg*. 2017;153:810–818. doi: 10.1016/j.jtcvs.2016.11.054.
133. Bagur R, Teefy PJ, Kiaii B, Diamantouros P, Chu MWA. First North American experience with the transfemoral ACURATE-neo™ self-expanding transcatheter aortic bioprosthesis. *Catheter Cardiovasc Interv*. 2017;90:130–138. doi: 10.1002/ccd.26802.
134. Jatene T, Castro-Filho A, Meneguz-Moreno RA, Siqueira DA, Abizaid AAC, Ramos AIO, Arrais M, Le Bihan DCS, Barretto RBM, Moreira AC, Sousa AGMR, Eduardo Sousa J. Prospective comparison between three TAVR devices: ACURATE neo vs. CoreValve vs. SAPIEN XT: a single heart team experience in patients with severe aortic stenosis. *Catheter Cardiovasc Interv*. 2017;90:139–146. doi: 10.1002/ccd.26837.
135. Kempfert J, Beyersdorf F, Schönburg M, Schuler G, Sorg S, Möllmann H, Mohr F, Walther T. Transapical aortic valve implantation using a new self-fexpandable bioprosthesis: initial outcomes. *Interact Cardiovasc Thorac Surg*. 2010;11:S123.
136. Schaefer A, Treede H, Schoen G, Deuschl F, Schofer N, Schneeberger Y, Blankenberg S, Reichenspurner H, Schaefer U, Conradi L. Improving outcomes: case-matched comparison of novel second-generation versus first-generation self-expandable transcatheter heart valves. *Eur J Cardiothorac Surg*. 2016;50:368–373. doi: 10.1093/ejcts/ezw021.
137. Pellegrini C, Husser O, Kim W, Holzamer A, Walther T, Rheude T, Trenkwalder T, Michel J, Kastrati A, Schunkert H, Burgdorf C, Hilker M, Möllmann H, Hengstenberg C. Tct-730: a multicenter analysis of incidence and predictors for permanent pacemaker implantations and new conduction abnormalities with a novel self-expandable transcatheter heart valve. *J Am Coll Cardiol*. 2016;68:B295.
138. Kempfert J, Holzhey D, Hofmann S, Girdauskas E, Treede H, Schröfel H, Thielmann M, Walther T. First registry results from the newly approved ACURATE TA™ TAVI system. *Eur J Cardiothorac Surg*. 2015;48:137–141. doi: 10.1093/ejcts/ezu367.
139. Kempfert J, Meyer A, Kim WK, Van Linden A, Arsalan M, Blumenstein J, Möllmann H, Walther T. Comparison of two valve systems for transapical aortic valve implantation: a propensity score-matched analysis. *Eur J Cardiothorac Surg*. 2016;49:486–492. doi: 10.1093/ejcts/ezv042.
140. Falk V, Walther T, Schwammenthal E, Strauch J, Aicher D, Wahlers T, Schäfers J, Linke A, Mohr FW. Transapical aortic valve implantation with a self-expanding anatomically oriented valve. *Eur Heart J*. 2011;32:878–887. doi: 10.1093/eurheartj/ehq445.
141. Holzhey D, Linke A, Treede H, Baldus S, Bleiziffer S, Wagner A, Börgermann J, Scholtz W, Vanoverschelde JL, Falk V. Intermediate follow-up results from the multicenter Engager European pivotal trial. *Ann Thorac Surg*. 2013;96:2095–2100. doi: 10.1016/j.athoracsur.2013.06.089.
142. Chamandi C, Regueiro A, Auffret V, Rodriguez-Gabella T, Chiche O, Barria A, Côté M, Philippon F, Puri R, Rodés-Cabau J. Reported versus "real" incidence of new pacemaker implantation post-transcatheter aortic valve replacement. *J Am Coll Cardiol*. 2016;68:2387–2389. doi: 10.1016/j.jacc.2016.08.065.
143. Durand E, Eltchaninoff H, Canville A, Bouhzam N, Godin M, Tron C, Rodriguez C, Litzler PY, Bauer F, Cribier A. Feasibility and safety of early discharge after transfemoral transcatheter aortic valve implantation with the Edwards SAPIEN-XT prosthesis. *Am J Cardiol*. 2015;115:1116–1122. doi: 10.1016/j.amjcard.2015.01.546.
144. Brignole M, Auricchio A, Baron-Esquivias G, Bordachar P, Boriani G, Breithardt OA, Cleland J, Deharo JC, Delgado V, Elliott PM, Gorenek B, Israel CW, Leclercq C, Linde C, Mont L, Padeletti L, Sutton R, Vardas PE, Zamorano JL, Achenbach S, Baumgartner H, Bax JJ, Bueno H, Dean V, Deaton C, Erol C, Fagard R, Ferrari R, Hasdai D, Hoes AW, Kirchhof P, Knuuti J, Kolh P, Lancellotti P, Linhart A, Nihoyannopoulos P, Piepoli MF, Ponikowski P, Sirnes PA, Tamargo JL, Tendera M, Torbicki A, Wijns W, Windecker S, Kirchhof P, Blomstrom-Lundqvist C, Badano LP, Aliyev F, Bänsch D, Baumgartner H, Bsata W, Buser P, Charron P, Daubert JC, Dobreanu D, Faerestrand S, Hasdai D, Hoes AW, Le Heuzey JY, Mavrakis H, McDonagh T, Merino JL, Nawar MM, Nielsen JC, Pieske B, Poposka L, Ruschitzka F, Tendera M, Van Gelder IC, Wilson CM; ESC Committee for Practice Guidelines (CPG). 2013 ESC guidelines on cardiac pacing and cardiac resynchronization therapy: the Task Force on cardiac pacing and resynchronization therapy of the European Society of Cardiology (ESC): developed in collaboration with the European Heart Rhythm Association (EHRA). *Eur Heart J*. 2013;34:2281–2329. doi: 10.1093/eurheartj/eht150.
145. Bagur R, Rodés-Cabau J, Gurvitch R, Dumont É, Velianou JL, Manazzoni J, Toggweiler S, Cheung A, Ye J, Natarajan MK, Bainey KR, DeLarochellière R, Doyle D, Pibarot P, Voisine P, Côté M, Philippon F, Webb JG. Need for

permanent pacemaker as a complication of transcatheter aortic valve implantation and surgical aortic valve replacement in elderly patients with severe aortic stenosis and similar baseline electrocardiographic findings. *JACC Cardiovasc Interv*. 2012;5:540–551. doi: 10.1016/j.jcin.2012.03.004.
146. Guetta V, Goldenberg G, Segev A, Dvir D, Kornowski R, Finckelstein A, Hay I, Goldenberg I, Glikson M. Predictors and course of high-degree atrioventricular block after transcatheter aortic valve implantation using the CoreValve Revalving System. *Am J Cardiol*. 2011;108:1600–1605. doi: 10.1016/j.amjcard.2011.07.020.
147. Chorianopoulos E, Krumsdorf U, Pleger ST, Katus HA, Bekeredjian R. Incidence of late occurring bradyarrhythmias after TAVI with the self-expanding CoreValve(®) aortic bioprosthesis. *Clin Res Cardiol*. 2012;101:349–355. doi: 10.1007/s00392-011-0398-9.
148. Nazif TM, Dizon JM, Hahn RT, Xu K, Babaliaros V, Douglas PS, El-Chami MF, Herrmann HC, Mack M, Makkar RR, Miller DC, Pichard A, Tuzcu EM, Szeto WY, Webb JG, Moses JW, Smith CR, Williams MR, Leon MB, Kodali SK; PARTNER Publications Office. Predictors and clinical outcomes of permanent pacemaker implantation after transcatheter aortic valve replacement: the PARTNER (Placement of AoRtic TraNscathetER Valves) trial and registry. *JACC Cardiovasc Interv*. 2015;8(pt A):60–69. doi: 10.1016/j.jcin.2014.07.022.
149. van der Boon RM, Van Mieghem NM, Theuns DA, Nuis RJ, Nauta ST, Serruys PW, Jordaens L, van Domburg RT, de Jaegere PP. Pacemaker dependency after transcatheter aortic valve implantation with the self-expanding Medtronic CoreValve System. *Int J Cardiol*. 2013;168:1269–1273. doi: 10.1016/j.ijcard.2012.11.115.
150. Naveh S, Perlman GY, Elitsur Y, Planer D, Gilon D, Leibowitz D, Lotan C, Danenberg H, Alcalai R. Electrocardiographic predictors of long-term cardiac pacing dependency following transcatheter aortic valve implantation. *J Cardiovasc Electrophysiol*. 2017;28:216–223. doi: 10.1111/jce.13147.
151. Pereira E, Ferreira N, Caeiro D, Primo J, Adão L, Oliveira M, Gonçalves H, Ribeiro J, Santos E, Leite D, Bettencourt N, Braga P, Simões L, Vouga L, Gama V. Transcatheter aortic valve implantation and requirements of pacing over time. *Pacing Clin Electrophysiol*. 2013;36:559–569. doi: 10.1111/pace.12104.
152. Simms AD, Hogarth AJ, Hudson EA, Worsnop VL, Blackman DJ, O'Regan DJ, Tayebjee MH. Ongoing requirement for pacing post-transcatheter aortic valve implantation and surgical aortic valve replacement. *Interact Cardiovasc Thorac Surg*. 2013;17:328–333. doi: 10.1093/icvts/ivt175.
153. Ramazzina C, Knecht S, Jeger R, Kaiser C, Schaer B, Osswald S, Sticherling C, Kühne M. Pacemaker implantation and need for ventricular pacing during follow-up after transcatheter aortic valve implantation. *Pacing Clin Electrophysiol*. 2014;37:1592–1601. doi: 10.1111/pace.12505.
154. Renilla A, Rubín JM, Rozado J, Moris C. Long-term evolution of pacemaker dependency after percutaneous aortic valve implantation with the CoreValve prosthesis. *Int J Cardiol*. 2015;201:61–63. doi: 10.1016/j.ijcard.2015.08.100.
155. Schernthaner C, Kraus J, Danmayr F, Hammerer M, Schneider J, Hoppe UC, Strohmer B. Short-term pacemaker dependency after transcatheter aortic valve implantation. *Wien Klin Wochenschr*. 2016;128:198–203. doi: 10.1007/s00508-015-0906-4.
156. Abramowitz Y, Kazuno Y, Chakravarty T, Kawamori H, Maeno Y, Anderson D, Allison Z, Mangat G, Cheng W, Gopal A, Jilaihawi H, Mack MJ, Makkar RR. Concomitant mitral annular calcification and severe aortic stenosis: prevalence, characteristics and outcome following transcatheter aortic valve replacement. *Eur Heart J*. 2017;38:1194–1203. doi: 10.1093/eurheartj/ehw594.
157. De Carlo M, Giannini C, Bedogni F, Klugmann S, Brambilla N, De Marco F, Zucchelli G, Testa L, Oreglia J, Petronio AS. Safety of a conservative strategy of permanent pacemaker implantation after transcatheter aortic CoreValve implantation. *Am Heart J*. 2012;163:492–499. doi: 10.1016/j.ahj.2011.12.009.
158. Fraccaro C, Buja G, Tarantini G, Gasparetto V, Leoni L, Razzolini R, Corrado D, Bonato R, Basso C, Thiene G, Gerosa G, Isabella G, Iliceto S, Napodano M. Incidence, predictors, and outcome of conduction disorders after transcatheter self-expandable aortic valve implantation. *Am J Cardiol*. 2011;107:747–754. doi: 10.1016/j.amjcard.2010.10.054.
159. Rodríguez-Olivares R, van Gils L, El Faquir N, Rahhab Z, Di Martino LF, van Weenen S, de Vries J, Galema TW, Geleijnse ML, Budde RP, Boersma E, de Jaegere PP, Van Mieghem NM. Importance of the left ventricular outflow tract in the need for pacemaker implantation after transcatheter aortic valve replacement. *Int J Cardiol*. 2016;216:9–15. doi: 10.1016/j.ijcard.2016.04.023.
160. Al-Azzam F, Greason KL, Krittanawong C, Williamson EE, McLeod CJ, King KS, Mathew V. The influence of native aortic valve calcium and transcatheter valve oversize on the need for pacemaker implantation after transcatheter aortic valve insertion. *J Thorac Cardiovasc Surg*. 2017;153:1056–1062.e1. doi: 10.1016/j.jtcvs.2016.11.038.
161. Erkapic D, Kim WK, Weber M, Möllmann H, Berkowitsch A, Zaltsberg S, Pajitnev DJ, Rixe J, Neumann T, Kuniss M, Sperzel J, Hamm CW, Pitschner HF. Electrocardiographic and further predictors for permanent pacemaker requirement after transcatheter aortic valve implantation. *Europace*. 2010;12:1188–1190. doi: 10.1093/europace/euq094.
162. Fujita B, Kütting M, Seiffert M, Scholtz S, Egron S, Prashovikj E, Börgermann J, Schäfer T, Scholtz W, Preuss R, Gummert J, Steinseifer U, Ensminger SM. Calcium distribution patterns of the aortic valve as a risk factor for the need of permanent pacemaker implantation after transcatheter aortic valve implantation. *Eur Heart J Cardiovasc Imaging*. 2016;17:1385–1393. doi: 10.1093/ehjci/jev343.
163. Gensas CS, Caixeta A, Siqueira D, Carvalho LA, Sarmento-Leite R, Mangione JA, Lemos PA, Colafranceschi AS, Caramori P, Ferreira MC, Abizaid A, Brito FS Jr; Brazilian Registry in Transcatheter Aortic Valve Implantation Investigators. Predictors of permanent pacemaker requirement after transcatheter aortic valve implantation: insights from a Brazilian registry. *Int J Cardiol*. 2014;175:248–252. doi: 10.1016/j.ijcard.2014.05.020.
164. Gonska B, Seeger J, Keßler M, von Keil A, Rottbauer W, Wöhrle J. Predictors for permanent pacemaker implantation in patients undergoing transfemoral aortic valve implantation with the Edwards Sapien 3 valve. *Clin Res Cardiol*. 2017;106:590–597. doi: 10.1007/s00392-017-1093-2.
165. Koos R, Mahnken AH, Aktug O, Dohmen G, Autschbach R, Marx N, Hoffmann R. Electrocardiographic and imaging predictors for permanent pacemaker requirement after transcatheter aortic valve implantation. *J Heart Valve Dis*. 2011;20:83–90.
166. Maan A, Refaat MM, Heist EK, Passeri J, Inglessis I, Ptaszek L, Vlahakes G, Ruskin JN, Palacios I, Sundt T, Mansour M. Incidence and predictors of pacemaker implantation in patients undergoing transcatheter aortic valve replacement. *Pacing Clin Electrophysiol*. 2015;38:878–886. doi: 10.1111/pace.12653.
167. Maeno Y, Abramowitz Y, Kawamori H, Kazuno Y, Kubo S, Takahashi N, Mangat G, Okuyama K, Kashif M, Chakravarty T, Nakamura M, Cheng W, Friedman J, Berman D, Makkar RR, Jilaihawi H. A highly predictive risk model for pacemaker implantation after TAVR [published online ahead of print April 7, 2017]. *JACC Cardiovasc Imaging*. doi: 10.1016/j.jcmg.2016.11.020. http://www.sciencedirect.com/science/article/pii/S1936878X17301523?via%3Dihub.
168. Mouillet G, Lellouche N, Yamamoto M, Oguri A, Dubois-Rande JL, Van Belle E, Gilard M, Laskar M, Teiger E. Outcomes following pacemaker implantation after transcatheter aortic valve implantation with CoreValve(®) devices: results from the FRANCE 2 Registry. *Catheter Cardiovasc Interv*. 2015;86:E158–E166. doi: 10.1002/ccd.25818.
169. Muñoz-García AJ, Hernández-García JM, Jiménez-Navarro MF, Alonso-Briales JH, Domínguez-Franco AJ, Fernández-Pastor J, Peña Hernández J, Barrera Cordero A, Alzueta Rodríguez J, de Teresa-Galván E. Factors predicting and having an impact on the need for a permanent pacemaker after CoreValve prosthesis implantation using the new Accutrak delivery catheter system. *JACC Cardiovasc Interv*. 2012;5:533–539. doi: 10.1016/j.jcin.2012.03.011.
170. Roten L, Wenaweser P, Delacrétaz E, Hellige G, Stortecky S, Tanner H, Pilgrim T, Kadner A, Eberle B, Zwahlen M, Carrel T, Meier B, Windecker S. Incidence and predictors of atrioventricular conduction impairment after transcatheter aortic valve implantation. *Am J Cardiol*. 2010;106:1473–1480. doi: 10.1016/j.amjcard.2010.07.012.
171. Kim WJ, Ko YG, Han S, Kim YH, Dy TC, Posas FE, Lee MK, Kim HS, Hong MK, Jang Y, Grube E, Park SJ. Predictors of permanent pacemaker insertion following transcatheter aortic valve replacement with the CoreValve Revalving System based on computed tomography analysis: an Asian multicenter registry study. *J Invasive Cardiol*. 2015;27:334–340.
172. Saia F, Lemos PA, Bordoni B, Cervi E, Boriani G, Ciuca C, Taglieri N, Mariani J Jr, Kalil Filho R, Marzocchi A. Transcatheter aortic valve implantation with a self-expanding nitinol bioprosthesis: prediction of the need for permanent pacemaker using simple baseline and procedural characteristics. *Catheter Cardiovasc Interv*. 2012;79:712–719. doi: 10.1002/ccd.23336.
173. Toutouzas K, Synetos A, Tousoulis D, Latsios G, Brili S, Mastrokostopoulos A, Karanasos A, Sideris S, Dilaveris P, Cheong A, Yu CM, Stefanadis C. Predictors for permanent pacemaker implantation after Core Valve implantation in patients without preexisting ECG conduction disturbances:

the role of a new echocardiographic index. *Int J Cardiol*. 2014;172:601–603. doi: 10.1016/j.ijcard.2014.01.091.
174. Schroeter T, Linke A, Haensig M, Merk DR, Borger MA, Mohr FW, Schuler G. Predictors of permanent pacemaker implantation after Medtronic CoreValve bioprosthesis implantation. *Europace*. 2012;14:1759–1763. doi: 10.1093/europace/eus191.
175. Akin I, Kische S, Paranskaya L, Schneider H, Rehders TC, Trautwein U, Turan G, Bänsch D, Thiele O, Divchev D, Bozdag-Turan I, Ortak J, Kundt G, Nienaber CA, Ince H. Predictive factors for pacemaker requirement after transcatheter aortic valve implantation. *BMC Cardiovasc Disord*. 2012;12:87. doi: 10.1186/1471-2261-12-87.
176. Latsios G, Gerckens U, Buellesfeld L, Mueller R, John D, Yuecel S, Syring J, Sauren B, Grube E. "Device landing zone" calcification, assessed by MSCT, as a predictive factor for pacemaker implantation after TAVI. *Catheter Cardiovasc Interv*. 2010;76:431–439. doi: 10.1002/ccd.22563.
177. Mouillet G, Lellouche N, Lim P, Meguro K, Yamamoto M, Deux JF, Monin JL, Bergoënd E, Dubois-Randé JL, Teiger E. Patients without prolonged QRS after TAVI with CoreValve device do not experience high-degree atrio-ventricular block. *Catheter Cardiovasc Interv*. 2013;81:882–887. doi: 10.1002/ccd.24657.
178. Rivard L, Schram G, Asgar A, Khairy P, Andrade JG, Bonan R, Dubuc M, Guerra PG, Ibrahim R, Macle L, Roy D, Talajic M, Dyrda K, Shohoudi A, le Polain de Waroux JB, Thibault B. Electrocardiographic and electrophysiological predictors of atrioventricular block after transcatheter aortic valve replacement. *Heart Rhythm*. 2015;12:321–329. doi: 10.1016/j.hrthm.2014.10.023.
179. Curtis AB, Worley SJ, Adamson PB, Chung ES, Niazi I, Sherfesee L, Shinn T, Sutton MS; Biventricular versus Right Ventricular Pacing in Heart Failure Patients with Atrioventricular Block (BLOCK HF) Trial Investigators. Biventricular pacing for atrioventricular block and systolic dysfunction. *N Engl J Med*. 2013;368:1585–1593. doi: 10.1056/NEJMoa1210356.
180. van Gils L, Tchetche D, Lhermusier T, Abawi M, Dumonteil N, Rodriguez Olivares R, Molina-Martin de Nicolas J, Stella PR, Carrie D, De Jaegere PP, Van Mieghem NM. Transcatheter heart valve selection and permanent pacemaker implantation in patients with pre-existent right bundle branch block. *J Am Heart Assoc*. 2017;6:e005028.
181. Amat-Santos IJ, Rodés-Cabau J, Urena M, DeLarochellière R, Doyle D, Bagur R, Villeneuve J, Côté M, Nombela-Franco L, Philippon F, Pibarot P, Dumont E. Incidence, predictive factors, and prognostic value of new-onset atrial fibrillation following transcatheter aortic valve implantation. *J Am Coll Cardiol*. 2012;59:178–188. doi: 10.1016/j.jacc.2011.09.061.
182. Auffret V, Regueiro A, del Trigo M, Campelo-Parada F, Abdul-Jawad Altisent O, Chiche O, Puri R, Rodés-Cabau J. Predictors of early cerebrovascular events in patients with severe aortic stenosis undergoing transcatheter aortic valve replacement: a systematic review and meta-analysis. *J Am Coll Cardiol*. 2016;68:673–684.
183. Tovia-Brodie O, Ben-Haim Y, Joffe E, Finkelstein A, Glick A, Rosso R, Belhassen B, Michowitz Y. The value of electrophysiologic study in decision-making regarding the need for pacemaker implantation after TAVI. *J Interv Card Electrophysiol*. 2017;48:121–130. doi: 10.1007/s10840-016-0218-2.
184. Urena M, Rodés-Cabau J. Managing heart block after transcatheter aortic valve implantation: from monitoring to device selection and pacemaker indications. *EuroIntervention*. 2015;11(suppl W):W101–W105. doi: 10.4244/EIJV11SWA30.
185. Leclercq F, Iemmi A, Lattuca B, Macia JC, Gervasoni R, Roubille F, Gandet T, Schmutz L, Akodad M, Agullo A, Verges M, Nogue E, Marin G, Nagot N, Rivalland F, Durrleman N, Robert G, Delseny D, Albat B, Cayla G. Feasibility and safety of transcatheter aortic valve implantation performed without intensive care unit admission. *Am J Cardiol*. 2016;118:99–106. doi: 10.1016/j.amjcard.2016.04.019.
186. Sideris S, Benetos G, Toutouzas K, Drakopoulou M, Sotiropoulos E, Gatzoulis K, Latsios G, Synetos A, Trantalis G, Tousoulis D, Kallikazaros I. Outcomes of same day pacemaker implantation after TAVI. *Pacing Clin Electrophysiol*. 2016;39:690–695. doi: 10.1111/pace.12871.
187. Chevreul K, Brunn M, Cadier B, Haour G, Eltchaninoff H, Prat A, Leguerrier A, Blanchard D, Fournial G, Iung B, Donzeau-Gouge P, Tribouilloy C, Debrux JL, Pavie A, Gilard M, Gueret P; FRANCE Registry Investigators. Cost of transcatheter aortic valve implantation and factors associated with higher hospital stay cost in patients of the FRANCE (FRench Aortic National CoreValve and Edwards) registry. *Arch Cardiovasc Dis*. 2013;106:209–219. doi: 10.1016/j.acvd.2013.01.006.
188. Udo EO, Zuithoff NP, van Hemel NM, de Cock CC, Hendriks T, Doevendans PA, Moons KG. Incidence and predictors of short- and long-term complications in pacemaker therapy: the FOLLOWPACE study. *Heart Rhythm*. 2012;9:728–735. doi: 10.1016/j.hrthm.2011.12.014.
189. Tompkins C, Cheng A, Dalal D, Brinker JA, Leng CT, Marine JE, Nazarian S, Spragg DD, Sinha S, Halperin H, Tomaselli GF, Berger RD, Calkins H, Henrikson CA. Dual antiplatelet therapy and heparin "bridging" significantly increase the risk of bleeding complications after pacemaker or implantable cardioverter-defibrillator device implantation. *J Am Coll Cardiol*. 2010;55:2376–2382. doi: 10.1016/j.jacc.2009.12.056.
190. Ponikowski P, Voors AA, Anker SD, Bueno H, Cleland JG, Coats AJ, Falk V, González-Juanatey JR, Harjola VP, Jankowska EA, Jessup M, Linde C, Nihoyannopoulos P, Parissis JT, Pieske B, Riley JP, Rosano GM, Ruilope LM, Ruschitzka F, Rutten FH, van der Meer P. 2016 ESC guidelines for the diagnosis and treatment of acute and chronic heart failure: the Task Force for the diagnosis and treatment of acute and chronic heart failure of the European Society of Cardiology (ESC) developed with the special contribution of the Heart Failure Association (HFA) of the ESC. *Eur Heart J*. 2016;37:2129–2200. doi: 10.1093/eurheartj/ehw128.
191. Meguro K, Lellouche N, Teiger E. Cardiac resynchronization therapy improved heart failure after left bundle branch block during transcatheter aortic valve implantation. *J Invasive Cardiol*. 2012;24:132–133.
192. Osmancik P, Stros P, Herman D, Kocka V, Paskova E. Cardiac resynchronization therapy implantation following transcatheter aortic valve implantation. *Europace*. 2011;13:290–291. doi: 10.1093/europace/euq336.

Circulation

American Heart Association.

Conduction Disturbances After Transcatheter Aortic Valve Replacement: Current Status and Future Perspectives

Vincent Auffret, Rishi Puri, Marina Urena, Chekrallah Chamandi, Tania Rodriguez-Gabella, François Philippon and Josep Rodés-Cabau

Circulation. 2017;136:1049-1069
doi: 10.1161/CIRCULATIONAHA.117.028352
Circulation is published by the American Heart Association, 7272 Greenville Avenue, Dallas, TX 75231

Print ISSN: 0009-7322. Online ISSN: 1524-4539

2.2.3 Synthèse

Cette revue de la littérature concernant les troubles conductifs post TAVI nous offre l'opportunité de proposer aux candidats au TAVI une prise en charge individualisé selon leurs facteurs de risque de trouble conductifs afin d'essayer d'en limiter l'incidence de survenue. Elle souligne également les limites des données de la science actuelle sur le sujet, mettant en évidence des pistes d'améliorations futures.

A la phase préopératoire, le dépistage de troubles conductifs asymptomatiques associés à la sténose aortique serrée, par une courte période (24-48h) de monitoring lors de l'hospitalisation pour bilan préopératoire, est un moyen simple et peu coûteux pour identifier des patients qui pourront bénéficier d'une implantation programmée avant la procédure et ne seront donc pas exposés au risque post-opératoire. Une stratégie approchante, basée sur un monitoring plus prolongé, est actuellement évaluée dans l'étude « Prolonged Continuous ECG Monitoring Prior to Transcatheter Aortic Valve Implantation » (PARE - NCT03561805). Par ailleurs, les facteurs de risque principaux de troubles conductifs étant représentés par la présence d'un bloc de branche droite du faisceau de His, l'implantation d'une valve auto-expansible (ou certaines valves à expansion mécanique encore peu utilisées) et un « oversizing » important prévisible de l'anneau ou de la chambre de chasse du ventricule, il est possible de réduire la survenue de trouble de conduction cardiaque par une meilleure sélection des patients. Les patients présentant un bloc de branche droite préexistant doivent se voir en priorité proposer une prothèse moins pourvoyeuse de troubles conductifs. L'analyse du scanner préopératoire doit également être minutieuse afin de prévoir les patients pour lesquels un risque important d'oversizing est présent afin d'adapter si possible le choix du type et de la taille de prothèse. Enfin, l'intérêt potentiel d'une évaluation systématique de la longueur du septum interventriculaire membraneux (60) ou d'une analyse précise de la localisation et du volume de calcification de diverses zones anatomiques d'intérêt tel que la chambre de chasse du ventricule gauche ou les cusps aortiques (61), mérite d'être évalué de façon prospective dans des études dédiées.

Pendant l'intervention, l'opérateur doit s'attacher à limiter les « agressions » du système de conduction cardiaque. L'élément le plus influent à ce stade semble être la profondeur d'implantation de la prothèse dans la chambre de chasse du ventricule gauche qui se doit d'être parfaitement maitrisée. Dans la pratique courante, cet élément est déjà pris en compte par les praticiens et des stratégies visant à limiter la profondeur d'implantation de la prothèse ont

démontré un impact positif sur le risque d'implantation d'un stimulateur cardiaque définitif après TAVI (62–64). Dans le même esprit, limiter les dilatations au ballon de la zone de largage de la prothèse dans des cas sélectionnés (patients à haut risque) pourrait permettre de réduire les complications conductives (65,66).

En fin d'intervention, en l'absence de bloc auriculoventriculaire de haut degré persistant, le maintien ou non de la sonde d'entrainement cardiaque temporaire est une question nécessitant de la part de l'opérateur une attention particulière. En effet, le maintien de cette sonde est généralement associé à un alitement plus prolongé avec sa morbidité propre, un risque de complications liées à la sonde elle-même plus important et nécessite une hospitalisation en secteur de soins intensifs avec un impact non négligeable sur le coût global de la procédure. L'opérateur doit donc juger de sa nécessité avec rigueur en tenant compte des caractéristiques de base du patient (présence d'un trouble conductif préexistant), du résultat de la procédure (profondeur d'implantation de la prothèse, autre complication nécessitant une hospitalisation en soins intensifs) et de l'éventuelle survenue/aggravation de troubles conductifs en perprocédure. Comme souligné dans notre revue de la littérature, il n'existe à ce jour pas de données solides sur le timing optimal de retrait de la sonde d'entrainement cardiaque temporaire, néanmoins il semble prudent de la maintenir en place au moins jusqu'au lendemain de la procédure chez les patients avec bloc de branche droit préexistant, en cas de bloc auriculoventriculaire de haut degré transitoire perprocédural ou encore en cas d'apparition/aggravation importante de troubles conductifs préexistant, notamment les patients avec un bloc de branche de novo soit très large (>150-160ms) soit associé à un bloc auriculoventriculaire du premier degré ou un allongement significatif de l'intervalle PR sur l'ECG (> 20-30ms).

En phase post-opératoire, l'élément le plus important est le respect des indications avec un haut niveau de preuve, émises par les recommandations internationales, pour l'implantation d'un stimulateur cardiaque définitif (64). Notre revue souligne essentiellement le manque de preuves scientifiques permettant de guider la prise en charge des patients. C'est probablement à ce stade que des études prospectives de cohortes de population voire des études randomisées seraient le plus utiles. Plusieurs objectifs peuvent être cités : identification de facteurs pronostiques de trouble conductif de haut degré retardé (> 48-72h après la procédure) afin de mieux sélectionner les candidats à une sortie précoce, évaluation de la valeur pronostique (notamment de la valeur prédictive négative) d'une exploration électrophysiologique systématique chez les patients avec troubles conductifs de novo ou aggravation de troubles

préexistant, impact de stratégies de management basées sur l'implantation de dispositifs de monitoring de l'ECG de longue durée qui ont démontré un taux d'arythmies cardiaques conduisant à une modification de la prise en charge médicale de près de 20% à 1 an dans la récente étude MARE (67), ou encore précision des facteurs pronostiques d'un pourcentage de stimulation ventriculaire élevé à long terme après implantation d'un stimulateur cardiaque post-TAVI, ce qui pourrait aider à préciser la place d'une technique comme la resynchronisation cardiaque en post-TAVI immédiat, etc...

2.3 Facteurs de risque de « mauvais résultats » après TAVI

2.3.1 Problématique

Comme nous l'avons vu dans le premier chapitre, le TAVI est une technique qui a été initialement développé pour prendre en charge des patients inopérables ou à très haut risque chirurgical. En conséquence, la mortalité à 1 an après TAVI dans plusieurs grandes études pivots au début de l'expérience était de 25 à 30% et au moins 10% des patients restaient très symptomatiques (grade 3 ou 4 de dyspnée selon la classification usuelle de la New-York Heart Association - NYHA[3]) à 6-12 mois de la procédure (13–15). De nombreuses études ont alors tenté d'évaluer les facteurs de risque de mortalité précoce et à moyen terme (1 an) après une procédure TAVI conduisant à démontrer l'impact délétère sur la survie de divers facteurs : fuite aortique para prothétique résiduelle modérée à sévère (15,68–70), broncho-pneumopathie chronique obstructive (68,71,72), insuffisance rénale chronique préexistante (70,73), ou encore hypertension pulmonaire (70,74,75).

Toutefois, le TAVI étant très majoritairement pratiqué chez des patients très âgés, chez qui la qualité de vie est tout aussi importante que l'espérance de vie, il paraissait intéressant de développer des modèles statistiques de prédiction du résultat « global » à court terme de la procédure incluant, outre la mortalité, le statut fonctionnel du patient, les éventuelles réhospitalisations ou encore les complications post-procédure susceptibles de retentir négativement sur la qualité de vie. Les études s'intéressant aux déterminants du statut

[3] Cette classification en 4 grades permet de quantifier l'essoufflement des patients, un grade plus important indiquant une dyspnée plus importante (grade 1: pas de dyspnée, grade 2 : dyspnée dans les efforts inhabituels de la vie quotidienne, grade 3 : dyspnée dans les efforts habituels de la vie quotidienne, grade 4 : dyspnée de repos).

fonctionnel ou de ce type de critère composite étant alors peu nombreuses (76,77), il nous apparaissait important de proposer notre contribution à la littérature.

2.3.2 Article original

Ce travail sur la cohorte rennaise de TAVI, publié dans *Archives of Cardiovascular Diseases*, s'inscrit dans ce contexte de manque de données concernant les facteurs prédictifs du pronostic global des patients. Son but principal était d'aider à mieux sélectionner les patients candidats à une procédure TAVI en identifiant, par analyse d'une cohorte de 163 patients traités entre 2009 et 2012, au moyen d'une méthode de régression logistique multivariée, les facteurs indépendamment associés à un critère composite de « mauvais résultats » associant les décès toutes causes, les AVC, les réhospitalisations pour insuffisance cardiaque ou en rapport avec la prothèse et une classe NYHA 3 ou 4 à 6 mois de la procédure.

Archives of Cardiovascular Disease (2014) 107, 10—20

Available online at ScienceDirect www.sciencedirect.com

Elsevier Masson France EM|consulte www.em-consulte.com/en

CLINICAL RESEARCH

Predictors of 6-month poor clinical outcomes after transcatheter aortic valve implantation

Facteurs prédictifs de mauvais résultat clinique à 6 mois de l'implantation d'une valve aortique percutanée

Vincent Auffret[a,b,c,d,*], Dominique Boulmier[a,b,c,d], Emmanuel Oger[e], Marc Bedossa[a,b,c,d], Erwan Donal[a,b,c,d], Marcel Laurent[a,b,c,d], Gwenaelle Sost[f], Xavier Beneux[g], Majid Harmouche[g], Jean-Philippe Verhoye[g], Hervé Le Breton[a,b,c,d]

[a] *Inserm, U1099, Rennes, France*
[b] *Université de Rennes 1, LTSI, Rennes, France*
[c] *CHU de Rennes, Service de Cardiologie et Maladies Vasculaires, Rennes, France*
[d] *Inserm, CIC-IT804, Rennes, France*
[e] *CHU de Rennes, Service de Pharmacologie Clinique, Rennes, France*
[f] *CHU de Rennes, Service de Gériatrie, Rennes, France*
[g] *CHU de Rennes, Service de Chirurgie Cardiaque, Thoracique et Vasculaire, Rennes, France*

Received 13 August 2013; received in revised form 27 October 2013; accepted 30 October 2013
Available online 18 December 2013

KEYWORDS
Transcatheter aortic valve implantation;
Aortic stenosis;
Aortic regurgitation;
Outcomes

Summary
Background. — Patient selection for transcatheter aortic valve implantation (TAVI) remains a major concern. Indeed, despite promising results, it is still unclear which patients are most and least likely to benefit from this procedure.
Aims. — To identify predictors of 6-month poor clinical outcomes after TAVI.

Abbreviations: AF, atrial fibrillation; AR, aortic regurgitation; AS, aortic stenosis; CI, confidence interval; EOA, effective orifice area; HR, hazard ratio; LVEF, left ventricular ejection fraction; MR, mitral regurgitation; NYHA, New York Heart Association; OR, odds ratio; RV, right ventricular; SAVR, surgical aortic valve replacement; sPAP, systolic pulmonary artery pressure; STS, Society of Thoracic Surgeons; TAVI, transcatheter aortic valve implantation; TEE, transoesophageal echocardiography; TTE, transthoracic echocardiography; TR, tricuspid regurgitation.

* Corresponding author. Service de Cardiologie, CHU de Rennes, 2, rue Henri-Le-Guilloux, 35000 Rennes, France.
E-mail address: vincent.auffret@chu-rennes.fr (V. Auffret).

1875-2136/$ — see front matter
http://dx.doi.org/10.1016/j.acvd.2013.10.005

Methods. — Patients who were discharged from our institution with a transcatheter-implanted aortic valve were followed prospectively. Our population was divided into two groups ('good outcomes' and 'poor outcomes') according to occurrence of primary endpoint (composite of all-cause mortality, all stroke, hospitalizations for valve-related symptoms or worsening heart failure from discharge to 6 months or 6-month New York Heart Association functional class III or IV). Patient characteristics were studied to find predictors of poor outcomes.
Results. — We included 163 patients (mean age, 79.9 ± 8.8 years; 90 men [55%]; mean logistic EuroSCORE, 18.4 ± 11.4%). The primary endpoint occurred in 49 patients (mean age, 83 ± 5 years; 31 men [63%]). By multivariable analysis, atrial fibrillation (odds ratio [OR] 3.94), systolic pulmonary artery pressure ≥ 60 mmHg (OR 7.56) and right ventricular dysfunction (OR 3.55) were independent predictors of poor outcomes, whereas baseline aortic regurgitation ≥ 2/4 (OR 0.07) demonstrated a protective effect.
Conclusion. — Atrial fibrillation, severe baseline pulmonary hypertension and right ventricular dysfunction (i.e. variables suggesting a more evolved aortic stenosis) were predictors of 6-month poor outcomes. Conversely, baseline aortic regurgitation ≥ 2/4 showed a protective effect, which needs to be confirmed in future studies. Our study highlights the need for a specific 'TAVI risk score', which could lead to better patient selection.

MOTS CLÉS
Valve aortique percutanée ;
Sténose aortique ;
Insuffisance aortique ;
Résultat

Résumé
Contexte. — La sélection des patients pour l'implantation d'une valve aortique transcathéter (TAVI) demeure un challenge clinique. En effet, malgré des résultats prometteurs, il reste difficile de savoir quels patients sont les moins susceptibles de tirer bénéfice de cette procédure.
Objectif. — Notre objectif était d'identifier des facteurs prédictifs d'un mauvais résultat 6 mois après TAVI.
Méthodes. — Nous avons prospectivement suivi les patients sortis de l'hôpital avec une valve aortique implantée par voie transcathéter. Notre population a été divisée en 2 groupes, « bon résultat » et « mauvais résultat », en fonction de la survenue du critère primaire qui était un critère composite des décès toutes causes, des accidents vasculaires cérébraux, des hospitalisations pour insuffisance cardiaque ou symptômes en rapport avec la valve entre la sortie de l'hospitalisation et le suivi à 6 mois ou une classe fonctionnelle New York Heart Association III ou IV à 6 mois. Les caractéristiques des patients ont été étudiées afin de déterminer des facteurs prédictifs de mauvais résultat.
Résultats. — Cent soixante-trois patients consécutifs (âge moyen : 79,9 ± 8,8 ans ; 90 hommes [55 %]) ont été inclus. L'EuroSCORE logistique moyen était de 18,4 ± 11,4 %. Quarante-neuf patients ont présenté le critère primaire. En analyse multivariée, la fibrillation atriale (OR 3,94), une pression artérielle pulmonaire systolique ≥ 60 mmHg (OR 7,56), une dysfonction ventriculaire droite (OR 3,55) étaient des facteurs prédictifs indépendants de mauvais résultat alors que l'insuffisance aortique préopératoire ≥ 2/4 (OR 0,07) présentait un effet protecteur.
Conclusion. — La fibrillation atriale, une pression artérielle pulmonaire systolique ≥ 60 mmHg et une dysfonction ventriculaire droite, des variables évoquant un rétrécissement aortique plus évolué, étaient des facteurs prédictifs de mauvais résultat à 6 mois après TAVI. À l'inverse, une insuffisance aortique préopératoire ≥ 2/4 présentait un effet protecteur qui doit être confirmé dans des études futures. Notre étude souligne la nécessité de développer un score de risque spécifique du TAVI qui pourrait améliorer la sélection des patients.

Introduction

Aortic stenosis (AS) is the most common valvular disease, with an increasing incidence in the elderly population [1]. Transcatheter aortic valve implantation (TAVI) was developed as an alternative to surgical aortic valve replacement (SAVR) in patients at prohibitive surgical risk. Several registries [2—4] showed functional improvement in patients with severe symptomatic AS treated with TAVI. TAVI demonstrated a 2-year survival advantage over medical therapy in inoperable patients [5] and non-inferiority against SAVR in high-risk patients [6]; it is now the standard of care for inoperable patients and a valid alternative to surgery for many high-risk patients [7].

Despite these promising results, a significant proportion of patients either die or have no functional benefits within the first months after TAVI [2,5,6,8]. Numerous predictors of mortality have been identified, such as postprocedural aortic regurgitation (AR) [2,3,6,9], chronic obstructive pulmonary disease [3], chronic kidney disease, pulmonary hypertension and postprocedural complications [9].

Moreover, recently, postprocedural AR and severe mitral regurgitation (MR) were identified as independent predictors of poor treatment response [8]. Nonetheless, data on predictors of functional outcomes after TAVI are scarce. Yet, given that this technique is generally intended for elderly patients, symptomatic improvement is as critical as the increase in life expectancy. A risk score to identify those patients who are least likely to benefit from TAVI should further improve the selection of TAVI candidates.

The goal of this prospective study was to identify predictors of 6-month poor outcomes after TAVI, defined as the clinical components of 'clinical efficacy', as outlined in the recommendations of the Valve Academic Research Consortium [10].

Methods

Patients

Patients with severe and symptomatic AS (effective orifice area [EOA] $\leq$1 cm^2) who underwent TAVI at our institution were prospectively enrolled. Exclusion criteria were death during the procedure or subsequent hospitalization, conversion to surgery or unsuccessful implantation (defined as impossibility to deliver and deploy a valve into the proper location for anatomical reasons). Before TAVI, these patients underwent an evaluation, which included a physical examination, blood tests, transthoracic and transoesophageal echocardiography (TTE and TEE, respectively) and computerized tomography. Indications, contraindications and anatomical requirements for TAVI have been described previously [7]. SAVR risk of mortality was estimated using the logistic EuroSCORE [11] and the Society of Thoracic Surgeons (STS) risk score [12]. Finally, TAVI indication was retained by a multidisciplinary 'Heart Team' based on the evaluation cited above. Patients were followed on-site before discharge, 1 month after implantation and either on-site or by their cardiologist 6 months after TAVI. Follow-up information was also obtained by telephone contact with deceased patients' physicians. Patients gave written informed consent before participation. The study was approved by the local ethics committee.

Endpoints

The primary endpoint was the clinical components of 'clinical efficacy' [10] (i.e. a composite of all-cause mortality, all stroke [disabling and non-disabling], hospitalizations for valve-related symptoms or worsening heart failure from discharge to 6 months or a 6-month New York Heart Association [NYHA] class III or IV). Secondary endpoints were clinical efficacy, as defined in the recommendations of the Valve Academic Research Consortium [10] (clinical components or valve-related dysfunction, i.e. mean aortic valve gradient $\geq$20 mmHg, EOA $\leq$0.9—1.1 cm^2 and/or Doppler velocity index < 0.35 m/s and/or moderate or severe prosthetic valve regurgitation), and 6-month all-cause mortality. The cohort was subsequently divided into two groups: 'good outcomes' and 'poor outcomes', according to the occurrence of the primary endpoint.

Atrial fibrillation (AF) was defined as any history of AF regardless of type of arrhythmia or presence of AF on at least one electrocardiogram during hospitalization for the preoperative assessment or the day before TAVI. Coronary artery disease was defined as presence of lesions with $\geq$50% diameter stenosis on pre-TAVI angiography and/or previous treatment with percutaneous coronary intervention or coronary artery bypass grafting. Complications were defined according to the recommendations of the Valve Academic Research Consortium [10].

Study devices and procedures

The two CE-approved prostheses and implantation techniques have been described previously [2,4]. The procedure was performed in a catheterization laboratory in a sterile environment by at least two interventional cardiologists, a cardiac surgeon and an anaesthesiologist. The choice of whether to use local or general anaesthesia was left at the discretion of the anaesthesiologist in charge of the patient. The type of anaesthesia used was not recorded routinely in our database, but was known for 81% (n=132) of patients, 66% of whom (n=87) underwent local anaesthesia. TEE was used for transapical cases, to accurately define the apical surgical access site. Fluoroscopy was used for valve positioning in all cases, with the help of TEE guidance only in transapical cases.

Echocardiography

TTE was performed according to the American Society of Echocardiography guidelines [13] by an experienced echocardiographer using a digital ultrasound scanner (Vivid7, GE Healthcare, Little Chalfont, UK; or iE33, Philips Healthcare, Andover, MA, USA).

In apical five-chamber view, peak and mean pressure gradients across the aortic valve were calculated using the Bernoulli equation. EOA was calculated using the continuity equation.

A multiparametric approach with both semiquantitative and quantitative variables was used to grade valvular regurgitation on a scale from 0 to 4, with higher grades indicating greater severity (0, no; 1, mild; 2, moderate; 3/4, severe). Baseline and postprocedural AR were graded in accordance with the European Society of Cardiology guidelines for native valves [14]. However, given the frequent eccentric and irregular jet of postprocedural AR, we also gave a heavy weighting to the circumferential extent of prosthetic AR in parasternal short-axis view, to provide an integrated assessment of postprocedural AR [10]. Thresholds were as follows: none, no regurgitant colour flow; mild extent, < 10%; moderate extent, 10—29%; severe extent, $\geq$30%. Before TAVI, we used TEE to measure the annulus diameter accurately and sometimes to grade AR or MR when TTE was not conclusive.

Pulmonary hypertension was defined as systolic pulmonary artery pressure (sPAP) $\geq$40 mmHg at rest, estimated using tricuspid regurgitation (TR) velocity [15]. Right atrial pressure was assessed using inferior vena cava diameter (in its long axis) and inspiratory collapse in the subcostal view [15]: a diameter $\leq$21 mm and a collapse > 50% with a sniff were used as cut-offs for normal right atrial pressure (i.e. 3 mmHg, range 0—5 mmHg), whereas a diameter > 21 mm and a collapse < 50% defined high right atrial pressure (15 mmHg, range 10—20 mmHg). In indeterminate cases,

in which the inferior vena cava diameter and collapse did not fit these definitions, an intermediate value of 8 mmHg (range 5—10 mmHg) was used. Right ventricular (RV) function was assessed in apical four-chamber view using tricuspid annular plane systolic excursion measured by M-mode, with a reference value for impaired RV systolic function of < 16 mm and an RV peak systolic velocity of the tricuspid annulus measured by tissue Doppler, with a value of ≥ 10 cm/s defining normal RV function [15]. Left ventricular ejection fraction (LVEF) was measured by Simpson's method from the four- and two-chamber views [13]. Left atrial end-systolic area was measured from the four-chamber apical view. LV end-diastolic and end-systolic diameters and end-diastolic septal thickness were measured by M-mode from parasternal views.

TTE was performed the day before TAVI, before discharge and 1 month and 6 months after TAVI.

Blood tests

Venous blood samples were obtained on the day before TAVI to determine concentrations of N-terminal pro B-type natriuretic peptide and serum creatinine. The estimated glomerular filtration rate was calculated using the abbreviated Modification of Diet in Renal Disease Study equation. Kidney disease was defined as moderate when the glomerular filtration rate was between 30 and 59 mL/min/1.73 m^2 and as severe when < 30 mL/min/1.73 m^2.

Statistical analysis

Numeric values are expressed as mean ± standard deviation. Normality was tested using the Kolmogorov-Smirnov test. Continuous variables were compared using the unpaired *t*-test or the Mann-Whitney U test, as appropriate. Chi-square analysis or Fisher's exact test was used to compare categorical variables. Patient characteristics were evaluated for poor outcomes. All baseline variables with a *P* value ≤ 0.2 in univariate analysis were entered into an ascending stepwise multivariable logistic regression analysis to identify independent predictors of poor outcomes and into an ascending stepwise Cox multivariable analysis to identify predictors of all-cause mortality. The likelihood ratio statistic was used at each step to define which variable should be included in or excluded from the model. Variables with a *P* value < 0.05 were added to or remained in the model, whereas variables with a *P* value ≥ 0.1 were removed. Results are presented as odds ratios (ORs) and hazard ratios (HRs). A *P* value ≤ 0.05 was considered significant. All probability values reported are two-sided. Statistical analysis was performed with the use of SPSS 21.0 software (SPSS, Inc., Chicago, IL, USA).

Results

Patients

From January 2009 to June 2012, 514 consecutive patients with severe and symptomatic AS were referred to our institution for pre-TAVI evaluation. After meetings of the Heart Team, TAVI indication was confirmed in 180 patients who underwent the procedure from February 2009 to July 2012. A total of 17 patients died during the procedure (*n* = 3) or the initial hospitalization (*n* = 6), were converted to surgery (*n* = 4: two annulus ruptures; two embolizations of the prosthesis in the left ventricle) or had unsuccessful implantation (*n* = 6: five non-fatal vascular access complications, one insufficient distance between valvular plane and a circumflex artery with an anomalous origin from the right sinus of Valsalva) and thus were excluded. Our study cohort included 163 surviving patients (Fig. 1). No patient was lost to follow-up.

The mean age of the study patients was 79.9 ± 8.8 years, 90 patients (55.2%) were men, the mean logistic EuroSCORE was 18.4 ± 11.4%, the mean STS risk score was 5.8 ± 3.1%, 118 patients (72.4%) were NYHA functional class III or IV, 86 patients (52.8%) had a history of acute heart failure and 71 patients (44%) had AF. The baseline characteristics of the study population are summarized in Table 1.

Procedural outcomes

The aortic valve prosthesis was inserted using the retrograde femoral artery approach (*n* = 132), the subclavian artery approach (*n* = 10), the transapical approach (*n* = 12) or the transaortic approach (*n* = 9). The implanted prosthesis was an Edwards SAPIEN (*n* = 8), an Edwards SAPIEN XT (*n* = 91) or a Medtronic CoreValve (*n* = 64). Valve size was 23 mm (*n* = 32), 26 mm (*n* = 63) or 29 mm (*n* = 4) for the Edwards devices and 26 mm (*n* = 20), 29 mm (*n* = 36) or 31 mm (*n* = 8) for the Medtronic CoreValve.

The mean total procedural time was 96 ± 31 minutes and the mean contrast agent volume was 238.8 ± 92.7 mL. Valve embolization in the aorta was observed in two cases and was managed with implantation of a second prosthesis. Acute kidney injury stage 2 or 3 arose in 10 patients (6.1%), including one who required temporary dialysis. Sixteen patients (9.8%, 15 CoreValve) received a new permanent pacemaker. Procedural outcomes are summarized in Table 2.

Mortality and poor outcomes

Eleven patients died (eight of cardiovascular causes) between discharge from hospital and 6-month follow-up. Thus, 6-month all-cause mortality rate was 6.7% for the study population and 11.1% for the 180 patients who underwent the procedure.

Twenty-three of 152 remaining study patients were NYHA functional class III or IV at 6-month follow-up. Hospitalization for heart failure occurred in 32 patients; no stroke occurred after the initial hospitalization. Eventually, 49 patients (30.1%) met the criteria for the 'poor outcomes' group. The 114 remaining patients (69.9%) formed the 'good outcomes' group.

All clinical characteristics with significant differences between groups are presented in Table 1. A total of 69 (42.3%) patients met the criteria for clinical efficacy.

Echocardiographical findings

Most patients had preserved LVEF (mean LVEF, 50.7 ± 14.8%) and only 25 patients (16%) had an LVEF ≤ 30%. Thirty-six patients (22.1%) had moderate or severe (≥ 2/4) AR at baseline. MR ≥ 2/4 was present in 65 patients (39.9%;

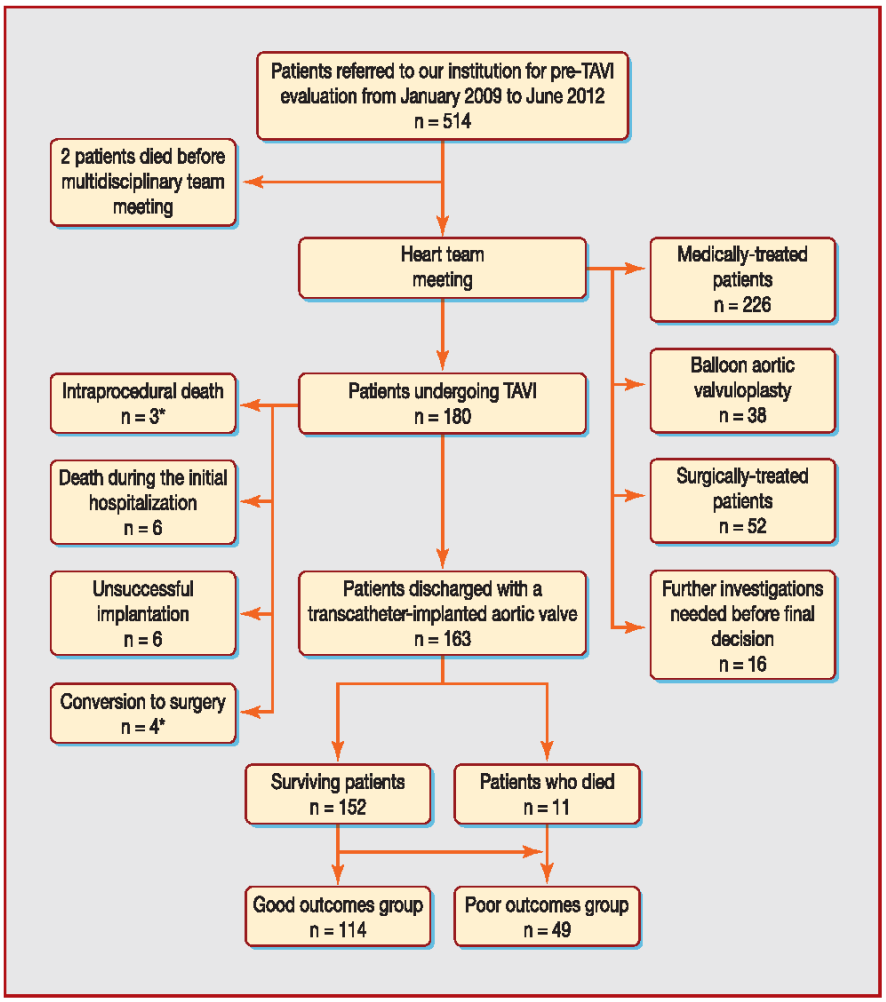

Figure 1. Flowchart. *: one patient died during surgical aortic valve replacement after aortic annulus rupture during transcatheter aortic valve implantation. †: one patient died during the initial hospitalization after conversion to surgery. TAVI: transcatheter aortic valve implantation.

moderate, $n=57$; severe, $n=8$). RV dysfunction was observed in 31 patients (19.0%) and 38 patients (23.3%) had TR $\geq$ 2/4 (moderate, $n=26$; severe, $n=12$). Pulmonary hypertension was diagnosed in 65.0% of patients; it was moderate (40 $\leq$ sPAP $\leq$ 59 mmHg) in 70 patients (42.9%) and severe (sPAP $\geq$ 60 mmHg) in 36 patients (22.1%). Overall, sPAP improved in 61 of the 106 patients (57.5%) with baseline pulmonary hypertension.

AR was common after TAVI, as 115 patients (70.6%) presented a leak, but AR $\geq$ 2/4 was present in only 30 patients (18.6%). Regarding patients with postprocedural AR $\geq$ 2/4, 9/16 patients (56.2%) in the good outcomes group compared with only 1/14 patients (7.1%) in the poor outcomes group had baseline AR $\geq$ 2/4. Echocardiographical findings are summarized in Table 3.

Predictors of 6-month poor outcomes

All variables with a P value $\leq$ 0.2 in univariate analysis for poor outcomes are listed in Table 4. These variables were entered into a stepwise multivariable logistic regression analysis that identified AF (OR 3.94, 95% confidence interval [CI] 1.67—9.29; $P=0.002$), RV dysfunction (OR 3.55, 95% CI 1.21—10.39; $P=0.02$) and severe baseline pulmonary hypertension (OR 7.56, 95% CI 2.58—22.17; $P<0.001$) as independent predictors of 6-month poor outcomes, whereas baseline AR $\geq$ 2/4 (OR 0.07, 95% CI 0.02—0.32; $P=0.001$) demonstrated a protective effect (Table 4).

Predictors of secondary endpoints

All variables with a P value $\leq$ 0.2 in univariate analysis for secondary endpoints are listed in Tables 5 and 6.

Independent predictors of clinical efficacy (Table 5) were AF (OR 4.09, 95% CI 1.99—8.39; $P<0.001$) and sPAP $\geq$ 60 mmHg (OR 3.84, 95% CI 1.52—9.72; $P=0.004$). Again, baseline AR $\geq$ 2/4 (OR 0.30, 95% CI 0.11—0.79; $P=0.015$) showed a protective effect.

In a stepwise Cox multivariable model, STS risk score (hazard ratio [HR] 1.32, 95% CI 1.11—1.57; $P=0.002$), prior

Table 1 Characteristics of the study patients at baseline.

Characteristics	All patients ($n=163$)	Good outcomes ($n=114$)	Poor outcomes ($n=49$)	P
Age (years)	79.9 ± 8.8	78.6 ± 9.7	82.8 ± 5.0	0.01
Men	90 (55.2)	59 (51.8)	31 (63.3)	0.24
Body surface area (m^2)	1.78 ± 0.2	1.77 ± 0.2	1.81 ± 0.3	0.63
Logistic EuroSCORE (%)	18.4 ± 11.4	17.4 ± 10.6	20.7 ± 12.7	0.12
STS risk score (%)	5.8 ± 3.1	5.4 ± 3.0	6.0 ± 3.0	0.002
NYHA class III or IV	118 (72.4)	76 (66.7)	42 (85.7)	0.02
Angina pectoris	32 (19.6)	25 (21.9)	7 (14.3)	0.36
Syncope	21 (12.9)	19 (16.7)	2 (4.1)	0.04
Previous acute heart failure	86 (52.8)	57 (50.0)	29 (59.2)	0.36
Clinical history				
CAD	85 (52.1)	64 (56.1)	21 (42.9)	0.17
Previous PCI	24 (14.7)	18 (15.8)	6 (12.2)	0.73
Previous BAV	29 (17.8)	16 (14.0)	13 (26.5)	0.09
Previous CABG	28 (17.2)	21 (18.4)	7 (14.3)	0.68
Previous SAVR	3 (1.8)	2 (1.8)	1 (2.0)	1.0
Cerebrovascular disease	24 (14.7)	17 (14.9)	7 (14.3)	1.0
PVD	32 (19.6)	26 (22.8)	6 (12.4)	0.18
Porcelain aorta	11 (6.7)	8 (7.0)	3 (6.1)	1.0
AF	71 (43.5)	37 (32.5)	34 (69.4)	< 0.0001
Chest wall irradiation	21 (12.9)	19 (16.7)	2 (4.1)	0.04
Hypertension	108 (66.3)	69 (60.5)	39 (79.6)	0.03
Diabetes mellitus	27 (16.6)	20 (17.5)	7 (14.3)	0.78
COPD	63 (38.9)	41 (36.3)	22 (44.9)	0.39
Chronic kidney disease				0.47
Moderate	66 (40.5)	43 (37.7)	23 (46.9)	
Severe	6 (3.7)	5 (4.4)	1 (2.0)	
NT-proBNP (pg/mL)	4281.3 ± 4378.4	4329.6 ± 4724.1	4172.1 ± 3518.2	0.36

Data are mean ± standard deviation or number (%). AF: atrial fibrillation; BAV: balloon aortic valvuloplasty; CABG: coronary artery bypass graft; CAD: coronary artery disease; COPD: chronic obstructive pulmonary disease; NT-proBNP: N-terminal prohormone of brain natriuretic peptide; NYHA: New York Heart Association; PCI: percutaneous coronary intervention; PVD: peripheral vascular disease; SAVR: surgical aortic valve replacement; STS: Society of Thoracic Surgeons.

valvuloplasty (HR 4.31, 95% CI 1.26—14.70; $P=0.02$), aortic annulus diameter (HR 1.50, 95% CI 1.12—2.00; $P=0.007$) and left atrial area (HR 1.12, 95% CI 1.01—1.25; $P=0.04$) were independent predictors of 6-month all-cause mortality (Table 6).

Discussion

TAVI is now the standard of care for 'inoperable' patients and a valid alternative to surgery for many high-risk patients [7]. Nevertheless, in recent studies [2,5], the percentage of patients who were either dead or severely symptomatic at 6 months was about 25%, highlighting that it is still unclear which patients are most likely to benefit from this procedure.

Indeed, although numerous studies have identified predictors of mortality [2,3,6,8,9], few of them have focused on predictors of functional results [8,16,17]. Thus, a strength of the present study was the identification of predictors of 'global' clinical 6-month poor outcomes after TAVI with both valves, in routine clinical practice and using all possible accesses. One of our main findings was the significant proportion of patients with 'poor outcomes'. Moreover, this is, to the best of our knowledge, the first study to highlight the potential independent effect of baseline AR on TAVI outcomes.

Atrial fibrillation

AF after TAVI has been associated with increased all-cause mortality [18]. In the study by Stortecky et al., this was mainly attributable to cardiac mortality, without differences in rates of systemic embolic events or fatal bleedings between patients with and without AF, and irrespective of the type of AF.

In our study, AF was an independent risk factor of 6-month poor outcomes because of increased rates of heart failure events and symptom sustainability. Given the preserved LVEF presented by our patients, it can be hypothesized that they were more likely to have heart failure with preserved ejection fraction. Indeed, AS, by increasing the pressure afterload and wall stress, first leads to LV hypertrophy and then to myocardial apoptosis and fibrosis, which are key factors in the progression towards heart failure [19]. AF, also related to myocardial fibrosis, might be a marker of

Table 2 Procedural characteristics and postprocedural outcomes.

Variables	All patients ($n=163$)	Good outcomes ($n=114$)	Poor outcomes ($n=49$)	P
Valve type				0.03
Edwards (SAPIEN and SAPIEN XT)	99 (60.7)	76 (66.7)	23 (46.9)	
Medtronic CoreValve	64 (39.2)	38 (33.3)	26 (53.1)	
Valve diameter				0.14
23 mm	32 (19.6)	23 (20.2)	9 (18.4)	
26 mm	83 (50.9)	62 (54.4)	21 (42.9)	
29 mm	40 (24.5)	26 (22.8)	14 (28.6)	
31 mm	8 (4.9)	3 (2.6)	5 (10.2)	
Vascular access				0.88
Transfemoral	132 (80.9)	92 (80.7)	40 (81.6)	
Subclavian	10 (6.1)	6 (5.3)	4 (8.2)	
Transapical	12 (7.4)	9 (7.9)	3 (6.1)	
Transaortic	9 (5.5)	7 (6.1)	2 (4.1)	
Procedural time (minutes)	96 ± 31	97 ± 34	95 ± 24	0.90
Total amount of contrast agent (mL)	238.8 ± 92.7	233.2 ± 85.1	252.8 ± 109.0	0.25
Need for second valve	2 (1.2)	1 (0.9)	1 (2.0)	0.51
Hospital stay (days)	9.2 ± 5.5	8.4 ± 4.6	11.0 ± 6.8	0.001
ICU stay (days)	3.5 ± 2.1	3.2 ± 1.9	4.2 ± 2.6	0.03
Bleeding				
Life-threatening or disabling	4 (2.5)	2 (1.8)	2 (4.1)	0.58
Major	34 (20.9)	24 (21.1)	10 (20.4)	1.0
Myocardial infarction	3 (1.8)	3 (2.6)	0 (0.0)	0.55
Stroke	4 (2.5)	3 (2.6)	1 (2.0)	1.0
Major vascular complication	16 (9.8)	10 (8.8)	6 (12.2)	0.57
Acute kidney injury, RIFLE stage 2 or 3	10 (6.1)	3 (2.6)	7 (14.3)	0.009
Need for permanent pacemaker implantation	16 (9.8)	6 (5.3)	10 (20.4)	0.007
Postoperative treatment				
Aspirin	143 (87.7)	102 (90.3)	41 (83.7)	0.35
Clopidogrel	93 (57.1)	74 (65.5)	19 (38.8)	0.003
Vitamin K antagonists	56 (34.4)	29 (25.7)	27 (55.1)	0.0006
Diuretics	94 (57.7)	61 (53.9)	33 (67.3)	0.16
Beta-blockers	87 (53.4)	60 (53.6)	27 (55.1)	0.99
ACE inhibitors/ARBs	80 (49.1)	62 (54.9)	18 (36.7)	0.05

Data are mean $\pm$ standard deviation or number (%). ACE: angiotensin-converting enzyme; ARB: angiotensin receptor blocker; ICU: intensive care unit.

such evolved AS, highlighting the need for rigorous echocardiographical screening before TAVI and tailored medication upon discharge for these patients.

Pulmonary hypertension

In TAVI series, the prevalence of sPAP > 60 mmHg ranged from 11% to 32% [9,20]. There is consistent evidence that pulmonary hypertension is an independent predictor of mortality in AS patients [9,21]. Worse functional results after TAVI have also been highlighted [22].

Diastolic dysfunction and AF are considered to be major determinants of pulmonary hypertension in patients with severe AS [21,23]. As previously discussed, these factors reflect the detrimental haemodynamic effects of evolved AS, leading to a vicious circle. Whether these effects can be relieved by TAVI is a major concern. Indeed, although TAVI has been shown to improve sPAP during the first year [23], Roselli et al. [21] demonstrated that, after this initial improvement, there was a progressive rise towards the preoperative level of sPAP in about 3.5 years after SAVR. Given the large number of TAVI candidates with reactive pulmonary hypertension, almost 50% of patients with sPAP > 60 mmHg [23], it suggests that patients with longstanding AS have pulmonary vasculature abnormalities that maintain pulmonary hypertension and worsen outcomes.

Right ventricular dysfunction

It has been shown that under the influence of various factors such as pericardiotomy, hypothermia, inflammation and prolonged cardiopulmonary bypass, RV function decreases after SAVR, which is not observed after TAVI [24]. Some authors have therefore recommended that RV dysfunction should prompt TAVI to be favoured over SAVR [24,25]. Nonetheless, there are no data supporting the fact that patients with pre-existing RV dysfunction experience functional improvement after TAVI. We showed that RV dysfunction was an

Table 3 Echocardiographical findings.

Variables	All patients ($n=163$)[a]	Good outcomes ($n=114$)	Poor outcomes ($n=49$)[b]	P
At baseline				
LVEF (%)	50.7 ± 14.8	50.2 ± 15.1	51.9 ± 14.0	0.48
LV end-diastolic diameter (mm)	50.1 ± 7.9	50.5 ± 7.9	49.3 ± 7.9	0.32
LV end-systolic diameter (mm)	36.1 ± 9.5	36.4 ± 9.9	35.5 ± 8.6	0.54
End-diastolic septal thickness (mm)	13.3 ± 2.6	13.3 ± 2.8	13.4 ± 2.4	0.96
Aortic annulus diameter (mm)	22.9 ± 2.1	22.7 ± 2.0	23.5 ± 2.1	0.05
Indexed aortic valve area (cm^2/m^2)	0.38 ± 0.10	0.38 ± 0.11	0.39 ± 0.09	0.27
Aortic mean gradient (mmHg)	50.8 ± 15.5	53.0 ± 15.9	45.7 ± 13.6	0.006
Moderate or severe AR	36 (22.1)	32 (28.1)	4 (8.2)	0.004
Moderate or severe MR	65 (39.9)	42 (36.8)	23 (46.9)	0.30
Left atrial area (cm^2)	28.0 ± 6.6	26.9 ± 6.5	30.5 ± 6.2	0.002
RV dysfunction	31 (19.0)	15 (15.2)	16 (32.7)	0.007
Moderate or severe TR	38 (23.3)	17 (14.9)	21 (42.9)	0.0002
Pulmonary hypertension	106 (65.0)	69 (60.5)	37 (75.5)	0.0007
40 mmHg ≤ sPAP ≤ 50 mmHg	70 (42.9)	53 (46.5)	17 (34.7)	0.173
sPAP ≥ 60 mmHg	36 (22.1)	16 (14.0)	20 (40.8)	< 0.001
Postoperative assessment				
Aortic valve area (cm^2)	1.87 ± 0.53	1.85 ± 0.53	1.90 ± 0.55	0.48
Aortic mean gradient (mmHg)	10.5 ± 4.2	10.9 ± 3.8	9.7 ± 4.9	0.01
Moderate or severe AR	30 (18.6)	16 (14.2)	14 (29.2)	0.04
Patient-prosthesis mismatch				0.33
Moderate	44 (27.0)	29 (26.4)	15 (31.3)	
Severe	8 (4.9)	4 (3.6)	4 (8.3)	
6-month follow-up				
LVEF (%)	55.9 ± 9.8	56.0 ± 9.6	55.6 ± 10.6	0.95
Aortic valve area (cm^2)	1.82 ± 0.6	1.77 ± 0.45	1.89 ± 0.69	0.81
Moderate or severe AR	29 (19.0)	19 (16.7)	10 (26.3)	0.21
Moderate or severe MR	25 (16.4)	15 (13.2)	10 (26.3)	0.15
Moderate or severe TR	21 (13.8)	7 (6.1)	14 (36.8)	< 0.001
Pulmonary hypertension	56 (36.8)	32 (28.1)	24 (63.2)	< 0.001

Data are mean ± standard deviation or number (%). AR, aortic regurgitation; LV: left ventricular; LVEF, left ventricular ejection fraction; MR: mitral regurgitation; RV, right ventricular; sPAP, systolic pulmonary artery pressure; TR, tricuspid regurgitation.
[a] $n=152$ at 6-month follow-up.
[b] $n=49$ at 6-month follow-up.

independent predictor of poor outcomes, which is in line with previous observations in the setting of SAVR [24].

Recently, Poliacikova et al. [25] reported the outcomes of 155 patients. In this study, RV dysfunction was noted in about 10% of patients and was not associated with an unfavourable prognosis. Nevertheless, a higher mortality rate was observed in patients with RV dysfunction, and low mortality rates in this study might have prevented this trend from reaching statistical significance. Besides, in our study, RV dysfunction was an independent predictor of functional outcomes, which were not assessed in the previous study. Consequently, we believe that RV function should be assessed carefully and taken into account during patient selection.

Aortic regurgitation

Our finding that patients with baseline AR ≥ 2/4 had a lower risk of poor outcomes may seem counterintuitive, as AR ≥ 2/4 has been shown to lower the event-free survival of patients with medically-managed AS [26]. However, there is no evidence that patients with such an AR have worse outcomes after SAVR [27].

AR is much more frequent after TAVI than after SAVR and a recent meta-analysis showed a pooled estimate of 12% for postprocedural AR ≥ 2/4 [28,29]. There is now consistent evidence that such an AR impacts negatively on survival and functional results after TAVI [2,3,6,8,28,29].

A haemodynamic study by Azadani et al. [30] showed substantial energy loss during diastole, even with mild AR, after implantation of a transcatheter valve resulting in higher LV workload. Indeed, postprocedural AR mimics the physiopathology of acute AR, subjecting a hypertrophied LV accustomed to pressure overload to volume overload [29]. The LV is unable to properly increase its end-diastolic volume because of impaired relaxation. Thus, the regurgitation volume precipitates an elevation in the already increased end-diastolic pressure, whereas forward stroke volume

Table 4 Univariate and multivariable predictors of poor outcomes.

Variables	Univariate OR (95% CI)	*P*	Multivariable OR (95% CI)	*P*
Age[a]	1.09 (1.03—1.16)	0.005	—	—
Logistic EuroSCORE[a]	1.03 (0.99—1.06)	0.09	—	—
STS risk score[a]	1.16 (1.04—1.29)	0.008	—	—
Syncope[b]	0.21 (0.05—0.95)	0.04	—	—
CAD[b]	0.59 (0.30—1.15)	0.12	—	—
PVD[b]	0.47 (0.18—1.23)	0.13	—	—
Prior valvuloplasty[b]	2.21 (0.97—5.05)	0.06	—	—
AF[b]	4.72 (2.29—9.72)	< 0.001	3.94 (1.67—9.29)	0.002
Chest wall irradiation[b]	0.21 (0.05—0.95)	0.04	—	—
Hypertension[b]	2.54 (1.16—5.60)	0.02	—	—
Valve type[b]	2.26 (1.14—4.48)	0.02	—	—
Annulus diameter[a]	1.20 (1.02—1.42)	0.03	—	—
Aortic mean gradient[a]	0.97 (0.95—0.99)	0.007	—	—
Left atrial area[a]	1.09 (1.03—1.16)	0.003	—	—
AR ≥ 2/4[b]	0.23 (0.08—0.69)	0.008	0.07 (0.02—0.32)	0.001
TR ≥ 2/4[b]	4.28 (1.99—9.20)	< 0.001	—	—
RV dysfunction[b]	3.20 (1.43—7.17)	0.005	3.55 (1.21—10.39)	0.02
sPAP ≥ 60 mmHg[b]	4.22 (1.94—9.19)	< 0.001	7.56 (2.58—22.17)	< 0.001

AF: atrial fibrillation; AR: aortic regurgitation; CAD: coronary artery disease; CI: confidence interval; OR: odds ratio; PVD: peripheral vascular disease; RV: right ventricular; sPAP: systolic pulmonary artery pressure; STS: Society of Thoracic Surgeons; TR: tricuspid regurgitation.

[a] Age: for each increase of 1 year; logistic EuroSCORE and STS risk score: for each increase of 1%; annulus diameter: for each increase of 1 mm; aortic mean gradient: for each increase of 1 mm Hg; left atrial area: for each increase of 1 cm^2.

[b] Reference values: for syncope, CAD, PVD, prior valvuloplasty, AF, chest wall irradiation, hypertension and RV dysfunction: absence of the variable; for valve type: Edwards valve; for AR: AR < 2/4; for TR: TR < 2/4; for sPAP: sPAP < 60 mmHg.

decreases. Furthermore, the increased LV filling pressure results in an additional reduction in coronary perfusion, which is already affected due to pre-existing myocardial hypertrophy. Eventually, these dramatic haemodynamic changes promote symptom sustainability.

We assume that patients with significant baseline AR may be 'tolerant' to postprocedural AR. This might be the result of less-altered myocardial compliance and LV remodelling. Future studies should investigate the potential independent effect of preoperative AR on TAVI outcomes.

Table 5 Univariate and multivariable predictors of clinical efficacy.

Variables	Univariate OR (95% CI)	*P*	Multivariable OR (95% CI)	*P*
Age[a]	1.07 (1.02—1.12)	0.01	—	—
Logistic EuroSCORE[a]	1.02 (0.99—1.05)	0.11	—	—
STS risk score[a]	1.12 (1.01—1.24)	0.04	—	—
Syncope[b]	0.38 (0.13—1.10)	0.07	—	—
PVD[b]	0.56 (0.24—1.26)	0.16	—	—
Prior valvuloplasty[b]	2.23 (0.99—5.06)	0.05	—	—
AF[b]	4.37 (2.25—8.48)	< 0.001	4.09 (1.99—8.39)	< 0.001
Chest wall irradiation[b]	0.50 (0.18—1.37)	0.18	—	—
Hypertension[b]	1.63 (0.83—3.20)	0.15	—	—
Annulus diameter[a]	1.20 (1.03—1.41)	0.02	—	—
Aortic mean gradient[a]	0.98 (0.96—0.99)	0.04	—	—
Left atrial area[a]	1.05 (0.99—1.10)	0.07	—	—
AR ≥ 2/4[b]	0.23 (0.08—0.69)	0.008	0.30 (0.11—0.79)	0.015
TR ≥ 2/4[b]	2.28 (1.09—4.78)	0.03	—	—
sPAP ≥ 60 mmHg[b]	3.12 (1.44—6.73)	0.004	3.84 (1.52—9.72)	0.004

AF: atrial fibrillation; AR: aortic regurgitation; CI: confidence interval; OR: odds ratio; PVD: peripheral vascular disease; sPAP: systolic pulmonary artery pressure; STS: Society of Thoracic Surgeons; TR: tricuspid regurgitation.

[a] Age: for each increase of 1 year; logistic EuroSCORE and STS risk score: for each increase of 1%; annulus diameter: for each increase of 1 mm; aortic mean gradient: for each increase of 1 mmHg; left atrial area: for each increase of 1 cm^2.

[b] Reference values: for syncope, PVD, prior valvuloplasty, AF, chest wall irradiation and hypertension: absence of the variable; for AR: AR < 2/4; for TR: TR < 2/4; for sPAP: sPAP < 60 mmHg.

Table 6 Univariate and multivariable predictors of all-cause mortality.

Variables	Univariate HR (95% CI)	*P*	Multivariable HR (95% CI)	*P*
Age[a]	1.08 (0.97–1.21)	0.16	–	–
STS risk score[a]	1.28 (1.09–1.50)	0.003	1.32 (1.11–1.57)	0.002
NYHA functional class III or IV[b]	3.91 (0.5–30.51)	0.19	–	–
Prior valvuloplasty[b]	4.00 (1.22–13.11)	0.02	4.31 (1.26–14.70)	0.02
AF[b]	2.39 (0.70–8.16)	0.17	–	–
Valve type[b]	2.85 (0.83–9.72)	0.10	–	–
Annulus diameter[a]	1.32 (1.02–1.72)	0.04	1.50 (1.12–2.00)	0.007
Left atrial area[a]	1.13 (1.03–1.24)	0.01	1.12 (1.01–1.25)	0.04
Permeability index[a]	0.82 (0.70–0.96)	0.01	–	–
MR $\geq$ 2/4[b]	2.68 (0.78–9.15)	0.12	–	–
sPAP $\geq$ 60 mmHg[b]	4.42 (1.35–14.47)	0.01	–	–

AF: atrial fibrillation; CI: confidence interval; OR: odds ratio; MT: mitral regurgitation; NYHA: New York Heart Association; sPAP: systolic pulmonary artery pressure; STS: Society of Thoracic Surgeons.
[a] Age: for each increase of 1 year; STS risk score: for each increase of 1%; annulus diameter: for each increase of 1 mm; left atrial area: for each increase of 1 cm^2; permeability index: for each increase of 1%.
[b] Reference values: for NYHA functional class: NYHA functional class I or II; for prior valvuloplasty and AF: absence of the variable; for valve type: Edwards valve; for MR: MR < 2/4; for sPAP: sPAP < 60 mmHg.

Limitations

When interpreting results of this study, some limitations need to be acknowledged. First, we have reported on the experience of a single tertiary-care referral centre with a small population. Thus, our results are primarily hypothesis-generating and ought to be confirmed in larger studies. Second, we had no standardized evaluation of frailty, which has recently been pointed out as a predictor of functional decline and mortality after TAVI [17]. Lastly, despite rigorous prospective follow-up, there was no external adjudication of events.

Conclusion

About one-third of patients in the present study had poor outcomes after TAVI. AF, severe baseline pulmonary hypertension and RV dysfunction (i.e. variables suggesting a more evolved AS) were predictors of 6-month poor outcomes. Conversely, baseline AR $\geq$ 2/4 showed a protective effect, which needs to be confirmed in future studies. Our study highlights the need for a specific 'TAVI risk score', which could lead to better selection of patients.

Disclosure of interest

The authors declare that they have no conflicts of interest concerning this article.

Acknowledgments

The authors are very grateful to Emmanuelle Babin-Lerede, Laurence Le Bouquin, Albane Piel and Raphael Martins for their continuous help for this study.

References

[1] Iung B, Baron G, Butchart EG, et al. A prospective survey of patients with valvular heart disease in Europe: The Euro Heart Survey on Valvular Heart Disease. Eur Heart J 2003;24:1231–43.
[2] Gilard M, Eltchaninoff H, Iung B, et al. Registry of transcatheter aortic-valve implantation in high-risk patients. N Engl J Med 2012;366:1705–15.
[3] Moat NE, Ludman P, de Belder MA, et al. Long-term outcomes after transcatheter aortic valve implantation in high-risk patients with severe aortic stenosis: the UK TAVI (United Kingdom Transcatheter Aortic Valve Implantation) Registry. J Am Coll Cardiol 2011;58:2130–8.
[4] Webb JG, Wood DA. Current status of transcatheter aortic valve replacement. J Am Coll Cardiol 2012;60:483–92.
[5] Makkar RR, Fontana GP, Jilaihawi H, et al. Transcatheter aortic-valve replacement for inoperable severe aortic stenosis. N Engl J Med 2012;366:1696–704.
[6] Kodali SK, Williams MR, Smith CR, et al. Two-year outcomes after transcatheter or surgical aortic-valve replacement. N Engl J Med 2012;366:1686–95.
[7] Vahanian A, Alfieri O, Andreotti F, et al. Guidelines on the management of valvular heart disease (version 2012). Eur Heart J 2012;33:2451–96.
[8] Gotzmann M, Pijakic A, Bojara W, et al. Transcatheter aortic valve implantation in patients with severe symptomatic aortic valve stenosis-predictors of mortality and poor treatment response. Am Heart J 2011;162:238–45, e1.
[9] Tamburino C, Capodanno D, Ramondo A, et al. Incidence and predictors of early and late mortality after transcatheter aortic valve implantation in 663 patients with severe aortic stenosis. Circulation 2011;123:299–308.
[10] Kappetein AP, Head SJ, Genereux P, et al. Updated standardized endpoint definitions for transcatheter aortic valve implantation: the Valve Academic Research Consortium-2 consensus document. Eur Heart J 2012;33:2403–18.
[11] Roques F, Nashef SA, Michel P, et al. Risk factors and outcome in European cardiac surgery: analysis of the EuroSCORE multinational database of 19,030 patients. Eur J Cardiothorac Surg 1999;15:816–22 [discussion 22–3].

[12] Shroyer AL, Coombs LP, Peterson ED, et al. The Society of Thoracic Surgeons: 30-day operative mortality and morbidity risk models. Ann Thorac Surg 2003;75:1856—64 [discussion 64—5].
[13] Lang RM, Bierig M, Devereux RB, et al. Recommendations for chamber quantification: a report from the American Society of Echocardiography's Guidelines and Standards Committee and the Chamber Quantification Writing Group, developed in conjunction with the European Association of Echocardiography, a branch of the European Society of Cardiology. J Am Soc Echocardiogr 2005;18:1440—63.
[14] Lancellotti P, Tribouilloy C, Hagendorff A, et al. European Association of Echocardiography recommendations for the assessment of valvular regurgitation. Part 1: aortic and pulmonary regurgitation (native valve disease). Eur J Echocardiogr 2010;11:223—44.
[15] Rudski LG, Lai WW, Afilalo J, et al. Guidelines for the echocardiographic assessment of the right heart in adults: a report from the American Society of Echocardiography endorsed by the European Association of Echocardiography, a registered branch of the European Society of Cardiology, and the Canadian Society of Echocardiography. J Am Soc Echocardiogr 2010;23:685—713 [quiz 86—8].
[16] Krane M, Deutsch MA, Piazza N, et al. One-year results of health-related quality of life among patients undergoing transcatheter aortic valve implantation. Am J Cardiol 2012;109:1774—81.
[17] Schoenenberger AW, Stortecky S, Neumann S, et al. Predictors of functional decline in elderly patients undergoing transcatheter aortic valve implantation (TAVI). Eur Heart J 2013;34:684—92.
[18] Stortecky S, Buellesfeld L, Wenaweser P, et al. Atrial fibrillation and aortic stenosis: impact on clinical outcomes among patients undergoing transcatheter aortic valve implantation. Circ Cardiovasc Interv 2013;6:77—84.
[19] Dweck MR, Boon NA, Newby DE. Calcific aortic stenosis: a disease of the valve and the myocardium. J Am Coll Cardiol 2012;60:1854—63.
[20] Buellesfeld L, Gerckens U, Schuler G, et al. 2-year follow-up of patients undergoing transcatheter aortic valve implantation using a self-expanding valve prosthesis. J Am Coll Cardiol 2011;57:1650—7.
[21] Roselli EE, Abdel Azim A, Houghtaling PL, et al. Pulmonary hypertension is associated with worse early and late outcomes after aortic valve replacement: implications for transcatheter aortic valve replacement. J Thorac Cardiovasc Surg 2012;144:1067—74 [e2].
[22] Ussia GP, Barbanti M, Petronio AS, et al. Transcatheter aortic valve implantation: 3-year outcomes of self-expanding CoreValve prosthesis. Eur Heart J 2012;33:969—76.
[23] Ben-Dor I, Goldstein SA, Pichard AD, et al. Clinical profile, prognostic implication, and response to treatment of pulmonary hypertension in patients with severe aortic stenosis. Am J Cardiol 2011;107:1046—51.
[24] Kempny A, Diller GP, Kaleschke G, et al. Impact of transcatheter aortic valve implantation or surgical aortic valve replacement on right ventricular function. Heart 2012;98:1299—304.
[25] Poliacikova P, Cockburn J, Pareek N, et al. Prognostic impact of pre-existing right ventricular dysfunction on the outcome of transcatheter aortic valve implantation. J Invasive Cardiol 2013;25:142—5.
[26] Zilberszac R, Gabriel H, Schemper M, et al. Outcome of combined stenotic and regurgitant aortic valve disease. J Am Coll Cardiol 2013;61:1489—95.
[27] Catovic S, Popovic ZB, Tasic N, et al. Impact of concomitant aortic regurgitation on long-term outcome after surgical aortic valve replacement in patients with severe aortic stenosis. J Cardiothorac Surg 2011;6:51.
[28] Athappan G, Patvardhan E, Tuzcu EM, et al. Incidence, predictors, and outcomes of aortic regurgitation after transcatheter aortic valve replacement: meta-analysis and systematic review of literature. J Am Coll Cardiol 2013;61:1585—95.
[29] Gotzmann M, Lindstaedt M, Mugge A. From pressure overload to volume overload: aortic regurgitation after transcatheter aortic valve implantation. Am Heart J 2012;163:903—11.
[30] Azadani AN, Jaussaud N, Matthews PB, et al. Energy loss due to paravalvular leak with transcatheter aortic valve implantation. Ann Thorac Surg 2009;88:1857—63.

2.3.3 Synthèse

Dans cette étude basée sur l'expérience initiale de notre centre, nous démontrions à l'époque que près d'un tiers des patients bénéficiant d'une procédure de TAVI présentaient des critères de mauvais résultat à court terme. Nous avons identifié plusieurs facteurs de risque dont l'impact pronostique délétère a depuis été largement confirmé dans de plus larges séries de patients : fibrillation atriale préexistante (78), dysfonction ventriculaire droite et hypertension pulmonaire (79,80), notamment. Cette étude nous a poussé à suggérer qu'il existait un continuum de gravité et d'évolution chez les patients porteurs d'une sténose aortique serrée; la maladie n'étant pas limitée à une simple atteinte valvulaire mais s'associant à des degrés divers d'atteinte des propriétés de relaxation musculaire cardiaque et de fibrose faisant le lit des arythmies atriales et du retentissement sur les pressions artérielles pulmonaires et la fonction ventriculaire droite. Notre hypothèse était que les facteurs de mauvais pronostic identifiés dans l'étude étaient en réalité les marqueurs de ces formes plus évoluées de cardiopathie valvulaire qui faisaient le lit du mauvais pronostic de ces patients. Cette hypothèse a depuis été formalisée, par d'autres auteurs, en une classification des dommages cardiaques induits par la sténose aortique serrée qui a démontré de manière récente, malgré l'évolution du profil de risque des patients traités au cours du temps, sa valeur pronostique importante pour prédire la mortalité après TAVI (80,81). Enfin, notre étude est, à notre connaissance, la première à avoir suggéré le caractère protecteur de la présence d'une fuite aortique significative avant TAVI par probable meilleure tolérance d'une éventuelle fuite para prothétique résiduelle post-opératoire. Cette hypothèse a également été confirmée dans de larges séries de patients (82,83).

Nous suggérions, dans notre conclusion, l'intérêt potentiel d'un score de risque spécifiquement dédié au TAVI afin de mieux identifier les patients à haut risque de mauvais résultats. Bien que le profil de risque des patients bénéficiant d'un TAVI ait graduellement diminué au cours du temps, la population traitée en pratique quotidienne reste majoritairement constituée d'octogénaires à risque chirurgical intermédiaire à élevé. Ainsi l'identification de la futilité de la procédure reste un enjeu crucial puisque plus de 5% des procédures réalisées dans une série récente pouvaient être considérées comme « futiles » (40). De nombreux scores développés à partir de populations de patients traités par TAVI, et destinés à des candidats à la technique, ont été publiés (35,84–88). Malheureusement, la plupart de ces scores s'attachent à prédire la mortalité hospitalière, à 30 jours ou à 1 an après TAVI sans intégrer d'élément plus global du pronostic des patients (84–88). Seul le score PARTNER prend en compte l'existence d'une faible qualité de vie ou d'une baisse de la qualité de vie à 6 mois post-TAVI comme

critère de mauvais résultat de la procédure (35). Outre des performances diagnostiques parfois modestes dans leur cohorte de développement et validation, il s'agit là probablement d'un premier frein à l'utilisation de ces scores qui ne prédisent que partiellement le mauvais résultat d'une procédure.

Au cours du temps, le concept émergent de fragilité gériatrique, prenant en compte la personne âgée dans sa globalité et évaluant différent paramètres de son statut physique et de son autonomie, a démontré sa pertinence pronostique pour prédire le devenir des patients traités par TAVI (33,89,90). Les paramètres de qualité de vie et la fragilité ont également démontré leur capacité à améliorer les performances diagnostiques de certains scores de risque spécifiques ou non du TAVI (91,92). Ces observations ont poussé certains auteurs à proposer une approche plus « holistique », combinant des scores de risque spécifique avec des paramètres de fragilité et des dysfonctions spécifiques d'organe, afin de mieux identifier le risque de futilité de la procédure (**Figure 32**)(33).

Table 3 **Integrated approach for estimating transcatheter aortic valve implantation-specific risk and futility**

Criteria	Low risk	Intermediate risk	High risk	Prohibitive risk
PARTNER TAVI score[a], OR FRANCE 2 TAVI score	<25% risk of mortality or lack of QOL improvement at 6 months Risk score: 0 (30-day mortality risk < 5%)	25–50% risk of mortality or lack of QOL improvement at 6 months Risk score: 1–5 (30-day mortality risk 5–15%)	>50% risk of mortality or lack of QOL improvement at 6 months Risk score: 6–7 (30-day mortality risk 15–25%)	Risk score ≥ 8 (30-day mortality risk > 25%)
Frailty[b]	None	1 index	≥2 indices	≥4 indices
Specific major organ system compromise not to be improved post-TAVI[c]	None	1 organ system	2 organ systems	≥3 organ systems

[a]http://h-outcomes.com/tavi-risk-calculator/.
[b]Frailty based on Katz Index (independence in feeding, bathing, dressing, transferring, toileting, and urinary incontinence)[30] and independence in ambulation (walk 5 m in <6 s).
[c]Examples of major organ system compromise:[34] Cardiac—severe LV systolic or diastolic dysfunction or RV dysfunction, and fixed pulmonary hypertension; CKD stage 3 or worse; pulmonary dysfunction with FEV1 < 50% or DLCO < 50% of predicted; CNS dysfunction (dementia, Alzheimer's disease, Parkinson's disease, and CVA with persistent physical limitation); GI dysfunction—Crohn's disease, ulcerative colitis, nutritional impairment, or serum albumin < 3.0; cancer—active malignancy; and liver—any history of cirrhosis, variceal bleeding, or elevated INR in the absence of VKA therapy.

Figure 32- Exemple d'approche globale d'évaluation de la futilité des procedures TAVI. Reproduite d'après Puri R et al (33).

Il faut toutefois souligner que de nombreux indices de fragilité existent et ont démontré une association avec les résultats du TAVI. L'addition d'un nombre limité de ces indices à des scores de risque n'améliore que de manière modeste leurs performances diagnostiques (33). Ainsi, dans la pratique quotidienne, il convient de réaliser un compromis entre une évaluation large, multidimensionnelle de la fragilité et l'usage de tests isolés plus simples. Ces éléments soulignent, malgré l'optimisation de l'évaluation du risque liée à l'introduction de ce concept

de fragilité, la difficulté de mesurer précisément l'impact de chaque caractéristique des patients au sein d'une population, certes à haut risque, mais restant hétérogène. Il s'agit là d'un second élément expliquant qu'aucun modèle prédictif de « mauvais résultat » de la procédure n'ait réellement émergé en routine clinique malgré près d'une décennie de recherche sur le sujet.

Enfin, les caractéristiques éminemment « mouvantes » de la population des patients TAVI avec l'évolution rapide de son profil de risque notamment, nous confronte probablement aux limites des modèles statistiques basés sur l'étude de cohortes de patients. Ces modèles, généralement issus d'une régression multivariée, sont développés à un instant *t* à partir d'une population aux caractéristiques figées traitée par des opérateurs dont l'expérience de la technique a pu s'accroitre par la suite et avec les outils endovasculaires disponibles à l'époque. Ainsi, ces modèles peuvent présenter des performances limitées dans une population différente de leur population de développement et n'intègrent pas l'expérience accrue des opérateurs ou les itérations successives du matériel utilisé. Ces limitations ouvrent donc la voie à l'application de nouveaux procédés analytiques basés sur l'intelligence artificielle ou faisant appel aux techniques de « Machine-Learning » qui permettent l'analyse de vastes bases de données et produisent des modèles qui peuvent être affinés à mesure que la base de données s'enrichit de nouveaux cas (93). Les données de santé disponibles n'ont jamais été aussi nombreuses et leur organisation en gigantesques bases de données, comme le Système National des Données de Santé (SNDS)[4] en France, devrait être la règle dans un avenir proche. Ces « big data » offriront alors un terrain d'expérimentation particulièrement propice à ces nouvelles méthodes analytiques (94–96).

2.4 Synthèse et perspectives

Dans ce deuxième chapitre, nous avons exposé, au travers de trois contributions originales, l'intérêt de l'étude de cohortes de patients, selon des méthodes statistiques usuelles, dans l'aide à la décision et l'optimisation des résultats des procédures TAVI. Ces méthodes, largement répandues dans le domaine scientifique médical, permettent en effet la mise en évidence de facteurs de risque d'événements post-opératoires permettant de mieux individualiser la stratégie de prise en charge d'un patient. Elles présentent également des limites, que nous avons évoquées dans la section précédente.

[4] https://www.snds.gouv.fr

Outre les limitations des méthodes statistiques classiques, il convient de souligner la richesse de la production scientifique médicale dans le domaine du TAVI. Une simple recherche sur la base de données Pubmed[5] en utilisant les termes « Transcatheter Aortic Valve » renvoie, à l'heure actuelle, à plus de 9000 références bibliographiques. Dans ce contexte, il est bien entendu impossible pour le clinicien de mémoriser toute l'information disponible, utile, et parfois même nécessaire, à une prise en charge individualisée optimale de son patient. Ce problème peut trouver sa solution dans l'utilisation de système d'assistance informatique, qui restituent au clinicien l'information pertinente à la résolution d'un problème clinique spécifique : les systèmes d'aide à la décision clinique (Clinical Decision-Support Systems - CDSS) qui seront abordés dans le prochain chapitre de ce travail.

[5] https://www.ncbi.nlm.nih.gov/pubmed/

Chapitre 3

Systèmes d'aide à la décision : Case-based reasoning

Le domaine médical et les sciences informatiques sont de nos jours de plus en plus interconnectés, notamment au travers du concept de gestes médico-chirurgicaux assistés par ordinateur (GMCAO) qui sont au cœur des travaux du Labex CAMI – Computer Assisted Medical Interventions- regroupant six laboratoires français (ICUBE, ISIR, LATIM, LIRMM, LTSI, TIMC) sur la thématique.

Une large part de la recherche actuelle porte sur l'élaboration de solutions d'assistance informatique particulières, désignés sous le terme de systèmes d'aide à la décision clinique (Clinical Decision Support System – CDSS) par l'utilisation de l'intelligence artificielle. D'une manière générale, les CDSS peuvent être définis comme des systèmes fournissant aux cliniciens, au personnel paramédical ou aux patients des informations, d'ordre générale sur une thématique particulière ou spécifiques du patient, traitées et présentées de manière pertinente et intelligente, dans le but d'améliorer la prise en charge sous ses différents aspects (diagnostic, planification d'une stratégie thérapeutique, traitement…)(97,98). Dans ce troisième chapitre, nous allons introduire l'intérêt potentiel des CDSS dans le contexte spécifique du TAVI. Ces travaux ont été menés au sein du LTSI de l'Université de Rennes 1 dans le cadre du projet européen H2020 EurValve[6]. Ce programme de recherche et d'innovation, financé par l'Union Européenne, avait pour but principal de produire, tester et valider un CDSS permettant la sélection de différentes stratégies thérapeutiques pour les pathologies valvulaires aortiques et mitrales, ainsi que la simulation, compréhension et comparaison de leurs bénéfices et risques potentiels. Dans ce chapitre, nous présentons nos travaux visant à proposer un type particulier de CDSS basé sur le raisonnement à base de cas (case-based reasoning-CBR).

Avant de présenter notre contribution et ses perspectives, nous rappellons brièvement les principes et la méthodologie des CBR.

[6] http://www.eurvalve.eu/

3.1 Système d'aide à la décision clinique : Case-Based Reasoning

3.1.1 CDSS et CBR

Les CDSS peuvent classiquement être divisés en 2 groupes: basés sur une connaissance *a priori* (« knowledge-based ») ou non (apprentissage automatique) (97,98). Les premiers sont les CDSS les plus couramment rencontrés en pratique courante dans le milieu médical. De nombreux d'entre eux sont issus de recherches préalables au cours desquelles les développeurs tentaient de produire des programmes capables de simuler la pensée d'un expert humain (97,99). Ces systèmes sont structurés autour de règles logiques de type « SI-ALORS » issues d'une base de connaissance. Un générateur d'inférences combine ces règles avec les données d'un patient pour produire une solution qu'il transmet à l'utilisateur via un mécanisme de communication permettant à ce dernier d'interagir en retour avec le système. Les CDSS « non-knowledge-based » utilisent notamment l'intelligence artificielle, via des procédés de machine-learning, permettant à l'ordinateur d'apprendre des expériences passées en reconnaissant des motifs particuliers dans les données cliniques.

Les systèmes basés exclusivement sur des règles peuvent s'avérer difficiles à implémenter, les règles les régissant devenant rapidement complexes et difficiles à paramétrer. En effet, il est aisé de « stocker » de l'expérience dans une approche basée sur des cas, alors que « coder » cette expérience sous forme de règles n'est pas réellement intuitif. Les CBR, utilisent des procédés dits de « lazy learning ». Contrairement aux procédés dits d'« eager learning » qui cherchent à établir des règles générales applicables à tout problème à partir de leur base de données, les procédés de « lazy learning » diffèrent le traitement de leur base de données, se contentant de la stocker, jusqu'à ce qu'une requête soit effectuée. Les CBR, associant ces deux procédés à une base de cas passés, peuvent être vus comme des CDSS hybrides permettant d'améliorer les performances globales du système (99). Ces approches basées sur l'étude de cas présentent certains avantages lorsque l'on cherche à créer un CDSS. Les CBR ont en particulier la propriété de s'adapter rapidement et automatiquement à l'augmentation de l'expérience alors que des systèmes basés sur des règles peuvent nécessiter d'analyser régulièrement le mode de raisonnement de l'utilisateur en fonction de l'évolution des connaissances.

Leur mode de fonctionnement se rapprochant du processus décisionnel d'un médecin qui s'appuie sur ses connaissances et son expérience, les CBR sont des systèmes particulièrement adaptés aux problématiques médicales dans lesquelles les connaissances sont

en perpétuelle évolution et où les cas sont constitués de très nombreuses caractéristiques rendant la généralisation du problème et l'établissement de modèles à partir de ce dernier extrêmement complexe (100). Des CBR ont ainsi été évalués dans certains domaines médicaux à des fins de classification, de diagnostic ou de planification. Néanmoins, la plupart de ces systèmes ne fonctionnent qu'à l'état de prototypes ne servant qu'à retrouver des cas similaires au problème courant laissant le soin à l'utilisateur d'adapter les solutions employées pour ces cas pour résoudre le problème courant (100). Cette limitation principale explique l'usage à ce jour plus limité des CBR dans le domaine médical que dans d'autre domaines.

3.1.2 Particularités du Case-Based Reasoning

Le principe du CBR repose sur l'hypothèse selon laquelle l'expérience passée est utile à la résolution d'un problème actuel. Il s'agit donc pour résoudre un problème de réutiliser les cas précédemment traités et mémorisés (101–104). Dans la cadre d'un CBR, un cas stocké comporte la description du problème traité, la solution qui a été proposée et les résultats obtenus par l'application de cette solution et peut être exprimé comme la paire (p,s) où p est le problème résolu et s la solution jugée utile à sa résolution. En d'autres termes, appliqué au TAVI, le CBR va proposer un ensemble de patients présentant un problème semblable à celui du patient à traiter. Ces patients similaires ou suffisamment proches du patient courant permettront au praticien de connaître quelle décision a été appliquée ainsi que ses conséquences afin de planifier la procédure de manière plus optimale.

Contrairement à d'autres méthodes de résolution de problème reposant sur l'intelligence artificielle, comme les réseaux neuronaux ou les règles de décision, qui tendent à sur généraliser le problème et ne peuvent donc pas adapter leur comportement aux caractéristiques les plus spécifiques de leur jeu de données, le CBR va lui chercher le ou les cas les plus spécifiques du problème à résoudre (101). Par ailleurs, le CBR présente l'avantage de pouvoir « apprendre » et évoluer en fonction des avancées médicales, au fur et à mesure de son utilisation. Cet apprentissage peut aller de la simple mémorisation d'un nouveau cas résolu à l'amélioration de l'organisation mémorielle ou des schémas de méta-apprentissage (101).

3.1.3 Cycle de base des CBR

Le cycle de résolution de problème utilisé par les CBR a classiquement été décrit comme le cycle des 4 « R » : « Retrieve, Reuse, Revise, Retain » (**Figure 33**) (103). Ce cycle débute par la présentation au système d'un nouveau problème à résoudre (un nouveau cas à diagnostiquer/traiter dans le domaine médical). Il existe alors une phase d'interprétation pendant laquelle le système construit la situation initiale en « traduisant » le cas dans le « langage » de présentation des connaissances qu'il utilise (« case representation »). Les cas (p,s) sont les représentations des expériences passées contenant leur contexte de survenue, les paramètres descriptifs importants ainsi que la solution appliquée pour traiter le cas et les conséquences des décisions prises (événements post-opératoires, suivi du patient).

Lors de la phase « *Retrieve* », le système cherche dans la base de cas, les cas les plus similaires au problème à résoudre. Cette recherche implique d'utiliser une mesure de similarité entre le nouveau cas et ceux enregistrés dans la base. Les cas retrouvés sont alors présentés par ordre décroissant de similarité avec le cas à résoudre. Transposé au TAVI, le système doit être en mesure de produire une liste de cas plus ou moins similaires au cas à traiter, chacun étant associé à une solution potentiellement différente et à un score de similarité avec le cas à résoudre.

A la phase « *Reuse* », les solutions utilisées dans les cas retrouvés les plus pertinents sont adaptées au cas présent pour suggérer la solution la plus adéquate. Ce cas devient alors le « cas résolu ». Il faut noter que de nombreux CBR ne réalisent pas une étape « *Reuse* » complète se limitant à des systèmes permettant de retrouver des cas similaires.

A la phase « *Revise* », la solution proposée a été mise en pratique sur le patient. Le « cas résolu » devient alors le « cas testé » (« revised case »). Le résultat obtenu (caractéristiques de procédures, résultat de celle-ci) après application de la solution est alors enregistré dans la base de données du CBR pour compléter le « cas testé ». Il est donc important d'identifier les complications ou échec afin de ne pas répéter la solution.

Enfin à la phase « *Retain* », le cas testé complet peut être, si son contenu informationnel est jugé pertinent (automatiquement ou par l'utilisateur selon les approches), ajouté à la mémoire du CBR pour être à son tour réutilisé ultérieurement. Cette étape est également appelée mémorisation.

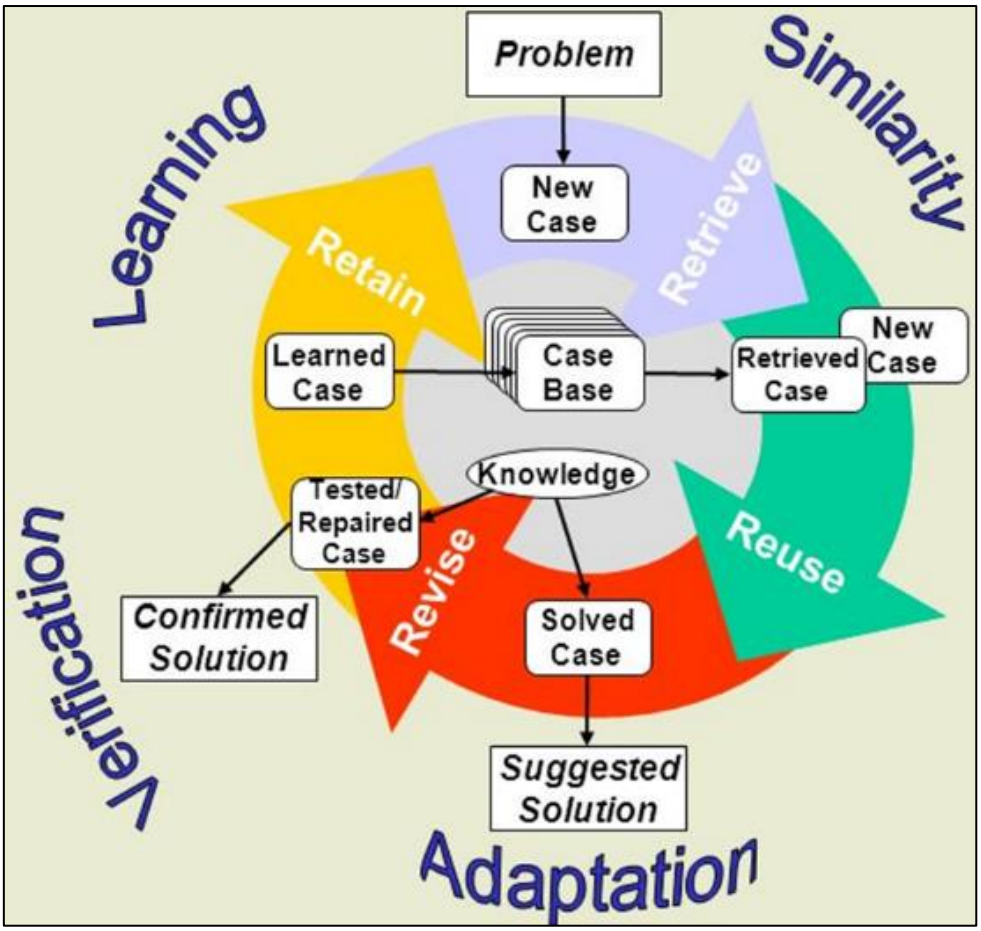

Figure 33 – Cycle de raisonnement classique d'un CBR.

Selon l'approche de CBR envisagée, chacune de ces phases peut être mise en œuvre de manière plus ou moins complexe et ainsi être divisée en un ensemble de sous-tâches pour lesquelles plusieurs algorithmes de résolution peuvent être utilisés (102). Ces éléments ne seront pas détaillés ici mais sont illustrés par la **Figure 34**.

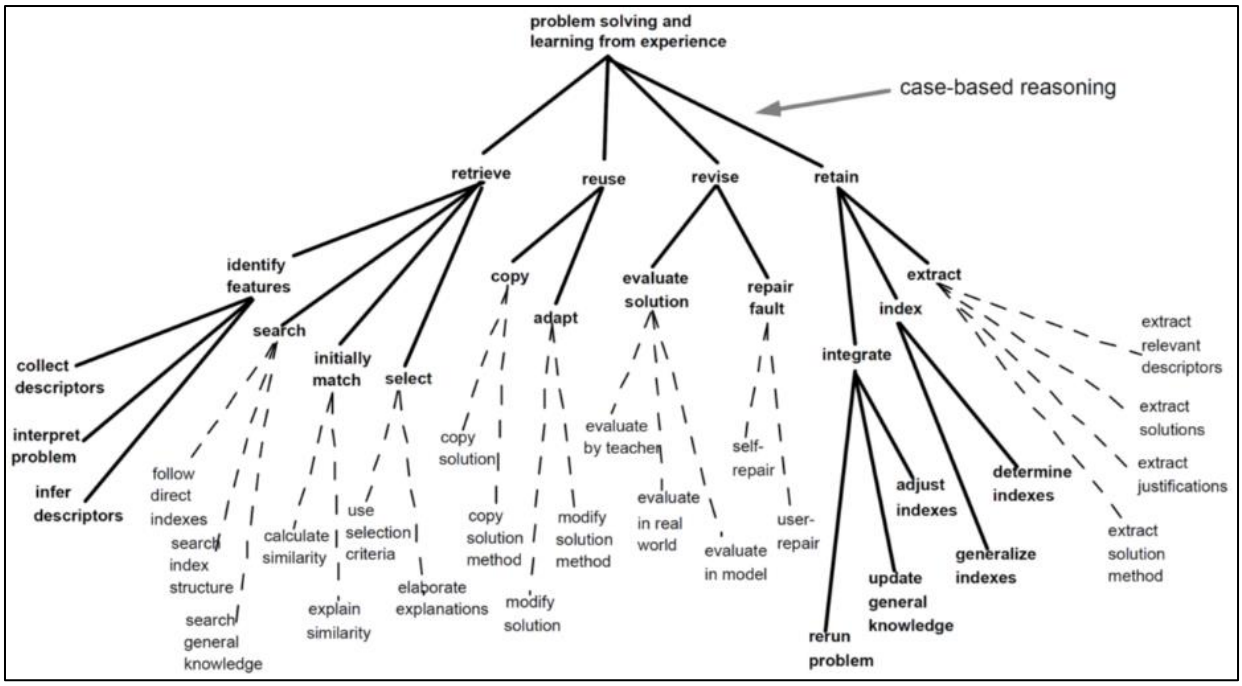

Figure 34 – Exemples de décomposition de tâches dans le cadre du CBR. Reproduite d'après Althoff KD et al (102). Les traits pleins relient les tâches à l'ensemble des sous-tâches les composant. Les traits pointillés relient les sous-tâches aux différentes méthodes utilisables pour les résoudre.

3.1.4 Eléments fondamentaux des CBR : notion de « Knowledge Container »

Les CBR sont articulés autour de quatre « modules de connaissance » distincts, capables d'interagir entre eux. Cette description a été initialement proposée par Richter, qui a introduit la notion de « Knowledge Container » (102,105). Ces quatre modules sont respectivement le vocabulaire, la mesure de similarité, les règles d'adaptation (ou de transformation de la solution) et enfin la base de cas (**Figure 35**). Les trois premiers modules contiennent principalement de la connaissance compilée ou exprimée (« expressed knowledge », soit des données plus stables) alors que le dernier module contient de la connaissance interprétée (« inferred knowledge ») par raisonnement à partir de la connaissance compilée dans le système. Ceci a pour conséquence de permettre la création quasi-immédiate d'information à partir de nouveaux cas faisant du CBR un outil particulièrement efficace pour gérer les connaissances dynamiques. De plus, le CBR permet le passage d'une connaissance d'un module vers un autre à mesure que cette connaissance devient plus fiable et plus « stable ». Ainsi, il est possible de faire fonctionner un CBR malgré un vocabulaire, une mesure de

similarité et/ou un container d'adaptation imparfaits si on dispose d'un nombre suffisamment grand de cas. Au cours du temps, le système apprend des cas et lorsqu'il est couplé à des techniques d'apprentissage, améliore son vocabulaire et sa mesure de similarité. L'amélioration de la connaissance dans ces containers permet alors au CBR de mieux différencier les cas disponibles et ainsi de réduire le nombre de cas nécessaires dans la base à la présentation de toutes les solutions potentielles au problème à résoudre. Si des connaissances deviennent disponibles au sein des règles de transformation de la solution, il est alors possible de réduire encore la base de cas puisque plusieurs solutions peuvent être proposées à partir d'un seul cas (102). La capacité d'apprentissage d'un CBR désigne donc essentiellement sa capacité à améliorer la structure et les performances de ces différents modules.

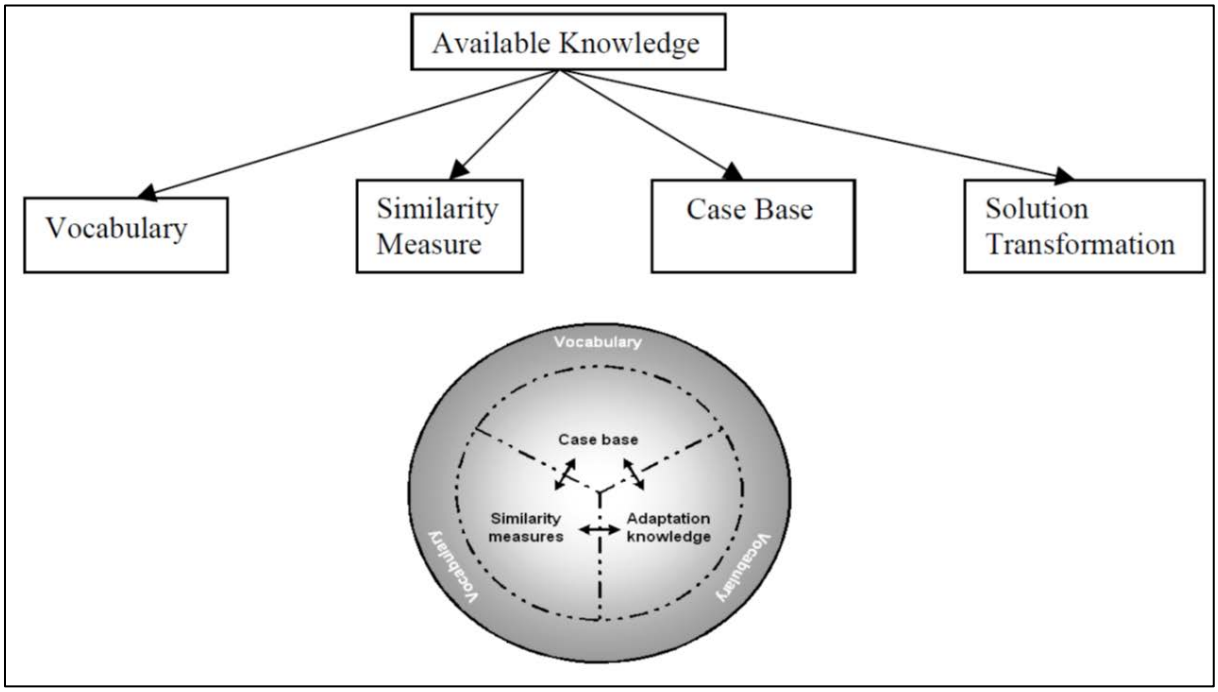

Figure 35 – Représentation de la distribution des connaissances dans un CBR en modules de connaissance (Knowledge Container) et leurs interactions. Reproduite d'après Richter M (105).

Le *vocabulaire* est le module le plus basique mais probablement le plus important puisqu'il définit explicitement et selon chaque problématique, les attributs utilisés pour décrire chaque cas, leurs valeurs potentielles et leur poids respectif. Il contient également généralement beaucoup de connaissance générale et accessible. Les étapes d'apprentissage et de maintenance du vocabulaire sont des processus difficiles à automatiser et qui passent le plus souvent par son

enrichissement (création d'un nouvel attribut ou calcul d'un attribut virtuel à partir d'attributs existants) ou l'exclusion d'attributs redondants/interdépendants, via l'intervention d'experts du domaine d'intérêt.

La *mesure de similarité (ou de dissimilarité, similarité = 1- dissimilarité)* représente une mesure de « distance », comprise entre 0 (non-similarité) et 1 (similarité), permettant de calculer la différence globale entre la question posée (le nouveau cas ou query, *q*) et un cas de la base de données (problème résolu, *p*) stocké conjointement avec sa solution (*s*). Il s'agit d'une mesure permettant de préciser de quelle manière deux cas sont similaires/proches. D'un point de vue mathématique, cette mesure de similarité utilise une mesure globale (*sim*) et plusieurs mesures locales entre les attributs. Elle est construite comme une fonction d'agrégation (*f*) des mesures locales sim_i calculées sur les différents attributs de sorte que :

$$\mathrm{sim}(q, p) = \Sigma(g_i \times \mathrm{sim}_i (q_i , p_i) \mid 1 \leq i \leq n).$$

où g désigne le facteur de ponderation $g = (g_1, \ldots, g_n)$ constitué de coefficients réels non négatifs normalisés de telle sorte que $\Sigma g_i = 1$ (105). Les mesures de similarité locales contiennent essentiellement des informations sur le domaine d'intérêt du CBR alors que la fonction d'agrégation contient des connaissances dites « utiles » spécifiques de la tâche à accomplir. Cette notion de connaissances « utiles » peut s'expliquer par le postulat de base sous-jacent à la mesure de similarité dans un CBR. En effet, l'exigence de base de la méthode est que la recherche du plus proche voisin (« nearest-neighbor ») de la question posée (*q*) renvoie de fait à la meilleure solution disponible dans la base. C'est-à-dire que pour le problème *q*, le cas (*p,s*) ait la propriété que *p* soit bien le plus proche voisin de *q* et que *s* soit la solution la plus « utile » à la résolution de *p*, contenue dans la base de cas. C'est ici qu'intervient le concept d'utilité qui peut être définit de deux façons :

(i) Par une relation de préférence définit sous la forme pref (p, s_1, s_2) qui se lit comme s_1 est préférée à (ou plus utile que) s_2 pour résoudre p.

(ii) Par une fonction de la forme u (p, s_1) qui renvoie à une valeur réelle d'utilité de s_1 pour p.

Il est commun de dire qu'une mesure de similarité correspond, ou au moins s'en approche, à l'utilité pour l'utilisateur. Ainsi l'équation *sim (q, p) = u (q, s)* est au moins approximativement vérifiée. Dans ce sens, il convient que les connaissances contenues dans la mesure de similarité soient en relation étroite avec l'utilité du CBR pour l'utilisateur, on parle donc de connaissances utiles (105).

De nombreuses mesures de distance comme celles de Minkowski, Camberra, Chebychev, Mahalanobis, Cosine ou Jaccard, peuvent être utilisées pour calculer cette fonction de similarité (106–108).

La mesure de similarité, tant locale que globale, est susceptible d'être améliorée par des procédés d'apprentissage que l'on classe en supervisés ou non. Les procédés non supervisés reconnaissent et regroupent, de manière automatique, des motifs identiques dans les données. La combinaison au CBR d'autres techniques d'intelligence artificielle (algorithme génétique, réseau de neurone, arbre de décision, etc…) dans des systèmes hybrides représente à cette fin un axe de recherche important (100). Les procédés supervisés font appel à une interaction avec l'expert. Ils permettent d'obtenir de l'information sur les relations de similarité, les pondérations des différents attributs ou encore les similarités locales. Par exemple, un moyen simple d'apprendre les relations de similarité locales est de corriger les erreurs du système dans la classification des plus proches voisins. Si un algorithme de classement propose le résultat suivant :

$$sim_{ord}=s_1 \geq s_2 \geq \ldots \geq s_k$$

Par interaction avec l'expert, ce résultat peut être modifié comme suit :

$$feedback_{ord}=s_3 \geq s_1 \geq s_5 \geq \ldots \geq s_k$$

Le système peut alors intégrer ce nouveau classement, considéré comme une amélioration qualitative, et ainsi apprendre de l'utilisateur. Pour superviser l'apprentissage de paramètres de similarité globale, il faut améliorer les pondérations de la fonction d'agrégation. Ceci peut être réalisé par de l'apprentissage « par renforcement », en réalisant des tests avec des questions dont la solution est connue. Ainsi, si le système donne un résultat satisfaisant avec les pondérations testées, celles-ci seront retenues et vice versa.

Comme évoqué précédemment, la *base de cas* contient les expériences passées sous la forme de paires (*p, s*) d'un problème *p* et de sa solution *s*. Cette base doit répondre à trois exigences distinctes. La première est qu'elle ne doit contenir que les cas dont l'utilité de *s* est maximale, ou tout du moins très bonne, pour la résolution de *p*. Ceci correspond à l'information contenue dans chaque cas. Les deux exigences suivantes sont conflictuelles :

(i) Une base doit être constituée d'autant de cas que possible car chaque cas peut potentiellement améliorer la compétence du système à trouver la solution.

(ii) Une base doit être aussi petite que possible car chaque nouveau cas peut augmenter le temps de recherche et ainsi diminuer l'efficience du système.

Ainsi, il faut accepter un compromis permettant d'obtenir un état optimal dans lequel l'ensemble des cas qui maximise la compétence du système est stocké dans la base de données sans impact négatif sur son efficience.

La base de cas peut donc également être améliorée par l'ajout de cas pertinents ou l'exclusion de cas ne contribuant pas ou très peu à la qualité de résolution de problème du système. Cette tâche désignée sous le nom de « case-base maintenance » est un élément central du fonctionnement des CBR (109) faisant proposer à certains auteurs un cycle de fonctionnement des CBR comportant deux étapes supplémentaires (*Review* et *Restore*) dédiées à cette tâche (110). De nombreux algorithmes ont été décrits pour automatiser cette tâche (111).

Les solutions proposées par la mesure de similarité peuvent être inappropriées, soit parce que la mesure de similarité est mal définie, soit parce qu'aucun cas présent dans la base n'a une utilité suffisante pour la résolution du problème posé (105). Pour répondre à ce problème, le dernier module de connaissances du CBR peut intégrer des règles d'adaptation (ou de transformation de la solution) prédéfinies, spécifiques de certaines tâches, codées par le développeur et stockées dans le système, afin de modifier une solution existante en une nouvelle solution voire de générer une nouvelle solution. Un bon moyen de représenter ces règles, notamment dans le contexte médical, est l'utilisation d'arbres de décision clinique. Une amélioration peut être obtenue par apprentissage de nouvelles règles d'adaptation à partir de la base de cas et représente donc essentiellement un transfert de connaissance entre les modules du CBR (105). Cependant, une modification des règles d'adaptation influence grandement les performances du CBR. En effet, toute modification des règles d'adaptation affecte la base de cas, le plus souvent en générant des cas redondants ou en entrainant l'exclusion de cas qui pourraient être utiles pour de futurs problèmes.

3.2 Application du CBR au TAVI

3.2.1 Contexte de nos travaux

Comme précédemment évoqué, nos travaux s'intègrent dans le Workpackage 5 du projet européen EurValve dont la finalité est de produire, tester et valider un système d'aide à

la décision clinique permettant la sélection de différentes stratégies thérapeutiques pour les pathologies valvulaires aortiques et mitrales, ainsi que la simulation, compréhension et comparaison de leurs bénéfices et risques potentiels.

Dans le cadre d'un précédent travail collaboratif, nous avions montré la possibilité d'adapter un système de type CBR au « workflow » global d'une procédure TAVI (99). Ce travail n'abordait pas la question spécifique des mesures de similarités et de leur évaluation. Seules une définition classique de la mesure de similarité et une représentation simple des cas avaient été envisagées. Dans le cadre de cette Thèse et du projet EurValve, nous avons conçu et développé un démonstrateur de CBR destiné à l'aide à la décision dans le cadre du TAVI, en orientant nos recherches sur l'aspect plus calculatoire de la définition et de l'optimisation d'une mesure de similarité adapté à la problématique clinique. Une interface graphique utilisateur a été spécifiquement développée afin de laisser un rôle central au praticien lors des phases *Reuse, Revise* et *Retain.* Cette interface propose au praticien des informations pertinentes pour sa prise de décision : n cas les plus similaires avec leurs résultats, mesure de similarité entre les cas, solutions suggérées. Concernant la phase *Retrieve,* qui a été automatisée, nous nous sommes intéressés aux questions du choix de la voie d'abord et de la prothèse (type et taille). Une base de cas de patients traités par TAVI au Centre Hospitalier Universitaire de Rennes a été créée. Outre les éléments cliniques pré procéduraux, les résultats et complications potentielles de la procédure, nous avons recueilli par une analyse dédiée de l'imagerie préopératoire (échocardiographie et surtout scanner) une liste d'attributs anatomiques prédéfinis, jugés pertinents pour répondre aux questions posées. Afin de créer une mesure de similarité adaptée à chaque problématique, nous avons notamment défini des arbres de décision tenant compte des connaissances cliniques des praticiens.

3.2.2 Article original

Ces travaux, ayant précédemment donnés lieu à la rédaction d'un acte de conférence (112), ont abouti à la rédaction de l'article suivant, récemment soumis pour publication dans Artificial Intelligence In Medicine.

Similarity measures and attributes selection for case-based reasoning in TAVI

Hélène Feuillâtre [1], Vincent Auffret [1], Miguel Castro [1], Florent Lalys [2], Hervé Le Breton [1], Mireille Garreau [1], Pascal Haigron [1]

Affiliations

[1] Univ Rennes, CHU Rennes, Inserm, LTSI – UMR 1099, F-35000 Rennes, France

[2] Therenva, F-35000 Rennes, France

Abstract

In a clinical decision support system, the purpose of case-based reasoning (CBR) is to help clinicians make convenient decisions for diagnosis or interventional gesture. Past experience, represented by a case-base of previous patients, is exploited to solve similar current problems through four steps—retrieve, reuse, revise, and retain. The proposed CBR has been focused on transcatheter aortic valve implantation (TAVI) to respond to clinical issues with regard to vascular access and prosthesis choices. Computing a relevant similarity measure is an essential processing step to obtain a set of retrieved cases from a case-base. Different similarity measures have been studied to better integrate the clinical knowledge, especially in terms of case representation, case selection, and decision tree. From a case-base of 69 patients, who underwent a TAVI procedure, two distinct analyses have been proposed to evaluate the system. The first one evaluated the suggested solution, and the second one, a set of similar cases. Results show that by using a dedicated similarity measure, with relevant and weighted attributes selected through a clinical decision tree, the set of retrieved cases, and consequently, the decision suggested by the CBR are improved.

Key words

Case-based reasoning; Similarity measure; Clinical decision tree; Transcatheter aortic valve implantation; Clinical decision support system

1. Introduction

Aortic stenosis (AS) represent the most common valvular heart disease [1]. According to the clinical guidelines [1,2], echocardiography is the key technique to diagnose the presence of AS, its severity, and prognostic. The "*heart team*", with their clinical expertise and different available guidelines about the management of severe AS, decides which intervention to apply to the patient: a surgical aortic valve replacement (SAVR) or a transcatheter aortic valve implantation (TAVI). Physicians have to consider several aspects, from patient and clinical features (e.g., risk score, comorbidity, and patient age) to anatomy and technical aspects (e.g., valve morphology, porcelain aorta). The "*heart team*" has to take several decisions about the patient. If TAVI is considered, the vascular access route and the choice of prosthesis have also to be determined. In this paper, a clinical decision support system (CDSS) [3] based on case reasoning is introduced, with the goal of helping practitioners to take decisions about the TAVI procedure.

Learning from past experiences, even with a limited number of previous patient cases, is the main concept of case-based reasoning (CBR). This accumulated knowledge plays an essential role in decision making when facing new problems. Indeed, the basic assumption of a CBR system is that similar cases should have similar solutions. The CBR is composed of four steps: *retrieve*, *reuse*, *revise*, and *retain* [4,5]. The retrieve step is mandatory and requires data processing to reliably evaluate the similarity between cases and recover relevant past cases. The other steps are defined according to the application and require user decisions on reuse, revision, and case retention after application and evaluation of the proposed solution.

Contrary to machine learning approaches, the CBR system does not need a substantial database. Even if the case-base increases according to the intended use of the CBR, the case maintenance (e.g., the retain step) has the aim to reduce the case-base by keeping only useful and relevant information [6,7]. In medical applications, CBR has the advantage of providing similar historical cases in addition to predictions. These similar cases provide a large amount of relevant information for decision making, such as the result of the procedure or the patient outcome after several months. In recent years, CBR has been considered as a useful decision support system for clinical questions [8,9].

CBR has already been applied in various domains, such as in statistical quality control [10], chemical engineering [11], signal-interpreting systems [12], or health science [8,9,13]. In the medical domain, according to a survey [9], CBR systems have different purposes such as diagnosis [14–16], classification [17–19], tutoring [20], planning [21,22], or knowledge acquisition [23]. Most of these CBR applications have been developed for specific diseases. Recently, CBR systems have been completed using artificial intelligence (AI) techniques. These hybrid CBR systems have been coupled

with rule-based reasoning (RBR) [15,16], fuzzy logic [24], data mining [25], neural networks [26], or genetic algorithms (GA) [8,14].

In the retrieve step, different techniques have been used to obtain similar cases. The most common retrieval technique has been the nearest neighbour retrieval (*k*-NN); however, a few CBR systems have used inductive or knowledge-guided approaches [8,27–29]. The similarity measure has represented a decisive part in the context of nearest neighbour retrieval.

Wilson and Martinez [30], Lesot et al. [31], and Choi et al. [32] presented different comparison studies about the similarity measures used in various applications (e.g., data mining, data analysis, or information retrieval). Other research works studied the similarity measures in CBR systems, such as Liao et al. [33], Núñez et al. [34], Avramenko and Kraslawki [11], or more recently, Gu et al. [14]. These different studies highlighted that the types of different attributes representing a case influenced the performance of the similarity measure, as did their degree of importance and the consideration of missing values.

In the retrieve step, most of the CBR systems used a similarity measure based on a generalised weighted distance metric. A distance measure was commonly used to compute the dissimilarity between the attributes of two cases. A diversity of distance measures was available such as the Minkowski, Camberra, Chebychev, Mahalanobis, Cosine, or Jaccard metrics [30–32]. A large number of CBR systems used the weighted Euclidean distance. Although most attributes are quantitative, the Euclidean distance and the other distance metrics are not suitable for all data types. The Euclidean distance is more appropriate for continuous quantitative values.

However, to overcome this problem, a few works [10,11] converted ordinal attributes to discrete values. An integer value was assigned to each category (for example, 1 for *Mild*, 2 for *Moderate*, 3 for *Heavy*, etc.). Afterwards, a distance measure between these integer values could be used to compute their degree of similarity. However, this type of discretisation was not suitable for a few cases. The ratio between each category could be different and this value inconsistent.

Another solution was to use a heterogeneous distance measure [14,30]. Wilson and Martinez [30] proposed a distance function, the heterogeneous Euclidean-overlap metric (HEOM), which used the overlap metric for qualitative (i.e., nominal) attributes and the normalised Euclidean metric for quantitative attributes (Section 3.2). The weighted heterogeneous Euclidean-overlap metric (WHEOM) represented the HEOM metric, where each attribute is weighted.

Wilson and Martinez explained that the HEOM metric corresponded to a simplistic approach for the qualitative attributes [30]. Indeed, the nominal or ordered attributes that were not similar

contributed considerably to the distance, conversely to the matching attributes. For this reason, they proposed to use another metric, the value difference metric (VDM) introduced by Stanfill and Waltz [35], instead of the overlap metric. The heterogeneous value difference metric (HVDM) mixed the advantageous property of the Euclidean distance and VDM on the quantitative and nominal attributes, respectively.

Increasingly numerous CBR systems have used a heterogeneous similarity measure with the Euclidean distance for the continuous quantitative attributes. However, they had a different approach for qualitative attributes. Sheraf-El-Deen et al. [15] and El-Fakdi et al. [36] used as a basis the WHEOM distance metric in their retrieve step, while Gu et al. [14] opted for the WHVDM metric. Guessoum et al. [37] determined the similarity between qualitative attributes thanks to a similarity matrix built from expert knowledge.

In addition to these metrics, the weight of the attributes in the similarity measure has an important impact in case retrieval. A majority of CBR systems have used weights to show the degree of importance of an attribute in the similarity measure. Several ways to establish weights exist. In medical CBR, a common approach has been to fix the weight thanks to expert knowledge [36]. Other works have used evolutionary algorithms, such as the GA [8,40]. Nonetheless, a few CBR systems have decided to give the same importance to each attribute [36].

The management of missing values is also an important issue in the similarity measure. When CBR is performed in a case with incomplete information, the result can be misrepresenting. Different approaches have been proposed [33,38,39]. A few CBR systems, such as that in El-Fakdi et al. [36], have chosen to discard the attribute when a value was missing. Other approaches estimated the distance between two case attributes when at least one of them was missing [37] or tried to complete the voids directly in the case-base, before using the CBR system.

The feasibility of designing CBR for TAVI has been previously reported in [36]. That work concentrated on the overall framework and its integration in the clinical workflow but did not focus on investigating the similarity functions. A classical definition of similarity measure was used, and only a simple representation of cases was considered. This study focuses on defining a relevant similarity measure to retrieve similar past cases. According to the decision to make, different issues have been addressed in defining the similarity measure, such as the choice of metrics, the selection of attributes, their degree of importance, and their mode of combination. In the design of the similarity measure, the experience and reasoning of physicians have been taken into account through the building of a clinical decision tree (CDT).

In the remainder of this paper, Section 2 provides a description of the CBR framework deployed for the planning of a TAVI procedure. The different similarity measures used to retrieve similar cases are described in Section 3. Different solutions about the selection and weighting of attributes and cases are formulated. The building of CDTs, which provide a hierarchical decision scheme about the attributes to use at different levels of decision, is explained. This section also presents criteria used for evaluation. In Section 4, results with a case-base of patients who underwent the TAVI procedure are presented. After the discussion in Section 5, Section 6 concludes and proposes the future work.

2. CBR framework

This section focuses on the concept of the proposed CBR in TAVI applications. The main goal of CBR is to support the practitioner in decision-making. The reasoning system does not provide the final decision but a suggestion. The final choice is still taken by the practitioner. The operation of CBR is based on the human–machine cooperation. CBR makes use of the complementarity between the practitioner (reasoning and decision to take) and the machine (computation). One of the first intentions of the clinical CBR is to integrate the reasoning of practitioners in the system. For TAVI, the decisions are related to the procedure characteristics (Figure 1): the implanted valve type, valve diameter, and type of planned access. When practitioners choose to perform this procedure, they obviously follow their own guidelines and decision trees, which they develop through experience. We choose to build decision trees that are very important in the reasoning process (Section 3) and to integrate them in the retrieve step, i.e., in the similarity measure.

2.1. Case Definition

A case, i.e., a patient, which is the central notion in a CBR system, represents the experience of physicians. It can be represented in various forms to be used in the retrieve step, such as a feature vector or a decision tree. The set of past cases is used to build the case-base CB. Each case $C_i(a, s, r) \in CB$ is composed of three categories of data specifically collected during the aortic valve intervention (Figure 1):

- the description of the problem represented by a feature vector $a = (a_1, a_2, \ldots, a_n)$, where n is the number of attributes (clinical attributes from patient characteristics and medical imaging such as the age or the diameter and calcification state of the aortic annulus),
- the solution s (procedure characteristics, such as the choice of the vascular access),

- the results r (procedure outcome, such as the procedure success, the annulus rupture, or the post-procedure aortic valve area).

Appendix A describes the different data considered in the CBR module. The clinical attributes are used in different steps of the CBR process: their resemblances between different patients are exploited to propose a relevant solution for decision support. These attributes contained in vector a can have different data types:

- continuous and discrete quantitative attributes such as diameter, area of the aortic annulus, or age,
- qualitative attributes that are ordered, called ordinal attributes, such as the tortuosity or the calcification of the different arteries,
- qualitative attributes that correspond to the Boolean category, such as the presence of calcification in the left ventricular outflow tract (LVOT).

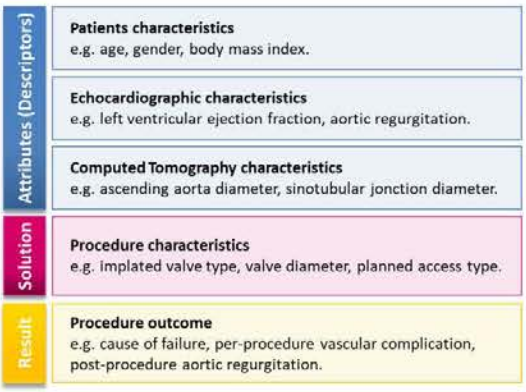

Figure 1: Example of clinical data in the TAVI database.

2.2. CBR solving cycle

The solution $C_{i,s}$ of the past cases C_i stored in the case-base is already known. However, the new case $C_c(a, \emptyset, \emptyset)$, from which the CBR will be executed, is not in the case-base ($C_c \notin CB$) and its solution $C_{c,s}$ is still unknown. The goal of CBR through the four steps (retrieve, reuse, revise, and retain) is to support the physician to make the most suitable decision about the solution $C_{c,s}$. From the current candidate patient C_c, the following steps (Figure 2) are performed:

- **RETRIEVE**: Owing to the computation of similarity measures from the attributes (Figure 1), a set of past similar cases is obtained. The *k*-nearest neighbour (*k*-NN) algorithm is used. The set of the k most similar cases can have different solutions and results. The design of similarity measures is detailed in Section 3.

- **REUSE**: From the set of k similar cases, the CBR suggests a solution s_s. In a classification problem, the suggested solution s_s represents the class corresponding to C_c. To determine the class of the current case C_c, a democracy voting weighted by the distance [36,41] but also by the rank of the similar cases is used (equation 1). $(s, C_{i,s})$ returns 1 if the class of the past case $C_{i,s}$ is similar to s and 0 otherwise. The rank $rank_i$ of the past case $C_i \in CB$ allows assigning more weight in the first similar cases for the class determination. $diss(C_c, C_i)$ represents the distance value between the current candidate case C_c and a past case C_i. The goal of this step is to help the practitioner to take the decision thanks to the comprehensive information provided by the graphical user interface (GUI).

$$Vote(s) = \sum_{i=1}^{k} \frac{1}{diss(C_c, C_i)} rank_i(s, C_{i,s}) \quad (1)$$

$$s_s = \arg\max_s (Vote(s))$$

- **REVISE**: The clinician has evaluated the suggested solution s_s and applied it. This suggested solution of the current case C_c becomes the confirmed solution $C_{c,s}$. The information about the solution $C_{c,s}$ and the result $C_{c,r}$ (i.e., the procedural outcomes) are completed into the current case $C_c(a, s, r)$ through the GUI.
- **RETAIN**: Useful experience is retained for future reuse. The user keeps the decision to add the current case C_c to the case-base through the GUI if it provides relevant knowledge.

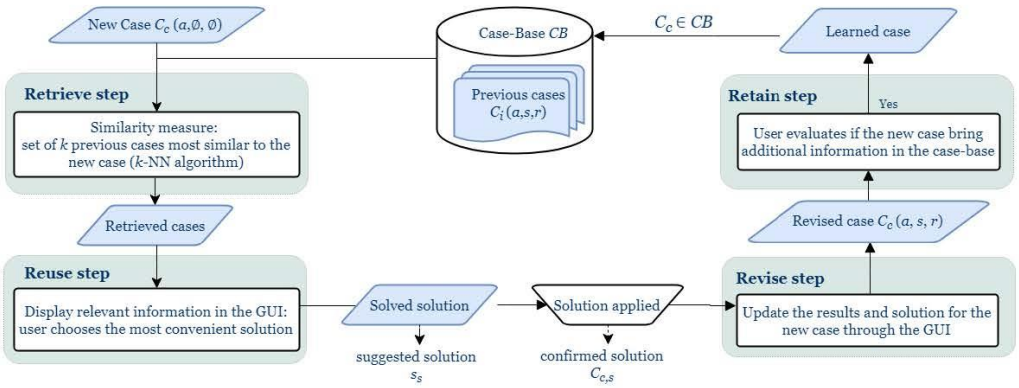

Figure 2: CBR steps.

The CBR module provides a user-friendly interface (Figure 3) to facilitate the visualisation of relevant information derived from the set of *k* similar cases and allows a complete integration of the practitioner in the reasoning system. The most relevant attributes, such as the procedure outcomes, are displayed for each similar case. The results of the reuse step (equation 1) are converted into a

percentage for each possible solution s. These percentages allow an easy determination of the suggested solution and of the level of confidence of the CBR in this solution.

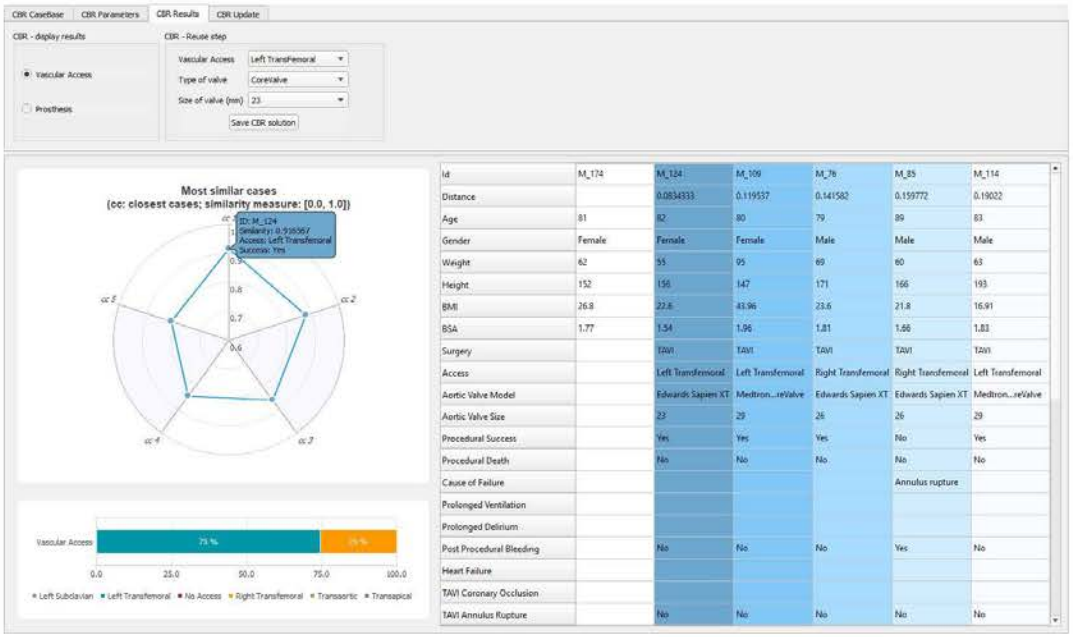

Id	M_174	M_124	M_109	M_76	M_85	M_114
Distance		0.0834333	0.119537	0.141582	0.159772	0.19022
Age	81	82	80	79	89	83
Gender	Female	Female	Female	Male	Male	Male
Weight	62	55	95	69	60	63
Height	152	156	147	171	166	193
BMI	26.8	22.6	43.96	23.6	21.8	16.91
BSA	1.77	1.54	1.96	1.81	1.66	1.83
Surgery		TAVI	TAVI	TAVI	TAVI	TAVI
Access		Left Transfemoral	Left Transfemoral	Right Transfemoral	Right Transfemoral	Left Transfemoral
Aortic Valve Model		Edwards Sapien XT	Medtron...reValve	Edwards Sapien XT	Edwards Sapien XT	Medtron...reValve
Aortic Valve Size		23	29	26	26	29
Procedural Success		Yes	Yes	Yes	No	Yes
Procedural Death		No	No	No	No	No
Cause of Failure					Annulus rupture	
Prolonged Ventilation						
Prolonged Delirium						
Post Procedural Bleeding		No	No	No	Yes	No
Heart Failure						
TAVI Coronary Occlusion						
TAVI Annulus Rupture		No	No	No	No	No

Figure 3: Screenshot of the GUI with the result of similarity measure.

3. Similarity measures

The quality of the results given by the CBR system depends mainly on the definition and the performance of the similarity measure. Defining a convenient similarity measure represents an important issue at the retrieval stage. The goal is to help the practitioner to take decisions about the vascular access (such as left or right trans-femoral and trans-apical), the type of prosthesis (e.g., Edwards Sapien XT or Medtronic CoreValve), and the size of the prosthesis (e.g., 23 mm, 26 mm, and 29 mm). Our approach relies on the definition of dedicated metrics from clinical attributes, available in the clinical database, combined with attribute selection and weight determination through CDTs.

3.1. Clinical decision trees (CDTs)

It is essential to consider relevant attributes in the similarity measure. According to the different levels of decision, the attributes in the case-base do not have the same importance. From expert knowledge and the literature (guidelines [1,2,42], expert consensus [43], and medical papers [44]), a few rules (which represent contraindications or preferences) and questions about the decision making process have been highlighted. They can be separated according to the type of decision: which vascular access, which type of prosthesis, and which size of prosthesis. A few rules may change

according to the hospitals and physicians and the improvement of devices (e.g., prosthesis and catheter) and new guidelines. These differences could easily be taken into account in the CDTs used in CBR.

Concerning the vascular access, the left and right trans-femoral accesses are used in most cases (more than 80% of the cases [43,44]). Then, the left trans-subclavian access or the trans-carotid access is preferred according to the hospital centre. In the current case-base, the trans-carotid was not available. The trans-aortic and trans-apical vascular accesses are increasingly infrequent because they are more invasive. They are highly contraindicated for elderly patients. Specific decision rules and conditions must be respected in hierarchical order, for each type of vascular access. For example, for the trans-femoral access, the diameter of the arteries is first examined to determine if these two accesses may be used during the intervention. If the diameters of the left and right arteries are adequate, the tortuosity and the calcification are next checked. Previous diseases on femoral arteries represent also a contraindication to use this vascular access. A previous aneurysm or thrombus means that arteries are frailer, and the risk of dissection is higher during the intervention.

The type and size of the prosthesis are linked. They both represent the characteristics of only one device. The different available prostheses do not have the same range of size. For example, the Medtronic CoreValve Classic exists in 23, 26, 29, and 31 mm while the Edward Sapien XT is available in 20, 23, 26, and 29 mm. As previously indicated, a few decision rules can be highlighted about these questions. The most important attributes for the size decision are the dimensions (area and diameter) of the annulus. A few indications exist for the prosthesis type. The choice depends on the vascular access selected previously. For example, if the trans-apical access is used, the Edward Sapien XT valve would be implanted, and operators would use the Medtronic CoreValve for the left trans-subclavian access. When both prosthesis types can be deployed, operators often chose according to his preference and practice. El-Fakdi et al. [36] have chosen in their CBR to separate firstly the choice of prosthesis type, and then the choice of the prosthesis size. In this approach, we propose only one decision for the prosthesis, as type and size are highly related. In this way, the considered CBR is constrained, thus avoiding the proposal of an incoherent combination of type and size of prosthesis.

The different attributes extracted from these rules are important in decision making. A few of them allow directly removing one possible solution. From these rules and the expert knowledge, relevant attributes are selected and a CDT is built (Figure 4) for each level of decision (type of access and prosthesis). Attributes in the root present a higher importance in the decision-making process than attributes near the leaves.

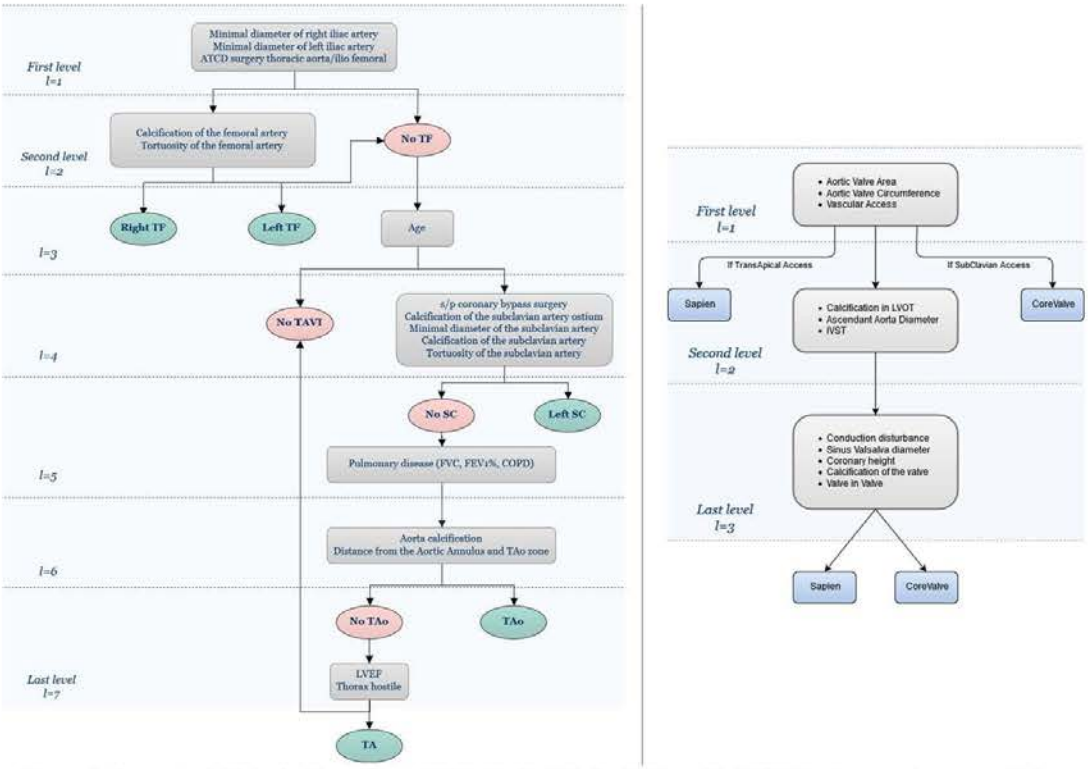

Figure 4: Example of attributes hierarchy in CDTs. On the left, the CDT used in TAVI for the vascular access choice. On the right, the CDT for the prosthesis choice (both type and size). TF: trans-femoral, SC: left trans-subclavian, TAo: trans-aortic, TA: trans-apical.

3.2. Metrics

To obtain similar cases, the similarity measures are generally computed through dissimilarity measures (equation 2) [30,41]. Most state-of-the-art similarity measures are based on a generalised weighted distance metrics (equation 3).

$$sim(C_c, C_i) = 1 - diss(C_c, C_i) \tag{2}$$

$$diss(C_c, C_i) = \frac{\sum_{a=a_1}^{a_n} w_a \, d\left(C_{c,a}, C_{i,a}\right)}{\sum_{a=a_1}^{a_n} w_a} \tag{3}$$

Let $diss(C_c, C_i)$ be the dissimilarity measure between cases C_c and C_i. Generally, the dissimilarity measure is computed with the weighted sum of the attribute differences and is in the range $[0,1]$. w_a corresponds to the weight of attribute a and $d\left(C_{c,a}, C_{i,a}\right)$ is the value that represents the difference between the attribute a in cases C_c and C_i. n represents the number of attributes of the case.

In the state-of-the-art, the ***HEOM*** (equation 4) [30] uses the overlap metric for qualitative (i.e., nominal) attributes and the normalised Euclidean metric for quantitative attributes (equation 5). The *HEOM* is defined as follows:

$$HEOM(C_c, C_i) = 1 - diss(C_c, C_i) \tag{4}$$

$$diss(C_c, C_i) = \sqrt{\sum_{a=a_1}^{a_n} d(C_{c,a}, C_{i,a})^2}$$

where $d(C_{c,a}, C_{i,a})$ defines the heterogeneous function between the attribute a of the two cases C_c and C_i:

$$d(C_{c,a}, C_{i,a}) = \begin{cases} overlap(C_{c,a}, C_{i,a}), & if\ C_{c,a}\ and\ C_{i,a}\ are\ qualitative \\ diff(C_{c,a}, C_{i,a}), & if\ C_{c,a}\ and\ C_{i,a}\ are\ quantitative \\ 1, & if\ C_{c,a}\ or\ C_{i,a}\ is\ unknown \end{cases} \tag{5}$$

where

$$overlap(C_{c,a}, C_{i,a}) = \begin{cases} 0, & if C_{c,a} = C_{i,a} \\ 1, & otherwise \end{cases}$$

and

$$diff(C_{c,a}, C_{i,a}) = \frac{|C_{c,a} - C_{i,a}|}{range_a}$$

Normalised attributes are used in the Euclidean distance function where the value $range_a = max_a - min_a$. max_a and min_a represent, respectively, the possible maximum and minimum values of the attributes. If these values are unknown, they are fixed according to the training set.

The generalised weighted heterogeneous measure (***GWHSM***) makes use of the Euclidean distance for numerical attributes and the Hamming distance for the categorical data (Equation 6) [36]. Attributes are discarded if the value is unknown in a case. Missing values do not play part in the similarity measure.

$$GWHSM(C_c, C_i) = 1 - diss(C_c, C_i) \tag{6}$$

$$diss(C_c, C_i) = \sqrt{\frac{\sum_{a=a_1}^{a_n} w_a\, d(C_{c,a}, C_{i,a})^2}{\sum_{a=a_1}^{a_n} w_a}}$$

$$\text{With } d(C_{c,a}, C_{i,a}) = \begin{cases} discard\ attribute & if\ C_{c,a}\ or\ C_{i,a}\ are\ unknown \\ d_C(C_{c,a}, C_{i,a}) & if\ C_{c,a} and\ C_{i,a}\ are\ categorical \\ |C_{c,a} - C_{i,a}| & if\ C_{c,a}\ and\ C_{i,a}\ are\ numerical \end{cases}$$

$$\text{Where } d_C(C_{c,a}, C_{i,a}) = \begin{cases} 1 & if\ C_{c,a} \neq C_{i,a} \\ 0 & if\ C_{c,a} = C_{i,a} \end{cases}$$

This last similarity measure, as explained, is already used in a CBR system applied in TAVI [36]. However, a few types of attributes are not considered. Hereafter, we propose different similarity measures that are dedicated to our clinical problem by taking into account the different data types of the selected attributes (Appendix A and Section 3.1.):

For the TAVI procedure, the proposed similarity measure does not consider non-ordered qualitative attributes. Nonetheless, if this type of attribute has to be used in a future development of the CBR (e.g., adaptation to other applications), the similarity measure can be improved by using the *VDM* [14]. Moreover, as previously explained, each attribute does not have the same influence in the decision-making process.

Firstly, we consider using a dedicated weighted heterogeneous similarity measure (***D_WHSM***).

$$D\_WHSM(C_c, C_i) = 1 - diss(C_c, C_i) \tag{7}$$

$$diss(C_c, C_i) = \sqrt{\frac{\sum_{a=a_1}^{a_n} w_a \, d(C_{c,a}, C_{i,a})^2}{\sum_{a=a_1}^{a_n} w_a}}$$

where

$$d(C_{c,a}, C_{i,a}) = \begin{cases} d_E(C_{c,a}, C_{i,a}) \ if \ C_{c,a} and \ C_{i,a} \ are \ quantitative \\ d_H(C_{c,a}, C_{i,a}) \ if \ C_{c,a} and \ C_{i,a} \ are \ binary \\ d_O(C_{c,a}, C_{i,a}) \ if \ C_{c,a} and \ C_{i,a} \ are \ ordinal \\ d_M(C_{c,a}, C_{i,a}) \ if \ C_{c,a} \ or \ C_{i,a} \ are \ missing \end{cases}$$

with

$$d_E(C_{c,a}, C_{i,a}) = \frac{|C_{c,a} - C_{i,a}|}{range_a}$$

$$d_H(C_{c,a}, C_{i,a}) = \begin{cases} 0, \ if C_{c,a} = C_{i,a} \\ 1, \ if C_{c,a} \neq C_{i,a} \end{cases} for \ C_{c,a}, C_{i,a} \in \{yes, \ no\}$$

$$d_O(C_{c,a}, C_{i,a}) = O[C_{c,a}][C_{i,a}]$$

$$d_M(C_{c,a}, C_{i,a}) = 0{,}5$$

As shown in equation 7, the Euclidean distance $d_E(C_{c,a}, C_{i,a})$ is computed for quantitative attributes and the Hamming distance $d_H(C_{c,a}, C_{i,a})$ is used for binary attributes. For each type of ordinal data, a distance matrix $d_O(C_{c,a}, C_{i,a})$ is built according to expert knowledge. The distance between attributes in the matrix is normalised in the range [0,1]. Table 1 presents an example of the similarity matrix used for the attribute relative to calcification. For instance, the distance between the attribute *Mild* and *Moderate* is 0.2, i.e., $d_O(C_{c,a}, C_{i,a}) = 0.2$ with $C_{c,a} = Mild$ and $C_{i,a} = Moderate$. Moreover, an online approach is preferred to manage the missing value d_M. The neutral approach, which gives directly the value 0.5 as distance between missing attributes, has been chosen.

Table 1: Example of distance matrix O used for the attribute calcification (ordinal data).

	No	Mild	Moderate	Heavy	Massive
No	0	0.15	0.5	0.90	1
Mild	0.15	0	0.2	0.5	0.7
Moderate	0.5	0.2	0	0.2	0.5
Heavy	0.90	0.5	0.2	0	0.15
Massive	1	0.7	0.5	0.15	0

Secondly, another type of similarity measure is proposed; this is the hierarchical heterogeneous similarity measure ***H_HSM***. The CDT is used in another way to determine the weight w_{a_l} of the selected attributes. In this case, the hierarchy of the CDT is exploited. Besides the selection of relevant attributes, *H_HSM* selects gradually the most similar cases. The expression of the metric $diss_l$ constituting *H_HSM* is adapted according to each level l of the CDT (equation 8).

$$diss_l(C_c, C_i) = \frac{\sum_{a_l=a_{1,l}}^{a_{n,l}} w_{a_l}\, d(C_{c,a_l}, C_{i,a_l})}{\sum_{a_l=a_{1,l}}^{a_{n,l}} w_{a_l}} \quad (8)$$

where $l \in [1, L]$ corresponds to the current level in the CDT and L is the height of the CDT. C_i with $i \in \left[0, {}^{m}/_{l}\right]$ represents a retained case in the case-base and m the total number of cases in the case-base. First, only attributes $a_l = (a_{1,l}, a_{2,l}, \ldots, a_{n,l})$ in the first level of the CDT ($l = 1$) are considered in the distance metric $diss_l$ (Figure 4). Next, a selection of cases is made. According to the distance value, only half on the most similar cases are kept. From these retained cases, the next value of the distance metric $diss_l$ is computed according to the next level of the CDT (l is incremented by 1). This next step takes into account the attributes present both in the previous levels and in the current level l of the CDT. This proposed *H_HSM* allows selecting the most relevant attributes and the most similar cases. Indeed, at a given level l only the most relevant attributes are used so that the least similar cases are directly removed for the next iteration.

3.3. Weighting scheme

The weight of the attribute represents an important part of the similarity measure. It allows showing the importance of an attribute in the decision making and scaling the different types of attributes

(e.g., continuous, discrete, or ordinal). Several weighting schemes are considered. All of them use a normalised weight w_a in the range $[0,1]$.

The basic approach is to consider that each attribute has the same influence. In this case, the weight w_a is set to the value 1 in the different similarity measure.

A more elaborated approach depending of expert knowledge is then considered. It relies on the exploitation of CDTs. The attributes in the first level of the CDT, such as the *aortic valve area* for the type and size of the prosthesis (Figure 4), have more importance in the decision making process than attributes in the other levels. The weights w_a are computed according to the attribute level l_a in the CDT and L, the total number of levels (equation 9). Attributes on the first level have their weight fixed at $w_a = 1$. For the other levels, the weight is subtracted by the inverse of the total number of levels, i.e., L, the height of the CDT. For instance, for the type and size of the prosthesis, the attributes present in the second level have a weight fixed to $w_a = 0.66$ and those in the third and last level have a weight value of $w_a = 0.33$.

$$w_a = (L - l_a + 1)/L \tag{9}$$

In order to compare similarity measures based on expert knowledge and the CDT, a learning-based approach is also used as weighting scheme. Using a GA to learn attribute weights, no prior knowledge is integrated in this last approach. GAs have already been adopted successfully in several CBR systems for weight determination [14,40]. In this approach, a floating-point chromosome representation is used to represent an individual. Each individual of the population in the GA represents a particular weight of the attributes of the similarity function. To calculate the fitness of each individual, the leave-one-out cross validation technique is employed. The average performance using the weights for the similarity function is calculated by repeatedly removing a case with a known solution from the case base, the so-called target case, retrieving the most similar case from the remaining cases in the case base and comparing the solution of the retrieved case with the actual solution of the target case. The fitness function is defined as the precision ($TP/(TP + FP)$) of the number of solutions correctly proposed. The used evolutionary operators are crossover, mutation, and elitism (elitist selection). The crossover rate is 0.9 and the mutation rate is 0.05. The population size is 60 and the number of generations used in the GA is 300. The proposed GA uses the roulette-wheel selection method. Elitism is used and ensures that the 50% fittest individuals are taken to the next generation.

3.4. Summary of similarity measures

From the metrics described in Section 3.2, several combinations with different weighting schemes and attribute selections are studied. Table 2 shows an overview of the different considered similarity measures.

Table 2: Similarity measures.

Similarity measure	Attribute selection	Attribute weight	Case selection
D_WHSM1	No	No	No
D_WHSM2	Yes - CDT	No	No
D_WHSM3	Yes - CDT	Yes – CDT Level	No
D_WHSM_GA	Yes - CDT	Yes - GA	No
H_HSM	Yes - CDT	Yes – Hierarchical process	Yes
H_WHSM	Yes - CDT	Yes – CDT Level and Hierarchical process	Yes
HEOM **[30]**	No	No	No
GWHSM **[36]**	Yes	No (set to 1 but can be modified manually by expert)	No
GWHSM_GA	Yes	Yes – GA	No

First of all, three different variants of the *D_WHSM* are considered to determine the influence of the attribute selection and the influence of the weight through the use of the CDT.

With the first version of the *D_WHSM* denoted ***D_WHSM1***, no attribute selection is performed (according to the case-base) and each attribute has the same importance in the decision making.

In ***D_WHSM2***, the second version of the weighted heterogeneous similarity measure, a selection of relevant attributes is applied. Only attributes present in the CDTs (Figure 4) are used. As previously, no weights are considered.

The third variant of the similarity measure, ***D_WHSM3***, fixed the weights of attributes thanks to the CDTs (equation 9).

Even if it is not the goal of this article, the last version of *D_WHSM*, denoted ***D_WHSM-GA***, used a standard GA to learn the attribute weights.

Next, two variants of the *H_HSM* are proposed. In the first one, ***H_HSM***, the weight w_{a_l} is set to 1 for each attribute (equation 8). In this configuration, the hierarchical process implies that the attributes are not taken into account in the same way. To fully combine the hierarchical and weighting-based schemes we also introduce the hierarchical weighted heterogeneous similarity measure ***H_WHSM***, where the weight w_{a_l} is fixed as in *D_WHSM3* (equation 9).

3.5. Evaluation approach

To evaluate the similarity measures performance through a leave-one-out cross validation, two evaluation criteria were considered.

The first way to evaluate the performance of the similarity measure was to analyse the set of k similar cases obtained after the retrieve step: the retrieve-based criterion. For each candidate case C_c, we have focused on the number of cases with the correct solution $C_{c,s}$ among the set of k retrieved cases.

Another way to evaluate the performance of the similarity measure was to analyse the rightness of the decision suggested by the CBR at the end of the reuse step: the reuse-based criterion. From the set of k most similar cases obtained through a given similarity measure, only one suggested solution was highlighted thanks to the equation 1. The candidate case C_c was assumed to be correctly classified when the suggested solution s_s was the same as the confirmed solution $C_{c,s}$, i.e., the one that has been applied during the intervention.

The evaluations have been performed on a real case-base of patients who underwent a TAVI procedure. To analyse the influence of the case-base content on the results, additional cases have also been generated from the real data. The data augmentation process was used to double the size of the case-base with the generated cases. From a real case $C_i(a, s, r) \in CB$ with CB the real case-base, all attributes $C_{i,a}$ describing the problem were modified to obtain the generated case. The solution $C_{i,s}$ and result $C_{i,r}$ were not changed. The distribution of generated cases remains the same as in real cases. The value of attributes resulting from measurement was randomly modified to be consistent with the solution of the case. For instance, the area of the aortic valve has been specified in the range recommended by the device manufacturer (Instruction For Use) for a given prosthesis size. Other quantitative attributes, such as the age, the weight and the height (and consequently the Body Mass Index and Body Surface Area), were also randomly modified until +/- 10% while

respecting a clinically coherent interval. Categorical attributes had their value randomly modified with the upper or lower grade (or left identical).

4. Results

The real case-base used for the evaluation is composed of 69 patients who underwent a TAVI procedure at the University Hospital of Rennes. For all patients, the attributes used in the CBR (patient and procedure characteristics) were directly obtained from data generally available in clinical routine (Annex A). There was no missing value in the dataset. Figure 5 shows the distribution of cases according to the two clinical decisions that have been considered: the vascular access and the prosthesis (both type and size). Five vascular accesses are represented in the case-base. The number of cases with trans-femoral access (both right and left side) is consistent with that in the literature (around 80%). Four combinations of prostheses are available: the *Edwards Sapien XT* in 23 mm and 26 mm and the *Medtronic CoreValve* in 26 mm and 29 mm.

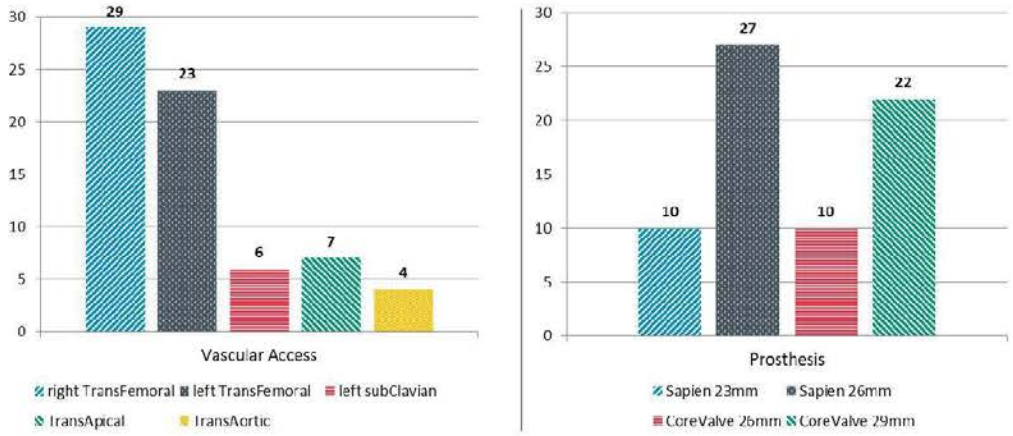

Figure 5: Distribution of cases in the real case-base according to the decision type (vascular access and prostheses).

The similarity measures have been evaluated through a leave-one-out cross validation. The similarity measures introduced in this work (*D_WHSM1*, *D_WHSM2*, *D_WHSM3*, *D_WHSM_GA*, *H_HSM*, and *H_WHSM*) have been compared with two state-of-the-art similarity measures: the *HEOM* metrics [30] and a generalised metrics *GWHSM* [36]. In the following, when not specified, the results reported were obtained from the real case-base of 69 cases.

4.1. Retrieve-based criterion

The first results relate to the global behaviour of the similarity measures when only the most similar case ($k = 1$) is retrieved. Figure 6 shows the true positive rate (TPR) and the false positive rate (FPR) obtained in the leave-one-out cross validation for different similarity measures when all decisions are considered (left: global decision, right: vascular access and prosthesis). The best results were obtained with *H_WHSM*. The other hierarchical similarity measure (*H_HSM*) gives slightly better solutions than *D_WHSM*. However, all *D_WHSM* measures surpass the state-of-the-art similarity measures (*HEOM* and *GWHSM*).

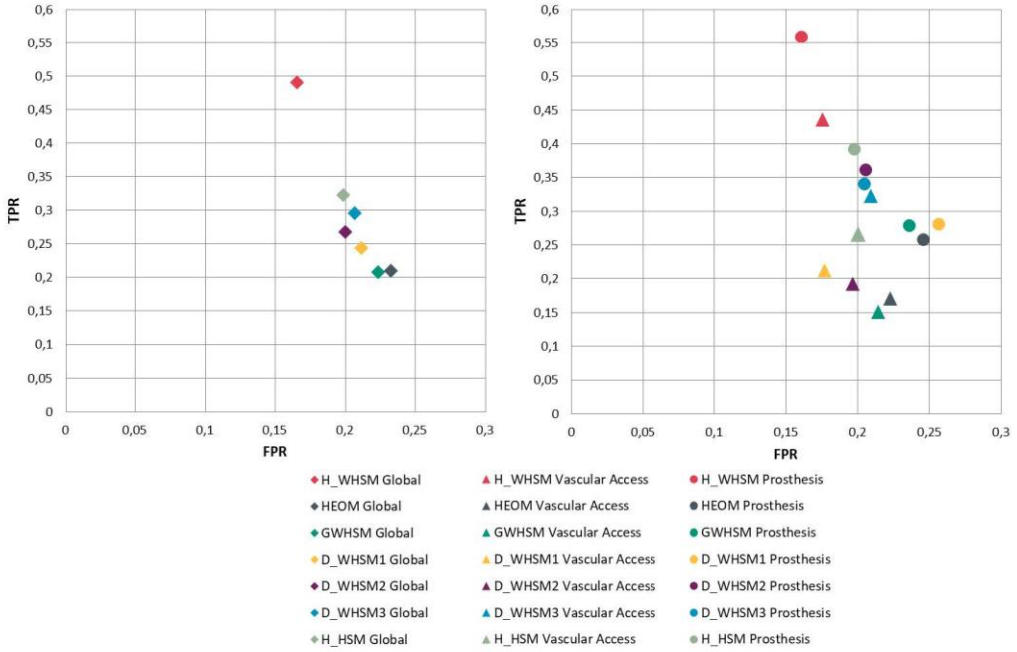

Figure 6: True Positive Rate (TPR) and False Positive Rate (FPR) for similarity measures according to the global decision when *k=1*.

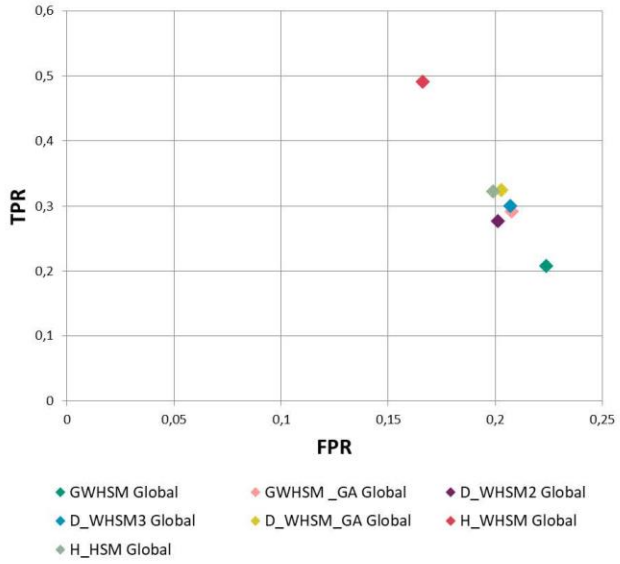

Figure 7: TPR and FPR of similarity measures using different weighting schemes according to the global decision when $k=1$.

The construction of the proposed similarity measures is based on an expert-based (*i.e.,* deductive) approach with the weighting and decision tree derived from clinical knowledge. Figure 7 compares their performance to that of similarity measures whose weights are obtained from a blind optimisation approach (GA). This approach was considered for two weighted heterogeneous similarity measures (*D_WHSM_GA* and *GWHSM_GA). D_WHSM_GA* shows only few differences with the *D_WHSM* variants: the TPR is around 0.3 and the FPR is around 0.2. With the help of a GA, *D_GWHSM_GA* reaches a performance approximately equivalent to that of *D_WHSM*. However, this is not enough to outperform *H_WHSM*. In addition, it is noted that the evaluation conditions were to the advantage of the GA weighting approach. Contrary to the deductive approach, it required a learning case-base, which was identical to the test case-base used to perform the leave-one-out cross validation.

After these global results, the CBR performance is examined through each possible solution available in the case-base. Figure 8 and Figure 9 show these specific results for the three similarity measures: *H_WHSM*, i.e., the one that exploits the most the CDT, and *HEOM* and *GWHSM*, the two state-of-the-art measures. The sensitivity and specificity of the similarity measures are computed for each possible solution when only one similar case is retained ($k = 1$). We set forth the hypothesis that this most similar case has a higher probability to have the correct solution. The sensitivity value for the trans-apical, trans-aortic, and left trans-subclavian accesses are close to, if not, zero for *HEOM*

and *GWHSM*. *H_WHSM* has a higher sensitivity for the different decisions expected for the left trans-femoral approach, obtaining a similar value to that of *GWHSM*. Moreover, the specificity values are almost always higher for *H_WHSM* than for *HEOM* and *GWHSM*, except for the trans-apical approach and the prosthesis Edward Sapien of 23 mm. We can also notice than the values for the trans-femoral approaches (both right and left) present the lower specificity values according to the solutions. Additional tests have been performed when the trans-femoral access, irrespective of the side, is considered as one single access. The sensitivity and the specificity of *H_WHSM* increase and reach, respectively, the values 1 and 0.81.

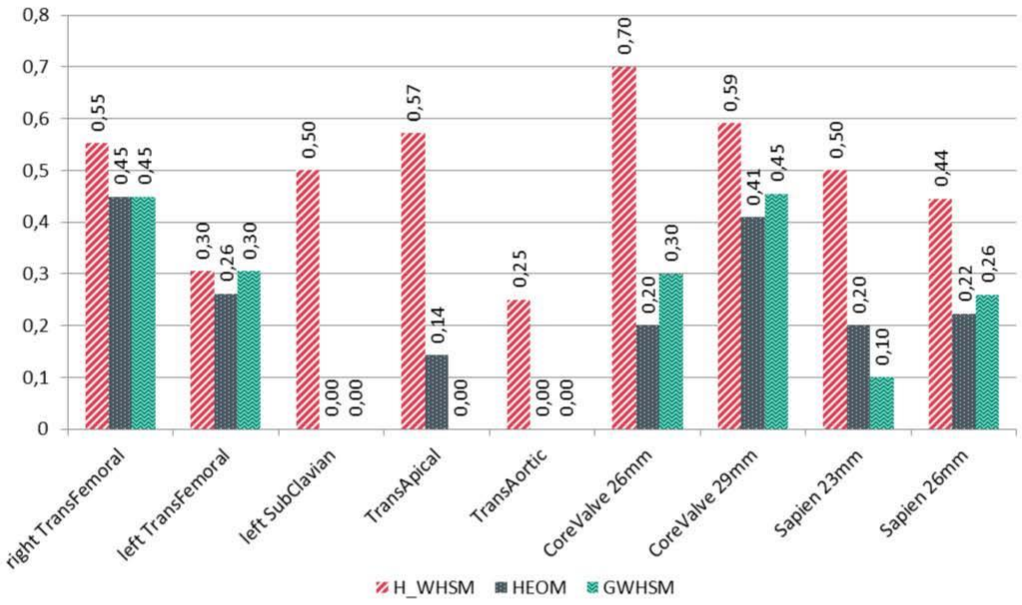

Figure 8: Sensitivity of similarity measures when one similar case is retained ($k=1$) for the different solutions.

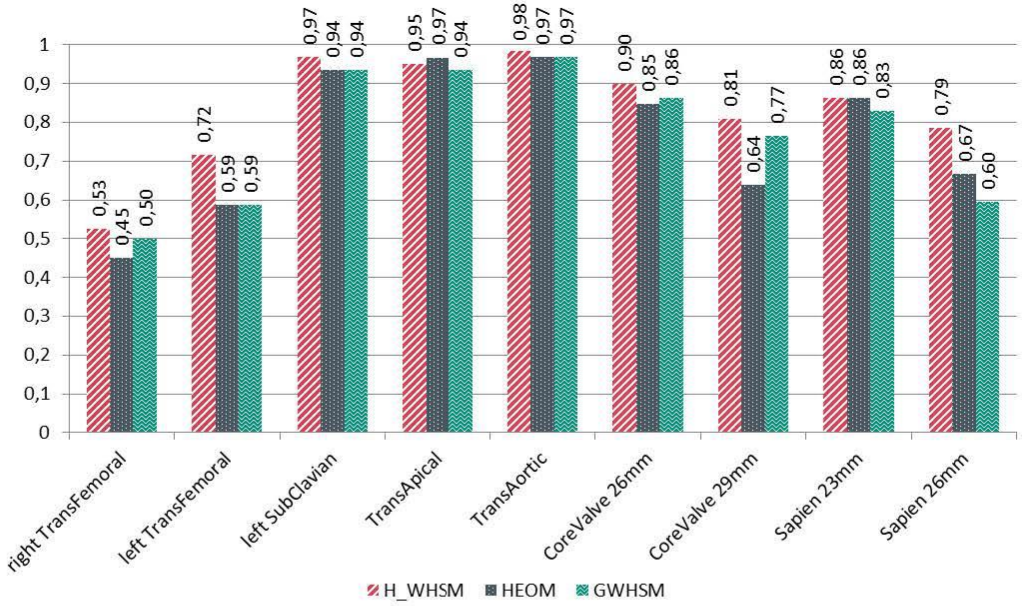

Figure 9: Specificity of similarity measures when one similar case is retained (k=1) for the different solutions.

As the value of k can be chosen by the user, the following results describe how the similarity measures behave when its value increases in the range $k \in [0; 7]$. The maximum number of most-similar cases (k=7) was fixed at 10% of the total number of real cases.

Figure 10 shows the average percentage of correct solutions that appear in one set of k retrieved cases. The left side displays all the proposed similarity measures and the right side the state-of-the-art similarity measures with *H_WHSM*. When $k = 4$, 42% of the four retrieved cases have on average the correct solution for the vascular access choice with *H_WHSM* (Figure 10A). This similarity measure gives for the different values of k a higher percentage than the other measures, thus *H_WHSM* outperformed them. For instance, the prosthesis decision obtains 42.74% for *H_WHSM* against 32.97%, 38.41%, 38.41%, and 36.96%, respectively, for *D_WHSM1*, *D_WHSM2*, *D_WHSM3,* and *H_HSM*. We can also notice that for the vascular access, the value of k shows little influence on the result, unlike the prosthesis choice (Figure 10B), which shows that the percentage tends towards $35-40$ % when the value of k increases.

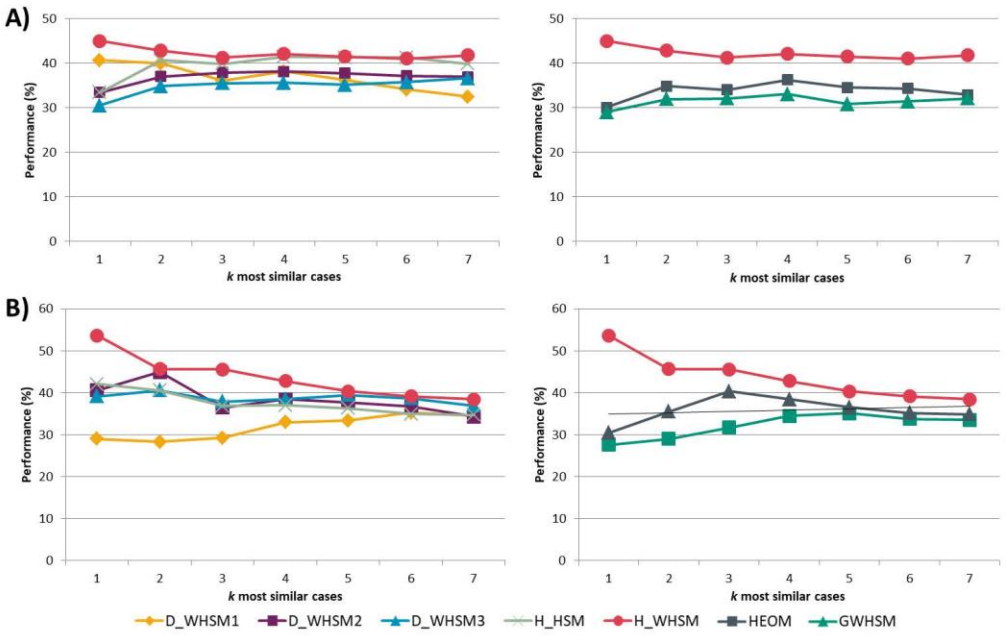

Figure 10: Average percentage of cases that present the correct solution in a set of k similar cases for the vascular access (A) and the prosthesis choice (B).

Hereafter, a candidate case C_c is now considered as correctly classified when the correct solution $C_{c,s}$ appears at least once among the k retrieved cases. This analysis represents a consistent indicator of performance as the final decision is left to the user. Figure 11 describes the percentage of cases correctly classified when $k \in [1; 7]$ for the two state-of-the-art similarity measures and the proposed *H_WHSM,* which outperformed the other proposed similarity measures. The performance increases significantly with the value of k reaching $90 - 100\%$ for each similarity measure. A sharp increase is shown between the lowest values of k. There is for instance a gap around 40% between $k = 1$ and $k = 3$. For the decision about vascular access (Figure 11A), the proposed measure improves the results for all k values. For the prosthesis choice (Figure 11B), *H_WHSM* gives a better classification when $k \in [1; 5]$. For the highest values of k, the measures present a similar performance. However, compared to *HEOM*, *H_WHSM* allows obtaining a better set of k retrieved cases.

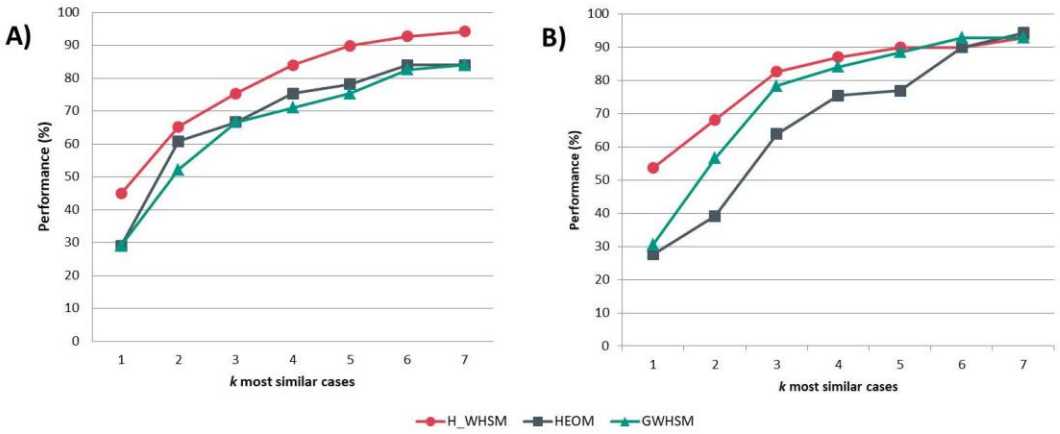

Figure 11: Percentage of cases where the correct decision appears at least once into the k most similar cases for the vascular access (A) and the prosthesis choice (B).

4.2. Reuse-based criterion

The reuse-based criterion is based on the suggested solution given by equation 1. Figure 12 shows the percentage of cases correctly classified according to the suggested solution for, respectively, the vascular access (Figure 12A) and the prosthesis choice (Figure 12B) decisions. The results obtained with the proposed similarity measures are displayed on the left side. As previously highlighted, the performance of *H_WHSM* gives the best percent of cases correctly classified for the different values of k. This last similarity measure is compared with the two state-of-the-art methods on the right side of Figure 12. Great differences between the percentages of cases correctly classified are shown. For example, when four most similar cases are selected ($k = 4$) for the prosthesis choice, $55{,}07\%$ of the suggested solutions are correct for *H_WHSM* against $30{,}43\%$ and $34{,}78\%$, respectively, for *HEOM* and *GWHSM*. Moreover, the percentage of cases correctly classified is almost stable for the different values of k. The voting rule adopted in the reuse step (equation 1) shows little sensitivity to k. The value of k has little influence regarding only the suggested solution.

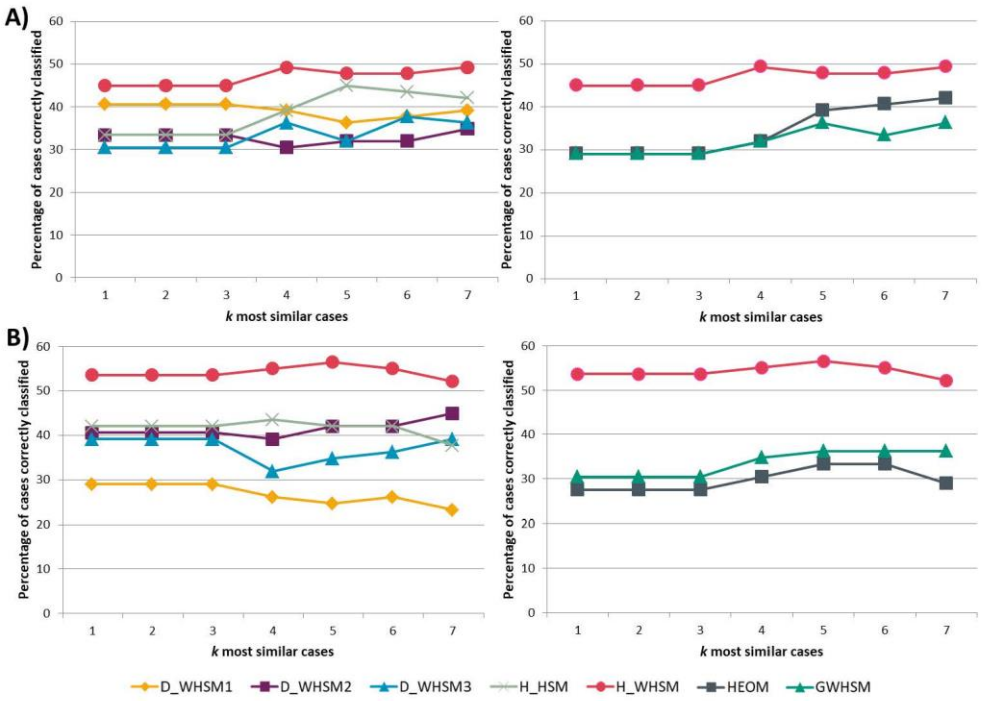

Figure 12: Percentage of suggested solution correctly classified for the vascular access choice (A) and the prosthesis choice (B).

Figure 13 describes for $k = 1$ and $k = 4$ the percentage of correctly classified suggested solution about prosthesis choice for three different case-bases composed of: (i) 69 real cases only, (ii) 69 generated cases only and (iii) both real and generated cases (138 cases). The same trend about similarity measures performance can be observed on the different case-bases. For the third case-base, the result obtained with *H_WHSM* increases to 91% when $k = 4$ and reaches 94% when $k = 1$.

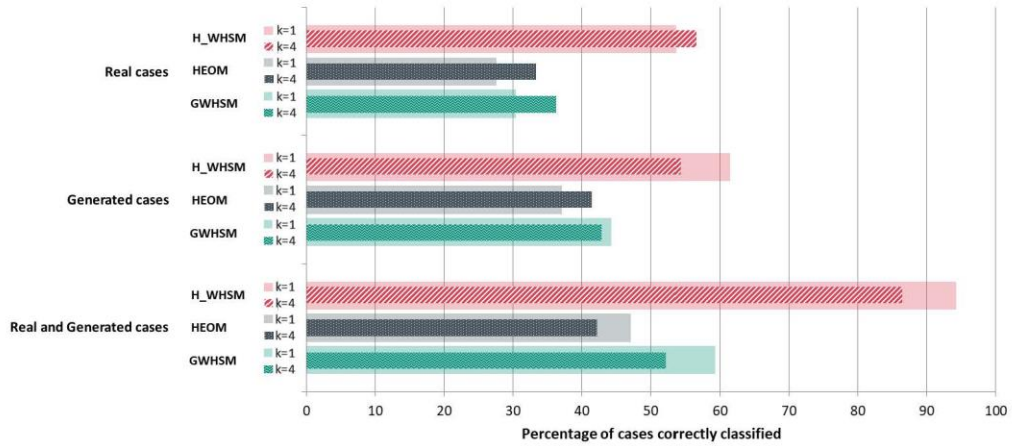

Figure 13: Percentage of suggested solutions correctly classified for the prosthesis choice obtained with three case-bases (real cases, generated cases, both real and generated cases).

5. Discussion

In this study, CBR was designed to help practitioners to take decisions about TAVI, and more specifically, decisions about the vascular access and the prosthesis. We focused on the similarity measure, which is a key component to retrieve cases. We examined the importance of considering CDTs and the selection of relevant attributes.

Six similarity measures (*D_WHSM1*, *D_WHSM2*, *D_WHSM3*, *D_WHSM_GA*, *H_HSM*, and *H_WHSM*) have been considered to determine the impact of a CDT on the set of k retrieved cases. Each similarity measure proposed one main change (Table 2). *D_WHSM1* represented a basic similarity measure, which used all the attributes of the case-base. This case-base did not have incoherent attributes (Appendix A). They were all related to the medical problem, but they remained generic, i.e., not linked to one decision. From *D_WHSM1* to *D_WHSM2*, the main change consisted in the selection of attributes through the CDT. The weighting scheme was modified in *D_WHSM3* and *D_WHSM_GA*. *H_HSM* included a CDT with a hierarchical approach, which selected progressively the most similar cases. Finally, *H_WHSM* was used to refine the weighting scheme in this last formulation.

In our approach, physicians play a major role. The CDT is used to fully integrate their reasoning. Moreover, the GUI allows them to interact easily with the CBR in order to take the most convenient decision. The GUI displays comprehensive information about which solutions have been applied to the k most similar patients and their outcomes, so that the final decision is left to the user.

Therefore, two types of evaluations have been performed. They were related to the set of similar cases (retrieve step) and to the suggested solution (reuse step). In these studies, the parameters or characteristics that could influence the results have been highlighted.

In the literature, most works evaluated their CBR on a given k through the suggested solution at the end of the reuse step (Section 3.1). The value of k could play a significant role in the result and may lead to different suggested solutions. In the proposed CBR, the choice of the number of similar cases is left to the user. Different values of k were tested to analyse its impact on the results. *H_WHSM*, the measure that outperformed the others, has the advantage of being stable in relation to the k value. For instance, retrieving 5 similar cases rather than 3 will have little influence on the suggested solution. However, it gives more information to the user about the coherence of the possible solutions.

The selection of relevant attributes and the weighting scheme was hypothesised to have a significant influence on the similarity measure. The behaviour of the CBR results for each k showed that *H_WHSM*, the similarity measure using the CDT, improved the relevance of the set of retrieved cases, and consequently, the reliability of the suggested solution.

To further examine the importance of using the CDT for the selection of attributes, we pointed out the results obtained with the two similarity measures that do not propose the selection of relevant attributes. *HEOM* [30] and *D_WHSM1* were among the worst measures regarding the true positive rate and the percentage of correct suggested solutions for all the decisions (Section 4.1). Moreover, the results with respect to the set of k retrieved cases (Section 4.1) obtained with *HEOM* [30] against those acquired with *D_WHSM2* and *D_WHHSM* showed that the selection of relevant attributes through the use of the CDT improved the retrieve step.

In addition, our results highlighted the importance of choosing a pertinent weighting scheme approach. Indeed, when comparing *D_WHSM2* with *D_WHSM3*, and *H_HSM* with *H_WHSM*, we saw that the weight had an impact on the determination of similar cases. *D_WHSM3*, which used a simple CDT-based weighting approach, resulted in a slight increase in sensitivity. However, the same weighting scheme used in *H_WHSM* substantially increased both the sensitivity and specificity as compared to *H_HSM*. We also considered a purely learning-based weighting approach in *D_WHSM_GA* and *GWHSM_GA*. The results obtained with both of them were better than those obtained with *GWHSM*, but they were significantly outperformed by those obtained with *H_WHSM*, although the test dataset was the same as the learning dataset. For this reason, we did not further investigate this learning approach. In further works, it could be interesting to combine it with the CDT, i.e., with selected attributes.

Using the CDT in the similarity measure permits to select gradually relevant past cases. This is the key point of the hierarchical metric. This case selection allows the most relevant attributes to be indirectly weighted. To show the influence of this characteristic, we have compared *D_WHSM2* with *H_HSM*, and *D_WHSM3* with *H_WHSM*. The hierarchical metric outperformed the *D_WHSM* metric. The same outcome can be established for *GWHSM* [36] and *HEOM* [30]. The sensitivity and specificity of *H_WHSM* were better than those of the two state-of-the-art similarity measures. We noted in Section 4.1 that for a few specific vascular accesses (trans-subclavian, trans-apical, trans-aortic), *HEOM* [30] and *GWHSM* [36] had a sensitivity value close to zero. With these two similarity measures, the CBR mostly suggested the wrong solution for each case having these particular vascular accesses. With the hierarchical measure *H_WHSM*, the correct decision was suggested in more cases, even if only few cases with these vascular accesses were available in the case-base.

Although CBR can be implemented with a small dataset, the information content available in the case-base has an impact on the result. We have shown that increasing the size of the case-base with a data augmentation approach (Section 4.2), and consequently the number of similar representative cases, allows improving the percentage of suggested solutions correctly classified (by reaching 94% for prosthesis choice for instance).

The case distribution could influence the CBR but could also lead to distorted results. The behaviour difference (according to k) between the two types of decisions (vascular access and prosthesis choice) in Figure 10 could thus be explained by the case representativeness of the real case-base. The issue related to the pre-processing (case maintenance) of the case-base has not been addressed in this work. As part of a future work, the enrichment of the case-base will be considered.

The different results have shown that the selection of relevant attributes have influenced the set of similar cases, and consequently, the suggested solution. We have shown this impact also in the specificity and sensitivity of *H_WHSM* (Figure 8 and Figure 9). Although the right and left trans-femoral accesses represented the majority of cases, their specificity was quite low according to the other access. With the attributes clinically available, the different similarity measures had difficulty to distinguish the right trans-femoral access from the left trans-femoral access. Only the clinical attributes related to the diameter of the femoral arteries were used in the case description to discern these two trans-femoral accesses. These attributes are ordinal data and are known to be operator dependent. To better characterise cases, further quantitative attributes related to the tortuosity and the calcification of each femoral artery could be extracted from CT images and included in the case-base.

These limitations could be reduced by completing the case-base with additional relevant attributes, consistently with the CDT (e.g. patient's clinical history). In addition, even if standard data available in clinical routine are used in the proposed approach, the issue of missing information might be raised, especially when physicians have to take the decision in emergencies. Missing data might consequently have an impact of the solution suggested by CBR. Different approaches to manage missing values exist. Although CBR already integrates a neutral approach in the similarity measure, the behaviour of the similarity measure when values are missing has still to be investigated.

6. Conclusion

CBR is an artificial intelligence approach that supports the user in decision making. The considered CBR has been designed for medical intervention, and more specifically, for the planning of TAVI procedures. Its goal is to help practitioners to take the most suitable decision about the vascular access and the prosthesis type.

In this work, we have shown that similarity measures specific to the problem being addressed improve the result over generic formulations. New similarity measures based on the CDT have been formulated and studied. We specially investigated the influence of the attribute selection, weighting scheme, and case selection for retrieving similar cases. We have shown that by taking into account the expert knowledge through the CDT, the CBR performance is increased. Promising results have been obtained with the hierarchical similarity measure *H_WHSM*.

This similarity measure could be enhanced. Commonly available clinical attributes were used in the studied similarity measures. Some relevant clinical attributes might be imprecise, such as tortuosity and calcification, or, even worse, missing. Thus, they might be differently evaluated by operators. High-level attributes computed from medical images or even statistical shape models could be used to make the attributes more sensitive and further improve the similarity measure.

7. Acknowledgements

This work was partially supported by the EU project EurValve Personalised Decision Support for Heart Valve Disease H2020 PHC-30-2015 689617, and by the French National Research Agency (ANR) in the framework of the Investissement d'Avenir Program through Labex CAMI (ANR-11- LABX-0004).

Conflict of interest

None declared.

Appendix A

The following attributes are used in the CBR. They were extracted from the data base of the University Hospital of Rennes. Some of them are used in the similarity measure. The others, which provide additional information to the physicians about the procedure outcomes, are displayed in the GUI.

Attribute Label	Code/Unit/Comment
1. Demographics	
- Gender	{Male, Female}
- Age	[Years]
- Height	[cm]
- Weight	[kg]
- BSA	[m^2]
- BMI	[kg/m^2]
2. Echocardiographic Measurements	
- LVEF	[%]
- Aortic valve dPmean	[mmHg]
- Aortic valve dPmax	[mmHg]
- Aortic valve regurgitation	{0,1,2,3,4}
3. CT Measurements	
- Diameter Ascending Aorta	[mm]
- Diameter Valve	[mm]
- Calcification of the Aorta	{No, Mild, Moderate, Heavy, Massive}
- Calcification of the Valve	{No, Mild, Moderate, Heavy, Massive}
- Extension of the calcifications in the LVOT	True, false
- End diastolic interventricular septum thickness	[mm]
- Minimal diameter of the right iliac artery	[mm]
- Minimal diameter of the left iliac artery	[mm]
- Calcification of the femoral arteries	{No, Mild, Moderate, Heavy, Massive}
- Tortuosity of the femoral arteries	{No, Mild, Moderate, Severe}
- Minimal diameter of the left subclavian artery	[mm]
- Calcification of the left subclavian artery	{No, Mild, Moderate, Heavy, Massive}
- Tortuosity of the left subclavian artery	{No, Mild, Moderate, Severe}
- Aortic valve area	[cm^2]
- Annulus diameter	[mm]
- Mid-sinus diameter	[mm]
- Sinotubular junction diameter	[mm]
- Left ventricule diameter at ED	[mm]
- Left ventricule diameter at ES	[mm]
4. Operative Data	
- Surgery	{TAVI}
- Access	{trans-apical, left trans-femoral, right trans-femoral, trans-aortic, left trans-subclavian}

-	Aortic valve size	[mm]
-	Model of aortic valve	Free text (CoreValve, Edwards, etc.)
-	Procedural Success	{true, false}
-	TAVI coronary occlusion	{true, false}
-	Cause of failure	Free text
-	Procedural death	{true, false}

References

[1] The Task Force for the Management of Valvular Heart Disease of the European Society of Cardiology (ESC) and the European Association for Cardio-Thoracic Surgery (EACTS). 2017 ESC/EACTS Guidelines for the management of valvular heart disease. Eur Heart J 2017.

[2] Nishimura RA, Otto CM, Bonow RO, Carabello BA, Erwin JP, Guyton RA, et al. 2014 AHA/ACC Guideline for the Management of Patients With Valvular Heart Disease. J Am Coll Cardiol 2014;63:e57–185. doi:10.1016/j.jacc.2014.02.536.

[3] Berner ES, editor. Clinical decision support systems: theory and practice. 2nd ed. New York, NY: Springer; 2007.

[4] Aamodt A, Plaza E. Case-Based Reasoning: Foundational Issues, Methodological Variations, and System Approaches. AI Commun 1994:39–59. doi:10.3233/AIC-1994-7104.

[5] Richter MM, Weber RO. Case-Based Reasoning. Berlin, Heidelberg: Springer Berlin Heidelberg; 2013. doi:10.1007/978-3-642-40167-1.

[6] Leake DB, Wilson DC. Remembering Why to Remember: Performance-Guided Case-Base Maintenance. In: Blanzieri E, Portinale L, editors. Adv. Case-Based Reason., vol. 1898, Berlin, Heidelberg: Springer Berlin Heidelberg; 2000, p. 161–72. doi:10.1007/3-540-44527-7_15.

[7] Wilson DC, Leake DB. Maintaining Case-Based Reasoners: Dimensions and Directions. Comput Intell 2001;17:196–213. doi:10.1111/0824-7935.00140.

[8] Choudhury N, Begum SA. A survey on case-based reasoning in medicine. Int J Adv Comput Sci Appl 2016;7:136–144.

[9] Begum S, Ahmed MU, Funk P, Xiong N, Folke M. Case-Based Reasoning Systems in the Health Sciences: A Survey of Recent Trends and Developments. IEEE Trans Syst Man Cybern Part C Appl Rev 2011;41:421–34. doi:10.1109/TSMCC.2010.2071862.

[10] Behbahani M, Saghaee A, Noorossana R. A case-based reasoning system development for statistical process control: Case representation and retrieval. Comput Ind Eng 2012;63:1107–17. doi:10.1016/j.cie.2012.07.007.

[11] Avramenko Y, Kraslawski A. Similarity concept for case-based design in process engineering. Comput Chem Eng 2006;30:548–57. doi:10.1016/j.compchemeng.2005.10.011.

[12] Perner P, editor. Case-based reasoning on images and signals. Berlin ; New York: Springer; 2008.

[13] Holt A, Bichindaritz I, Schmidt R, Perner P. Medical applications in case-based reasoning. Knowl Eng Rev 2005;20:289. doi:10.1017/S0269888906000622.

[14] Gu D, Liang C, Zhao H. A case-based reasoning system based on weighted heterogeneous value distance metric for breast cancer diagnosis. Artif Intell Med 2017. doi:10.1016/j.artmed.2017.02.003.

[15] Sharaf-El-Deen DA, Moawad IF, Khalifa ME. A New Hybrid Case-Based Reasoning Approach for Medical Diagnosis Systems. J Med Syst 2014;38. doi:10.1007/s10916-014-0009-1.

[16] Saraiva R, Perkusich M, Silva L, Almeida H, Siebra C, Perkusich A. Early diagnosis of gastrointestinal cancer by using case-based and rule-based reasoning. Expert Syst Appl 2016;61:192–202. doi:10.1016/j.eswa.2016.05.026.

[17] Begum S, Barua S, Filla R, Ahmed MU. Classification of physiological signals for wheel loader operators using Multi-scale Entropy analysis and case-based reasoning. Expert Syst Appl 2014;41:295–305. doi:10.1016/j.eswa.2013.05.068.
[18] Montani S, Leonardi G, Ghignone S, Lanfranco L. Flexible case-based retrieval for comparative genomics. Appl Intell 2013;39:144–52. doi:10.1007/s10489-012-0399-z.
[19] Miotto R, Weng C. Case-based reasoning using electronic health records efficiently identifies eligible patients for clinical trials. J Am Med Inform Assoc 2015;22:e141–50. doi:10.1093/jamia/ocu050.
[20] Doyle D, Cunningham P, Walsh P. AN EVALUATION OF THE USEFULNESS OF EXPLANATION IN A CASE-BASED REASONING SYSTEM FOR DECISION SUPPORT IN BRONCHIOLITIS TREATMENT. Comput Intell 2006;22:269–81. doi:10.1111/j.1467-8640.2006.00288.x.
[21] Petrovic S, Khussainova G, Jagannathan R. Knowledge-light adaptation approaches in case-based reasoning for radiotherapy treatment planning. Artif Intell Med 2016;68:17–28. doi:10.1016/j.artmed.2016.01.006.
[22] Brown D, Aldea A, Harrison R, Martin C, Bayley I. Temporal case-based reasoning for type 1 diabetes mellitus bolus insulin decision support. Artif Intell Med 2018;85:28–42. doi:10.1016/j.artmed.2017.09.007.
[23] Gu D, Liang C, Li X, Yang S, Zhang P. Intelligent Technique for Knowledge Reuse of Dental Medical Records Based on Case-Based Reasoning. J Med Syst 2010;34:213–22. doi:10.1007/s10916-008-9232-y.
[24] El-Sappagh S, Elmogy M, Riad AM. A fuzzy-ontology-oriented case-based reasoning framework for semantic diabetes diagnosis. Artif Intell Med 2015;65:179–208. doi:10.1016/j.artmed.2015.08.003.
[25] Huang M-J, Chen M-Y, Lee S-C. Integrating data mining with case-based reasoning for chronic diseases prognosis and diagnosis. Expert Syst Appl 2007;32:856–67. doi:10.1016/j.eswa.2006.01.038.
[26] Biswas SK, Chakraborty M, Singh HR, Devi D, Purkayastha B, Das AK. Hybrid case-based reasoning system by cost-sensitive neural network for classification. Soft Comput 2017;21:7579–96. doi:10.1007/s00500-016-2312-x.
[27] Shin K, Han I. A case-based approach using inductive indexing for corporate bond rating. Decis Support Syst 2001;32:41–52. doi:10.1016/S0167-9236(01)00099-9.
[28] Watson I, Marir F. Case-based reasoning: A review. Knowl Eng Rev 1994;9:327. doi:10.1017/S0269888900007098.
[29] Main J, Dillon TS, Shiu SCK. A Tutorial on Case Based Reasoning. In: Pal SK, Dillon TS, Yeung DS, editors. Soft Comput. Case Based Reason., London: Springer London; 2001, p. 1–28. doi:10.1007/978-1-4471-0687-6_1.
[30] Wilson DR, Martinez TR. Improved heterogeneous distance functions. J Artif Intell Res 1997;6:1–34.
[31] Lesot MJ, Rifqi M, Benhadda H. Similarity measures for binary and numerical data: a survey. Int J Knowl Eng Soft Data Paradig 2009;1:63. doi:10.1504/IJKESDP.2009.021985.
[32] Choi S-S, Cha S-H, Tappert CC. A survey of binary similarity and distance measures. J Syst Cybern Inform 2010;8:43–48.
[33] Liao TW, Zhang Z, Mount CR. Similarity measures for retrieval in case-based reasoning systems. Appl Artif Intell 1998;12:267–88. doi:10.1080/088395198117730.
[34] Núñez H, Sànchez-Marrè M, Cortés U, Comas J, Martínez M, Rodríguez-Roda I, et al. A comparative study on the use of similarity measures in case-based reasoning to improve the classification of environmental system situations. Environ Model Softw 2004;19:809–19. doi:10.1016/j.envsoft.2003.03.003.
[35] Stanfill C, Waltz D. Toward memory-based reasoning. Commun ACM 1986;29:1213–28. doi:10.1145/7902.7906.

[36] El-Fakdi A, Gamero F, Meléndez J, Auffret V, Haigron P. eXiTCDSS: A framework for a workflow-based CBR for interventional Clinical Decision Support Systems and its application to TAVI. Expert Syst Appl 2014;41:284–94. doi:10.1016/j.eswa.2013.05.067.

[37] Guessoum S, Laskri MT, Lieber J. RespiDiag: A Case-Based Reasoning System for the Diagnosis of Chronic Obstructive Pulmonary Disease. Expert Syst Appl 2014;41:267–73. doi:10.1016/j.eswa.2013.05.065.

[38] Di Nuovo AG. Missing data analysis with fuzzy C-Means: A study of its application in a psychological scenario. Expert Syst Appl 2011;38:6793–7. doi:10.1016/j.eswa.2010.12.067.

[39] Lin J-H, Haug PJ. Exploiting missing clinical data in Bayesian network modeling for predicting medical problems. J Biomed Inform 2008;41:1–14. doi:10.1016/j.jbi.2007.06.001.

[40] Grech A, Main J. A Case-Based Reasoning Approach to Formulating University Timetables Using Genetic Algorithms. In: Khosla R, Howlett RJ, Jain LC, editors. Knowl.-Based Intell. Inf. Eng. Syst., vol. 3681, Berlin, Heidelberg: Springer Berlin Heidelberg; 2005, p. 76–83. doi:10.1007/11552413_12.

[41] Cunningham P. A Taxonomy of Similarity Mechanisms for Case-Based Reasoning. IEEE Trans Knowl Data Eng 2009;21:1532–43. doi:10.1109/TKDE.2008.227.

[42] Authors/Task Force Members, Vahanian A, Alfieri O, Andreotti F, Antunes MJ, Baron-Esquivias G, et al. Guidelines on the management of valvular heart disease (version 2012): The Joint Task Force on the Management of Valvular Heart Disease of the European Society of Cardiology (ESC) and the European Association for Cardio-Thoracic Surgery (EACTS). Eur Heart J 2012;33:2451–96. doi:10.1093/eurheartj/ehs109.

[43] Otto CM, Kumbhani DJ, Alexander KP, Calhoon JH, Desai MY, Kaul S, et al. 2017 ACC Expert Consensus Decision Pathway for Transcatheter Aortic Valve Replacement in the Management of Adults With Aortic Stenosis. J Am Coll Cardiol 2017. doi:10.1016/j.jacc.2016.12.006.

[44] Cahill TJ, Chen M, Hayashida K, Latib A, Modine T, Piazza N, et al. Transcatheter aortic valve implantation: current status and future perspectives. Eur Heart J 2018. doi:10.1093/eurheartj/ehy244.

3.3 Synthèse et perspectives

Dans ce chapitre, nous nous sommes intéressés à l'apport d'un type particulier de systèmes d'aide à la décision clinique, le case-based reasoning, dans le contexte du TAVI. Comme évoqué précédemment, cet intérêt se justifie par la difficulté potentielle pour les cliniciens de disposer, au moment voulu, du maximum d'informations pertinentes à la planification et à la réalisation de la procédure.

Nous avons démontré la faisabilité d'un système de type CBR dans le contexte du TAVI ainsi que l'importance d'une définition optimale de la mesure de similarité utilisée pour optimiser les solutions suggérées par le CBR afin d'aider le praticien dans sa prise de décision. En effet, l'utilisation de mesures de similarité spécifiquement dédiées à la problématique clinique améliore significativement les performances du CBR comparativement à des mesures plus générales. Notre travail souligne l'importance de l'expérience clinique pour définir des arbres de décision reproduisant le raisonnement clinique, utilisables par le CBR, et pondérer correctement les différents attributs considérés. Ceci nous a permis de créer des mesures de similarités spécifiques de chaque problématique abordée en identifiant et pondérant les attributs adéquats. Les mesures de similarité de notre CBR pourraient encore être affinées par l'adjonction aux attributs disponibles actuellement en routine des attributs de plus haut niveau (*e.g*. descripteurs de forme, de calcifications), plus objectifs, spécifiques de zones anatomiques et issus d'une analyse plus fine de l'imagerie préopératoire par scanner.

Enfin, nous nous sommes limités dans nos travaux à étudier les aspects de choix de la prothèse et de la voie d'abord pour établir la faisabilité de notre méthode et étudier l'impact de la mesure de similarité. Néanmoins, on peut aisément imaginer que la méthodologie « CBR » puisse être transposée à d'autres problématiques plus complexes comme par exemple l'identification de patients à haut risque de complications ou de mauvais résultats de la procédure comme nous l'évoquions dans le chapitre précédent. Ainsi, des CBR destinés à ces aspects, et intégrant les nombreux facteurs prédictifs mis en évidence dans la littérature par les méthodes statistiques « traditionnelles », pourraient être des outils utiles à la prise de décision en pratique quotidienne.

Chapitre 4

Apport de la simulation numérique à l'aide à la décision

La simulation numérique s'est établie comme un outil pertinent dans de nombreux domaines industriels. Elle permet d'améliorer sensiblement les coûts, l'efficacité et les performances des systèmes. En outre, les améliorations de capacités de calcul et des techniques de modélisation permettent de s'attaquer à des problèmes toujours plus complexes. Il est ainsi cohérent d'envisager l'utilisation des simulations numériques dans le domaine médical.

La simulation numérique offre la possibilité de s'adapter à l'évolution rapide des dispositifs. Elle est actuellement principalement exploitée dans un but de conception de ces dispositifs. Elle permet également théoriquement de simuler différentes conditions opératoires et de représenter les gestes opératoires du clinicien. Ainsi, la simulation numérique personnalisée est une piste pour fournir au médecin une compréhension approfondie des phénomènes mécaniques afin de l'assister dans ses prises de décision. Néanmoins, dans ce but, elle doit être en mesure de considérer différentes anatomies, et de s'adapter à chaque patient ce qui pose des problèmes de paramétrage et de validation de son caractère prédictif.

Le domaine du TAVI semble à ce titre un champ d'investigation pour la simulation numérique puisque la planification de la procédure soulève de nombreuses questions à propos du choix de la prothèse, son déploiement, son positionnement avant et après largage, sa performance à long terme et des complications possibles. L'analyse de l'imagerie préopératoire est aujourd'hui la pierre angulaire de la planification du geste et fournit de nombreuses informations anatomiques essentielles à la procédure mais très peu de connaissances sur les nombreuses interactions matériel endovasculaire/tissus intervenant pendant le geste. Malgré l'expérience clinique qui s'est développée autour du TAVI, une analyse plus complète des mécanismes est nécessaire pour apporter de nouvelles réponses aux questions de planification. La simulation biomécanique semble être une piste particulièrement intéressante dans ce contexte pour anticiper les interactions des dispositifs endovasculaires et les conséquences de certaines décisions lors de l'intervention même s'il existe encore des obstacles scientifiques et techniques à franchir pour appliquer les méthodes de simulation numérique sur des problèmes cliniques.

Dans ce contexte, dans le cadre d'une collaboration entre le LTSI (Laboratoire Traitement du Signal et de l'Image – Université de Rennes 1, INSERM), le CIS (Centre

Ingénierie et Santé – Ecole des mines de Saint-Etienne, CNRS) et la société ANSYS, nous nous sommes intéressés à une approche de simulation numérique par méthode des éléments finis, pour prédire la configuration spatiale des outils utilisés lors de la procédure TAVI. Ces travaux de simulation ont également fait appel à des procédés de traitement d'image mis en œuvre par le LTSI et la société Therenva.

Dans ce dernier chapitre, nous présentons dans un premier temps une revue de l'état de l'art sur les méthodes de simulation numérique spécifique patient appliquées au TAVI. Dans un second temps, nous abordons les notions de traitement de l'image qui ont été nécessaires à la réalisation de ce travail et les illustrons par deux contributions originales portant sur la segmentation de l'imagerie 3D préopératoire et sur le recalage de cette imagerie 3D avec l'imagerie 2D peropératoire. Enfin, nous proposons une approche de simulation spécifique patient portant sur les déformations du guide rigide au cours d'une procédure TAVI et ses interactions avec le ventricule gauche.

4.1 Etat de l'art

4.1.1 Revue de la littérature

L'article de bibliographie suivant, publié dans « International Journal of Advances in Engineering Sciences and Applied Mathematics», expose les problématiques encadrant le TAVI et dresse l'état de l'art des études de simulation numérique qui contribuent à les résoudre.

Review of Patient-Specific Simulations of Transcatheter Aortic Valve Implantation

P. Vy[1,2,3,4*], V. Auffret[3,4,5], P. Badel[2], M. Rochette[1], H. Le Breton[3,4,5], P. Haigron[3,4], S. Avril[2]

[1] ANSYS France, Villeurbanne, F-69100, France
[2] Ecole Nationale Supérieure des Mines de Saint-Etienne, CIS-EMSE, CNRS:UMR5307, LGF, F-42023 Saint Etienne, France
[3] INSERM, U1099, Rennes, F-35000, France
[4]Université de Rennes 1, LTSI, F-35000 Rennes, France
[5]CHU Rennes, Service de Cardiologie et Maladies Vasculaires, Rennes, F-35000, France
[*] Author for correspondence. E-mail address: phuoc.vy@ansys.com

Keywords

Heart valve, aortic valve, finite element analysis, patient-specific, numerical simulation, transcatheter aortic valve implantation

Abstract

Transcatheter Aortic Valve Implantation (TAVI) accounts for one of the most promising new cardiovascular procedures. This minimally invasive technique is still at its early stage and is constantly developing thanks to imaging techniques, computer science, biomechanics and technologies of prosthesis and delivery tools. As a result, patient-specific simulation can find an exciting playground in TAVI. It canexpress its potential by providing the clinicians with powerful decision support, offering great assistance in their workflow. Through a review of the current scientific field, we try to identify the challenges and future evolutions of patient-specific simulation for TAVI. This review article is an attempt to summarize and coordinate data scattered across the literature about patient-specific biomechanical simulation for TAVI.

Introduction

Aortic Stenosis (AS) is a cardiovascular disease affecting the heart's aortic valve. *Surgical aortic valve replacement* (AVR or SAVR) is the current standard treatment. Unfortunately, it requires thoracotomy and cardiopulmonary bypass to reach and repair the damaged zone. These difficult procedures can be especially life-threatening for elderly patients and require a long recovery period. Fig.1 shows a picture of an on-going AVR.

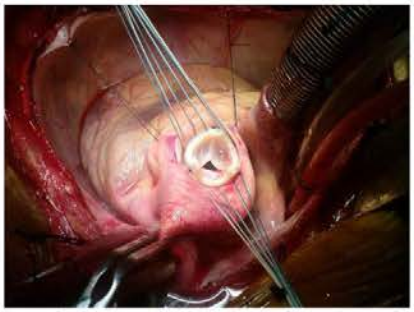

Fig.1 AVR, surgical implantation of a bioprosthetic valve, cf section 1 for more detail (reproduced with permission of Dr. Sukumar Mehta)

Transcatheter Aortic Valve Implantation (TAVI) has emerged as a promising solution for AS treatment. This novel technique consists in delivering a bioprosthesis into the heart, through the patient's arteries. This minimally invasive procedure significantly shortens recovery time and can successfully treat inoperable or very high-risk patients. Indeed, TAVI has proven to be superior to AVR in such populations [1][2][3]. However, TAVI is a recent procedure, with the earliest implantations dating back to 2002 [4], leading TAVI prostheses to continue struggling to outperform AVR prostheses in various aspects [5]. Indeed, this method of treatment has been limited to high-risk patients due to numerous concerns, such as complications that are particularly difficult to deal with [6][7] and limited follow-up data about prosthesis durability.

In order to predict the complications that may occur, a promising approach is taking into account the specific details of the anatomy and characteristics of arteries, as they can differ greatly from one individual to another. Therefore, patient-specific simulations are powerful tools in this context. There is little doubt that patient-specific simulation will help TAVI expand its recommended patient population. Still, TAVI is challenging to model and simulate accurately. Patient-specific simulation studies only started a few years ago[8]. As a result, comparative studies on large-scale data are lacking and there is no reliable and proven model. Instead, those studies are dedicated to developing increasingly accurate models. This review article will shed some light on these advances.

The first part of this review provides general information for readers who are unfamiliar with TAVI. It details the context of AS, the procedure of TAVI and the common complications that follow it. The second part will offer an overview of the evolution and new aspects in patient-specific simulation. The third part will look at the choices made in each study to model TAVI. The last part will expose how simulation results have been exploited so far.

1. Clinical context

This first section provides clarification about the general context of *Aortic Stenosis* (AS) and *Transcatheter Aortic Valve Implantation* (TAVI). It is mainly intended for readers unfamiliar with the cardiovascular field. As it expands the points in the introduction, readers may skip to the second section concerning patient-specific simulation.

1.1. Aortic Stenosis

General considerations

The heart pumps blood and guarantees the necessary blood irrigation across the human body. In other words, the heart provides mechanical energy to make the blood flow. Naturally, an obstacle in the blood vessels or failure of a component of the heart may dissipate this mechanical energy. The heart will be forced to compensate this energy loss to maintain adequate blood flow. This additional burden can exceed the heart's capacity and lead to heart failure. This is precisely the situation that happens in the case of AS.

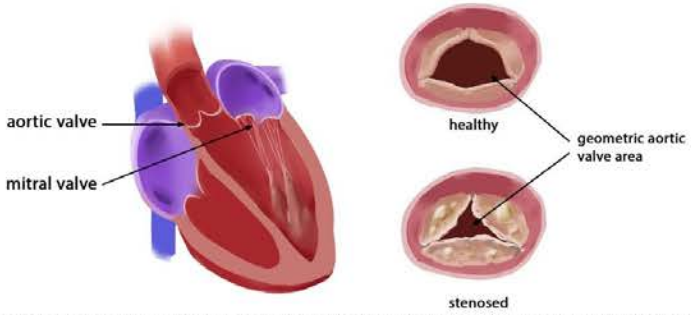

fig.2 Left, aortic valve anatomy; right,upper view of fully open healthy and calcified valve during systole

The heart includes four valves which are essential to its pumping function. In particular, the Aortic Valve separates the left ventricle from the aorta. Through three mobile leaflets, which open during the left ventricle contraction (systole) and close during the left ventricle relaxation (diastole), it maintains a unidirectional blood flow from the heart to the aorta. Then the aorta and further arteries lead to all the tissues that require blood: the heart itself, the brain, organs, muscles, etc.

AS is defined by a decreased effective area of the aortic valve and is considered severe when this area is below $1cm^2$ or $0.6cm^2/m^2$ [9]. It is the most common valvular disease with increasing incidence in aging population affecting almost 10% of octogenarians[10][11]. In a large majority of cases, this is because of heavy calcifications of its leaflets. Fig.2 shows how the calcified valve behaves in comparison to a normal valve during systole. In a way, AS is the apparition of an obstacle right at the start of the arterial system. From a fluid dynamic point of view, the flow cross-section (aortic valve area) of the blood is significantly reduced at the passage of the calcified aortic valve. The reduction of this area may cause a turbulent mixing phenomenon, which is depicted in Fig.3. It shows a side view of the aortic valve. The central jet velocity increases at the choke point as its pressure drops. Then, the central jet progressively loses velocity and recovers pressure. A portion of the central jet is redirected to the turbulent mixing zone, where part of the initial energy provided by the heart is dissipated into heat [12][13][14]. The turbulent mixing zone is at the interface of the central jet and the recirculation zone, where vorticities helps closing the valve at the end of systole. Lacking energy, the central jet may not recover enough pressure. From a clinical point of view, the patient would eventually suffer low cardiac output and low arterial pressure, as the remaining mechanical energy is insufficient to pump the blood to meet the body's needs. In practice, however, a compensation mechanism allows the heart to maintain adequate cardiac output through left ventricular hypertrophy before reaching heart failure.

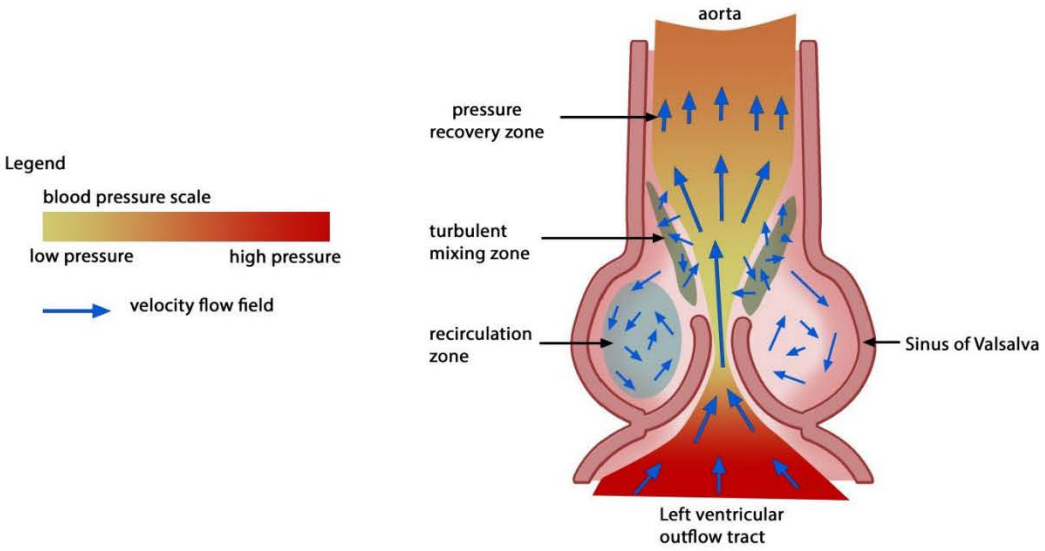

Fig.3 Side cut view of aortic valve. Dissipation of mechanical energy is mainly located in the turbulent mixing zone

Symptoms

AS has a slow onset as the heart can only tolerate reduction of the aortic valve area to some extent. Symptoms usually appear when AS is at a severe stage and quickly progresses thereafter [15]. Severe AS requires urgent treatment [16]. As previously stated, the heart eventually fails to provide the necessary mechanical energy to maintain an adequate cardiac output and end-diastolic left ventricular pressure rises. This situation is called congestive heart failure and can lead to a fatal outcome. The most common symptoms of severe AS are shortness of breath (dyspnea), chest pain and syncope typically during exercise but acute congestive heart failure (pulmonary edema) and even sudden cardiac death may also occur.

Causes

The main mechanism is the growth of calcifications on the leaflets known as degenerative AS which usually concerns the elderly. The calcifications stiffen the leaflets as they grow on it and hinder the opening and/or the closing of the valve. Another cause is the congenital defect known as bicuspid valve. The aortic valve possesses two leaflets instead of three, resulting in faster degeneration of the aortic valve. Indeed, bicuspid aortic valve alone is not sufficient to cause severe aortic stenosis by itself, but rather, accelerates the degeneration and calcification of the aortic valveleading to an earlier onset of aortic stenosis [17].

Standard treatment

Surgical Aortic Valve Replacement (AVR or SAVR) is established as the gold standard for the treatment of AS. The surgeon accesses the heart through thoracotomy and cardiopulmonary bypass. The native calcified leaflets are removed and a prosthesis is sewn into the aortic root, cf Fig.1. TAVI prosthesis are limited to bio-prosthesis (leaflets sewn into a stent c.f. Fig.5), because the percutaneous access through arteries requires crimping the prosthesis to fit in the vessels (c.f. section 1.2).On the other hand, AVR prosthesis can have different designs that do not require to be crimped, thanks to the direct access to the heart through thoracotomy. Therefore, it is possible to implant mechanical valve with high structural durability that can outlast bio-prosthesis. However, mechanical prosthesis necessitates lifelong anti-coagulant treatments to prevent thrombosis. Such prosthesis is the bi-leaflet valve given in the Fig. 4-C.

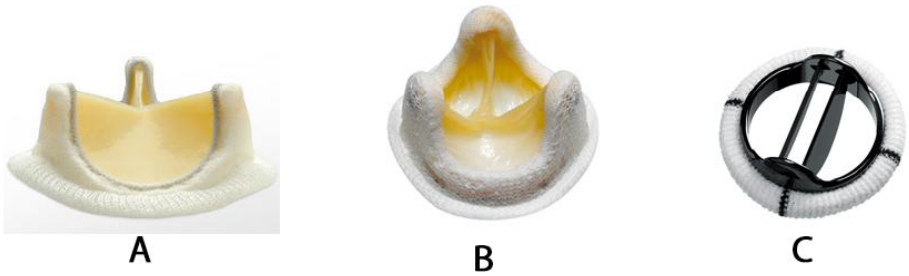

Fig.4 AVR prostheses; A –face view of bioprosthesis; B –upper view of bioprosthesis; C - bi leaflet-mechanical

The advantages of AVR are that the surgeon has total control over the tools, calcifications and position of implantation of the prosthesis. Additionally, this treatment is well documented and reliable as it has a long history of practice[20][21]. The burden on the patient's body and potential severe postoperative complications in elderly and often frail patients are the main weaknesses of this treatment. Thus, it is estimated that one third of patients cannot undergo this treatment because of high-risk comorbidities [10].

Socio-economic impact

The growth of calcifications is a relatively slow process and requires years to become life-threatening. Except for patients with bicuspid valves, it is usually elderly patients over 70 years of age who are concerned by AS. This is precisely the reason why AVR is not sufficient to face this disease. Elderly patients may suffer comorbidities and thus be exposed to high risks during open-heart surgeries. They would then require lengthy recovery times and follow-ups, inducing further costs for the hospital facilities. The cost of AVR intervention is around $26,900 [22], however, the total cost of the treatment includes the hospitalization following the surgery. Therefore, the cost increases significantly for high-risk patients: from $106,277 (for non-high risk) to $144,183 over the course of 5 years, according to M. Clark *et al.*[23].

The increase of life expectancy also increases the prevalence of this disease in the general population [24][25]. As the proportion of elderly population steadily increases, the number of patients is expected to increase to 1.4 million patients in North America by 2050[26]. Indeed, the authors applied the estimated prevalence of AS in elder patient population and applied it to prediction of the population evolution. Thus, it is crucial to find new solutions to treat the oncoming increase of patients more efficiently.It is estimated that 67,500 AVR were performed in 2010 in the United States [23]. A statistical study estimated that the number of severe symptomatic AS amounted to 540,000 in North America in 2013[26].

1.2. What exactly is TAVI?

A recent alternative to the AVR is the minimally invasive TAVI, *Transcatheter Aortic Valve Implantation*, sometimes called PAVR, *Percutaneous Aortic Valve Replacement*. Rather than removing the calcified valve, the goal of TAVI is to deposit a prosthesis (TAV) over the diseased leaflets. ~~Examples of TAV are displayed in Fig.4~~. In order to deliver it onto the impaired valve, the prosthesis is moved through the artery. The prosthesis is crimped in a catheter to fit into the artery, hence the term Transcatheter. Thus, the procedure rests upon complex high-technology prosthesis which can change size. The two most popular models are displayed in Fig.5. Thorough review of new-generation prosthesis can be found in [27].

Fig.5 TAV prostheses: left is SAPIEN (Edwards Lifesciences™); right is CoreValve (Medtronic™)

TAVI can be used to treat inoperable patients, i.e. patients with chest malformation, repeated open-chest surgeries or serious underlying illness. For now, rather than directly competing with each other, both procedures are complementary, with their own strengths and weaknesses. To date, TAV durability is not well documented with only a few reports with a follow-up to 5 years post procedure. The PARTNER trial[2]showed that TAVI was superior to classic medical treatment and non-inferior to AVR for its 1-year all-cause mortality primary endpoint and the more recent CoreValve US PIVOTAL trial that enrolled patients at slightly lower risk, although still considered high risk, even demonstrated the superiority of TAVI over AVR for the same endpoint[1]. Currently, TAVI is only recommended for inoperable or high-risk patients, as assessed by a "Heart Team" including interventional and non-interventional cardiologists, cardiac surgeons, anesthesiologists, geriatricians, etc. Nonetheless, TAVI offers room for improvement. Better reliability of TAVI would broaden the eligible population, lessen the burden on patients and potentially result in a lower financial cost in the long run. In order to observe the full scope of the hurdles encountered by TAVI, the following parts will describe the procedure. This will help with understanding the complications that can arise from TAVI.

Setting up the guidewire

The procedure involves steering tools through sinuous arteries to the valve location. Once a stiff guidewire is set up into the left ventricle, the tools are easily brought on a catheter gliding over the guidewire. The guidewires are preferably inserted through the femoral artery but TAVI may be performed by sub-clavian, carotid, direct aortic and transapical approach, as seen on Fig.6. There is a recent increase of prosthesis models, some of them are specialized for a specific type of approaches, such as Engager (Medtronic™)which is specifically designed for transapical approach[27].

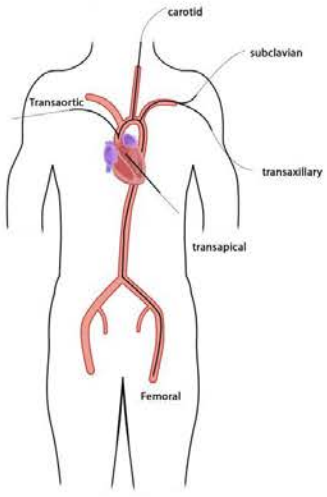

Fig.6 Map of vascular access for TAVI

Predilatation

Once the stiff guidewire is inserted into the left ventricle, it is possible to deploy the prosthesis. However in some cases, the calcified aortic valve does not allow the prosthesis passage. In order to force the valve opening, a predilatation is usually performed. This step is called *aortic valvuloplasty* or *balloon valvuloplasty*. A balloon is brought to the calcified valve and expanded as shown in Fig.7.

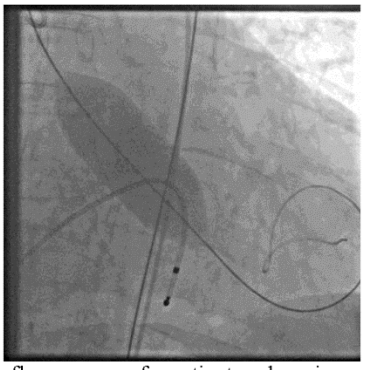

Fig.7 X-ray fluoroscopy of a patient undergoing predilatation

The pressure at the heart output is so high that deploying a balloon without precaution may tear the heart valve and damage the aorta. Hence, it is necessary to suspend the blood flow with "Burst stimulation". The heart is stimulated at a very high rate by a temporary pacemaker introduced in the right ventricle through the femoral vein. The heart twitches uncoordinatedly without pumping blood, allowing balloon deployment.

Prosthesis Deployment

The two most popular TAVI prostheses worldwide are SAPIEN (Edwards Sapien, Edwards Lifesciences, Irvine, CA, USA) and CoreValve (CoreValve, Medtronic, Minneapolis, MN, USA). These devices are displayed in Fig.5. Those two prostheses have different deployment mechanisms. SAPIEN is *balloon expandable*, meaning a balloon deployment is necessary to implant it. Another burst stimulation is required during this step. The deployment is fast but the position cannot be corrected once it begins. CoreValve is *self-expandable*, it adopts its final shape as it is released from the sheath. The medical team releases CoreValve progressively (10%, 25%, 50%, etc.) and continuously adjusts its position during the deployment which may still be challenging because of difficulties to predict the final position of the prosthesis once deployed.

Whichever prosthesis is chosen, it is brought to the middle of the native valve along the guidewire. When the medical team is ready, the prosthesis is unsheathed and carefully deployed. While this procedure sounds promising, some challenges remain. Its performance is still uncertaincompared to AVR for non-high risk patient, while its current operation cost is far higher[22]. Complications following TAVI exist and increase the mortality rate. It is critical for the development of TAVI that the cost of the devices decreases and that its complications are addressed.

1.3. TAVI Challenges

Thanks to the efforts of Cribier *et al.*[4],the first TAVI was executed in 2002. However, 13 years of evolution in procedures, prosthesis, and delivering tools are too limited to completely erase complications. This part lists the main complications encountered in the TAVI procedure reported[7].

Positional shift

AVR allows total control of the tools, the implantation site and the anchoring of the prosthesis by the surgeon. In the opposite case, tools in TAVI are remotely inserted in a way that offers little control for the operator. Concretely, the AVR surgeon can precisely cut the aorta to position the prosthesis, while TAVI only allows for

the length of insertion for the prosthesis deployment. As a result, the prosthesis can shift during its implantation. An experimental study showed the SAPIEN shift longitudinally during deployment[28]. Although minor for most cases, a significant shift can unexpectedly occur and lead to complications [29]. It must be noted that different models of stent induce different shifts. It was observed that SAPIEN 3 and the former version SAPIEN XT do not behave the same way[30].

Moreover, the angle of deployment and the shift between the center of the aortic valve and the prosthesis prior to implantation are difficult to control. Fig.8 shows a TAV in a slanted starting configuration for deployment. It may be difficult for inexperienced teams to accurately predict the outcome of deployment. Hence, one of the major issues of TAVI is the positioning reliability of the prosthesis inside the native valve. Because of an unreliable control of the implantation, this can lead to a variety of different complications.

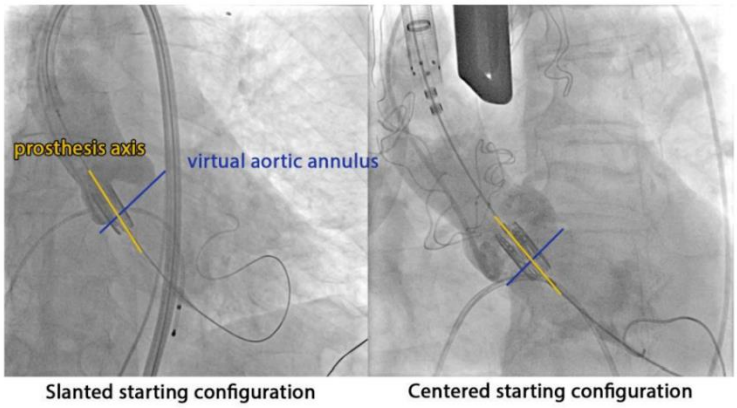

Fig.8 Misaligned starting position of TAV for the deployment in two different patients receiving a SAPIEN™

Coronary occlusion & Migration

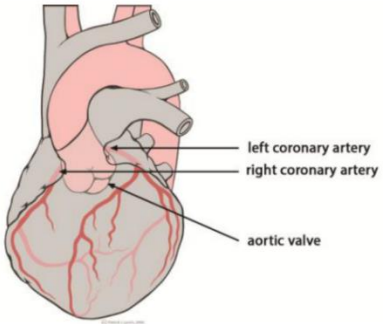

Fig.9 Heart with highlighted aorta and coronary arteries (illustration from Patrick J. Lynch)

Coronary arteries supply the heart with blood. They begin in the aorta, few millimeters,around 12 mm on average, above the valve as seen in Fig.9[31]. A misplaced prosthesis may block the coronary, which will lead to myocardial infarction. *Coronary occlusion* also occurs when the calcified native leaflet shifts towards the coronary artery [32] or when a calcification migrates into the coronary [33]. Migration of TAV can also happen due to misplacement, either into the aorta if the prosthesis is deployed too high, or into the left ventricle when excessively low [29].

Mitral valve injury

The mitral valve is right beside the aortic valve, c.f. Fig.2. It has two leaflets which are linked to papillary muscles on the heart wall. The "super stiff" guidewire placed in the ventricle may injure the mitral valve or its muscles. Low prosthesis may also hinder the mitral valve, and cause serious degradation to it [7].

Atrioventricular block

A nerve network is spread through the heart, allowing polarization of the heart muscle and triggering the heart contraction. If the prosthesis is too low, it may lead to *atrioventricular block*, which is a disturbance of the nerve network, and induce conduction abnormalities. In this case, the patient needs a permanent pacemaker. This complication happens more often in TAVI than in AVR and three time more often in CoreValve than in SAPIEN prosthesis[34]. This is an additional cost because this complication can appear up to 6 days after the intervention, prolonging the duration of hospitalization for monitoring.

Prosthesis mismatch

AS is a decrease of the opening valve area. The goal of TAVI is to restore the valve area. However, a small enlargement of the opening area may not bring significant benefit to the patient. Sometimes, the overall impact of the TAVI can be negative instead of alleviating the patient's situation. Those situations are referred as *prosthesis mismatch*. It is a significant problem when implanting a new prosthesis inside an already existing one (valve-in-valve maneuver) or a bicuspid valve [35]. The prosthesis functional area will be smaller than the maximum aortic valve area of the anatomy. Also, the prosthesis may not be fully deployed inside bicuspid valves. Otherwise, mismatch still remains a rare occurrence compared to classic surgery[36][37]. *Prosthesis mismatch* can also occur when the chosen prosthesis is undersized. However, an oversized prosthesis may result in other problems, e.g. aortic injury. Hence, the expertise of the medical team is crucial to determine the best compromise limiting the risk of complications.

Aortic injury

The aortic root containing the valve may rupture following the implantation of the prosthesis. This complication is particularly difficult to study because of its low frequency (~1%) and many types of rupture can arise [38]. Aggressive oversizing of the prosthesis was said to be related to this [6]. However, Hayashida *et al.*[39] suggested that the calcification layout on the aortic root is a strong reason for the aortic rupture[39]. Indeed, dislodged calcification may push vulnerable area of the aortic root.

Leaks

Paravalvular leaks remain a big hurdle in TAVI. They are less likely to occur during AVR. Leaks cause regurgitation which burdens the heart and may be correlated with long term prognosis and late mortality [40]. In engineering concepts, leaks contribute to significant energy loss in diastole [5][35]. Much like the previous complications, paravalvular leaks may be related to an inadequate sizing of the prosthesis, as oversized prostheses are said to reduce leaks [7]. The stent must adapt to the shape of the aorta wall. This depends significantly on the calcification scattered on the native valve. As the leaflets are designed to open and close correctly when totally circular, the stent must also be as round as possible to prevent a central leak [41].

There are different types of leaks, which are represented in Fig.10[42]. *Transvalvular leaks* come from an insufficient coaptation of the prosthesis leaflets. In other words, the leaflets do not seal the valve because gaps appear between the leaflets. It may happen when the deployed stent is not circular enough [43]. *Paravalvular leaks* appear from the gaps between the stent and the aortic wall. Lastly, *supra-skirtal leaks* occur in a similar way as paravalvular leaks. A skirt is sewn on the stent frame of the prosthesis to seal the gap between the leaflets and the stent. However, if the prosthesis is placed too low, the skirt does not fulfill its function.

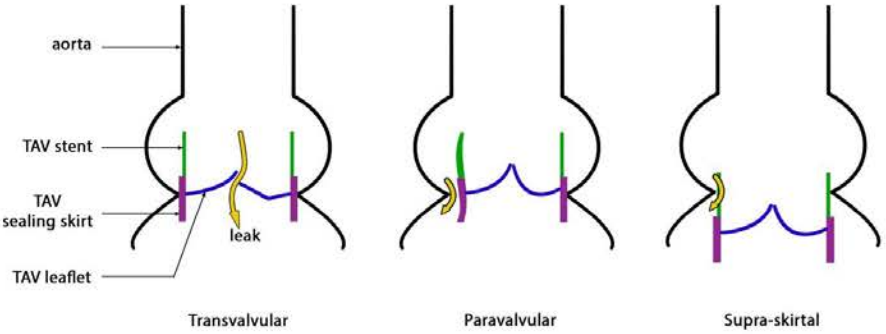

Fig.10 Side section of a leaking TAV; left, transvalvular leak; middle, paravalvular leak; right, supra-skirtal leak [42]

Calcification migration

Embolic stroke is one of the main concerns of TAVI. During the insertion of delivery tools, the thick catheters may dislodge calcification from the aorta. Besides this, during the balloon dilatation or prosthesis deployment, the native valves are crushed and will release calcific debris which may migrate to the brain [44]. Hopefully, new devices such as embolic filters may reduce these complications [45]. Claret Medical's device, Sentinel, has received approval for the American market. Studies to evaluate its performance are still ongoing.

Financial challenge

TAVI has quickly been adopted across 40 countries. It is estimated that over 50,000 TAVI procedures had been performed since 2002 [46]. However, the current market of TAVI prosthesis is extremely limited. The few available models are costly. Currently, the performance of TAVI does not justify the healthcare expenditure for non-high risk patients [22]. Lowering the cost and improving the performance of TAVI are necessary steps to broaden its use.

Current medical research is focused on preventing those complications. Patient-specific simulation is a very relevant path to explore in order to predict the complications. The next part reviews the TAVI finite-element models that have been created so far and how they can help clinical workflow.

2. State of the art

2.1. Beneficial impact of patient-specific simulations

TAVI has yet to overcome the problems described in the previous section. It has a strong potential because it can treat a broader population than AVR can. Also, the minimally-invasive procedure itself leaves the patient in a better condition than patients recovering from thoracotomy. However, TAVI cannot guarantee total relief of aortic valve dysfunction. In such cases, the degradation of the patient's condition does not stop and leads to further hospitalization. We can distinguish two ways to overcome complications. One way would be the improvement of the TAVI procedure itself. This can be achieved through various ways such as the development of prostheses, delivery tools, tracking tools, and imaging devices.

Some anatomies are more prone to complications than others. Therefore, another aspect to improve on is the planning and patient selection criteria in order to reject those with high risk anatomies. Accurate selection will help to make the best out of TAVI by treating patients who require minimally invasive intervention while avoiding high risk patients. Thanks to the continuous medical research in TAVI, the sources of complications are better understood. *In vitro*, *in vivo* and numerical simulation clarified many phenomena [47]. In practice, those problems are very difficult to avoid, as their mechanisms cannot be fully handled with current decision support tools. Some patients who seem perfectly fine to receive TAVI turn out to be problematic cases, e.g. aortic rupture [39]. In other words, despite a better understanding of the phenomena, complications still remain highly complex problems. Thus, the knowledge of complications cannot be easily generalized. It is of utmost

importance to study case-by-case complication risk. The medical team handling the surgery needs strong expertise of TAVI to ensure success. Large differences were reported between inexperienced, beginning medical teams in comparison to experienced ones [48]. Moreover, different models of prostheses behave differently. Medical teams experienced with one TAV model may not easily use another one. For all those reasons, medical teams can benefit from quantitative tools to aid the surgical planning, assessing and comparing AVR and TAVI postoperative performance.

Different approaches are available to predict risk. The statistical risk assessment can prove to be a helpful decisional tool as it can provide risk scores to predict failure of intervention. Statistical risk models are developed using post-data results of previous intervention. For instance, Euroscore is aninternationally used risk model to evaluate the risk of death after heart surgery, and uses a manageable amount of parameters such as age, gender, comorbidities, etc. Risk scores can also be applied to TAVI [49]. In the end, risk scores provide limited information about the type of complication and how it may be solved. Though risk scores are an asset to spread the use of TAVI, it does not invite development in complication management. Moreover, statistical models are restricted in the amount of input parameters, and as previously said, complications are difficult to generalize. Another drawback is the evolution of tools and prosthesis type. It is safe to assume that the quality of prosthesis models may impact the risk. Then, new models cannot benefit from statistical risk assessment since post-op data would be non-existent.

On the other hand, numerical simulations take into account intricate input data and can offer a better grasp of complications. Thus, this method can provide finer risk assessment than statistical risk models and better insight on the complication mechanisms.

2.2. Chronology of TAVI simulation

Papers concerning TAVI and aortic valve simulation were primarily retrieved from PubMed and Google Scholar, using the keywords: Transcatheter Aortic Valve Implantation simulation, Finite Element Aortic Valve, Fluid-structure Aortic Valve. Additionally, backward and forward snowballing was performed to extend the bibliography. Some of the following studies are not patient-specific. However, those models of simulation may be adapted to patient-specific geometries to design a patient-specific planning procedure. Papers closely concerning TAVI are reported in tab.1.

We can observe an increase of numerical simulation studies concerning TAVI during the last decade. We found that the first simulation study concerning TAVI prosthesis was made by Dwyer *et al.* (2009) to characterize the blood ejection force that can migrate the prosthesis[50]. However, the first study using patient specific data for TAVI was proposed by Sirois *et al.* (2011)[8]. Though numerical study of TAVI is recent, the use of simulation had already been developed in numerous applications. For instance, studies about kinematics of native aortic valve greatly helped TAVI studies. Some of the relevant studies remotely concerning TAVI are reported in tab.2.

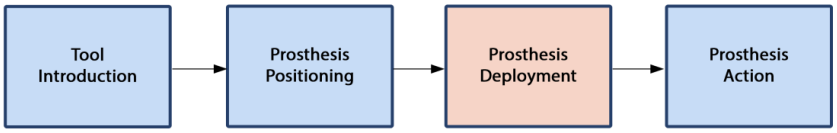

Fig.11 Different stage of TAVI procedure

TAVI simulation studies usually concern only one step of the procedure. Fig.11 summarizes the main steps of TAVI. As the previous table reports it, most of the papers focus on the prosthesis deployment step. This is a critical step because it predicts the final prosthesis configuration. Indeed, most complications are dependent on how and where the prosthesis is anchored in the aortic root. A realistic deployment simulation should take into account input data such as prosthesis configuration prior to deployment. Anticipation of the prosthesis behavior during this critical step is greatly beneficial for medical teams. Currently, they have to choose the starting position of the deployment without any certitude regarding how the prosthesis will behave during implantation. However, no simulation study has been done yet on the insertion of tools and prosthesis starting configurations.

Even though simulations are not advanced enough to predict where the prosthesis will land depending on the starting position yet, they can provide invaluable insight on possible outcomes and optimal prosthesis sizing. Additionally, final prosthesis configuration is a preliminary input for the following step, which consists in simulating the prosthesis function in the patient anatomy. The goal of the next step is the hemodynamic

assessment for the performance of the valve. This can help choosing the best procedure between TAVI and AVR. It would also be possible to find the optimal final position of the prosthesis. Indeed, Groves *et al.* [62]showed that the position of the prosthesis impacts the quality of hemodynamics such as blood velocity and coronary perfusion[62].

The deployment of balloon-expandable TAV is mainly a structural problem, where blood flow can be neglected thanks to burst stimulation and the speed of the deployment. As a result, published studies largely exploit Finite Element Method (FE) in order to simulate the prosthesis' expansion. On the other hand, neglecting blood flow is a less obvious choice for self-expanding TAV, as its deployment is slow and the TAV is liable to slightly migrate with blood pressure. In this case, methods encompassing blood flowmay be considered. For instance, CFD simulation (Computational Fluid Dynamic) can simulate the blood flow. It seems that there is a strong interaction between the blood and valve as it pushes the leaflets. Therefore, a strong coupling is needed between the fluid aspect and structural aspect. A relevant approach is FSI simulation (Fluid-Structure Interaction).Moreover, the complex mechanical behavior of a self-expanding stent is an additional challenge for researchers. Very few studies concern self-expanding TAV for now, but more is expected to come. Indeed, a large proportion of new prosthesis models are using self-expandable technology : CENTERA, Acurate, Jena Valve, Portico, UCL TAV, Foldavalve, etc [63][27].

When prosthesis deployment is successfully simulated, studies attempt to extract useful criteria in order to estimate the prosthesis performance. Simple criteria can be assumed from the deployment data, e.g. stresses, strains and shape of the stent and leaflets. However, they remain too limited to reliably predict performance. As a result, some papers tackle the next step, following the deployment step. Sirois *et al.* [8]were the first to suggest a CFD simulation after FE deployment to characterize the blood flow. Auricchio *et al.*[57] performed another step to close the valve through FE simulation[57]. In both studies, the movement of the leaflet was obtained through FE simulation and originated from uniform pressure upon the leaflets, instead of the action of the blood. This type of model is called "dry" model as it replaces fluid by prescribed pressure.

However, FE simulations may fail to reproduce the complete in vivo behavior and thus provide inaccurate data. A more exhaustive type of simulation would be Fluid-Structure Interaction (FSI) as it couples fluid mechanics to structural analysis. FSI techniques are still maturing in order to study healthy native aortic valve behavior, but numerous results and hypothesis can be applied again to TAVI simulations since those healthy valve models are very advanced. Results from those studies that can be applied to TAVI are reported in tab.2.

FSI has not been fully implemented in the context of TAVI yet. One exception is the study by Kemp *et al.* [56], which studies a custom-designed TAV prosthesis. Even though careful consideration of the fluid through CFD or FSI is a reasonable idea, current models might be insufficient to provide reliable data, as Sotiropoulos *et al.* and Stewart *et al.* pointed out[64][65]. As FSI progresses, we can expect FSI studies of TAVI performance to appear. Still, it is not clear whether the FSI gain in accuracy for hemodynamic assessment can justify the computational cost, but FSI is used more and morein applications such as mechanical aortic valve prosthesis [66].

3. Method of simulation

In this section, various aspects needed to define simulations are reviewed. Main points of those different aspects have their dedicated part: meshing the valve, mechanical properties of the tissues and boundary condition. For readers seeking complementary points of view on heart valve simulation, reviews from W. Sun *et al.*, G. Marom *et al.*, Votta *et al.*, Tseng *et al.* can be particularly useful[89][90][66][47].

3.1. Geometry

Imaging challenges

Simulation studies have shown that geometry can significantly impact the results. In particular, it was found that asymmetry in geometrical configuration of the leaflet impacts the leaflet stress, and consequently, the valve durability [68]. It has been shown in numerous studies that the sinus of Valsalva also influences stress distribution for both the aortic wall and leaflets [69][77][79]. In addition, the aortic wall deformation significantly participates in the valve opening [70][71]. All this evidence concurs on the importance of accurate

geometry representation of both the aortic wall and leaflets. However, accurate imaging of the leaflet and aortic wall is challenging because of its motion throughout the cardiac cycle. Therefore, imaging techniques and image processing knowledge play a large role in the extraction of patient-specific anatomy. Indeed, image processing is required to extract relevant elements from patient anatomy. For instance, the pulmonary artery usually overlaps with the aorta. This can disturb the extracted valve geometry.

Several imaging techniques are available in clinical practice, such as echocardiography or magnetic resonance imaging (MRI). Currently, the main technique being used to obtain 3D geometry for TAVI simulation is the multi-slice computed tomography (MSCT or CT). On the other hand, FSI simulation usually prefers MRI, as it may also provide fluid data (4D MRI flow imaging). Even though echocardiography is widely used clinically to assess valvulopathy, 3D echocardiography has poor spatial resolution and is not sufficient for geometrical reconstruction alone.

Before a TAVI, patients usually undergo a CT scan for the planning of procedure. Because classic CT scans are not instantaneous, they fail to grasp the quick movement of the leaflets. However, "Gated CT scans" are synchronized with the ECG (electrical heart activity). Those scans allow accurate representation of the leaflets at a specific phase of the cardiac cycle, provided the patient ECG is regular. Those synchronized scans allow finer 3D reconstruction of the anatomical architecture of the patient. However, the drawback of CT scans is the radiation exposure and nephrotoxic contrast media injection in the patient.

Aortic wall & native leaflet reconstruction

Numerical simulations of TAVI opted for CT scans, but there is no agreement on the extraction method. We report numerous different software: VTK, Mimics (Materialise, Leuven, Belgium), Avizo (VSG, Burlington, MA), ITKsnap etc. Tab.3 reports in the second column the image processing software used in various studies. It is difficult to automatically extract the fine details of anatomy, such as leaflets, even though synchronized CT scans offer good quality. Therefore, most studies manually traced those parts, or used geometric reconstruction from landmarks. Capelli *et al.* [51] and Wang *et al.* [58] extracted the native leaflets directly from CT. However, Capelli *et al.*[51]mentioned the difficulties and the efforts required to extract them. Indeed, Osirix and Avizo are both general segmentation software, but require expertise from the operator. This is why imaging processing techniques are crucial to introduce patient-specific simulation in the clinical field as an easy-to-use planning tool.

Studies used various phases of the cardiac cycle, usually either at peak systole or peak diastole, when the motion of the leaflet is minimal. Capelli *et al.* [51] and Wang *et al.* [52]reconstructed the leaflet in its systole phase[52]. Wang *et al.* [58]used diastole instead. It is worth noting that Morganti *et al.* [59]reconstructed the native healthy leaflet from manual landmarks, and projected calcifications upon it. Indeed, at the start of the simulated deployment, the native leaflets were completely open. However, it was open well beyond the case of a severe aortic stenosis. The starting configuration should be stress-free, meaning that the effort to push the calcified leaflets open may have been underestimated.

After extraction of the geometry, it is necessary to produce a proper mesh for calculation. Other software is usually needed. This step can either be made on dedicated meshers like ICEM CFD (Ansys, Inc., Canonsburg, PA, USA) and HyperMesh (Altair Engineering, Inc., MI) or on solver preprocessors such as Abaqus (Simulia, Dassault Systems, Providence, RI, USA). Aortic wall and calcification are often meshed with tetrahedral elements while leaflets are usually meshed with quadrilateral shell elements with reduced integration.

Zero-pressure issue

In simulations, the initial input geometry of the model should often be in a stress-free state. However, it is important to keep in mind that the scanned anatomy is physiologically loaded, as the artery bears the systemic arterial pressure and other loads. Therefore, the scanned geometry of the patient taken as such in the simulation would be inaccurate, because this geometry is actually the result of loadings while the simulation model should consider it as unloaded. Some studies transformed scanned geometry to find the state of the valve without blood pressure. This state is often referred as the "no-load" state or "zero-pressure" state. This state can be achieved by excising the aortic valve out from the subject.

Some FE studies suggested exploiting the zero-pressure state[52][81][82]. Wang*et al.*[52]proposed a straightforward method to determine the zero-pressure state. Experimentation has been made to determine the

relationship between the aorta diameter and blood pressure. Labrosse *et al.* [82] used a mathematical model for the geometry of the aortic valve and dimensions of the unpressurized aortic valve provided by prior experimental studies [91]. Conti *et al.* [81]used a mathematical model as well. However, the dimensions of the model were identified from their MRI data. The mesh from MRI data underwent an iterative algorithm to identify the zero-pressure dimensions.

However, arteries and valves may also be subject to complex internal stress. It was found that radially cutting arteries will make them spring open[92]. Such configuration is referred as the "no-stress" state. W. Huang showed that the inner wall of arteries is in compression and that the outer wall is in tension[93]. Zhao *et al.* showed how the no-stress state impacted simulations data[94]. X. Huang *et al.* suggested a method to compute the no-stress state, proving the feasibility of computing no-stress configurations[95]. However, simulation studies concerning TAVI have not exploited no-stress configuration yet.

Calcifications

Another geometrical detail that is difficult to grasp, yet which has crucial importance, is the calcification. Synchronized CT-scan may provide a precise layout of the calcifications. There are different possibilities to represent them in the mesh. Capelli, Morganti and Wang modeled calcifications as "zones" projected onto the leaflet, c.f. Fig.12 (left)[51][59][52]. The reconstructed native leaflet geometry is overlapped with CT-scan containing calcification data as described in [59]. It is assumed that the calcifications intersect the valve geometry and give the positions of calcific shell elements.These calcified zones were thicker compared to a healthy leaflet, as if calcification grew from both sides of the leaflet. In other words, a calcified zone encompassed both the normal leaflet layer and its calcifications. Calcifications on the aortic wall were ignored in the study[51], however they might be relevant as the aortic wall has been shown to participate to valve opening [70]. Although Wang *et al.*used such equivalent zones (leaflet+calcification) in their first study [52], theyconsidered the calcifications as separate from leaflet in their next study [58].Indeed,they hypothesized that calcification did not have fixed thickness and grew on one side of the leaflet, c.f. fig.12 (right). Also, Wang*et al.* projected calcifications on the aorta. Similar method was also previously applied by Russ *et al*, where segmented calcification elements were tied to the closest element by constraint [54].

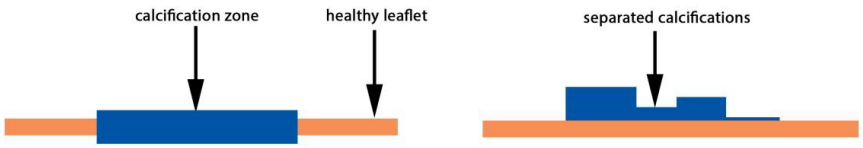

Fig.12 Calcification models; left is used in most studies; right is used by Russ *et al.* and Wang *et al.* [54][58]

The level of description of calcified aortic valve undoubtedly requires further study. Another question about anatomy is how much of the surrounding tissues should be modeled. Indeed, the aortic valve is connected to the ventricle below, and connected to the aortic artery above. Wang *et al.* [52]suggested including a part of the myocardium into the simulation. However, no subsequent studies followed this recommendation.

TAVI tools

Depending on the simulated step (tool insertion, deployment or post-deployment) and the hypotheses, different tools should be modeled. Most studies focus only on the deployment stage, which does not require the prosthesis leaflets. All papers reported about TAVI reconstructed at least the prosthesis stent. As it was stated previously, and also reported in Tab.3, most studies focused on the Edwards SAPIEN (Edwards Lifesciences, Irvine, California). As of today, the SAPIEN is the only available balloon-expandable prosthesis.

So far, CoreValve (Medtronic Inc., Minneapolis, Minnesota) stents are included in few studies [53][54][61]. These studies proposed an accurate mathematical model for the geometry. It has been reused by Tzamtzis *et al.*[55]. Lastly, a generic self-expandable stent has been designed by Gunning *et al.*[60]. This new model was motivated by the fact that many new commercial devices use this mechanism.

In both TAV prostheses, leaflets were sometimes modeled. The usual approach is defining the leaflet through a mathematical model, and morphing it to adapt to the stent [57].

In the case of a balloon-expandable stent, the balloon should be modeled as well. In most cases, it is modeled as a simple rigid cylinder whose nodes are constrained to expand. There are some exceptions, however, as Auricchio *et al.* and Wang *et al.* modeled the balloon with a realistic geometry[57][58].

Summary

While zero-pressure and no-stress states might be important in Abdominal Aortic Aneurysm for accurate prediction of aortic rupture [96], no study has proven its importance in the context of TAVI yet. Grande-Allen (2000) suggested the hypothesis that the residual stress was negligible in comparison with the valve and root stresses, and so far no study has challenged it[69]. Another notable point of the geometry section is the lack of an automated method to extract patient-specific geometry. Leaflet and valve extraction is an image processing technique and an image processing question that has no definite answer yet. Because of the small size and the transient nature of those details, they are difficult to extract from scans. Efforts are currently made to automatize the extraction of patient-specific geometries[97]. Some studies explore the use of parametric models whose dimensions are fitted with image recordings. For instance, Haj-Ali *et al.* &Rankin *et al.* suggested various parametric models[98][99]. Zheng *et al.* & Pouch *et al.* elaborated methods to extract leaflets[100][101]. In the study from Mansi *et al.*[102], an automated method can accurately extract the mitral valve.The spread of these fully automated tools is a necessary step: Not only would it make patient-specific simulations easy-to-use for medical teams, but it could also help exploit large patient data sets for validation studies. So far, no study has used such tools yet, but we can expect new studies featuring new methods in the future. Additionally, the use of patient-specific simulation in the clinical framework raises the issue of computational time and model complexity. The complexity of the model should not induce an impractical, long duration of computation in order to meet the clinical needs. However, the current stage of development of numerical simulation is not advanced enough to tackle this issue.

3.2. Mechanical properties

Detailing constitutive equations of each material model is beyond the scope of the present review article. Readers are referred to the review articles for a general description of the different material models widely used in simulations[90][89]. A short explanation is given in the following section.

Aorta & leaflets

We can observe different types of constitutive mechanical models. Linear elasticity (LE) is a model where stresses and strains are linearly related. A typical stress-strain curve is straight as shown in Fig.13 left. Linear elasto-plasticity (EP) is a model where the material can have permanent deformations. Tab.4 reports the different material models used for the aorta, leaflet, calcifications and prosthesis in the studies related to TAVI simulation. Concerning non-linear elastic behavior, several models are available. Hyperelasticity (HE) is a more complex model where the stress is related to strain energy density. It is often used to model non-linear elastic stress-strain responses, as shown in Fig.13 right.Another class of models used to describe soft biological tissues are the models based on the law of mixture (composite or mixture theory). Those multi-layered models take into account the contribution of all the structural constituents in the mechanical behavior of the material (elastic fibers, smooth muscle cells, fibrillar collagen). Those models are commonly applied in cardiovascular mechanics [103][104][105][106].

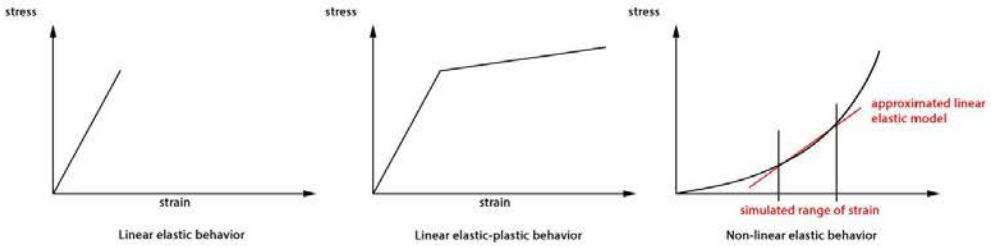

Fig.13 Mechanical models used in numerical simulations for TAVI

All the studies agree that anisotropic and hyperelastic models are required for biological soft tissues in TAVI simulations. Russ *et al.* compared rigid, linear-elastic and hyper-elastic isotropic models in a special deployment simulation[54]. Despite the fact that the hyperelastic model is supposed to have the highest accuracy, the difference found with a linearized elastic model seems negligible given the conditions of the deployment (5.5% deformation error from hyper-elastic versus 5.8% for linear-elastic). A simplifying hypothesis can reasonably be adopted. Because aortic root does not significantly deform during implantation, linearization of the material properties seems viable. Proper linearization requires finding the adequate level of loading on the aorta during implantation and using the corresponding Young's modulus, as seen in Fig.13 (right).

The use of hyperelastic laws may emphasize the sensitivity of simulations to the lack of zero-pressure state. Indeed, hyperelastic model of soft tissues shows a small stiffness at very low strain (horizontal slope) and high stiffness at higher strain (steeper slope). Therefore the mechanical response of hyperelastic material changes significantly depending on its level of strain. However, we have seen in the previous section that the geometry, taken as it is, has an initial loading in the patient. This load induces a pre-strain that increases the stiffness of the aortic wall, if the physiological configuration is erroneously used as a zero-pressure configuration. Surprisingly, among the papers using hyperelastic constitutive models for the aortic wall, only Wang *et al.* [52] explicitly computed the zero-pressure state of the aortic valve. Then again, other aspects of simulation models that need better adjustment may have a stronger impact on the simulation. Therefore, the development of zero-pressure models in the context of TAVI might not have the highest priority so far.

The TAVI simulations that take the native leaflets into account often use the same model for both the aortic wall and the leaflets. In opposition, it is common in FSI studies to use a linear elastic model for the aortic wall and a hyperelastic one for the leaflets. As a matter of fact, biological material models were an important aspect in studies for dynamic analysis of aortic valve behavior. This is understandable given the importance of native leaflets in the latter type of studies, which are precisely focused on the motion of the leaflets. Indeed, some TAVI studies do not even take native leaflets into account. In the case they do, the native leaflets end up tightly crushed by the stent. The anisotropic model appeared relatively late in TAVI studies compared to dynamic aortic valve studies. Auricchio *et al.* [57]& Wang *et al.* [58]are the first TAVI simulations to propose an anisotropic hyperelastic model. The aorta is represented as a composite material including 2 families of fibers [110]. Moreover, a failure criterion based on maximum stress for rupture was implemented.

Meanwhile, concerning studies about the motion of leaflets, De Hart *et al.* and Driessen *et al.* thoroughly tested the fiber-reinforced anisotropic hyperelastic material model for the leaflets[74][114]. Marom *et al.* studied the impact of assigning different material parameters between the three leaflets[86]. Koch *et al.* compared various constitutive material models[83]. Four cases were tested: isotropic linear elasticity, transversely linear elasticity, isotropic hyperelasticity and transversely hyperelasticity. The limitation of those studies lies in the fact that a perfectly healthy aortic valve is considered. In the case of patient-specific simulation, the incertitude on the material parameter may be more impactful compared to the type of material model chosen.

Calcifications

Capelli *et al.*[51] and Morganti *et al.* [59]considered calcified zones, the calcified zone material being an equivalent model which encompasses the leaflet and the calcification characteristics. Thus, they used a linear elastic material, stiffer than a healthy leaflet and less stiff than pure calcification. Young's modulus (10 MPa) was chosen according to Loree *et al.*[115]. Capelli *et al.*[51]also suggested a method to represent the effect of

calcification against the opening of the valve. The calcified nodes at the junction between the leaflet and the wall were completely tied. However, a limit on maximum stress induced a rupture of this junction and the leaflet may deform more easily.

Both studies from Wang *et al.*[52][58] used linear elastic model. The first study used calcified leaflet zones but included a very stiff material model (Young's modulus of 60 GPa). This choice is based on the study of Ebenstein *et al.*[108] that reported high elastic modulus from nanoindentation experiments. It seems reasonable that the material model obtained from nanoindentation relates to a relatively 'pure' calcification. However, that choice would seem more appropriate in the second study of Wang *et al.*[58], where the leaflet and calcifications are separate entities. Instead, Wang*et al.*[58]used a stiffness (Young's modulus of 12.6 MPa) based on another study [111].

Prosthesis

Edward's SAPIEN series are balloon expandable models. The former stents are made in stainless steel. Tzamtzis *et al.*[55]used a linear elastic-plastic to represent X2 CrNiMo-18-15-13 alloy. However, the latest models (e.g. SAPIEN 3) include a cobalt chromium frame. Morganti *et al.* [59]used updated mechanical characteristics for the cobalt chromium alloy.

On the other hand, Medtronic's CoreValve series is a self-expanding prosthesis. Its mechanical behavior is very complex, as it depends on its thermo-mechanical history. CoreValve complexity is not popular in patient-specific simulations, since most of them feature the Sapien prosthesis. Still, Russ *et al.* simulated the deployment of a CoreValve stent[54]. However, the study assigned it a linear elastic-plastic behavior. Tzamtzis *et al.* [55]made a set of mechanical experiments to determine the mechanical response of CoreValve in a 37°C environment. He considered a complex mechanical model for NiTi material, which was developed by Auricchio *et al.* [116]. Gunning *et al.* simulated a realistic self-expanding stent deployment[60]. They applied the same material model on a custom-designed stent from the study by Tzamtzis *et al.*[55].

Friction

Apart from constitutive material models, it may be necessary to define the friction behavior between the different parts of the model. Indeed, friction plays an essential role in the prosthesis stability, as it counteracts pressure gradient [50]. Tab.5 reports the coefficient of friction used in TAVI simulations. Exceptionally, Morganti (2014) does not assign friction[59]. However, the stent is vertically constrained so that it does not migrate.

It is important to note that leaflets and calcifications are not always taken into account in those studies. It is believed that those can give support to the prosthesis [50]. Therefore, the tuning of friction coefficients by the different studies may come from the need to encompass the effect of the missing calcifications and leaflets over the support.

Summary

Studies exploit progressively more advanced constitutive material models. Some of them, however, may come with additional costs. For instance, complex models may require more efforts to adjust and more computational time. Also, more realistic models may increase the sensitivity of the simulation to other aspects which were previously neglected. It is suspected that the use of hyperelastic models increases the sensitivity to the initial geometry of the model, which should take into account the zero-pressure state. Studies are needed to clarify this aspect.

Lastly, a hurdle to patient-specific simulation is the identification of the patient specific mechanical characteristics. The mechanical response of the aorta may vary from patient to patient, with different ages and diseases. Invasive measurement of a patient's aortic valve mechanical properties for simulations before TAVI does not seem a viable option. Efforts are made to develop methods to assess in-vivo material properties such as vascular elastography. Wittek *et al.* & Flamini *et al.* proposed a method to assess aorta mechanical properties from 4D ultrasound data[117][118]. The constitutive model parameters of patient-specific arteries can be obtained from inverse FE method and measurement of the artery wall strain from blood pressure changes. However, these methods do not seem applicable to the aortic valve yet. Different degrees of calcification may

also lead to very variable properties too. Thus, TAVI simulation lacks in the patient-specific material aspect. The choice of material model will remain a challenging question in TAVI simulation.

3.3. Boundary conditions

Boundary conditions are an important input in the model to perform reliable simulations. Like geometry of anatomy and mechanical properties of tissues, the complexity of human physiologic conditions does not allow exact representation in the simulations. This is even more evident in patient-specific cases, where a lot of parameters are inaccessible. Therefore, it is often necessary to assume the physiological conditions to define simplified boundary conditions. This aspect of simulation may be the most arbitrary, because there is a very broad range of possibilities to define boundary conditions. Depending on the focus of the simulation study, hypotheses concerning the boundary conditions must be taken accordingly. In the present review article, we will focus on TAV deployment conditions.

Surrounding tissues

TAVI simulations only consider a small portion of anatomy: the aortic valve. However, the valve is, in reality, connected to surrounding tissues. It is necessary to define how the modeled valve interacts with the external environment that is excluded from the simulation model. In the case of TAVI simulation, there is no consensus about boundary conditions applied on the extremities of the geometry. Capelli *et al.*[51]constrains every degree of freedom of the nodes along the extremities, fixing in space the ends of the model. Morganti *et al.*[59]constrains the aorta and the balloon to not move vertically. However nodes can move radially. Wang *et al.* [52]expands the geometry zone to the myocardium. Only the upper edge of the aorta (distal side) is constrained in all translations. In other words, we observe either totally fixed nodes, or plane-constrained nodes. However, when experimental data are observed, more complex details appear. The same way the arteries bear circumferential pre-stress, they also bear axial pre-stretch [119]. In studies of aortic valve motion, we observe more varied conditions. Labrosse *et al.* imposed an axial pre-stretch by prescribing axial displacement to the distal edge[82]. So far, TAVI studies neglected the interaction between the aortic wall and the surrounding tissues. Only the extremities of the model were considered, but it must be kept in mind that those interactions may have to be modeled. Sturla *et al.* suggested to wrap the aortic root with a virtual fully recoverable foam, the external surface of the foam being fixed[87].

Blood flow

TAVI studies usually concern classical solid FE analysis, so they do not take into consideration the fluid dynamics. The usual approach to model blood interaction is the use of spatially uniform prescribed pressure. The in-vivo aortic wall is constantly loaded with a minimal blood pressure. However, no simulation of TAVI included this pressure. Wang *et al.* [52]justified the omission of blood pressure by the decrease of blood pressure during rapid pacing (heart burst stimulation) during deployment. The study suggested that pressure decreases from 80-120mmHg down to 0-20mmHg. Nonetheless, the reported experimental decrease of pressure is smaller than this estimate: from 62-94 mmHg down to 34-64 mmHg [120].

In the case that prosthesis action is also studied, it is necessary to model the transvalvular pressure. The usual method is applying a uniform pressure on the surface of the TAV leaflets. Sirois *et al.*[8] and Auricchio *et al.* [57] prescribed pressure only on the leaflets to determine the motion of the leaflets and the closed state respectively. The review of Sun *et al.* and the studies of Marom *et al.* and Sturla *et al.* explained the merit of using FSI simulation compared to FE "dry" models[89][84][87]. For example, the momentum of blood flow produces a closing impulse that is not modeled in "dry" FE [76]. The prosthesis leaflets may be overly opened when simulating systole. The blood flow model grants damping that smooth the movement of the leaflets.

Deployment steps& Balloon expansion

An efficient and reliable simulation requires modeling boundary conditions as closely as necessary to the real conditions of the procedure. Deployment is usually composed of two steps. The crimping of the stent consists in compressing the stent so that its size fits in the arteries. Then, a balloon inside the prosthesis expands it (in the case of SAPIEN). Little to no data is given about the method to center the balloon during deployment. It seems that a number of studies arbitrarily align the balloon in the center of the valve. In practice, the balloon centers

itself during expansion. However, the boundary conditions at the edge of geometry are often in total constraint, so they likely prevent the balloon from 'auto-centering'. As previously stated, current models focus on the results of the deployment, such as stresses and deformations. It does not matter that the prosthesis does not take a realistic path during the deployment, as long as the prosthesis is correctly positioned in the end of simulation. However, a more realistic description of the boundary conditions of the balloon could allow realistic simulation of the migrations which may occur during deployment.

The models of the balloon expansion in simulation studieswere relatively simple for a long time. However, recent studies suggest that the expansion model is important. Capelli *et al.* [51]and Auricchio *et al.* [57]used a uniform pressure expansion to deploy the balloon. Morganti *et al.*[59]and Wang *et al.* [52] initially used a plain cylinder. Its nodes were constrained in displacement in order to simulate the deployment. In the case of a CoreValve deployment, Russ *et al.* [54]suggested a rare method of deployment. It did not use a balloon, and displacements were directly applied to the stent. In order to crimp the prosthesis, the extremities of the stent frame were stretched. Then, the deployment consisted in squeezing the extremities. Eventually, this idea was not exploited in other studies.

While most balloon inflations were straightforward in previous studies, Wang *et al.* [58]challenged the use of uniform pressure expansion. Instead, the balloon was inflated based on a volume variable method [121]. This method was originally applied to angioplasty, and focused on the transitory radial force during the expansion. It showed that the force is influenced more by the diameter of the balloon than by the filling pressure. In practice, TAVI operators do not control the pressure, but rather the injected volume inside the balloon. Furthermore, the operators can choose to use an oversized balloon and prosthesis, without completely filling the balloon, in order to facilitate deployment. That is something that may not be simulated realistically with uniform pressure.

Summary

Boundary conditions represent a very large question in numerical simulation. There is no definite answer as to what should be simplified or neglected and what should be accurately modeled. The method of simulation itself limits the choice, as FE analysis does not allow realistic models of blood flow. While it may not be a problem for quick balloon-expandable deployment, it may be so for self-expanding prostheses. Indeed, those prostheses "swim" along their guidewire and are constantly moving with the blood flow during the deployment.

Many physiological conditions cannot be entirely grasped. Heart Burst Stimulation is not modeled at all, yet the geometrical model may greatly change as it contracts the muscle fibers. However, modeling the myocardium activation in the deployment for in-vivo tissues obviously seem a cumbersome task compared to how it may benefit to the accuracy of the simulation. Moreover, accurate descriptions of deployment tools are missing in the current studies, such as the guidewire of the TAV. Balloons are always spatially fixed, while in practice they are free to move along their guidewire. Hence, current studies completely neglect the aspect of deployment where the prosthesis is liable to migrate. However small, the prosthesis migration has different degrees across the different type of prosthesis. Medical teams are interested in it to plan their prosthesis delivery[28].

4. Data analysis

4.1. Simulation outputs

The stresses induced on the aortic wall are relevant to assess the risk of aortic injury, and were often reported[51][52][57][59][60]. Stresses on the stent are also relevant as they may be related to the prosthesis durability. Also, contact force between the stent and the aortic wall is relevant to assess the risk of migration of the prosthesis. However, patient-specific simulation did not systematically report contact force.

An important result of simulation is the final shape of the geometries. Wang *et al.* [52][58]and Morganti *et al.* [59]reported the gaps between the deployed stent and the aortic wall. Indeed, these gaps are crucial to predicting paravalvular leaks. Morganti *et al.*[59]showed that those leaks could be estimated for the case of two patients, by observing their retrograde blood flow.

When calcified native leaflets are modeled, the observation of their final shape can inform clinicians on the occurrence of coronary occlusion. Indeed, coronary occlusion sometimes happens from the displacement of bulky calcified leaflets over the coronary ostium [6].

The final shape of the stent also greatly impacts the behavior of the prosthesis leaflets [43]. The behavior of the leaflets determines the stress distribution and the transvalvular leaks. Transvalvular leaks are believed to be related to the coaptation area between the leaflets during diastole. Auricchio *et al.* [57]and Gunning *et al.* [60]simulated the valve closure at diastole by prescribing pressure at each side of the leaflets.

Clinicians usually evaluate the severity of stenosis through pressure gradient, which is the difference of pressure at both sides of the valve. Sirois *et al.*[8] and Capelli *et al.* [51]suggested measuring the geometric orifice area of the aortic valve before and after deployment of the prosthesis. Sadly, the conditions of measurement were not specified. Subsequent patient-specific TAVI simulations dropped this aspect. While geometric area has a strong correlation with energy loss at systole, a more precise fluid mechanics simulation of the implanted prosthesis could be relevant during the whole cardiac cycle. Sirois *et al.*[8]computed turbulent kinetic energy from CFD simulation.

One of the interests of simulating deployment without focusing on the starting deployment position is the search for the optimal position of the landing site. Several studies tested several positions of implantation and compared their performances. Capelli *et al.*[51]showed that geometric orifice area could vary according to the implantation depth. Auricchio *et al.* [57]compared two extreme positions of prosthesis in terms of aortic wall stress, TAV leaflets stress, and coaptation area. There is no CFD study on this aspect yet. However, Groves *et al.* showed through experimental setup that the position of TAV had an impact on the flow[62]. The position of the valve changed the aortic wall stress and residence time of blood particles in the aortic root. It is speculated that the residence time of blood within the aortic root also influenced the coronary perfusion. Those studies on the optimal position of prosthesis pave the way towards the use of patient-specific simulation for clinical planning.

Dwyer *et al.* [50]expressed concern over the orientation of the TAV prosthesis. Indeed, it has a free axis of rotation, as it may rotate around its guidewire, c.f. Fig.14. Gunning *et al.*[60]studied the impact of this orientation on the prosthesis.

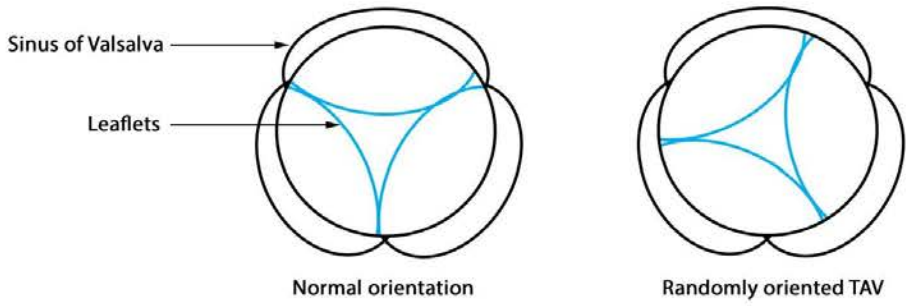

Fig.14 Upper view of aortic valve, orientation of prosthesis compared to sinus configuration

4. 2. Perspectives

Currently, the presented parameters already offer interesting insight to clinicians. There is no doubt that they can still be further developed. Some examples are given in this section.

The native leaflets are tied and aligned at the base of a sinus, which plays a role in the normal function of the valve (c.f. Fig.14). The sinus shape evens out the stress, and helps the valve closure during diastole [69][77][79]. The impact of orientation on the motion of leaflets has not been studied yet.

Atrioventricular Block is supposed to be related to the stress distribution on the aortic wall. Larger models to obtain a precise map of stresses would help predicting this complication.

Current models of TAV post-operative action are still lacking as it was partially treated very recently by very few studies. As mentioned in the boundary condition section, FE "dry" simulation neglects the aortic wall deformation and focuses on a specific phase of the cardiac cycle, while differences in deformation between the wall and the stent may result in unwanted friction.

Conclusion

TAVI simulations are still in an active period as new studies offer increasingly accurate models. Models significantly differ from each other, from the choice in geometry, mechanical properties and boundary conditions. Current studies lack statistical data to firmly justify those choices. Therefore they may not be reliable enough to offer precise quantitative estimations, though they can help medical teams [58]. Precaution is still needed when applying current models to clinical use.

Current patient-specific simulations put an emphasis on the end of deployment step and prosthesis action. However, they do not tackle the placement shift and migration that occur during deployment. Yet, these are major issues in TAVI as misplacement can have catastrophic outcomes, e.g. coronary occlusion, supra-skirtal leaks, and ventricle migration. Choosing the best starting positions for the deployment is a big concern for medical teams, especially in cases in which the deployment mechanism does not allow for recapture of the prosthesis or is difficult to predict. Thus, numerous challenges are awaiting patient-specific simulations.

Disclosure

P. Vy and M. Rochette are full-time employees of ANSYS France. H. Le Breton hadreceived speaker honorarium from Edwards Lifesciences.

References

[1] D. H. Adams, J. J. Popma, M. J. Reardon, S. J. Yakubov, J. S. Coselli, G. M. Deeb, T. G. Gleason, M. Buchbinder, J. Hermiller, N. S. Kleiman, S. Chetcuti, J. Heiser, W. Merhi, G. Zorn, P. Tadros, N. Robinson, G. Petrossian, G. C. Hughes, J. K. Harrison, J. Conte, B. Maini, M. Mumtaz, S. Chenoweth, and J. K. Oh, "Transcatheter Aortic-Valve Replacement with a Self-Expanding Prosthesis.," *N. Engl. J. Med.*, vol. 370, pp. 1790–8, 2014.

[2] C. Smith and M. Leon, "Transcatheter versus Surgical Aortic-Valve Replacement in High-Risk Patients," *N. Engl. J. Med.*, vol. 364, no. 23, pp. 2187–98, 2011.

[3] M. B. Leon, C. R. Smith, M. Mack, D. C. Miller, J. W. Moses, L. G. Svensson, E. M. Tuzcu, J. G. Webb, G. P. Fontana, R. R. Makkar, D. L. Brown, P. C. Block, R. A. Guyton, A. D. Pichard, J. E. Bavaria, H. C. Herrmann, P. S. Douglas, J. L. Petersen, J. J. Akin, W. N. Anderson, D. Wang, and S. Pocock, "Transcatheter aortic-valve implantation for aortic stenosis in patients who cannot undergo surgery.," *N. Engl. J. Med.*, vol. 363, no. 17, pp. 1597–1607, 2010.

[4] A. Cribier, H. Eltchaninoff, A. Bash, N. Borenstein, C. Tron, F. Bauer, G. Derumeaux, F. Anselme, F. Laborde, and M. B. Leon, "Percutaneous transcatheter implantation of an aortic valve prosthesis for calcific aortic stenosis: First human case description," *Circulation*, vol. 106, no. 24, pp. 3006–3008, 2002.

[5] A. N. Azadani, N. Jaussaud, P. B. Matthews, L. Ge, T. S. Guy, T. a M. Chuter, and E. E. Tseng, "Energy loss due to paravalvular leak with transcatheter aortic valve implantation.," *Ann. Thorac. Surg.*, vol. 88, no. 6, pp. 1857–1863, 2009.

[6] J. B. Masson, J. Kovac, G. Schuler, J. Ye, A. Cheung, S. Kapadia, M. E. Tuzcu, S. Kodali, M. B. Leon, and J. G. Webb, "Transcatheter Aortic Valve Implantation. Review of the Nature, Management, and Avoidance of Procedural Complications," *JACC Cardiovasc. Interv.*, vol. 2, no. 9, pp. 811–820, 2009.

[7] J. Shannon, M. Mussardo, A. Latib, K. Takagi, A. Chieffo, M. Montorfano, and A. Colombo, "Recognition and management of complications during transcatheter aortic valve implantation.," *Expert Rev. Cardiovasc. Ther.*, vol. 9, pp. 913–926, 2011.

[8] E. Sirois, Q. Wang, and W. Sun, "Fluid Simulation of a Transcatheter Aortic Valve Deployment into a Patient-Specific Aortic Root," *Cardiovasc. Eng. Technol.*, vol. 2, no. 3, pp. 186–195, 2011.

[9] A. Vahanian, O. Alfieri, F. Andreotti, M. J. Antunes, G. Barón-Esquivias, H. Baumgartner, M. A. Borger, T. P. Carrel, M. De Bonis, A. Evangelista, V. Falk, B. Iung, P. Lancellotti, L. Pierard, S. Price, H. J. Schäfers, G. Schuler, J. Stepinska, K. Swedberg, J. Takkenberg, U. O. Von Oppell, S. Windecker, J. L. Zamorano, M. Zembala, J. J. Bax, C. Ceconi, V. Dean, C. Deaton, R. Fagard, C. Funck-Brentano, D. Hasdai, A. Hoes, P. Kirchhof, J. Knuuti, P. Kolh, T. McDonagh, C. Moulin, B. a. Popescu, Ž. Reiner, U. Sechtem, P. A. Sirnes, M. Tendera, A. Torbicki, L. Von Segesser, L. P. Badano, M. Bunc, M. J. Claeys, N. Drinkovic, G. Filippatos, G. Habib, a. Pieter Kappetein, R. Kassab, G. Y. H. Lip, N. Moat, G. Nickenig, C. M. Otto, J. Pepper, N. Piazza, P. G. Pieper, R. Rosenhek, N. Shuka, E. Schwammenthal, J. Schwitter, P. T. Mas, P. T. Trindade, and T. Walther, "Guidelines on the management of valvular heart disease (version 2012)," *Eur. Heart J.*, vol. 33, no. 19, pp. 2451–2496, 2012.

[10] B. Iung, G. Baron, E. G. Butchart, F. Delahaye, C. Gohlke-Bärwolf, O. W. Levang, P. Tornos, J. L. Vanoverschelde, F. Vermeer, E. Boersma, P. Ravaud, and A. Vahanian, "A prospective survey of patients with valvular heart disease in Europe: The Euro Heart Survey on valvular heart disease," *Eur. Heart J.*, vol. 24, no. 13, pp. 1231–1243, 2003.

[11] G. W. Eveborn, H. Schirmer, G. Heggelund, P. Lunde, and K. Rasmussen, "The evolving epidemiology of valvular aortic stenosis. The Tromso Study," *Heart*. 2012.

[12] C. Clark, "Energy losses in flow through stenosed valves.," *J. Biomech.*, vol. 12, no. December 1978, pp. 737–746, 1979.

[13] D. Garcia and L. Kadem, "Orifice Area , Effective Orifice Area , or Gorlin Area ?," 2006.

[14] P. Dyverfeldt, M. D. Hope, E. E. Tseng, and D. Saloner, "Magnetic resonance measurement of turbulent kinetic energy for the estimation of irreversible pressure loss in aortic stenosis," *JACC Cardiovasc. Imaging*, vol. 6, no. 1, pp. 64–71, 2013.

[15] C. MD, G. EW, B. BH, C. CJ, Q. JA, and B. R. Jr., "Rate of progression of severity of valvular aortic stenosis in the adult.," *Am. Heart J.*, vol. 98, no. 6, pp. 689–700, 1979.

[16] J. Turina, O. Hess, F. Sepulcri, and H. P. Krayenbuehl, "Spontaneous course of aortic valve disease.," *Eur. Heart J.*, vol. 8, no. 5, pp. 471–483, 1987.

[17] C. M. Otto, "Timing of aortic valve surgery CatherineMOtto," *Circulation*, pp. 211–218, 2000.

[18] P. Kleine, M. J. Hasenkam, H. Nygaard, M. Perthel, D. Wesemeyer, and J. Laas, "Tilting disc versus bileaflet aortic valve substitutes: intraoperative and postoperative hemodynamic performance in humans.," 2000.

[19] V. Goyal, S. Devgarha, S. Kalla, and C. P. Srivastava, "Comparative evaluation of hemodynamic performance in early post-operative period of tilting disc vs. bileaflet mechanical valve at mitral position — A prospective study," *Indian J. Thorac. Cardiovasc. Surg.*, vol. 25, no. 2, pp. 52–55, Jun. 2009.

[20] W. S. EDWARDS and L. SMITH, "Aortic valve replacement with a subcoronary ball valve.," *Surg. Forum*, vol. 9, pp. 309–313, 1958.

[21] W. S. Edwards, "Aortic valve replacement with a subcoronary ball valve--early experiments.," *Med. Instrum.*, vol. 11, no. 2, pp. 77–79, 1977.

[22] M. Neyt, H. Van Brabandt, S. Van De Sande, and S. Devriese, "Transcatheter Aortic Valve Implantation (TAVI): a Health Technology Assessment Update," 2011.

[23] M. A. Clark, F. G. Duhay, A. K. Thompson, M. J. Keyes, L. G. Svensson, R. O. Bonow, B. T. Stockwell, and D. J. Cohen, "Clinical and economic outcomes after surgical aortic valve replacement in Medicare patients," *Risk Manag. Healthc. Policy*, vol. 5, pp. 117–126, 2012.

[24] B. A. Carabello and W. J. Paulus, "Aortic stenosis," *The Lancet*, vol. 373, no. 9667. pp. 956–966, 2009.

[25] B. Iung and A. Vahanian, "Epidemiology of valvular heart disease in the adult.," *Nat. Rev. Cardiol.*, vol. 8, no. 3, pp. 162–172, 2011.

[26] R. L. J. Osnabrugge, D. Mylotte, S. J. Head, N. M. Van Mieghem, V. T. Nkomo, C. M. Lereun, A. J. J. C. Bogers, N. Piazza, and a. P. Kappetein, "Aortic stenosis in the elderly: Disease prevalence and number of candidates for transcatheter aortic valve replacement: A meta-analysis and modeling study," *J. Am. Coll. Cardiol.*, vol. 62, no. 11, pp. 1002–1012, 2013.

[27] A. Ielasi, A. Latib, and M. Tespili, "Current and new-generation transcatheter aortic valve devices: an update on emerging technologies.," *Expert Rev. Cardiovasc. Ther.*, vol. 11, pp. 1393–405, 2013.

[28] D. Dvir, I. Lavi, H. Eltchaninoff, D. Himbert, Y. Almagor, F. Descoutures, A. Vahanian, C. Tron, A. Cribier, and R. Kornowski, "Multicenter evaluation of Edwards SAPIEN positioning during transcatheter aortic valve implantation with correlates for device movement during final deployment.," *JACC. Cardiovasc. Interv.*, vol. 5, no. 5, pp. 563–70, May 2012.

[29] C. Cao, "Migration of transcatheter valve into the left ventricle," 2012.

[30] G. Schymik, H. Schröfel, M. Heimeshoff, A. Luik, M. Thoenes, and L. Mandinov, "How to Adapt the Implantation Technique for the New SAPIEN 3 Transcatheter Heart Valve Design," *J. Interv. Cardiol.*, vol. 28, no. 1, pp. 82–89, 2015.

[31] L. Lehmkuhl, B. Foldyna, K. Von Aspern, C. Lücke, M. Grothoff, S. Nitzsche, J. Kempfert, M. Haensig, A. Rastan, T. Walther, F.-W. Mohr, and M. Gutberlet, "Inter-individual variance and cardiac cycle dependency of aortic root dimensions and shape as assessed by ECG-gated multi-slice computed tomography in patients with severe aortic stenosis prior to transcatheter aortic valve implantation: is it crucial for," *Int. J. Cardiovasc. Imaging*, vol. 29, no. 3, pp. 693–703, Mar. 2013.

[32] H. B. Ribeiro, L. Nombela-Franco, M. Urena, M. Mok, S. Pasian, D. Doyle, R. Delarochellière, M. Côté, L. Laflamme, H. Delarochellière, R. Allende, E. Dumont, and J. Rodés-Cabau, "Coronary obstruction following transcatheter aortic valve implantation: A systematic review," *JACC: Cardiovascular Interventions*, vol. 6, no. 5. pp. 452–461, 2013.

[33] R. G. Seipelt, G. Hanekop, F. A. Schoendube, and W. Schillinger, "Heart team approach for transcatheter aortic valve implantation procedures complicated by coronary artery occlusion.," *Interact. Cardiovasc. Thorac. Surg.*, vol. 14, no. 4, pp. 431–3, 2012.

[34] G. C. M. Siontis, P. Jüni, T. Pilgrim, S. Stortecky, L. Büllesfeld, B. Meier, P. Wenaweser, and S. Windecker, "Predictors of Permanent Pacemaker Implantation in Patients With Severe Aortic Stenosis Undergoing TAVR," *J. Am. Coll. Cardiol.*, vol. 64, no. 2, pp. 129–140, 2014.

[35] A. N. Azadani, N. Jaussaud, P. B. Matthews, L. Ge, T. a M. Chuter, and E. E. Tseng, "Transcatheter aortic valves inadequately relieve stenosis in small degenerated bioprostheses.," *Interact. Cardiovasc. Thorac. Surg.*, vol. 11, pp. 70–77, 2010.

[36] M. A. Clavel, J. G. Webb, P. Pibarot, L. Altwegg, E. Dumont, C. Thompson, R. De Larochellière, D. Doyle, J. B. Masson, S. Bergeron, O. F. Bertrand, and J. Rodés-Cabau, "Comparison of the

Hemodynamic Performance of Percutaneous and Surgical Bioprostheses for the Treatment of Severe Aortic Stenosis," *J. Am. Coll. Cardiol.*, vol. 53, no. 20, pp. 1883–1891, 2009.

[37] S. H. Ewe, M. Muratori, V. Delgado, M. Pepi, G. Tamborini, L. Fusini, R. J. M. Klautz, P. Gripari, J. J. Bax, M. Fusari, M. J. Schalij, and N. A. Marsan, "Hemodynamic and clinical impact of prosthesispatient mismatch after transcatheter aortic valve implantation," *J. Am. Coll. Cardiol.*, vol. 58, no. 18, pp. 1910–1918, 2011.

[38] M. Pasic, A. Unbehaun, S. Buz, T. Drews, and R. Hetzer, "Annular Rupture During Transcatheter Aortic Valve Replacement," *JACC Cardiovasc. Interv.*, vol. 8, no. 1, pp. 1–9, 2015.

[39] K. Hayashida, E. Bouvier, T. Lefèvre, T. Hovasse, M.-C. Morice, B. Chevalier, M. Romano, P. Garot, A. Farge, P. Donzeau-Gouge, and B. Cormier, "Potential mechanism of annulus rupture during transcatheter aortic valve implantation.," *Catheter. Cardiovasc. Interv.*, vol. 82, no. 5, pp. E742–6, Nov. 2013.

[40] P. Généreux, S. J. Head, R. Hahn, B. Daneault, S. Kodali, M. R. Williams, N. M. Van Mieghem, M. C. Alu, P. W. Serruys, A. P. Kappetein, and M. B. Leon, "Paravalvular leak after transcatheter aortic valve replacement: The new achilles' heel? A comprehensive review of the literature," *Journal of the American College of Cardiology*, vol. 61, no. 11. pp. 1125–1136, 2013.

[41] R. Zegdi, V. Ciobotaru, M. Noghin, G. Sleilaty, A. Lafont, C. Latrémouille, A. Deloche, and J.-N. Fabiani, "Is it reasonable to treat all calcified stenotic aortic valves with a valved stent? Results from a human anatomic study in adults.," *J. Am. Coll. Cardiol.*, vol. 51, no. 5, pp. 579–84, Feb. 2008.

[42] B. E. Stähli, W. Maier, R. Corti, T. F. Lüscher, R. Jenni, and F. C. Tanner, "Aortic regurgitation after transcatheter aortic valve implantation: mechanisms and implications.," *Cardiovasc. Diagn. Ther.*, vol. 3, no. 1, pp. 15–22, 2013.

[43] W. Sun, K. Li, and E. Sirois, "Simulated elliptical bioprosthetic valve deformation: implications for asymmetric transcatheter valve deployment.," *J. Biomech.*, vol. 43, no. 16, pp. 3085–90, Dec. 2010.

[44] P. Kahlert, F. Al-Rashid, P. Döttger, K. Mori, B. Plicht, D. Wendt, L. Bergmann, E. Kottenberg, M. Schlamann, P. Mummel, D. Holle, M. Thielmann, H. G. Jakob, T. Konorza, G. Heusch, R. Erbel, and H. Eggebrecht, "Cerebral embolization during transcatheter aortic valve implantation: A transcranial doppler study," *Circulation*, vol. 126, no. 10, pp. 1245–1255, 2012.

[45] C. K. Naber, A. Ghanem, A. A. Abizaid, A. Wolf, J. M. Sinning, N. Werner, G. Nickenig, T. Schmitz, and E. Grube, "First-in-man use of a novel embolic protection device for patients undergoing transcatheter aortic valve implantation," *EuroIntervention*, vol. 8, no. 1, pp. 43–50, 2012.

[46] J. G. Webb and D. A. Wood, "Current status of transcatheter aortic valve replacement," *J. Am. Coll. Cardiol.*, vol. 60, no. 6, pp. 483–492, 2012.

[47] E. E. Tseng, A. Wisneski, A. N. Azadani, and L. Ge, "Engineering perspective on transcatheter aortic valve implantation," *Interv. Cardiol.*, vol. 5, pp. 53–70, 2013.

[48] J.G. Webb, "Percutaneous aortic valve replacement in selected high risk patients with aortic stenosis," 2007.

[49] I. B., L. C., H. D., E. H., C. K., D.-G. P., F. J., L. P., L. a., L. M., P. a., T. E., L. M., V. a., and G. M., "Predictive factors of early mortality after transcatheter aortic valve implantation: Individual risk assessment using a simple score," *Heart*, vol. 100, no. 13, pp. 1016–1023, 2014.

[50] H. a Dwyer, P. B. Matthews, A. Azadani, N. Jaussaud, L. Ge, T. S. Guy, and E. E. Tseng, "Computational fluid dynamics simulation of transcatheter aortic valve degeneration.," *Interact. Cardiovasc. Thorac. Surg.*, vol. 9, pp. 301–308, 2009.

[51] C. Capelli, G. M. Bosi, E. Cerri, J. Nordmeyer, T. Odenwald, P. Bonhoeffer, F. Migliavacca, a M. Taylor, and S. Schievano, "Patient-specific simulations of transcatheter aortic valve stent implantation.," *Med. Biol. Eng. Comput.*, vol. 50, no. 2, pp. 183–92, Feb. 2012.

[52] Q. Wang, E. Sirois, and W. Sun, "Patient-specific modeling of biomechanical interaction in transcatheter aortic valve deployment.," *J. Biomech.*, vol. 45, no. 11, pp. 1965–71, Jul. 2012.

[53] R. Hopf, M. Gessat, V. Falk, and E. Mazza, "Reconstruction of Stent Induced Loading Forces on the Aortic Valve Complex," pp. 104–111, 2012.

[54] C. Russ, R. Hopf, S. Hirsch, S. Sundermann, V. Falk, G. Szekely, and M. Gessat, "Simulation of transcatheter aortic valve implantation under consideration of leaflet calcification.," *Conf. Proc. IEEE Eng. Med. Biol. Soc.*, vol. 2013, pp. 711–4, Jan. 2013.

[55] S. Tzamtzis, J. Viquerat, J. Yap, M. J. Mullen, and G. Burriesci, "Numerical analysis of the radial force produced by the Medtronic-CoreValve and Edwards-SAPIEN after transcatheter aortic valve implantation (TAVI).," *Med. Eng. Phys.*, vol. 35, no. 1, pp. 125–30, Jan. 2013.

[56] I. Kemp, K. Dellimore, R. Rodriguez, C. Scheffer, D. Blaine, H. Weich, and a. Doubell, "Experimental validation of the fluid-structure interaction simulation of a bioprosthetic aortic heart valve," *Australas. Phys. Eng. Sci. Med.*, vol. 36, no. 3, pp. 363–373, 2013.

[57] F. Auricchio, M. Conti, S. Morganti, and a Reali, "Simulation of transcatheter aortic valve implantation: a patient-specific finite element approach.," *Comput. Methods Biomech. Biomed. Engin.*, vol. 17, no. 12, pp. 1347–57, Jan. 2014.

[58] Q. Wang, S. Kodali, C. Primiano, and W. Sun, "Simulations of transcatheter aortic valve implantation: implications for aortic root rupture.," *Biomech. Model. Mechanobiol.*, Apr. 2014.

[59] S. Morganti, M. Conti, M. Aiello, a Valentini, a Mazzola, a Reali, and F. Auricchio, "Simulation of transcatheter aortic valve implantation through patient-specific finite element analysis: Two clinical cases.," *J. Biomech.*, no. 2012, Jun. 2014.

[60] P. S. Gunning, T. J. Vaughan, and L. M. McNamara, "Simulation of Self Expanding Transcatheter Aortic Valve in a Realistic Aortic Root: Implications of Deployment Geometry on Leaflet Deformation," *Ann. Biomed. Eng.*, vol. 42, no. 9, pp. 1989–2001, 2014.

[61] M. Gessat, R. Hopf, T. Pollok, C. Russ, T. Frauenfelder, S. H. Sundermann, S. Hirsch, E. Mazza, G. Szekely, and V. Falk, "Image-based mechanical analysis of stent deformation: Concept and exemplary implementation for aortic valve stents," *IEEE Trans. Biomed. Eng.*, vol. 61, no. c, pp. 4–15, 2014.

[62] E. M. Groves, A. Falahatpisheh, J. L. Su, and A. Kheradvar, "The Effects of Positioning of Transcatheter Aortic Valves on Fluid Dynamics of the Aortic Root," *ASAIO J.*, vol. 60, pp. 545–552, 2014.

[63] A. Kheradvar, E. M. Groves, C. J. Goergen, S. H. Alavi, R. Tranquillo, C. a. Simmons, L. P. Dasi, K. J. Grande-Allen, M. R. K. Mofrad, A. Falahatpisheh, B. Griffith, F. Baaijens, S. H. Little, and S. Canic, "Emerging Trends in Heart Valve Engineering: Part II. Novel and Standard Technologies for Aortic Valve Replacement," *Ann. Biomed. Eng.*, 2014.

[64] F. Sotiropoulos, "Computational Fluid Dynamics for Medical Device Design and Evaluation: Are We There Yet?," *Cardiovascular Engineering and Technology*, vol. 3, no. 2, pp. 137–138, 2012.

[65] S. F. C. Stewart, E. G. Paterson, G. W. Burgreen, P. Hariharan, M. Giarra, V. Reddy, S. W. Day, K. B. Manning, S. Deutsch, M. R. Berman, M. R. Myers, and R. a. Malinauskas, "Assessment of CFD Performance in Simulations of an Idealized Medical Device: Results of FDA's First Computational Interlaboratory Study," *Cardiovasc. Eng. Technol.*, vol. 3, no. 2, pp. 139–160, 2012.

[66] E. Votta, T. B. Le, M. Stevanella, L. Fusini, E. G. Caiani, A. Redaelli, and F. Sotiropoulos, "Toward patient-specific simulations of cardiac valves: State-of-the-art and future directions," *J. Biomech.*, vol. 46, no. 2, pp. 217–228, 2013.

[67] S. Krucinski, I. Vesely, M. a. Dokainish, and G. Campbell, "Numerical simulation of leaflet flexure in bioprosthetic valves mounted on rigid and expansile stents," *J. Biomech.*, vol. 26, no. 8, pp. 929–943, 1993.

[68] K. J. Grande, R. P. Cochran, P. G. Reinhall, and K. S. Kunzelman, "Stress variations in the human aortic root and valve: the role of anatomic asymmetry.," *Ann. Biomed. Eng.*, vol. 26, no. 4, pp. 534–545, 1998.

[69] K. J. Grande-Allen, R. P. Cochran, P. G. Reinhall, and K. S. Kunzelman, "Re-creation of sinuses is important for sparing the aortic valve: a finite element study.," *J. Thorac. Cardiovasc. Surg.*, vol. 119, no. 4 Pt 1, pp. 753–763, 2000.

[70] R. Gnyaneshwar, R. K. Kumar, and K. R. Balakrishnan, "Dynamic analysis of the aortic valve using a finite element model.," *Ann. Thorac. Surg.*, vol. 73, no. 01, pp. 1122–9, 2002.

[71] I. C. Howard, E. a Patterson, and a Yoxall, "On the opening mechanism of the aortic valve: some observations from simulations.," *J. Med. Eng. Technol.*, vol. 27, no. 6, pp. 259–266, 2003.

[72] M. a. Nicosia, R. P. Cochran, and K. S. Kunzelman, "Coupled fluid-structure finite element modeling of the aortic valve and root," *Proc. Second Jt. 24th Annu. Conf. Annu. Fall Meet. Biomed. Eng. Soc. [Engineering Med. Biol.*, vol. 2, no. 5, pp. 1278–1279, 2002.

[73] C. Carmody, G. Burriesci, I. Howard, and E. Patterson, "The use of LS-DYNA fluid-structure interaction to simulate fluid-driven deformation in the aortic valve.," no. 0, pp. 11–20, 2003.

[74] J. De Hart, F. P. T. Baaijens, G. W. M. Peters, and P. J. G. Schreurs, "A computational fluid-structure interaction analysis of a fiber-reinforced stentless aortic valve," *J. Biomech.*, vol. 36, no. 5, pp. 699–712, 2003.

[75] G. Arcidiacono, a. Corvi, and T. Severi, "Functional analysis of bioprosthetic heart valves," *J. Biomech.*, vol. 38, no. 7, pp. 1483–1490, 2005.

[76] D. R. Hose, A. J. Narracott, J. M. T. Penrose, D. Baguley, I. P. Jones, and P. V. Lawford, "Fundamental mechanics of aortic heart valve closure," *J. Biomech.*, vol. 39, no. 5, pp. 958–967, 2006.

[77] A. Ranga, O. Bouchot, R. Mongrain, P. Ugolini, and R. Cartier, "Computational simulations of the aortic valve validated by imaging data: evaluation of valve-sparing techniques.," *Interact. Cardiovasc. Thorac. Surg.*, vol. 5, no. 4, pp. 373–378, 2006.

[78] E. J. Weinberg and M. R. Kaazempur Mofrad, "Transient, three-dimensional, multiscale simulations of the human aortic valve.," *Cardiovasc. Eng.*, vol. 7, no. 4, pp. 140–155, 2007.

[79] S. Katayama, N. Umetani, S. Sugiura, and T. Hisada, "The sinus of Valsalva relieves abnormal stress on aortic valve leaflets by facilitating smooth closure," *J. Thorac. Cardiovasc. Surg.*, vol. 136, no. 6, pp. 1528–1535.e1, 2008.

[80] F. Viscardi, C. Vergara, L. Antiga, S. Merelli, A. Veneziani, G. Puppini, G. Faggian, A. Mazzucco, and G. B. Luciani, "Comparative Finite Element Model Analysis of Ascending Aortic Flow in Bicuspid and Tricuspid Aortic Valve," *Artif. Organs*, vol. 34, no. 12, pp. 1114–1120, 2010.

[81] C. a Conti, E. Votta, A. Della Corte, L. Del Viscovo, C. Bancone, M. Cotrufo, and A. Redaelli, "Dynamic finite element analysis of the aortic root from MRI-derived parameters.," *Med. Eng. Phys.*, vol. 32, no. 2, pp. 212–221, 2010.

[82] M. R. Labrosse, K. Lobo, and C. J. Beller, "Structural analysis of the natural aortic valve in dynamics: From unpressurized to physiologically loaded," *J. Biomech.*, vol. 43, no. 10, pp. 1916–1922, 2010.

[83] T. M. Koch, B. D. Reddy, P. Zilla, and T. Franz, "Aortic valve leaflet mechanical properties facilitate diastolic valve function.," *Comput. Methods Biomech. Biomed. Engin.*, vol. 13, no. 2, pp. 225–234, 2010.

[84] G. Marom, R. Haj-Ali, E. Raanani, H. J. Schäfers, and M. Rosenfeld, "A fluid-structure interaction model of the aortic valve with coaptation and compliant aortic root," *Med. Biol. Eng. Comput.*, vol. 50, no. 2, pp. 173–182, 2012.

[85] I. Borazjani, "Fluid-structure interaction, immersed boundary-finite element method simulations of bio-prosthetic heart valves," *Comput. Methods Appl. Mech. Eng.*, vol. 257, pp. 103–116, 2013.

[86] G. Marom, M. Peleg, R. Halevi, M. Rosenfeld, E. Raanani, A. Hamdan, and R. Haj-Ali, "Fluid-structure interaction model of aortic valve with porcine-specific collagen fiber alignment in the cusps.," *J. Biomech. Eng.*, vol. 135, no. 10, pp. 101001–6, 2013.

[87] F. Sturla, E. Votta, M. Stevanella, C. a. Conti, and A. Redaelli, "Impact of modeling fluid-structure interaction in the computational analysis of aortic root biomechanics," *Med. Eng. Phys.*, vol. 35, no. 12, pp. 1721–1730, 2013.

[88] M. Y. S. Kuan and D. M. Espino, "Systolic fluid-structure interaction model of the congenitally bicuspid aortic valve: assessment of modelling requirements.," *Comput. Methods Biomech. Biomed. Engin.*, no. August, pp. 37–41, 2014.

[89] W. Sun, C. Martin, and T. Pham, "Computational modeling of cardiac valve function and intervention.," *Annu. Rev. Biomed. Eng.*, vol. 16, pp. 53–76, 2014.

[90] G. Marom, "Numerical Methods for Fluid – Structure Interaction Models of Aortic Valves," 2014.

[91] M. Swanson and R. E. Clark, "Dimensions and geometric relationships of the human aortic valve as a function of pressure.," *Circ. Res.*, vol. 35, no. 6, pp. 871–882, 1974.

[92] C. J. Chuong and Y. C. Fung, "Three-dimensional stress distribution in arteries.," *J. Biomech. Eng.*, vol. 105, no. 3, pp. 268–274, 1983.

[93] W. Huang and R. T. Yen, "Zero-stress states of human pulmonary arteries and veins.," *J. Appl. Physiol.*, vol. 85, no. 3, pp. 867–873, 1998.

[94] J. Zhao, J. Day, Z. F. Yuan, and H. Gregersen, "Regional arterial stress-strain distributions referenced to the zero-stress state in the rat.," *Am. J. Physiol. Heart Circ. Physiol.*, vol. 282, no. 2, pp. H622–H629, 2002.

[95] X. Huang, C. Yang, C. Yuan, F. Liu, G. Canton, J. Zheng, P. K. Woodard, G. a Sicard, and D. Tang, "Patient-specific artery shrinkage and 3D zero-stress state in multi-component 3D FSI models for carotid atherosclerotic plaques based on in vivo MRI data.," *Mol. Cell. Biomech.*, vol. 6, no. 2, pp. 121–134, 2009.

[96] L. Speelman, E. M. H. Bosboom, G. W. H. Schurink, J. Buth, M. Breeuwer, M. J. Jacobs, and F. N. van de Vosse, "Initial stress and nonlinear material behavior in patient-specific AAA wall stress analysis.," *J. Biomech.*, vol. 42, no. 11, pp. 1713–9, Aug. 2009.

[97] S. Grbic, T. Mansi, R. Ionasec, I. Voigt, H. Houle, M. John, M. Schoebinger, N. Navab, and D. Comaniciu, "Image-based computational models for TAVI planning: From CT images to implant deployment," in *Lecture Notes in Computer Science (including subseries Lecture Notes in Artificial Intelligence and Lecture Notes in Bioinformatics)*, 2013, vol. 8150 LNCS, no. PART 2, pp. 395–402.

[98] R. Haj-Ali, G. Marom, S. Ben Zekry, M. Rosenfeld, and E. Raanani, "A general three-dimensional parametric geometry of the native aortic valve and root for biomechanical modeling," *J. Biomech.*, vol. 45, no. 14, pp. 2392–2397, 2012.

[99] J. S. Rankin, M. C. Bone, P. M. Fries, D. Aicher, H. J. Schäfers, and P. S. Crooke, "A refined hemispheric model of normal human aortic valve and root geometry," *J. Thorac. Cardiovasc. Surg.*, vol. 146, no. 1, 2013.

[100] Y. Zheng, M. John, R. Liao, A. Nöttling, J. Boese, J. Kempfert, T. Walther, G. Brockmann, and D. Comaniciu, "Automatic aorta segmentation and valve landmark detection in C-Arm CT for transcatheter aortic valve implantation," *IEEE Trans. Med. Imaging*, vol. 31, no. 12, pp. 2307–2321, 2012.

[101] A. M. Pouch, H. Wang, M. Takabe, B. M. Jackson, C. M. Sehgal, J. H. Gorman, R. C. Gorman, and P. A. Yushkevich, "Automated segmentation and geometrical modeling of the tricuspid aortic valve in 3D echocardiographic images," in *Lecture Notes in Computer Science (including subseries Lecture Notes in Artificial Intelligence and Lecture Notes in Bioinformatics)*, 2013, vol. 8149 LNCS, no. PART 1, pp. 485–492.

[102] T. Mansi, I. Voigt, B. Georgescu, X. Zheng, E. A. Mengue, M. Hackl, R. I. Ionasec, T. Noack, J. Seeburger, and D. Comaniciu, "An integrated framework for finite-element modeling of mitral valve biomechanics from medical images: Application to MitralClip intervention planning," *Med. Image Anal.*, vol. 16, no. 7, pp. 1330–1346, 2012.

[103] A. Valentín, J. D. Humphrey, and G. A. Holzapfel, "A Multi-Layered Computational Model of Coupled Elastin Degradation, Vasoactive Dysfunction, and Collagenous Stiffening in Aortic Aging," *Ann. Biomed. Eng.*, vol. 39, no. 7, pp. 2027–2045, Jul. 2011.

[104] N. Xiao, J. D. Humphrey, and C. A. Figueroa, "Multi-scale computational model of three-dimensional hemodynamics within a deformable full-body arterial network," *J. Comput. Phys.*, vol. 244, pp. 22–40, Jul. 2013.

[105] S. Roccabianca, C. A. Figueroa, G. Tellides, and J. D. Humphrey, "Quantification of regional differences in aortic stiffness in the aging human," *J. Mech. Behav. Biomed. Mater.*, vol. 29, pp. 618–634, Jan. 2014.

[106] D. Klepach, L. C. Lee, J. F. Wenk, M. B. Ratcliffe, T. I. Zohdi, J. L. Navia, G. S. Kassab, E. Kuhl, and J. M. Guccione, "Growth and remodeling of the left ventricle: A case study of myocardial infarction and surgical ventricular restoration," *Mech. Res. Commun.*, vol. 42, pp. 134–141, Jun. 2012.

[107] Y.-C. Fung, *Biomechanics*. 1993.

[108] D. M. Ebenstein, D. Coughlin, J. Chapman, C. Li, and L. a. Pruitt, "Nanomechanical properties of calcification, fibrous tissue, and hematoma from atherosclerotic plaques," *J. Biomed. Mater. Res. - Part A*, vol. 91, pp. 1028–1037, 2009.

[109] G. a Holzapfel, T. C. Gasser, and R. W. Ogden, "A new constitutive framework for arterial wall mechanics and a comperative study of material models," *J. Elast.*, vol. 61, pp. 1–48, 2000.

[110] T. C. Gasser, R. W. Ogden, and G. a Holzapfel, "Hyperelastic modelling of arterial layers with distributed collagen fibre orientations.," *J. R. Soc. Interface*, vol. 3, no. 6, pp. 15–35, Feb. 2006.

[111] G. a. Holzapfel, G. Sommer, and P. Regitnig, "Anisotropic Mechanical Properties of Tissue Components in Human Atherosclerotic Plaques," *J. Biomech. Eng.*, vol. 126, no. 5, p. 657, 2004.

[112] A. P. S. Selvadurai, "Deflections of a rubber membrane," *J. Mech. Phys. Solids*, vol. 54, no. 6, pp. 1093–1119, 2006.

[113] O. H. Yeoh, "Some Forms of the Strain Energy Function for Rubber," *Rubber Chemistry and Technology*, vol. 66, no. 5. pp. 754–771, 1993.

[114] N. J. Driessen, R. a Boerboom, J. M. Huyghe, C. V Bouten, and F. P. Baaijens, "Computational analyses of mechanically induced collagen fiber remodeling in the aortic heart valve.," *J. Biomech. Eng.*, vol. 125, no. 4, pp. 549–557, 2003.

[115] H. M. Loree, S. Y. Park, and R. T. L. E. E. B, "STATIC CIRCUMFERENTIAL TANGENTIAL MODULUS TISSUE," vol. 27, no. 2, 1994.

[116] F. Auricchio and R. L. Taylor, "Shape-memory alloys : modelling and numerical simulations the finite-strain superelastic behavior," vol. 7825, no. 96, 1997.

[117] A. Wittek, K. Karatolios, P. Bihari, T. Schmitz-Rixen, R. Moosdorf, S. Vogt, and C. Blase, "In vivo determination of elastic properties of the human aorta based on 4D ultrasound data," *J. Mech. Behav. Biomed. Mater.*, vol. 27, pp. 167–183, 2013.

[118] V. Flamini, A. P. Creane, C. M. Kerskens, and C. Lally, "Imaging and finite element analysis: A methodology for non-invasive characterization of aortic tissue," *Med. Eng. Phys.*, vol. 37, no. 1, pp. 48–54, 2015.

[119] L. Cardamone, A. Valentín, J. F. Eberth, and J. D. Humphrey, "Origin of axial prestretch and residual stress in arteries," *Biomech. Model. Mechanobiol.*, vol. 8, no. 6, pp. 431–446, 2009.

[120] C. Schramm, A. Huber, and K. Plaschke, "The accuracy and responsiveness of continuous noninvasive arterial pressure during rapid ventricular pacing for transcatheter aortic valve replacement.," *Anesth. Analg.*, vol. 117, no. 1, pp. 76–82, Jul. 2013.

[121] C. Capelli, J. Nordmeyer, S. Schievano, P. Lurz, S. Khambadkone, S. Lattanzio, A. M. Taylor, L. Petrini, F. Migliavacca, and P. Bonhoeffer, "How do angioplasty balloons work: a computational study on balloon expansion forces.," *EuroIntervention*, vol. 6, no. 5, pp. 638–42, Nov. 2010.

Annexes

Study	Patient-specific	Subject	TAVI step	Deployment type
Dwyer 2009 [50]	No	Migration forces on TAV	Post-op	-
Sun 2010 [43]	No	Stress in leaflet and hemodynamics for elliptical TAV	Post-op	-
Sirois 2011 [8]	Yes	Hemodynamics before and after TAVI	Deployment & post-op	Balloon expandable
Capelli 2012 [51]	Yes	TAV deployment for valve-in- valve and bicuspid cases	Deployment	Balloon expandable
Wang 2012 [52]	Yes	TAV deployment	Deployment	Balloon expandable
Hopf 2012 [53]	Yes	Post-op stress & displacement extraction	Post-op	-
Russ 2013 [54]	Yes	TAV deployment sensitivity study	Deployment	Self expandable
Tzamtzis 2013 [55]	No	TAV radial force	Deployment	Both
Kemp 2013 [56]	No	TAV hemodynamics	Post-op	-
Auricchio 2014 [57]	Yes	TAV deployment	Deployment	Balloon expandable
Wang 2014 [58]	Yes	Aortic Rupture	Deployment	Balloon expandable
Morganti 2014 [59]	Yes	TAV deployment	Deployment	Balloon expandable
Gunning 2014 [60]	Yes	TAV deployment	Deployment	Self expandable
Gessat 2014 [61]	Yes	Post-op stress & displacement extraction	Post-op	-

Tab.1 Simulation studies closely related to TAVI

Study	Type	Subject	Cardiac cycle concerned
Krucinski 1993 [67]	FE	Leaflet flexure	Full
Grande-Allen 1998 [68]	FE	Asymmetry of leaflets	Diastole
Grande-Allen 2000 [69]	FE	Sinus & stress	Diastole
Gyaneshwar 2002 [70]	FE	Dynamic analysis of leaflet & aortic root	Full
Howard 2003 [71]	FE	Dynamic analysis of leaflet & aortic root	Full

Nicosia 2003 [72]	FSI	Patient-specific aortic valve model	Full
Carmody 2003 [73]	FSI	Valve-ventricle coupling	Full
De Hart 2003 [74]	FSI	Leaflet material models : fiber-reinforced vs homogeneous	Full
Arcidiacono 2005 [75]	FE	Prosthesis material : isotropic vs anisotropic	Full
Hose 2006 [76]	FSI	Closure impulse	Diastole
Ranga 2006 [77]	FSI	Sinus	Full
Weinberg 2007 [78]	FE	Multiscale analysis	Full
Katayama 2008 [79]	FSI	Sinus	Full
Viscardi 2010 [80]	CFD	Comparison : bicuspid vs tricuspid	Full
Conti 2010 [81]	FE	Dynamic FE analysis	Full
Labrosse 2010 [82]	FE	Dynamic FE analysis	Full (shortened diastole)
Koch 2010 [83]	FE	Leaflet material	Diastole
Marom 2012 [84]	FSI	Importance of FSI over "dry" FE	Mid-diastole
Kemp 2013 [56]	FSI	Experimental validation	Full
Borazjani 2013 [85]	FSI	Comparison : mechanical prosthesis / bioprosthesis	Full
Marom 2013 [86]	FSI	Collagen fiber network asymmetry	Full
Sturla 2013 [87]	FSI	Comparison "dry" FE / FSI	Full
Kuan 2014 [88]	FSI	2D study of bicuspid valve	Full

Tab.2 Numerical simulations about motion of healthy native aortic valve

Study	Imaging software	mesher	native leaflet	Calcification	Prosthesis
Sirois 2011 [8]	VTKPointpicker	HyperMesh	yes	no	SAPIEN
Capelli 2012 [51]	Mimics	?	yes	yes	SAPIEN
Wang 2012 [52]	Avizo	HyperMesh	yes	yes	SAPIEN
Russ 2013 [54]	Philips Heart Navigator	ICEM CFD	yes	yes	CoreValve
Auricchio 2014 [57]	ITKsnap	Matlab	no	no	SAPIEN
Wang 2014 [58]	Avizo	HyperMesh	yes	yes	SAPIEN

Morganti 2014 [59]	ITKsnap	Matlab	yes	yes	SAPIEN
Gunning 2014 [60]	Mimics	Abaqus	no	no	Custom self-expandable

Tab.3 Conditions for geometric reconstruction in numerical models

Study	Aorta/Leaflet	Calcification	Prosthesis	Zero-pressure
Sirois 2011 [8]	HE (Fung) [107]	none	?	no
Capelli 2012 [51]	HE (Mooney-Rivlin)	LE	EP (E=193 MPa) stainless steel	no
Wang 2012 [52]	HE [96]	LE [108]	EP cobalt-chromium (E=243 GPa)	yes
Russ 2013 [54]	Rigid/LE/HE	LE	EP Nitinol	no
Auricchio 2014 [57]	HE [109]	none	EP stainless steel	no
Wang 2014 [58]	HE [110]	LE [111]	EP stainless steel [55]	?
Morganti 2014 [59]	HE [112][113]	LE	EP cobalt-chromium (E=233GPa)	no
Gunning 2014 [60]	HE (Mooney-Rivlin)	none	HE Nitinol [55]	no

Tab.4 Material models used in TAVI simulations

Study	Friction Coefficient
Capelli 2012 [51]	0.25
Wang 2012 [52]	0.1
Russ 2013 [54]	0.2
Auricchio 2014 [57]	0.2
Morganti 2014 [59]	Vertical constraint instead of friction
Gunning 2014 [60]	0.25

Tab.5 Coefficient of friction reported in simulation studies

4.1.2 Synthèse

Cette revue de la littérature démontre la tendance actuelle des études de simulation numérique personnalisée à s'intéresser principalement au déploiement de la prothèse et à son impact sur les complications per et post procédurales qui constituent les préoccupations principales des cliniciens. La plupart des études évaluent le résultat du déploiement de la prothèse selon les recommandations des fabricants. Ainsi, des études ont évalué les interactions entre la prothèse et le tissu aortique natif pour prédire le fonctionnement de la prothèse et ses conséquences. L'analyse des forces de contact entre la prothèse et les tissus natifs environnants a été utilisée pour prédire le risque de troubles conductifs post-procédure dans une série de 112 patients implantés de valves auto-expansibles. Elle se montre plus efficace qu'un facteur de risque classiquement décrit comme la profondeur d'implantation, pour prédire cette complication (113). Une telle analyse a également été proposée pour prédire le risque de rupture d'anneau liée aux calcifications (114). La simulation du déplacement des cusps aortiques calcifiées a également été proposée pour évaluer le risque d'occlusion coronaire liée au TAVI (115). Plusieurs études de simulation utilisant la méthode des éléments finis se sont intéressées à la distance entre le stent ou sa jupe externe et les tissus natifs comme une mesure de substitution de la fuite aortique post procédure (115,116). Certaines études ont tenté d'affiner les résultats en modifiant les positions de déploiement de la prothèse (117,118), en tenant compte de techniques comme la post-dilatation (115), ou encore en associant à la méthode des éléments finis une évaluation de la mécanique des fluides (118). En résumé, l'aspect du positionnement de la prothèse commence à être abordé en littérature par l'angle du post-déploiement « Quel est l'impact du positionnement final sur les performances ? » mais pas encore par celui du pré-déploiement « Quels éléments déterminent le positionnement final ? »

Il semble pourtant pertinent d'évaluer cet aspect afin notamment de prévoir les cas de positionnement complexe de la prothèse plutôt que d'y être directement confronté pendant la procédure. L'expérience clinique montre que ces cas d'angulation insatisfaisante entre la prothèse et la racine aortique ne sont pas si rares et qu'il est toujours difficile de prévoir le mouvement de bascule de la prothèse dans ces conditions. Par ailleurs, tenter des manœuvres de correction ou réaliser une analyse prolongée du comportement de la prothèse selon les manipulations de l'opérateur sur les outils n'est tout simplement pas possible en peropératoire en raison des risques de mauvaise tolérance hémodynamique ou de complications lors de cette phase de déploiement. Compte tenu de ces limitations, la simulation numérique personnalisée semble donc une piste prometteuse en complément des techniques de planification usuelle pour

tenter de répondre aux questions suivantes : « Comment les outils se positionnent dans la valve aortique et comment influencer leur positionnement ? ».

Comme nous l'avons rappelé dans le premier chapitre, la prothèse et son cathéter de pose sont amenés au niveau de la valve aortique grâce à un guide rigide[7] qui franchit la sténose valvulaire et prend appui dans le ventricule gauche. Des manipulations des opérateurs sur ce guide peuvent ainsi produire des mouvements fins de la prothèse. Par exemple, une poussée sur le guide va lui faire prendre un appui plus prononcé sur le ventricule gauche ce qui aura pour effet de faire légèrement remonter la prothèse en position plus aortique. Si cette poussée est couplée à une poussée sur le cathéter de pose, on peut assister à une « co-axialisation » de la prothèse avec la racine aortique notamment lorsque celle-ci présente une anatomie horizontale. La limite de ces manœuvres sur le guide réside dans le fait de ne pas créer de tension excessive sur le ventricule gauche qui induirait un risque de rupture trop important. L'expérience montre donc que le guide rigide permet de modifier le positionnement de la prothèse. Ainsi le positionnement du guide lui-même tant au niveau valvulaire que ventriculaire gauche pourrait influencer le positionnement final de la prothèse et donc les résultats de la procédure. Au-delà de la conception des dispositifs et de l'analyse et la compréhension de leurs effets, des questions subsistent quant à la possibilité de rendre les approches de simulation numérique prédictives et spécifiques patient afin de planifier la procédure. Par conséquent, l'objectif de notre travail a été de produire un modèle de simulation numérique personnalisé permettant de prédire le positionnement initial dans la valve aortique du guide rigide au cours d'une procédure TAVI ainsi que ses interactions avec le ventricule gauche. Outre l'aspect calculatoire complexe de ce type de modèle, il représente également un challenge dans la définition de ses conditions aux limites, son paramétrage et sa validation qui nécessite une collaboration étroite entre ingénieurs et cliniciens pour sa mise en œuvre.

4.2 Exploitation des données d'imagerie

L'approche que nous proposons s'appuie sur l'exploitation des données d'imagerie acquises en routine clinique. La structure anatomique tridimensionnelle (3D) en entrée de la simulation numérique est issue du scanner préopératoire. Le paramétrage du modèle du guide interagissant avec la structure anatomique est réalisé par confrontation à l'imagerie

[7] Dénomination « clinique » de ce guide qui présente en réalité des propriétés mécaniques (rigidité) variables dans ses différentes portions.

bidimensionnelle (2D) peropératoire. La validation du modèle de simulation numérique impliquant la comparaison de ses résultats avec la réalité clinique, en l'occurrence l'angiographie peropératoire, certaines méthodes de traitement des images pré et peropératoires ont été nécessaires à sa réalisation. Il est donc utile d'en rappeler ici les grands principes.

L'anatomie 3D spécifique du patient étant issue de l'imagerie tomographique préopératoire, il était nécessaire de pouvoir la repositionner dans un repère commun avec celui de l'angiographie 2D peropératoire. Ce processus de traitement d'image est appelé recalage. Afin de faciliter cette procédure, nous devions par ailleurs extraire de l'ensemble du volume 3D préopératoire, un volume limité à la région d'intérêt du ventricule et de l'aorte ascendante. Ce processus est quant à lui désigné sous le terme de segmentation.

Dans les sections suivantes, nous rappellerons les grands principes de ces deux étapes du traitement de l'image et présenterons les contributions originales produites dans le cadre de cette Thèse sur ces problématiques de traitement de l'image.

4.2.1 Segmentation

A) Généralités

La segmentation d'image est une opération de traitement d'images qui a pour but de rassembler des pixels entre eux suivant des critères prédéfinis. Les pixels reflétant l'information d'intérêt sont ainsi regroupés afin de constituer une partition de l'image.

Les méthodes de segmentation couramment utilisées dans le domaine médical, notamment dans la segmentation des structures vasculaires, se distinguent par leur finalité qui est de détecter une « région » ou des « contours ». Le seuillage est la technique de segmentation la plus simple et la plus utilisée au quotidien dans le domaine médical (119). Elle permet de séparer en deux classes les intensités de chacun des pixels contenus dans une image, grâce à un seuil défini par l'utilisateur ou automatiquement. La croissance de région (« region growing » consiste à faire « grossir » une région de pixels à partir d'un point de départ, appelé germe (120,121). Ces méthodes sont généralement semi-automatiques, nécessitant une initialisation par l'utilisateur. Les approches « région » ont pour inconvénient d'incorporer facilement des pixels voisins de même intensité mais appartenant à un organe ou une structure voisine et différente de celle étudiée. Pour remédier à ce problème elles peuvent être combinées à des méthodes basées contours.

Les approches basées contours cherchent à exploiter le fait qu'il existe une transition détectable entre deux régions connexes et se basent sur les propriétés locales des bords. Cette méthode nécessite un prétraitement obligatoire pour éviter de détecter le bruit (filtre de Canny par exemple (122)). Malgré ce filtrage, les images sont souvent difficiles à exploiter sauf si elles sont très contrastées. Les contours extraits sont la plupart du temps morcelés et peu précis, il faut alors utiliser des techniques de reconstruction de contours par interpolation ou connaître a priori la forme de l'objet recherché. Des méthodes ont ainsi été développées telles que les contours actifs utilisant des modèles déformables (*snakes* (123)), les courbes de niveaux (*level set*(124,125)).

Certaines approches peuvent également faire appel à des méthodes « basées Atlas » permettant d'intégrer de la connaissance *a priori* (126). Celles-ci reposent sur une base de données au sein de laquelle les structures anatomiques d'intérêt ont été segmentées manuellement par un expert. L'atlas contient à la fois le résultat des délinéations manuels et les images associées (connaissance a priori). Un recalage élastique entre les images de l'atlas et l'image à segmenter permet ainsi d'estimer le champ de déformation à appliquer à une délinéation de l'atlas pour la transposer sur l'image à traiter et ainsi la segmenter.

B) Segmentation des structures vasculaires

Une revue de la littérature rapporte les travaux sur les techniques de segmentation de la lumière vasculaire utilisées dans le cadre d'examens 3D (127). Cette revue présente les techniques de segmentation selon trois axes : les modèles qui permettent d'intégrer une connaissance a priori sur les structures vasculaires (géométrie, apparence), les caractéristiques ou primitives détectables dans l'image, et les schémas d'extraction qui combinent modèles, primitives et algorithmes d'optimisation pour parvenir au résultat de segmentation. Les trois grandes classes de primitives vasculaires et leurs filtres et détecteurs utilisés pour évaluer un modèle vasculaire sont :

- les primitives isotropes, n'exploitant pas l'élongation présumée d'un vaisseau sanguin (128–130) et faisant intervenir une caractérisation locale de l'intensité du vaisseau d'intérêt,
- les primitives exploitant la géométrie 3D locale (131) et impliquant notamment les méthodes dérivatives telles que l'étude de la Hessienne multi-échelle (132,133), les

méthodes intégratives fondées sur l'étude des moments d'inertie (134–136), et l'optimisation locale d'un modèle hybride (137–139),

- les primitives 2D évaluant les sections orthogonales des vaisseaux d'intérêt ; les méthodes reposent généralement sur l'évaluation de la position médiale (128,131) et d'une détection plus ou moins grossière de la frontière de la lumière vasculaire utilisant par exemple la technique du ray-casting (140).

Après ces techniques de prétraitement d'images, les algorithmes d'extraction mis en œuvre pour la segmentation de la lumière vasculaire à proprement parler peuvent aussi se classer en trois groupes:

- Les algorithmes de croissance de région; cette catégorie comprend la croissance de région classique (141,142), fondée sur des critères d'inclusion voxel par voxel, mais aussi les algorithmes de propagation par front (143,144) où la cohérence spatiale du processus est contrôlée. De tels algorithmes procèdent de manière itérative et progressive, permettant notamment l'inclusion de critères adaptatifs améliorant la robustesse et la précision du résultat final.
- Les méthodes de contours actifs (145,146); cette catégorie inclut un certain nombre de méthodes paramétriques (*snakes*) (147) spécifiquement adaptées aux structures fines telles que les vaisseaux sanguins, ainsi que des approches implicites telles que des méthodes par ensembles de niveaux (*level-sets*) (148) dédiées à la segmentation vasculaire.
- Les approches fondées sur la ligne centrale; ces algorithmes visent avant tout à extraire la structure médiale des vaisseaux cibles; on distingue les méthodes par suivi direct, qui segmentent itérativement le vaisseau en suivant pas-à-pas sa ligne centrale (135,140), et les processus d'optimisation tels que les méthodes par chemins minimaux (149,150).

Dans la pratique courante, la plupart des logiciels dédiés à l'analyse des structures vasculaires propose une segmentation automatique à l'aide des algorithmes cités précédemment. Dans les cas où la segmentation automatique n'est pas possible (images peu ou pas contrastées, artéfacts), les logiciels utilisés en routine offrent la possibilité d'une interaction avec l'utilisateur qui devra alors extraire certaines informations manuellement.

C) Développement et validation d'une segmentation automatique de l'aorte ascendante

Afin de faciliter la réalisation de simulations à partir de l'anatomie 3D du patient, extraite du scanner préopératoire, il nous fallait disposer d'une méthode de segmentation la plus automatisée possible de la région d'intérêt. Les segmentations du ventricule gauche et de l'aorte ascendante étaient réalisées séparément avant d'être importées dans le logiciel de modélisation 3D ANSYS SpaceClaim (ANSYS, Canonsburg, PA, Etats-Unis) où elles étaient associées. Concernant le ventricule, la segmentation était réalisée de manière interactive par l'utilisation du logiciel 3D-Slicer (151). Pour l'aorte ascendante, nous avons tiré profit de travaux initiés dans le cadre de mon Master 2 abordant la problématique de l'assistance peropératoire et de la réalité augmentée dans le cadre des procédures TAVI en utilisant le logiciel Endosize (Therenva, Rennes, France) (152). Ces travaux ont contribué à développer une méthode de segmentation hybride impliquant des méthodes basées sur des modèles géométriques et statistiques de détection des lignes centrales, associées à une méthode de contours actifs 3D et permettant la détection automatique de points d'intérêt anatomiques. La validation de cette méthode par rapport à des mesures d'experts est présentée dans l'article original suivant.

MINIMALLY INVASIVE THERAPY & ALLIED TECHNOLOGIES
https://doi.org/10.1080/13645706.2018.1488734

Taylor & Francis
Taylor & Francis Group

ORIGINAL ARTICLE

Automatic aortic root segmentation and anatomical landmarks detection for TAVI procedure planning

Florent Lalys[a], Simon Esneault[a], Miguel Castro[b,c], Lucas Royer[a], Pascal Haigron[b,c], Vincent Auffret[b,c,d] and Jacques Tomasi[d]

[a]Therenva, Rennes, France; [b]INSERM, Rennes, France; [c]Signal and Image Processing Laboratory (LTSI), University Rennes 1, Rennes, France; [d]Department of Cardiothoracic and Vascular Surgery, CHU Rennes, Rennes, France

ABSTRACT

Purpose: Minimally invasive trans-catheter aortic valve implantation (TAVI) has emerged as a treatment of choice for high-risk patients with severe aortic stenosis. However, the planning of TAVI procedures would greatly benefit from automation to speed up, secure and guide the deployment of the prosthetic valve. We propose a hybrid approach allowing the computation of relevant anatomical measurements along with an enhanced visualization.

Material and methods: After an initial step of centerline detection and aorta segmentation, model-based and statistical-based methods are used in combination with 3D active contour models to exploit the complementary aspects of these methods and automatically detect aortic leaflets and coronary ostia locations. Important anatomical measurements are then derived from these landmarks.

Results: A validation on 50 patients showed good precision with respect to expert sizing for the ascending aorta diameter calculation (2.2 ± 2.1 mm), the annulus diameter (1.31 ± 0.75 mm), and both the right and left coronary ostia detection (1.96 ± 0.87 mm and 1.80 ± 0.74 mm, respectively). The visualization is enhanced thanks to the aorta and aortic root segmentation, the latter showing good agreement with manual expert delineation (Jaccard index: 0.96 ± 0.03).

Conclusion: This pipeline is promising and could greatly facilitate TAVI planning.

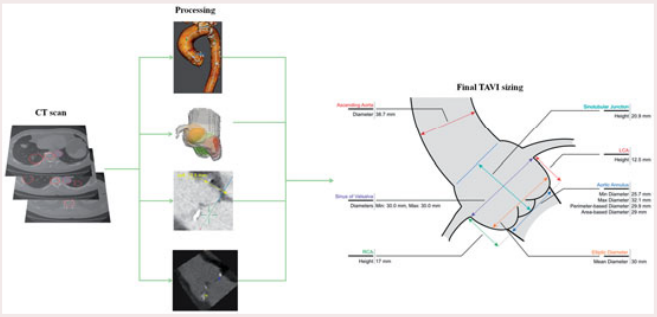

ARTICLE HISTORY
Received 4 September 2017
Accepted 21 May 2018

KEYWORDS
TAVI; statistical-based methods; active contour models; endovascular procedures

Introduction

Minimally invasive trans-catheter aortic valve implantation (TAVI) is an emerging technique that is especially suitable for high-risk patients with severe aortic stenosis, but that has also the potential to be applied to lower surgical-risk patients [1]. However, exact targeting remains very important, since complications can appear due to a misplaced valve. Adverse effects arising from a misplaced valve can be reduced with improved patient selection and aortic sizing. Specifically, it is crucial to decide the suitable type and dimensions of the prosthesis based on the aortic root geometry. For this type of pre-procedural planning, computed tomography angiography (CTA) scan has been accepted as the modality of choice.

Using CTA, a number of studies have proposed imaging pipelines to extract the aortic valve anatomical parameters and derived clinical measurements. While solutions using manual interactions have been first proposed to guide TAVI planning [2,3], automatic planning can reduce the inconsistency in

CONTACT Florent Lalys florent.lalys@therenva.com Therenva, 4 rue Jean Jaures, 35000 Rennes, France

sizing due to inter-observer variability [4]. From the TAVI planning, many steps can be independently decomposed, from the segmentation of the thoracic aorta to the automatic detection of key anatomical landmarks. For thoracic aorta segmentation, multi-atlas-based segmentation with Hough transform have been proposed in non-contrast CT [5] or with 3 D level set approaches [6] in CTA. For aortic root segmentation, 3 D normalized cuts [7,8] have been used. Korosoglou et al. [9] used a model-based segmentation approach to highlight the usefulness of software-assisted pre-procedural assessment, while Gao et al. [10] automatically segment the aortic root following an atlas-based approach.

Automatic detection of landmarks is essential for TAVI planning but often laborious to extract. From these measurements, annulus radius and orientation, and distance from annulus plane to right and left coronary ostia can be derived. Zheng et al. [11,12] proposed a learning-based approach to automatically detect major landmarks with marginal space learning based on the C-arm CT. Model-based approach has been followed by Waechter et al. [13] to locate coronary ostia and annulus plane. Ionasec et al. [14] also proposed a valve model to detect landmarks but their work was based on 4 D CT. Automatic measurements of aortic annulus diameters have been proposed with 3 D transesophageal echocardiography (TEE) [15] or ultrasound images [16–18]. Grbic et al. [19] employed robust machine learning algorithms to estimate the valve model parameters from non-contrast CT including information on valve leaflets and calcium. Segmentation of aortic valve from TEE using an improved probability estimation and continuous max-flow approach has also been proposed [20], or using a combination of shape-based B-Spline explicit active surface and generalized Hough transform [21].

From the literature, it has been demonstrated that automated landmarks detection allows standardizing the planning, reducing inter-observer variation and reducing sizing time. While specific aspects of TAVI planning have been mostly studied independently to date, and often with imaging modalities that are not adopted by the cardio-vascular community, there is no standardized automated solution that encompasses the different steps that compose the TAVI planning, i.e., segmentation of the thoracic aorta, extraction of aorta centerlines, aortic root segmentation and major anatomical landmarks detection. The purpose of this work is to propose a complete TAVI planning tool based on an image processing pipeline that exploits the complementary aspects of state-of-the-art detection approaches.

Material and methods

The proposed image-processing pipeline consists of four main steps and is depicted in Figure 1. The input data are the pre-procedural electrocardiographic (ECG)-gated CTA, widely adopted by cardio-vascular surgeons. They are loaded into the EndoSize® software (Therenva, Rennes, France) [22], a CE- and FDA-marked validated medical device for planning and sizing of endovascular procedures. After initial centerline extraction and aorta segmentation, a method for automatic detection of aortic leaflets is presented, as well as a method for the automatic detection of the coronary artery ostia. For enhanced 3 D visualization and landmarks adjustment, we also propose a 3 D segmentation of the aortic root. The final step includes a refinement of anatomical landmarks position. Each step is independently presented and validated using a large dataset of patients operated for TAVI.

Step no. 1 and step no. 2 – enterline extraction and aorta segmentation

The only required user interaction is the placement of one seed point approximatively set in the aortic root. A volume of interest (VOI) is set in order to keep the ascending aorta, the aortic arch and the descending aorta, using volumes resolution of $1 \times 1 \times 1$ mm. Then, after a rough segmentation of the whole aorta using a binary threshold (100 HU to 600 HU), a dynamic programming approach is applied in the Hough space for localizing key center points in the aorta. We exploit here the 3-D tubular shape characteristic of the aorta, where appearance of the ascending and descending aortas in axial slices approximates a circular shape. The objective is to choose one point in the Hough accumulator of each axial image. A dynamic programming approach is employed to find the optimal combination of points from the Hough accumulators by taking both the center coordinates and the radius as input parameters. We finally used a fast-marching-based minimal path extraction to refine the centerline detection in case of errors.

Starting from the detected centerline, the aorta is also automatically segmented. As this step has already been presented in a previous paper [22], it will not be described in detail here. This segmentation of the upper part of the aorta is mainly used for visualization purposes (Figure 2), but is also useful to determine the ascending aorta diameter, which is a key parameter for TAVI planning. Min, max and mean diameter of each slice perpendicular to the centerline are made available to the user.

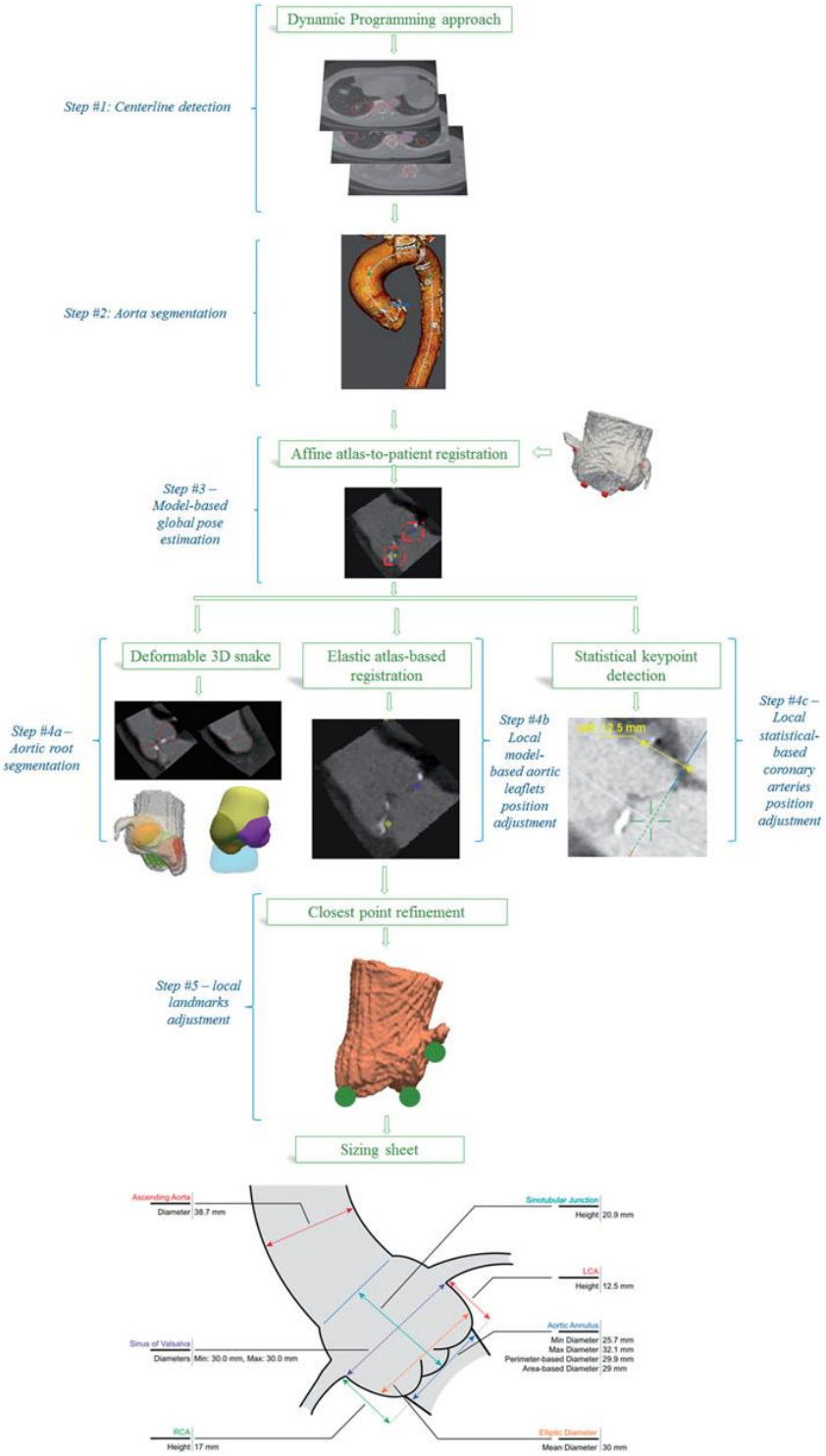

Figure 1. Workflow of segmentation/detection within the TAVI planning software.

Step no. 3 – Global pose estimation

The processing pipeline then focuses on the aortic root. From the final segmented aorta, its centerline, and the user seed point, a second VOI centered on the aortic root is derived with a tube mask of constant diameter (computed according to the maximum aorta diameter) along the centerline and smoothed

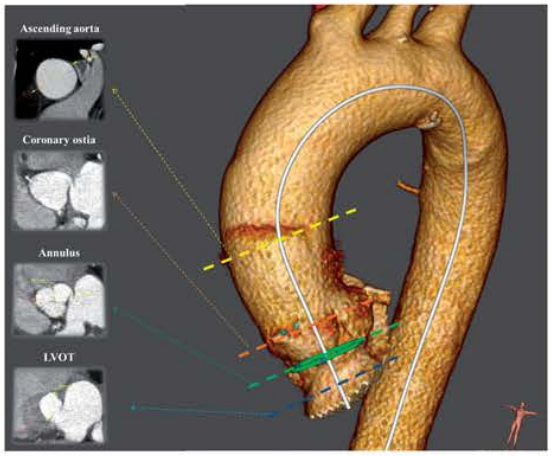

Figure 2. Visualization of the different aorta levels.

using anisotropic diffusion. Then, the global pose of the aortic root was estimated following a model-based approach. Due to computation time constraint, a single low resolution atlas (average model) of the aortic root was constructed offline using 25 volumes following the standard iterative methodology of atlas creation [23], resulting in a volume with both an average unbiased shape and average intensity (size $26 \times 26 \times 26$, $2\,mm^3$ isotropic resolution). Internal experiments were conducted and showed that from 25 patients, the accuracy of the global pose did not change significantly. Eight key points were positioned on the patient's images by an expert and warped into the atlas coordinate system: the left and right coronary ostia, the three aortic cusps leaflets and three seed points approximatively corresponding to the barycenter of the cusps. Then, the key points information was transferred to the patient coordinate system by an affine intensity-based registration algorithm (metric: cross-correlation, optimizer: Powell, isotropic scaling), where calcifications were masked out using a simple threshold (intensity >800 HU). From the position, orientation, and scale of the average shape, we can infer a first rough estimation of the position of each of the eight anatomical keypoints.

Step no. 4 – Local landmarks detection and aortic root segmentation

The eight key points are further either refined or directly used as seed points under the guidance of their own specific detectors.

Step no. 4a – Aortic root segmentation: Starting from 2 mm diameter spheres initialized from seed points in the barycenter of the three cusps (computed from step *no.*3), 3D deformable models were employed to accurately segment the aortic root by constraining smooth boundaries. Specifically, a 3D gradient vector flow snake [24] with a descent gradient optimizer was employed, with proper internal and external energy tuned to keep a smooth curvature along the cusps (alpha =0.1, beta =3, gamma =0.01, number of iterations =200). Combining these segmentations allows extracting the entire aortic root, and is useful to remove all unnecessary arterial structures (e.g., heart, coronary arteries) for proper visualization.

Step no. 4b – Leaflet position adjustment: Similar to hierarchical approaches, and using the positions initialized in step *no.*3, the three aortic cusps leaflets are refined in a smaller 2cm diameter VOI. Three high resolution atlases (size $26 \times 26 \times 26$, $0.6\,mm^3$ isotropic resolution) were constructed using the same learning database of 25 patients, and deformable registration (diffeomorphic demons' algorithm, cross-correlation similarity metric, gradient descent optimizer, rigid registration initialization) was used to warp final landmark positions on the different patient local VOIs.

Step no. 4c – Coronary ostia position adjustment: A training phase is necessary to learn the relationship between the image and the coronary ostia location. We used a combination of 3D Haar-like features, histogram of gradient (HoG) and speeded up robust features (SURF) trained using a Support Vector Machine (gaussian kernel) on an external database of 100 patients originally intended for thoracic endovascular aneurysm repair (TEVAR). Even if patients treated with TAVI have usually more calcifications than patients with TEVAR, no significant differences exist for coronary anatomy between both groups. The correct position is automatically detected on the new volume by restraining the area of research in a smaller 2 cm diameter VOI around the positions estimated from step *no.* 3.

Step no. 5 – Landmarks position refinement

To take advantage of all previous methods, results from the different steps were combined. Landmark positions found in step *no.* 4b and step *no.* 4c were further locally refined using the aortic root segmentation from step *no.* 4a, which is well suitable to precisely detect boundaries. Specifically, landmarks were adjusted to the closest point of the 3 D aortic root surface. Important TAVI measurements were then derived from these landmarks. The annulus plane was defined as the plane connecting the three

leaflets. Given the annulus plane, the annulus to ostia distance was also computed for both coronary ostia.

Evaluation

Anonymized electrocardiogram-gated CTA scans (Siemens Healthcare, Munich, Germany) with resolution of $0.87 \times 0.87 \times 0.62$ mm, 75 ml of contrast media, from 50 symptomatic patients (80 ± 5 years old, 65% male) originally intended for pre-operative planning of TAVI at the Rennes University Hospital were systematically obtained during a one-year period between 2015 and 2016. All patients had a tricuspid valve. All steps were independently evaluated. Centerline detection was qualitatively assessed. To be correctly detected, a centerline has to include the ascending aorta, the aortic arch and the descending aorta and has to have all points within the aorta. For aorta segmentation, we computed the maximum ascending aorta diameter, which is another important measure to derive from the planning. The aortic root landmarks detection was compared to a manual expert delineation throughout the pipeline to evaluate the influence of each step. Due to the high inter-observer variability, the same expert (an engineer but with a long background in TAVI planning) annotated the training and test patients. In addition to the position of the landmarks, the annulus radius and the annulus to ostia heights were evaluated. The impact of each step was iteratively validated using a paired sample *t*-test. Finally, the accuracy of the aortic root segmentation was assessed by comparing the segmentation results with manual delineations using the Jaccard index.

Results

Centerline detection and aorta segmentation

Aorta centerlines from 48 patients out of 50 were correctly extracted based on the initial seed point only (Figure 3). For the two remaining patients, very late contrast injections were noticed that highlight other neighboring structures. Qualitatively, aorta segmentations were also conclusive for the entire database (Figure 3), and an error of 2.2 ± 2.1 mm was found when comparing the automatic maximum ascending aorta diameter with the expert sizing.

Anatomical landmarks detection

Landmarks detection showed very accurate results for aortic leaflets detection, and accurate results for coronary ostia detection (Figure 4). Each additional step showed statistically lower errors than the previous step ($p < .05$). Aortic leaflets detection showed errors of 1.96 ± 0.84 mm, 2.34 ± 0.78 mm and 1.23 ± 1.12 mm for the right, left and non-coronary ostia, respectively. The annulus diameter, derived from aortic leaflet detection and the centerline, showed an error of 1.31 ± 0.75 mm, while right and left coronary ostia heights showed errors of 1.96 ± 0.87 mm and 1.80 ± 0.74 mm, respectively.

Figure 3. Examples of centerlines extraction and aorta segmentation for nine patients.

Aortic root segmentation

Aortic root segmentation showed accurate results compared to manual delineations: average Jaccard index of 0.96 ± 0.03, average false-positive ratio of $4.0 \pm 2.3\%$ and an average false-negative ratio of $0.6 \pm 0.2\%$.

Discussion

A TAVI planning tool with automatic measurements is presented that allows for simplified planning. One

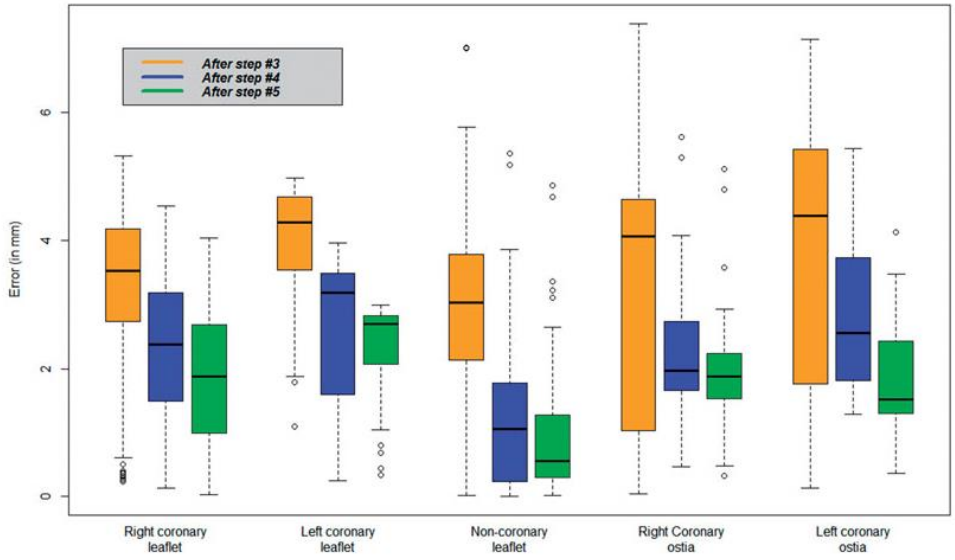

Figure 4. Difference (in mm) between automatic landmark detection and expert positioning at each step of the pipeline.

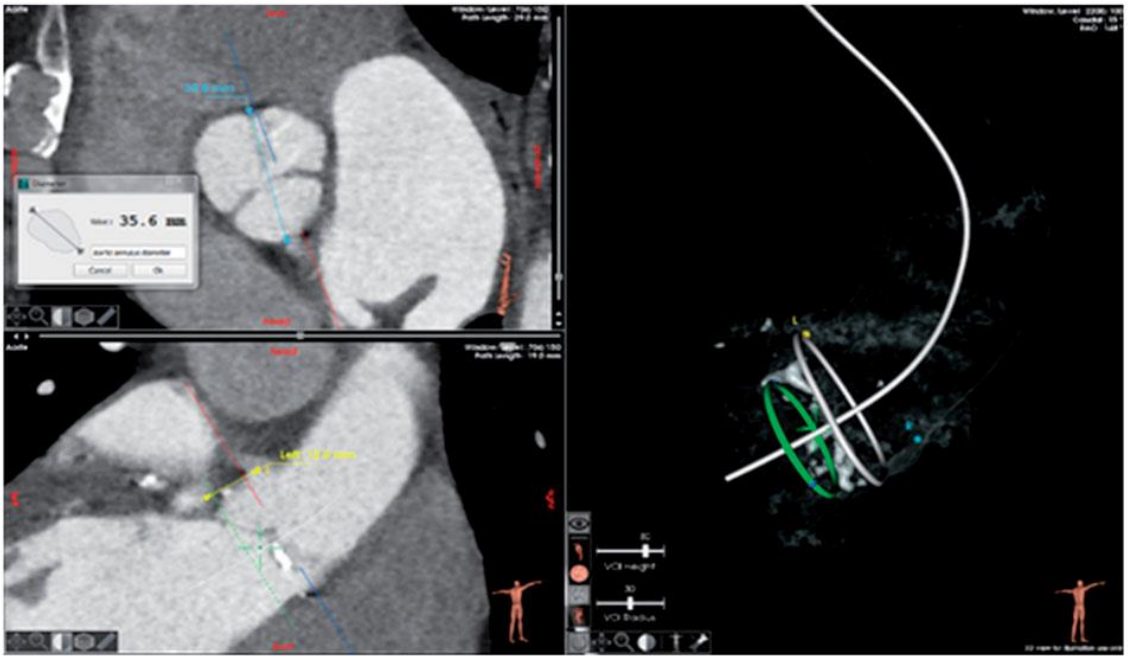

Figure 5. Visualization of the measurement step within the EndoSize® TAVI module.

simple user interaction is needed to directly access the dedicated VOI and retrieve a list of key anatomical measurements, which considerably reduces user interactions compared to traditional TAVI sizing. In certain cases, and according to physician's practice, slight adjustments might be necessary. The visualization is also simplified thanks to the aortic root segmentation, allowing the generation of additional visualization modalities such as valve close-up, half pipe or calcification view (Figure 5). The pipeline showed descent computation burden, with an average total processing time of <8 s on a 3.0 GHz Quad Core 2 CPU, totally compatible with clinical routine. The next step of the software includes the choice of access sites before the generation of a summarized sizing sheet. A set of commercial prosthetic aortic valves is then proposed to be able to choose the most suitable one. This step is of high importance because of the recent development of a large set of available valve prostheses [25]. A clinical study is currently under consideration to evaluate the

time and accuracy obtained with/without the use of this automatic pipeline.

The choice of using various approaches for detecting anatomical landmarks was driven by two main observations: First, model-based approaches may not be adapted for VOIs including arteries, as the registration is driven by the aortic root boundaries more than by arteries. Second, even if supervised discriminative machine learning techniques are robust to different field-of-views and contrast injections, they are not as accurate when dealing with strong intensity differences (i.e., calcifications). Due to the high anatomical variability, our database of 100 patients was not sufficient for this problem. For our aortic root segmentation method, active contour models are robust to noise and less sensitive to large intensity gaps than other image processing methods. Step *no.*5 was therefore useful to constrain landmarks on the aortic root surface. The succession of steps was validated by systematically quantifying errors for each landmark and the derived measures.

Compared to other studies, our current framework demonstrated similar accuracies, but proposes a wide set of automatic measurement and visualization tools that no study has presented to date. While segmentations are difficult to compare due to database heterogeneity or metrics used, it is however possible to confront our landmark detection results with the literature. For aortic leaflets detection based on C-arm CT, Zheng et al. [11,12] achieved a mean detection error of 2.09 ± 1.18 mm, and a 2.07 ± 1.53 mm detection error for coronary ostia, which is very close to our results. Using pre-operative CT, Waechter et al. [13] obtained impressive accuracy for coronary ostia detection (error of 1.2 ± 0.6 mm for the left ostia, 1.0 ± 0.8 mm for the right ostia); however, the validation is performed on only 20 patients and no results on centerline detection and ascending aorta segmentation are proposed. Elattar et al. [26] reported a 2.81 ± 2.08 mm error between automatic landmarks detection and the reference landmarks, comparable with the inter-observer variability of 2.38 ± 1.56 mm, while Liang et al. [27] reported a mean error of 0.69 mm for aortic valve leaflets detection. Considering the high inter-observer variability discussed in the work of Zhao et al. [4] and Elattar et al. [26], a TAVI sizing can be considered accurate enough with results <3 mm, which is the case in this study.

This study suffers from some limitations. First, the manual delineation was performed by a single surgeon, while intra- and inter-expert variability would have been informative. The on-going clinical study includes three surgeons of different experience levels and will allow us to quantify those variabilities. Second, this workflow is well suitable for patients with a tricuspid valve, and the lack of patients with bicuspid valves prevented us to train and validate a specific workflow. Finally, the set of parameters used for the different processing steps has been tuned and validated on clinical data from one single site, and could not be fully optimized when experimenting on CTA with different contrast injection protocols or resolutions.

Conclusion

We proposed and evaluated a hybrid approach for TAVI planning allowing the computation of relevant anatomical measurements. After a minimal user interaction, it is possible to detect the aorta centerline, segment the aorta, detect key anatomical landmarks and segment the aortic root in an automatic fashion. The first model-based pose estimation, the atlas-based leaflets detection, the statistical-based coronary ostia detection, and the automatic segmentation of the aortic root are suitable to directly access the dedicated VOI, propose a set of automatic measurements and enhance the visualization of the aortic root. With an upcoming clinical evaluation, the proposed pipeline is promising and could simplify TAVI planning.

Declaration of interest

Florent Lalys has disclosed those interests fully to Taylor & Francis, and has in place an approved plan for managing any potential conflicts arising from this arrangement.

Funding

This research is sponsored by Therenva, France, and may lead to the development of products.

References

[1] Lindman BR, Pibarot P, Arnold SV, et al. Transcatheter versus surgical aortic valve replacement in patients with diabetes and severe aortic stenosis at high risk for surgery: an analysis of the PARTNER trial (placement of aortic transcatheter valve). J Am Coll Cardiol. 2014;63:1090–1099.

[2] Gessat M, Merk DR, Falk V, et al. A planning system for transapical aortic valve implantation. In: Miga MI, Wong KH, editors; SPIE Proceedings Vol. 7261: Medical Imaging 2009: Visualization, Image-Guided Procedures, and Modeling, Lake Buena Vista, FL, United States, 2009; p. 72611E.

[3] Karar ME, Gessat M, Walther T, et al. Towards a new image guidance system for assisting transapical

minimally invasive aortic valve implantation. Conf Proc IEEE Eng Med Biol Soc. 2009;2009:3645–3648.
[4] Zhao F, Xie X, Roach M. Computer vision techniques for transcatheter intervention. IEEE J Transl Eng Health Med. 2015;3:1900331.
[5] Isgum I, Staring M, Rutten A, et al. Multi-atlas-based segmentation with local decision fusion #x2014;application to cardiac and aortic segmentation in ct Scans. IEEE Trans Med Imaging. 2009;28:1000–1010.
[6] Kurugol S, San Jose Estepar R, Ross J, et al. Aorta segmentation with a 3D level set approach and quantification of aortic calcifications in non-contrast chest CT. Conf Proc IEEE Eng Med Biol Soc. 2012;2012:2343–2346.
[7] Elattar MA, Wiegerinck EM, Planken RN, et al. Automatic segmentation of the aortic root in CT angiography of candidate patients for transcatheter aortic valve implantation. Med Biol Eng Comput. 2014;52:611–618.
[8] Elattar M, Wiegerinck E, Planken N, et al. Automated normalized cut segmentation of aortic root in ct angiography. In: Romero LMR, editor. XIII Mediterranean Conference on Medical and Biological Engineering and Computing 2013. Sevilla, Spain: Springer International Publishing; 2014; p. 1821–1824.
[9] Korosoglou G, Gitsioudis G, Waechter-Stehle I, et al. Objective quantification of aortic valvular structures by cardiac computed tomography angiography in patients considered for transcatheter aortic valve implantation. Cathet Cardiovasc Intervent. 2013;81:148–159.
[10] Gao X, Kitslaar PH, Scholte AJHA, et al. Automatic aortic root segmentation in CTA whole-body dataset; 2016. San Diego (CA), United States: SPIE Medical Imaging; p. 97850F–97857F.
[11] Zheng Y, John M, Liao R, et al. Automatic aorta segmentation and valve landmark detection in C-arm CT for transcatheter aortic valve implantation. IEEE Trans Med Imaging. 2012;31:2307–2321.
[12] Zheng Y, John M, Liao R, et al. Automatic aorta segmentation and valve landmark detection in C-arm CT: application to aortic valve implantation. Med Image Comput Comput-Assist Interv. 2010;13:476–483.
[13] Waechter I, Kneser R, Korosoglou G, et al. Patient specific models for planning and guidance of minimally invasive aortic valve implantation. Med Image Comput Comput-Assist Interv. 2010;13:526–533.
[14] Ionasec RI, Georgescu B, Gassner E, et al. Dynamic model-driven quantitative and visual evaluation of the aortic valve from 4D CT. Med Image Comput Comput-Assist Interv. 2008;11:686–694.
[15] Bersvendsen J, Beitnes JO, Urheim S, et al. Automatic measurement of aortic annulus diameter in 3-dimensional transoesophageal echocardiography. BMC Med Imaging. 2014;14:31–35.
[16] Dong B, Guo Y, Wang B, et al. Aortic valve segmentation from ultrasound images based on shape constraint CV model. Conf Proc IEEE Eng Med Biol Soc. 2013;2013:1402–1405.
[17] Guo Y, Dong B, Wang B, et al. Semiautomatic segmentation of aortic valve from sequenced ultrasound image using a novel shape-constraint GCV model. Med Phys. 2014;41:072901.
[18] Nie Y, Luo Z, Cai J, et al. A novel aortic valve segmentation from ultrasound image using continuous max-flow approach. Conf Proc IEEE Eng Med Biol Soc. 2013;2013:3311–3314.
[19] Grbic S, Ionasec R, Mansi T, et al. Advanced intervention planning for transcatheter aortic valve implantations (TAVI) from CT using volumetric models. In: IEEE 10th International Symposium on Biomedical Imaging: From nano to macro; 2013. San Francisco (CA). p. 1424–1427.
[20] Cai J, Zhuang X, Nie Y, et al. Real-time aortic valve segmentation from transesophageal echocardiography sequence. Int J CARS. 2015;10:447–458.
[21] Queiros S, Papachristidis A, Morais P, et al. Fully automatic 3D-TEE segmentation for the planning of transcatheter aortic valve implantation. IEEE Trans Biomed Eng. 2016;64:1711–1720.
[22] Kaladji A, Lucas A, Kervio G, et al. Sizing for endovascular aneurysm repair: clinical evaluation of a new automated three-dimensional software. Ann Vasc Surg. 2010;24:912–920.
[23] Rueckert D, Frangi AF, Schnabel JA. Automatic construction of 3-D statistical deformation models of the brain using nonrigid registration. IEEE Trans Med Imaging. 2003;22:1014–1025.
[24] Xu C, Prince JL. Snakes, shapes, and gradient vector flow. IEEE Trans Image Process Publ IEEE SS. 1998;7:359–369.
[25] Melnick G, Guerios EE, Agreli G. Modular aortic valve prosthesis for transcatheter aortic valve implantation: a novel concept with a new implantation method. Minim Invasive Ther Allied Technol. 2017;26:60–64.
[26] Elattar M, Wiegerinck E, van Kesteren F, et al. Automatic aortic root landmark detection in CTA images for preprocedural planning of transcatheter aortic valve implantation. Int J Cardiovasc Imaging. 2016;32:501–511.
[27] Liang L, Martin C, Wang Q, et al. Estimation of aortic valve leaflets from 3D CT images using local shape dictionaries and linear coding. Proc. SPIE 9784, Medical Image 2016: Image Process. 2016:978432.

4.2.2 Synthèse

Cet article présente une méthode hybride de segmentation de l'aorte. Notre contribution s'est focalisée sur la définition d'une approche simplifiée de sizing pour le TAVI et son évaluation. Suite à une interaction utilisateur très limitée, la méthode mise en œuvre combine différentes techniques automatiques (seuillage, programmation dynamique, contours actifs 3D, approches basées Atlas) pour fournir au praticien les informations pertinentes et utiles.

Cette méthode a pu être validée sur 50 patients. La précision de la segmentation automatique et sa rapidité (temps de calcul <8 sec) nous permettent aujourd'hui de l'utiliser en routine clinique pour le « sizing » de la région d'intérêt indispensable avant chaque procédure et justifie son choix dans notre approche de simulation numérique personnalisée.

4.3 Recalage

Une fois la segmentation obtenue, il nous fallait, comme précédemment évoqué, pouvoir la mettre en correspondance avec la référence angiographique afin de pouvoir valider les résultats de notre simulation. Ceci peut être réalisé par un procédé de traitement d'image appelé recalage. Dans cette section, nous rappellerons tout d'abord les principes généraux du recalage avant de présenter nos travaux portant sur l'influence des conditions d'acquisition des images pré- et peropératoire sur les résultats du recalage dans un second temps.

4.3.1 Généralités

Le recalage désigne la mise en correspondance dans un référentiel commun, par l'estimation d'une transformation géométrique, de données issues de modalités d'imagerie différentes.

Le recalage permet de mettre en correspondance des images issues de modalités différentes (IRM, TDM, angiographie…) et de dimensionnalités différentes (3D, 2D…). Il peut être défini comme la recherche de la transformation spatiale des points d'une image, en s'appuyant sur les points physiques correspondants d'une autre image, pour que les deux images soient alignées dans le même repère. Ainsi, en recalage, on distingue toujours deux images, l'une étant la référence et l'autre l'image à transformer.

L'image de référence est aussi appelée image cible et l'image à transformer est appelée image source ou image flottante. Dans le cadre de la simulation considérée ici, il s'agit de mettre

en correspondance les images tomographiques 3D préopératoires avec une image fluoroscopique 2D de référence acquise en peropératoire (ce peut également être le cas de la réalité augmentée par fusion d'images pour faciliter la navigation endovasculaire). Néanmoins, selon l'équipement radiologique considéré, l'image peropératoire de référence peut être en 2D (un cliché dans une incidence fixe) ou 3D (acquisition rotationnelle).

Le recalage est un problème complexe et très vaste. L'objectif de cette section n'est pas d'en faire l'état de l'art mais d'en rappeler les principes généraux et de voir quelles sont les méthodes retenues dans notre application. Ces principes et méthodes sont détaillés dans des travaux dédiés (153,154).

Soient une image source A (image transformée) et une image cible B (image de référence) et leur domaine respectif Ω_A et Ω_B. Le recalage a pour but d'estimer la transformation T :

$$T{:}\Omega_A \rightarrow \Omega_B$$

de telle manière que $A \circ T$ soit similaire à B selon un critère prédéfini (fonction d'énergie). Les méthodes de recalage se distinguent entre elles selon 4 critères :

- Les primitives : ce sont les informations extraites de l'image qui sont exploitées pour constituer un critère de distance et contrôler le recalage,
- Le critère de similarité ou de distance : ce critère permet d'évaluer la ressemblance ou la dissemblance entre l'image cible et l'image source transformée, il dépend des primitives et est caractérisé par une valeur extrémale (minimale pour les primitives géométriques et maximale pour les intensités)
- Le modèle de transformation: définit la façon dont l'image est géométriquement modifiée,
- La méthode d'optimisation : c'est la méthode qui permet d'effectuer la résolution numérique afin de déterminer la meilleure solution pour la transformation recherchée. Il s'agit le plus souvent d'un processus itératif qui peut être sensible aux conditions initiales (paramètres de la transformation initiale) afin de converger correctement et rapidement vers le minimum global (paramètres de la transformation / solution recherchée).

A) Primitives

Le choix des primitives utilisées pour guider le recalage est crucial. Il est conditionné par la nature des images à traiter. On distingue deux approches. L'approche géométrique consiste à extraire des primitives géométriques (points, contours) et leur mise en correspondance se fait en minimisant une distance pour diminuer itérativement la dissemblance entre l'image observée et l'image résultant de la transformation recherchée. L'approche iconique utilise l'ensemble de l'information portée par l'image en se basant le plus souvent sur les niveaux de gris et leur mise en correspondance se fait en maximisant le critère de similarité basé sur l'intensité de l'image pour augmenter la ressemblance entre les images.

a) Approche géométrique

L'approche géométrique consiste à trouver les structures communes dans les deux images c'est-à-dire à identifier dans les deux images les primitives géométriques comme les points, les courbes, les surfaces, les volumes, … et à mettre en correspondance ces primitives. Le recalage d'images se fait en deux grandes étapes: la segmentation et la mise en correspondance ou le recalage proprement dit. La segmentation peut être manuelle, semi-automatique voire automatique. A partir de la détection de ces primitives, une multitude d'approches ont été reportées pour réaliser le recalage. On peut citer entre autres la minimisation de la distance euclidienne, la minimisation de la carte de distances (155), les méthodes d'interpolation/approximation (156) et l'algorithme de type ICP (157) (algorithme du point le plus proche itéré – *Iterative Closest Point*).

b) Approche iconique

Cette approche utilise l'information d'intensité attribuée à chaque pixel de l'image, soit en comparant directement les niveaux de gris des images, soit en associant à chaque pixel une valeur déterminée à partir des niveaux de gris et en comparant ces ensembles de valeurs (158). Cette approche ne nécessite pas de réduction préalable de données comme l'approche géométrique qui utilise des sous-ensembles de l'image. Par conséquent la quantité de données est importante. Cette approche consiste essentiellement à optimiser un critère de similarité fondé uniquement sur des comparaisons d'intensités. La méthode de bas niveau est une autre appellation de l'approche iconique. Elle est notamment bien adaptée en recalage multimodal.

c) Approche hybride

L'utilisation conjointe des deux précédentes approches vise à améliorer la robustesse de l'algorithme de recalage en combinant les avantages liés à chaque type d'information. Le terme

d'appariement permettant de mettre en correspondance les objets à recaler est alors composé d'une contribution liée aux informations iconiques et d'une contribution liée aux points de repère géométriques (159,160).

B) Critère de similarité

Comme mentionné précédemment le critère de similarité dépend des primitives. C'est à partir de celles-ci que la fonction de coût est déterminée. Le processus de recalage se fait par la suite en optimisant cette fonction que l'on cherche soit à minimiser pour les distances (approche géométrique) ou à maximiser pour les intensités (approche iconique).

Dans les primitives géométriques, le critère est la distance entre les primitives. La méthode de mesure dépend des sous-ensembles considérés mais le plus souvent la stratégie d'optimisation cherche à minimiser cette distance qui représente le décalage entre les deux images. Dans le cas de points appariés et identifiés dans les deux images, la distance euclidienne est classiquement utilisée. Pour les ensemble de points (courbes), il existe plusieurs méthodes : carte de distance (155), moyenne du carrée de la distance (161), distance de Hausdorff (162).

Pour les approches basées intensité, la similarité peut être mesurée par de nombreuses méthodes également : critère de similarité quadratique, information mutuelle mesure basée sur le coefficient de corrélation, critère de similarité robuste. Dans ces cas, la stratégie d'optimisation cherche à maximiser le critère de similarité.

C) Modèle de transformation

Le choix de la transformation est orienté par la nature de la correspondance géométrique que l'on désire établir entre l'image source et l'image cible. On distingue principalement deux types de transformations.

a) Recalage rigide global et transformations linéaires

Le recalage rigide global consiste à rechercher la transformation géométrique qui permet d'aligner globalement les structures. Le recalage rigide est surtout utilisé pour des objets rigides. Néanmoins, il est possible de l'utiliser pour comparer globalement des objets déformables.

Les transformations utilisées dans le recalage rigide global sont appelées linéaires car pouvant s'écrire sous la forme d'un produit matriciel. Les transformations linéaires incluent plus généralement plusieurs types de transformations qui peuvent être combinées entre elles. Ces transformations peuvent être formulées sous forme de matrice et autoriser une représentation en coordonnées homogènes, très utilisées en géométrie projective pour la représentation des scènes 3D.

Le recalage rigide ou linéaire revient à résoudre l'expression suivante:

$$T = \arg\min_{T \in E} C\,(I, T \circ J)$$

Avec :

T : la transformation recherchée

arg min : la fonction d'optimisation

C : Mesure de similarité

I : image de référence (considérée comme une fonction)

J : image flottante (considérée comme une fonction)

E : espace de recherche

- Transformations rigides

Très utilisées dans le domaine médical pour recaler des images multimodales mono-patient, ce sont les transformations telles que la rotation et la translation (ou isométrie lorsqu'elles sont combinées). Elles permettent de conserver le parallélisme, les angles et les distance sont alors préservés.

- Transformations affines

La transformation affine est la transformation linéaire la plus générale. Elle préserve les segments et peut être une composition de transformations telles que rotation, translation, changement d'échelle ou encore projection. La transformation affine par morceau est aussi utilisée dans le recalage inter-sujets.

- Transformations projectives

Cette transformation est une transformation affine particulière. La projection est essentiellement utilisée dans le domaine du recalage 3D/2D, comme le recalage de données IRM ou Scanner X et de radiographies (163).

b) Transformations non-linéaires

Ici la transformation est définie explicitement en chaque pixel de l'image par un vecteur de déplacement. On parle aussi de transformation élastique, non-rigide. Citons les modèles élastique (164), fluide (165), le flux optique (166) et le modèle de diffusion dont le modèle des démons (167) qui est l'un des plus connus dans le recalage déformable.

D) Algorithme d'optimisation

Les méthodes d'optimisation permettent d'estimer les paramètres de la transformation afin de minimiser ou maximiser le critère de similarité (intensité ou distance). Cette estimation peut être complexe et différentes stratégies peuvent être employées afin d'obtenir une solution satisfaisante dans un temps de calcul raisonnable. On distingue 4 classes de méthodes: méthodes directes, continues, discrètes et heuristiques (168).

4.3.2 Recalage 3D/2D

Une récente revue de la littérature (169) spécifiquement destinée aux méthodes de recalage 3D/2D pour les interventions guidés par l'image, reprenant le papier princeps de Maintz et Viergever (153) propose une classification des différentes méthodes de recalage selon huit critères : modalité d'image, dimensionnalité des images, nature des primitives utilisées, transformation géométrique, procédure d'optimisation, nature du sujet à recaler, applications.

Dans le cadre d'un recalage 3D/2D impliquant un scanner X préopératoire et une fluoroscopie X peropératoire, on parle de recalage « quasi intra-modal ». Il s'agit d'estimer la transformation qui permet de mettre en correspondance les données 3D et 2D (**Figure 37**).

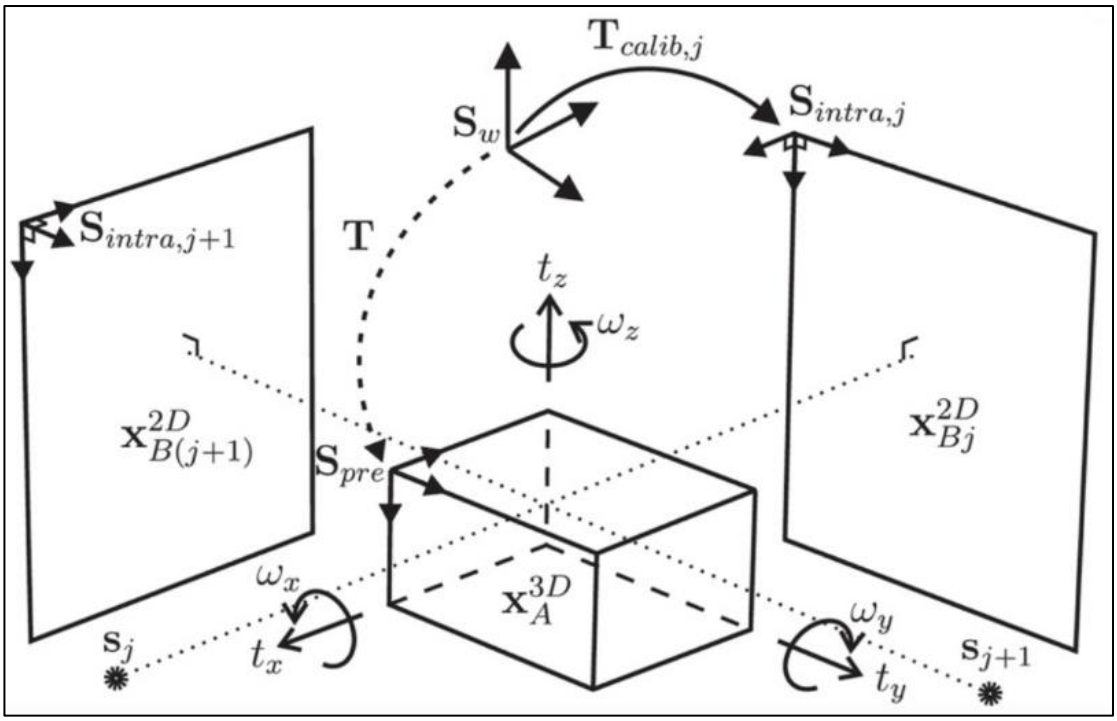

Figure 36- Décomposition géométrique du recalage d'une image 3D avec une image 2D fluoroscopique. S*j* et S_{J+1} sont les directions du faisceau de rayons X par rapport aux images 2D j et (j+1) définies par les systèmes de coordonnées $S_{intra,j}$ et $S_{intra,j+1}$ respectivement. S_w est le système de coordonnées intraopératoire et S_{pre} le système préopératoire. $T_{calib,j}$ est la transformation rigide entre $S_{intra,j}$ et S_w. T est la transformation rigide entre S_{pre} et S_w estimée par le recalage. La transformation rigide T est définie par 6 paramètres tx, ty, tz, ωx, ωy et ωz. Reproduite d'après Markelj et al (169).

Le recalage consiste plus précisément à estimer une transformation géométrique globale 3D-2D combinant une projection perspective ou conique et une transformation rigide 3D-3D représentant la relation spatiale entre l'anatomie du patient (décrite dans le repère d'imagerie 3D pré-opératoire) et l'ensemble source-détecteur du C-arm (repère 3D per-opératoire). Si les matrices de projection sont connues, ce qui est souvent le cas en pratique quotidienne où elles sont issues du système d'acquisition fluoroscopique, le recalage consiste alors à estimer la transformation rigide 3D/3D.

Les primitives utilisées pour le recalage peuvent être de nature extrinsèque ou intrinsèque. Dans le cas des primitives extrinsèques, il s'agit d'utiliser des marqueurs externes à l'image, comme des éléments radio-opaques non soumis à déformation entre les deux images, qui permettent de faciliter le recalage. Les primitives de nature intrinsèque exploitent quant à

elles les structures anatomiques observables dans les images. Trois classes de primitives peuvent être distinguées : basées sur la géométrie (« *feature-based* »), sur l'intensité (« *intensity-based* ») ou sur les gradients (« *gradient-based* ») (169).

Dans le présent travail, la méthode utilisée est basée sur une code de recalage développé au sein du LTSI (170,171). Ce code repose sur une approche géométrique (« *feature-based* ») faisant, comme nous l'avons précédemment évoqué, intervenir une segmentation préalable des structures d'intérêt. Cette méthode de recalage consiste à minimiser la distance entre des points de la structure 3D projetée et des courbes décrivant la structure 2D (typiquement les lignes centrales). Ce type de méthode présente l'intérêt de ne pas avoir à réaliser un appariement de points caractéristiques qui impliquerait dans le cas des structures considérées des opérations manuelles. Toutefois leur robustesse et leur rapidité de mise en œuvre sont directement liées à la qualité de la segmentation.

L'approche de recalage mise en œuvre combine la génération des contours projetés à partir d'une description de la structure anatomique 3D préopératoire au moyen d'un C-arm « virtuel » (**Figure 38**) et l'optimisation de la correspondance entre la projection de la description anatomique 3D préopératoire et de son observation dans l'image 2D per-opératoire (**Figure 39**). Pour réaliser cette optimisation, le logiciel de recalage estime itérativement la pose du C-arm virtuel pour minimiser un critère de distance défini par la distance euclidienne 2D entre le contour de la projection 3D de la segmentation et le contour 2D de la structure d'intérêt dans l'angiographie. Le contourage de la région d'intérêt sur l'angiographie, a été réalisé manuellement par un expert. Une carte de distance à partir du contour 2D de l'aorte est calculée par la méthode de Chamfer. La minimisation du critère de distance est alors réalisée par un algorithme d'optimisation de Powell.

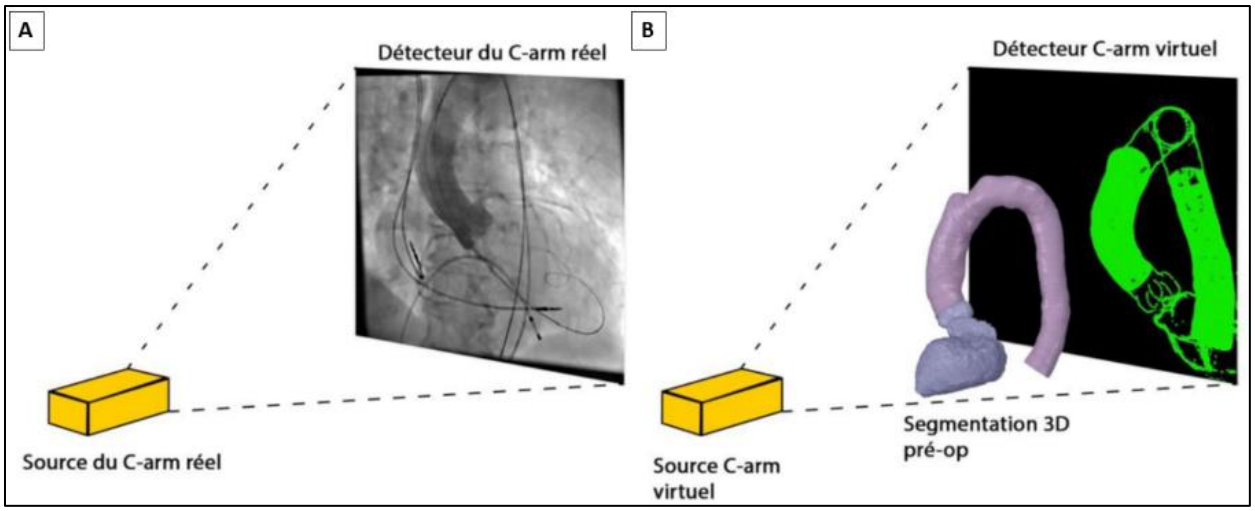

Figure 37 – Phase de projection et de transformation rigide 3D/3D du recalage.

A- Projection per-opératoire. B-Projection virtuelle de la simulation.

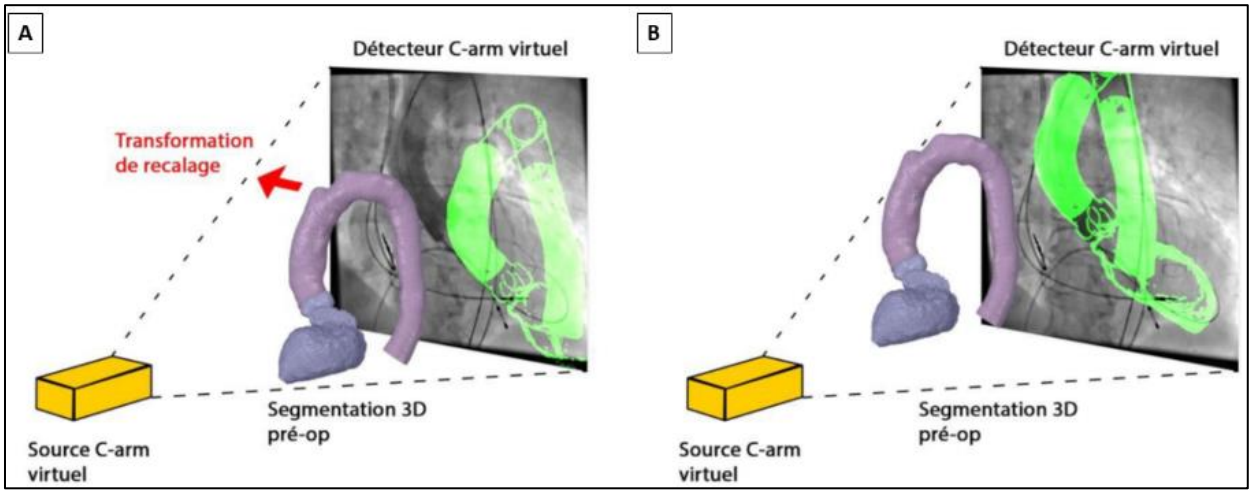

Figure 38 – Phase d'optimisation du recalage. A- L'initialisation du recalage produit une projection insatisfaisante. B- Une nouvelle angulation du C-arm virtuel par rapport à la structure anatomique 3D segmentée (issue du scanner préopératoire) produit une projection plus proche de l'image peropératoire.

4.3.3 Influence des conditions d'acquisition des images sur les résultats du recalage.

Une contrainte importante à considérer dans le contexte du TAVI dans une optique de recalage est le mouvement perpétuel de la région d'intérêt qu'il soit d'origine cardiaque ou respiratoire. Cet élément étant potentiellement de nature à modifier les résultats du recalage, il nous paraissait important d'en évaluer l'influence sur notre stratégie afin d'utiliser secondairement les données d'entrée les plus appropriées possible au processus de recalage que la finalité soit l'augmentation de l'image peropératoire (assistance à la navigation), le paramétrage ou la validation de la simulation.

L'article suivant, soumis pour publication dans le « Journal of Medical Imaging», évalue ainsi le résultat de notre stratégie de recalage en utilisant différentes données d'entrée, prenant en compte les mouvements aortiques et respiratoires. Notre hypothèse principale était que l'utilisation d'images fluoroscopiques peropératoires acquises dans des conditions proches

de celles du volume tridimensionnel utilisé pour la segmentation aboutirait à un meilleur résultat du processus de recalage. Les données d'entrée 3D provenaient du scanner préopératoire et pouvaient varier par leur synchronisation ou non à l'électrocardiogramme et, pour les données synchronisées, par la phase du cycle cardiaque (R-R) à laquelle elles étaient acquises. Les données d'entrée 2D provenaient de l'angiographie peropératoire. Différentes caractéristiques liées à l'acquisition des images pouvaient varier: qualité de l'injection dans l'aorte ascendante, position du diaphragme, instant du cycle cardiaque considéré. Nous avons ainsi évalué sept stratégies en utilisant la position du diaphragme dans les images angiographiques pour tenir compte du mouvement respiratoire en partant du principe que les données tomodensitométriques préopératoires étaient acquises au cours d'une apnée télé-inspiratoire (le diaphragme étant alors en position basse). Les mouvements liés au cycle cardiaque ont été évalués grâce aux données DICOM des fichiers fluoroscopiques qui donnaient accès à l'électrocardiogramme. Les images pouvaient ainsi être rapprochées du volume 3D correspondant à la même phase du cycle cardiaque selon la stratégie de recalage évaluée. Les sept stratégies ont été évaluées sur les données de 25 patients traités au CHU de Rennes sur leur précision globale par la mesure du coefficient de Dice ainsi que par la mesure de l'erreur de re-projection au niveau de points d'intérêt spécifiques (en l'occurrence les premiers millimètres des artères coronaires).

Influence of Aortic and Respiratory Motion on 3D/2D Registration During Transcatheter Aortic Valve Implantation

Authors: Vincent Auffret[1,2,3], Miguel Castro[1,2], Long-Hung Nguyen-Duc[1,2], Hervé Le Breton[1,2,3], Pascal Haigron[1,2]

[1] Université de Rennes 1, LTSI, Rennes, France

[2] INSERM U 1099, Rennes, France

[3] Service de Cardiologie et Maladies Vasculaires, CHU Pontchaillou, Rennes, France

Vincent Auffret and Miguel Castro contributed equally to this work.

Corresponding author: Dr Vincent Auffret, MD, MSc
Address: Cardiology and Vascular Diseases Department, Pontchaillou University Hospital
2 rue Henri Le Guilloux, 35033 Rennes, France.
Email address: vincent.auffret@chu-rennes.fr
Phone number: + 33 299 282 505
Fax: +33 299 282 503

Abstract

Purpose: Patient-specific numerical simulation, and advanced visualization and guidance technology like the augmented angio-navigation can add useful information in relatively complex transcatheter aortic valve implantation (TAVI) procedures. The registration between a three dimensional (3D) model and two dimensional (2D) angiography of the aorta during TAVI procedures is the first step towards augmented fluoroscopy. In this paper, we propose to study the influence of the aortic and respiratory motion on the registration of pre- and intraoperative data during TAVI procedure.

Methods: We studied the registration between 3D pre-operative computed tomography angiography (CTA) and 2D intra-operative fluoroscopy. We considered seven strategies to define the best input data to register, taking into account the aortic and respiratory motion in different manners. Every strategies used the same rigid 3D/2D registration algorithm and differed on the preoperative data, and on the criteria to select the intraoperative frame to register: based on contrast enhancement, temporal data using the cardiac cycle, and the respiratory cycle to account for the movement of the diaphragm. The proposed strategies of registration were evaluated on 25 datasets from patients affected by severe aortic stenosis who underwent TAVI.

Results: Feasibility of the proposed strategies ranged from 68% to 100% of cases. All strategies had comparable mean Dice coefficients ranging from 0.945 to 0.954. Re-projection target registration error for the left and right coronary arteries ranged from 1.75 mm (interquartile range: 0.76-2.74) to 3.26 mm (2.2-4.3), and from 2.53 mm (1.22-3.84) to 4.03 mm (3.16-4.89), respectively. There was no obvious superiority of one strategy over the other in terms of accuracy.

Conclusion: Our work suggest that the conditions of acquisition of the input data in terms of phases of the cardiac, and respiratory cycles, may actually play a limited role in the results of a 3D CTA / 2D fluoroscopy registration for TAVI.

Index Terms— Image Registration, Transcatheter Aortic Valve Implantation, Aortic valve stenosis, computed tomography, fluoroscopy.

Introduction

Aortic stenosis (AS) is the most common valvular disease, with an increasing incidence in the elderly population [1]. Transcatheter aortic valve implantation (TAVI) was developed as an alternative to surgical aortic valve replacement (SAVR) in patients at prohibitive surgical risk. It is now the standard of care for inoperable patients and high-risk patients and a valid alternative to surgery for many intermediate risk patients [2]. Fluoroscopy is the standard imaging technique for guiding TAVI procedures. In order to visualize the aortic root under fluoroscopy a contrast agent need to be injected. To avoid multiple angiographic projections (and injections of a contrast agent), a perpendicular view of the valve, which separately depict all three aortic cusps in one plane (i.e. the deployment projection), is usually determined using the pre-operative computed tomography angiography (CTA). Fluoroscopy-guided procedures pose issues regarding precise location and tracking of anatomical structures such as the valvular plane, which may lead to valve misplacement that further promotes complications and poor prognosis. Registration and fusion of the pre-operative aortic CTA and the intra-operative fluoroscopic angiogram might help to overcome these difficulties. Registration strategies relying on the cone-beam computed tomography (CBCT) or on multiple fluoroscopic frames face issues related to the need for repeated cardiac pacing, multiple contrast injection, synchronization, and X-ray exposure. Therefore, using a single angiographic frame for 3D/2D registration in the setting of TAVI, may be best-suited to the usual clinical workflow, assuming pre- and per-operative data are correctly selected according to the cardiac and respiratory cycle. Moreover, in recent years, there has been an increasing interest surrounding patient-specific numerical simulation strategies regarding the positioning, deployment and performances of transcatheter heart valves [3]. These strategies usually rely on pre-operative CTA data, and may need to be validated through registration with per-operative fluoroscopic data, which implies determining the best input data to register.

In this paper, we propose to study the influence of the aortic and respiratory motion when registering pre- and intra-operative data during TAVI procedure.

Methods

Data acquisition

Anonymized electrocardiogram (ECG)-gated CTA and fluoroscopic data of 25 patients (mean age 81 years old, 40% female) with severe aortic valve stenosis who underwent TAVI at Rennes University Hospital were used for this study. All patients undergoing TAVI at our institution gave written informed consent for the procedures and anonymous collection of their data, which were gathered in an electronic database. The institutional review board waived specific consent for this study due to its retrospective and observational nature.

Cardiac CT angiography was performed with a GE Discovery (General Electric Healthcare, Boston, Massachusetts, USA) scanner. First, images of the aortic root were acquired using retrospective ECG gating, and then data were acquired cranio-caudally without ECG gating extending from the distal part of the common carotid arteries to the femoral arteries for the assessment of vascular access. Seventy to 150 ml of iodinated contrast media (Iomeron 200 or 400 MCT, Bracco Imaging, Konstanz, Germany; Xenetix 350, Guerbet, Villepinte, France) was injected at a flow rate of 4.0 ml/s followed by a flushing bolus of 70 ml 0.9% saline solution. For each patient, two type of reconstructions were performed: a small and large field of view (FOV) data set for the assessment of the aortic root (heart reconstruction) and the iliofemoral access, respectively. Reconstructed slice thickness was 0.75mm and slice increment 0.4mm was applied for small FOV reconstruction and 0.8mm increment for large

FOV reconstruction. The aortic root volume was reconstructed every 10% of the cardiac cycle (from one R peak to the next R peak on the ECG).

Fluoroscopic sequences were routinely acquired during TAVI procedures at a rate of 15 frames/second during the injection of 20-30ml of iodinated contrast agent at a flow rate of 10-15ml/sec.

Data synchronisation

The temporal synchronization between a fluoroscopic frame extracted from a sequence and a reconstructed volume from the CTA was performed using the ECG signal registered in the DICOM files of both modalities. A particular moment in the cardiac cycle, expressed as a percentage of time between two R-waves on the ECG signal, was associated with the closest corresponding reconstructed volume and with the closest corresponding frame in the fluoroscopic sequence.

Contrast Feature Curve

Given an angiography sequence of with N frames, an expert cardiologist manually delineated a region of interest (ROI) around the aortic root. This ROI was designed to measure the evolution of the level of contrast throughout the sequence. For each frame, we calculated the mean gray level in the ROI to construct a contrast feature curve of the entire sequence. In general, this curve contains a dominant peak for a sequence during contrast injection as seen in *Figure 1*. The subset of images that contained a sufficient level of contrast to perform manual contouring of the aortic root was selected.

Automatic detection of diaphragm movement

The preoperative CTA being performed during an end-inspiratory apnea, patients' lungs are full of air with the diaphragm in his lowest position. To find similar conditions during the

intraoperative phase, we had to be able to extract the movement of the diaphragm from the fluoroscopic sequence. In such a sequence, the aortic root movement can be seen as a combination of the respiratory and the cardiac movements. Under the assumption of independence between the two components of the movement, we extracted the diaphragm motion from the sequence. We used an image-based method to track the diaphragm. We previously described this method to track the calcifications of the aortic valve in fluoroscopic images [4]. We delineated a ROI around the diaphragm, at the interface between lungs and the abdomen in the fluoroscopic sequence, and tracked it. The evolution of the position of this ROI over time was then plotted. The end-inspiratory phase was arbitrary defined as the subset of frames where the diaphragm is between its lowest position and 15% above it. This usually corresponded to only a few frames (<10) within each sequence. *Figure 2* shows the results of the automatic detection of diaphragm movement, and contrast level detection in two extreme cases. In the first case, the frames with the higher mean level of contrast coincide with the end-inspiratory phase, and our assumption was that these frames were highly reliable for registration purpose. The second case depicts the worst possible association between the contrast injection and the diaphragm position, the best-contrasted frames coinciding with the expiratory phase.

Aortic root segmentation algorithm

The 3D volume was loaded into the EndoSize software [5], a CE- and FDA-marked validated medical device for planning and sizing of endovascular procedures. The software uses a previously described automatic segmentation algorithm [6]. Briefly, it only requires the placement of one seed point approximatively set in the aortic root by the user. This point is used to extract the aorta centerline. Starting from the detected centerline, the aorta is also automatically segmented using a region growing algorithm that allows removing all neighbouring tissues [6]. Then, starting from 2mm diameter spheres initialized from seed points

in the barycentre of the three cusps, 3D deformable models are employed to accurately segment the aortic root by constraining smooth boundaries. Specifically, a 3D gradient vector flow snake [7] with a descending gradient optimizer is employed with proper internal and external energy tuned to keep a smooth curvature along the cusps. Combining these segmentations allows extracting the entire ascending aorta, and is useful to remove all unnecessary arterial structures (e.g. heart, coronary arteries) for proper visualization.

Because of the larger FOV used for data acquisition, applying this algorithm to non-ECG-gated data yielded larger segmented volumes than those obtained with the smaller ECG-gated FOV. Therefore, to maintain comparability between strategies, we only used the first 5cm of the aortic root segmentation for each registration performed. Moreover, this strategy was deemed appropriate because the anatomic features of interest in the TAVI setting are located in this aortic root region.

Registration Method and Steps

Numerous 3D/2D registration methods are described in the literature to perform the registration between 3D volumes and 2D fluoroscopic frames [8,9]. Usually, the 3D/2D geometrical transformation can be expressed as the combination of a 3D/3D rigid transformation and a 3D/2D projection. In this study, a feature-based approach was used to estimate the rigid transformation combining 3 translations and 3 rotations. The angular position of the intra-operative imaging device and the intrinsic perspective projection parameters were extracted from the DICOM headers of the fluoroscopic sequence in order to initialize the registration algorithm. An expert interventional cardiologist manually contoured the aortic root visualized on the fluoroscopic frame. This 2D contour was the feature used to compute the distance metric for the registration. It was defined as the Euclidean 2D distance between the contour of the projected 3D pre-operative aorta segmentation and the 2D aorta

contour observed in the angiography. A distance map was computed from the 2D aortic contour with the Chamfer operator. The minimization of the distance criterion was iteratively performed using a Powell optimization algorithm until the estimate of the 3D/2D transform was satisfactory [10]. *Figure 3* summarizes the workflow of the proposed registration method.

Registration strategies

A graphical interface was created in matlab to help the expert choose the adequate frame in the fluoroscopic sequence for each strategy. To this purpose, the contrast feature curve, the diaphragm movement graph, and the ECG signal were simultaneously plotted (*Figure 4*).

We considered seven strategies to define the best input data to register, taking into account the aortic and respiratory motion in different manners. Each strategy involved the same registration algorithm, and differed on the pre-operative data, and on the criteria to select the intra-operative fluoroscopic frame to register. These strategies were based on contrast enhancement, temporal data using the cardiac cycle (ECG) and the respiratory cycle to take into account the movement of the diaphragm. Strategies were named as follow and their respective input data are further detailed hereafter:

1) Contrast enhancement

2) Contrast enhancement + diaphragm

3) Contrast enhancement at 70% of the cardiac cycle

4) Contrast enhancement at 70% of the cardiac cycle + diaphragm

5) Temporal match at 70% of the cardiac cycle + diaphragm

6) Contrast favored over temporal match

7) Temporal match favored over contrast

1) Contrast enhancement: In this strategy, input data are obtained from the pre-operative CTA without ECG-gating and from an intra-operative fluoroscopic sequence. An expert interventional cardiologist manually selected the frame with the best contrast enhancement in the angiographic sequence without taking into account respiratory motion. To precisely identify this frame, the mean grey level in the aorta during the intra-operative sequence was plotted as described above. The minimum value of the mean grey level correspond to the maximum spread of contrast agent in the aortic root, which helped the expert select the reference image to register (see *figure* 1). This strategy correspond to the red line in *Figure 5*.
2) Contrast enhancement + diaphragm: This strategy used the same preoperative input data as the previous one which was registered to the per-operative frame with the best contrast enhancement during the end-inspiratory phase. Tracking of the diaphragm movement as previously described was used to identify the end-inspiratory phase during which, we selected the most contrasted frame as described for the first strategy. This strategy correspond to the orange line in *Figure 5*.
3) Contrast enhancement + end-diastolic phase: Pre-operative data were acquired from the ECG-gated CTA using an end-diastolic volume (mostly 70% of the cardiac cycle), which usually correspond to the moment when the heart is the less mobile. Intra-operative data were the same as in the first strategy.
4) Contrast enhancement + end-diastolic phase + diaphragm: Pre-operative data were the same as in the previous strategy and per-operative data were the same as in the second strategy.
5) Temporal match + end-diastolic phase + diaphragm: Pre-operative data remained the same as in the two previous strategies and the intra-operative frame was chosen using

the DICOM headers contained in the fluoroscopic sequence. During the end-inspiratory phase, we selected a frame corresponding to the end-diastolic CTA volume, which was previously chosen, without taking into account contrast enhancement. This strategy corresponds to the yellow line in *Figure 5*.

6) Contrast favored over temporal match: During the end-inspiratory phase, we chose the most contrasted frame in the fluoroscopic sequence using the method described above (orange line in *Figure 5*). Using the DICOM headers contained in the fluoroscopic sequence, the percentage of the cardiac cycle corresponding to this frame was identified, and finally the closest pre-operative volume was selected for registration among the volumes obtained from ECG-gated CTA and reconstructed every 10% of the cardiac cycle.
7) Temporal match favored over contrast: Within the end-inspiratory phase, using the ECG data of the DICOM headers of the fluoroscopic sequence, we selected the peroperative frame, which was the closest to a pre-operative reconstructed volume of the aorta (in percentage of the cardiac cycle). These data were then selected for registration without further consideration for contrast. This strategy corresponds to the green line in *Figure 5*.

Evaluation of registration strategies

During a standard TAVI procedure, the C-arm of the X-ray system is kept in the same angulations when the optimal fluoroscopic projection for deployment has been selected. For this reason, we considered the evaluation on the coordinate system of the fluoroscopic projection used for deployment to be appropriate, as previously described [11]. Strategies were evaluated by calculating the Dice coefficient (*Figure 6*) and computing the 2D re-projection target registration error (TRE), using as landmark points coronary arteries (*Figure 7*). To this purpose, the proximal segments of coronary arteries were segmented from preoperative 3D

volumes and their centreline was calculated. Six points belonging to the centreline of the proximal segment of coronary arteries were marked in the angiographic images by the expert interventional cardiologist. The Euclidian distance between those manually placed points and the nearest point of the centreline of the 3D re-projected volumes was computed.

All evaluations were made on a workstation equipped with an Intel Xeon processor (2.44GHz GHz) with 48 Gigabytes of RAM.

Results

Feasibility of the registration strategies

Not all strategies could be performed in all patients either because the end-inspiratory phase did not coincide with the contrast injection, or because the same fluoroscopic frame or the same phase of the cardiac cycle were selected for different strategies. *Table 1* summarizes the total number of cases tested per strategy. Feasibility of the proposed strategies ranged from 68% of cases for strategies 3 and 7 to 100% of cases for strategy 1 and 2.

Dice coefficient

Table 2 reports the mean ± standard deviation of each strategy's Dice coefficient. All strategies had comparable mean Dice coefficients ranging from 0.945 (strategies 5 and 6) to 0.954 (strategy 1) suggesting the accuracy of the whole matching process involving the segmentation of input 3D data, the 3D/2D registration, and the delineation of the 2D intraoperative image.

Re-projection target registration error

Re-projection TRE for the left and right coronary arteries are depicted in *Figure 8* and *Figure 9*, respectively. TRE values were higher for the right coronary artery, likely because it is more

mobile than the left coronary artery during the cardiac cycle. Strategies had median TRE ranging from 1.75 mm (interquartile range: 0.76-2.74) to 3.26 mm (2.2-4.3) for the left coronary artery, and from 2.53 mm (1.22-3.84) to 4.03 mm (3.16-4.89) for the right coronary artery. Strategy 6, which favoured contrast while accounting for temporal matching on the cardiac cycle, and the respiratory cycle, seemed to display the best results, overall. However, these results were close to strategy 1 based on non-ECG-gated data.

Discussion

To the best of our knowledge, this is the first study investigating the influence of diaphragm movement, and the cardiac cycle on the performance of a registration of 3D CTA with X-ray fluoroscopy for image fusion during TAVI. Based on data of 25 patients who underwent TAVI, we did not demonstrate a significant impact of different input data on the results of a preoperative 3D / per-operative 2D images' registration. Seven strategies were evaluated, each accounting for cardiac and respiratory motions in a different manner, and yielded rather comparable results in terms of 3D/2D matching. Interestingly, the strategy relying on non-ECG-gated pre-operative data achieved the higher Dice coefficient and a TRE comparable with those of other strategies, suggesting that if ECG-gating is required for accurate pre-procedural vascular sizing of the aortic root and annulus, it provides little additional value in performing registration of the segmented pre-operative 3D data to per-operative 2D data. This finding may be of importance as, in clinical practice, non-ECG data usually involves volumes acquired on a larger FOV, which allows the segmentation and registration of the entire aorto-iliac vasculature, thus enabling to assist clinicians with image fusion from the ilio-femoral vascular access to the prosthesis deployment, during all steps of TAVI procedures [12].

Advanced visualization and guidance technology involving patient-specific 3D models of the aorta can greatly facilitate TAVI procedures by combining a high spatial resolution with

excellent soft-tissue contrast imaging (CTA) with a high temporal resolution modality lacking anatomical information (fluoroscopy) for real-time feedback [12,13]. To date, different approaches for image-based guidance have been published. Only some of them take into account in some way the aortic and/or respiratory motion. Schrofel et al. proposed a method based on a manual alignment of the 3D pre-operative data to two fluoroscopic images acquired at different angulations [14]. This approach is based only on bones structures; the fluoroscopic images are then shown synchronized with the ECG to compensate the movement of the heart-beat. Several previous studies were based on intra-operative cone-beam computed tomography (CBCT) volumes, which were obtained in the complex environment of a hybrid operating room. John et al proposed such a system that allows a straightforward registration of a contrast-enhanced 3D CBCT, which, being acquired on the same imaging system, is inherently registered with the fluoroscopic per-operative image [15]. However, despite the reported success, this strategy requires an additional contrast agent injection, and, to minimize cardiac and respiratory motion, is performed during rapid cardiac pacing after stopping the patient ventilation during a TAVI procedure performed under general anaesthesia. Therefore, this approach is limited in routine practice as TAVI is increasingly performed under local anaesthesia [16], and because of concerns regarding the risk of acute kidney injury associated with the additional contrast injection, as well as potential consequences of repeated runs of rapid pacing (arterial hypotension with increased risk of myocardial injury, stroke…). Miao et al. demonstrated the high accuracy of a hybrid method combining a feature/landmark-based method with an intensity-based method for 3D / 2D registration during TAVI [17]. However, in this work, cardiac and/or respiratory motions were only considered as a potential source of ghost artefacts in digitally subtracted images, which may have high gradients, therefore affecting their registration algorithm because of the gradient-based similarity measure used. Liao et al. further refined both method, proposing a fully automatic system for contrast-based

3D/2D registration between the 3D model and 2D angiography [13]. The framework relied on an automatic detection of contrast agent injection, which triggered the 3D / 2D registration. Automatic calculation of the 3D / 2D transformation was performed for each injected acquisition of the aortic root to compensate the patient's movements and the aortic deformation due to the insertion of the devices. Rapid pacing was assumed for valve deployment. Thus the workflow was not suited for self-expandable prosthesis implantation during which pacing is usually not performed at the deployment phase. Moreover, motion compensation was achieved within 2.5s after availability of the most contrasted frame, which did not allow live use of the method during TAVI procedures. Lv et al continued to develop this approach adding an iterative motion model to guide the 3D/2D registration [11]. They used an image-based automatic motion-phase detection, taking advantage of the pseudo-periodic property of the aortic motion, greatly improving the results of the registration compared with the naïve frame-by-frame method, especially in frames without reliable contrast. Their key idea was to periodically update the patient-specific motion-model using frames already registered, starting from the frames with most contrast. The constructed motion-model from this initial cardiac cycle was then used to supervise the registration of the frames in other cycles with less contrast, and was iteratively updated. To overcome the issue of additional contrast injection of these strategies relying on an intra-operative CBCT, Lu et al. proposed the use of a native CBCT to register the pre-operative CTA [18]. The limited visibility of the target structures requires the use of anatomical landmarks, such as heart surface, wall calcifications, spine and bone borders, thoracic cavity for registration [19]. Furthermore, insufficient quality of the CBCT image may hinder registration, and necessitate highly trained operators, making the workflow less straightforward [12]. Finally, given the rapid expansion of TAVI indications, a significant proportion of procedures is performed in standard catheterization laboratory room without CBCT availability [16]. Thus, methods registering the

pre-operative CTA to the per-operative fluoroscopy seem to represent the best option for a large availability in clinical practice. Recently, Vernikouskaya et al. published such a patient-specific method [12]. The initial registration of the two datasets was performed during the femoral puncture, and sheath introduction using routinely acquired (with less than 10ml of contrast agent) angiograms in 2 different projections. This initial registration was not accurate for the thoracic region, mainly because the patient's position on the CTA and the catheterization tables may differ. A manual correction based on two non contrast-enhanced fluoroscopic sequences recorded in left (40°) and right (30°) anterior oblique was applied, yielding adequate superposition of the 3D anatomic model. Further refinement was achieved by correcting the registration after each routinely acquired aortogram during the procedure. Using this technique in 20 TAVI candidates, authors demonstrated encouraging clinical results in terms of reduction of contrast agent injection, X-ray dose, and fluoroscopy time [12]. Besides its potential benefits at the procedural stage, image registration and fusion may also be useful during procedural planning. Indeed, we recently reported a patient-specific simulation of the stiff guidewire's deformations during TAVI, which involved 3D/2D registration to import and validate the simulation results into the intra-operative coordinate system [20]. As patient-specific simulation is rapidly gaining interest as a complementary planning tool in the TAVI setting [3], defining the best data to use in 3D / 2D image registrations may be crucial in a near future. Most above-discussed studies attempted to minimize the cardiac and respiratory movements, sometimes emphasizing the importance of similar condition of acquisition of pre- and per operative data regarding results of the registration [18]. On the contrary, our results suggest that registering images acquired at the same or nearly the same respiratory and cardiac phases may actually be of limited importance as compared with the accuracy of the registration algorithm itself to achieve adequate superposition of pre-operative 3D data on per-operative 2D images.

Several limitations of the present work should be acknowledged. First, all data came from a limited number of patients treated in a single-centre. Pre-operative CTA were acquired with the arms of the patients in an upward position over their head. TAVI procedure being performed with the arms down along the body, some prosthesis manufacturers started recommending the acquisition of the pre-operative CTA in this position. Whether our results hold true with such conditions of acquisition, or with CTA with different contrast injection protocols or resolution, is unknown. Furthermore, we evaluated the influence of the cardiac cycle and respiratory motion on a single rigid registration strategy. The TRE reported in the present work sometimes exceeded the usual clinically-acceptable 3-mm cut-off for 3D / 2D registration in the TAVI setting [13]. This may be explained by the use of a single rigid transformation. Nevertheless, the integration of non-rigid transformations in the 3D/2D registration process still remains challenging. Moreover, it should be highlighted that the main objective of this study was not to evaluate the accuracy of the distance/similarity function used for registration but rather the influence of the input data on the results of the registration process.

Conclusion

In the present study, using seven strategies, we evaluated the influence of numerous input data for 3D pre-operative CTA / 2D per-operative fluoroscopy registration in the setting of TAVI. Our results suggest that accounting for the respiratory motion, and cardiac cycle in various ways plays a marginal role in the results of a 3D CTA / 2D fluoroscopy registration for TAVI. Interestingly, the use of non-ECG-gated 3D CTA, which usually allow the segmentation of larger volumes in clinical practice, achieved similar results to those obtained with ECG-gated data.

Compliance with Ethical Standards

Funding: This study received no extra-mural funding.

Conflict of Interest: The authors declare that they have no conflict of interest.

Ethical approval: All procedures performed in this study in accordance with the ethical standards of the institutional and/or national research committee and with the 1964 Helsinki declaration and its later amendments or comparable ethical standards. For the present retrospective study, the institutional review board waved specific consent due to its observational nature.

Informed consent: All patients undergoing TAVI at our institution gave written informed consent for the procedures and anonymous collection of their data, which were gathered in an electronic database. The institutional review board waived specific consent for this study due to its retrospective and observational nature.

References

1. Iung B, Baron G, Butchart EG, Delahaye F, Gohlke-Barwolf C, Levang OW, Tornos P, Vanoverschelde J-L, Vermeer F, Boersma E, Ravaud P, Vahanian A. A prospective survey of patients with valvular heart disease in Europe: The Euro Heart Survey on Valvular Heart Disease. *Eur Heart J* 2003;24:1231–1243.

2. Baumgartner H, Falk V, Bax JJ, De Bonis M, Hamm C, Holm PJ, Iung B, Lancellotti P, Lansac E, Rodriguez Munoz D, Rosenhek R, Sjogren J, Tornos Mas P, Vahanian A, Walther T, Wendler O, Windecker S, Zamorano JL. 2017 ESC/EACTS Guidelines for the management of valvular heart disease. *Eur Heart J* 2017;38:2739–2791.

3. Vy P, Auffret V, Badel P, Rochette M, Le Breton H, Haigron P, Avril S. Review of patient-specific simulations of transcatheter aortic valve implantation. *Int J Adv Eng Sci Appl Math* 2016;8:2–24.

4. Nguyen DLH, Garreau M, Auffret V, Le Breton H, Verhoye JP, Haigron P. Intraoperative tracking of aortic valve plane. *Conf Proc IEEE Eng Med Biol Soc* 2013;2013:4378–4381.

5. Kaladji A, Lucas A, Kervio G, Haigron P, Cardon A. Sizing for endovascular aneurysm repair: clinical evaluation of a new automated three-dimensional software. *Ann Vasc Surg* 2010;24:912–920.

6. Lalys F, Esneault S, Castro M, Royer L, Haigron P, Auffret V, Tomasi J. Automatic aortic root segmentation and anatomical landmarks detection for TAVI procedure planning. *Minim Invasive Ther Allied Technol* 2018:1–8.

7. Xu C, Prince JL. Snakes, shapes, and gradient vector flow. *IEEE Trans Image Process* 1998;7:359–369.

8. Markelj P, Tomazevic D, Likar B, Pernus F. A review of 3D/2D registration methods for image-guided interventions. *Med Image Anal* 2012;16:642–661.

9. Song G, Han J, Zhao Y, Wang Z, Du H. A Review on Medical Image Registration as an Optimization Problem. *Curr Med Imaging Rev* 2017;13:274–283.

10. Dumenil A, Kaladji A, Castro M, Esneault S, Lucas A, Rochette M, Goksu C, Haigron P. Finite-element-based matching of pre- and intraoperative data for image-guided endovascular aneurysm repair. *IEEE Trans Biomed Eng* 2013;60:1353–1362.

11. Lv X, Liao R, Liu Y, Miao S. A framework for automatic, accurate, and fast 2-D+T/3-D registration applied to trans-catheter aortic valve implantation (TAVI) procedures. *Proc ISBI* 2012:956–959.

12. Vernikouskaya I, Rottbauer W, Seeger J, Gonska B, Rasche V, Wohrle J. Patient-specific registration of 3D CT angiography (CTA) with X-ray fluoroscopy for image fusion during transcatheter aortic valve implantation (TAVI) increases performance of the procedure. *Clin Res Cardiol* 2018;107:507–516.

13. Liao R, Miao S, Zheng Y. Automatic and efficient contrast-based 2-D/3-D fusion for trans-catheter aortic valve implantation (TAVI). *Comput Med Imaging Graph* 2013;37:150–161.

14. Schröfel H, Bakker N., Van den Boomen R. Transcatheter aortic valve implantation in a hybrid operating room using HeartNavigator. *MEDICAMUNDI, Philips Healthcare Nederland BV* 2010;54.

15. John M, Liao R, Zheng Y, Nottling A, Boese J, Kirschstein U, Kempfert J, Walther T. System to guide transcatheter aortic valve implantations based on interventional. *Med Image Comput Comput Assist Interv* 2010;13:375–382.

16. Auffret V, Lefevre T, Van Belle E, Eltchaninoff H, Iung B, Koning R, Motreff P, Leprince P, Verhoye JP, Manigold T, Souteyrand G, Boulmier D, Joly P, Pinaud F, Himbert D, Collet JP, Rioufol G, Ghostine S, Bar O, Dibie A, Champagnac D, Leroux L, Collet F, Teiger E, Darremont O, Folliguet T, Leclercq F, Lhermusier T, Olhmann P, Huret B, Lorgis L, Drogoul L, Bertrand B, Spaulding C, Quilliet L, Cuisset T, Delomez M, Beygui F, Claudel J-P, Hepp A, Jegou A, Gommeaux A, Mirode A, Christiaens L, Christophe C, Cassat C, Metz D, Mangin L, Isaaz K, Jacquemin L, Guyon P, Pouillot C, Makowski S, Bataille V, Rodés-Cabau J, Gilard M, Le Breton H. Temporal Trends in Transcatheter Aortic Valve Replacement in France: FRANCE 2 to FRANCE TAVI. *J Am Coll Cardiol* 2017;70:42–55.

18. Lu Y, Sun Y, Liao R, Ong SH. A pre-operative CT and non-contrast-enhanced C-arm CT registration framework for trans-catheter aortic valve implantation. *Comput Med Imaging Graph* 2014;38:683–695.

19. Ierardi AM, Duka E, Radaelli A, Rivolta N, Piffaretti G, Carrafiello G. *Fusion of CT Angiography or MR Angiography with Unenhanced CBCT and Fluoroscopy Guidance in Endovascular Treatments of Aorto-Iliac Steno-Occlusion: Technical Note on a Preliminary Experience.* United States; 2016:111–116.

20. Vy P, Auffret V, Castro M, Badel P, Rochette M, Haigron P, Avril S. Patient-specific simulation of guidewire deformation during transcatheter aortic valve implantation. *Int J Numer Method Biomed Eng* 2018;34:e2974.

Figures legends

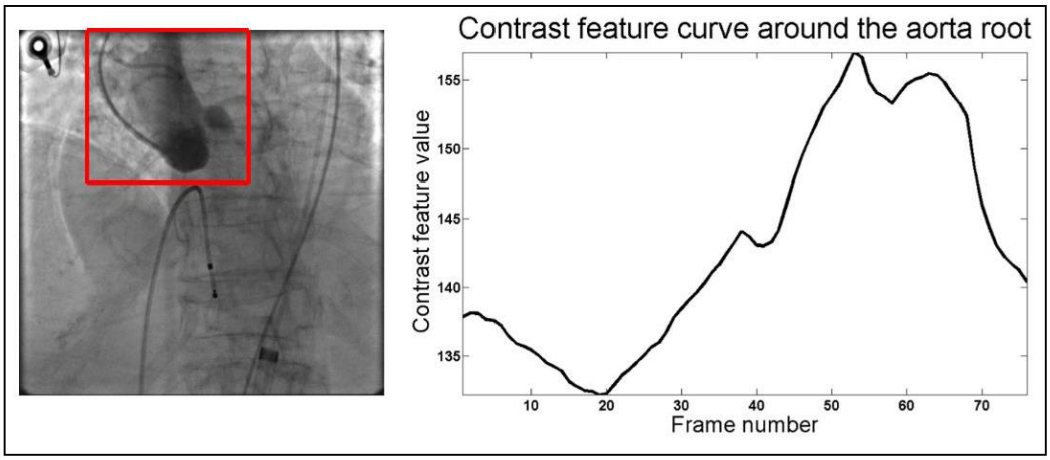

Figure 1 – Contrast feature curve.

Red rectangle in the left picture corresponds to the region of interest marked over a frame of the fluoroscopic sequence. In the right image, the contrast feature curve of the fluoroscopic sequence.

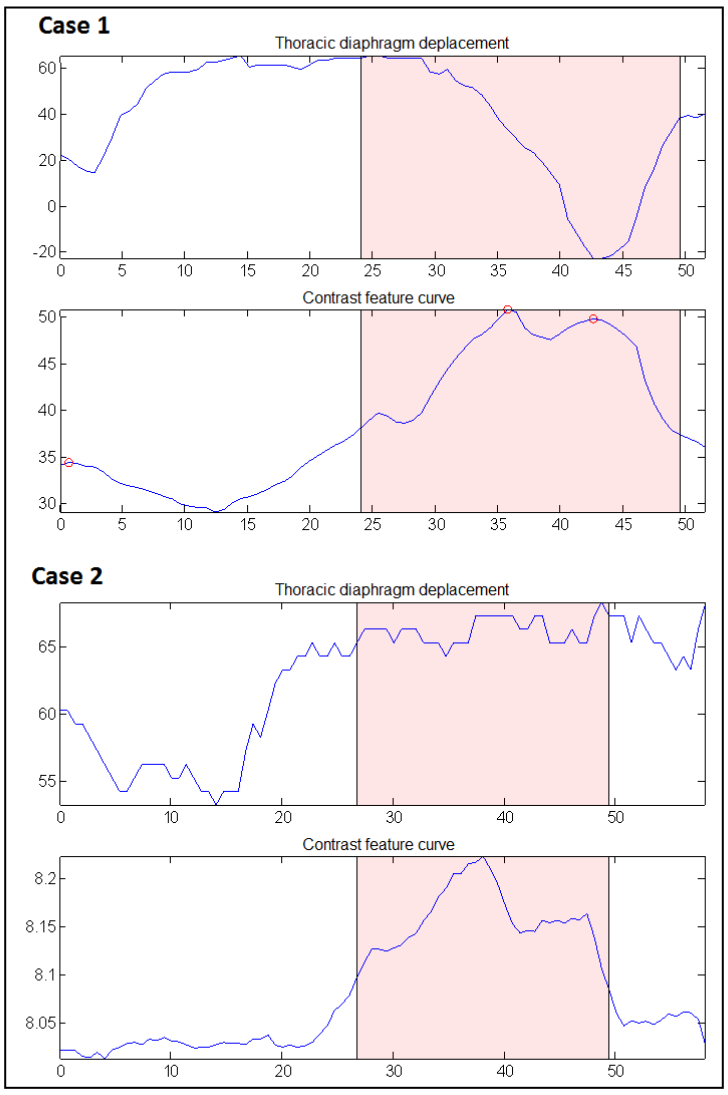

Figure 2 – Automatic detection of diaphragm movement synchronized with the contrast feature curve in a fluoroscopic sequence.

Case 1: The frames with most contrast coincides with the inhalation phase. Case 2:

The worst alignment between the contrast injection and the diaphragm movement.

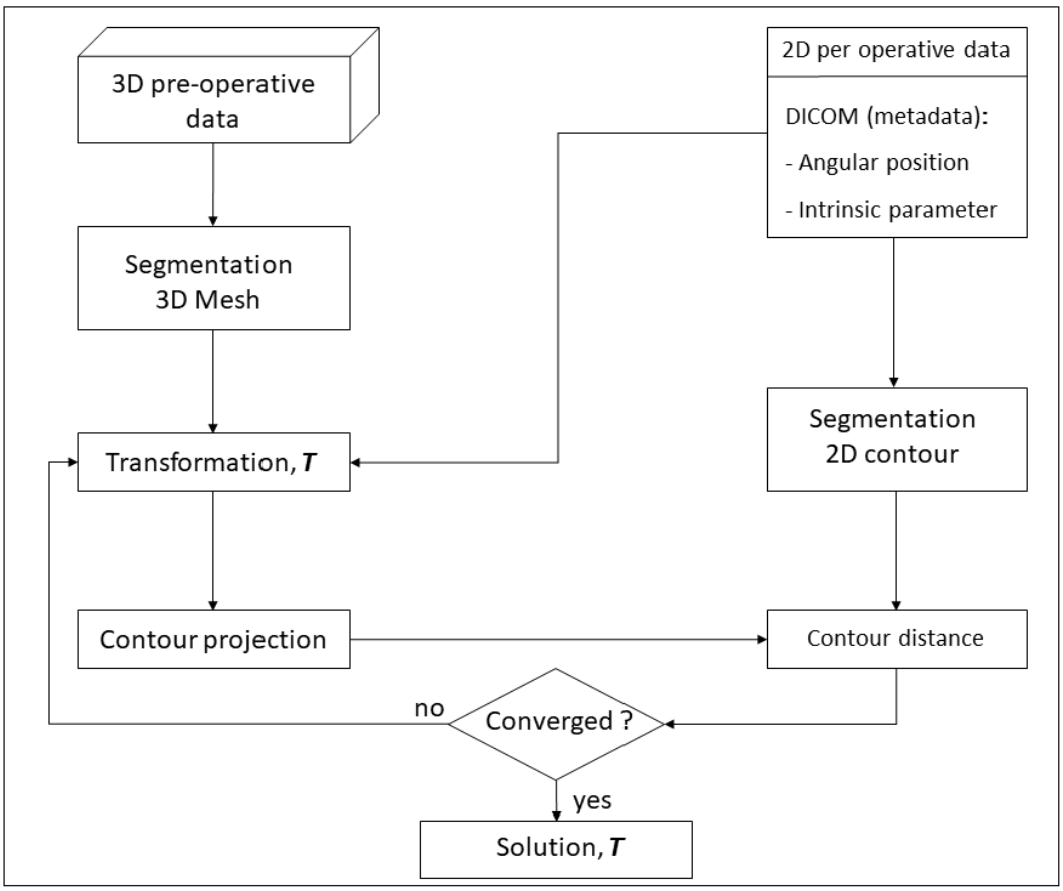

Figure 3 - Workflow of the proposed registration method.

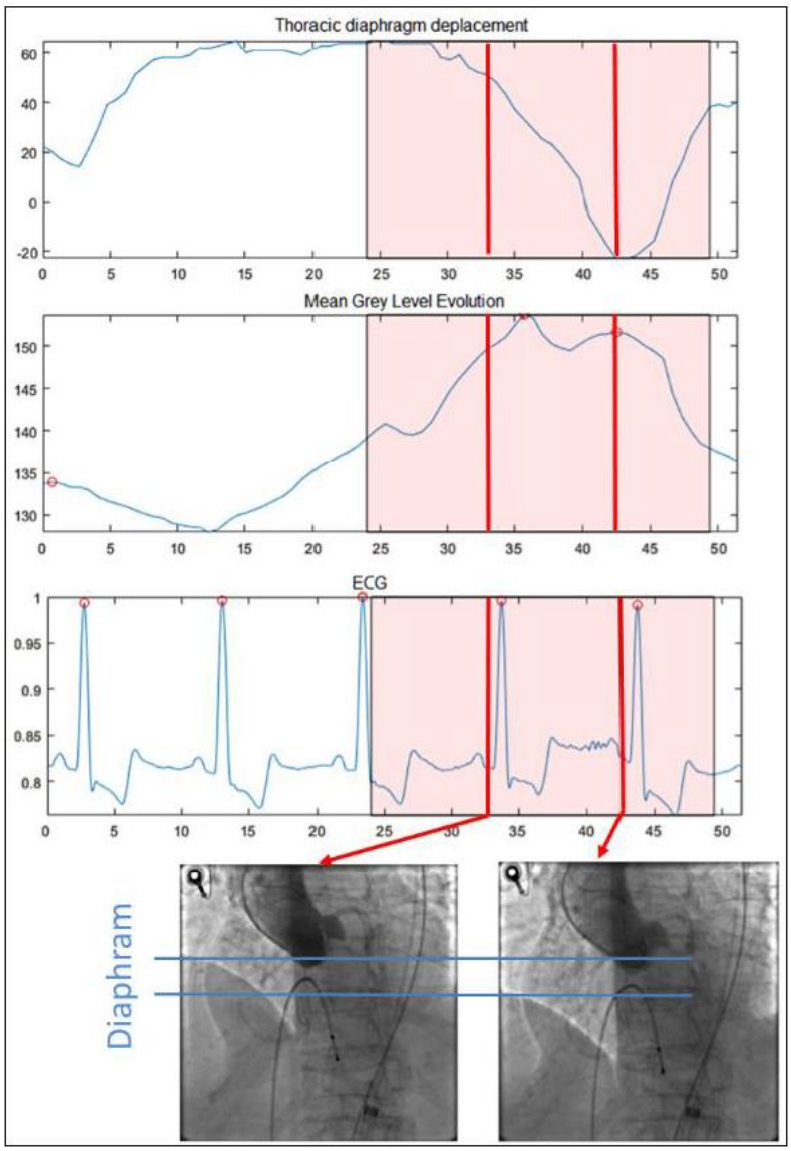

Figure 4 – Matlab-created graphical interface.

Movement of the diaphragm (top) synchronized with the contrast feature curve (middle) and the corresponding ECG (bottom) during the angiogram acquisition.

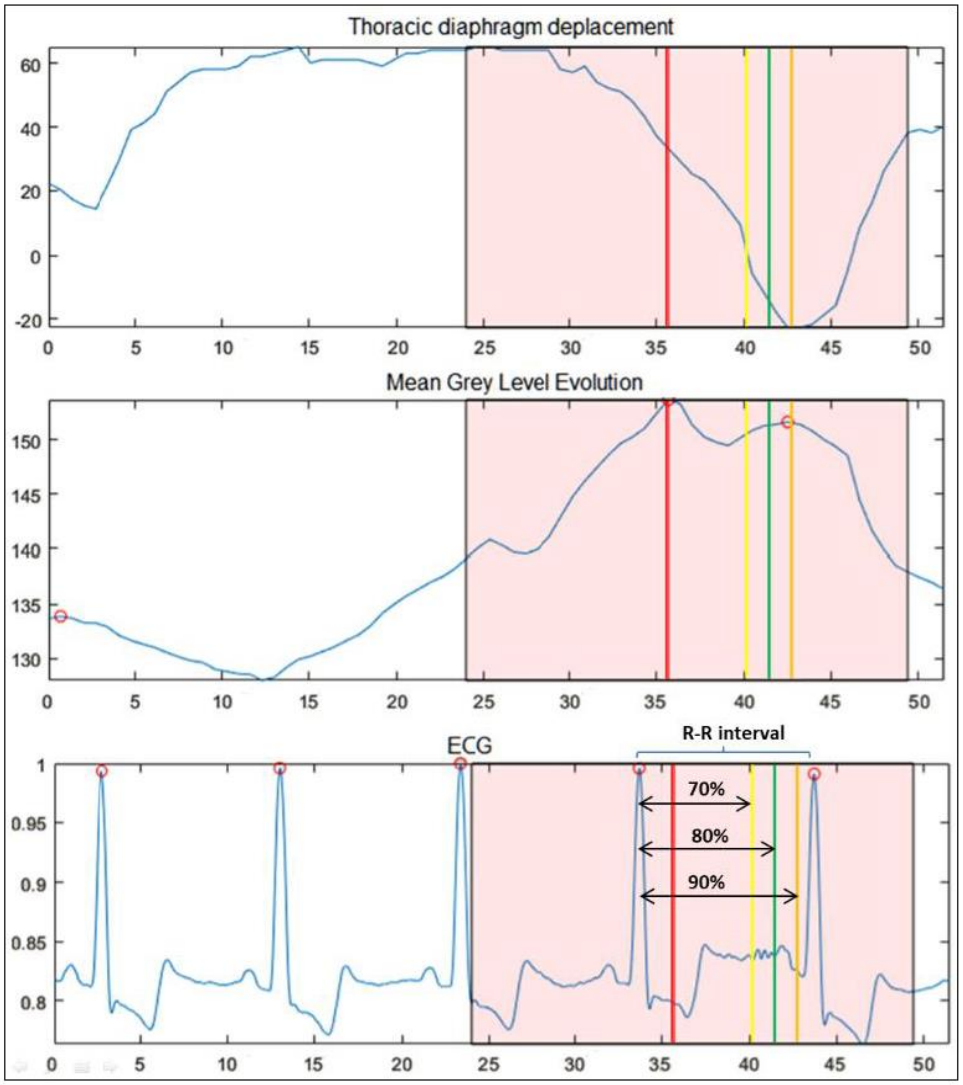

Figure 5 – Registration strategies.

Illustration of the proposed registration strategies. The red line corresponds to strategies 1 and 3. The yellow line corresponds to strategy 5. The green line corresponds to strategy 7. The orange line corresponds to strategies 2, 4 and 6.

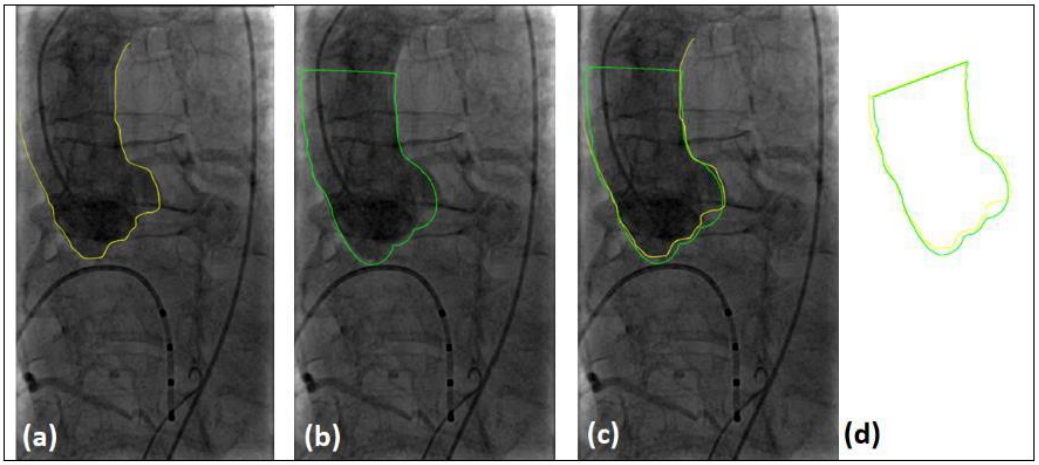

Figure 6 – Dice coefficient.

Registration between the CTA volume and the fluoroscopic frame. (a) The yellow line represents the contour of the aortic root manually extracted. (b) The green line represents the outline of the 3D volume projected on the angiography. (c) 3D/2D Registration result. (d) Comparison of both contours and calculation of the Dice Coefficient.

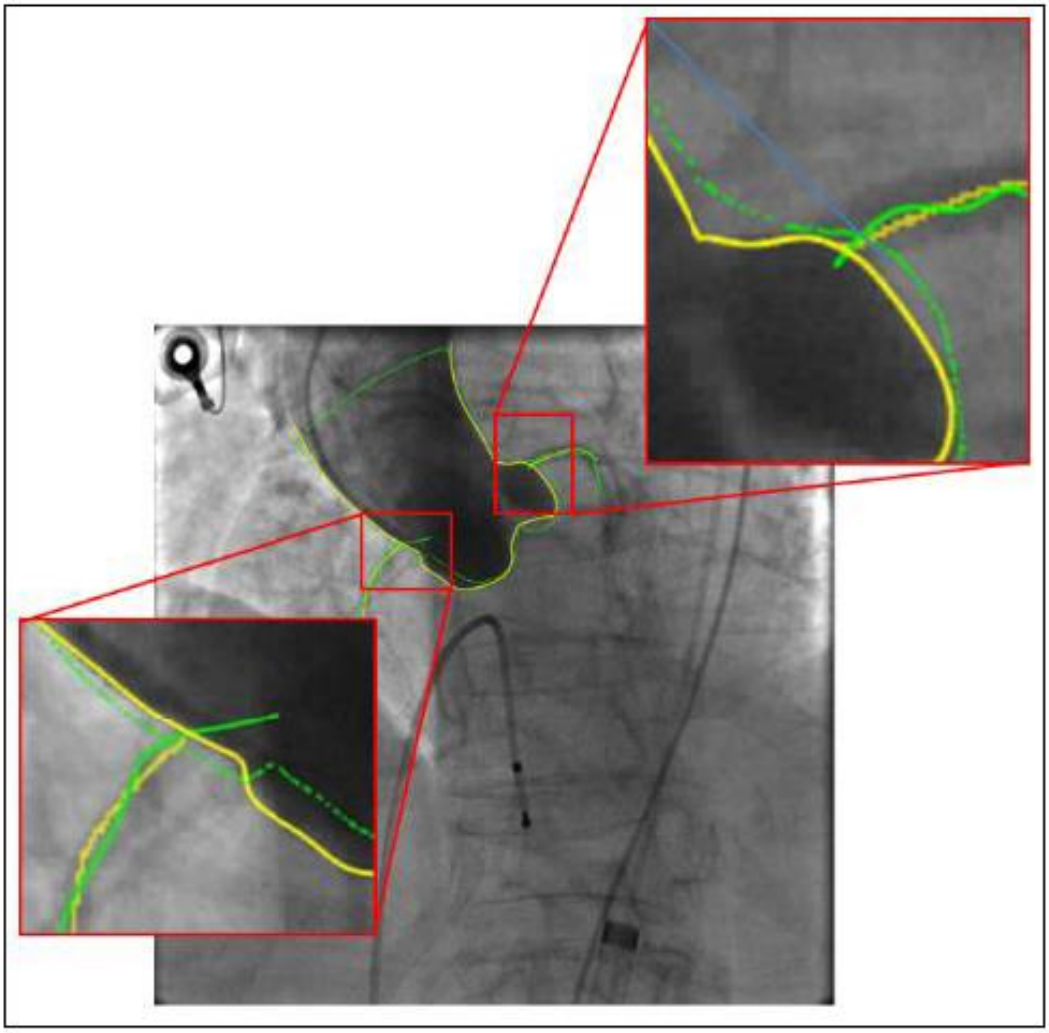

Figure 7 – Target registration error of the coronary arteries centrelines.

The yellow line represents the manually delineated centreline. The green line represents the automatically detected centreline from the 3D segmentation. Target registration error was defined as the Euclidian distance between those manually placed points and the nearest point of the centreline of the 3D re-projected volumes was computed.

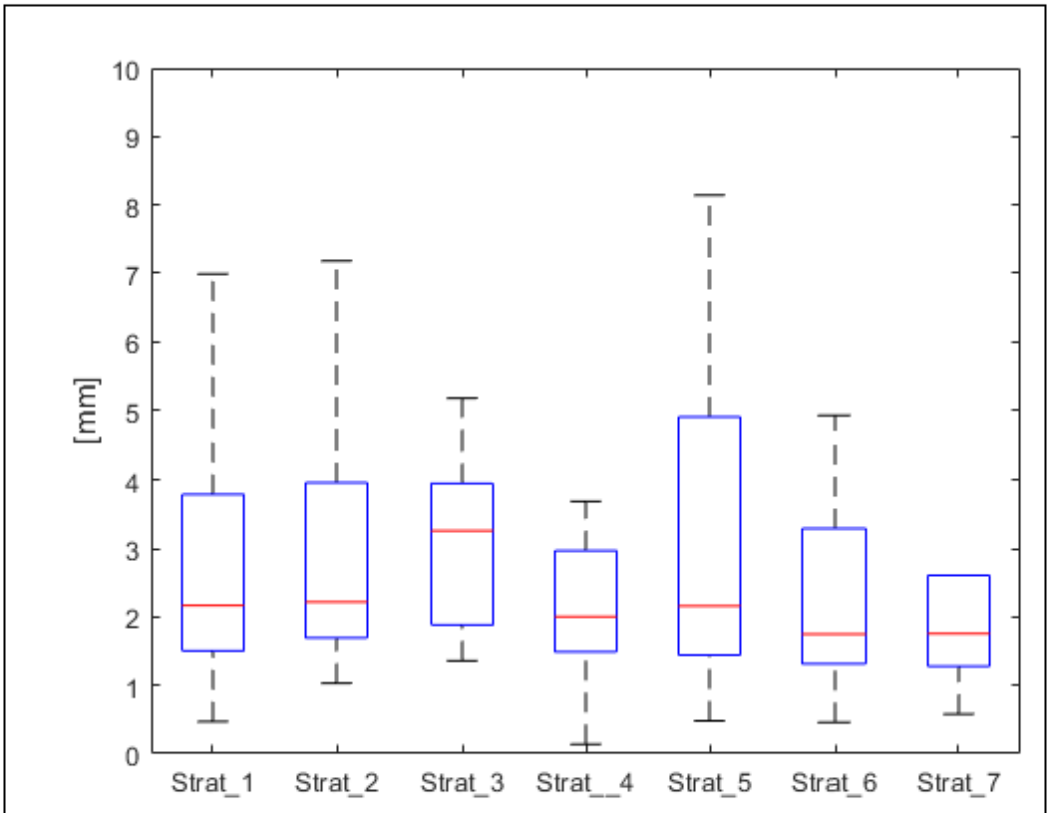

	Strat_1	Strat_2	Strat_3	Strat_4	Strat_5	Strat_6	Strat_7
error	2.6880	3.0150	3.4600	3.1920	3.1680	2.4220	3.1050
std	1.8190	1.9870	2.3990	2.5770	2.2580	2.0550	2.9100
max	6.9950	7.4410	8.9200	9.4890	8.1400	8.9200	8.9200
min	0.4680	1.0350	0.1390	0.7210	0.4800	0.4620	0.5790

Figure 8 – Target registration error of the left coronary artery for each strategy

The limits of each box represent the 25th and 75th percentiles, the whisker represents the min and the max value, and the red line represents the median value. Each boxplot is represented without the outliers. The table reports the mean error with its standard deviation (std) and range (min-max).

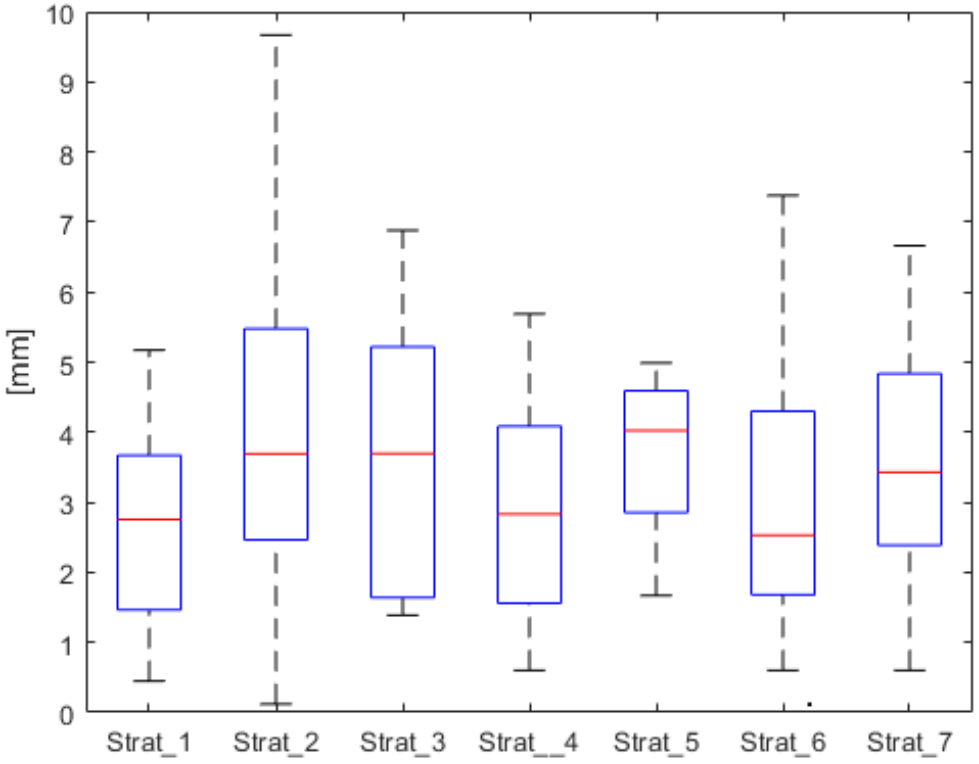

	Strat_1	Strat_2	Strat_3	Strat_4	Strat_5	Strat_6	Strat_7
error	2.6670	4.0400	3.2410	3.2090	4.2210	3.4860	4.0520
std	1.3930	2.5790	2.0550	1.6530	2.3950	3.0720	2.9040
max	5.1710	9.6650	6.5730	6.8810	10.2590	13.6350	13.0250
min	0.4450	0.1230	1.2560	0.6040	1.6660	0.6040	0.6040

Figure 9 – Target registration error of the right coronary artery for each strategy

The limits of each box represent the 25th and 75th percentiles, the whisker represents the min and the max value, and the red line represents the median value. Each boxplot is represented without the outliers. The table reports the mean error with its standard deviation (std) and range (min-max).

Table 1 - Summary of the total number of cases tested for each strategy.	
Strategy	**Number of cases**
Strategy 1: Contrast enhancement	25
Strategy 2: Contrast enhancement + diaphragm	25
Strategy 3: Contrast enhancement + end-diastolic phase	17
Strategy 4: Contrast enhancement + end-diastolic phase + diaphragm	20
Strategy 5: Temporal match during end-diastolic phase + diaphragm	21
Strategy 6: Contrast favored over temporal match	20
Strategy 7: Temporal match favored over contrast	17

Table 2 - Dice Coefficient after registration using the proposed strategies		
Strategy	**Mean Dice coefficient**	**Standard deviation**
1	0.954	0.015
2	0.948	0.018
3	0.948	0.015
4	0.948	0.019
5	0.945	0.017
6	0.945	0.025
7	0.953	0.019

4.3.4 Synthèse

Dans cette étude, nous avons évalué l'impact des mouvements cardiaques et respiratoires sur le résultat d'un processus de recalage 3D/2D en utilisant des données d'entrée permettant de prendre en compte ces paramètres. Nos différentes stratégies prenaient en compte ou non le mouvement respiratoire et privilégiaient un recalage basé sur la qualité de l'injection dans l'image 2D (contraste) ou un recalage basé sur la correspondance des images en termes de phase du cycle cardiaque à laquelle elles étaient acquises. En ce qui concerne l'image 2D peropératoire, le critère de qualité d'injection, l'emporte sur les critères de situation temporelle dans le cycle cardio-respiratoire. Pour les données 3D préopératoires, l'utilisation d'un large volume non synchronisé semble licite pour la mise en correspondance 3D/2D et permet de couvrir les structures d'intérêt pour le modèle de simulation numérique personnalisé

4.4 Simulation numérique

4.4.1 Rationnel médical et présentation du modèle de simulation

Après la présentation des éléments essentiels de traitement de l'image de notre travail dans les sections précédentes, nous présentons ici le modèle de simulation numérique, développé dans le cadre d'un travail conjoint avec le CIS (Centre Ingénierie et Santé – Ecole des mines de Saint-Etienne, CNRS) et la société ANSYS, utilisant la méthodes des éléments finis en résolution quasi-statique implicite, associée à une méthode semi-interactive d'initialisation pour accélérer et stabiliser le calcul. Les étapes de création de ce modèle, dépassant le cadre de ce travail, ne seront pas rapportées en détail ici mais peuvent être retrouvées dans la Thèse de Doctorat de P. Vy (« Simulation numérique personnalisée du positionnement des guides dans les procédures d'implantation de valve aortique percutanée », CIS, Mécanique et Ingénierie, Ecole des Mines de Saint-Etienne) et seront néanmoins rappelées dans la première contribution originale présentée dans cette section.

Comme nous l'avons précédemment rappelé, le guide rigide utilisé au cours des procédures TAVI joue un rôle non négligeable dans le positionnement initial de la prothèse et de son cathéter porteur au cours d'une procédure TAVI. Ses interactions avec le ventricule gauche peuvent par ailleurs en cas de trop grande « agressivité » être source d'une complication grave : la rupture ventriculaire gauche. Malgré ce rationnel à l'étude du comportement du guide rigide au cours des procédures, la littérature à ce sujet reste pauvre probablement car le cathéter

porteur des prothèses, plus épais et structurellement plus raide, est perçu comme ayant une influence plus importante sur le déroulement et les résultats de la procédure, par les cliniciens. Les problèmes et les questionnements liés au guide rigide ne sont donc pas systématiquement mis en lumière par la littérature, mais ils justifient cependant de la création et de l'utilisation grandissante de guides rigides dédiés au TAVI tel que le modèle SAFARI (Boston Scientific). Ainsi, il existe une zone d'incertitude sur le comportement du guide qui présente un potentiel médical pour éviter les complications (*e.g*. la perforation du ventricule) et pour offrir la plus grande stabilité de déploiement de la prothèse possible durant l'intervention. L'analyse de l'insertion du guide se conçoit donc, en tant qu'étape préliminaire d'une simulation plus large incluant la prothèse et son cathéter, par les données qu'elle peut apporter sur l'impact non-négligeable du guide sur les premières estimations de la position initiale de la prothèse et sur ses interactions avec le ventricule gauche. Dans cet esprit, notre modèle de simulation numérique doit répondre à un problème mécanique complexe faisant intervenir des éléments dont les caractéristiques biomécaniques précises sont difficiles voire impossible à obtenir comme bien souvent dans le contexte médical. Il convient donc d'accepter un compromis entre le coût de la prédiction et sa justesse. En d'autres termes, le problème mécanique doit être simplifié afin d'être moins coûteux en temps de calcul tout en restant représentatif des phénomènes observés au cours des procédures TAVI. Pour ce faire, nous avons dû avoir recours à plusieurs hypothèses simplificatrices.

Tout d'abord, les mouvements des structures anatomiques d'intérêt et leur effet sur le guide ont été négligés en faisant l'hypothèse que les déplacements induits sur ce dernier sont quasi-statiques car la faible masse du guide génère des forces d'inertie négligeables par rapport aux forces de contact mises en jeu. Seule la forme finale du guide a été prédite par l'équilibre statique final de la simulation puisqu'il nous paraissait injustifié de simuler l'ensemble de la montée du guide en termes d'utilité pour un outil de planification. Suite à nos observations peropératoires, les parois aortiques ne se déformant pas ou très peu sous l'effet du seul guide rigide, nous avons également considéré les parois de l'aorte et du ventricule comme rigides ce qui permet de ne pas tenir compte de paramètres comme la pression artérielle ou le degré de vasoconstriction dans la simulation. Les calcifications sont exclues car elles occupent peu de volume pour bloquer le trajet du guide. Les feuillets de la valve ne sont pas pris en compte dans cette première approche. Leur observation est en effet confrontée à la limite de la résolution spatio-temporelle du CT pré-opératoire et leurs propriétés mécaniques complexes sont difficilement caractérisables pour un patient spécifique. Le guide rigide a été considéré comme

une poutre élastique dont la caractérisation mécanique a été calquée sur celle de l'Amplatz Super Stiff. On suppose que le matériau du guide garde un comportement élastique malgré les grands déplacements générés par la flexion du guide. L'extrémité distale du guide est définie par un arrondi caractérisé par un angle et un rayon de courbure. Le contact du guide avec la paroi est considéré sans frottement car son revêtement polymère les réduit fortement. Enfin concernant les conditions aux limites, la relation entre le guide et le désilet d'introduction de la prothèse, considéré comme rigide et remontant jusque dans l'aorte abdominale, est modélisée par un pivot glissant. Ceci permet d'exclure l'aorte et les artères fémorales de la simulation. La position et l'orientation du guide à la sortie du désilet étant des données inconnues en pré-opératoire, nous avons jugé acceptable de les fixer arbitrairement considérant que les erreurs de prédiction situées loin de la valve aortique avaient un effet négligeable sur la justesse de la simulation au niveau valvulaire.

La contribution suivante présente le modèle numérique développé et sa validation par confrontation à l'imagerie interventionnelle de patients traités par TAVI au CHU de Rennes. Nous avons exploité dans le cadre de ce travail des images acquises en routine clinique lors de procédures de TAVI transfémoral réalisées dans une salle hybride (Thera Image) en sélectionnant des images présentant une injection de qualité suffisante au niveau de l'aorte ascendante.

Received: 13 November 2017 | Revised: 11 February 2018 | Accepted: 19 February 2018
DOI: 10.1002/cnm.2974

RESEARCH ARTICLE - APPLICATION

WILEY

Patient-specific simulation of guidewire deformation during transcatheter aortic valve implantation

Phuoc Vy[1,2,3,4] | Vincent Auffret[3,4,5] | Miguel Castro[3,4] | Pierre Badel[2] | Michel Rochette[1] | Pascal Haigron[3,4] | Stéphane Avril[2]

[1] ANSYS France, 69100 Villeurbanne, France

[2] Ecole Nationale Supérieure des Mines de Saint-Etienne, CIS-EMSE, INSERM: U1059, SAINBIOSE, 42023 Saint-Etienne, France

[3] INSERM, U1099, 35000 Rennes, France

[4] LTSI, Université de Rennes 1, 35000 Rennes, France

[5] CHU Rennes, Service de Cardiologie et Maladies Vasculaires, 35000 Rennes, France

Correspondence
Pascal Haigron, LTSI, Université de Rennes 1, campus de Beaulieu bat.22, 35000 Rennes, France.
Email: pascal.haigron@univ-rennes1.fr

Abstract

Transcatheter aortic valve implantation is a recent mini-invasive procedure to implant an aortic valve prosthesis. Prosthesis positioning in transcatheter aortic valve implantation appears as an important aspect for the success of the intervention. Accordingly, we developed a patient-specific finite element framework to predict the insertion of the stiff guidewire, used to position the aortic valve. We simulated the guidewire insertion for 2 patients based on their pre-operative CT scans. The model was designed to primarily predict the position and the angle of the guidewires in the aortic valve, and the results were successfully compared with intraoperative images.

The present paper describes extensively the numerical model, which was solved by using the ANSYS software with an implicit resolution scheme, as well as the stabilization techniques which were used to overcome numerical instabilities. We performed sensitivity analysis on the properties of the guidewire (curvature angle, curvature radius, and stiffness) and the conditions of insertion (insertion force and orientation). We also explored the influence of the model parameters. The accuracy of the model was quantitatively evaluated as the distance and the angle difference between the simulated guidewires and the intraoperative ones. A good agreement was obtained between the model predictions and intraoperative views available for 2 patient cases. In conclusion, we showed that the shape of the guidewire in the aortic valve was mainly determined by the geometry of the patient's aorta and by the conditions of insertion (insertion force and orientation).

1 | INTRODUCTION

Transcatheter aortic valve implantation (TAVI) is a mini-invasive procedure to replace aortic valves in the context of *aortic stenosis*. This procedure consists in delivering a fully collapsible replacement valve (*prosthesis*) onto the native aortic valve through a catheter (*sheath*). A *stiff guidewire* is first inserted in the patient's aorta with access via the femoral artery. The function of the guidewire is that of a rail along which the sheath can glide. This function is essential to ensure the navigation along the aortic arch up to the heart.

The first TAVI procedure was achieved in 2002 by Alain Cribier.[1] Since then, TAVI has permitted the treatment of patients who cannot benefit of an open heart surgery.[2,3] Nowadays, TAVI shows excellent 1-year outcomes for both

high-risk and intermediate-risk patients.[4] Building up on these excellent results, TAVI procedures might drastically increase in the future.

Despite this situation, a number of aspects remain to be improved, including the long-term durability and the management of possible complications. Research efforts by medical teams are focused on identifying the mechanisms of complications and determining the strategies to handle them.[5,6] It was shown that the risk of complications may be increased in case of inappropriate positioning of the delivery system in the valvular plane. For instance, paravalvular leaks,[7-9] atrioventricular block,[10] and coronary occlusion[11] could be related to the invalid implantation position of the prosthesis within the native aortic valve.

Patient-specific numerical simulations can help clinicians during preoperative planning and intraoperative navigation, as shown by different reviews recently published.[12-14] Several studies have already proved the feasibility of simulating prosthesis deployment within patient-specific anatomy. Bosmans et al validated a self-expanding prosthesis deployment model by comparing it with postoperative data. They obtained an accurate prediction of the final shape of the prosthesis.[15] Wang et al simulated balloon-expandable valve deployment within several patient-specific aortic valve geometries.[16] They illustrated how the interaction between calcifications and Valsalva sinuses could possibly induce aortic rupture. Simulation was instrumental in the decision of the medical team for the simulated patient cases. Auricchio et al suggested the measurement of the coaptation area of prosthesis leaflets to estimate the risk of transvalvular leaks.[17] Morganti et al simulated the deformed geometry of deployed prosthesis within the aortic valve.[18] They were able to predict risks of perivalvular leaks by studying the contacts between the stent and the aortic valve leaflet.

Recently, Morganti et al confirmed that the implantation depth and release angle had a crucial role on determining valve anchoring, device deformation, and risk of regurgitation.[19] This highlights the importance of correctly positioning the delivery system before and during deployment. However, the simulation of delivery tools (prosthesis, sheath, and guidewire) before deployment has not been tackled yet despite their importance on the outcome of the procedure. Such simulation raises many difficult challenges, so we focus on a single tool as a preliminary step toward this goal. To our best knowledge, the stiff guidewire used in TAVI was never simulated, despite the valuable information that can be provided on the mechanical behavior related to tool alignment. To address this issue, we introduce a novel simulation approach of the stiff guidewire in this paper. This novel simulation approach aims at predicting guidewire deformation and positioning in the first stage of TAVI procedures. The paper is organized as follows. In section 2, the mechanical problem is first formulated from a physical analysis of the stiff guidewire insertion. Then, a numerical model solving this problem is defined. Finally, the methods for our sensitivity analysis and validation are described. The simulation results are reported in section 3 and are discussed in section 4.

2 | MATERIALS AND METHODS

The purpose of the model is to predict the shape of a stiff guidewire inserted into a patient-specific aortic and ventricular geometry. The mechanical problem consists in determining the stresses and strains of a beam (the guidewire) constrained to fit within a cavity (aorta and left ventricle). The problem is solved with the finite element (FE) method by using an implicit scheme.

2.1 | Mechanical problem formulation

2.1.1 | Assumption on motions

Respiratory and cardiac movements may distort the complete structure.[20-22] However, the proposed approach was to neglect the dynamic effects of this motion on the guidewire. In addition, guidewire motion was assumed quasi-static because its low mass produced small inertial force compared with the contact forces. Only the final position of the guidewire was predicted by the final static equilibrium of the simulation.

2.1.2 | Mechanical properties

According to intraoperative observations, stiff guidewire insertion led to marginal deformations of the aorta. Thus, the aortic wall and the ventricle were assumed to remain rigid. Under this assumption, it was not necessary to model the influence of blood pressure, prestress within the vascular muscles, and the nonlinear behavior of the aortic wall over large deformations. Despite this, a model with linear elastic tissues was tested for the sake of feasibility proof.

Amplatz Super Stiff and Amplatz Extra Stiff guidewires, commonly recommended for the Corevalve™ and SAPIEN™ prostheses, respectively, were modeled in this study. The elastic properties of the Amplatz Super stiff guidewire used in CoreValve™ implantation were characterized in prior studies.[23,24] Figure 1B shows the bending stiffness along the guidewire. We did not observe any permanent deformation on the stiff guidewire caused by the intervention. Excluding gothic aortic arches, we assume that the usual curvature of the aortic arch is not sufficient to cause plastic strains.

The guidewires were designed with a straight end and may perforate the ventricular wall. To minimize the perforation risk, the guidewire has to be curved at its end before the intervention. To that purpose, clinicians manually deform the guidewire to create a curved end, as shown in Figure 1A. The obtained deformation is permanent (plastic deformation).

This predeformation of the guidewire tip was unknown for both patients considered in this study. Therefore, we investigated the impact of this predeformation through a sensitivity analysis where we varied both the angle and the radius of curvature. The straight floppy part at the end of the guidewire (Figure 1A) had a length of 40 mm. The length between the end and point C (Figure 1A) was set to 120 mm in agreement to the usual practice in the Rennes University Hospital. This corresponded to the transition between the floppy tip and the stiff body of the guidewire (Figure 1B).

2.1.3 | Contacts and boundary conditions

Interactions between the guidewire and the aortic wall result in contact forces. Friction (tangent) contact forces were neglected because the guidewire had a PTFE coating to reduce friction.

In the model, a slipping rail constrained the direction and the orientation of the proximal end (base) of the guidewire in the thoracic aorta. Translations and rotations applied by the operator were modeled as Dirichlet boundary conditions applied at the extreme distal node of the guidewire.

During actual TAVI procedures, the proximal end of the guidewire is free in the left ventricle, while the distal end is moved by the operator. Usually, during its introduction through the femoral dilator, the curved end of the guidewire can take different orientations, as shown in Figure 1C and D. Nevertheless, it remains possible to adjust the orientation when the guidewire reaches the ventricular cavity. We defined the model to take into account the possibility of different orientations in the ventricular cavity.

2.1.4 | Summary of physical parameters

The *physical parameter* input in the model is summarized in Table 1. They include the aortic geometry, the guidewire stiffness, the angle and radius of the curved tip, the axial force applied to the distal end of the guidewire, and the initial

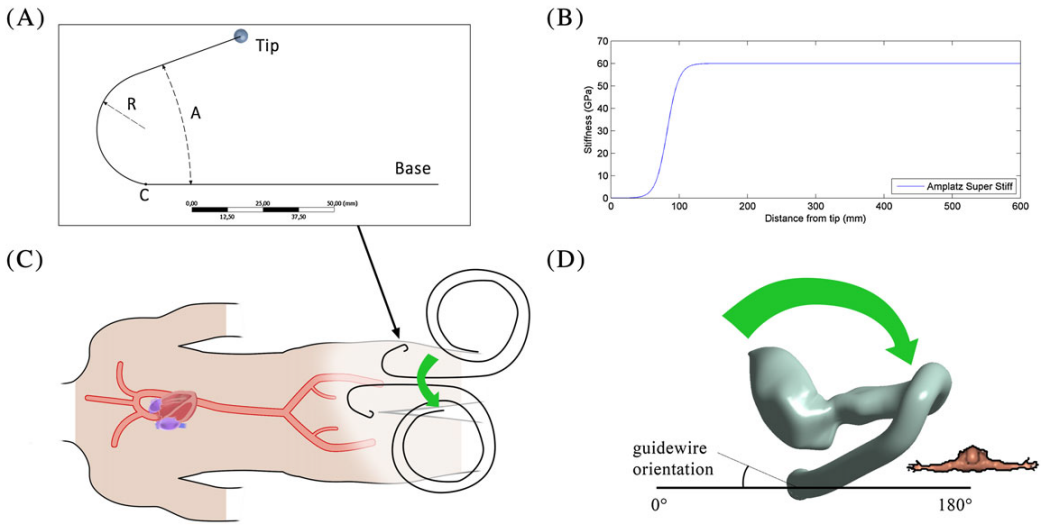

FIGURE 1 A, Model of guidewire predeformation; A, angle; R, radius of curvature; C, start of the curved shape; the tip has a rigid sphere to avoid convergence issues arising from contacts (cf. section 2.2.4). B, Stiffness profile along the guidewire based on (Luboz et al, 2011; Harrison et al, 2011). C and D, illustration of the orientation of the guidewire tip from different views

TABLE 1 Variation of parameters organized as sets of simulation, each focusing on the effect of an individual parameter

	Simulation						
Physical Parameters Focus	**1 Angle**	**2 Radius**	**3 Radius**	**4 Stiffness**	**5 Orientation**	**6 Insertion Depth**	**7-12 Numerical Param.**
Guidewire properties							
Angle (°)	20-120	20	80	20	20	20	20
Radius (mm)	30	15-30	15-30	30	25	25	30
Base stiffness (GPa)	60	60	60	20-100	60	60	60
Insertion conditions							
Force (N)	0.1-0.2	0.1-0.2	0.1-0.2	Max	0.1-0.2	Max	0.2
Orientation (°)	90	90	90	90	0-180	90	90
Initial depth (mm)	−40	−40	−40	−40	−40	7	−40

Numerical parameters Focus	**1-6 Physical param.**	**7 FKN**	**8 FTOLN**	**9 Mesh**	**10 Decay ratio**	**11 Decay/loadstep**	**12 Substep/predictor**
Contact conditions							
Stiffness coefficient (N/mm3)	1	0.1-10	1	1	0.1	0.1	1
Penetration tolerance	2	2	0.5-4	2	2	2	2
Model and solver parameters							
Mesh element size	0.4	0.7	0.7	0.4-0.7	0.7	0.7	0.7
Decay ratio	0.87	0.87	0.87	0.87	0.75-0.9	0.7-0.87	0.87
Number of loadsteps	125	125	125	125	125	50-125	125
Number of substeps	1	1	1	1	10	1	1-10
Predictor	On	Off	On	On	On	On	On/off

orientation. A sensitivity analysis was performed on these physical parameters to determine how they affect the model predictions. This analysis is designed to provide insights on the behavior of the guidewire rather than provide exact recommendation on the parameters. Indeed, those parameters are difficult to control precisely. The geometry of the stiff guidewire is approximately created as the clinician manually deforms it without any precise tool, or selected in a restricted catalog of preshaped guidewire. Likewise, the orientation of the stiff guidewire can be adjusted during its insertion but it is difficult to measure.

2.2 | Discretization and resolution method

2.2.1 | Patient-specific geometry

All patients who undergo TAVI at Rennes University Hospital provide informed consent to participate in the French National Transcatheter Aortic Valve Registry, FRANCE-TAVI,[25] allowing anonymous collection and processing of their clinical data. These interventions are commonly performed under fluoroscopic control. The 2D visualization of the aortic root can only be achieved via the injection of a contrast agent. The images used in the present study were retrospectively collected after the procedures of 2 patients who underwent TAVI at Rennes University Hospital. For both, a CoreValve prosthesis (Medtronic™) was implanted from retrograde trans-femoral access. These retrospective cases were chosen as both had intraoperative images of sufficient quality to permit their registration to the 3D preoperative CT images and to be used for the comparison with numerical simulations. The intraoperative images consisted of digitally subtracted angiography acquired during the protocol when the guidewire was inserted in the ventricle of the patient. The ascending thoracic aorta appeared clearly enough in these images, thanks to the contrast injection (Figure 2A).

A 3D preoperative CT image was routinely acquired for clinical assessment before TAVI interventions. The unsynchronized CT angioscan acquisition was performed by using Discovery CT750HD (General Electric™) (Figure 2B). A

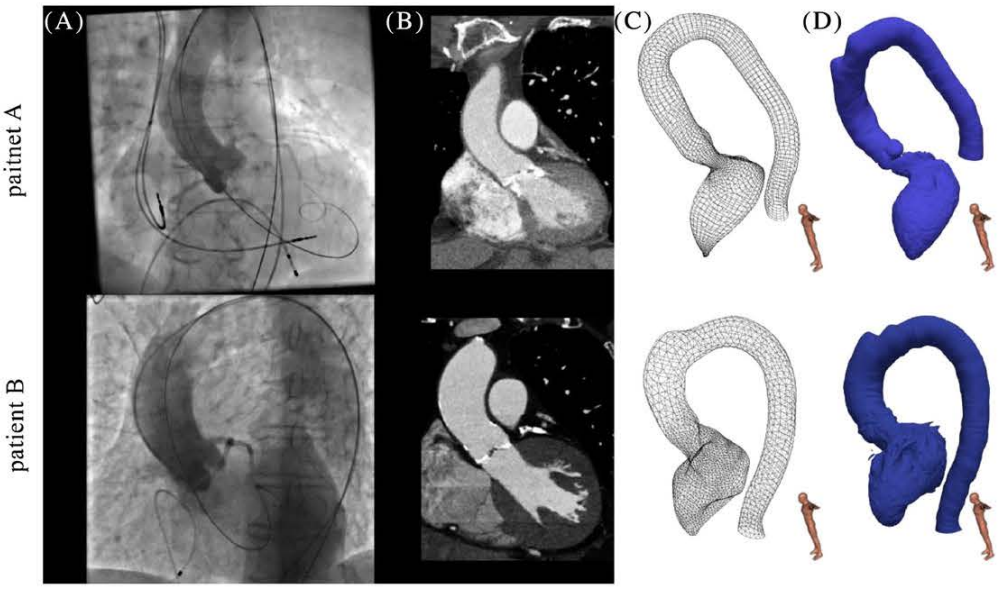

FIGURE 2 A, Intraoperative angiography of aortic root. B, Reformatted slice showing the aortic valve from preoperative CT scan. C, Finite element mesh from segmentation of CT scan. D, Segmentation from CT scan

3D reconstructed image of cardiac structures is shown in Figure 2C. In addition, the clinical protocol included a synchronized CT-scan showing exclusively the aortic valve. In our study, it was assumed that the ventricle geometry obtained in the unsynchronized CT image was fully dilated and close to diastolic state. This was verified by superimposing the synchronized and unsynchronized CT images.

Three-dimensional reconstruction of the left ventricle and aorta was interactively performed by using 3D slicer.[26] The aortic section was smoothed but did not behave well at the supra-aortic trunks (Figure 2D). Moreover, the automatic segmentation created an irregular rough surface that is unlike the real aorta or ventricle. The surface was smoothed and imported in ANSYS by using Spaceclaim, the integrated CAD module of Ansys. Only the aorta was segmented, leaving aside collateral branches and the supra-aortic trunk. The aorta was segmented from the aortic root to the distal thoracic aorta. The artifacts from the supra-aortic trunks were interactively smoothed, and a more realistic mesh was recovered (Figure 2C). This correction must be carefully performed to limit the impact on the results. We assumed that the interactions between the guidewire and the abdominal aorta, the iliac, and the femoral artery had a marginal effect on the position of the guidewire at the aortic valve because of the long sheaths specifically used in TAVI procedures.

This paper mainly focuses on the investigation of patient #1. The investigation of patient #2, reported in Appendix A, was aimed at the verification of the applicability of the model on different geometries.

2.2.2 | Meshing

The geometry was meshed in ANSYS. The rigid aorta was meshed with quadrilateral and triangle contact elements (TARGE170) as shown in Figure 1C. The default mesh had 9610 nodes for patient #1. The guidewire was meshed with quadratic 3-node beam elements based on Timoshenko beam theory (BEAM189) and line contact elements (CONTA175).

2.2.3 | Resolution scheme

Neglecting friction and plasticity, the problem was conservative. However, due to contacts and large deflections of the guidewire, it turned to be highly nonlinear. The simulations were performed on the commercial software ANSYS 17.1 with full Newton-Raphson method and sparse matrix direct solver. Time substeps ensuring convergence of the resolution were defined automatically by ANSYS. A bisection—subdivision of a substep—was performed when more than 26 equilibrium iterations were required to converge a substep. The minimum allowed time step was 5.10^{-3} s for every simulation.

2.2.4 | Boundary conditions and stabilization techniques

The resolution was achieved in 3 stages, as illustrated in Figure 3. Stage I consisted in deforming the guidewire to match the shape of the centerline of the aorta. Stage II consisted in releasing the kinematic constraints applied at stage I, leading to contact between the guidewire and the aortic wall. In stage III, the end of the guidewire could be moved (axial force or rotation) to simulate the action of an operator.

At stage II, the sudden release of the kinematic constraints is often too abrupt for the Newton Raphson algorithm to face contact nonlinearities. Hence, stabilization techniques were introduced. To this end, springs were connected to the nodes of the guidewire. Longitudinal and torsional springs were compared, with torsional springs turning out to be more successful. For each stabilized node, 3 torsional springs prevented rotations about x y, and z axes. They were defined with COMBIN14 elements. They were attached to guidewire nodes at 1 end and to a virtual anchoring node (created for that purpose) at the other end. Anchoring nodes had their displacement coupled with that of the respective guidewire nodes. Their rotations, however, were tied to the guidewire rotations with a delay of one loadstep. Torsional springs had high initial stiffness (11.36 N mm rad^{-1}) so that kinematic constraints could be removed without inducing sudden large displacement. The spring stiffness was decreased at each loadstep by a *decay ratio*. At the end of the stage II, all torsional springs had a null stiffness.

Two options were considered for the reaction force at the distal end of the guidewire. The first option consisted in adjusting the position of the guidewire during the whole simulation to maintain the desired reaction force. This method will be referred as *natural insertion*. Conversely, the *forced insertion* consisted in maintaining the initial depth of insertion throughout stage II.

The distal end of the guidewire was arbitrarily assigned to remain tangential to the centerline of the aorta. It happened that the actual position of guidewires observed intraoperatively at the bottom of the descending thoracic aorta may noticeably deviate from the centerline and be in contact with the wall. However, this was sufficiently far from the aortic root to induce a marginal impact on the results of this study.

Contacts were activated during stage II. Frictionless contact between patient geometry and stiff guidewire was enforced by using an augmented Lagrangian algorithm. The main parameters determining the behavior of the contact were the *contact stiffness coefficient* (FKN) and the *penetration tolerance* (FTOLN). Contact stiffness influenced the contact force applied on the bodies to prevent interpenetration. Nodes with higher penetration than the tolerance do not satisfy the contact compatibility, which is also a convergence criterion. This means that the solver has to repeat the equilibrium iteration with a higher contact force. Numerous preliminary simulations showed that direct contact between the node at the tip of the guidewire and the ventricle led to divergence of the Newton-Raphson algorithm. This issue was addressed by defining a small rigid sphere at the tip of the guidewire (cf. Figure 1A). In general, irregular contact zones such as kinks may lead to large variation of the stiffness matrix of the model which would lead to the failure of the resolution algorithm.

2.2.5 | Summary of numerical parameters

Numerical parameters are summarized in 1. They include the *mesh density*, the *number of loadsteps*, the *initial number of substeps*, the *predictor* (parameter to speed up the process of solving a substep by extrapolating better initial equilibrium iteration), the *depth of insertion*, the *decay ratio* of stabilization springs, the *contact stiffness*, and the *penetration tolerance*.

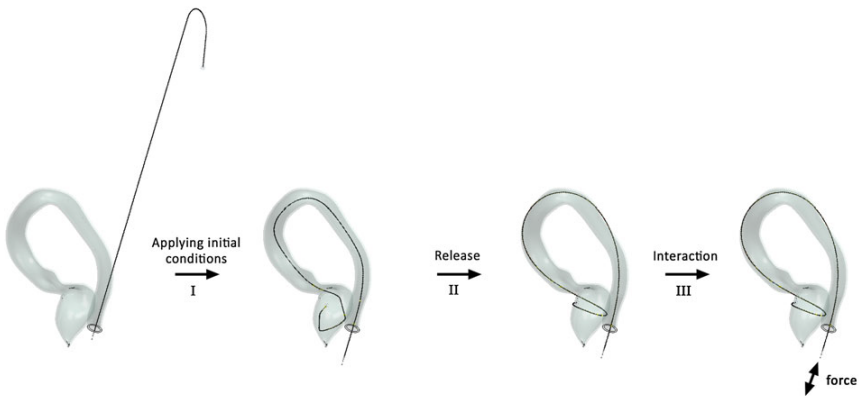

FIGURE 3 Illustration of the simulation stages. After applying initial conditions, the guidewire was constrained on the centerline. After the constraints were relaxed, the guidewire reached its final equilibrium. Then, insertion force could be varied

2.3 | Sensitivity analysis

2.3.1 | Evaluation criteria

The success of model predictions was assessed based on the following characteristics: robustness, computation time, and accuracy.

Robustness

The robustness denoted the ability of the simulation to converge in a mathematically satisfying equilibrium solution regardless of the variation of the input parameters. Convergence or divergence of the solution on a specific range of parameters was a straightforward indicator of robustness. It was observed in preliminary simulations that among all physical parameters, the axial insertion force was the main restriction for robustness (as it induced compression of the guidewire that reached its critical buckling load, which is an instability that cannot be handled with implicit resolution). Thus, maximum converging insertion force was deemed to be a relevant indicator of robustness when varying other parameters and results were presented accordingly.

Computation time

The simulations on ANSYS 17.1 were performed on a HP Z800 Workstation having 2 processors Intel® Xeon® E5620 and 12 GB of RAM. The computation time is reported as the duration of stages I and II of the simulation.

Accuracy

We defined the accuracy of the prediction as the degree of similarity between the simulation result and intraoperative data. The primary output of the simulation was the position and angle of the simulated guidewire in the aortic valve plane. The intraoperative image was a 2D fluoroscopic image, so this comparison was performed by projecting the simulation results according to the current pose of the C-arm. An example of measurement is shown in Figure 4B, where the projection of the simulation is overlapped with the intraoperative view. The aortic valve plane was manually defined according to the contour of the contrast injection. The distance between the simulation and the data was measured at the aortic valve plane in pixels (pixel size for the intraoperative data used here: 0.308 and 0.308 mm at the C-arm detector). The difference of angle was measured in degree.

A 3D/2D registration was necessary to bring the simulation results into the intraoperative coordinate system, as shown in Figure 4B. It is composed of a transformation representing the C-arm pose, a transformation positioning the preoperative CT-scan in the 3D space and a transformation corresponding to the projection performed during the generation of intraoperative images. Numerous 3D/2D registration methods can be found in the literature to obtain such transformation.[27] In this study, a rigid transform combining 3 translations and 3 rotations was iteratively defined. The

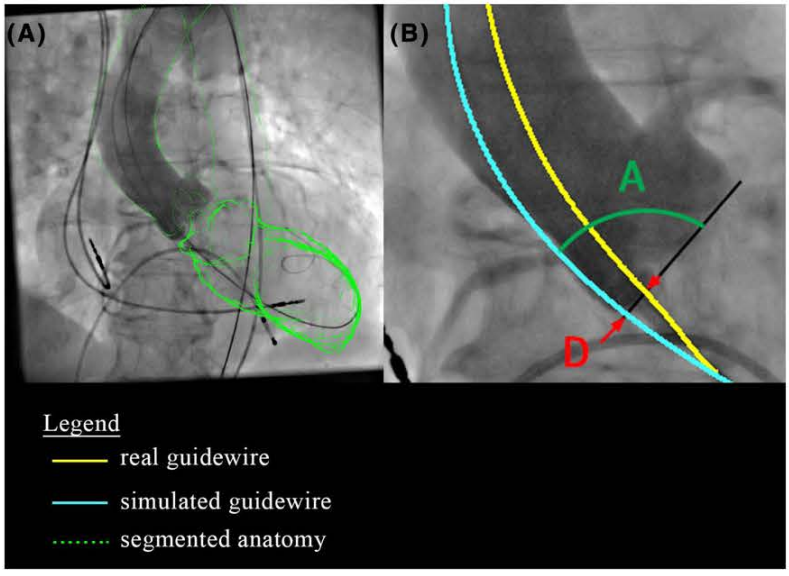

FIGURE 4 A, Projection of 3D preoperative geometry on the intraoperative 2D view according to the registration transforms. B, Intraoperative guidewire is drawn with a yellow line; simulated guidewire appear with a cyan line. The aortic valve plane is manually drawn. The distance *D* and angle *A* of the guidewires are measured at the intersection with the valve plane

C-arm pose and the intrinsic perspective projection parameters were extracted from the DICOM header of the intraoperative data to initialize the registration algorithm.

The aortic root of the 2D intraoperative image (Figure 2A) was manually contoured by an expert. The criterion for registration was the Euclidean 2D distance between the contour of the projected 3D preoperative aorta and the 2D aorta contour observed in the fluoroscopy. A distance map was computed from the 2D aortic contour with the Chamfer operator. The minimization of the distance criterion was iteratively performed by using a Powell optimization algorithm until the estimate of the 3D/2D transform was satisfactory.[28] The resulting projection is shown in Figure 4A. Two intraoperative angiographies at different pose of the C-arm were available and considered in the registration process for patient 2.

2.3.2 | Variations of input parameters

The simulations reported in Table 1 are sorted according to the variation of input parameters. Sets #1 to 6 are related to the exploration of physical parameters. Sets #7 to 12 are related to numerical parameters. The geometry of patient #1 was thoroughly studied under the 12 simulation sets.

Simulation set #1 explored the curvature angle of the guidewire tip from 20° to 120° with a 20° step at a fixed radius of curvature of 30 mm. Sets #2 and 3 explored the radius of curvature from 15 to 30 mm with a 5-mm step at a fixed angle of 20° and 80°, respectively. Set #4 explored the stiffness of the guidewire, which varied from 20 to 100 GPa. Set #5 explored the orientation from 0 to 180° with a fixed guidewire shape. Set #6 tested the forced insertion method to increase the initial depth of insertion. The guidewire was initially 47 mm deeper when using the *forced insertion* method. An insertion force of 0.1 to 0.2 N as indicated in Table 1 means that the stiff guidewire was inserted to reach a reaction force of 0.20 N and then retracted. This allowed comparing the shape of the guidewire at 0.20 and 0.10 N. Sets #4 and #6 simply had the guidewire inserted as much as possible until divergence. Finally, the model with linear elastic tissues was tested for feasibility. The tissues had an elastic modulus of 2 MPa and a Poisson's ratio of 0.49. Arbitrary boundary conditions were defined to maintain the anatomy. Elastic supports (0.15 N mm^{-3}) were defined on the thoracic aorta and the apex of the ventricle. The guidewire had a curvature of 20° and a radius of 25 mm. It was inserted with a natural insertion method to reach 0.05 and 0.1 N. The registration of the simulated deformed aorta was not performed, and accuracy evaluation was not available.

Set #7 explored the contact stiffness coefficient (FKN) from 0.1 to 10. Set #8 explored the penetration tolerance (FTOLN) from 0.5 to 4 mm. Set #9 explored the mesh density of the guidewire (1.4 node/mm, 2.5 node/mm, and 5 node/mm). The stiffness of the torsional stabilization springs was adjusted to provide the same initial level of support. Set #10 explored the decay ratio from 0.75 to 0.9.

In set #11, the decay ratio was adjusted with the number of loadsteps so that the stabilization springs reached the same stiffness at their complete deactivation across all simulations of the set (10^{-4} N mm rad^{-1}). Thus, the number of loadsteps was explored while keeping the release rate of the stabilization springs consistent. Finally, set #12 explored the relationship between the number of substep and the predictor.

3 | RESULTS

From a qualitative point of view, the model was able to converge on a large range of parameters. Table 2 reports the computation times, including minimum, maximum, and mean values, along with the diverged simulations. Table 3 reports the minimum, maximum, standard deviation, and mean values of accuracy measurements, ie, angle difference and distance rounded at the nearest pixel.

3.1 | Sensitivity to physical parameters

3.1.1 | Influence of the stiff guidewire properties

The sets investigating the effect of the curvature angle and radius (#1, #2, and #3) converged. The maximum insertion force for convergence of set #4 is reported in Table 4B. A linear regression analysis between the maximum insertion force and the stiffness of the guidewire was performed. The regression coefficient is 0.004 N/GPa, and the coefficient of determination is 0.9984.

Computation times were similar across those simulations (between 3000 and 4000 s). The simulated guidewires (#1, #2, and #3) projected on intraoperative image are shown in Figure 5B to D. The standard deviation of the angle difference and distance was low, less than 1° of angle difference and 3 px of distance. The curvature radius

TABLE 2 Computation time of simulations required to reach static equilibrium and remove all stabilization

Set	1		2		3	
Param.	Angle (°)	Computation Time (s)	Radius (mm)	Computation Time (s)	Radius (mm)	Computation Time (s)
Min	60	2,772	20	3,045	30	3,289
Max	120	3,522	30	3,521	25	4,279
Avr		3,239		3,352		3,703
Set	**4**		**5**		**6**	
Param.	**Stiffness (GPa)**	**Computation time (s)**	**Orientation (°)**	**Computation time (s)**	**Depth (mm)**	**Computation time (s)**
Min	100	3,435	0	3,081	−47	4,638
Max	20	4,707	180	3,982	7	9,572
Avr		3,835		3,401		7,105
Set	**7**		**8**		**9**	
Param.	**Contact stiffness (N/mm3)**	**Computation time (s)**	**Penetration (mm)**	**Computation time (s)**	**Mesh (node/mm)**	**Computation time (s)**
Min	3	2,846	0.5	3,521	1.4	4,056
Max	1	4,113	10	3,702	5	14,928
Avr		3,386		3,624		7,873
Set	**10**		**11**		**12**	
Param.	**Decay**	**Computation time (s)**	**Decay/loadstep**	**Computation time (s)**	**Substep/predictor**	**Computation time (s)**
Min	0.87	31,540	0.7929/75	1,821	1/on	3,521
Max	0.8	36,623	0.8402/100	2,547	10/off	14,382
Avr		33,623		2,166		7,221

Diverged simulations					
Sets	**12**		**7**	**2bis (patient 2)**	
Param.	**Substep**	**Predictor**	**FKN**	**Angle**	**Radius**
Values	10	On	0.1	20	20

of the guidewire produced the highest standard deviation. The curvature angle produced the lowest standard deviation. The projections of set #4 were not reported in the figures because the simulated guidewire shapes were too similar.

3.1.2 | Influence of the insertion conditions

Set #5 investigating the orientation converged. It required a computation time ranging from 3081 to 3982 seconds. Figure 5E shows the guidewires of set #5. The deformation of the tip is noticeably influenced by the orientation of the guidewire. The standard deviation was 2° and 4.4 px for angle difference and distance, respectively. Set #6 converged when the insertion depth was less than −18 mm or included in a range between −3.9 and 10.8 mm. Further range was not tested. The domain of convergence can be observed in the force versus displacement curve in Figure 6D. The simulated guidewires at the edge of the domain of convergence are projected in Figure 6A to C. The variation of insertion depth resulted in a large standard deviation (6.8° and 12.7 px). However, simulated guidewires from forced insertion obtained higher differences with the intraoperative guidewire. The differences produced when varying the insertion force from 0.10 to 0.20 N (natural insertion) for set #1 are reported in Table 4A. The simulated guidewires are projected

TABLE 3 Accuracy evaluation of simulation sets from the projection of simulated guidewire on intraoperative image

Set	1	Angle	2	Radius	3	Radius
Parameters	Angle Difference (°)	Distance (px)	Angle Difference (°)	Distance (px)	Angle Difference (°)	Distance (px)
Min	3.6	2	−0.5	1	−0.4	0
Max	4.4	3	−2.3	6	−1.6	5
Mean	3.9	2.3	−0.8	3.3	−0.7	2.3
Std	0.3	0.3	1.3	2.2	0.9	2.2
Set	**4**	**Stiffness**	**5**	**Orientation**	**6**	**Depth**
Parameters	**Angle difference (°)**	**Distance (px)**	**Angle difference (°)**	**Distance (px)**	**Angle difference (°)**	**Distance (px)**
Min	0	4	−0.4	3	−0.3	0
Max	0.6	5	2.8	13	−9.9	18
Mean	0.1	4.6	0.3	5.2	−5.1	9
Std	0.3	0.5	2	4.4	6.8	12.7
Set	**7**	**FKN**	**8**	**FTOLN**	**9**	**Mesh**
Parameters	**Angle difference (°)**	**Distance (px)**	**Angle difference (°)**	**Distance (px)**	**Angle difference (°)**	**Distance (px)**
Min	0	0	0.5	2	0	1
Max	−0.4	0	1.5	2	−0.5	1
Mean	−0.3	0	1	2	−0.2	1
Std	0.2	0	0.5	0	0.3	0
Set	**10**	**Decay**	**11**	**Decay / loadstep**	**12**	**Substep/predictor**
Parameters	**Angle difference (°)**	**Distance (px)**	**Angle difference (°)**	**Distance (px)**	**Angle difference (°)**	**Distance (px)**
Min	1.4	4	1.7	4	0.7	2
Max	2.1	4	2	4	1	2
Mean	1.8	4	1.9	4	0.9	2
Std	0.3	0	0.2	0	0.2	0

in Figure 5A and B. The mean values for the angle difference increased by 3.3° and distance by 1 px with the increasing force. The standard deviations remained similar for both 0.10 and 0.20 N.

3.2 | Sensitivity to numerical parameters

We observe from Table 3 that sets #7 to #12 produce very small standard deviation (less than 0.5° and 0 px). We deduce that the variation of the numerical parameters has negligible influence on the accuracy. Instead, they show a strong influence on convergence and computation time. Excessively low contact stiffness resulted in divergence. Using predictor with a large number of substep slowed the simulation and occasionally led to divergence. The decay ratio should be adjusted so that the torsional springs are deactivated with stiffness around 10^{-4} N mm rad^{-1}. The mesh density had a negligible impact on computation time. Each set is detailed in the following paragraphs.

3.2.1 | Contact conditions

In set #7, contact stiffness coefficient of 0.1 diverged. All simulations of set #8 converged. The physical parameters were angle = 100°, radius = 30 mm, and force = 0.22 N with predictor activated. The standard deviations from both contact stiffness coefficient and penetration tolerance variation were negligible, less than 0.5° for angle difference and 0 px for distance.

TABLE 4 Detailed measurements for sets #1 and #4

(a) Comparison of Insertion Force 0.10 N and 0.20 N (Set #1)				
Set #1	**Insertion Force 0.10 N**		**Insertion Force 0.20 N**	
Angle (°)	**Angle Difference (°)**	**Distance (px)**	**Angle Difference (°)**	**Distance (px)**
20	3.6	3	0.9	2
40	3.6	2	1	1
60	3.8	2	0.9	1
80	4	3	0.5	0
100	3.9	2	0	1
120	4.4	2	0.2	1
Mean	3.9	2.3	0.6	1.0
Standard deviation	0.3	0.5	0.4	0.6

(b) Maximum force insertion appears linearly dependent on stiffness of the guidewire (set #4)			
Set #4 Stiffness (GPa)	**Angle difference (°)**	**Distance (px)**	**Maximum force (N)**
20	0.1	5	0.08
40	0	5	0.16
60	-0.2	5	0.24
80	0.6	4	0.32
100	0.1	4	0.39
Mean	0.1	4.6	
Standard deviation	0.3	0.5	

3.2.2 | Model and solver parameter

Concerning set #9, the coarser mesh (1.4 node/mm) had the shortest total computation time (4056 s). The finer mesh (5 node/mm) had the longest computation time (14,928 s). Maximum insertion force of the finer mesh was 0.01 N above that of the coarser mesh. A large fraction of the computation time was spent to compute the last increments of insertion force. The standard deviation was negligible for both angle difference (0.3°) and distance (0 px).

The physical parameters for set #10 were angle = 20°, radius = 30 mm, and force = 0.20 N with a mesh density of 0.14 node/mm and 10 substeps per loadstep. The fastest simulation ran with a decay ratio of 0.87. During the deactivation of the stabilization springs at loadstep 124, their stiffness was near 10^{-4} N mm rad^{-1}. Lower decay ratio generated instability at each loadstep, which resulted in an increased computation time. Higher decay ratio slowed down the removal of stabilization springs. If the spring stiffness was still too high during the loadstep of complete deactivation of stabilization springs, instabilities arose and increased the computation time. The projections of set #9 appeared undistinguishable one from another. Careful inspection showed that very few pixels were positioned differently. The standard deviation was negligible for both angle difference (0.3°) and distance (0 px).

The physical parameters for set #11 were angle = 20°, radius = 25 mm, and force = 0.15 N. The best computation time was 1821 seconds (decay ratio = 0.7929, 75 loadsteps). The projections of the simulations appeared undistinguishable except small differences in the ventricle. The standard deviation was negligible for both angle difference (0.2°) and distance (0 px).

Finally, the physical parameters for set #11 were angle = 20°, radius = 30 mm, and force = 0.20 N. A simulation using predictor and 10 substeps per loadstep diverged. The use of predictor and the increase of the substep number did not seem to impact the accuracy of the prediction because the standard deviations were low (0.2° for angle difference and 0 px for distance). Predictor was beneficial if the number of substeps was set to 1. Conversely, predictor severely hindered the simulation when the number of substeps was set to 10.

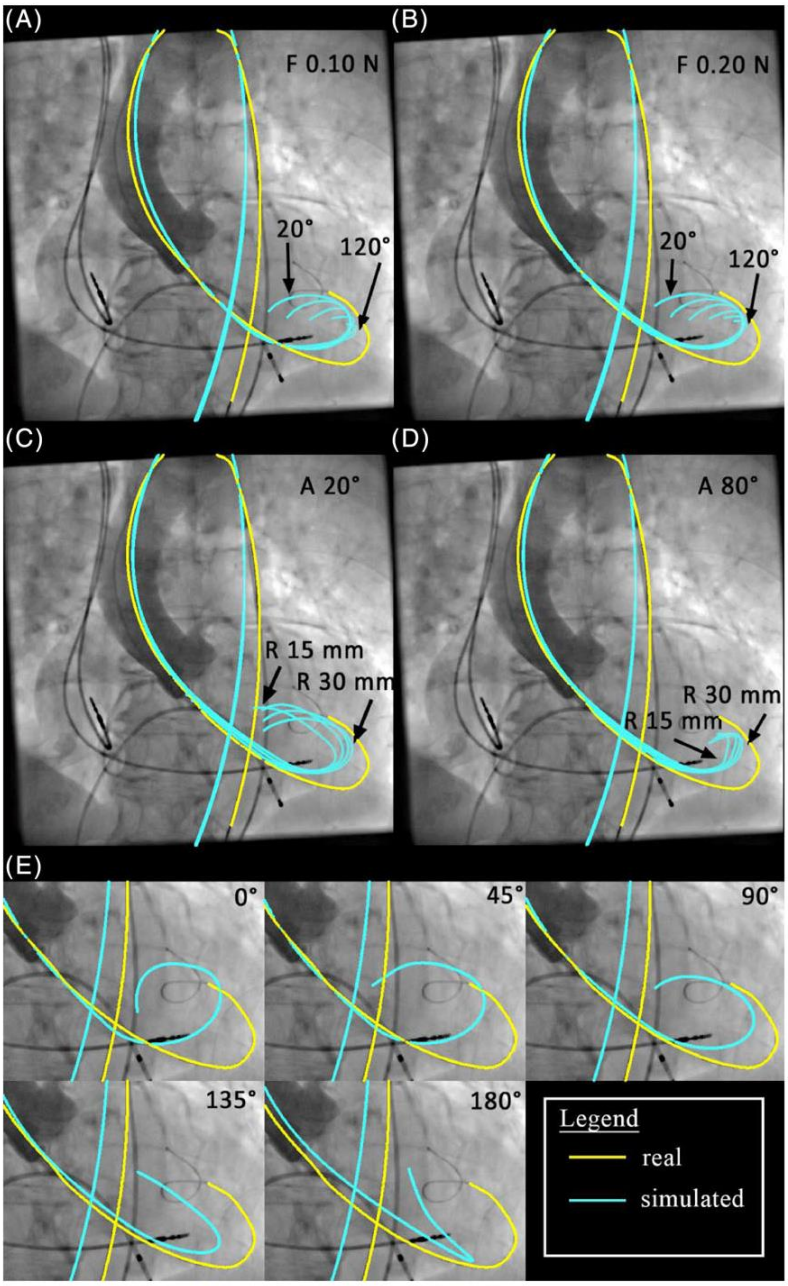

FIGURE 5 Projection of simulated guidewires. A, Set #1 exploring angle curvature at 0.10 N insertion force. B, Set #1 exploring angle curvature at 0.20 N insertion force. C, Set #2 exploring radius at 20° angle curvature. D, Set #3 exploring radius at 80° angle curvature. E, Set #5 exploring orientation

4 | DISCUSSION

4.1 | Summary

This study presented an FE modeling framework for predicting the shape of a stiff guidewire inserted into a patient-specific geometry of the left ventricle and aortic arch. The model was solved with an implicit resolution scheme in ANSYS. Then, the performance of the model was evaluated in accuracy, robustness, and speed of resolution. Nonlinearity associated with contacts proved to be a challenging problem for the implicit resolution method. Therefore, stabilization techniques were proposed to enhance the robustness of the model and overcome instabilities. The model was able to explore a wide range of parameters and provide insights on the behavior of the inserted guidewire. The results of the simulations were compared with intraoperative 2D images. Very good agreement could be obtained with respect to the intraoperative guidewire position after a thorough sensitivity analysis of the simulation problem. The guidewire properties which

a) b) c) Projections of simulated guidewires at the edges of the convergence domain reported in d). Natural insertion simulations matched closer to intra-operative data than forced insertion simulations.

d) Force-displacement graph of the insertion of guidewire. Forced insertion method allows exploring isolated domain of convergence.

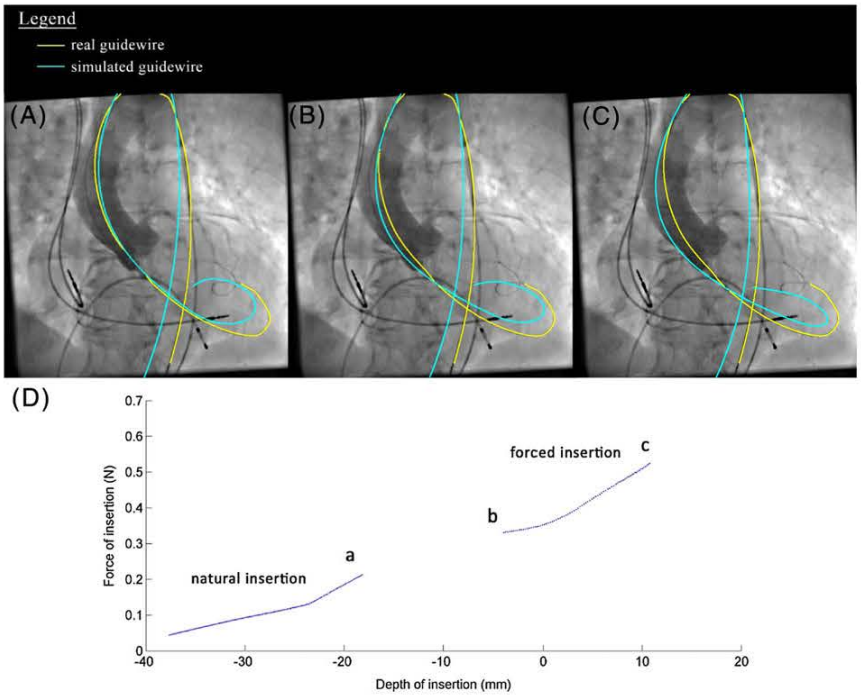

FIGURE 6 A to C, Projections of simulated guidewires at the edges of the convergence domain reported in (D). Natural insertion simulations matched closer to intraoperative data than forced insertion simulations. D, Force-displacement graph of the insertion of guidewire. Forced insertion method allows exploring isolated domain of convergence

produced the most accurate predictions were the following: curvature of 100° and curvature radius of 30 mm and insertion force of 0.20 N with a 90° orientation.

The main conclusion of the sensitivity analysis was that the patient anatomy itself mostly determined the shape of the guidewire and had a more significant impact than the guidewire curvature properties. This can be explained by the high compliance of the guidewire in its curved part compared with the straight body of the guidewire.

Excluding the patient's geometry, the influence of the physical parameters on the prediction was intricate and prevented from extracting general trends. This was especially the case for the shape of the guidewire in the left ventricle. Therefore, numerical simulations appeared to be useful to understand the insertion and navigation of endovascular tools in the aortic arch and left ventricle.

4.2 | Contribution and comparison with bibliography

Transcatheter aortic valve implantation interventions heavily rely on the experience of medical teams. Thus, numerical models can be a relevant objective complementary support. Most of the published work was focused on the numerical deployment of the prosthesis regardless of its predeployment positioning. To the best of our knowledge, no study was performed on the position of delivery tools and prosthesis at the aortic valve. Yet, it is important to deal with the position of the prosthesis because it is a concern for the success of the deployment.

Similar studies were performed by Dumenil et al and Gindre et al for the insertion of guidewires during endovascular aneurysm repair.[28,29] Other studies were dedicated to the insertion of catheter during mini-invasive treatment of cerebrovascular disease.[30-33] Among them, Lawton et al described a computationally efficient FE model based on an in-house resolution method.[34] The catheter was modeled as a thin rod, and the vessels were assumed rigid like in the present study. Schafer et al presented a method to determine the shape of the guidewire by using shortest path algorithms.[35]

Each problem was unique and raised different challenges. Cerebrovascular intervention raised challenges by navigating into a complex maze of thin arteries. Transcatheter aortic valve implantation and endovascular aneurysm repair raised more concerns on the correct placement of a prosthesis in large vessels. During TAVI, unlike other medical contexts, the guidewire is pushed against the ventricle wall. The force exerted against the guidewire; its curvature and its properties could influence its shape. Beyond the insertion of a stiff guidewire alone, it must be kept in mind that the insertion of the prosthesis and its sheath could also deform the aortic arch.

Models for cerebrovascular treatment navigation usually featured in-house implicit resolution schemes, which seemed to be successful when the vessels were rigid and little stress was generated. Conversely, models for aneurysm repair showed that explicit resolution was successful to predict the large deformations of the tools and the arteries. Likewise, simulation model for the deployment of prosthesis mainly used explicit resolution scheme so far. Despite the widespread use of explicit schemes for similar problems, we successfully used an implicit resolution scheme which is expected to provide more reliable results about stresses, strains, and contact forces.

4.3 | Interpretation of results

The main findings can be summarized as follows. Concerning the physical parameters, the results showed that the insertion force, orientation, and curvature radius strongly impacted the guidewire deformation and position at the plane of aortic valve. The curvature angle and stiffness of the guidewire had a weak influence on the inserted shape. The tests over the numerical parameters showed that they had negligible impact on the accuracy. The base of the guidewire was assumed to have little impact on the accuracy at the aortic valve, so its position was arbitrarily chosen. As such, the base of the simulated guidewire did not match the intraoperative image. The comparison of the simulation in the ventricle was not conclusive. The intraoperative ventricle appeared radio transparent so the quality of registration could not be assessed in this volume. However, all things considered, the model could reach very good accuracy in predicting the position and angle of the guidewire at the aortic valve.

Throughout the development of the model, we observed convergence difficulties for insertion force above approximately 0.20 N by using natural insertion method. A force displacement graph was plotted in Figure 6D and illustrated the domain where the simulation diverged. An analysis on the guidewire stiffness showed that the maximum insertion force was strongly correlated to the stiffness. However, the guidewire shape at the maximum insertion force was nearly identical whatever the stiffness. Using the forced insertion method, the simulation could overcome the instabilities and reach an insertion force between 0.3 and 0.5 N. However, those simulations were even more different from the intraoperative 2D image, shifting the guidewire at the aortic valve more than 10 px. Beyond 0.5 N, the simulation encountered again convergence difficulties.

The insertion of a beam against a wall might be prone to buckling effects, which can create convergence difficulties for an implicit resolution method. Euler's critical buckling load is given by the formula:

$$F = \frac{\pi 2EI}{(KL)2} \tag{1}$$

where L is the length of the beam, E is the Young's modulus of the beam (60 GPa), I is the area moment of inertia of the cross section (0.0491 mm^4), and K is the column effective length factor which was assumed to be equal to 2 as we considered one end highly constrained by contact force on the aortic wall (fixed) and the floppy tip of the guidewire free to move. Equation 1 is consistent with the correlation observed in set #4 between the stiffness of the guidewire and the maximum insertion force. To have a rough evaluation of the critical load for the guidewire, we measured that the length of the guidewire which may be subject to buckling was about 180 mm. Figure 7 shows the major contact zones on the guidewire and the measurement (in green). We obtained a critical load around 0.22 N and the proportionality coefficient relating E to F ($\pi 2I/(KL)2$) equal to 0.0037 N/GPa. This theoretical critical load was in the same range order as the maximum axial forces reached before divergence of our simulations (~0.2 N). Coincidentally, the theoretical proportionality coefficient was also in the same range as the coefficient deduced from set #4 (0.0040 N/GPa).

4.4 | Limitations

One of the main limitations of this study was related to the available data. The preoperative 3D image was unsynchronized with heart cycle, and the valve leaflets could not be extracted. The valve calcifications as seen in Figure 2B have been neglected and may impact the simulation. They could be added as rigid bodies. However, we observed that the

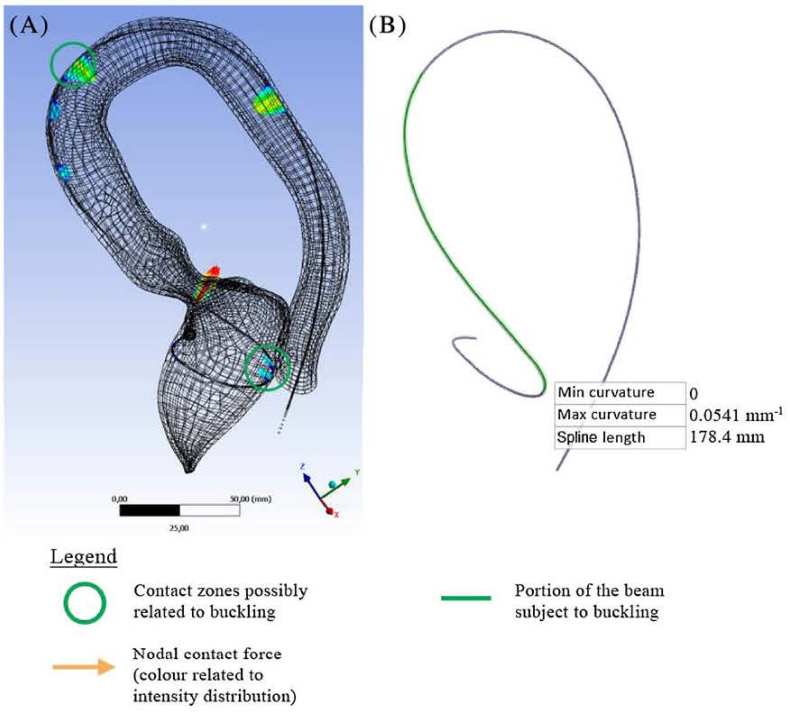

FIGURE 7 A, Contact force distribution along the simulated guidewire from set #6 (Figure 6A). The green circles highlight contact zones which may produce a buckling effect. B, Measurement of the portion of the guidewire hypothetically subjected to buckling

simulated guidewire did not touch the segmented calcifications in those patient cases specifically. The shape of the ventricle was approximate due to heartbeat effects. The creation process of the patient mesh also increased the uncertainties on the geometry of the model. The model required information on the conditions of insertion that could not be obtained from the intraoperative data, such as the inserted length of the guidewire, the insertion force, the orientation, and the shape of the curvature of the guidewire. Last, there was a possible mismatch between the model geometry and intraoperative image because of heartbeat and breathing motions. The 2D/3D registration was focused on the ascending aorta, where the contrast due to injection was highest. In the near future, the comparison of the numerical model with intraoperative images of a larger cohort of patients should provide a clearer evaluation of the reliability of the simulations and the validity of the assumptions. Finally, despite the importance of modeling the guidewire deformation, the prosthesis and the sheath should be included into the model in future studies.

The Timoshenko beam formulation was not necessarily the most appropriate choice due to the occurrence of shear-locking in field-inconsistent elements. The effect of shear-locking on accuracy and robustness was mitigated by the use of 3-node quadratic element but certainly affected the speed of the simulation. A possible direction for future works would be the improvement of the performances by including new element formulations.

4.5 | Application perspectives

The simulation framework offered interesting insights on the behavior of the guidewire and provided data to improve TAVI simulation outcomes accuracy. The framework is currently not at the stage where it can provide strategies to completely correct misalignment of the prosthesis at the aortic valve but tries to contribute toward this goal.

The prosthesis alignment is greatly determined by the sheath in comparison with the guidewire. The latter still contributes to both the alignment and the stability of the prosthesis. In exceptional cases, this small contribution is enough to allow experienced clinicians improving the alignment of self-expandable prosthesis by manipulating the guidewire. The insights provided by this simulation framework could be applied to predict whether this kind of maneuver is feasible or beneficial for a given patient anatomy and a given guidewire curvature.

In addition, the handling of the guidewire carries a risk of ventricle damage. The simulation framework could help studying the behavior of the contact between the guidewire and the ventricle to help choosing the guidewire curvature associated with the best stability and the safest distribution of contact forces on the ventricular wall. Currently, there is no general agreement regarding guidewire curvature. Increasingly more clinicians use preshaped guidewire (SAFARI™), and some center systematically use the smallest size for simplicity. Some clinicians report that small-sized preshape is

prone to unwanted migration within the ventricle and provides less stability to the prosthesis deployment. The current simulation framework has only been assessed for geometrical parameters at the aortic valve. Future works could be directed toward the improvement of prediction in the ventricle.

Finally, the centerline of the aortic valve is the starting point to visualize the prosthesis deployment. The simulated guidewire is a possible improvement to help the clinicians guess more accurately the alignment of the prosthesis in the preoperative planning stages and approach more cautiously anatomies which produce severe misalignment and have higher risks of complication. As the model matures, sheath and prosthesis may be included to help the clinician making more accurate predictions. Retrograde trans-femoral access is associated with the highest survival rate, but there could be exceptional patient cases where other accesses provide safer positioning of the prosthesis. Future works could also compare the impact of vascular accesses on prosthesis positioning.

5 | CONCLUSION

This paper presented a unique simulation framework to predict the angle and the position of a stiff guidewire in the aortic valve. The accuracy of the model was evaluated with patient intraoperative data, and good agreement could be reached. The sensitivity analysis concluded that the shape of the guidewire was mainly determined by the patient geometry and the insertion conditions. The unique use of implicit resolution scheme in this particular context required stabilization techniques to guarantee convergence. However, divergence still occurred when the guidewire was subject to buckling. A larger number of patient cases will be simulated in the future to ascertain the reliability of this method.

ACKNOWLEDGEMENTS

This work was partly supported by the French ANR within the Investissements d'Avenir program (Labex CAMI) under reference ANR-11-LABX-0004. This work has been partially conducted in the experimental platform TherA-Image (Rennes, France) supported by Europe FEDER.

ORCID

Phuoc Vy http://orcid.org/0000-0003-3813-7611

REFERENCES

1. Cribier A, Eltchaninoff H, Bash A, et al. Percutaneous transcatheter implantation of an aortic valve prosthesis for calcific aortic stenosis: first human case description. *Circulation*. 2002;106(24):3006-3008. https://doi.org/10.1161/01.CIR.0000047200.36165.B8
2. Smith C, Leon M. Transcatheter versus surgical aortic-valve replacement in high-risk patients. *N Engl J Med*. 2011;364(23):2187-2198. https://doi.org/10.1056/NEJMoa1109071
3. Leon MB, Smith CR, Mack M, et al. Transcatheter aortic-valve implantation for aortic stenosis in patients who cannot undergo surgery. *N Engl J Med*. 2010;363(17):1597-1607. https://doi.org/10.1056/NEJMoa1008232
4. Thourani VH, Kodali S, Makkar RR, et al. Transcatheter aortic valve replacement versus surgical valve replacement in intermediate-risk patients: a propensity score analysis. *The Lancet*. 2016;143(1):64-71. https://doi.org/10.1016/S0140-6736(16)30073-3
5. Masson JB, Kovac J, Schuler G, et al. Transcatheter aortic valve implantation. Review of the nature, management, and avoidance of procedural complications. *J Am Coll Cardiol Intv*. 2009;2(9):811-820. https://doi.org/10.1016/j.jcin.2009.07.005
6. Shannon J, Mussardo M, Latib A, et al. Recognition and management of complications during transcatheter aortic valve implantation. *Expert Rev Cardiovasc Ther*. 2011;9(7):913-926. https://doi.org/10.1586/erc.11.84
7. Généreux P, Head SJ, Hahn R, et al. Paravalvular leak after transcatheter aortic valve replacement: the new Achilles' heel? A comprehensive review of the literature. *J Am Coll Cardiol*. 2013;61(11):1125-1136.
8. Zegdi R, Ciobotaru V, Noghin M, et al. Is it reasonable to treat all calcified stenotic aortic valves with a valved stent? Results from a human anatomic study in adults. *J Am Coll Cardiol*. 2008;51(5):579-584. https://doi.org/10.1016/j.jacc.2007.10.023
9. Stähli BE, Maier W, Corti R, Lüscher TF, Jenni R, Tanner FC. Aortic regurgitation after transcatheter aortic valve implantation: mechanisms and implications. *Cardiovascular diagnosis and therapy*. 2013;3(1):15-22. https://doi.org/10.3978/j.issn.2223-3652.2013.02.01
10. Siontis GCM, Jüni P, Pilgrim T, et al. Predictors of permanent pacemaker implantation in patients with severe aortic stenosis undergoing TAVR. *J Am Coll Cardiol*. 2014;64(2):129-140. https://doi.org/10.1016/j.jacc.2014.04.033

11. Ribeiro HB, Nombela-Franco L, Urena M, et al. Coronary obstruction following transcatheter aortic valve implantation: a systematic review. *J Am Coll Cardiol Intv*. 2013;6(5):452-461.
12. Sun W, Martin C, Pham T. Computational modeling of cardiac valve function and intervention. *Annu Rev Biomed Eng*. 2014;16(1):53-76. https://doi.org/10.1146/annurev-bioeng-071813-104517
13. Tseng EE, Wisneski A, Azadani AN, Ge L. Engineering perspective on transcatheter aortic valve implantation. *Interv Cardiol*. 2013;5(1):53-70. https://doi.org/10.2217/ica.12.73
14. Vy P, Auffret V, Badel P, et al. Review of patient-specific simulations of transcatheter aortic valve implantation. *International Journal of Advances in Engineering Sciences and Applied Mathematics*. 2016;8(1):2-24. https://doi.org/10.1007/s12572-015-0139-9
15. Bosmans B, Famaey N, Verhoelst E, Bosmans J, Vander Sloten J. A validated methodology for patient specific computational modeling of self-expandable transcatheter aortic valve implantation. *J Biomech*. 2016;49(13):2824-2830. https://doi.org/10.1016/j.jbiomech.2016.06.024
16. Wang Q, Kodali S, Primiano C, Sun W. Simulations of transcatheter aortic valve implantation: implications for aortic root rupture. *Biomech Model Mechanobiol*. 2014;14(1):29-38. https://doi.org/10.1007/s10237-014-0583-7
17. Auricchio F, Conti M, Morganti S, Reali A. Simulation of transcatheter aortic valve implantation: a patient-specific finite element approach. *Comput Methods Biomech Biomed Engin*. 2014;17(12):1347-1357. https://doi.org/10.1080/10255842.2012.746676
18. Morganti S, Conti M, Aiello M, et al. Simulation of transcatheter aortic valve implantation through patient-specific finite element analysis: two clinical cases. *J Biomech*. 2014;2012(11):2547-2555. https://doi.org/10.1016/j.jbiomech.2014.06.007
19. Morganti S, Brambilla N, Petronio AS, Reali A, Bedogni F, Auricchio F. Prediction of patient-specific post-operative outcomes of TAVI procedure: the impact of the positioning strategy on valve performance. *J Biomech*. 2015;49(12):2513-2519. https://doi.org/10.1016/j.jbiomech.2015.10.048
20. Wang Y, Riederer SJ, Ehman RL. Respiratory motion of the heart: kinematics and the implications for the spatial resolution in coronary imaging. Magnetic resonance in medicine: official journal of the Society of Magnetic Resonance in Medicine/Society of Magnetic Resonance in Medicine *Magn Reson Med* 1995; 33(5):713–719. https://doi.org/10.1002/mrm.1910330517
21. Weber TF, Tetzlaff R, Rengier F, et al. Respiratory displacement of the thoracic aorta: physiological phenomenon with potential implications for thoracic endovascular repair. *Cardiovasc Intervent Radiol*. 2009;32(4):658-665. https://doi.org/10.1007/s00270-009-9553-3
22. Jurencak T, Turek J, Kietselaer BLJH, et al. MDCT evaluation of aortic root and aortic valve prior to TAVI. What is the optimal imaging time point in the cardiac cycle? *Eur Radiol*. 2015;25(7):1975-1983. https://doi.org/10.1007/s00330-015-3607-5
23. Luboz V, Zhai J, Odetoyinbo T, et al. Simulation of endovascular guidewire behaviour and experimental validation. *Comput Methods Biomech Biomed Engin*. 2011;14(6):515-520. https://doi.org/10.1080/10255842.2010.484003
24. Harrison GJ, How TV, Vallabhaneni SR, et al. Guidewire stiffness: what's in a name? *J Endovasc Ther*. 2011;18(6):797-801. https://doi.org/10.1583/11-3592.1
25. Auffret V, Lefevre T, Van Belle E, et al. Temporal trends in transcatheter aortic valve replacement in France. *J Am Coll Cardiol*. 2017;70(1):42-55. https://doi.org/10.1016/j.jacc.2017.04.053
26. Kikinis R, Pieper SD, Vosburgh KG. 3D slicer: a platform for subject-specific image analysis, visualization, and clinical support. In: Jolesz FA, ed. *Intraoperative Imaging and Image-Guided Therapy*. New York, NY: Springer New York; 2014:277-289.
27. Markelj P, Tomaževič D, Likar B, Pernuš F. A review of 3D/2D registration methods for image-guided interventions. *Med Image Anal*. 2012;16(3):642-661. https://doi.org/10.1016/j.media.2010.03.005
28. Dumenil A, Kaladji A, Castro M, et al. Finite element-based matching of pre- and intra-operative data for image-guided endovascular aneurysm repair. *IEEE Transactions on Bio-Medical Engineering*. 2012;60(c):1353-1362. https://doi.org/10.1109/TBME.2012.2235440
29. Gindre J, Bel-Brunon A, Kaladji A, et al. Finite element simulation of the insertion of guidewires during an EVAR procedure: example of a complex patient case, a first step toward patient-specific parameterized models. *International Journal for Numerical Methods in Biomedical Engineering*. 2015;20(4):n/a-n/a. https://doi.org/10.1002/cnm.2716):e02716
30. Wang YP, Chui CK, Cai YY, Mak KH. Topology supported finite element method analysis of catheted guidewire navigation in reconstructed coronary arteries. 1997; 24.
31. Lenoir J, Cotin S, Duriez C, Neumann P. Interactive physically-based simulation of catheter and guidewire. *Computers and Graphics (Pergamon)*. 2006;30(3):417-423. https://doi.org/10.1016/j.cag.2006.02.013
32. Nowinski WL, Chui CK. Simulation of interventional neuroradiology procedures. Proceedings - International Workshop on Medical Imaging and Augmented Reality, MIAR 2001 2001:87–94. https://doi.org/10.1109/MIAR.2001.930269
33. Cotin S, Duriez C, Lenoir J, Neumann P, Dawson S. New approaches to catheter navigation for interventional radiology simulation. *Lecture Notes in Computer Science (including subseries Lecture Notes in Artificial Intelligence and Lecture Notes in Bioinformatics)* 2005; 3750 LNCS(June 2017):534–542. https://doi.org/10.1007/11566489_66
34. Lawton W, Raghavan R, Ranjan SR, Viswanathan RR. Tubes in tubes: catheter navigation in blood vessels and its applications. *International Journal of Solids and Structures*. 2000;37(22):3031-3054. https://doi.org/10.1016/S0020-7683(99)00067-0

35. Schafer S, Singh V, Noël PB, Walczak AM, Xu J, Hoffmann KR. Real-time endovascular guidewire position simulation using shortest path algorithms. *Int J Comput Assist Radiol Surg*. 2009;4(6):597-608. https://doi.org/10.1007/s11548-009-0385-z

How to cite this article: Vy P, Auffret V, Castro M, et al. Patient-specific simulation of guidewire deformation during transcatheter aortic valve implantation. *Int J Numer Meth Biomed Engng*. 2018;34:e2974. https://doi.org/10.1002/cnm.2974

APPENDIX A

The simulation framework was tested on another patient geometry to verify its applicability. The rigid aorta of patient #2 was meshed with 10,294 contact elements (TARGE170) as seen in Figure 1C. The simulation set investigated the robustness of the model regarding the variation of the guidewire curvature radius. The radius ranged from 5 to 30 mm with a 5-mm step.

Most of the simulations converged at 0.20 N insertion force. The exception was radius 20 mm as the simulation could only reach 0.10 N. Figure A shows the projection of the simulated guidewires in 2 different incidences. The accuracy is reported in Table A.

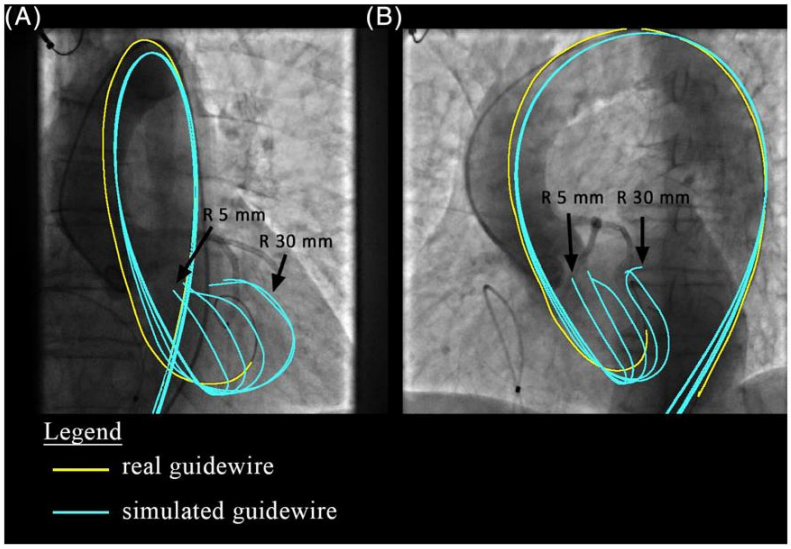

FIGURE A Superimposition of set #2bis related to the second patient case. Angle curvature was fixed at 20° and the insertion force at 0.20 N. A, Superimposition of simulated guidewires on incidence 1. B, Superimposition of simulated guidewires on incidence 2

TABLE A Test of guidewire radius for the second patient

Set #2bis Radius (mm)	Angle Difference (°)	Distance (px)	Maximum Force (N)
5	−5.2	23	0.2
10	−5.9	24	0.2
15	−5.7	23	0.2
20	−5.3	24	0.1
25	−3.4	20	0.2
30	−0.7	14	0.2
Mean	−4.4	21.3	
Standard deviation	1.5	2.9	

4.4.2 Synthèse

L'étude précédente valide sur deux patients la capacité du modèle numérique à prédire correctement la position du guide rigide au niveau de la valve aortique en dépit de l'incertitude des paramètres d'entrée (paramètres physiques peropératoires notamment). L'étude montre que les conditions d'insertion (force d'insertion et orientation) sont les paramètres contrôlables ayant le plus fort impact sur la position du guide suivi par la géométrie du guide (rayon et angle de courbure). Il semble également que la position des zones de contact avec l'aorte est un facteur important pour la forme du guide. Malgré les erreurs locales sur la rugosité de la paroi ou la mauvaise estimation de l'épaisseur des parois, la simulation peut fournir une bonne approximation de la forme générale du guide tant que la géométrie globale de l'anatomie du patient est respectée. Cette analyse reste cependant limitée par le faible nombre de cas étudiés et devra être confirmée par une analyse à plus large échelle. Enfin, les temps de simulation sont actuellement de l'ordre de 30 minutes ne permettant pas d'effectuer des analyses de sensibilité dans un contexte d'application médicale et devront donc être réduits par exemple en améliorant le choix des conditions initiales du modèle.

4.4.3 Application potentielle : étude des forces de contact

Au-delà de son rôle comme étape préliminaire d'une simulation de déploiement de prothèse, notre modèle présente l'intérêt de permettre l'évaluation de l'impact de différentes géométries (préformation) de guide sur les forces de contact pariétales au niveau ventriculaire gauche. Ce type d'évaluation pourrait être utile afin d'identifier les anatomies de patients et géométries de guide à risque de perforation ventriculaire et à l'inverse le type de guide offrant le support optimal au déploiement de la prothèse pour un patient donné. Pour explorer ces aspects, nous avons réalisé une analyse de sensibilité observant l'influence du rayon de courbure sur la répartition des forces de contact durant l'insertion du guide. Cette étude a fait l'objet de l'acte de conférence suivant (Computing In Cardiology 2017).

Study of the Behavior of Different Guidewire Shapes in a Patient-specific Numerical Model for Transcatheter Aortic Valve Implantation

Phuoc Vy[1,2,3,4], Vincent Auffret[3,4,5], Miguel Castro[3,4], Pierre Badel[2], Michel Rochette[1], Pascal Haigron[3,4], Stéphane Avril[2], Hervé Le Breton[3,4,5]

[1]ANSYS France, Villeurbanne, France
[2]Ecole Nationale Supérieure des Mines de Saint-Etienne, CIS-EMSE, INSERM:U1059, SAINBIOSE, Saint-Etienne, France
[3]INSERM, U1099, Rennes, France
[4]LTSI, Université de Rennes 1, Rennes, France
[5]CHU Rennes, Service de Cardiologie et Maladies Vasculaires, Rennes

Abstract

Transcatheter Aortic Valve Implantation is a mini-invasive procedure to replace aortic valves. The approach consists in delivering a fully collapsible bioprosthesis to the native valve site through a catheter. Stiff guidewires are required to deliver, stabilize and deploy the prosthesis by fitting in the left ventricular apex but they can also damage the ventricular wall of the patient. Nowadays, guidewires of different sizes, stiffness and shapes are available. In order to find the most appropriate guidewire for each patient, modelling could provide a better understanding of the interactions between the guidewire and the patient's left ventricle walls. Our objective was to explore the influence of guidewire shape on the contact conditions using numerical simulations.

We have developed a Finite Element model to simulate the stiff guidewire inserted into the left ventricle. The model was solved using the ANSYS software with an implicit resolution scheme. We explored different shapes for the distal end of the guidewire. We observed the distribution of the contact forces. An adequate curvature size resulted in smaller maximum pressure.

1. Introduction

Aortic stenosis (AS) is a widespread cardiovascular disease with increasing incidence in aging population, affecting almost 10% of octogenarians [1]. Symptoms of severe AS include dyspnea, chest pain, syncope, acute congestive heart failure, and sudden death. Severe symptomatic AS requires timely aortic valve replacement. Transcatheter Aortic Valve Implantation (TAVI) is a mini-invasive procedure to replace aortic valves and showed similar results as surgical treatment among intermediate or high surgical-risk patients [2-4]. The most common approach for TAVI is the femoral artery. Using a dedicated catheter, a stiff guidewire is inserted from the femoral artery to the left ventricle to assist the navigation of the prosthesis along the aortic arch. The fully crimped prosthesis is delivered by a catheter which glides over the guidewire to reach the aortic valve.

To provide support to the delivery catheter, the tip of the stiff guidewire lies against the ventricular wall, which can lead to left ventricular perforation if too much pressure is applied on the guidewire or if the shape of the guidewire does not suit the left ventricle. However, subtle manipulations of the guidewire allow fine adjustments of the prosthesis position before its deployment and are essential to the success of the procedure. Nevertheless, surgeons have a limited perception on the intra-operative behaviour of the guidewire. The most suitable guidewire shape and the amount of pressure that can be safely applied to this guidewire remain unclear in clinical practice.

The understanding of the behaviour of the tools appears as a key to better control the procedure. Studying the interactions between the guidewire and the ventricular wall could help choose an appropriate guidewire shape to decrease the risk of ventricular perforation. Several simulation studies have already simulated prosthesis deployment within the patient-specific aortic valve [5]. These numerical models seemed in agreement with the decision of the medical team for the simulated patient cases. However, to the best of our knowledge, there is no numerical study about the relationship between guidewire shape and its interaction with the ventricle. To address this lack, a contact analysis was performed on two retrospective patient cases using numerical simulation of guidewire insertion.

2. Materials and methods

2.1. Geometries

Images were retrospectively collected after the procedure of two patients (noted case A and B) who underwent TAVI in the cardiovascular department of the Rennes University Hospital. An intra-operative angiography was acquired during the protocol (Figure 1a) but the precise shape of the guidewire pre-deformed by the practitioner was unknown. A pre-operative CT-scan was segmented to extract the thoracic aorta and the left ventricle. The geometry was smoothed and imported in ANSYS for numerical simulation (Figure 1b).

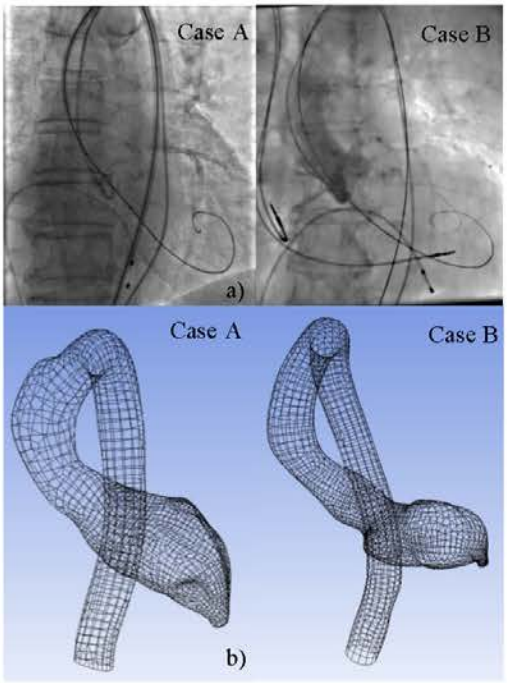

Figure 1. Patient-specific geometry of patient case A (left) and patient case B (right) a) intra-operative angiography b) simulation mesh.

The influence of the shape of the guidewire pre-deformation was studied by varying its radius of curvature from 15mm to 30mm (Figure 2a).

2.2. Assumptions

The CT image showed a fully dilated ventricle at diastole. The guidewire did not induce noticeable deformation of the aortic and ventricular walls according to our observations of the angiography. Thus, they were assumed rigid. The insertion of the guidewire in the ventricle was assumed to be quasi-static because the contact forces outweighed the inertia effects. Friction forces were neglected because the guidewire had a PTFE coating designed to reduce friction. It was assumed that deformation of the guidewire far from the ventricle marginally impacted the result of the study.

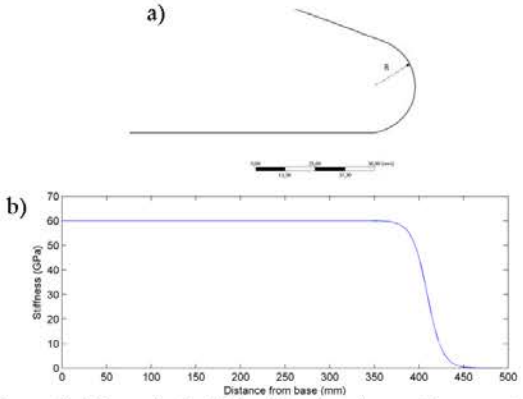

Figure 2. Numerical stiff guidewire shape a) geometry b) stiffness of the guidewire.

2.2. Numerical model

The numerical model was defined on the commercial software ANSYS 17.1. The simulations were performed with full Newton-Raphson method and sparse matrix direct solver.

The geometry was meshed in ANSYS. The patient mesh included 8341 nodes and 2794 contact element. The guidewire mesh had 4165 nodes and 1388 elements. The average distance between the nodes was 0.2 mm. The patient mesh was rigid and the guidewire behaviour was modelled with a linear elastic model. The stiffness profile of the guidewire is given in Figure 2b.

The guidewire was maintained tangential to the centerline at the exit point of the femoral sheath used for tools insertion in the abdominal aorta. Its longitudinal displacement was constrained and the corresponding insertion force was evaluated. Contact was numerically enforced using Augmented Lagrangian method. The simulation results were compared to intra-operative views in order to qualitatively assess the accuracy of the simulation.

2.3. Contact analysis

The contact analysis concerned the region of the guidewire inserted in the ventricle (Figure 3). The nodal contact force along the region of interest was plotted. The maximum contact force was qualitatively compared among the contact zones. The general reaction force of the ventricle acting on the guidewire was evaluated by the vector sum of the nodal forces.

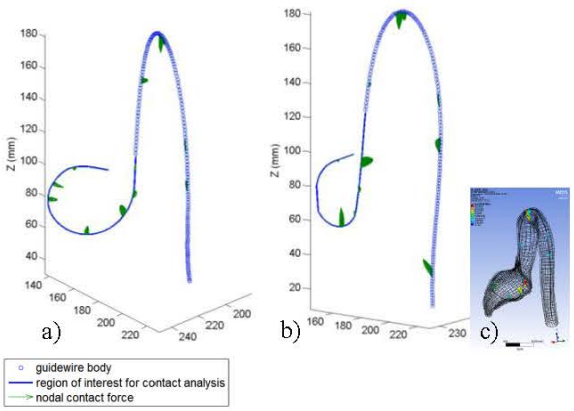

Figure 3. Side view of guidewire insertion in the ventricle with an insertion force of 0.20 N a) large curvature (30 mm) b) small curvature (15 mm) c) overview of the mesh orientation.

3. Results

3.1 Comparison to intra-operative data

The pre-operative geometries were registered on the intra-operative angiography by matching the contour of the contrast-injected aortic root. The intra-operative guidewire curvature was unknown but simulated guidewires with a 30 mm radius showed satisfying match in the region of interest (Figure 4).

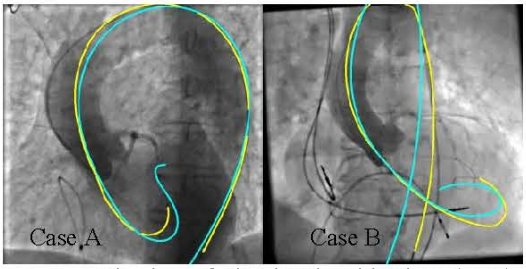

Figure 4. Projection of simulated guidewires (cyan) on intra-operative guidewires (yellow).

3.2 Contact results

Figure 5 shows the comparison between a small and a large curvature (noted R15 and R30 for 15 mm and 30 mm), as well as the comparison of a low and high insertion force (noted F0.10 and F0.20 for 0.10 N and 0.20 N) on patient case A. Figure 6 shows the comparison of the curvature size on patient case B at an insertion force of 0.20 N.

In case A with F0.10, the larger curvature had a higher maximum force than the small curvature near the aortic valve. However, it did decrease the contact force applied on the ventricular wall from 0.018 N to 0.007 N (around 375 mm on guidewire length). This effect can also be observed in Figure 3, at the bottom of the curvature. The larger curvature increased the number of contact zone along the guidewire (from 5 to 8 in case A, from 3 to 8 in case B). Case B shows a decrease of maximum nodal force from 0.025 N down to 0.019N by using a larger curvature. The length of the guidewire in contact increased from 72.8 mm to 94.9 mm. The sum of the norm of the contact force remained 0.16N.

Increasing the insertion force resulted in different behavior according to the curvature size (Figure 7). The vector sum increased for small curvature. This suggested that the contact forces were more directional. This is supported by an increased reaction force at the ventricular wall resulting from higher insertion force (Figure 5b around 380 mm). In the larger curvature case, insertion resulted in higher contact force at the tip of the guidewire and in a shifting of the contact zone toward the left of Figure 5a. In other word, the guidewire slid on the wall with a coiling movement as opposed to the small curved guidewire, which was simply pushing deeper in the ventricular wall.

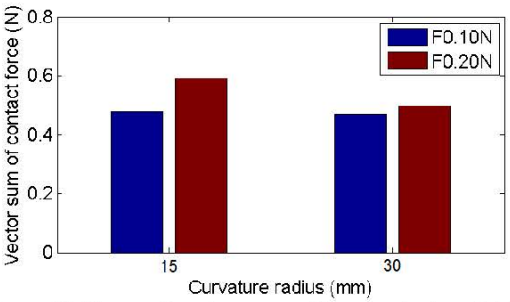

Figure 7. Norm of vector sum of the contact nodal force in the ventricle for case A.

4. Conclusion

This study outlined qualitative trends describing the behavior of a stiff guidewire in the left ventricle. The largest curvature size for the guidewire shape provided a sliding effect which limited the magnitude of contact force on the ventricular wall. In the opposite, a small curvature increased the contact force in a concentrated area on the ventricular wall.

Numerical model could be used in a patient-specific method to determine the safest guidewire shape. Our preliminary results have to be confirmed by further studies. They should address the issues related to material properties of the patient's vascular structures, the range of curvature sizes of the guidewire and the validation on a representative set of cases.

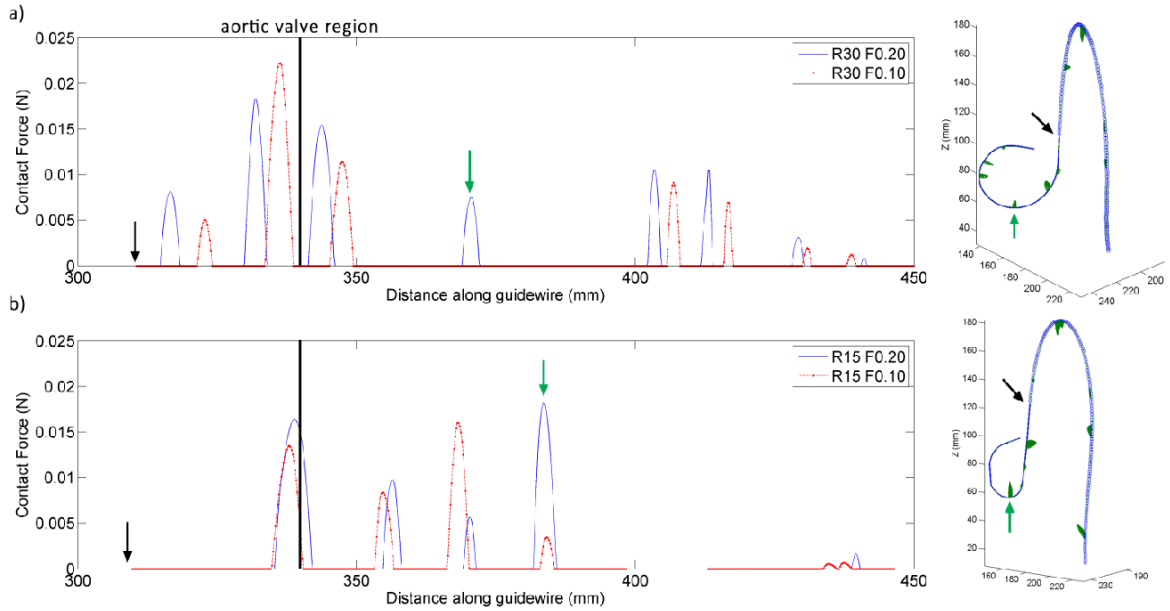

Figure 5. Contact forces along the guidewire in case A with an insertion force of 0.10 N and 0.20 N for a) large curvature (30 mm) and b) small curvature (15 mm). A 3D view of the simulated guidewire is shown in the right. Arrows on the graph are reflected back on the 3D view.

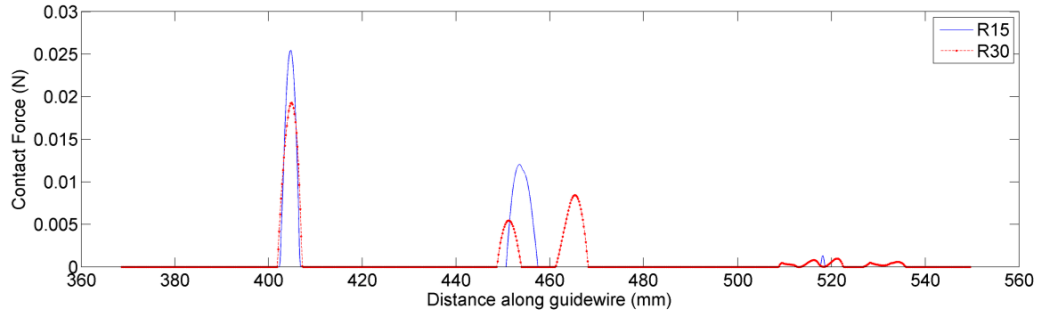

Figure 6. Contact forces along the guidewire in case B with an insertion force 0.20 N for large curvature (30 mm) and small curvature (15 mm).

Acknowledgements

This work has been conducted in the experimental platform TherA-Image (Rennes, France) supported by Europe FEDER.

References

[1] Eveborn GW, Schirmer H, Heggelund G, Lunde P, Rasmussen K. The evolving epidemiology of valvular aortic stenosis. The Tromso Study. Heart 2012;99:396-400.
[2] Leon MB et al. Transcatheter or Surgical Aortic-Valve Replacement in Intermediate-Risk patients. N Engl J Med 2016;374:1609-20.
[3] Siontis GCM et al. Transcatheter aortic valve implantation vs. surgical aortic valve replacement for treatment of severe aortic stenosis: a meta-analysis of randomized trials. European Heart Journal 2016;37:3503-12.
[4] Reardon MJ et al. Surgical or Transcatheter Aortic-Valve Replacement in Intermediate-Risk Patients. N Engl J Med 2017;376:1321-31.
[5] Wang Q et al. Simulations of transcatheter aortic valve implantation: implications for aortic root rupture. Biomech. Model. Mechanobiol. 2015;14:29-38.

Address for correspondence.

Phuoc VY
CIC-IT de Rennes
CHU de Rennes
Centre cardio pneumologique
Rue Henri Le Guilloux
35033 Rennes
phuoc.vy@ansys.com

4.5 Bilan et perspectives

Nous avons évoqué dans ce chapitre nos travaux de traitement de l'image pour leur contribution à la personnalisation de la simulation numérique et à sa confrontation aux données de l'imagerie peropératoire. Il faut également rappeler que ces travaux peuvent avoir un apport intéressant pour le clinicien dans le cadre de la réalité augmentée peropératoire. Cette technique fait en effet souvent intervenir des processus de recalage et fusion d'image et le « *tracking* » automatique de structures dans les images afin « d'augmenter » l'angiographie 2D peropératoire par la projection de données segmentées 3D préopératoires en assurant pour les interventions cardiaques une compensation automatique et en temps réel du mouvement des structures d'intérêt. Ces aspects font également l'objet de travaux par notre équipe mais ceux-ci ne faisaient pas partie du cadre de cette Thèse (172,173).

Nous avons présenté l'intérêt potentiel de la simulation numérique spécifique patient pour l'aide à la décision dans le contexte du TAVI. Notre modèle numérique de simulation de l'insertion du guide rigide se montre prometteur pour la prédiction de la position du guide au niveau de la valve aortique ainsi que pour évaluer ses interactions avec les parois ventriculaires. Néanmoins, plusieurs limites persistent comme des incertitudes sur certains paramètres physiques d'insertion *in vivo* (s'apparentant aux conditions initiales du modèle) ou le fait que le modèle n'ait été validé que sur un nombre limité de cas.

Pour pallier aux incertitudes concernant les paramètres d'entrée, nous avons depuis l'étude de validation de notre modèle poursuivi nos travaux par son évaluation sur un fantôme physique crée par impression 3D à partir de l'anatomie d'un patient utilisée dans notre étude de validation. Ces travaux *in vitro* ont permis l'évaluation de nombreuses conditions d'insertion différentes et la validation du modèle numérique en comparaison au fantôme physique notamment dans des zones éloignées de la région d'intérêt (aorte descendante). En effet, les acquisitions sur fantôme ont été faites à l'aide d'un CBCT 3D en salle hydride, permettant ainsi de récupérer précisément la position du guide dans l'aorte abdominale et de connaitre exactement la longueur de guide insérée.

Des validations *in vivo* sur un plus grand nombre de cas restent toutefois nécessaires. Il convient également de garder à l'esprit que dans l'objectif de simuler un déploiement de prothèse complet, notre modèle ne constitue qu'une étape préliminaire, nécessaire à la simulation ultérieure du cathéter porteur et de la prothèse, mais en aucun cas suffisant en soit. Le développement de ce type de modèle pourrait néanmoins pour affiner sa validation et son

paramétrage nécessiter des acquisitions peropératoires en CBCT 3D qui ne font actuellement pas partie du « workflow » clinique (augmentation de l'irradiation et de la quantité de produit de contraste injectée pour le patient). Ainsi, le développement des modèles numériques reste à la fois un défi du côté médical pour surmonter les difficultés d'acquisition des données peropératoires et un défi du côté développement pour surmonter les carences de ces données d'entrée.

Conclusion

Cette Thèse a abordé la question de l'aide à la décision dans le domaine du remplacement valvulaire aortique percutané (TAVI). Cette technique d'émergence récente est actuellement en plein essor ouvrant de nombreuses possibilités de recherche. L'évolution rapide du profil des patients traités vers des patients à plus faible risque chirurgical, qui bénéficiaient jusqu'alors d'une chirurgie de remplacement valvulaire aortique aux résultats largement éprouvés, impose notamment de sélectionner au mieux les patients, de planifier méticuleusement et d'individualiser les procédures et de les réaliser en minimisant les risques de complications. Pour ce faire, les cliniciens s'appuient actuellement sur un certain empirisme issu de leur expérience passée et sur l'analyse impliquant de nombreuses opérations manuelles sur les données de l'imagerie préopératoire, notamment du scanner, apportant des informations anatomiques brutes. Afin d'accompagner le médecin dans cette tâche de planification, il est possible d'envisager des outils l'aidant dans l'analyse de l'imagerie, lui restituant les données essentielles et pertinentes au cas traité voire augmentant l'information disponible grâce à des éléments simulés.

Partant de ce postulat, cette Thèse s'inscrit essentiellement dans la phase préopératoire du geste ne traitant pas des aspects d'aide à la décision en cours de procédure (ce qui constitue plus exactement une aide à la réalisation du geste) ou en post-procédure. Dans une première étape, nous avons rappelé le contexte actuel du TAVI en France afin de permettre la compréhension des problématiques auxquelles il expose les cliniciens notamment en termes de sélection des patients et de complications potentielles de la procédure.

Ces aspects ont ensuite été développés dans un deuxième chapitre s'intéressant à l'apport des approches d'analyse statistique et d'étude de cohorte de patients, classiques dans le domaine médical, pour l'identification de facteurs pronostiques ou prédictifs d'événement après TAVI. Nous avons dans cette partie centré notre propos sur deux complications particulières par leur fréquence (troubles conductifs) ou leurs conséquences fonctionnelles potentielles (AVC) qui en font des problématiques quotidiennes pour les cliniciens. Nous avons également abordé le problème de la sélection des patients par l'identification de facteurs de risque de mauvais résultat « global » après TAVI. Ce chapitre a démontré l'intérêt des méthodes d'analyse habituelles dans le domaine médical pour apporter aux cliniciens des informations utiles à ces décisions en terme de planification de la procédure. Nous y avons également abordé certaines limites de ces techniques tenant notamment aux caractéristiques des

modèles statistiques utilisés mais également à l'absence d'outils permettant l'organisation, la mise à jour et la restitution des informations pertinentes au regard des abondantes données engrangées dans la littérature.

De nouvelles approches analytiques faisant notamment appel à des procédées de « machine-learning » et tirant profit de l'organisation des données de santé en larges bases de données pourraient dans un avenir proche pallier un certain nombre de ces limitations. Dans le cadre de cette Thèse, nous nous sommes plutôt focalisés dans une troisième partie sur l'apport potentiel d'un système d'aide à la décision basé sur le « case-based reasoning » pour l'organisation et la restitution des informations pertinentes au traitement d'un cas particulier. La faisabilité globale de ce type d'approche dans le cadre du TAVI ayant été précédemment démontrée, nous avons ciblé, dans notre contribution, une partie plus analytique de l'élaboration des CBR portant sur l'optimisation de la mesure de similarité entre le problème à résoudre (cas du patient à traiter) et les solutions (cas des patients traités et stratégies thérapeutiques qui leurs ont été appliquées) en s'attachant à la problématique « simple » du choix de la voie d'abord et de la prothèse. Nos travaux peuvent être interprétés comme une première étape à la mise en œuvre d'un outil d'aide à la décision plus large capable d'inclure et restituer de manière pertinente des informations pronostiques issues des recherches médicales selon les procédés statistiques classiques, des données anatomiques précises issues de l'imagerie voire des données « augmentées » par des procédées de simulation biomécanique afin d'aider le clinicien à répondre à des questions plus complexes de sélection des candidats à une procédure TAVI ou d'individualisation dans la réalisation de ces procédures.

Dans une dernière partie, nous nous sommes intéressés au potentiel de la simulation numérique en tant qu'outil d'aide à la décision. En effet, par l'augmentation des informations préopératoires liées à une plus grande exploitation des données anatomiques habituellement recueillies, la simulation semble être une stratégie prometteuse pour extraire des indicateurs pertinents (risque de complications, performances hémodynamiques de la prothèse) afin de mieux planifier et réaliser la procédure (choix de la prothèse, d'outils complémentaires de prévention de certaines complications, anticipation du résultats de certaines manœuvres). En l'absence de travaux sur cette étape de la procédure, il nous paraissait opportun de tenter de prédire la déformation et la position du guide rigide inséré puisqu'il présente une influence certaine sur la position de la prothèse et que les interactions des cliniciens avec ce dernier sont suffisamment importantes pour ne pouvoir être ignorées. Ainsi, au-delà de son impact sur le déploiement de la prothèse, les connaissances concernant le comportement mécanique du guide

et ses interactions avec l'aorte et le ventricule gauche étaient très limitées bien qu'elles présentent un intérêt dans la compréhension des rares mais gravissimes cas de perforation ventriculaire gauche.

La construction de notre modèle de simulation a nécessité de formuler une représentation de la réalité au travers d'hypothèses et des lois qui la gouvernent. En tenant compte de l'objectif du modèle et des compromis entre robustesse, justesse et coût de calcul, ces hypothèses ont été émises au regard des données d'imagerie pré-opératoires et per-opératoires, sur le comportement des tissus du patient et des outils. Après une première validation de ce modèle sur des données de patients traités, nous avons montré qu'il pourrait avoir un intérêt pour la prédiction du comportement du guide dans le ventricule gauche et ainsi permettre le choix du guide le plus adapté à l'anatomie de chaque patient.

Toutefois, il faut garder à l'esprit que notre travail constitue une première étape dans la mise au point d'un modèle de simulation plus global du déploiement des prothèses. L'ajout d'éléments, comme le cathéter de pose dans une prochaine étape, nécessitera vraisemblablement un travail conséquent de révision des hypothèses réalisées pour la mise au point du modèle actuel. Un autre défi réside dans le temps nécessaire à la mise au point du modèle à partir de données brutes. Des efforts concernant la reconstruction de la géométrie de simulation, le recalage, l'ajustement préliminaire des paramètres pour la robustesse et la rapidité du calcul devront donc être réalisés pour envisager l'utilisation de la simulation numérique en pratique courante. Quoi qu'il en soit, les progrès à venir de l'imagerie préopératoire, les évolutions constantes du matériel d'implantation et l'arrivée prochaine sur le marché de nouvelles valves aux mécanismes de déploiement divers, offrent un vaste champ d'exploration à la simulation numérique afin d'améliorer notre perception des informations préopératoires, la planification du geste et *in fine* sa réalisation.

Annexe 1

Appendice complémentaire de "Temporal Trends in Transcatheter Aortic Valve Replacement in France: FRANCE 2 to FRANCE TAVI."

Supplementary appendix

Auffret et al. Temporal Trends in Transcatheter Aortic Valve Implantation in France: from FRANCE 2 to FRANCE TAVI.

Tables of content

I- France TAVI scientific committee

Chairperson

Pr Hervé LE BRETON

Cardiologists

Pr Hélène ELTCHANINOFF
Pr Martine GILARD
Pr Bernard IUNG
Pr Herve LE BRETON
Dr Thierry LEFEVRE
Pr Eric VAN BELLE

Cardiac surgeons

Pr Marc LASKAR
Pr Pascal LEPRINCE

Methodologist

Pr Bernard IUNG

Statistician

Vincent BATAILLE

II- List of FRANCE TAVI participating centers and key personnel

Centers	Key personnel
Institut Hospitalier Jacques Cartier-Massy-805 patients	Interventional cardiologists : Bernard CHEVALIER, Philippe GAROT, Thomas HOVASSE, Thierry LEFEVRE Cardiac surgeons : Patrick DONZEAU GOUGE, Arnaud FARGE, Mauro ROMANO Non-interventional cardiologists : Bertrand CORMIER, Erik BOUVIER
CHU de Lille-Lille-573 patients	Interventional cardiologists : Jean-Jacques BAUCHART, Jean-Christophe BODART, Cédric DELHAYE, David HOUPE, Robert LALLEMANT, Fabrice LEROY, Arnaud SUDRE, Eric VAN BELLE Cardiac surgeons : Francis JUTHIER, Mohamed KOUSSA, Dr Thomas MODINE, Natacha ROUSSE Non-interventional cardiologists : Jean-Luc AUFFRAY, Marjorie RICHARDSON
CHU de Rouen-Rouen-541 patients	Interventional cardiologists : Jacques BERLAND, Hélène ELTCHANINOFF, Mathieu GODIN, René KONING Cardiac surgeon : Jean-Paul BESSOU
CHU de Nantes-Nantes-490 patients	Interventional cardiologists: Vincent LETOCART, Thibaut MANIGOLD, Cardiac surgeon: Jean-Christian ROUSSEL Non-interventional cardiologist: Philippe JAAFAR
CHU de Clermont-Ferrand-Clermont-Ferrand-449 patients	Interventional cardiologists: Nicolas COMBARET, Geraud SOUTEYRAND Cardiac surgeons: Nicolas D'OSTREVY, Andréa INNORTA Non-interventional cardiologists: Guillaume CLERFOND, Charles VORILHON
CHU de Rennes-Rennes-417 patients	Interventional cardiologists : Vincent AUFFRET, Marc BEDOSSA, Dominique BOULMIER, Hervé LE BRETON, Guillaume LEURENT Cardiac surgeons : Amedeo ANSELMI, Majid HARMOUCHE, Jean-Philippe VERHOYE Non-interventional cardiologists : Erwan DONAL
Hopital Saint Joseph-Marseille-406 patients	Interventional cardiologists : Jacques BILLE, Patrick JOLY, Cardiac surgeon : Rémi HOUEL Non-interventional cardiologists : Bertrand VILETTE
CHU d'Angers-Angers-397 patients	Interventional cardiologists :Wissam ABI KHALIL, Stéphane DELEPINE Cardiac surgeons : Olivier FOUQUET, Dr Frédéric PINAUD Non-interventional cardiologist : Frédéric ROULEAU
CHU Bichat-Paris-388 patients	Interventional cardiologists: Jérémie ABTAN, Dr Dominique HIMBERT, Marina URENA Cardiac surgeons : Soleiman ALKHODER, Walid GHODBANE Non-interventional cardiologists: Dimitri ARANGALAGE, Eric BROCHET, Coppelia GOUBLAIRE
CHU La Pitié Salpêtrère-Paris-388 patients	Interventional cardiologist : Olivier BARTHELEMY, Rémi CHOUSSAT, Jean-Philippe COLLET Cardiac surgeon : Guillaume LEBRETON, Pascal LEPRINCE, Chiro MASTRIOANNI Non-interventional cardiologist : Richard ISNARD
CHU Louis Pradel-Lyon-385 patients	Interventional cardiologists : Raphael DAUPHIN, Olivier DUBREUIL, Guy DURAND DE GEVIGNEY, Gérard FINET, Brahim HARBAOUI, Sylvain RANC, Gilles RIOUFOL, Cardiac surgeons: Fadi FARHAT, Olivier JEGADEN, Jean-François OBADIA, Matteo POZZI
Centre cardiologique Marie Lannelongue-Le	Interventional cardologists : Saïd GHOSTINE, Philippe

Plessis Robinson-380 patients	BRENOT, Sahbi FRADI Cardiac surgeons : Alexandre AZMOUN, Philippe DELEUZE Non-interventionals cardiologists : Martin KLOECKNER
Clinique Saint-Gatien-Tours-379 patients	Interventional cardiologists : Olivier BAR, Didier BLANCHARD, Christophe BARBEY, Stephan CHASSAING Cardiac surgeons: Didier CHATEL, Olivier LE PAGE, Arnaud TAURAN Non-interventional cardiologists : Didier BRUERE, Laurent BODSON, Yvon MEURISSE, Aurélien SEEMANN
Institut mutualiste Montsouris-Paris-377 patients	Interventional cardiologists :Nicolas AMABILE, Christophe CAUSSIN, Alain DIBIE, Simon ELHADDAD, Luc DRIEU, Alice OHANESSIAN François PHILIPPE, Aurélie VEUGEOIS Cardiac surgeon :Matthieu DEBAUCHEZ, Konstantinos ZANNIS Non-intervertional cardiologist : Daniel CZITROM, Chrystelle DIAKOV, François RAOUX
Clinique du Tonkin-Lyon-337 patients	Interventional cardiologists: Didier CHAMPAGNAC, Yves LIENHART, Patrick STAAT, Oualid ZOUAGHI Cardiac surgeons: Vincent DOISY, Jean Philippe FRIEH, Fabrice WAUTOT Non-interventional cardiologists : Julie DEMENTHON, Olivier GARRIER, Fadi JAMAL, Pierre Yves LEROUX
CHU de Bordeaux-Bordeaux-323 patients	Interventional cardiologists : Frédéric CASASSUS, Lionel LEROUX, Benjamin SEGUY Cardiac surgeon : Laurent BARANDON, Louis LABROUSSE, Julien PELTAN Non-interventional cardiologists : Claire CORNOLLE, Marina DIJOS, Stéphane LAFITTE
Hôpital privé Clairval-Marseille-305 patients	Interventional cardiologists : Gilles BAYET, Claude CHARMASSON, Frédéric COLLET Cardiac surgeons : Alain VAILLANT, Jacques VICAT Non-interventional cardiologist : Marie Paule GIACOMONI
CHU Mondor-Créteil-304 patients	Interventional cardiologist : Emmanuel TEIGER Cardiac surgeon : Eric BERGOEND Non-interventional cardiologist : Céline ZERBIB
Clinique Saint-Augustin-Bordeaux-300 patients	Interventional cardiologist : Olivier DARREMONT, Jean Louis LEYMARIE Cardiac surgeon : Philippe CLERC, Emmanuel CHOUKROUN, Nicolas ELIA, Jean-Philippe GRIMAUD, Jean-Philippe GUIBAUD, Stéphane WROBLEWSKI Non-interventional cardiologists : Eric ABERGEL, Emmanuel BOGINO, Christophe CHAUVEL, Patrick DEHANT, Marc SIMON
CHU de Nancy-Nancy-292 patients	Interventional cardiologists : Michel ANGIOI, Julien LEMOINE, Simon LEMOINE, Batric POPOVIC Cardiac surgeons : Thierry FOLLIGUET, Pablo MAUREIRA Non-interventional cardiologists : Olivier HUTTIN, Christine SELTON SUTY
CHU de Montpellier-Nîmes-Montpellier-Nîmes-289 patients	Interventional cardiologists : Guillaume CAYLA, Delphine DELSENY, Florence LECLERCQ, Gilles LEVY, Jean Christophe MACIA, Eric MAUPAS, Christophe PIOT, François RIVALLAND, Gabriel ROBERT, Laurent SCHMUTZ, Frédéric TARGOSZ Cardiac surgeons : Bernard ALBAT, Arnaud DUBAR, Nicolas DURRLEMAN, Thomas GANDET, Emmanuel MUNOS Non-interventional cardiologists : Stéphane CADE, Frédéric CRANSAC
CHU de Toulouse-Toulouse-285 patients	Interventional cardiologists : Frédéric BOUISSET, Thibault

	LHERMUSIER Cardiac surgeons : Etienne GRUNENWALD, Bertrand MARCHEIX Non-interventional cardiologist : Pauline FOURNIER
CHU de Strasbourg-Strasbourg-278 patients	Interventional cardiologists : Olivier MOREL, Patrick OHLMANN Cardiac surgeons : Michel KINDO, Minh Tam HOANG Non-interventional cardiologists: Hélène PETIT, Hafida SAMET, Anne TRINH
Hôpital privé Saint Martin-Caen-264 patients	Interventional cardiologists : Bruno HURET, Guillaume LECOQ, Jean François MORELLE, Pascal RICHARD Cardiac surgeons : Thierry DERIEUX, Emmanuel MONIER Non-interventional cardiologist : Cédric JORET
CHU de Dijon-Dijon- 262 patients	Interventional cardiologist : Luc LORGIS Cardiac surgeon : Olivier BOUCHOT Non-interventional cardiologist : Jean Christophe EICHER
Institut Arnaud Tzanck-Saint Laurent du Var-238 patients	Interventional cardiologists : Laurent DROGOUL, Pierre MEYER Cardiac surgeons : Stéphane LOPEZ, Michel TAPIA, Jacques TEBOUL Non-interventional cardiologists : Jean-Pierre ELBEZE, Alain MIHOUBI
CHU de Grenoble-Grenoble-236 patients	Interventional cardiologists : Bernard BERTRAND, Gérald VANZETTO, Olivier WITTENBERG Cardiac surgeons: Vincent BACH, Cécile MARTIN Non-interventional cardiologists : Carole SAUIER, Charlotte CASSET
CHU de Brest-Brest-235 patients	Interventional cardiologists : Philippe CASTELLANT, Martine GILARD Cardiac surgeons : Eric BEZON, Jean-Noel CHOPLAIN, Ahmed KALLIFA, Bahaa NASR Non-interventional cardiologists : Yannick JOBIC
Hôpital Européen Georges Pompidou-Paris-205 patients	Interventional cardiologists:, Dr Didier BLANCHARD, Antoine LAFONT, Jean-Yves PAGNY, Christian SPAULDING Cardiac surgeons : Ramzi ABI AKAR, Jean-Noël FABIANI, Rachid ZEGDI Non-interventional cardiologists : Alain BERREBI, Tania PUSCAS
CHU de Tours-Tours-199 patients	Interventional cardiologists :Bernard DESVEAUX, Fabrice IVANES, Laurent QUILLIET, Christophe SAINT ETIENNE Cardiac surgeon : Thierry BOURGUIGNON Non-interventional cardiologists : Blandine AUPY, Romain PERAULT
CHU La Timone-Marseille-193 patients	Interventional cardiologists : Jean-Louis BONNET, Thomas CUISSET, Marc LAMBERT Cardiac surgeons : Dominique GRISOLI, Nicolas JAUSSAUD Non-interventional cardiologist : Erwan SALAUN
Polyclinique du Bois-Lille-183 patients	Interventional cardiologist : Maxence DELOMEZ, Cardiac surgeon : Amine LAGHZAOUI Non-interventional cardiologist : Christine SAVOYE
CHU de Caen-Caen-173 patients	Interventional cardiologists: Farzin BEYGUI, Mathieu BIGNON, Vincent ROULE, Rémy SABATIER Cardiac surgeons : Calin IVASCAU, Vladimir SAPLACAN Non-interventional cardiologists : Dr Eric SALOUX
Infirmerie protestante-Lyon-170 patients	Interventional cardiologists : Damien BOUCHAYER, Jean-Philippe CLAUDEL, Guillaume TREMEAU Cardiac surgeons : Camille DIAB, Joel LAPEZE, Franck PELISSIER, Thomas SASSARD

	Non-interventional cardiologists : Catherine MATZ, Nicolas MONSARRAT
Clinique de la Sauvegarde-Lyon-167 patients	Interventional cardiologists: Ivan CAREL, Alain HEPP, Franck SIBELLAS Cardiac surgeon: Alain CURTIL
Hôpital privé Parly 2-Le Chesnay-167 patients	Interventional cardiologists : Grégoire DAMBRIN, Xavier FAVEREAU, Arnaud JEGOU Cardiac surgeons : Gabriel GHORAYEB, Laurent GUESNIER, Wassim KHOURY, Christophe KUCHARSKI, Bruno POUZET, Claude VAISLIC Non-interventional cardiologists : Riadh CHEIKH-KHELIFA, Loïc HILPERT, Philippe MARIBAS
Hôpital privé de Bois-Bernard-CH Lens-Bois-Bernard / Lens-166 patients	Interventional cardiologists : Antoine GOMMEAUX, Gery HANNEBICQUE, Philippe HOCHART, Marc PARIS, Max PECHEUX Cardiac surgeon : Olivier FABRE, Laurent GUESNIER
CHU d'Amiens-Amiens-156 patients	Interventional cardiologists : Laurent LEBORGNE, Anfani MIRODE, Marcel PELTIER, Faouzi TROJETTE Cardiac surgeon : Doron CARMI Non-interventional cardiologist : Christophe TRIBOUILLOY
CHU de Poitiers-Poitiers-150 patients	Interventional cardiologists : Luc CHRISTIAENS, Jean MERGY Cardiac surgeon : Pierre CORBI Non-interventional cardiologist : Pascale RAUD RAYNIER
Hôpital Clinique Claude Bernard-Metz-107 patients	Interventional cardiologists : Sylvain CARILLO, Charles CHRISTOPHE, Arnaud HUEBER, Fédéric MOULIN Cardiac surgeon : Georges PINELLI
CHU de Limoges-Limoges-86 patients	Interventional cardiologist : Claude CASSAT, Nicole DARODES Cardiac surgeon : Francis PESTEIL
CHU de Reims-Reims-85 patients	Interventional cardiologist : Damien METZ Cardiac surgeon : Chadi ALUDAAT Non-interventional cardiologist : Frédéric TOROSSIAN
CH d'Annecy-Annecy-85 patients	Interventional cardiologists : Loïc BELLE, Lionel MANGIN Cardiac surgeon : Nicolas CHAVANIS Non-interventional cardiologist : Chrystelle AKRET
CHU de Saint Etienne-Saint Etienne-73 patients	Interventional cardiologists : Alexis CERISIER, Karl ISAAZ Cardiac surgeons:Jean Pierre FAVRE, Jean François FUZELLIER Non-interventional cardiologist : Romain PIERRARD
CH de Mulhouse- Mulhouse- 72 patients	Interventional cardiologists : Laurent JACQUEMIN, Olivier ROTH , Jean Yves WIEDEMANN Cardiac surgeons : Nicolas BISCHOFF, Georghe GAVRA Non-inerventional cardiologist: Nicolas BOURRELY
Centre cardiologique du Nord-Saint Denis-20 patients	Interventional cardiologist : Franck DIGNE, Philippe GUYON, Mohammed NAJJARI, Victor STRATIEV Cardiac surgeon: Nicolas BONNET, Patrick MESNILDREY Non-interventional cardiologists: David ATTIAS, Julien DREYFUS, Daniel KARILA COHEN, Thierry LAPERCHE, Julien NAHUM, Aliocha SCHEUBLE
Clinique Sainte Clotilde- Saint Denis de La Réunion -18 patients	Interventional cardiologists: Christophe POUILLOT, Geoffrey RAMBAUD Cardiac surgeon: Eric BRAUBERGER Non-interventional cardiologist: Michel AH HOT
Clinique Ambroise Paré-Neuilly sur Seine- 6 patients	Interventional cardiologists: Philippe ALLOUCH, Fabrice BEVERELLI, Serge MAKOWSKI, Julien ROSENCHER Cardiac surgeons: Stéphane AUBERT, Jean Michel GRINDA, Thierry WALDMAN

III- Definitions used in the FRANCE TAVI database

Variables	Definitions
Baseline characteristics	
Peripheral arterial disease:	Intermittent claudication, > 50% diameter stenosis or occlusion of a carotid artery, previous or planned intervention of the aorta, lower limb arteries or carotid arteries. Previous amputation for arterial causes.
Chronic pulmonary disease:	Chronic use of bronchodilators or corticosteroids for respiratory causes
Severe renal failure	Serum creatinine ≥ 200 µmol/l
Procedural characteristics	
Device success:	VARC-2 definition[1] : Absence of procedural mortality AND correct positioning of a single prosthetic heart valve into the proper anatomical location AND intended performance of the prosthetic heart valve (no prosthesis–patient mismatch AND mean aortic valve gradient <20 mmHg or peak velocity < 3 m/s, AND no moderate or severe prosthetic valve regurgitation)
Outcomes	
Mortality:	VARC-2 definition[1]: <u>Cardiovascular mortality:</u> Any of the following criteria Death due to proximate cardiac cause (e.g. myocardial infarction, cardiac tamponade, worsening heart failure) Death caused by non-coronary vascular conditions such as neurological events, pulmonary embolism, ruptured aortic aneurysm, dissecting aneurysm, or other vascular disease All procedure-related deaths, including those related to a complication of the procedure or treatment for a complication of the procedure All valve-related deaths including structural or non-structural valve dysfunction or other valve-related adverse events Sudden or unwitnessed death Death of unknown cause <u>Non-cardiovascular mortality:</u> Any death in which the primary cause of death is clearly related to another condition (e.g. trauma, cancer, suicide)
Valve migration:	VARC-2 definition[1]: After initial correct positioning, the valve prosthesis moves upwards or downwards, within the aortic annulus from its initial position, with or without consequences
Vascular complication:	Vascular access site complication requiring surgery or percutaneous intervention.
Major bleeding:	Overt bleeding either associated with a drop in the hemoglobin level of at least 3.0 g/dl or requiring transfusion of ≥ two units of whole blood/red blood cells OR bleeding causing hypovolemic shock or severe hypotension requiring vasopressors or surgery
Renal failure:	Increase in serum creatinine to ≥1.5× increase compared with baseline OR increase of ≥0.3 mg/dl (≥26.4 mmol/L)

IV- Supplementary Table 1– Baseline characteristics and in-hospital outcomes of included vs. excluded patients.

Characteristics	Included patients (n=16969)	Excluded patients (n=389)	p value
Clinical characteristics			
Registry			< 0.001
France 2, n (%)	4165 (24.5)	36 (9.3)	
France TAVI, n (%)	12804 (75.5)	353 (90.7)	
Age, y	83.2 ± 7.2 *(n=16969)*	84.7 ± 7.0 *(n=389)*	0.753
Median (IQR)	84.6 (80.1 – 88.0)	86.1 (82.1 – 89.1)	
Male sex, n./ total n. (%)	8425/16969 (49.7)	176/389 (45.2)	0.118
Body-mass index, kg/m²	26.4 ± 5.2 *(n=16779)*	25.8 ± 5.3 *(n=361)*	0.334
Logistic EuroSCORE, %	18.9 ± 12.9 *(n=16386)*	18.1 ± 13.8 *(n=365)*	0.012 *
Median (IQR)	15.5 (10.0 – 24.5)	14.0 (9.0 – 23.0)	
NYHA class III or IV, n./ total n. (%)	11393/16398 (69.5)	199/368 (54.1)	0.365
≥ 2 APE within previous year, n./ total n.(%)	2199/16180 (13.6)	22/359 (7.5)	< 0.001
Clinical history, n./ total n. (%)			
Previous myocardial infarction < 90 days	289/16780 (1.7)	3/375 (0.8)	0.188
Previous CABG	2171/16833 (12.9)	50/378 (13.2)	0.545
Previous SAVR	628/16808 (3.7)	9/373 (2.4)	0.751
Previous permanent pacemaker	2404/16800 (14.3)	37/378 (9.8)	0.232
Atrial fibrillation	3833/15227 (25.2)	27/172 (15.7)	0.032
Previous stroke/TIA	1806/16780 (10.8)	35/375 (9.3)	0.478
Diabetes mellitus	4316/16766 (25.7)	84/376 (22.3)	0.959
Peripheral vascular disease	3992/16787 (23.8)	81/375 (21.6)	0.747
Chronic pulmonary disease	3560/16790 (21.2)	75/376 (20.0)	0.654
Serum creatinine > 200 µmol/l	989/16336 (6.1)	26/336 (7.7)	0.363
Renal dialysis	339/16592 (2.0)	11/372 (3.0)	0.399
Life expectancy < 1yr, n./ total n. (%)	452/16410 (2.8)	4/376 (1.1)	0.127
Imaging findings			
Ejection fraction, %	54.7 ± 13.7 *(n=16426)*	54.1 ± 11.1 *(n=362)*	0.967
Median (IQR)	59 (45 – 65)	60 (45 – 60)	
Aortic valve area, cm²	0.69 ± 0.25 *(n=15480)*	0.75 ± 0.62 *(n=343)*	< 0.001
Aortic annulus, mm	23.3 ± 2.6 *(n=15168)*	23.0 ± 2.4 *(n=351)*	0.561
Aortic mean gradient, mm Hg	47.4 ± 16.0 *(n=16387)*	46.9 ± 15.4 *(n=358)*	0.120
Moderate or severe AR, n./ total n. (%)	2853/14049 (20.3)	62/287 (21.6)	0.893
Moderate or severe MR, n./ total n. (%)	3219/14438 (22.3)	56/280 (20.0)	0.146
Severe PH (sPAP > 60 mm Hg), n (%)	1699/12969 (13.1)	39/331 (11.8)	0.792
In-hospital outcomes			
All-cause death	901/16969 (5.3)	25/389 (6.4)	0.363

Annulus rupture	66/16722 (0.4)	2/370 (0.5)	0.606
Aortic dissection	56/16722 (0.3)	0/425 (0.0)	-
Valve migration	195/16722 (1.2)	2/370 (0.5)	0.302
Tamponade	312/16722 (1.9)	1/370 (0.3)	0.072
Stroke	332/16722 (2.0)	4/370 (1.1)	0.322
STEMI	61/16722 (0.4)	0/370 (0.0)	-
Permanent pacemaker implantation†	2316/14229 (16.3)	18/331 (5.4)	0.067
Pulmonary embolism	23/16722 (0.1)	0/370 (0.0)	-
Renal failure	675/16722 (4.0)	5/370 (1.4)	0.284
Renal dialysis	140/16722 (0.8)	0/370 (0.0)	-
Echocardiographic findings			
Aortic valve area, cm²	1.78 ± 0.54 *(n=6899)*	1.83 ± 0.54 *(n=61)*	0.257
Aortic mean gradient, mm Hg	10.4 ± 6.1 *(n=14165)*	10.9 ± 6.3 *(n=328)*	0.119
Moderate or severe AR, n./total n. (%)	1684/14618 (11.5)	29/329 (8.8)	0.514

APE= Acute pulmonary edema; AR=Aortic regurgitation; CABG= coronary artery bypass graft; IQR= interquartile range; MR=Mitral regurgitation; SAVR= surgical aortic valve replacement; sPAP= systolic pulmonary artery pressure; STEMI= ST-segment elevation myocardial infarction; TIA= transient ischemic attack.

* Test performed using log-transformed variable.

† Number are given for patients without prior permanent pacemaker

V- Supplementary Table 2- Baseline characteristics and in-hospital outcomes of patients with versus without reported 30-day follow-up.

Characteristics	Patients with reported 30-day mortality (n=12489)	Patients without reported 30-day mortality (n=4480)	p value
Clinical characteristics			
Registry			0.173
France 2, n (%)	3277 (26.2)	888 (19.8)	
France TAVI, n (%)	9212 (73.8)	3592 (80.2)	
Age, y	83.3 ± 7.0 *(n=12489)*	83.2 ± 7.7 *(n=4480)*	0.507
Median (IQR)	84.5 (80.1 – 88.0)	84.7 (80.1 – 88.1)	
Male sex, n./ total n. (%)	6171/12489 (49.4)	2254/4480 (50.3)	0.584
Body-mass index, kg/m²	26.4 ± 5.2 *(n=12379)*	26.3 ± 5.1 *(n=4400)*	0.280
Logistic EuroSCORE, %	18.9 ± 12.7 *(n=12109)*	18.7 ± 13.3 *(n=4277)*	0.600*
Median (IQR)	15.8 (10.0 – 24.9)	15.0 (9.5 – 24.0)	
NYHA class III or IV, n./ total n. (%)	8226/12140 (67.8)	3167/4258 (74.4)	0.619
≥ 2 APE within previous year, n./ total n.(%)	1601/11978 (13.4)	598/4202 (14.2)	0.790
Clinical history, n./ total n. (%)			
Previous myocardial infarction < 90 days	207/12400 (1.7)	82/4380 (1.9)	0.681
Previous CABG	1589/12438 (12.8)	582/4395 (13.2)	0.805
Previous SAVR	419/12423 (3.4)	209/4385 (4.8)	0.174
Previous permanent pacemaker	1720/12414 (13.9)	684/4386 (15.6)	0.092
Atrial fibrillation	2831/11404 (24.8)	1002/3823 (26.2)	0.873
Previous stroke/TIA	1353/12416 (10.9)	453/4364 (10.4)	0.482
Diabetes mellitus	3264/12405 (26.3)	1052/4361 (24.1)	0.161
Peripheral vascular disease	2737/12423 (22.0)	1255/4364 (28.9)	0.089
Chronic pulmonary disease	2573/12413 (20.7)	987/4377 (22.6)	0.332
Serum creatinine > 200 µmol/l	736/12222 (6.0)	253/4114 (6.2)	0.826
Renal dialysis	242/12292 (2.0)	97/4300 (2.3)	0.351
Life expectancy < 1yr, n./ total n. (%)	400/12062 (3.3)	52/4348 (1.2)	0.212
Imaging findings			
Ejection fraction, %	54.8 ± 13.8 *(n=12228)*	54.2 ± 13.7 *(n=4254)*	0.494
Median (IQR)	59 (45 – 65)	57 (45 – 65)	
Aortic valve area, cm²	0.69 ± 0.25 *(n=11515)*	0.69 ± 0.24 *(n=3965)*	0.878
Aortic annulus, mm	23.3 ± 2.6 *(n=11511)*	23.3 ± 2.7 *(n=3657)*	0.967
Aortic mean gradient, mm Hg	47.4 ± 15.9 *(n=12153)*	47.5 ± 16.4 *(n=4234)*	0.255
Moderate or severe AR, n./ total n. (%)	2217/10470 (21.2)	636/3579 (17.8)	0.594
Moderate or severe MR, n./ total n. (%)	2454/10834 (22.7)	765/3604 (21.2)	0.637
Severe PH (sPAP > 60 mm Hg), n (%)	1242/9780 (12.7)	457/3109 (14.7)	0.157

In-hospital outcomes			
All-cause death	698/12489 (5.6)	203/4480 (4.5)	0.122
Annulus rupture	45/12399 (0.4)	21/4323 (0.5)	0.376
Aortic dissection	42/12399 (0.3)	14/4323 (0.3)	0.939
Valve migration	144/12399 (1.2)	51/4323 (1.2)	0.786
Tamponade	220/12399 (1.8)	92/4323 (2.1)	0.308
Stroke	242/12399 (2.0)	90/4323 (2.1)	0.543
STEMI	51/12399 (0.4)	10/4323 (0.2)	0.415
Permanent pacemaker implantation†	1673/10628 (15.7)	643/3601 (17.9)	0.381
Pulmonary embolism	16/12399 (0.1)	7/4323 (0.2)	0.766
Renal failure	546/12399 (4.4)	129/4323 (3.0)	0.175
Renal dialysis	111/12399 (0.9)	29/4323 (0.7)	0.600
Echocardiographic findings			
Aortic valve area, cm²	1.75 ± 0.53 *(n=5265)*	1.88 ± 0.54 *(n=1634)*	0.476
Aortic mean gradient, mm Hg	10.3 ± 6.0 *(n=10870)*	10.5 ± 6.3 *(n=3295)*	0.791
Moderate or severe AR, n./total n. (%)	1375/11016 (12.5)	309/3602 (8.6)	0.011

APE= Acute pulmonary edema; AR=Aortic regurgitation; CABG= coronary artery bypass graft; IQR= interquartile range; MR=Mitral regurgitation; SAVR= surgical aortic valve replacement; sPAP= systolic pulmonary artery pressure; STEMI= ST-segment elevation myocardial infarction; TIA= transient ischemic attack.

* Test performed using log-transformed variable.

† Number are given for patients without prior permanent pacemaker

VI- Supplementary Table 3 - Baseline characteristics of Edwards SAPIEN valves recipients according to year of inclusion within centers involved in both registries.

Characteristics	FRANCE 2		FRANCE TAVI			p for trend
	2010 (n=958)	2011/2012 (n=1533)	2013 (n=1466)	2014 (n=1868)	2015 (n=3015)	
Clinical characteristics						
Age, y	82.8±7.2 *(n=958)*	83.0±7.1 *(n=1533)*	83.1±7.6 *(n=1466)*	83.3±7.2 *(n=1868)*	82.9±7.4 *(n=3023)*	0.667
Median (IQR)	84.1 (79.1-87.9)	84.4 (79.7-87.8)	84.6 (80.2-87.9)	84.5 (80.3-88.1)	84.3 (80.0-87.7)	
Male sex, n./ total n. (%)	455/958 (47.5)	687/1533 (44.8)	683/1466 (46.6)	925/1868 (49.5)	1513/3015 (50.2)	0.002
Body-mass index, kg/m²	25.8±5.0 *(n=953)*	26.0±4.8 *(n=1530)*	26.5±5.2 *(n=1447)*	26.6±5.3 *(n=1852)*	26.6±5.2 *(n=2952)*	< 0.001
Logistic EuroSCORE, %	23.7±14.6 *(n=923)*	20.2±13.7 *(n=1483)*	18.5±12.1 *(n=1400)*	18.0±11.9 *(n=1799)*	16.8±11.4 *(n=2883)*	< 0.001 *
Median (IQR)	20.6 (12.8-31.7)	16.5 (10.4-26.8)	16.0 (10.0-24.0)	15.0 (10.0-23.0)	13.9 (9.0-21.0)	
< 10, n (%)	142 (15.4)	338 (22.8)	314 (22.4)	425 (23.6)	830 (28.8)	
10-19, n (%)	297 (32.2)	566 (38.2)	560 (40.0)	756 (42.0)	1223 (42.4)	
20-39, n (%)	364 (39.4)	439 (29.6)	435 (31.1)	521 (29.0)	699 (24.3)	
≥ 40, n (%)	120 (13.0)	140 (9.4)	91 (6.5)	97 (5.4)	131 (4.5)	
NYHA class III or IV, n./ total n. (%)	729/958 (76.1)	1120/1531 (73.2)	1021/1447 (70.6)	1244/1805 (68.9)	1833/2867 (63.9)	< 0.001
≥ 2 APE within previous year, n./ total n.(%)	142/954 (14.9)	176/1520 (11.6)	190/1431 (13.3)	245/1773 (13.8)	361/2876 (12.6)	0.836
Clinical history, n./ total n. (%)						
Coronary artery disease, n./ total n. (%) **	421/955 (44.1)	707/1521 (46.5)	559/1375 (40.7)	759/1785 (42.5)	1144/2723 (42.0)	0.094
Previous myocardial infarction <90 days	16/957 (1.7)	18/1527 (1.2)	29/1453 (2.0)	26/1850 (1.4)	38/2947 (1.3)	0.588
Previous CABG	196/955 (20.5)	228/1521 (15.0)	170/1461 (11.6)	199/1859 (10.7)	282/2951 (9.6)	< 0.001
Previous SAVR	5/955 (0.5)	25/1521 (1.6)	26/1462 (1.8)	46/1855 (2.5)	96/2941 (3.3)	< 0.001
Previous permanent pacemaker	143/951 (15.0)	193/1525 (12.7)	195/1456 (13.4)	268/1855 (14.5)	381/2953 (12.9)	0.557
Atrial fibrillation	246/940 (26.2)	373/1513 (24.7)	324/1312 (24.7)	424/1674 (25.3)	557/2398 (23.2)	0.019

Previous stroke/TIA	94/955 (9.8)	160/1521 (10.5)	157/1456 (10.8)	221/1854 (11.9)	304/2950 (10.3)	0.759
Diabetes mellitus	262/955 (27.4)	366/1521 (24.1)	382/1454 (26.2)	465/1849 (25.2)	778/2948 (26.4)	0.745
Peripheral vascular disease	309/957 (32.3)	382/1527 (25.0)	301/1460 (20.6)	389/1859 (20.9)	613/2953 (20.8)	< 0.001
Chronic pulmonary disease	251/955 (26.3)	359/1521 (23.6)	318/1459 (21.8)	355/1857 (19.1)	449/2949 (15.2)	< 0.001
Serum creatinine ≥ 200 µmol/l	111/957 (11.6)	93/1527 (6.1)	71/1433 (5.0)	116/1805 (6.4)	141/2822 (5.0)	< 0.001
Renal dialysis	32/955 (3.4)	24/1521 (1.6)	34/1450 (2.3)	47/1838 (2.6)	50/2864 (1.8)	0.128
Life expectancy < 1yr, n./ total n. (%)	22/955 (2.3)	27/1521 (1.8)	69/1390 (5.0)	48/1776 (2.7)	90/2842 (3.2)	0.011
Imaging findings						
Ejection fraction, %	52.8±14.2 *(n=943)*	54.5±13.8 *(n=1507)*	54.9±13.8 *(n=1433)*	54.8±13.5 *(n=1822)*	55.5±13.4 *(n=2900)*	< 0.001
Median (IQR)	55.0 (42.0-65.0)	58.0 (45.0-65.0)	60.0 (45.0-65.0)	60.0 (45.0-65.0)	60.0 (46.0-65.0)	
< 50%, n (%)	335 (35.5)	444 (29.5)	404 (28.2)	490 (26.9)	750 (25.9)	
Aortic valve area, cm²	0.65±0.18 *(n=910)*	0.66±0.17 *(n=1455)*	0.67±0.23 *(n=1359)*	0.69±0.23 *(n=1700)*	0.71±0.25 *(n=2653)*	< 0.001
Aortic annulus, mm	21.5±1.8 *(n=878)*	21.9±2.0 *(n=1437)*	23.0±2.5 *(n=1300)*	23.3±2.4 *(n=1654)*	23.6±2.6 *(n=2646)*	< 0.001
Aortic mean gradient, mm Hg	48.2±17.0 *(n=941)*	49.0±16.4 *(n=1492)*	47.8±15.7 *(n=1431)*	47.3±15.5 *(n=1804)*	47.4±15.9 *(n=2862)*	< 0.001
Moderate or severe AR, n./ total n. (%)	153/894 (17.1)	267/1451 (18.4)	217/1103 (19.7)	310/1627 (19.1)	471/2343 (20.1)	0.996
Moderate or severe MR, n./ total n. (%)	212/901 (23.5)	346/1459 (23.7)	271/1273 (21.3)	346/1631 (21.2)	559/2350 (23.8)	0.250
Severe PH (sPAP > 60 mm Hg), n (%)	115/767 (15.0)	147/1171 (12.6)	150/1147 (13.1)	181/1469 (12.3)	261/2161 (12.1)	0.088

APE= acute pulmonary edema; AR=Aortic regurgitation; CABG= coronary artery bypass graft; IQR= interquartile range; MR=Mitral regurgitation; PH= Pulmonary hypertension; SAVR= surgical aortic valve replacement; sPAP= systolic pulmonary artery pressure; TIA= transient ischemic attack.

* Test performed using log-transformed variable.

** Presence of at least one significant lesion (≥50%) on the pre-procedural coronary angiogram.

VII- Supplementary Table 4 - Baseline characteristics of Medtronic CoreValve recipients according to year of inclusion within centers involved in both registries.

Characteristics	FRANCE 2		FRANCE TAVI			p for trend
	2010 (n=420)	2011/2012 (n=852)	2013 (n=1027)	2014 (n=1270)	2015 (n=1230)	
Clinical characteristics						
Age, y	81.5±7.5 *(n=420)*	82.8±7.3 *(n=852)*	83.1±7.4 *(n=1027)*	83.1±7.3 *(n=1270)*	83.3±6.9 *(n=1230)*	0.001
Median (IQR)	82.9 (77.4-86.8)	84.3 (79.4-87.7)	84.4 (80.2-87.8)	84.4 (79.6-88.1)	84.4 (80.5-87.9)	
Male sex, n./ total n. (%)	250/420 (59.5)	520/852 (61.0)	535/1027 (52.1)	606/1270 (47.7)	583/1230 (47.4)	< 0.001
Body-mass index, kg/m²	26.7±5.2 *(n=419)*	26.3±5.2 *(n=852)*	26.5±5.3 *(n=1017)*	26.4±5.3 *(n=1260)*	26.6±5.4 *(n=1194)*	0.810
Logistic EuroSCORE, %	22.0±14.9 *(n=402)*	20.9±14.6 *(n=835)*	18.9±13.1 *(n=991)*	17.5±12.4 *(n=1221)*	16.6±12.2 *(n=1205)*	< 0.001 *
Median (IQR)	19.5 (10.9-29.7)	16.9 (10.4-28.2)	15.0 (10.0-26.0)	14.3 (9.0-22.0)	13.0 (8.4-21.0)	
< 10, n (%)	90 (22.4)	189 (22.6)	246 (24.8)	363 (29.7)	393 (32.6)	
10-19, n (%)	119 (29.6)	296 (35.4)	379 (38.2)	447 (36.6)	464 (38.5)	
20-39, n (%)	141 (35.1)	266 (31.9)	279 (28.2)	343 (28.1)	297 (24.7)	
≥ 40, n (%)	52 (12.9)	84 (10.1)	87 (8.8)	68 (5.6)	51 (4.2)	
NYHA class III or IV, n./ total n. (%)	311/420 (74.0)	630/850 (74.1)	672/994 (67.6)	782/1230 (63.6)	678/1126 (60.2)	< 0.001
≥ 2 APE within previous year, n./ total n.(%)	49/420 (11.7)	85/847 (10.0)	130/976 (13.3)	136/1214 (11.2)	145/1145 (12.7)	0.129
Clinical history, n./ total n. (%)						
Coronary artery disease, n./ total n. (%) **	172/420 (41.0)	371/851 (43.6)	413/946 (43.7)	507/1182 (42.9)	482/1092 (44.1)	0.800
Previous myocardial infarction <90 days	1/420 (0.2)	14/852 (1.6)	25/1008 (2.5)	18/1256 (1.4)	24/1213 (2.0)	0.118
Previous CABG	79/420 (18.8)	146/851 (17.2)	141/1021 (13.8)	145/1266 (11.5)	130/1213 (10.7)	< 0.001
Previous SAVR	17/420 (4.0)	16/851 (1.9)	52/1019 (5.1)	100/1264 (7.9)	118/1212 (9.7)	< 0.001
Previous permanent pacemaker	62/420 (14.8)	149/847 (17.6)	186/1016 (18.3)	181/1263 (14.3)	167/1212 (13.8)	0.036
Atrial fibrillation	132/416 (31.7)	232/839 (27.7)	258/945 (27.3)	249/1155 (21.6)	211/978 (21.6)	< 0.001

Previous stroke/TIA	45/420 (10.7)	71/851 (8.3)	115/1017 (11.3)	146/1258 (11.6)	120/1214 (9.9)	0.512
Diabetes mellitus	113/420 (26.9)	222/851 (26.1)	257/1015 (25.3)	321/1256 (25.6)	316/1213 (25.8)	0.680
Peripheral vascular disease	127/420 (30.2)	198/852 (23.2)	227/1017 (22.3)	262/1263 (20.7)	268/1212 (22.1)	0.006
Chronic pulmonary disease	108/420 (25.7)	213/851 (25.0)	236/1022 (23.1)	259/1260 (20.6)	173/1214 (14.3)	< 0.001
Serum creatinine ≥ 200 µmol/l	37/420 (8.8)	68/852 (8.0)	60/991 (6.1)	63/1210 (5.2)	47/1147 (4.1)	< 0.001
Renal dialysis	12/420 (2.9)	27/851 (3.2)	22/1013 (2.2)	20/1251 (1.6)	11/1161 (1.0)	< 0.001
Life expectancy < 1yr, n./ total n. (%)	28/420 (6.7)	17/851 (2.0)	35/1001 (3.5)	30/1228 (2.4)	49/1148 (4.3)7	0.396
Echocardiographic findings						
Ejection fraction, %	51.5±15.0 *(n=416)*	51.6±14.4 *(n=840)*	53.4±13.9 *(n=987)*	54.3±13.4 *(n=1238)*	55.6±12.7 *(n=1162)*	< 0.001
Median (IQR)	55.0 (40.0-60.0)	53.5 (40.0-61.0)	55.0 (45.0-64.0)	57.0 (45.0-65.0)	60.0 (50.0-65.0)	
< 50%, n (%)	155 (37.3)	329 (39.2)	347 (35.2)	359 (29.0)	285 (24.5)	
Aortic valve area, cm²	0.69±0.20 *(n=390)*	0.70±0.20 *(n=766)*	0.69±0.26 *(n=941)*	0.69±0.25 *(n=1140)*	0.71±0.24 *(n=1068)*	0.056
Aortic annulus, mm	23.0±2.4 *(n=390)*	23.0±2.4 *(n=740)*	24.1±2.8 *(n=911)*	23.7±2.9 *(n=1104)*	24.0±2.8 *(n=1038)*	< 0.001
Aortic mean gradient, mm Hg	46.9±15.8 *(n=407)*	46.6±16.1 *(n=813)*	46.5±16.3 *(n=995)*	46.7±15.9 *(n=1236)*	46.5±16.2 *(n=1149)*	0.805
Moderate or severe AR, n./ total n. (%)	81/395 (20.5)	179/796 (22.5)	178/746 (23.9)	258/1066 (24.2)	261/860 (30.3)	< 0.001
Moderate or severe MR, n./ total n. (%)	88/395 (22.3)	151/794 (19.0)	195/847 (23.0)	245/1092 (22.4)	213/885 (24.1)	0.016
Severe PH (sPAP > 60 mm Hg), n (%)	42/312 (13.5)	76/647 (11.7)	117/800 (14.6)	137/985 (13.9)	98/826 (11.9)	0.859

APE= acute pulmonary edema; AR=Aortic regurgitation; CABG= coronary artery bypass graft; IQR= interquartile range; MR=Mitral regurgitation; PH= Pulmonary hypertension; SAVR= surgical aortic valve replacement; sPAP= systolic pulmonary artery pressure; TIA= transient ischemic attack.

* Test performed using log-transformed variable.

*** Presence of at least one significant lesion (≥50%) on the pre-procedural coronary angiogram.

VIII- Supplementary Table 5 – Baseline characteristics of transfemoral TAVI recipients according to year of inclusion within centers involved in both registries.

Characteristics	FRANCE 2		FRANCE TAVI			p for trend
	2010 (n=1036)	2011/2012 (n=1712)	2013 (n=1976)	2014 (n=2533)	2015 (n=3562)	
Clinical characteristics						
Age, y	82.6±7.4 *(n=1036)*	83.3±6.9 *(n=1712)*	83.6±7.1 *(n=1976)*	83.5±7.2 *(n=2533)*	83.4±7.0 *(n=3562)*	0.022
Median (IQR)	84.1 (78.8-87.8)	84.7 (80.0-88.0)	84.9 (80.7-88.2)	84.8 (80.5-88.3)	84.6 (80.5-88.0)	
Male sex, n./ total n. (%)	495/1036 (47.8)	798/1712 (46.6)	927/1976 (46.9)	1191/2533 (47.0)	1676/3562 (47.1)	0.833
Body-mass index, kg/m²	26.1±5.1 *(n=1032)*	26.2±5.1 *(n=1711)*	26.5±5.2 *(n=1954)*	26.5±5.2 *(n=2513)*	26.6±5.2 *(n=3474)*	0.002
Logistic EuroSCORE, %	22.4±14.8 *(n=993)*	20.1±13.7 *(n=1666)*	18.0±11.9 *(n=1890)*	17.1±11.4 *(n=2431)*	16.1±10.8 *(n=3444)*	< 0.001*
Median (IQR)	19.4 (11.4-29.8)	16.2 (10.4-26.8)	15.0 (10.0-23.0)	14.0 (9.4-22.0)	13.0 (8.7-20.5)	
< 10, n (%)	194 (19.5)	379 (22.8)	451 (23.9)	656 (27.0)	1076 (31.2)	
10-19, n (%)	321 (32.3)	638 (38.3)	764 (40.4)	996 (41.0)	1434 (41.6)	
20-39, n (%)	353 (35.5)	495 (29.7)	561 (29.7)	672 (27.6)	803 (23.3)	
≥ 40, n (%)	125 (12.6)	154 (9.2)	114 (6.0)	107 (4.4)	131 (3.8)	
NYHA class III or IV, n./ total n. (%)	799/1036 (77.1)	1284/1708 (75.2)	1350/1934 (69.8)	1635/2448 (66.8)	2086/3340 (62.5)	< 0.001
≥ 2 APE within previous year, n./ total n.(%)	134/1034 (13.0)	195/1703 (11.5)	241/1904 (12.7)	306/2420 (12.6)	417/3386 (12.3)	0.243
Clinical history, n./ total n. (%)						
Coronary artery disease, n./ total n. (%) **	407/1035 (39.3)	726/1704 (42.6)	716/1839 (38.9)	967/2408 (40.2)	1300/3187 (40.8)	0.559
Previous myocardial infarction <90 days	12/1035 (1.2)	28/1708 (1.6)	38/1947 (2.0)	36/2504 (1.4)	47/3482 (1.4)	0.951
Previous CABG	161/1035 (15.6)	240/1704 (14.1)	208/1965 (10.6)	249/2521 (9.9)	298/3486 (8.6)	< 0.001
Previous SAVR	20/1035 (1.9)	26/1704 (1.5)	57/1964 (2.9)	117/2517 (4.7)	180/3478 (5.2)	< 0.001
Previous permanent pacemaker	150/1030 (14.6)	261/1704 (15.3)	302/1956 (15.4)	360/2516 (14.3)	459/3485 (13.2)	0.052
Atrial fibrillation	301/1020 (29.5)	453/1687 (26.9)	475/1807 (26.3)	574/2297 (25.0)	641/2806 (22.8)	< 0.001

Previous stroke/TIA	100/1035 (9.7)	156/1704 (9.2)	209/1960 (10.7)	298/2514 (11.9)	348/3485 (10.0)	0.315
Diabetes mellitus	283/1035 (27.3)	404/1704 (23.7)	494/1956 (25.3)	626/2509 (25.0)	899/3483 (25.8)	0.866
Peripheral vascular disease	227/1035 (21.9)	280/1708 (16.4)	293/1959 (15.0)	373/2518 (14.8)	532/3487 (15.3)	< 0.001
Chronic pulmonary disease	275/1035 (26.6)	407/1704 (23.9)	429/1966 (21.8)	479/2517 (19.0)	492/3486 (14.1)	< 0.001
Serum creatinine ≥ 200 µmol/l	114/1035 (11.0)	117/1708 (6.9)	100/1931 (5.2)	132/2435 (5.4)	136/3330 (4.1)	< 0.001
Renal dialysis	35/1035 (3.4)	36/1704 (2.1)	41/1951 (2.1)	44/2501 (1.8)	44/3369 (1.3)	< 0.001
Life expectancy < 1yr, n./ total n. (%)	39/1035 (3.8)	32/1704 (1.9)	86/1893 (4.5)	59/2449 (2.4)	122/3361 (3.6)	0.280
Echocardiographic findings						
Ejection fraction, %	52.3±14.6 *(n=1020)*	53.3±14.3 *(n=1689)*	54.4±13.9 *(n=1913)*	54.9±13.5 *(n=2466)*	55.7±13.1 *(n=3413)*	< 0.001
Median (IQR)	55.0 (40.0-65.0)	55.0 (45.0-65.0)	57.0 (45.0-65.0)	60.0 (46.0-65.0)	60.0 (49.0-65.0)	
< 50%, n (%)	367 (36.0)	569 (33.7)	591 (30.9)	661 (26.8)	866 (25.4)	
Aortic valve area, cm²	0.66±0.18 *(n=977)*	0.67±0.18 *(n=1599)*	0.67±0.22 *(n=1828)*	0.68±0.23 *(n=2295)*	0.71±0.25 *(n=3147)*	< 0.001
Aortic annulus, mm	21.9±2.1 *(n=957)*	22.1±2.2 *(n=1563)*	23.3±2.7 *(n=1761)*	23.4±2.6 *(n=2227)*	23.6±2.7 *(n=3087)*	< 0.001
Aortic mean gradient, mm Hg	48.2±17.2 *(n=1012)*	48.8±16.5 *(n=1655)*	47.8±16.2 *(n=1928)*	47.4±15.8 *(n=2456)*	47.5±16.1 *(n=3383)*	0.001
Moderate or severe AR, n./ total n. (%)	190/974 (19.5)	315/1616 (19.5)	313/1467 (21.3)	449/2184 (20.6)	607/2670 (22.7)	0.193
Moderate or severe MR, n./ total n. (%)	229/976 (23.5)	378/1625 (23.3)	383/1682 (22.8)	484/2215 (21.9)	655/2707 (24.2)	0.863
Severe PH (sPAP > 60 mm Hg), n (%)	117/812 (14.4)	172/1324 (13.0)	219/1549 (14.1)	259/1999 (13.0)	305/2499 (12.2)	0.118

APE= acute pulmonary edema; AR=Aortic regurgitation; CABG= coronary artery bypass graft; IQR= interquartile range; MR=Mitral regurgitation; PH= Pulmonary hypertension; SAVR= surgical aortic valve replacement; sPAP= systolic pulmonary artery pressure; TIA= transient ischemic attack.

* Test performed using log-transformed variable.

*** Presence of at least one significant lesion (≥50%) on the pre-procedural coronary angiogram.

IX- Supplementary Table 6 – Baseline characteristics of the FRANCE TAVI population according to the type of implanted valve.

Characteristics	Medtronic CoreValve (n=4465)	Edwards SAPIEN (n=8232)	p value
Clinical characteristics			
Age, y	83.3±7.1 *(n=4465)*	83.4±7.2 (n=8232)	0.926
Median (IQR)	84.5 (80.3-88.0)	84.7 (80.4-88.1)	
Male sex, n./ total n. (%)	2215/4465 (49.6)	4044/8232 (49.1)	0.632
Body-mass index, kg/m²	26.5±5.3 *(n=4398)*	26.5±5.2 (n=8118)	0.729
Logistic EuroSCORE, %	18.1±12.9 *(n=4321)*	17.9±12.0 (n=7918)	0.001 *
Median (IQR)	15.0 (9.0-24.0)	15.0 (9.7-23.0)	
< 10, n (%)	1202 (27.8)	2010 (25.4)	
10-19, n (%)	1616 (37.4)	3228 (40.8)	
20-39, n (%)	1214 (28.1)	2237 (28.2)	
≥ 40, n (%)	289 (6.7)	443 (5.6)	
NYHA class III or IV, n./ total n. (%)	2802/4253 (65.9)	5397/7881 (68.5)	0.126
≥ 2 APE within previous year, n./ total n.(%)	622/4211 (14.8)	1076/7726 (13.9)	0.024
Clinical history, n./ total n. (%)			
Coronary artery disease, n./ total n. (%) **	1808/4130 (43.8)	3246/7729 (42.0)	0.456
Previous myocardial infarction < 90 days	100/4410 (2.3)	136/8110 (1.7)	0.122
Previous CABG	551/4437 (12.4)	882/8143 (10.8)	0.063
Previous SAVR	366/4429 (8.3)	193/8127 (2.4)	< 0.001
Previous permanent pacemaker	682/4424 (15.4)	1115/8129 (13.7)	0.033
Atrial fibrillation	968/3922 (24.6)	1788/7114 (25.1)	0.858
Previous stroke/TIA	502/4421 (11.4)	881/8106 (10.9)	0.521
Diabetes mellitus	1141/4408 (25.9)	2111/8106 (26.0)	0.183
Peripheral vascular disease	1018/4420 (23.0)	1822/8104 (22.5)	0.089
Chronic pulmonary disease	922/4419 (20.9)	1608/8117 (19.8)	0.033
Serum creatinine ≥ 200 µmol/l	220/4226 (5.2)	414/7848 (5.3)	0.748
Renal dialysis	73/4348 (1.7)	162/7991 (2.0)	0.207
Life expectancy < 1yr, n./ total n. (%)	124/4298 (2.9)	225/7858 (2.9)	0.889
Echocardiographic findings			
Ejection fraction, %	54.7±13.4 (n=4305)	55.4±13.6 (n=7967)	0.957
Median (IQR)	58.0 (45.0-65.0)	60.0 (46.0-65.0)	
< 50%, n (%)	1236 (28.7)	2141 (26.9)	
Aortic valve area, cm²	0.70±0.30 (n=4009)	0.69±0.24 (n=7458)	0.172
Aortic annulus, mm	24.0±2.9 (n=3961)	23.5±2.5 (n=7278)	<0.001
Aortic mean gradient, mm Hg	46.6±16.2 (n=4299)	47.4±15.7 (n=7936)	0.272
Moderate or severe AR, n./ total n. (%)	872/3493 (25.0)	1234/6550 (18.8)	< 0.001

Moderate or severe MR, n./ total n. (%)	853/3646 (23.4)	1508/6769 (22.3)	0.188
Severe PH (sPAP > 60 mm Hg), n (%)	466/3389 (13.8)	810/6249 (13.0)	0.170

APE= Acute pulmonary edema; AR=Aortic regurgitation; CABG= coronary artery bypass graft; IQR= interquartile range; MR=Mitral regurgitation; PH= Pulmonary hypertension; SAVR= surgical aortic valve replacement; sPAP= systolic pulmonary artery pressure; TIA= transient ischemic attack.

* Test performed using log-transformed variable.

** Presence of at least one significant lesion (≥50%) on the pre-procedural coronary angiogram.

X- Supplementary Table 7 – Baseline characteristics of the FRANCE TAVI population according to the approach.

Characteristics	TF (n=10602)	Non-TF (n=2202)	p value
Clinical characteristics			
Age, y	83.7±7.0 *(n=10602)*	81.9±8.0 *(n=2202)*	<0.001
Median (IQR)	84.9 (80.8-88.2)	83.3 (78.2-87.3)	
Male sex, n./ total n. (%)	5013/10602 (47.3)	1301/2202 (59.1)	< 0.001
Body-mass index, kg/m²	26.6±5.2 *(n=10448)*	26.4±5.4 *(n=2175)*	0.074
Logistic EuroSCORE, %	17.4±11.7 *(n=10218)*	20.7±14.5 *(n=2123)*	
Median (IQR)	14.0 (9.1-22.0)	17.0 (10.0-27.0)	< 0.001 *
< 10, n (%)	2784 (27.3)	460 (21.7)	
10-19, n (%)	4121 (40.3)	773 (36.4)	
20-39, n (%)	2791 (27.3)	678 (31.9)	
≥ 40, n (%)	522 (5.1)	212 (10.0)	
NYHA class III or IV, n./ total n. (%)	6834/10135 (67.6)	1435/2131 (67.3)	0.228
≥ 2 APE within previous year, n./ total n.(%)	1390/9965 (14.0)	325/2073 (15.7)	0.001
Clinical history, n./ total n. (%)			
Coronary artery disease, n./ total n. (%) **	4015/9904 (40.5)	1078/2057 (52.4)	< 0.001
Previous myocardial infarction < 90 days	184/10440 (1.8)	54/2182 (2.5)	0.010
Previous CABG	1064/10491 (10.1)	377/2193 (17.2)	< 0.001
Previous SAVR	468/10474 (4.5)	91/2185 (4.2)	0.315
Previous permanent pacemaker	1500/10467 (14.3)	307/2188 (14.0)	0.771
Atrial fibrillation	2341/9211 (25.4)	422/1908 (22.1)	0.513
Previous stroke/TIA	1138/10447 (10.9)	257/2184 (11.8)	0.136
Diabetes mellitus	2679/10440 (25.7)	592/2177 (27.2)	0.195
Peripheral vascular disease	1810/10434 (17.4)	1043/2195 (47.5)	< 0.001
Chronic pulmonary disease	2028/10454 (19.4)	523/2187 (23.9)	< 0.001
Serum creatinine ≥ 200 µmol/l	484/10087 (4.8)	151/2091 (7.2)	< 0.001
Renal dialysis	170/10297 (1.7)	65/2146 (3.0)	< 0.001
Life expectancy < 1yr, n./ total n. (%)	291/10190 (2.9)	65/2071 (3.1)	0.721
Echocardiographic findings			
Ejection fraction, %	55.4±13.6 *(n=10239)*	54.2±13.5 *(n=2139)*	0.001
Median (IQR)	60.0 (46.0-65.0)	58.0 (45.0-65.0)	
< 50%, n (%)	2770 (27.1)	630 (29.5)	
Aortic valve area, cm²	0.69±0.26 *(n=9605)*	0.71±0.27 *(n=1964)*	0.001
Aortic annulus, mm	23.6±2.7 *(n=9390)*	24.0±2.6 *(n=1950)*	< 0.001
Aortic mean gradient, mm Hg	47.5±16.0 *(n=10239)*	45.3±14.8 *(n=2101)*	< 0.001
Moderate or severe AR, n./ total n. (%)	1739/8370 (20.8)	379/1748 (21.7)	0.550

Moderate or severe MR, n./ total n. (%)	1994/8687 (23.0)	375/1811 (20.7)	0.060
Severe PH (sPAP > 60 mm Hg), n (%)	1080/8068 (13.4)	200/1647 (12.1)	0.416

APE= Acute pulmonary edema; AR=Aortic regurgitation; CABG= coronary artery bypass graft; IQR= interquartile range; MR=Mitral regurgitation; PH= Pulmonary hypertension SAVR= surgical aortic valve replacement; sPAP= systolic pulmonary artery pressure; TIA= transient ischemic attack.

* Test performed using log-transformed variable.

** Presence of at least one significant lesion (≥50%) on the pre-procedural coronary angiogram.

XI- Supplementary Table 8 - Outcomes of the FRANCE TAVI population according to the type of implanted valve.

Outcomes	Medtronic CoreValve (n=4465)	Edwards SAPIEN (n=8232)	p value
In-hospital outcomes			
Time from implantation to discharge,			<0.001 *
Median (IQR)	8 (6-11) (n=4439)	7 (5-10) (n=8128)	
1-5 days	897/4439 (20.2)	2218/8128 (27.3)	
6-9 days	2035/4439 (45.8)	3660/8128 (45.0)	
≥ 10 days	1507/4439 (34.0)	2250/8128 (27.7)	
Complications, n./total n. (%)			
Death			
From all-cause	244/4465 (5.5)	315/8232 (3.8)	< 0.001
Cause of death			
CV death	172/244 (70.5)	197/315 (62.5)	ref
Non CV death	63/244 (25.8)	95/315 (30.2)	0.073
Unknown	9/244 (3.7)	23/315 (7.3)	0.030
Annulus rupture	8/4413 (0.2)	44/8038 (0.6)	0.005
Aortic dissection	22/4413 (0.5)	24/8038 (0.3)	0.082
Valve migration	84/4413 (1.9)	52/8038 (0.7)	<0.001
Tamponade	87/4413 (2.0)	162/8038 (2.0)	0.617
Stroke	100/4413 (2.3)	145/8038 (1.8)	0.169
STEMI	16/4413 (0.4)	11/8038 (0.1)	0.014
Permanent pacemaker implantation**	939/3703 (25.4)	903/6886 (13.1)	< 0.001
Pulmonary embolism	9/4413 (0.2)	8/8038 (0.1)	0.141
Renal failure	181/4424 (4.1)	292/8038 (3.6)	0.444
Renal dialysis	36/4424 (0.8)	50/8038 (0.6)	0.356
Echocardiographic findings			
Aortic valve area, cm²	1.76±0.62 (n=1527)	1.77±0.52 (n=3138)	< 0.001
Aortic mean gradient, mm Hg	9.2±7.0 (n=3736)	10.9±5.8 (n=6863)	< 0.001
Moderate or severe AR, n./total n. (%)	587/3877 (15.1)	522/7045 (7.4)	< 0.001
Moderate or severe MR, n./total n. (%)	576/3290 (17.5)	933/6176 (15.1)	0.049
Vital status after 30-days †			< 0.001
Dead, n./total n. (%)	225/3224 (6.6)	263/5725 (4.5)	< 0.001
Alive, n./total n. (%)	3100/3224 (91.7)	5285/5725 (92.3)	ref
Unknown, n./total n. (%)	57/3224 (1.7)	177/5725 (3.1)	< 0.001
Cause of death			
CV death, n (%)	154/225 (68.4)	153/263 (58.2)	ref
Non CV death, n (%)	59/225 (26.2)	86/263 (32.7)	0.029

Unknown, n (%)	12/225 (5.3)	24/263 (9.1)	0.036

* Test performed using log-transformed variable.

** Number are given for patients without prior permanent pacemaker

† In a subgroup of 9107 subjects from 35 centers with sufficient follow-up data (centers in which vital status after 30 days was known for at least 90% of the patients)

AR= Aortic regurgitation; CV= Cardiovascular; MR=Mitral regurgitation; STEMI= ST-segment elevation myocardial infarction.

XII- Supplementary Table 9 – Outcomes of the FRANCE TAVI population according to the approach.

Outcomes	TF (n=10602)	Non-TF (n=2202)	p value
In-hospital outcomes			
Time from implantation to discharge,			< 0.001 *
Median (IQR)	7 (5-10) *(n=10500)*	9 (7-13) *(n=2172)*	
1-5 days	2905 (27.7)	227 (10.4)	
6-9 days	4867 (46.3)	877 (40.4)	
≥ 10 days	2728 (26.0)	1068 (49.2)	
Complications, n./total n. (%)			
Death			
From all-cause	408/10602 (3.9)	154/2202 (7.0)	< 0.001
Cause of death			
CV death	284/408 (69.6)	86/154 (55.9)	ref
Non CV death	103/408 (25.2)	57/154 (37.0)	0.005
Unknown	21/408 (5.2)	11/154 (7.1)	0.161
Annulus rupture	50/10408 (0.5)	2/2149 (0.1)	0.031
Aortic dissection	37/10408 (0.4)	9/2149 (0.4)	0.653
Valve migration	115/10408 (1.1)	24/2149 (1.1)	0.892
Tamponade	227/10408 (2.2)	29/2149 (1.4)	0.021
Stroke	200/10408 (1.9)	49/2149 (2.3)	0.266
STEMI	20/10408 (0.2)	7/2149 (0.3)	0.265
Permanent pacemaker implantation**	1570/8846 (17.8)	300/1835 (16.4)	0.012
Pulmonary embolism	14/10408 (0.1)	4/2149 (0.2)	0.602
Renal failure	355/10408 (3.4)	125/2149 (5.8)	< 0.001
Renal dialysis	60/10408 (0.6)	26/2149 (1.2)	0.002
Echocardiographic findings			
Aortic valve area, cm²	1.77±0.55 *(n=4013)*	1.70±0.57 *(n=711)*	0.908
Aortic mean gradient, mm Hg	10.3±6.4 *(n=8963)*	10.4±6.1 *(n=1721)*	0.577
Moderate or severe AR, n./total n. (%)	940/9193 (10.2)	179/1814 (9.9)	0.799
Moderate or severe MR, n./total n. (%)	1294/7940 (16.3)	225/1604 (14.0)	0.071
Vital status after 30-days †			
Dead, n./total n. (%)	359/7575 (4.7)	134/1637 (8.2)	< 0.001
Alive, n./total n. (%)	7005/7575 (92.5)	1475/1637 (90.1)	ref
Unknown, n./total n. (%)	211/7575 (2.8)	28/1637 (1.7)	0.033
Cause of death			
CV death, n (%)	239/359 (66.6)	71/134 (53.0)	ref
Non CV death, n (%)	93/359 (25.9)	54/134 (40.3)	0.003

Unknown, n (%)	27/359 (7.5)	9/134 (6.7)	0.784

* Test performed using log-transformed variable.

** Number are given for patients without prior permanent pacemaker

† In a subgroup of 9212 subjects from 35 centres with sufficient follow-up data (centres in which vital status after 30 days was known for at least 90% of the patients)

AR= Aortic regurgitation; MR=Mitral regurgitation; STEMI= ST-segment elevation myocardial infarction.

XIII- Supplementary Table 10 - Baseline characteristics of the FRANCE TAVI population according to centers' participation in the FRANCE 2 registry.

Characteristics	Patients from centres involved in both registries (n=9982)	Patients from centres involved in FRANCE TAVI only (n=2822)	p value
Clinical characteristics			
Age, y	83.1±7.3 *(n=9982)*	84.2±6.5 *(n=2822)*	0.026
Median (IQR)	84.4 (80.2-87.9)	85.3 (81.2-88.5)	
Male sex, n./ total n. (%)	4899/9982 (49.1)	1415/2822 (50.1)	0.329
Body-mass index, kg/m²	26.5±5.3 *(n=9828)*	26.5±5.2 *(n=2795)*	0.847
Logistic EuroSCORE, %	17.5±12.0 *(n=9600)*	19.3±13.2 *(n=2741)*	0.270 *
Median (IQR)	14.2 (9.4-22.2)	16.0 (10.0-25.0)	
< 10, n (%)	2602 (27.1)	642 (23.4)	
10-19, n (%)	3879 (40.4)	1015 (37.0)	
20-39, n (%)	2592 (27.0)	877 (32.0)	
≥ 40, n (%)	527 (5.5)	207 (7.6)	
NYHA class III or IV, n./ total n. (%)	6299/9575 (65.8)	1970/2666 (73.9)	0.977
≥ 2 APE within previous year, n./ total n.(%)	1224/9515 (12.9)	491/2523 (19.5)	
Clinical history, n./ total n. (%)			
Coronary artery disease, n./ total n. (%) **	3903/9204 (42.4)	1190/2757 (43.2)	0.463
Previous myocardial infarction < 90 days	162/9828 (1.7)	76/2794 (2.7)	0.176
Previous CABG	1075/9874 (10.9)	366/2810 (13.0)	0.054
Previous SAVR	438/9855 (4.4)	121/2804 (4.3)	0.782
Previous permanent pacemaker	1388/9856 (14.1)	419/2799 (15.0)	0.602
Atrial fibrillation	2030/8544 (23.8)	733/2575 (28.5)	0.063
Previous stroke/TIA	1075/9852 (10.9)	320/2779 (11.5)	0.637
Diabetes mellitus	2535/9839 (25.8)	736/2778 (26.5)	0.381
Peripheral vascular disease	2073/9868 (21.0)	780/2761 (28.3)	0.151
Chronic pulmonary disease	1810/9865 (18.4)	741/2776 (26.7)	< 0.001
Serum creatinine ≥ 200 µmol/l	499/9511 (5.3)	136/2667 (5.1)	0.610
Renal dialysis	184/9680 (1.9)	51/2763 (1.9)	0.987
Life expectancy < 1yr, n./ total n. (%)	328/9488 (3.5)	28/2773 (1.0)	
Echocardiographic findings			
Ejection fraction, %	54.9±13.5 *(n=9647)*	55.9±13.9 *(n=2731)*	0.115
Median (IQR)	60.0 (45.0-65.0)	60.0 (45.0-65.0)	
< 50%, n (%)	2658 (27.6)	742 (27.2)	
Aortic valve area, cm²	0.69±0.24 *(n=8962)*	0.70±0.33 *(n=2607)*	0.581
Aortic annulus, mm	23.5±2.7 *(n=8753)*	24.0±2.7 *(n=2587)*	0.064

Aortic mean gradient, mm Hg	47.2±15.8 *(n=9581)*	47.2±16.0 *(n=2759)*	0.629
Moderate or severe AR, n./ total n. (%)	1707/7819 (21.8)	411/2299 (17.9)	0.277
Moderate or severe MR, n./ total n. (%)	1835/8160 (22.5)	534/2338 (22.8)	0.367
Severe PH (sPAP > 60 mm Hg), n (%)	947/7464 (12.7)	333/2251 (14.8)	0.208

APE= Acute pulmonary edema; AR=Aortic regurgitation; CABG= coronary artery bypass graft; IQR= interquartile range; MR=Mitral regurgitation; PH= Pulmonary hypertension; SAVR= surgical aortic valve replacement; sPAP= systolic pulmonary artery pressure; TIA= transient ischemic attack.

* Test performed using log-transformed variable.

** Presence of at least one significant lesion (≥50%) on the pre-procedural coronary angiogram.

XIV- Supplementary Table 11- Procedural characteristics of the FRANCE TAVI population according to centers' participation in the FRANCE 2 registry.

Characteristics	Patients from centres involved in both registries (n=9982)	Patients from centres involved in FRANCE TAVI only (n=2822)	p value
Location			
Catheterization laboratory, n (%)	5978/9950 (60.1)	1595/2796 (57.0)	ref
Operating room, n (%)	564/9950 (5.7)	61/2796 (2.2)	< 0.001
Hybrid room, n (%)	3408/9950 (34.2)	1140/2796 (40.8)	0.072
General anesthesia, n./total n. (%)	5194/9888 (52.5)	1337/2757 (48.5)	0.326
TEE guidance, n./total n. (%)	2871/8875 (32.4)	801/2498 (32.1)	0.837
Transfemoral approach, n (%)	8073/9982 (80.9)	2529/2822 (89.6)	< 0.001
Valve type			
Edwards SAPIEN, n (%) *	6349/9982 (63.6)	1883/2822 (66.7)	ref
Medtronic CoreValve, n (%)	3527/9982 (35.3)	938/2822 (33.3)	0.773
Others, n (%)	106/9982 (1.1)	1/2822 (0.0)	< 0.001
Need for a 2nd valve, n./total n. (%)	186/9982 (1.9)	50/2822 (1.8)	0.997
Conversion to surgery, n./total n. (%)	55/9814 (0.6)	10/2743 (0.4)	0.246
Device success, n./total n. (%)	9485/9795 (96.8)	2654/2749 (96.5)	0.549

TEE= Transesophageal echocardiography.
* Including all iterations (SAPIEN, SAPIEN XT, SAPIEN 3)

XV- Supplementary Table 12- Outcomes of the FRANCE TAVI population according to centers' participation in the FRANCE 2 registry.

Outcomes	Patients from centers involved in both registries (n=9982)	Patients from centers involved in FRANCE TAVI only (n=2822)	p value
In-hospital outcomes			
Time from implantation to discharge,			0.869 *
Median (IQR)	8 (6-11) *(n=9913)*	7 (5-10) *(n=2759)*	
1-5 days	2430 (24.5)	702 (25.4)	
6-9 days	4399 (44.4)	1345 (48.8)	
≥ 10 days	3084 (31.1)	712 (25.8)	
Complications, n./total n. (%)			
Death			
From all-cause	421/9982 (4.2)	141/2822 (5.0)	0.143
Cause of death			
CV death	269/421 (63.9)	101/141 (71.6)	ref
Non CV death	125/421 (29.7)	35/141 (24.8)	0.198
Unknown	27/421 (6.4)	5/141 (3.5)	0.142
Annulus rupture	36/9814 (0.4)	16/2743 (0.6)	0.376
Aortic dissection	33/9814 (0.3)	13/2743 (0.5)	0.294
Valve migration	114/9814 (1.2)	25/2743 (0.9)	0.284
Tamponade	190/9814 (1.9)	66/2743 (2.4)	0.306
Stroke	189/9814 (1.9)	60/2743 (2.2)	0.516
STEMI	22/9814 (0.2)	5/2743 (0.2)	0.718
Permanent pacemaker implantation**	1506/8367 (18.0)	364/2314 (15.7)	0.256
Pulmonary embolism	14/9814 (0.1)	4/2743 (0.2)	0.856
Renal failure	412/9814 (4.2)	68/2743 (2.5)	0.302
Renal dialysis	70/9814 (0.7)	16/2743 (0.6)	0.666
Echocardiographic findings			
Aortic valve area, cm^2	1.71±0.54 *(n=3610)*	1.93±0.56 *(n=1114)*	0.031
Aortic mean gradient, mm Hg	10.5±6.5 *(n=8263)*	9.8±5.7 *(n=2421)*	0.249
Moderate or severe AR, n./total n. (%)	940/8513 (11.0)	179/2494 (7.2)	0.029
Moderate or severe MR, n./total n. (%)	1186/7357 (16.1)	333/2187 (15.2)	0.721
Vital status after 30-days †			
Dead, n./total n. (%)	405/7916 (5.1)	88/1296 (6.8)	0.233
Alive, n./total n. (%)	7290/7916 (92.1)	1190/1296 (91.8)	ref
Unknown, n./total n. (%)	221/7916 (2.8)	18/1296 (1.4)	0.013
Cause of death			

CV death, n (%)	247/405 (61.0)	63/88 (71.6)	ref
Non CV death, n (%)	126/405 (31.1)	21/88 (23.9)	0.151
Unknown, n (%)	32/405 (7.9)	4/88 (4.5)	0.198

* Test performed using log-transformed variable.

** Number are given for patients without prior permanent pacemaker

† In a subgroup of 9212 subjects from 35 centers with sufficient follow-up data (centers in which vital status after 30 days was known for at least 90% of the patients)

AR= Aortic regurgitation; CV= Cardiovascular; MR=Mitral regurgitation; STEMI= ST-segment elevation myocardial infarction.

XVI- Online-only references

1. Kappetein AP, Head SJ, Généreux P, et al. Updated standardized endpoint definitions for transcatheter aortic valve implantation: The Valve Academic Research Consortium-2 consensus document. *Eur Heart J* 2012; **33**(19): 2403-18b.

Annexe 2

Appendice complémentaire de "Predictors of Early Cerebrovascular Events in Patients With Aortic Stenosis Undergoing Transcatheter Aortic Valve Replacement."

Online supplemental appendix

Auffret et al, Predictors of Cerebrovascular Events Post-TAVR.

Search strategy: MEDLINE (PubMed database)

(("Transcatheter Aortic Valve Replacement"[MESH]) OR (transcatheter aortic valve) OR (TAVI) OR (TAVR) OR (Transcutaneous aortic valve) OR (Percutaneous aortic valve)) AND ("2000/01/01"[Date - Publication]: "2015/12/09"[Date - Publication]) AND Humans[Mesh] NOT review[Publication Type]) NOT editorial[Publication Type]) NOT comment[Publication Type]) NOT case reports[Publication Type]

Supplemental Table 1- Reporting of stroke by included studies.

First Author[ref]	Stroke definition	Stroke adjudication	In-hospital all stroke	In-hospital major stroke	In-hospital stroke/TIA	30d all stroke	30d major stroke	30d stroke/TIA
Leker[e1]	NA	Neurologist	No	No	Yes	No	No	No
Stortecky[e2]	VARC	Neurologist	No	No	No	No	No	Yes
Stangl[e3]	VARC	NA	No	No	No	No	Yes	No
O'Connor[e4]	NA	NA	No	No	No	Yes	No	No
Sherif[e5]	NA	NA	No	No	No	Yes	No	No
Nuis[e6]	VARC	NA	Yes	No	No	No	No	No
Abramowitz[e7]	VARC-2	NA	No	No	No	No	No	Yes
Yamamoto[e8]	VARC	NA	No	No	No	No	Yes	Yes
Konigstein[e9]	VARC-2	NA	No	No	No	No	No	Yes
Yamamoto[e10]	VARC	Independent CEC	No	No	No	Yes	Yes	No
Nombela-Franco[e11]	VARC	NA	No	No	No	No	No	Yes
Conrotto[e12]	VARC	NA	Yes	No	Yes	No	No	No
Minha[e13]	VARC-2	NA	Yes	No	No	No	No	No
Barbash[e14]	VARC-2	NA	Yes	No	No	No	No	No
Chopard[e15]	VARC-2	Independent CEC	No	No	No	Yes	No	No
Maan[e16]	NA	NA	No	No	No	Yes	No	Yes
Yankelson[e17]	VARC-2	Neurologist	No	No	No	Yes	No	No
Abdel-Wahab[e18]	VARC	NA	Yes	No	No	No	No	No
Abramowitz[e19]	VARC	NA	No	No	No	No	No	Yes
Gautier[e20]	NA	NA	No	No	No	Yes	No	No
Mancio[e21]	VARC	NA	No	No	No	No	No	Yes
Snow[e22]	NA	NA	No	No	Yes	No	No	No
Stefanini[e23]	VARC	CEC	No	No	No	Yes	Yes	No
Allende[e24]	VARC-2	NA	No	No	No	Yes	No	Yes
Ferro[e25]	NA	NA	Yes	No	No	No	No	No
Nguyen[e26]	NA	NA	Yes	No	No	No	No	No
Oguri[e27]	VARC	Independent CEC	Yes	Yes	No	No	No	No
Sinning[e28]	NA	NA	Yes	No	No	No	No	No
Bosmans[e29]	NA	NA	No	No	No	Yes	No	No
Eltchaninoff[e30]	NA	NA	No	No	No	Yes	No	No
Ewe[e31]	NA	NA	Yes	No	No	No	No	No
Frohlich[e32]	NA	NA	Yes	No	Yes	No	No	No
Imnadze[e33]	VARC-2	NA	No	No	No	Yes	No	No
Lotfi[e34]	VARC-2	NA	No	No	No	Yes	No	No
Mack[e35]	VARC-2	Independent cardiologist	Yes	No	Yes	No	No	No
Muensterer[e36]	VARC	NA	Yes	No	Yes	No	No	No
Petronio[e37]	NA	NA	Yes	No	No	No	No	No
Schymik[e38]	VARC-2	NA	No	No	No	Yes	Yes	Yes
Seiffert[e39]	VARC	NA	No	No	No	Yes	Yes	Yes
Walters[e40]	VARC-2	Independent CEC	No	No	No	Yes	No	No
Webb[e41]	VARC-2	NA	No	No	No	Yes	Yes	Yes

Abdel-Wahab[e42]	VARC	Independent CEC	No	No	No	Yes	Yes	No
Swedish report[e43]	NA	NA	Yes	No	No	No	No	No
Chieffo[e44]	VARC	NA	No	No	No	No	Yes	No
Collas[e45]	NA	NA	No	No	No	No	No	Yes
Kasel[e46]	VARC	NA	Yes	No	Yes	No	No	Yes
Ludman[e47]	NA	NA	No	No	Yes	No	No	No
Sabaté[e48]	VARC	NA	Yes	Yes	Yes	No	No	No
Watanabe[e49]	VARC-2	NA	No	No	Yes	No	No	No
Wenaweser[e50]	VARC	CEC	No	No	No	Yes	No	No
Wenaweser[e51]	VARC-2	Independent CEC	No	No	No	Yes	Yes	Yes
Lange[e52]	NA	NA	No	No	No	No	No	Yes
Makkar[e53]	PARTNER Trial/Registry	Independent CEC	No	No	No	Yes	No	Yes
Geisbusch[e54]	NA	NA	Yes	No	No	No	No	No
Barbanti[e55]	VARC	NA	Yes	Yes	Yes	Yes	Yes	Yes
Hahn[e56]	PARTNER Trial/Registry	Independent CEC	Yes	No	No	Yes	No	No
Lasa[e57]	NA	NA	Yes	No	No	No	No	No
Stundl[e58]	VARC-2	NA	Yes	No	No	No	No	No
Watanabe[e59]	VARC-2	NA	No	No	Yes	No	No	No
Durand[e60]	VARC	Independent CEC	No	No	No	Yes	Yes	Yes
Huczek[e61]	VARC-2	Blinded adjudication	No	No	Yes	No	No	No
Poliacikova[e62]	VARC	NA	Yes	No	No	Yes	No	No
Stabile[e63]	VARC-2	Independent CEC	No	No	No	Yes	Yes	No
Ussia[e64]	VARC	NA	Yes	Yes	Yes	Yes	Yes	Yes

CEC=Clinical event committee; NA= Not available; TIA=Transient ischemic attack; VARC= Valve Academic Research Consortium

Supplemental Table 2- Clinical and procedural characteristics of studies included for the evaluation of baseline predictors.

First Author[ref]	Age (years)	Male Sex (%)	Logistic EuroSCORE	STS-PROM	Prior stroke (%)	Prior AF (%)	Approach (%)	Valve type (%)	BPD (%)	TV-in-TV (%)	In-hospital or 30d all-cause mortality (%)
Leker[e1]	80.6±6.3	44.4	25.3±16.1	ND	ND	ND	TF (81) SC (19)	MCV (100)	ND	ND	2.8
Stortecky[e2]	82.5±5.8	49.0	24.3±14.2	6.8±5.3	8.0	27.0	TF (79) TA (20) SC (1)	MCV (58) ESV (42)	28.0	2.0	6.4
Stangl[e3]	79.0±8.0	42.0	19.9±15.4	ND	10.0	19.0	TF (100)	MCV (83) ESV (17)	ND	ND	3.0
O'Connor[e4]	82.4±7.9	51.3	23.1±14.7	ND	16.2	ND	TF (70) TA (23) Others (7)	MCV (33) ESV (66) Portico (<1)	ND	ND	6.5
Sherif[e5]	81.7±6.1	42.2	20.6±13.4	ND	7.9	25.0	TF (88) TA (9) SC (3)	MCV (78) ESV (22)	ND	ND	8.1
Nuis[e6]	80.0±8.0	50.0	13.8 (10.0-22.0)	5.0 (3.4-7.3)	23.0	30.0	TF (97) SC (3)	MCV (100)	16.4	5.1	8.4
Abramowitz[e7]	82.1±6.8	60.5	ND	7.9±4.6	12.7	33.8	TF (85) TA (6) Others (9)	ESV (100)	8.9	3.0	2.9
Yamamoto[e8]	84.1±7.3	44.0	24.1±11.9	12.5±8.5	11.0	ND	TF (96) Others (4)	MCV (95) ESV (5)	ND	2.0	8.0
Konigstein[e9]	82.0±5.7	42.0	24.0±14.0	ND	10.0	30.0	TF (100)	MCV (75) ESV (25)	ND	ND	ND
Yamamoto[e10]	82.8±7.0	50.9	22.0±14.3	ND	9.9	ND	TF (75) TA (18) SC (7)	MCV (33) ESV (67)	ND	2.2	9.6
Nombela-Franco[e11]	81.0±8.0	50.7	ND	6.5 (4.3-9.7)	ND	26.0	TF (68) TA (30) Others (2)	MCV (33) ESV (64) Portico (1)	17.8	3.1	8.7
Conrotto[e12]	82 (81-83)	49.5	22.0 (20.0-24.0)	10.0 (9.0-12.0)	14.3	ND	TF (58) TA (23) SC (19)	MCV (53) ESV (47)	ND	ND	5.7
Minha[e13]	83.4±7.6	49.5	ND	9.7±4.6	16.8	42.1	TF (75) TA (22) Others (3)	MCV (ND) ESV (ND)	6.8	ND	9.2
Barbash[e14]	84.0±7.6	48.8	28.9±24.0	10.5±4.6	21.0	38.5	TF (74) TA (25) TAo (1)	MCV (ND) ESV (ND)	4.3	1.1	9.2
Chopard[e15]	82.8±7.0	50.6	21.8±14.0	14.1±11.5	9.9	25.9	TF (73) TA (18) Others (9)	MCV (34) ESV (66)	ND	ND	9.3
Maan[e16]	84.2±6.8	47.0	14.3±12.2	6.9±3.8	18.0	48.9	TF (ND) TA (59) Others (ND)	ESV (100)	ND	ND	6.6
Yankelson[e17]	83.0±5.6	40.5	24.3±14.1	ND	10.0	31.1	TF (98) TA (ND) Others (ND)	MCV (ND) ESV (ND)	ND	ND	3.2
Abdel-Wahab[e18]	81.7±6.2	42.0	20.5±13.1	ND	8.0	24.7	TF (87) TA (9) Others (4)	MCV (81) ESV (19)	ND	ND	8.3
Abramowitz[e19]	83.1±5.4	39.0	26.3±13.1	ND	8.4	ND	TF/SC (100)	MCV (100)	ND	ND	2.4
Gautier[e20]	81.1±.7.7	53.8	26.7±14.4	ND	ND	ND	ND	MCV (ND) ESV (ND)	ND	ND	12.0

Mancio[e21]	79.0±9.0	52.0	ND	6.0±5.0	ND	32.0	TF/SC (96) TA (4)	MCV (87) ESV (13)	ND	ND	6.6
Snow[e22]	81.3±7.6	53.2	18.1 (12.1-28.1)	ND	ND	ND	ND	MCV (48) ESV (52)	ND	ND	6.3
Stefanini[e23]	82.5±5.8	44	23.4±13.8	6.9±5.3	8.0	29.0	TF (78) TA (21) SC (1)	MCV (54) ESV (45) Symetis (1)	ND	2.0	6.3
Allende[e24]	80.5±7.2	49.9	17.6 (11.0-27.0	6.5 (5.0-12.0)	12.6	30.4	TF (76) TA (ND) Others (ND)	MCV (49) ESV (51)	ND	ND	7.2
Ferro[e25]	82 (77-87)	53.5	18.9 (12.4-28.7)	ND	17.9	24.2	TF (70) TA (ND) Others (ND)	MCV (ND) ESV (ND)	ND	ND	5.5
Nguyen[e26]	82.2±8.2	55.8	ND	12.1±6.4	16.2	ND	TF (62) TA (31) Others (7)	ND	ND	ND	3.4
Oguri[e27]	82.8±7.1	51.5	19.1 (11.7-28.4)	9.7 (5.9-20.4)	9.9	26.3	TF (74) TA (18) Others (8)	MCV (34) ESV (66)	ND	2.2	7.9
Sinning[e28]	81.8±6.2	41.8	20.7±13.0	ND	8.2	25.2	TF (87) TA (9) Others (4)	MCV (75) ESV (25)	ND	ND	8.4

Values are mean ± standard deviation or median (interquartile range). AF= Atrial fibrillation; BPD= Balloon post-dilation; ESV= Edwards Sapien valve; MCV= Medtronic CoreValve; ND= No data; SC= Subclavian; STS-PROM= Society of Thoracic Surgeon-Predicted Risk of Mortality; TA=Transapical; Tao=Transaortic; TF=Transfemoral; TV-in-TV= Transcatheter valve within a transcatheter valve.

Supplemental Table 3- Clinical and procedural characteristics of studies included for the evaluation of procedural predictors.

First Author[ref]	Age (years)	Male Sex (%)	Logistic EuroSCORE	STS-PROM	Prior stroke (%)	Prior AF (%)	Approach (%)	Valve type (%)	BPD (%)	TV-in-TV (%)	In-hospital or 30d all-cause mortality (%)
Bosmans[e29]	83.0±5.5	ND	30.9±16	ND	ND	ND	TF (53) TA (47)	MCV (43) ESV (57)	ND	ND	12.0
Eltchaninoff[e30]	82.3±7.3	56.6	25.6±11.4	18.9±12.8	9.4	ND	TF (66) TA (29) SC (5)	MCV (36) ESV (64)	ND	ND	12.7
Ewe[e31]	80.6±7.9	50.0	21.3±11.8	8.7±3.6	11.5	21.2	TF (44) TA (56)	ESV (100)	ND	ND	4.8
Frohlich[e32]	83 (77-87)	52.7	18.0 (12.0-27.7)	ND	15.1	20.6	TF (71) TA (19) Others (10)	MCV (49) ESV (51)	ND	2.3	5.6
Imnadze[e33]	80.8±6.2	43.2	23.7±13.3	8.0±6.3	12.3	ND	TF (21) TA (79)	MCV (2) ESV (89) Symetis (9)	ND	ND	3.9
Lotfi[e34]	80.7±6.4	41.2	26.2±14.6	ND	ND	23.2	TF (55) TA (45)	MCV (55) ESV (45)	ND	ND	9.8
Mack[e35]	84 (78-88)	50.0	ND	7.0 (5-11)	13.0	41.0	TF (64) TA (29) Others (7)	ESV (100)	ND	2.9	5.5
Muensterer[e36]	80.1±7.2	46.3	19.5±12.7	6.0±4.3	11.7	ND	TF (88) SC (12)	MCV (100)	ND	2.0	8.4
Nombela-Franco[e11]	81.0±8.0	50.7	ND	6.5 (4.3-9.7)	ND	26.0	TF (68) TA (30) Others (2)	MCV (33) ESV (64) Portico (1)	17.8	3.1	8.7
Petronio[e37]	83 (78-86)	44.0	20.1 (12.8-30.5)	ND	7.8	ND	TF (89) SC (11)	MCV (100)	ND	3.9	3.9
Schymik[e38]	81.9±5.4	43.5	23.1±16.2	ND	ND	ND	TF (59) TA (41)	MCV (19) ESV (80) Symetis (1)	ND	ND	6.3
Seiffert[e39]	81 (80-81)	44.5	22.7 (21.2-24.2)	8.3 (7.7-8.9)	19.3	33.2	TF (46) TA (54)	MCV (14) ESV (86)	ND	ND	10.1
Stortecky[e2]	82.5±5.8	49.0	24.3±14.2	6.8±5.3	8.0	27.0	TF (79) TA (20) SC (1)	MCV (58) ESV (42)	28.0	2.0	6.4
Walters[e40]	82.7±ND	52.7	27.8±ND	ND	ND	ND	TF (52) TA (48)	ESV (100)	ND	ND	7.8
Webb[e41]	83.6±5.0	46.0	21.6±	7.4±	7.3	27.5	TF (64) TA (33) TAo (3)	ESV (100)	3.3	ND	5.3
Abdel-Wahab[e42]	80.8±11.3	35.7	21.8±13.8	5.9±3.4	ND	28.2	TF (100)	MCV (50) ESV (50)	34.4	3.3	4.6
Swedish report[e43]	ND	55.5	ND	ND	ND	ND	TF (74) TA (22) SC (4)	MCV (58) ESV (42)	ND	3.8	14.0
Chieffo[e44]	82.0±6.9	47.1	21.9±13.0	9.1±7.1	12.1	ND	TF (100)	MCV (50) ESV (50)	ND	ND	7.6
Collas[e45]	83 (79-87)	47.0	22.8 (14.4-33.7)	ND	15.0	ND	TF (74) TA (19) Others (7)	MCV (47) ESV (53)	ND	2.0	9.0
Kasel[e46]	80.7±5.9	33.0	22.0±14.6	9.6±7.4	ND	13.0	TF (100)	MCV (50) ESV (50)	ND	ND	4.0
Ludman[e47]	81.3±7.6	47.3	21.9±13.7	ND	9.1	26.6	TF (71) TA (19)	MCV (48) ESV (52)	ND	2.4	6.3

Sabaté[e48]	81.0±6.0	46.0	17.0±11.0	ND	10.0	29.0	Others (10) TF (79) TA (21)	MCV (43) ESV (57)	13.0	1.0	9.0
Watanabe[e49]	83.1±7.2	45.0	22.1±11.9	ND	ND	ND	TF (100)	MCV (47) ESV (53)	ND	1.6	9.1
Wenaweser[e50]	82.0±6.5	42.5	24.6±15.3	6.4±4.9	9.0	26.0	TF (77) TA (21) SC (2)	MCV (65) ESV (35)	ND	2.0	7.5
Wenaweser[e51]	82.4±6.2	48.5	20.2±12.7	8.2±7.1	11.9	ND	TF (100)	MCV (58) ESV (42)	ND	ND	3.6
Lange[e52]	80.3±7.1	37.0	20.2±13.0	6.1±4.1	13.2	23.3	TF (61) TA (31) Others (8)	MCV (69) ESV (31)	16.6	2.6	9.5
Makkar[e53]	84.5±7.2	52.4	26.5±16.2	11.5±4.3	ND	ND	TF (58) TA (42)	ESV (100)	ND	2.5	6.0
Nuis[e6]	80.0±8.0	50.0	13.8 (10.0-22.0)	5.0 (3.4-7.3)	23.0	30.0	TF (97) Others (3)	MCV (100)	16.4	5.1	8.4
Geisbusch[e54]	81.0±5.0	47.6	ND	ND	12.0	ND	TF (93) SC (7)	MCV (100)	ND	ND	9.9
Barbanti[e55]	81.6±6.5	47.5	ND	7.1 (4-13)	11.3	5.4	TF (81) SC (14) TAo (5)	MCV (100)	20.0	4.9	4.1
Hahn[e56]	84.4±7.2	52.9	27.0±16.3	11.5±4.2	ND	50.6	ND	ESV (100)	12.0	ND	3.3
Lasa[e57]	81.2±4.7	49.7	25.8±10.5	ND	ND	34.4	TF (61) TA (39)	ESV (100)	13.0	ND	ND
Stundl[e58]	81.4±6.6	54.4	ND	6.8 (4.4-10.7)	ND	ND	TF (97) TAo (2) SC (1)	MCV (100)	37.6	7.0	5.3
Watanabe[e59]	84 (81-88)	44.9	22.0±12.2	ND	ND	ND	TF (51) TA (25) Others (24)	ESV (100)	10.4	2.1	12.8
Durand[e60]	83.6±6.1	47.9	20.1±12.0	7.2±5.3	8.6	28.4	TF (81) TA (18) SC (1)	MCV (19) ESV (81)	ND	ND	8.6
Huczek[e61]	78.6±7.6	51.0	23.1±16.9	ND	22.0	26.0	TF (81) TA (11) Others (8)	MCV (66) ESV (34)	ND	ND	8.3
Poliacikova[e62]	81.8±6.7	54.4	ND	ND	ND	17.4	ND	MCV (100)	ND	ND	4.7
Stabile[e63]	80.7±5.3	33.3	24.2±10.1	10.1±6.0	ND	ND	ND	ESV (100)	ND	ND	2.5
Ussia[e64]	81.0±4.0	46.0	21.0±13.0	7.3±4.0	13.0	13.0	TF (97) SC (3)	MCV (100)	5.0	4.0	10.0
Barbash[e14]	84.0±7.6	48.8	28.9±24.0	10.5±4.6	21.0	38.5	TF (74) TA (25) Others (1)	ND	4.3	1.1	9.2
Chopard[e15]	82.8±7.0	50.6	21.8±14.0	14.1±11.5	9.9	25.9	TF (73) TA (18) Others (9)	MCV (34) ESV (66)	ND	ND	9.3
Yankelson[e17]	83.0±5.6	40.5	24.3±14.1	ND	10.0	31.1	TF (98) TA (ND) Others (ND)	MCV (ND) ESV (ND)	ND	ND	3.2

Values are mean ± standard deviation or median (interquartile range). Abbreviations as in supplementary table 2.

Supplemental Figure 1- Individual meta-analyses of baseline predictors of short-term cerebrovascular events after TAVR.

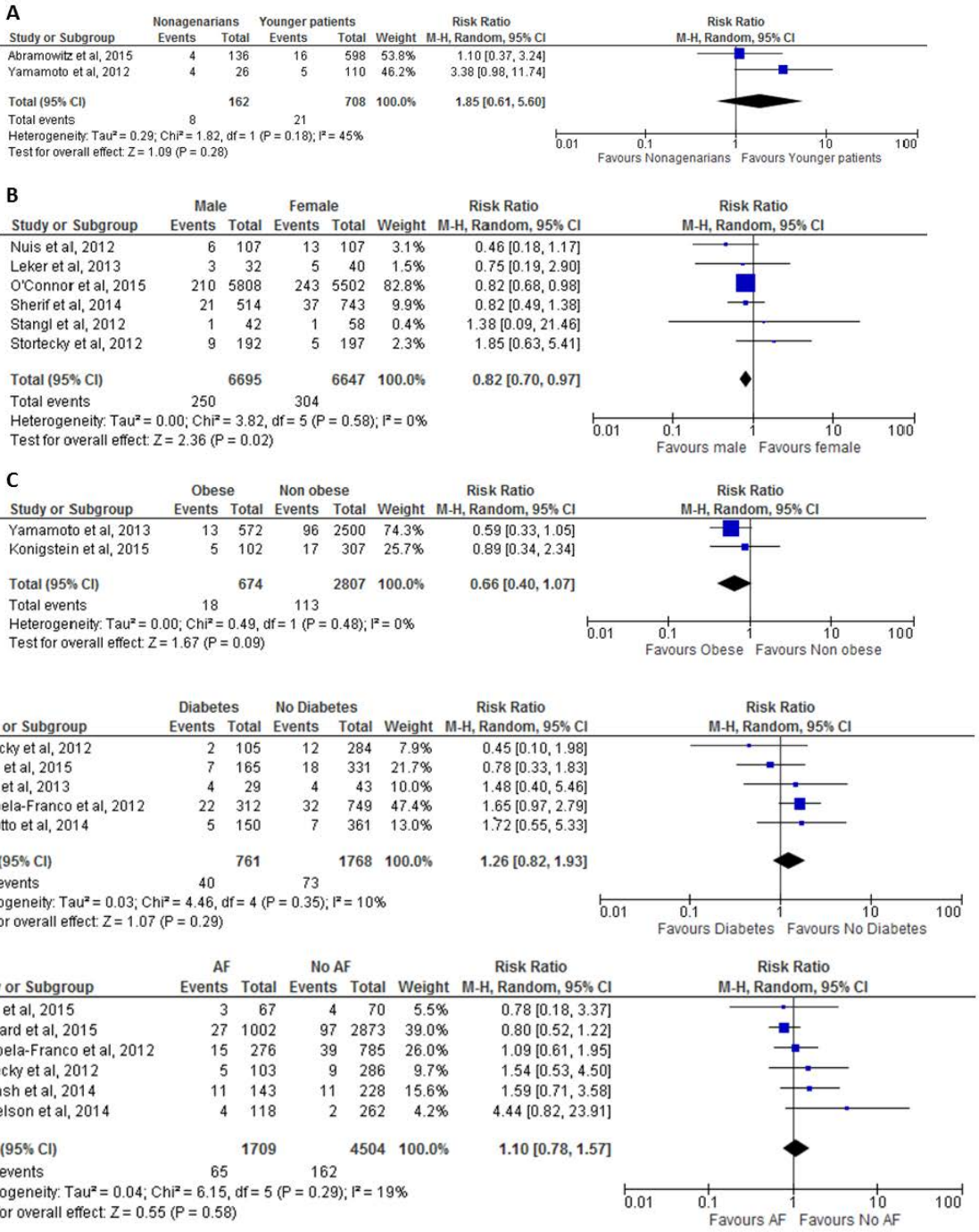

F

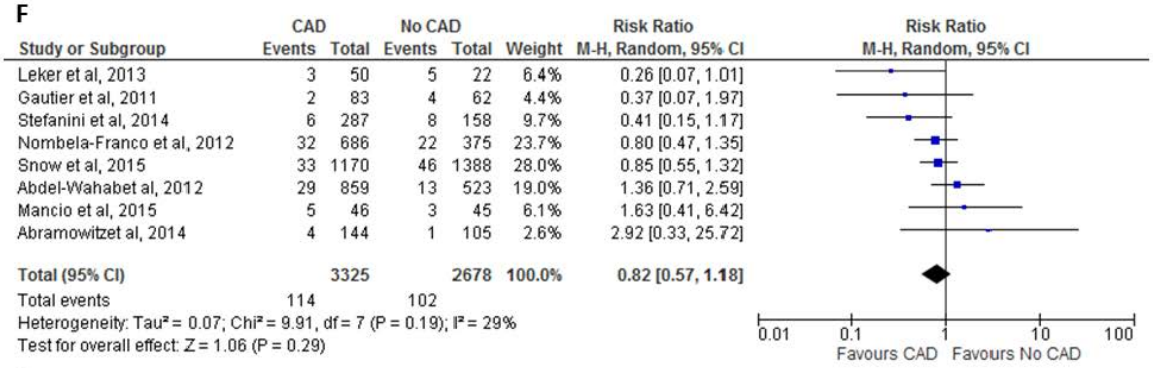

G

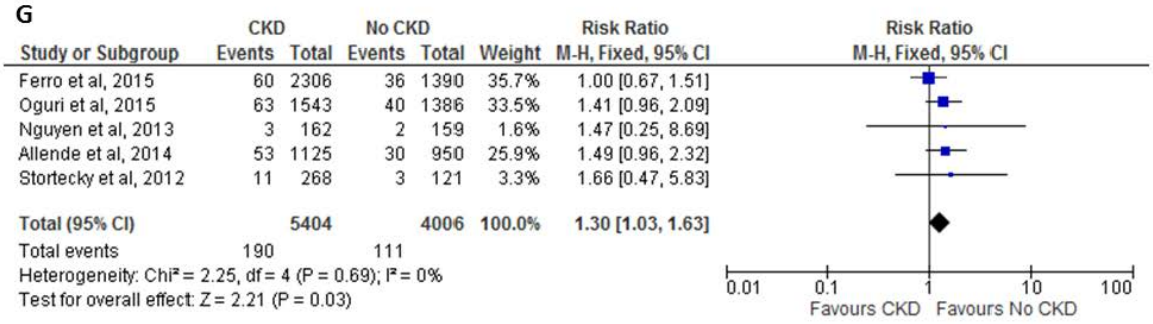

H

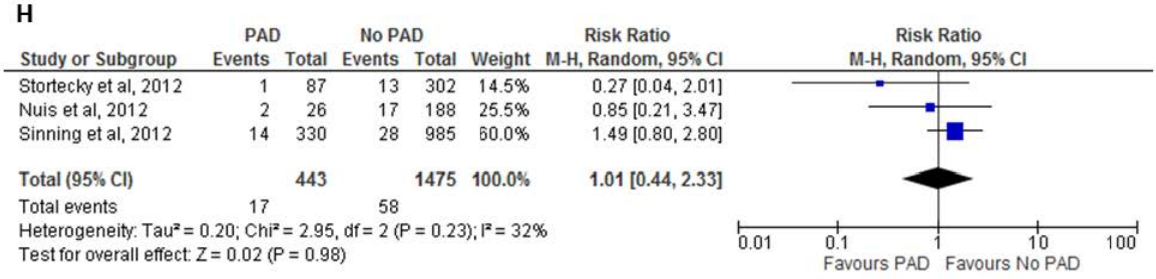

AF= Atrial fibrillation; CAD= Coronary artery disease; CKD= Chronic kidney disease; PAD= Peripheral artery disease; TAVR= Transcatheter aortic valve replacement.

Supplemental Figure 2- Sensitivity analysis for sex excluding small studies (n<200) using A) a random effect model and B) a fixed effect model.

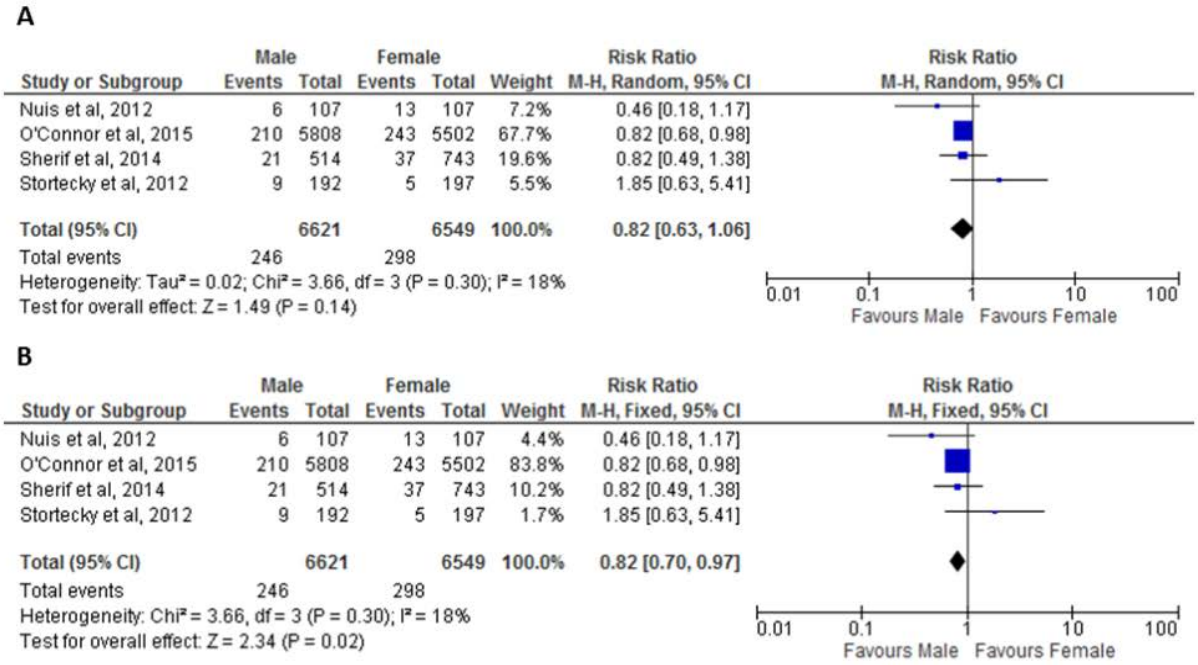

Supplemental Figure 3- Individual meta-analyses of procedural predictors of short-term cerebrovascular events after TAVR.

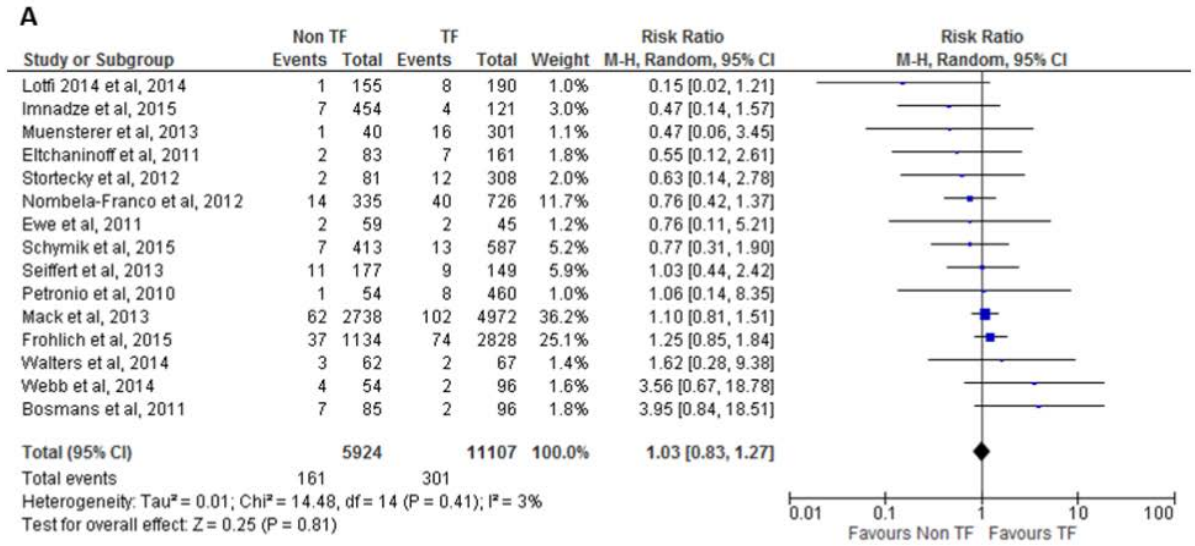

B

Study or Subgroup	MCV Events	MCV Total	ESV Events	ESV Total	Weight	Risk Ratio M-H, Random, 95% CI
Seiffert et al, 2013	1	45	19	281	1.8%	0.33 [0.05, 2.39]
Abdel-Wahab et al, 2014	3	117	7	121	3.9%	0.44 [0.12, 1.67]
Wenaweser et al, 2014	9	324	9	232	8.1%	0.72 [0.29, 1.78]
Ludman et al, 2015	50	1896	54	2031	38.6%	0.99 [0.68, 1.45]
Wenaweser et al, 2011	6	130	3	70	3.7%	1.08 [0.28, 4.18]
Swedish Report, 2013	2	122	1	87	1.2%	1.43 [0.13, 15.48]
Collas et al, 2015	25	401	19	460	18.7%	1.51 [0.84, 2.70]
Sabaté et al, 2013	20	610	17	806	15.8%	1.55 [0.82, 2.94]
Kasel et al, 2014	6	50	3	50	3.9%	2.00 [0.53, 7.56]
Chieffo et al, 2013	6	204	2	204	2.7%	3.00 [0.61, 14.69]
Watanabe et al, 2013	4	150	1	170	1.5%	4.53 [0.51, 40.11]
Total (95% CI)		**4049**		**4512**	**100.0%**	**1.16 [0.89, 1.52]**
Total events	132		135			

Heterogeneity: Tau² = 0.01; Chi² = 10.46, df = 10 (P = 0.40); I² = 4%
Test for overall effect: Z = 1.12 (P = 0.26)

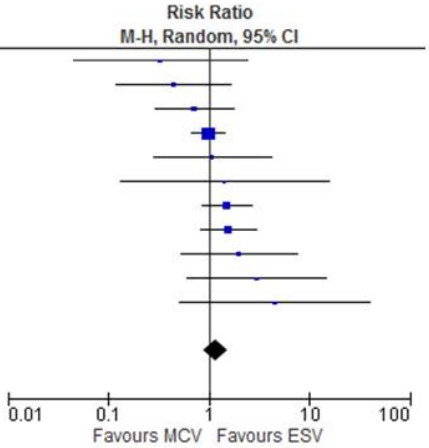

C

Study or Subgroup	First half Events	First half Total	Second half Events	Second half Total	Weight	Risk Ratio M-H, Random, 95% CI
Lange et al, 2012	11	210	8	210	10.8%	1.38 [0.56, 3.35]
Nombela-Franco et al, 2012	33	532	21	529	30.0%	1.56 [0.92, 2.66]
Ludman et al, 2015	56	1688	48	2285	59.2%	1.58 [1.08, 2.31]
Total (95% CI)		**2430**		**3024**	**100.0%**	**1.55 [1.16, 2.08]**
Total events	100		77			

Heterogeneity: Tau² = 0.00; Chi² = 0.08, df = 2 (P = 0.96); I² = 0%
Test for overall effect: Z = 2.94 (P = 0.003)

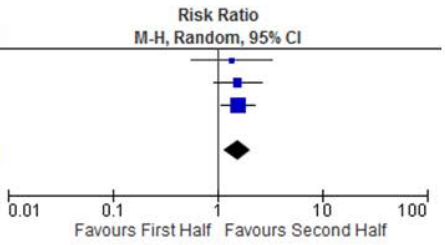

D

Study or Subgroup	TV-in-TV Events	TV-in-TV Total	No TV-in-TV Events	No TV-in-TV Total	Weight	Risk Ratio M-H, Random, 95% CI
Nuis et al, 2012	1	11	18	203	20.2%	1.03 [0.15, 6.99]
Makkar et al, 2013	3	63	93	2491	59.0%	1.28 [0.42, 3.92]
Stortecky et al, 2012	1	7	13	382	20.8%	4.20 [0.63, 27.83]
Total (95% CI)		**81**		**3076**	**100.0%**	**1.56 [0.66, 3.70]**
Total events	5		124			

Heterogeneity: Tau² = 0.00; Chi² = 1.42, df = 2 (P = 0.49); I² = 0%
Test for overall effect: Z = 1.02 (P = 0.31)

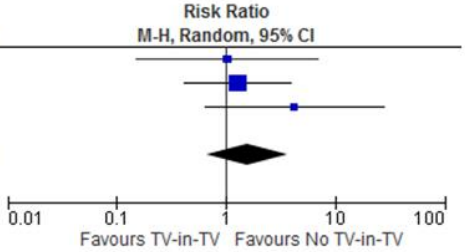

E

Study or Subgroup	Embolization/Migration Events	Embolization/Migration Total	No Embolization/Migration Events	No Embolization/Migration Total	Weight	Risk Ratio M-H, Random, 95% CI
Nuis et al, 2012	1	20	18	194	17.5%	0.54 [0.08, 3.83]
Geisbusch et al, 2010	3	21	13	191	39.1%	2.10 [0.65, 6.77]
Makkar et al, 2013	3	26	93	2528	43.4%	3.14 [1.06, 9.26]
Total (95% CI)		**67**		**2913**	**100.0%**	**1.97 [0.81, 4.77]**
Total events	7		124			

Heterogeneity: Tau² = 0.16; Chi² = 2.71, df = 2 (P = 0.26); I² = 26%
Test for overall effect: Z = 1.50 (P = 0.13)

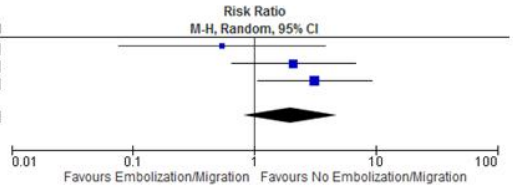

F

Study or Subgroup	BPD Events	BPD Total	No BPD Events	No BPD Total	Weight	Risk Ratio M-H, Random, 95% CI
Nuis et al, 2012	1	35	18	179	3.8%	0.28 [0.04, 2.06]
Watanabe et al, 2015	1	49	9	421	3.6%	0.95 [0.12, 7.38]
Stundl et al, 2015	2	85	3	141	4.7%	1.11 [0.19, 6.48]
Barbanti et al, 2014	8	272	27	1104	24.5%	1.20 [0.55, 2.62]
Hahn et al, 2014	13	264	63	1871	43.7%	1.46 [0.82, 2.62]
Stortecky et al, 2012	7	108	7	281	14.2%	2.60 [0.93, 7.24]
Lasa et al, 2014	2	24	4	133	5.5%	2.77 [0.54, 14.30]
Total (95% CI)		**837**		**4130**	**100.0%**	**1.43 [0.97, 2.10]**
Total events	34		131			

Heterogeneity: Tau² = 0.00; Chi² = 5.06, df = 6 (P = 0.54); I² = 0%
Test for overall effect: Z = 1.82 (P = 0.07)

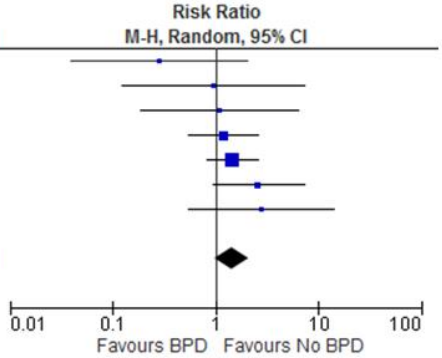

G

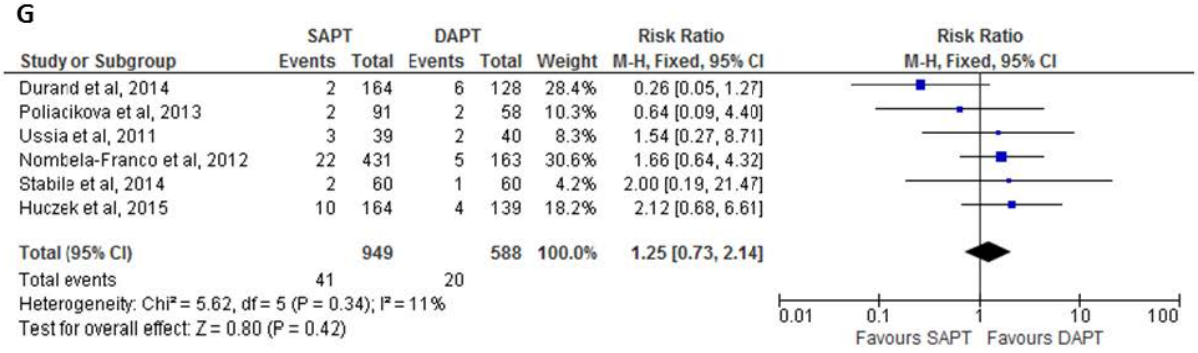

H

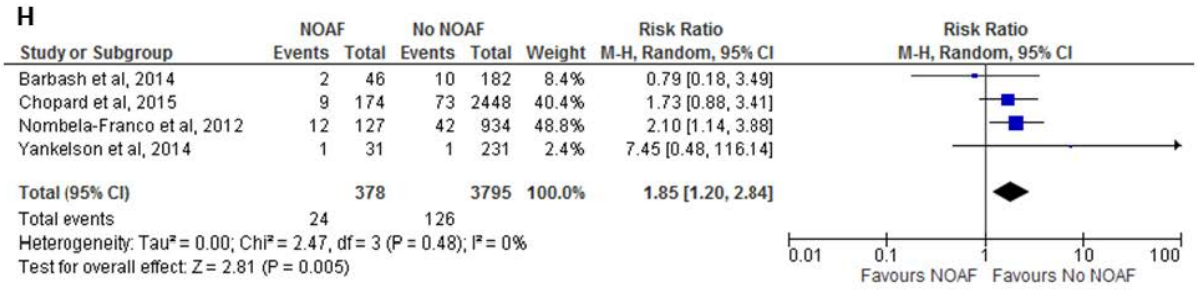

BPD=Balloon post-dilation; DAPT=Dual antiplatelet therapy; ESV=Edwards-Sapien valve; MCV=Medtronic Corevalve; NOAF=New-onset atrial fibrillation; SAPT= Single antiplatelet therapy; TAVR= Transcatheter aortic valve replacement; TF= Transfemoral; TVE/M= Transcatheter valve embolization or migration; TV-in-TV= Transcatheter valve within a transcatheter valve.

Supplemental online references.

1. Ludman PF, Moat N, de Belder MA et al. Transcatheter Aortic Valve Implantation in the United Kingdom: Temporal Trends, Predictors of Outcome, and 6-Year Follow-Up: A Report From the UK Transcatheter Aortic Valve Implantation (TAVI) Registry, 2007 to 2012. Circulation 2015;131:1181-90.

2. Stortecky S, Windecker S, Pilgrim T et al. Cerebrovascular accidents complicating transcatheter aortic valve implantation: frequency, timing and impact on outcomes. EuroIntervention 2012;8:62-70.

3. Nombela-Franco L, Webb JG, de Jaegere PP et al. Timing, predictive factors, and prognostic value of cerebrovascular events in a large cohort of patients undergoing transcatheter aortic valve implantation. Circulation 2012;126:3041-53.

4. Nuis RJ, Van Mieghem NM, Schultz CJ et al. Frequency and causes of stroke during or after transcatheter aortic valve implantation. Am J Cardiol 2012;109:1637-43.

5. Leker RR, Eichel R, Verber A, Cohen JE, Lotan C, Danenberg HD. Stroke complicating transcatheter aortic valve implantation: Incidence, risk factors and outcome. Int J Stroke 2013;8:235-239.

6. Stangl V, Baldenhofer G, Knebel F et al. Impact of gender on three-month outcome and left ventricular remodeling after transfemoral transcatheter aortic valve implantation. Am J Cardiol 2012;110:884-90.

7. O'Connor SA, Morice MC, Gilard M et al. Revisiting Sex Equality With Transcatheter Aortic Valve Replacement Outcomes: A Collaborative, Patient-Level Meta-Analysis of 11,310 Patients. J Am Coll Cardiol 2015;66:221-8.

8. Sherif MA, Zahn R, Gerckens U et al. Effect of gender differences on 1-year mortality after transcatheter aortic valve implantation for severe aortic stenosis: Results from a multicenter real-world registry. Clin Res Cardiol 2014;103:613-620.

9. Abramowitz Y, Chakravarty T, Jilaihawi H et al. Comparison of Outcomes of Transcatheter Aortic Valve Implantation in Patients ≥90 Years Versus <90 Years. Am J Cardiol 2015;116:1110-1115.

10. Yamamoto M, Meguro K, Mouillet G et al. Comparison of effectiveness and safety of transcatheter aortic valve implantation in patients aged >/=90 years versus <90 years. Am J Cardiol 2012;110:1156-63.

11. Konigstein M, Havakuk O, Arbel Y et al. The obesity paradox in patients undergoing transcatheter aortic valve implantation. Clin Cardiol 2015;38:76-81.

12. Yamamoto M, Mouillet G, Oguri A et al. Effect of body mass index on 30- and 365-day complication and survival rates of transcatheter aortic valve implantation (from the French aortic national corevalve and edwards 2 [FRANCE 2] registry). Am J Cardiol 2013;112:1932-1937.

13. Conrotto F, D'Ascenzo F, Giordana F et al. Impact of diabetes mellitus on early and midterm outcomes after transcatheter aortic valve implantation (from a multicenter registry). Am J Cardiol 2014;113:529-34.

14. Minha S, Magalhaes MA, Barbash IM et al. The impact of diabetes mellitus on outcome of patients undergoing transcatheter aortic valve replacement. IJC Metabolic and Endocrine 2015;9:54-60.

15. Barbash IM, Minha S, Ben-Dor I et al. Predictors and clinical implications of atrial fibrillation in patients with severe aortic stenosis undergoing transcatheter aortic valve implantation. Catheter Cardiovasc Interv 2015;85:468-77.

16. Chopard R, Teiger E, Meneveau N et al. Baseline Characteristics and Prognostic Implications of Pre-Existing and New-Onset Atrial Fibrillation After Transcatheter Aortic Valve Implantation: Results From the FRANCE-2 Registry. JACC Cardiovasc Interv 2015;8:1346-1355.

17. Maan A, Heist EK, Passeri J et al. Impact of atrial fibrillation on outcomes in patients who underwent transcatheter aortic valve replacement. Am J Cardiol 2015;115:220-6.

18. Yankelson L, Steinvil A, Gershovitz L et al. Atrial fibrillation, stroke, and mortality rates after transcatheter aortic valve implantation. Am J Cardiol 2014;114:1861-6.

19. Abdel-Wahab M, Zahn R, Horack M et al. Transcatheter aortic valve implantation in patients with and without concomitant coronary artery disease: comparison of characteristics and early outcome in the German multicenter TAVI registry. Clin Res Cardiol 2012;101:973-81.

20. Abramowitz Y, Banai S, Katz G et al. Comparison of early and late outcomes of TAVI alone compared to TAVI plus PCI in aortic stenosis patients with and without coronary artery disease. Catheter Cardiovasc Interv 2014;83:649-654.

21. Gautier M, Pepin M, Himbert D et al. Impact of coronary artery disease on indications for transcatheter aortic valve implantation and on procedural outcomes. EuroIntervention 2011;7:549-555.

22. Mancio J, Fontes-Carvalho R, Oliveira M et al. Coronary Artery Disease and Symptomatic Severe Aortic Valve Stenosis: Clinical Outcomes after Transcatheter Aortic Valve Implantation. Front Cardiovasc Med 2015;2:18.

23. Snow TM, Ludman P, Banya W et al. Management of concomitant coronary artery disease in patients undergoing transcatheter aortic valve implantation: The United Kingdom TAVI Registry. Int J Cardiol 2015;199:253-260.

24. Stefanini GG, Stortecky S, Cao D et al. Coronary artery disease severity and aortic stenosis: clinical outcomes according to SYNTAX score in patients undergoing transcatheter aortic valve implantation. Eur Heart J 2014;35:2530-40.

25. Allende R, Webb JG, Munoz-Garcia AJ et al. Advanced chronic kidney disease in patients undergoing transcatheter aortic valve implantation: insights on clinical outcomes and prognostic markers from a large cohort of patients. Eur Heart J 2014;35:2685-96.

26. Ferro CJ, Chue CD, De Belder MA et al. Impact of renal function on survival after transcatheter aortic valve implantation (TAVI): An analysis of the UK TAVI registry. Heart 2015;101:546-552.

27. Nguyen TC, Babaliaros VC, Razavi SA et al. Impact of varying degrees of renal dysfunction on transcatheter and surgical aortic valve replacement. J Thorac Cardiovasc Surg 2013;146:1399-406.

28. Oguri A, Yamamoto M, Mouillet G et al. Impact of chronic kidney disease on the outcomes of transcatheter aortic valve implantation: results from the FRANCE 2 registry. EuroIntervention 2015;10:e1-9.

29. Sinning JM, Horack M, Grube E et al. The impact of peripheral arterial disease on early outcome after transcatheter aortic valve implantation: Results from the German Transcatheter Aortic Valve Interventions Registry. Am Heart J 2012;164:102-110.e1.

30. Bosmans JM, Kefer J, De Bruyne B et al. Procedural, 30-day and one year outcome following corevalve or edwards transcatheter aortic valve implantation: Results of the belgian national registry. Interact Cardiovasc Thorac Surg 2011;12:762-767.

31. Eltchaninoff H, Prat A, Gilard M et al. Transcatheter aortic valve implantation: Early results of the FRANCE (FRench Aortic National CoreValve and Edwards) registry. Eur Heart J 2011;32:191-197.

32. Ewe SH, Delgado V, Ng AC et al. Outcomes after transcatheter aortic valve implantation: transfemoral versus transapical approach. Ann Thorac Surg 2011;92:1244-51.

33. Fröhlich GM, Baxter PD, Malkin CJ et al. Comparative Survival after Transapical, Direct Aortic, and Subclavian Transcatheter Aortic Valve Implantation (Data from the UK TAVI Registry). Am J Cardiol 2015;116:1555-1559.

34. Imnadze G, Franz N, Hofmann S et al. Benefits of Best for Groin Strategy Leading to a Transapical TAVI Dominance. Thorac Cardiovasc Surg 2015;63:487-492.

35. Lotfi S, Dohmen G, Gotzenich A et al. Midterm outcomes after transcatheter aortic valve implantation. Innovations (Phila) 2014;9:343-7.

36. Mack MJ, Brennan JM, Brindis R et al. Outcomes following transcatheter aortic valve replacement in the United States. JAMA 2013;310:2069-2077.

37. Muensterer A, Mazzitelli D, Ruge H et al. Safety and efficacy of the subclavian access route for TAVI in cases of missing transfemoral access. Clin Res Cardiol 2013;102:627-636.

38. Petronio AS, De Carlo M, Bedogni F et al. Safety and efficacy of the subclavian approach for transcatheter aortic valve implantation with the CoreValve revalving system. Circ Cardiovasc Interv 2010;3:359-366.

39. Schymik G, Wurth A, Bramlage P et al. Long-term results of transapical versus transfemoral TAVI in a real world population of 1000 patients with severe symptomatic aortic stenosis. Circ Cardiovasc Interv 2015;8.

40. Seiffert M, Schnabel R, Conradi L et al. Predictors and outcomes after transcatheter aortic valve implantation using different approaches according to the valve academic research consortium definitions. Catheter Cardiovasc Interv 2013;82:640-52.

41. Walters DL, Sinhal A, Baron D et al. Initial experience with the balloon expandable Edwards-SAPIEN Transcatheter Heart Valve in Australia and New Zealand: The SOURCE ANZ registry: Outcomes at 30 days and one year. Int J Cardiol 2014;170:406-412.

42. Webb J, Gerosa G, Lefevre T et al. Multicenter evaluation of a next-generation balloon-expandable transcatheter aortic valve. J Am Coll Cardiol 2014;64:2235-43.

43. Abdel-Wahab M, Mehilli J, Frerker C et al. Comparison of balloon-expandable vs self-expandable valves in patients undergoing transcatheter aortic valve replacement: the CHOICE randomized clinical trial. JAMA 2014;311:1503-14.

44. TAVI annual report 2011. Scand Cardiovas J 2013;47:95-102.

45. Chieffo A, Buchanan GL, Van Mieghem NM et al. Transcatheter aortic valve implantation with the Edwards SAPIEN versus the Medtronic CoreValve Revalving system devices: a multicenter collaborative study: the PRAGMATIC Plus Initiative (Pooled-RotterdAm-Milano-Toulouse In Collaboration). J Am Coll Cardiol 2013;61:830-6.

46. Collas VM, Dubois C, Legrand V et al. Midterm clinical outcome following Edwards SAPIEN or Medtronic Corevalve transcatheter aortic valve implantation (TAVI): Results of the Belgian TAVI registry. Catheter Cardiovasc Interv 2015;86:528-535.

47. Kasel AM, Cassese S, Ischinger T et al. A prospective, non-randomized comparison of SAPIEN XT and CoreValve implantation in two sequential cohorts of patients with severe aortic stenosis. Am J Cardiovasc Dis 2014;4:87-99.

48. Sabate M, Canovas S, Garcia E et al. In-hospital and mid-term predictors of mortality after transcatheter aortic valve implantation: data from the TAVI National Registry 2010-2011. Rev Esp Cardiol 2013;66:949-58.

49. Watanabe Y, Hayashida K, Yamamoto M et al. Transfemoral aortic valve implantation in patients with an annulus dimension suitable for either the Edwards valve or the CoreValve. Am J Cardiol 2013;112:707-13.

50. Wenaweser P, Pilgrim T, Roth N et al. Clinical outcome and predictors for adverse events after transcatheter aortic valve implantation with the use of different devices and access routes. Am Heart J 2011;161:1114-24.

51. Wenaweser P, Stortecky S, Heg D et al. Short-term clinical outcomes among patients undergoing transcatheter aortic valve implantation in Switzerland: The Swiss TAVI registry. EuroIntervention 2014;10:982-989.

52. Lange R, Bleiziffer S, Mazzitelli D et al. Improvements in transcatheter aortic valve implantation outcomes in lower surgical risk patients: a glimpse into the future. J Am Coll Cardiol 2012;59:280-7.

53. Makkar RR, Jilaihawi H, Chakravarty T et al. Determinants and outcomes of acute transcatheter valve-in-valve therapy or embolization: a study of multiple valve implants in the

U.S. PARTNER trial (Placement of AoRTic TraNscathetER Valve Trial Edwards SAPIEN Transcatheter Heart Valve). J Am Coll Cardiol 2013;62:418-30.

54. Geisbusch S, Bleiziffer S, Mazzitelli D, Ruge H, Bauernschmitt R, Lange R. Incidence and management of CoreValve dislocation during transcatheter aortic valve implantation. Circ Cardiovasc Interv 2010;3:531-6.

55. Barbanti M, Petronio AS, Capodanno D et al. Impact of balloon post-dilation on clinical outcomes after transcatheter aortic valve replacement with the self-expanding CoreValve prosthesis. JACC Cardiovasc Interv 2014;7:1014-21.

56. Hahn RT, Pibarot P, Webb J et al. Outcomes with post-dilation following transcatheter aortic valve replacement: the PARTNER I trial (placement of aortic transcatheter valve). JACC Cardiovasc Interv 2014;7:781-9.

57. Lasa G, Gaviria K, Sanmartin JC, Telleria M, Larman M. Postdilatation for treatment of perivalvular aortic regurgitation after transcatheter aortic valve implantation. Catheter Cardiovasc Interv 2014;83:E112-8.

58. Stundl A, Rademacher MC, Descoups C et al. Balloon post-dilation and valve-in-valve implantation for the reduction of paravalvular leakage with use of the self-expanding CoreValve prosthesis. EuroIntervention 2015;11.

59. Watanabe Y, Hayashida K, Lefèvre T et al. Is postdilatation useful after implantation of the Edwards valve? Catheter Cardiovasc Interv 2015;85:667-676.

60. Durand E, Blanchard D, Chassaing S et al. Comparison of two antiplatelet therapy strategies in patients undergoing transcatheter aortic valve implantation. Am J Cardiol 2014;113:355-60.

61. Huczek Z, Kochman J, Grygier M et al. Pre-procedural dual antiplatelet therapy and bleeding events following transcatheter aortic valve implantation (TAVI). Thromb Res 2015;136:112-117.

62. Poliacikova P, Cockburn J, De Belder A, Trivedi U, Hildick-Smith D. Antiplatelet and antithrombotic treatment after transcatheter aortic valve implantation - Comparison of regimes. J Invasive Cardiol 2013;25:544-548.

63. Stabile E, Pucciarelli A, Cota L et al. SAT-TAVI (single antiplatelet therapy for TAVI) study: A pilot randomized study comparing double to single antiplatelet therapy for transcatheter aortic valve implantation. Int J Cardiol 2014;174:624-627.

64. Ussia GP, Scarabelli M, Mul M et al. Dual antiplatelet therapy versus aspirin alone in patients undergoing transcatheter aortic valve implantation. Am J Cardiol 2011;108:1772-1776.

Annexe 3

Appendice complémentaire de "Conduction Disturbances After Transcatheter Aortic Valve Replacement: Current Status and Future Perspectives."

SUPPLEMENTAL MATERIAL

Auffret et al. Conductions disturbances post-TAVR

Supplemental Tables

Supplemental Table 1- Predictors of new-onset left bundle branch block following transcatheter aortic valve replacement among studies with a multivariable analysis			
Author, [Online ref], n of patients	**Valve type (%)**	**Incidence, n (%)**	**Multivariable predictors: OR (95% CI)**
Aktug et al,[1], n=139	Edwards SAPIEN/SAPIEN XT (52) Medtronic CoreValve (48)	40 (29)	Depth of implantation: 1.15 per mm (1.004-1.31)
Bernardi et al, [2], n=761	Medtronic CoreValve (76) Edwards SAPIEN XT (24)	268 (35.2)	Medtronic CoreValve: 2.9 (1.8-4.7)* Balloon pre-dilation: 1.8 (1.2-2.6)*
Boerlage-Van Dijk et al, [3], n=121	Medtronic CoreValve (100)	47 (39)	26 mm valve size (vs. 23 mm): 4.1 (1.3-12.3) Depth of implantation: 1.3 per mm (1.1-1.6)
Carrabba et al,[4] , n=92	Medtronic CoreValve (100)	34 (37)	Baseline LVEDV: 0.79/mL (0.62-1.2)
Franzoni et al, [5], n=238	Edwards SAPIEN/SAPIEN XT (63) Medtronic CoreValve (37)	63 (26.5)	Medtronic CoreValve: 7.2 (2.9-17.4)
Hein-Rothweiler et al, [6], n=225	Edwards SAPIEN XT (100)	52 (23.1)	First-degree AV block: 3.9 (1.6-9.6) Annular calcification: 3.0 (1.4-6.7) Area cover index: 1.8/% (1.3-2.7) LCA to annulus distance: 0.65 per mm (0.44-0.96)
Houthuizen et al, [7], n=679	Medtronic CoreValve (57) Edwards SAPIEN/SAPIEN XT (43)	233 (34.3)	Medtronic CoreValve: 8.51 (5.53-13.11) Diabetes mellitus: 1.52 (1.01-2.29)
Katsanos et al, [8], n=94	Edwards SAPIEN/SAPIEN XT (100)	15 (16)	Overexpansion > 15% of native annulus area: 5.3 (1.4-19.9) Depth of implantation: 1.4 per mm (1.1-1.8)
Khawaja et al, [9], n=185	Medtronic CoreValve (100)	105 (56.8)	Baseline RBBB: 0.25 (0.13-0.49) Valve-in-Valve: 0.05 (0.01-0.29)
Nishiyama et al, [10], n=90	Edwards SAPIEN XT (100)	20 (22)	Valve area / LVOT area: 3.0 (1.03–8.7)
Schymik et al, [11], n=634	Edwards SAPIEN/SAPIEN XT (81) Medtronic CoreValve (19)	197 (31.1)	Medtronic CoreValve: 2.5 (1.7-3.8)* Female gender: 1.57 (1.08-2.3)* Previous CABG: 1.6 (1.0-2.7)*
Urena et al, [12], n=202	Edwards SAPIEN/SAPIEN XT (100)	61 (30.2)	Baseline QRS duration: 1.24 per 4ms (1.01-1.51)* Prosthesis ventricular depth: 1.37/ per mm (1.06-1.77)*
Urena et al, [13], n=668	Edwards SAPIEN/SAPIEN XT/ SAPIEN 3 (100)	128 (19.2)	Transapical approach: 1.9 (1.15-3.16)* 29 mm valve size: 3.12 (1.22-7.97)*
Van der Boon et al,[14], n=549	Edwards SAPIEN/SAPIEN XT (50.5)	185 (33.7)	Depth of implantation: 1.16 per mm (1.10-1.24)
	Medtronic CoreValve (49.5)		

* Predictors of new-onset persistent left bundle branch block.

AV : atrioventricular ; CABG : coronary artery bypass graft ; LCA : left coronary artery ; LVEDV : left ventricular end-diastolic volume ; LVOT : left ventricular outflow tract ; RBBB : right bundle branch block

Supplemental Table 2– Impact of new-onset left bundle branch block on mortality among studies with a multivariable analysis				
Author, [Online ref], n of patients	**Valve type (%)**	**Mortality rate at follow-up**		**Multivariable OR/HR (95% CI)**
		LBBB (%)	No-LBBB (%)	
Carrabba et al, [4], n=92	Medtronic CoreValve (100)	11.8	12.1	0.98 (0.27-3.61)
Houthuizen et al, [7], n=679	Medtronic CoreValve (57) Edwards SAPIEN/SAPIEN XT (43)	37.8	24	1.54 (1.12-2.10)
Schymik et al, [11], n=634	Edwards SAPIEN/SAPIEN XT (81) Medtronic CoreValve (19)	20.8	13	1.84 (1.35-2.02)
Urena et al, [13], n=668	Edwards SAPIEN/SAPIEN XT (100)	27.8	28.4	0.87 (0.55-1.37)

CI: confidence interval; HR: hazard-ratio; LBBB: left bundle branch block; OR: odds-ratio.

Supplemental Table 3 – Impact of new-onset left bundle branch block on the occurrence of advanced atrioventricular block or permanent pacemaker implantation among studies with a multivariable analysis				
Author, [Online ref], n of patients	**Valve type (%)**	**HAVB/PPI rate at follow-up**		**Multivariable OR/HR (95% CI)**
		LBBB (%)	No-LBBB (%)	
Akin et al, [15], n=45*	Medtronic CoreValve (100)	74	17	24.9 (1.6-392.6)
Schymik et al, [11], n=634	Edwards SAPIEN/SAPIEN XT (81) Medtronic CoreValve (19)	14.2	9.4	NS
Urena et al, [13], n=668	Edwards SAPIEN/SAPIEN XT (100)	13.4	3.0	4.29 (2.03-9.07)

*Rates of pacemaker at 7-day post-TAVR.

Abbreviations as in supplemental Table 2

Supplemental Table 4- Predictors of permanent pacemaker implantation following transcatheter aortic valve replacement among studies with a multivariable analysis			
Author, [Online ref], n of patients	**Valve type (%)**	**Incidence, n (%)**	**Multivariable predictors: OR/HR (95% CI)**
Abramowitz et al,[16] , n=606	Edwards SAPIEN/SAPIEN XT (70) Edwards SAPIEN 3 (22) Medtronic CoreValve (8)	70 (11.6)	Severe mitral annular calcification: 2.8 (1.1-7.5) Baseline RBBB: 6.9 (3.3-14.6) Medtronic CoreValve: 4.9 (1.4-16.9)
Akin et al, [15], n=45	Medtronic CoreValve (100)	23 (51)	New-onset LBBB (within 60 min of TAVR): 24.9 (1.6-392.6) First-degree AV block > 200 ms (within 60 min of TAVR): 11.4 (1.1-97.6) QRS duration > 120 ms (within 60 min of TAVR): 14.3 (1.5-135.9)
Al-Azzam et al, [17], n=300	Edwards SAPIEN/SAPIEN XT (66) Medtronic CoreValve (19) Edwards SAPIEN 3 (15)	59 (19.7)	Baseline RBBB: 4.5 (1.6-8.6) Medtronic CoreValve: 4.1 (1.5-11)
Bagur et al, [18], n=411	Edwards SAPIEN/SAPIEN XT (100)	30 (7.3)	Baseline RBBB: 8.6 (3.1-23.7)
Bleiziffer et al,[19] , n=159	Medtronic CoreValve (78) Edwards SAPIEN (22)	35 (22)	Intraoperative AV block: 4.8 (2.0-11.9)
Boerlage-Van Dijk et al,[3], n=105	Medtronic CoreValve (100)	23 (22)	Baseline RBBB: 8.5 (1.6-44.9) Mitral annular calcification: 1.3 (1.1-1.6)
Calvi et al, [20], n=162	Medtronic CoreValve (100)	42 (26)	Baseline RBBB: 16.5 (3.3-82.3)
D'Ancona et al,[21] , n=322	Edwards SAPIEN (100)	20 (6.2)	Age: 1.08 (0.9-1.1)
De Carlo et al, [22], n=275	Medtronic CoreValve (100)	66 (24)	Depth of implantation: 1.2 per mm (1.03-1.3) Baseline RBBB: 3.7 (1.5-9.2) Left anterior hemiblock: 2.3 (1.1-5.1) Longer PR interval: 1.02 per ms (1.0-1.04)
De Torres-Alba et al,[23] , n=162	Edwrads SAPIEN 3 (100)	31 (19.1)	Implantation height (% of stent in the aorta): 0.95 (0.91-0.99)
Erkapic et al,[24] , n=50	Medtronic CoreValve (72) Edwards SAPIEN (28)	17 (34)	Baseline RBBB: NR Medtronic CoreValve: NR
Fadahunsi et al, [25], n=9785	Edwards SAPIEN/SAPIEN XT (88) Medtronic CoreValve (12)	651 (6.7)	Age: 1.07/5years (1.01-1.2) Prior conduction defect:1.9 (1.6-2.3) Medtronic CoreValve: 7.6 (6.0-9.6)
Fraccaro et al, [26], n=64	Medtronic CoreValve (100)	25 (39)	Depth of implantation: 1.2 (1.01–1.4) Baseline RBBB: 6.1(1.0–36.5)
Fujita et al, [27], n=162	Edwards SAPIEN XT (61) Medtronic CoreValve (39)	16 (9.9)	Baseline RBBB: 12.6 (2.4-66.8) Left coronary cusp calcium volume > 209mm^3: 7.5 (1.5-36.1)
Gensas et al, [28], n=353	Medtronic CoreValve (86) Edwards SAPIEN XT (14)	89 (25.2)	Baseline RBBB: 4.4 (2.2-8.8) Medtronic CoreValve: 4.2 (1.6-11.5) Balloon pre-dilation: 1.8 (1.02-3.0)
Giustino et al, [29], n=947	Edwards SAPIEN/SAPIEN XT (53) Medtronic CoreValve (47)	164 (17.3)	Age: 1.08 per year (1.04-1.12) Male sex:1.7 (1.1-2.7) Body-mass index: 1.08 per unit (1.02-1.13) TF-TAVR: 0.5 (0.3-0.9) Medtronic CoreValve: 2.6 (1.6-4.3) Balloon post-dilation: 9.2 (5.5-15.5) Diameter cover index > 8 units: 3.2 (1.6-6.7)
Gonska et al, [30], n=283	Edwards SAPIEN 3 (100)	52 (18.4)	First degree AV block: 4.0 (1.7-9.1) Baseline RBBB: 4.6 (1.5-13.2)
Guetta et al, [31], n=70	Medtronic CoreValve (100)	25 (36)	Baseline RBBB: 42.9 (14.1-155.8) Depth of implantation (>6mm): 22.2 (5.2-95.6)
Hamdan et al, [32], n=73	Medtronic CoreValve (92) Medtronic Engager (8)	21 (29)	Membranous septum length: 1.43 (1.1-1.8) Calcification in basal septum: 4.9 (1.2-20.5) Difference between membranous septum length and depth of implantation: 1.39 (1.2-1.7)
Husser et al, [33], n=208	Edwards SAPIEN 3 (100)	34 (16)	Baseline RBBB: 12.0 (3.4-42.0) Atrial fibrillation: 4.0 (1.6-10.2) Heart rate on admission: 0.94 (0.91-0.98) Previous unspecific IVCD: 10.0 (1.6-61.1) COPD: 4.7 (1.5-14.4) Depth of implantation at the nonseptal side: 1.1 (1.06-1.13)
Katsanos et al, [8], n=94	Edwards SAPIEN/SAPIEN XT (100)	15 (16)	Overexpansion > 15% of native annulus area: 5.3 (1.4-19.9) Depth of implantation: 1.4 per mm (1.1-1.8)
Khawaja et al, [9], n=243	Medtronic CoreValve (100)	81 (33.3)	Perprocedural AV block: 6.3 (3.6-11.2) Balloon predilation: 2.7 (2.0-3.5) 29 mm valve size: 2.5 (1.2-5.1) Interventricular septum thickness: 1.18 (1.1-3.1)

			Prolonged baseline QRS duration: 3.5 (1.6-7.4)
Kim et al, [34], n=117	Medtronic CoreValve (100)	23 (19.7)	Depth of implantation: 1.3 (1.03-1.5) Perimeter stretching index: 1.5 (1.2-1.9)
Koos et al, [35], n=80	Medtronic CoreValve (72) Edwards SAPIEN (28)	17 (21)	Baseline RBBB Medtronic CoreValve
Lange et al,[36] , n=237	Medtronic CoreValve (100)	50 (21.1)	Baseline RBBB: 46.7 (8.8-249.0) Valvuloplasty balloon of 25mm (vs. 18/20 mm): 5.5 (1.0-29.0)
Latsios et al, [37], n=67	Medtronic CoreValve (100)	32 (47)	Male sex: 0.08 (0.01-0.48) LVEF: 0.92 (0.86-0.98) Device landing zone calcification (Agatston score): 1.06 (1.02-1.11)
Ledwoch et al, [38], n=1147	Medtronic CoreValve (100)	386 (33.7)	No prior valve surgery: 0.3 (0.1-0.8) Porcelain aorta : 1.6 (1.1-2.4) Medtronic CoreValve: 2.9 (1.7-4.7)
Lopez-Aguilera et al, [39], n=181	Medtronic CoreValve (100)	33 (25)	Baseline RBBB: 9.9 (2.3-42.9) Depth of implantation: 1.15 per mm (1.02-1.28)
Maan et al, [40], n=110	Edwards SAPIEN/SAPIEN XT (100)	31 (28.2)	Baseline RBBB: 4.9 (1.3-18.5) Valve size /LVOT diameter ratio (%): 1.06 (1.00-1.11)
Maeno et al, [41], n=240	Edwards SAPIEN 3 (100)	35 (14.6)	Baseline RBBB: 14.3 (5.0-40.9) Difference between membranous septal length and valve implantation: 1.7 (1.4-2.1) Membranous septum length: 0.6 (0.5-0.8) Non-coronary cusp-device landing zone calcification:1.04 (1.02-1.06)
Mauri et al, [42], n=229	Edwards SAPIEN 3 (100)	33 (14.4)	Baseline RBBB: 16.9 (3.0-95.5) LVOT calcification below the left coronary cusp>13.7 mm^3: 3.7 (1.3-10.6) LVOT calcification below the right coronary cusp>4.8 mm^3: 4.7 (1.6-14.1) Implantation depth > 25.5% ventricular part of the stent frame: 15.7 (5.7-43.5)
Mouillet et al,[43] , n=79	Medtronic CoreValve (100)	21 (27)	Post-TAVR QRS duration: NR (1.008-1.009)
Mouillet et al,[44], n=833	Medtronic CoreValve (100)	252 (30.3)	Baseline RBBB: 2.3 (1.7-3.1)
Munoz-Garcia et al, [45], n=174	Medtronic CoreValve (100)	48 (27.6)	Baseline RBBB: 3.5 (1.7-7.3)

			Depth of implantation: 1.2 (1.1-1.3) Use of the traditional delivery system (vs Accutrack): 27 (2.8-257)
Nazif et al, [46], n=1973	Edwards SAPIEN (100)	173 (8.8)	Baseline RBBB: 7.0 (4.9-10.1) Prosthesis diameter/LVOT diameter: 1.3 /0.1 increment (1.1-1.5) LVEDD: 0.68 per cm (0.53-0.87)
Nishiyama et al, [10], n=90	Edwards SAPIEN XT (100)	20 (22)	Valve area / LVOT area: 3.0 (1.03–8.7)
Ramazzina et al, [47], n=97	Medtronic CoreValve (61) Edwards SAPIEN (39)	35 (36)	Medtronic CoreValve: 25.7 (5.3-125.4) Atrial fibrillation: 0.13 (0.03-0.54) Diabetes mellitus: 0.16 (0.04-0.70)
Rodriguez-Olivares et al, [48], n=302	Medtronic CoreValve (67) Edwards SAPIEN XT (13) Boston Scientific Lotus (12) Edwards SAPIEN 3 (8)	68 (22.5)	Baseline RBBB: 2.9 (1.2-6.9) Newer-generation valves: 2.1 (1.0-4.5) LVOT oversizing: 1.03 per 1% (1.005-1.065) Depth of implantation: 1.2 per mm (1.09-1.3)
Roten et al, [49], n=67	Medtronic CoreValve (61) Edwards SAPIEN (39)	23 (34)	Baseline RBBB: 7.3 (2.4-22.2)
Saia et al, [50], n=60	Medtronic CoreValve (100)	17 (28.3)	Interventricular septum thickness: 0.52 (0.32-0.85) Depth of implantation: 1.4 (1.03-1.8)
Schroeter et al, [51], n=88	Medtronic CoreValve (100)	32 (36)	Age > 75 years: 4.6 (1.2-17.0) Valve oversizing > 4 mm: 2.2 (0.6-7.3) Atrial fibrillation: 5.2 (2.0-13.8) Pre-TAVR heart rate <65 per min: 2.9 (1.1-7.9)
Schymik et al, [11], n=634	Edwards SAPIEN/SAPIEN XT (81) Medtronic CoreValve (19)	69 (10.8)	Baseline RBBB: 6.2 (3.8-10.3) Permanent atrial fibrillation: 1.8 (1.1-2.6) Medtronic CoreValve: 2.4 (1.6-3.8)
Tarantini et al, [52], n=189	Edwards SAPIEN XT (85) Edwards SAPIEN 3 (15)	22 (11.6)	Edwards SAPIEN 3 (vs. SAPIEN XT): 7.5 (1.2-48.0)
Toutoutzas et al, [53], n=113	Medtronic CoreValve (100)	44 (38.9)	Depth of implantation: 1.5 (1.2-1.9) LVOT diameter/annulus diameter: 0.85 (0.77-0.92)
Urena et al, [13], n=668	Edwards SAPIEN/SAPIEN XT (100)	29 (4.3)	New-onset persistent LBBB: 4.29 (2.03-9.07)
Van der Boon et al, [14], n=549	Edwards SAPIEN/SAPIEN XT (50.5) Medtronic CoreValve (49.5)	73 (13.3)	Baseline RBBB: 7.2 (3.3-15.9)
Van Mieghem et al, [54], n=864	Boston Scientific Lotus (100)	259 (30.0)	Baseline RBBB: 3.3 (1.8-5.9) STS score: 1.03 (1.00-1.05)

			Diabetes mellitus:1.4 (1.01-2.0) Oversizing of the aortic annulus (% of the diameter): 1.02 (1.00-1.03)
Zaman et al, [55], n=93	Boston Scientific Lotus (100)	27 (28)	Baseline RBBB: 2.8 (1.1-7.0) Depth of implantation below the non-coronary cusp > 5 mm: 2.4 (1.0-5.7)

COPD: Chronic obstructive pulmonary disease; IVCD: intraventricular conduction disturbance; LBBB: left bundle branch block; LVEF: left ventricular ejection fraction; LVEDD: left ventricular end-diastolic diameter; TAVR: transcatheter aortic valve replacement. Other abbreviations as in Supplemental Table 1.

Supplemental Table 5 – Impact of permanent pacemaker implantation on mortality (studies with a multivariable analysis)

Author,[Online ref], n of patients	Valve type (%)	Mortality rate at follow-up		Multivariable OR/HR (95% CI)
		PPI (%)	No-PPI (%)	
Buellesfeld et al, [56], n=305	Medtronic CoreValve (87) Edwards SAPIEN/SAPIEN XT (13)	19.4	18.0	1.06 (0.60-1.84)
Carrabba et al, [4], n=92	Medtronic CoreValve (100)	NR	NR	0.74 (0.18-3.02)
Dizon et al, [57], n=2531	Edwards SAPIEN (100)	26.3	20.0	1.38 (1 .00-1.89)
Fadahunsi et al, [25], n=9785	Edwards SAPIEN/SAPIEN XT (88) Medtronic CoreValve (12)	24.1	19.6	1.31 (1.09-1.58)
Giustino et al, [29], n=1062	Edwards SAPIEN/SAPIEN XT (53) Medtronic CoreValve (47)	28.7	21.8	1.11 (0.74-1.67)
Urena et al, [58], n=1556	Edwards SAPIEN/SAPIEN XT (55) Medtronic CoreValve (45)	20.6	22.2	1.02 (0.74-1.42)

PPI: permanent pacemaker implantation. Other abbreviations as in Supplemental Table 2.

Supplemental Table 6 – Ongoing studies evaluating conduction disturbances post-TAVR and their management strategies.

Trials	Design	N	Interventions	Primary Endpoint
HESITATE (NCT02659137)	Prospective, single-center, non-randomized	100	EPS during the procedure Surface ECG:1 day before TAVR, 1 hour after TAVR, at discharge, at 6 weeks, at 6 months, at 12 months.	Presence of a conduction disturbance in the His-bundle on occurrence of a LBBB on surface ECG by registering the HV-time during the TAVR procedure. Evaluate the location of LBBB
NCT02559011	Prospective, single-center, non-randomized	100	Insertion of an implantable cardiac monitoring device (Medtronic REVEAL LinQ™) at least 4 weeks before the procedure. Interrogation of the device just prior to readmission for TAVI and thereafter at 1, 3, 6, and 12 months of follow-up	Establish the incidence of new onset atrial fibrillation and complete AV-block within 12 months after TAVI.
LBBB-TAVI NCT02482844	Prospective, multicenter, non-randomized	200	All TAVR patients with a NOP-LBBB observed beyond 24 hours after the procedure will be included and will benefit from an EPS. If HV delay exceed 70ms or in case of infra-hisian block, patients will undergo PPI. An implantable monitoring device will be implanted in other cases	Rate and timing of appearance of high-degree AVB post TAVR.
MARE NCT02153307	Prospective, multicenter, non-randomized	80	Patients with NOP-LBBB (of a duration of at least 48 h which persists at hospital discharge, at least 3 days and up to 15 days after the procedure) will receive an implantable loop recorder (Medtronic REVEAL LinQ™)	Rate and time of onset of high degree AVB, Incidence of arrhythmic events leading to a change in treatment or major adverse event
TAVISTIM NCT02337140	Prospective, non-randomized	165	EPS before and after TAVR. ECG monitoring for 24h post-TAVR. At 24 hours, implantation of a pacemaker (SorinGroup KORA DR) in AAI-Safe R mode in case of severe conduction disturbances. Repeated EPS at 24h in patients with NOP-LBBB. If HV > 70ms: PPI.	Confirm appropriate pacing indication in patients with conduction disorders after TAVR (i.e. more than 1% of ventricular pacing or at least one DDD mode switch in the memories within 2 months of the procedure; in non-implanted patients, the non-indication for pacing will be confirmed in the absence of clinical event and 24-hour Holter ECG recording abnormality)
PPM in TAVR NCT02994667	Prospective, single-center, non-randomized	50	Enrollment of all consecutive patients who undergo PPI for new conduction disturbances after TAVR. All pacemaker will be equipped of algorithms to minimize right ventricular pacing	Incidence of ventricular pacing at 90-day post-TAVR
NCT02700633	Retrospective, multicenter, non-randomized	4000	Comparison of patients undergoing PPI before discharge post-TAVR vs. patients not undergoing PPI before discharge post-TAVR.	Comparison of 30-day mortality between groups

AVB: Atrioventricular block; ECG: Electrocardiogram; EPS: Electrophysiological study; NOP-LBBB: New-onset persistent left bundle branch block; PPI: Pacemaker implantation; TAVR: Tanscatheter aortic valve replacement.

Supplemental Figure 1

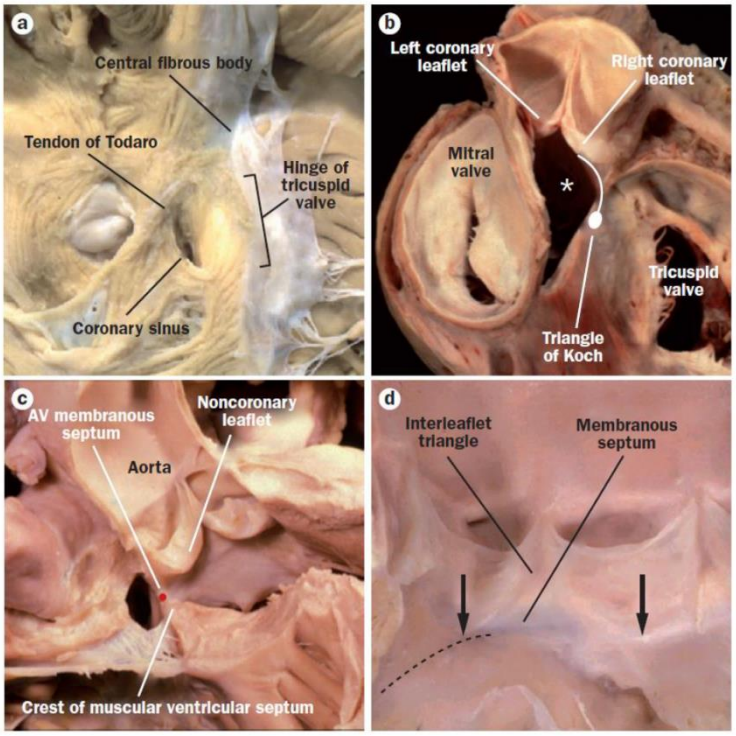

Figure legend

Anatomy and relationship between the aortic valvular complex and the atrioventricular conduction system.

a | A view of the right side of the atrial and ventricular septa, illustrating the landmarks of the triangle of Koch. The atrioventricular node is located at the apex of the triangle, and the bundle of His penetrates the central fibrous body. **b** | The course of the axis as it penetrates, created by removing the noncoronary sinus of the aortic root, which reveals the deep diverticulum (star) that interposes between the mitral valve and the ventricular septum. The location of the atrioventricular node (oval), and the course of the conduction axis (line emanating from the oval) are marked. **c** | The position of the bundle of His as it is sandwiched between the membranous and muscular parts of the ventricular septum (red circle), created by dissecting away the right ventricular outflow tract to reveal the posterior components of the aortic root. **d** | The opened aortic root viewed from the left ventricle. The basal attachments of the right and noncoronary leaflets of the aortic valve (arrows), with the location of the most-superior part of the left bundle branch as it originates from the branching component of the conduction axis (broken black line).

Reproduced from Van der Boon RM et al. Nat Rev Cardiol. 2012;9:454-463 with permission from the publisher.

Supplemental references

1. Aktug O, Dohmen G, Brehmer K, Koos R, Altiok E, Deserno V, Herpertz R, Autschbach R, Marx N, Hoffmann R. Incidence and predictors of left bundle branch block after transcatheter aortic valve implantation. *Int J Cardiol*. 2012;160:26-30
2. Bernardi FL, Ribeiro HB, Carvalho LA, Sarmento-Leite R, Mangione JA, Lemos PA, Abizaid A, Grube E, Rodes-Cabau J, de Brito FS, Jr. Direct transcatheter heart valve implantation versus implantation with balloon predilatation: Insights from the brazilian transcatheter aortic valve replacement registry. *Circ CardiovascInterv*. 2016;9 pii: e003605
3. Boerlage-Van Dijk K, Kooiman KM, Yong ZY, Wiegerinck EM, Damman P, Bouma BJ, Tijssen JG, Piek JJ, Knops RE, Baan J, Jr. Predictors and permanency of cardiac conduction disorders and necessity of pacing after transcatheter aortic valve implantation. *Pacing Clin Electrophysiol*. 2014;37:1520-1529
4. Carrabba N, Valenti R, Migliorini A, Marrani M, Cantini G, Parodi G, Dovellini EV, Antoniucci D. Impact on left ventricular function and remodeling and on 1-year outcome in patients with left bundle branch block after transcatheter aortic valve implantation. *Am J Cardiol*. 2015;116:125-131
5. Franzoni I, Latib A, Maisano F, Costopoulos C, Testa L, Figini F, Giannini F, Basavarajaiah S, Mussardo M, Slavich M, Taramasso M, Cioni M, Longoni M, Ferrarello S, Radinovic A, Sala S, Ajello S, Sticchi A, Giglio M, Agricola E, Chieffo A, Montorfano M, Alfieri O, Colombo A. Comparison of incidence and predictors of left bundle branch block after transcatheter aortic valve implantation using the corevalve versus the edwards valve. *Am J Cardiol*. 2013;112:554-559
6. Hein-Rothweiler R, Jochheim D, Rizas K, Egger A, Theiss H, Bauer A, Massberg S, Mehilli J. Aortic annulus to left coronary distance as a predictor for persistent left bundle branch block after tavi. *Catheter Cardiovasc Interv*. 2017;89:E162-E168

7. Houthuizen P, Van Garsse LA, Poels TT, de Jaegere P, van der Boon RM, Swinkels BM, Ten Berg JM, van der Kley F, Schalij MJ, Baan J, Jr., Cocchieri R, Brueren GR, van Straten AH, den Heijer P, Bentala M, van Ommen V, Kluin J, Stella PR, Prins MH, Maessen JG, Prinzen FW. Left bundle-branch block induced by transcatheter aortic valve implantation increases risk of death. *Circulation.* 2012;126:720-728

8. Katsanos S, van Rosendael P, Kamperidis V, van der Kley F, Joyce E, Debonnaire P, Karalis I, Bax JJ, Marsan NA, Delgado V. Insights into new-onset rhythm conduction disorders detected by multi-detector row computed tomography after transcatheter aortic valve implantation. *Am J Cardiol.* 2014;114:1556-1561

9. Khawaja MZ, Rajani R, Cook A, Khavandi A, Moynagh A, Chowdhary S, Spence MS, Brown S, Khan SQ, Walker N, Trivedi U, Hutchinson N, De Belder AJ, Moat N, Blackman DJ, Levy RD, Manoharan G, Roberts D, Khogali SS, Crean P, Brecker SJ, Baumbach A, Mullen M, Laborde JC, Hildick-Smith D. Permanent pacemaker insertion after corevalve transcatheter aortic valve implantation: Incidence and contributing factors (the uk corevalve collaborative). *Circulation.* 2011;123:951-960

10. Nishiyama T, Tanosaki S, Tanaka M, Yanagisawa R, Yashima F, Kimura T, Arai T, Tsuruta H, Murata M, Aizawa Y, Kohno T, Maekawa Y, Hayashida K, Takatsuki S, Fukuda K. Predictive factor and clinical consequence of left bundle-branch block after a transcatheter aortic valve implantation. *Int J Cardiol.* 2017;227:25-29

11. Schymik G, Tzamalis P, Bramlage P, Heimeshoff M, Wurth A, Wondraschek R, Gonska BD, Posival H, Schmitt C, Schrofel H, Luik A. Clinical impact of a new left bundle branch block following tavi implantation: 1-year results of the tavik cohort. *Clin Res Card.* 2015;104:351-362

12. Urena M, Mok M, Serra V, Dumont E, Nombela-Franco L, DeLarochelliere R, Doyle D, Igual A, Larose E, Amat-Santos I, Cote M, Cuellar H, Pibarot P, de Jaegere P, Philippon F, Garcia del Blanco B, Rodes-Cabau J. Predictive factors and long-term clinical consequences of persistent left bundle branch block following transcatheter aortic valve implantation with a balloon-expandable valve. *J Am Coll Cardiol.* 2012;60:1743-1752

13. Urena M, Webb JG, Cheema A, Serra V, Toggweiler S, Barbanti M, Cheung A, Ye J, Dumont E, Delarochellière R, Doyle D, Al Lawati HA, Peterson M, Chisholm R, Igual A, Ribeiro HB, Nombela-Franco L, Philippon F, Del Blanco BG, Rodés-Cabau J. Impact of new-onset persistent left bundle branch block on late clinical outcomes in patients undergoing transcatheter aortic valve implantation with a balloon-expandable valve. *JACC Cardiovasc Interv*. 2014;7:128-136

14. Van Der Boon RMA, Houthuizen P, Urena M, Poels TT, Van Mieghem NM, Brueren GRG, Altintas S, Nuis RJ, Serruys PW, Van Garsse LAFM, Van Domburg RT, Cabau JR, De Jaegere PPT, Prinzen FW. Trends in the occurrence of new conduction abnormalities after transcatheter aortic valve implantation. *Catheter Cardiovasc Interv*. 2015;85:144-152

15. Akin I, Kische S, Paranskaya L, Schneider H, Rehders TC, Trautwein U, Turan G, Bansch D, Thiele O, Divchev D, Bozdag-Turan I, Ortak J, Kundt G, Nienaber CA, Ince H. Predictive factors for pacemaker requirement after transcatheter aortic valve implantation. *BMC Cardiovasc Dis*. 2012;12:87

16. Abramowitz Y, Kazuno Y, Chakravarty T, Kawamori H, Maeno Y, Anderson D, Allison Z, Mangat G, Cheng W, Gopal A, Jilaihawi H, Mack MJ, Makkar RR. Concomitant mitral annular calcification and severe aortic stenosis: Prevalence, characteristics and outcome following transcatheter aortic valve replacement. *Eur Heart J*. 2017;38:1194-1203

17. Al-Azzam F, Greason KL, Krittanawong C, Williamson EE, McLeod CJ, King KS, Mathew V. The influence of native aortic valve calcium and transcatheter valve oversize on the need for pacemaker implantation after transcatheter aortic valve insertion. *J Thorac Cardiovasc Surg*. 2017;153:1056-1062.e1051

18. Bagur R, Rodes-Cabau J, Gurvitch R, Dumont E, Velianou JL, Manazzoni J, Toggweiler S, Cheung A, Ye J, Natarajan MK, Bainey KR, DeLarochelliere R, Doyle D, Pibarot P, Voisine P, Cote M, Philippon F, Webb JG. Need for permanent pacemaker as a complication of transcatheter aortic valve implantation and surgical aortic valve replacement in elderly patients with severe aortic stenosis and similar baseline electrocardiographic findings. *JACC Cardiovasc Interv*. 2012;5:540-551

19. Bleiziffer S, Ruge H, Horer J, Hutter A, Geisbusch S, Brockmann G, Mazzitelli D, Bauernschmitt R, Lange R. Predictors for new-onset complete heart block after transcatheter aortic valve implantation. *JACC Cardiovasc Interv.* 2010;3:524-530

20. Calvi V, Conti S, Pruiti GP, Capodanno D, Puzzangara E, Tempio D, Di Grazia A, Ussia GP, Tamburino C. Incidence rate and predictors of permanent pacemaker implantation after transcatheter aortic valve implantation with self-expanding corevalve prosthesis. *J Interv Card Electrophysiol.* 2012;34:189-195

21. D'Ancona G, Pasic M, Unbehaun A, Hetzer R. Permanent pacemaker implantation after transapical transcatheter aortic valve implantation. *Interact Cardiovasc Thorac Surg* 2011;13:373-376

22. De Carlo M, Giannini C, Bedogni F, Klugmann S, Brambilla N, De Marco F, Zucchelli G, Testa L, Oreglia J, Petronio AS. Safety of a conservative strategy of permanent pacemaker implantation after transcatheter aortic corevalve implantation. *Am Heart J.* 2012;163:492-499

23. De Torres-Alba F, Kaleschke G, Diller GP, Vormbrock J, Orwat S, Radke R, Reinke F, Fischer D, Reinecke H, Baumgartner H. Changes in the pacemaker rate after transition from edwards sapien xt to sapien 3 transcatheter aortic valve implantation: The critical role of valve implantation height. *JACC Cardiovasc Interv* 2016;9:805-813

24. Erkapic D, Kim WK, Weber M, Mollmann H, Berkowitsch A, Zaltsberg S, Pajitnev DJ, Rixe J, Neumann T, Kuniss M, Sperzel J, Hamm CW, Pitschner HF. Electrocardiographic and further predictors for permanent pacemaker requirement after transcatheter aortic valve implantation. *Europace.* 2010;12:1188-1190

25. Fadahunsi OO, Olowoyeye A, Ukaigwe A, Li Z, Vora AN, Vemulapalli S, Elgin E, Donato A. Incidence, predictors, and outcomes of permanent pacemaker implantation following transcatheter aortic valve replacement: Analysis from the u.S. Society of thoracic surgeons/american college of cardiology tvt registry. *JACC Cardiovasc Interv.* 2016;9:2189-2199

26. Fraccaro C, Buja G, Tarantini G, Gasparetto V, Leoni L, Razzolini R, Corrado D, Bonato R, Basso C, Thiene G, Gerosa G, Isabella G, Iliceto S, Napodano M. Incidence, predictors, and

outcome of conduction disorders after transcatheter self-expandable aortic valve implantation. *Am J Cardiol.* 2011;107:747-754

27. Fujita B, Kutting M, Seiffert M, Scholtz S, Egron S, Prashovikj E, Borgermann J, Schafer T, Scholtz W, Preuss R, Gummert J, Steinseifer U, Ensminger SM. Calcium distribution patterns of the aortic valve as a risk factor for the need of permanent pacemaker implantation after transcatheter aortic valve implantation. *Eur Heart J Cardiovasc Imaging.* 2016;17:1385-1393

28. Gensas CS, Caixeta A, Siqueira D, Carvalho LA, Sarmento-Leite R, Mangione JA, Lemos PA, Colafranceschi AS, Caramori P, Ferreira MC, Abizaid A, Brito FS, Jr. Predictors of permanent pacemaker requirement after transcatheter aortic valve implantation: Insights from a brazilian registry. *Int J Cardiol.* 2014;175:248-252

29. Giustino G, Van der Boon RM, Molina-Martin de Nicolas J, Dumonteil N, Chieffo A, de Jaegere PP, Tchetche D, Marcheix B, Millischer D, Cassagneau R, Carrie D, Van Mieghem NM, Colombo A. Impact of permanent pacemaker on mortality after transcatheter aortic valve implantation: The pragmatic (pooled rotterdam-milan-toulouse in collaboration) pacemaker substudy. *EuroIntervention.* 2016;12:1185-1193

30. Gonska B, Seeger J, Kessler M, von Keil A, Rottbauer W, Wohrle J. Predictors for permanent pacemaker implantation in patients undergoing transfemoral aortic valve implantation with the edwards sapien 3 valve. *Clin Res Card.* 2017;106:590-597

31. Guetta V, Goldenberg G, Segev A, Dvir D, Kornowski R, Finckelstein A, Hay I, Goldenberg I, Glikson M. Predictors and course of high-degree atrioventricular block after transcatheter aortic valve implantation using the corevalve revalving system. *Am J Cardiol.* 2011;108:1600-1605

32. Hamdan A, Guetta V, Klempfner R, Konen E, Raanani E, Glikson M, Goitein O, Segev A, Barbash I, Fefer P, Spiegelstein D, Goldenberg I, Schwammenthal E. Inverse relationship between membranous septal length and the risk of atrioventricular block in patients undergoing transcatheter aortic valve implantation. *JACC Cardiovasc Interv.* 2015;8:1218-1228

33. Husser O, Pellegrini C, Kessler T, Burgdorf C, Thaller H, Mayr NP, Kasel AM, Kastrati A, Schunkert H, Hengstenberg C. Predictors of permanent pacemaker implantations and new-onset conduction abnormalities with the sapien 3 balloon-expandable transcatheter heart valve. *JACC Cardiovasc Interv.* 2016;9:244-254

34. Kim WJ, Ko YG, Han S, Kim YH, Dy TC, Posas FE, Lee MK, Kim HS, Hong MK, Jang Y, Grube E, Park SJ. Predictors of permanent pacemaker insertion following transcatheter aortic valve replacement with the corevalve revalving system based on computed tomography analysis: An asian multicenter registry study. *J Invasive Cardiol.* 2015;27:334-340

35. Koos R, Mahnken AH, Aktug O, Dohmen G, Autschbach R, Marx N, Hoffmann R. Electrocardiographic and imaging predictors for permanent pacemaker requirement after transcatheter aortic valve implantation. *J Heart Valve Dis.* 2011;20:83-90

36. Lange P, Greif M, Vogel A, Thaumann A, Helbig S, Schwarz F, Schmitz C, Becker C, D'Anastasi M, Boekstegers P, Pohl T, Laubender RP, Steinbeck G, Kupatt C. Reduction of pacemaker implantation rates after corevalve(r) implantation by moderate predilatation. *EuroIntervention.* 2014;9:1151-1157

37. Latsios G, Gerckens U, Buellesfeld L, Mueller R, John D, Yuecel S, Syring J, Sauren B, Grube E. "Device landing zone" calcification, assessed by msct, as a predictive factor for pacemaker implantation after tavi. *Catheter Cardiovasc Interv.* 2010;76:431-439

38. Ledwoch J, Franke J, Gerckens U, Kuck KH, Linke A, Nickenig G, Krulls-Munch J, Vohringer M, Hambrecht R, Erbel R, Richardt G, Horack M, Zahn R, Senges J, Sievert H. Incidence and predictors of permanent pacemaker implantation following transcatheter aortic valve implantation: Analysis from the german transcatheter aortic valve interventions registry. *Catheter Cardiovasc Interv.* 2013;82:E569-577

39. Lopez-Aguilera J, Segura Saint-Gerons JM, Mazuelos Bellido F, Suarez de Lezo Herreros de Tejada J, Pineda SO, Pan Alvarez-Ossorio M, Romero Moreno MA, Pavlovic D, Suarez de Lezo Cruz Conde J. Effect of new-onset left bundle branch block after transcatheter aortic valve implantation (corevalve) on mortality, frequency of re-hospitalization, and need for pacemaker. *Am J Cardiol.* 2016;118:1380-1385

40. Maan A, Refaat MM, Heist EK, Passeri J, Inglessis I, Ptaszek L, Vlahakes G, Ruskin JN, Palacios I, Sundt T, Mansour M. Incidence and predictors of pacemaker implantation in patients undergoing transcatheter aortic valve replacement. *Pacing Clin Electrophysiol.* 2015;38:878-886

41. Maeno Y, Abramowitz Y, Kawamori H, Kazuno Y, Kubo S, Takahashi N, Mangat G, Okuyama K, Kashif M, Chakravarty T, Nakamura M, Cheng W, Friedman J, Berman D, Makkar RR, Jilaihawi H. A highly predictive risk model for pacemaker implantation after tavr. *JACC. Cardiovascular imaging.* 2017

42. Mauri V, Reimann A, Stern D, Scherner M, Kuhn E, Rudolph V, Rosenkranz S, Eghbalzadeh K, Friedrichs K, Wahlers T, Baldus S, Madershahian N, Rudolph TK. Predictors of permanent pacemaker implantation after transcatheter aortic valve replacement with the sapien 3. *JACC Cardiovasc Interv.* 2016;9:2200-2209

43. Mouillet G, Lellouche N, Lim P, Meguro K, Yamamoto M, Deux JF, Monin JL, Bergoend E, Dubois-Rande JL, Teiger E. Patients without prolonged qrs after tavi with corevalve device do not experience high-degree atrio-ventricular block. *Catheter Cardiovasc Interv.* 2013;81:882-887

44. Mouillet G, Lellouche N, Yamamoto M, Oguri A, Dubois-Rande JL, Van Belle E, Gilard M, Laskar M, Teiger E. Outcomes following pacemaker implantation after transcatheter aortic valve implantation with corevalve® devices: Results from the france 2 registry. *Catheter Cardiovasc Interv.* 2015;86:E158-E166

45. Munoz-Garcia AJ, Hernandez-Garcia JM, Jimenez-Navarro MF, Alonso-Briales JH, Dominguez-Franco AJ, Fernandez-Pastor J, Pena Hernandez J, Barrera Cordero A, Alzueta Rodriguez J, de Teresa-Galvan E. Factors predicting and having an impact on the need for a permanent pacemaker after corevalve prosthesis implantation using the new accutrak delivery catheter system. *JACC Cardiovasc Interv.* 2012;5:533-539

46. Nazif TM, Dizon JM, Hahn RT, Xu K, Babaliaros V, Douglas PS, El-Chami MF, Herrmann HC, Mack M, Makkar RR, Miller DC, Pichard A, Tuzcu EM, Szeto WY, Webb JG, Moses JW, Smith CR, Williams MR, Leon MB, Kodali SK. Predictors and clinical outcomes of

permanent pacemaker implantation after transcatheter aortic valve replacement: The partner (placement of aortic transcatheter valves) trial and registry. *JACC Cardiovasc Interv.* 2015;8:60-69

47. Ramazzina C, Knecht S, Jeger R, Kaiser C, Schaer B, Osswald S, Sticherling C, Kuhne M. Pacemaker implantation and need for ventricular pacing during follow-up after transcatheter aortic valve implantation. *Pacing Clin Electrophysiol.* 2014;37:1592-1601

48. Rodriguez-Olivares R, van Gils L, El Faquir N, Rahhab Z, Di Martino LF, van Weenen S, de Vries J, Galema TW, Geleijnse ML, Budde RP, Boersma E, de Jaegere PP, Van Mieghem NM. Importance of the left ventricular outflow tract in the need for pacemaker implantation after transcatheter aortic valve replacement. *Int J Cardiol.* 2016;216:9-15

49. Roten L, Wenaweser P, Delacretaz E, Hellige G, Stortecky S, Tanner H, Pilgrim T, Kadner A, Eberle B, Zwahlen M, Carrel T, Meier B, Windecker S. Incidence and predictors of atrioventricular conduction impairment after transcatheter aortic valve implantation. *Am J Cardiol.* 2010;106:1473-1480

50. Saia F, Lemos PA, Bordoni B, Cervi E, Boriani G, Ciuca C, Taglieri N, Mariani J, Jr., Kalil Filho R, Marzocchi A. Transcatheter aortic valve implantation with a self-expanding nitinol bioprosthesis: Prediction of the need for permanent pacemaker using simple baseline and procedural characteristics. *Catheter Cardiovasc Interv.* 2012;79:712-719

51. Schroeter T, Linke A, Haensig M, Merk DR, Borger MA, Mohr FW, Schuler G. Predictors of permanent pacemaker implantation after medtronic corevalve bioprosthesis implantation. *Europace.* 2012;14:1759-1763

52. Tarantini G, Mojoli M, Purita P, Napodano M, D'Onofrio A, Frigo A, Covolo E, Facchin M, Isabella G, Gerosa G, Iliceto S. Unravelling the (arte)fact of increased pacemaker rate with the edwards sapien 3 valve. *EuroIntervention.* 2015;11:343-350

53. Toutouzas K, Synetos A, Tousoulis D, Latsios G, Brili S, Mastrokostopoulos A, Karanasos A, Sideris S, Dilaveris P, Cheong A, Yu CM, Stefanadis C. Predictors for permanent pacemaker implantation after core valve implantation in patients without preexisting ecg conduction disturbances: The role of a new echocardiographic index. *Int J Cardiol.* 2014;172:601-603

54. Van Mieghem N, van Gils L, Wöhrle J, Hildick-Smith D, Bleiziffer S, Blackman D, Abdel-Wahab M, Linke A, Ince H, Wenaweser P, Werner N, Allocco DJ, Dawkins KD, Falk V. Tct-733 predictors of permanent pacemaker implantation in patients treated in routine clinical practice with the repositionable and fully retrievable lotus valve. *J Am Coll Cardiol.* 2016;68:B296-B296

55. Zaman S, McCormick L, Gooley R, Rashid H, Ramkumar S, Jackson D, Hui S, Meredith IT. Incidence and predictors of permanent pacemaker implantation following treatment with the repositionable lotus transcatheter aortic valve. *Catheter Cardiovasc Interv.* 2017; 90:147-154

56. Buellesfeld L, Stortecky S, Heg D, Hausen S, Mueller R, Wenaweser P, Pilgrim T, Gloekler S, Khattab AA, Huber C, Carrel T, Eberle B, Meier B, Boekstegers P, Juni P, Gerckens U, Grube E, Windecker S. Impact of permanent pacemaker implantation on clinical outcome among patients undergoing transcatheter aortic valve implantation. *J Am Coll Cardiol.* 2012;60:493-501

57. Dizon JM, Nazif TM, Hess PL, Biviano A, Garan H, Douglas PS, Kapadia S, Babaliaros V, Herrmann HC, Szeto WY, Jilaihawi H, Fearon WF, Tuzcu EM, Pichard AD, Makkar R, Williams M, Hahn RT, Xu K, Smith CR, Leon MB, Kodali SK. Chronic pacing and adverse outcomes after transcatheter aortic valve implantation. *Heart.* 2015;101:1665-1671

58. Urena M, Webb JG, Tamburino C, Munoz-Garcia AJ, Cheema A, Dager AE, Serra V, Amat-Santos IJ, Barbanti M, Imme S, Briales JH, Benitez LM, Al Lawati H, Cucalon AM, Garcia Del Blanco B, Lopez J, Dumont E, Delarochelliere R, Ribeiro HB, Nombela-Franco L, Philippon F, Rodes-Cabau J. Permanent pacemaker implantation after transcatheter aortic valve implantation: Impact on late clinical outcomes and left ventricular function. *Circulation.* 2014;129:1233-1243

Bibliographie

1. Cinquin P. Medical imaging and computer-assisted interventions. Rev Prat. 1996;46(3):319-23.

2. Cinquin P, Bainville E, Barbe C, Bittar E, Bouchard V, Bricault L, et al. Computer assisted medical interventions. IEEE Eng Med Biol Mag. 1995;14(3):254-63.

3. Otto CM, Prendergast B. Aortic-valve stenosis--from patients at risk to severe valve obstruction. N Engl J Med. 21 août 2014;371(8):744-56.

4. Iung B. A prospective survey of patients with valvular heart disease in Europe: The Euro Heart Survey on Valvular Heart Disease. Eur Heart J. 2003;24(13):1231-43.

5. Nguyen V, Michel M, Eltchaninoff H, Gilard M, Dindorf C, Iung B, et al. Implementation of Transcatheter Aortic Valve Replacement in France. J Am Coll Cardiol. 17 avr 2018;71(15):1614-27.

6. Makkar RR, Fontana GP, Jilaihawi H, Kapadia S, Pichard AD, Douglas PS, et al. Transcatheter aortic-valve replacement for inoperable severe aortic stenosis. N Engl J Med. 2012;366(18):1696-704.

7. Kodali SK, Williams MR, Smith CR, Svensson LG, Webb JG, Makkar RR, et al. Two-year outcomes after transcatheter or surgical aortic-valve replacement. N Engl J Med. 2012;366(18):1686-95.

8. Cribier A. Percutaneous Transcatheter Implantation of an Aortic Valve Prosthesis for Calcific Aortic Stenosis: First Human Case Description. Circulation. 2002;106(24):3006-8.

9. Grube E, Schuler G, Buellesfeld L, Gerckens U, Linke A, Wenaweser P, et al. Percutaneous aortic valve replacement for severe aortic stenosis in high-risk patients using the second- and current third-generation self-expanding CoreValve prosthesis: device success and 30-day clinical outcome. J Am Coll Cardiol. 3 juill 2007;50(1):69-76.

10. Lefevre T, Kappetein AP, Wolner E, Nataf P, Thomas M, Schachinger V, et al. One year follow-up of the multi-centre European PARTNER transcatheter heart valve study. Eur Heart J. janv 2011;32(2):148-57.

11. Thomas M, Schymik G, Walther T, Himbert D, Lefevre T, Treede H, et al. Thirty-day results of the SAPIEN aortic Bioprosthesis European Outcome (SOURCE) Registry: A European registry of transcatheter aortic valve implantation using the Edwards SAPIEN valve. Circulation. 6 juill 2010;122(1):62-9.

12. Eltchaninoff H, Prat A, Gilard M, Leguerrier A, Blanchard D, Fournial G, et al. Transcatheter aortic valve implantation: Early results of the FRANCE (FRench Aortic National CoreValve and Edwards) registry. Eur Heart J. 2011;32(2):191-7.

13. Leon MB, Smith CR, Mack M, Miller DC, Moses JW, Svensson LG, et al. Transcatheter aortic-valve implantation for aortic stenosis in patients who cannot undergo surgery. N Engl J Med. 21 oct 2010;363(17):1597-607.

14. Smith CR, Leon MB, Mack MJ, Miller DC, Moses JW, Svensson LG, et al. Transcatheter versus surgical aortic-valve replacement in high-risk patients. N Engl J Med. 9 juin 2011;364(23):2187-98.

15. Gilard M, Eltchaninoff H, Iung B, Donzeau-Gouge P, Chevreul K, Fajadet J, et al. Registry of transcatheter aortic-valve implantation in high-risk patients. N Engl J Med. 3 mai 2012;366(18):1705-15.

16. Adams DH, Popma JJ, Reardon MJ, Yakubov SJ, Coselli JS, Deeb GM, et al. Transcatheter aortic-valve replacement with a self-expanding prosthesis. N Engl J Med. 8 mai 2014;370(19):1790-8.

17. Leon MB, Smith CR, Mack MJ, Makkar RR, Svensson LG, Kodali SK, et al. Transcatheter or Surgical Aortic-Valve Replacement in Intermediate-Risk Patients. N Engl J Med. 28 avr 2016;374(17):1609-20.

18. Reardon MJ, Van Mieghem NM, Popma JJ, Kleiman NS, Sondergaard L, Mumtaz M, et al. Surgical or Transcatheter Aortic-Valve Replacement in Intermediate-Risk Patients. N Engl J Med. 6 avr 2017;376(14):1321-31.

19. Reinohl J, Kaier K, Reinecke H, Schmoor C, Frankenstein L, Vach W, et al. Effect of Availability of Transcatheter Aortic-Valve Replacement on Clinical Practice. N Engl J Med. 17 déc 2015;373(25):2438-47.

20. Gaede L, Blumenstein J, Liebetrau C, Dorr O, Kim W-K, Nef H, et al. Outcome after transvascular transcatheter aortic valve implantation in 2016. Eur Heart J. 21 févr 2018;39(8):667-75.

21. Mack MJ, Leon MB, Thourani VH, Makkar R, Kodali SK, Russo M, et al. Transcatheter Aortic-Valve Replacement with a Balloon-Expandable Valve in Low-Risk Patients. N Engl J Med. 17 mars 2019;

22. Popma JJ, Deeb GM, Yakubov SJ, Mumtaz M, Gada H, O'Hair D, et al. Transcatheter Aortic-Valve Replacement with a Self-Expanding Valve in Low-Risk Patients. N Engl J Med. 17 mars 2019;

23. Baumgartner H, Falk V, Bax JJ, De Bonis M, Hamm C, Holm PJ, et al. 2017 ESC/EACTS Guidelines for the management of valvular heart disease. Eur Heart J. 21 sept 2017;38(36):2739-91.

24. Auffret V, Lefevre T, Van Belle E, Eltchaninoff H, Iung B, Koning R, et al. Temporal Trends in Transcatheter Aortic Valve Replacement in France: FRANCE 2 to FRANCE TAVI. J Am Coll Cardiol. juill 2017;70(1):42-55.

25. Blackstone EH, Suri RM, Rajeswaran J, Babaliaros V, Douglas PS, Fearon WF, et al. Propensity-matched comparisons of clinical outcomes after transapical or transfemoral transcatheter aortic valve replacement: A placement of aortic transcatheter valves (PARTNER)-I trial substudy. Circulation. 2015;131(22):1989-2000.

26. Thourani VH, Kodali S, Makkar RR, Herrmann HC, Williams M, Babaliaros V, et al. Transcatheter aortic valve replacement versus surgical valve replacement in intermediate-risk patients: a propensity score analysis. Lancet. 28 mai 2016;387(10034):2218-25.

27. Lanz J, Greenbaum A, Pilgrim T, Tarantini G, Windecker S. Current state of alternative access for transcatheter aortic valve implantation. EuroIntervention J Eur Collab Work Group Interv Cardiol Eur Soc Cardiol. 31 août 2018;14(AB):AB40-52.

28. Greenbaum AB, Babaliaros VC, Chen MY, Stine AM, Rogers T, O'Neill WW, et al. Transcaval Access and Closure for Transcatheter Aortic Valve Replacement: A Prospective Investigation. J Am Coll Cardiol. 7 févr 2017;69(5):511-21.

29. Blanke P, Weir-McCall JR, Achenbach S, Delgado V, Hausleiter J, Jilaihawi H, et al. Computed Tomography Imaging in the Context of Transcatheter Aortic Valve Implantation (TAVI)/Transcatheter Aortic Valve Replacement (TAVR): An Expert Consensus Document of the Society of Cardiovascular Computed Tomography. JACC Cardiovasc Imaging. janv 2019;12(1):1-24.

30. D'Agostino RS, Jacobs JP, Badhwar V, Fernandez FG, Paone G, Wormuth DW, et al. The Society of Thoracic Surgeons Adult Cardiac Surgery Database: 2019 Update on Outcomes and Quality. Ann Thorac Surg. janv 2019;107(1):24-32.

31. Auffret V, Regueiro A, del Trigo M, Campelo-Parada F, Abdul-Jawad Altisent O, Chiche O, et al. Predictors of early Cerebrovascular Events in Patients with Severe Aortic Stenosis Undergoing Transcatheter Aortic Valve Replacement: A Systematic Review and Meta-Analysis. J Am Coll Cardiol. 2016;

32. Auffret V, Puri R, Urena M, Chamandi C, Rodriguez-Gabella T, Philippon F, et al. Conduction Disturbances After Transcatheter Aortic Valve Replacement: Current Status and Future Perspectives. Circulation. 12 sept 2017;136(11):1049-69.

33. Puri R, Iung B, Cohen DJ, Rodes-Cabau J. TAVI or No TAVI: identifying patients unlikely to benefit from transcatheter aortic valve implantation. Eur Heart J. 21 juill 2016;37(28):2217-25.

34. Arnold SV, Afilalo J, Spertus JA, Tang Y, Baron SJ, Jones PG, et al. Prediction of Poor Outcome After Transcatheter Aortic Valve Replacement. J Am Coll Cardiol. 25 oct 2016;68(17):1868-77.

35. Arnold SV, Reynolds MR, Lei Y, Magnuson EA, Kirtane AJ, Kodali SK, et al. Predictors of poor outcomes after transcatheter aortic valve replacement: results from the PARTNER (Placement of Aortic Transcatheter Valve) trial. Circulation. 24 juin 2014;129(25):2682-90.

36. Arnold SV, Spertus JA, Lei Y, Green P, Kirtane AJ, Kapadia S, et al. How to define a poor outcome after transcatheter aortic valve replacement : Conceptual framework and empirical observations from the placement of Aortic Transcatheter Valve (PARTNER) trial. Circ Cardiovasc Qual Outcomes. 2013;6(5):591-7.

37. Zusman O, Kornowski R, Witberg G, Lador A, Orvin K, Levi A, et al. Transcatheter Aortic Valve Implantation Futility Risk Model Development and Validation Among Treated Patients With Aortic Stenosis. Am J Cardiol. 15 déc 2017;120(12):2241-6.

38. van Mourik MS, Vendrik J, Abdelghani M, van Kesteren F, Henriques JPS, Driessen AHG, et al. Guideline-defined futility or patient-reported outcomes to assess treatment success after TAVI: what to use? Results from a prospective cohort study with long-term follow-up. Open Heart. 2018;5(2):e000879.

39. Lantelme P, Eltchaninoff H, Rabilloud M, Souteyrand G, Dupre M, Spaziano M, et al. Development of a Risk Score Based on Aortic Calcification to Predict 1-Year Mortality After Transcatheter Aortic Valve Replacement. JACC Cardiovasc Imaging. janv 2019;12(1):123-32.

40. Lantelme P, Courand P-Y, Harbaoui B. Predicting Futility for Transcatheter Aortic Valve Replacement Procedures: Where Do We Stand? JACC Cardiovasc Interv. 13 août 2018;11(15):1536-7.

41. Auffret V, Boulmier D, Oger E, Bedossa M, Donal E, Laurent M, et al. Predictors of 6-month poor clinical outcomes after transcatheter aortic valve implantation. Arch Cardiovasc Dis. janv 2014;107(1):10-20.

42. Durko AP, Reardon MJ, Kleiman NS, Popma JJ, Van Mieghem NM, Gleason TG, et al. Neurological Complications After Transcatheter Versus Surgical Aortic Valve Replacement in Intermediate-Risk Patients. J Am Coll Cardiol. 30 oct 2018;72(18):2109-19.

43. Kapadia SR, Huded CP, Kodali SK, Svensson LG, Tuzcu EM, Baron SJ, et al. Stroke After Surgical Versus Transfemoral Transcatheter Aortic Valve Replacement in the PARTNER Trial. J Am Coll Cardiol. 13 nov 2018;72(20):2415-26.

44. Patel PA, Patel S, Feinman JW, Gutsche JT, Vallabhajosyula P, Shah R, et al. Stroke After Transcatheter Aortic Valve Replacement: Incidence, Definitions, Etiologies and Management Options. J Cardiothorac Vasc Anesth. avr 2018;32(2):968-81.

45. Nombela-Franco L, Webb JG, de Jaegere PP, Toggweiler S, Nuis RJ, Dager AE, et al. Timing, predictive factors, and prognostic value of cerebrovascular events in a large cohort of patients undergoing transcatheter aortic valve implantation. Circulation. 18 déc 2012;126(25):3041-53.

46. Vlastra W, Jimenez-Quevedo P, Tchetche D, Chandrasekhar J, de Brito FSJ, Barbanti M, et al. Predictors, Incidence, and Outcomes of Patients Undergoing Transfemoral Transcatheter Aortic Valve Implantation Complicated by Stroke. Circ Cardiovasc Interv. mars 2019;12(3):e007546.

47. Arnold SV, Zhang Y, Baron SJ, McAndrew TC, Alu MC, Kodali SK, et al. Impact of Short-Term Complications on Mortality and Quality of Life After Transcatheter Aortic Valve Replacement. JACC Cardiovasc Interv. 25 févr 2019;12(4):362-9.

48. Miller DC, Blackstone EH, Mack MJ, Svensson LG, Kodali SK, Kapadia S, et al. Transcatheter (TAVR) versus surgical (AVR) aortic valve replacement: occurrence, hazard, risk factors, and consequences of neurologic events in the PARTNER trial. J Thorac Cardiovasc Surg. avr 2012;143(4):832-843.e13.

49. Kapadia S, Agarwal S, Miller DC, Webb JG, Mack M, Ellis S, et al. Insights Into Timing, Risk Factors, and Outcomes of Stroke and Transient Ischemic Attack After Transcatheter Aortic Valve Replacement in the PARTNER Trial (Placement of Aortic Transcatheter Valves). Circ Cardiovasc Interv. sept 2016;9(9).

50. Haussig S, Mangner N, Dwyer MG, Lehmkuhl L, Lucke C, Woitek F, et al. Effect of a Cerebral Protection Device on Brain Lesions Following Transcatheter Aortic Valve Implantation in Patients With Severe Aortic Stenosis: The CLEAN-TAVI Randomized Clinical Trial. Jama. août 2016;316(6):592-601.

51. Lansky AJ, Schofer J, Tchetche D, Stella P, Pietras CG, Parise H, et al. A prospective randomized evaluation of the TriGuard™ HDH embolic DEFLECTion device during transcatheter aortic valve implantation: Results from the DEFLECT III trial. Eur Heart J. 2015;36(31):2070-8.

52. Giustino G, Sorrentino S, Mehran R, Faggioni M, Dangas G. Cerebral Embolic Protection During TAVR: A Clinical Event Meta-Analysis. J Am Coll Cardiol. 31 janv 2017;69(4):465-6.

53. Seeger J, Kapadia SR, Kodali S, Linke A, Wohrle J, Haussig S, et al. Rate of peri-procedural stroke observed with cerebral embolic protection during transcatheter aortic valve replacement: a patient-level propensity-matched analysis. Eur Heart J. 24 déc 2018;

54. Jochheim D, Zadrozny M, Ricard I, Sadry TM, Theiss H, Baquet M, et al. Predictors of cerebrovascular events at mid-term after transcatheter aortic valve implantation - Results from EVERY-TAVI registry. Int J Cardiol. 1 oct 2017;244:106-11.

55. Werner N, Zeymer U, Schneider S, Bauer T, Gerckens U, Linke A, et al. Incidence and Clinical Impact of Stroke Complicating Transcatheter Aortic Valve Implantation: Results From the German TAVI Registry. Catheter Cardiovasc Interv Off J Soc Card Angiogr Interv. oct 2016;88(4):644-53.

56. Kleiman NS, Maini BJ, Reardon MJ, Conte J, Katz S, Rajagopal V, et al. Neurological Events Following Transcatheter Aortic Valve Replacement and Their Predictors: A Report From the CoreValve Trials. Circ Cardiovasc Interv. sept 2016;9(9).

57. Bosmans J, Bleiziffer S, Gerckens U, Wenaweser P, Brecker S, Tamburino C, et al. The Incidence and Predictors of Early- and Mid-Term Clinically Relevant Neurological Events after Transcatheter Aortic Valve Replacement in Real-World Patients. J Am Coll Cardiol. 2015;66(3):209-17.

58. Thourani VH, O'Brien SM, Kelly JJ, Cohen DJ, Peterson ED, Mack MJ, et al. Development and Application of a Risk Prediction Model for In-Hospital Stroke After Transcatheter Aortic Valve Replacement: A Report From The Society of Thoracic Surgeons/American College of Cardiology Transcatheter Valve Therapy Registry. Ann Thorac Surg. 7 déc 2018;

59. Auffret V, Regueiro A, Campelo-Parada F, Del Trigo M, Chiche O, Chamandi C, et al. Feasibility, safety, and efficacy of transcatheter aortic valve replacement without balloon predilation: A systematic review and meta-analysis. Catheter Cardiovasc Interv Off J Soc Card Angiogr Interv. 1 nov 2017;90(5):839-50.

60. Hamdan A, Guetta V, Klempfner R, Konen E, Raanani E, Glikson M, et al. Inverse Relationship Between Membranous Septal Length and the Risk of Atrioventricular Block in Patients Undergoing Transcatheter Aortic Valve Implantation. JACC Cardiovasc Interv. 17 août 2015;8(9):1218-28.

61. Maeno Y, Abramowitz Y, Kawamori H, Kazuno Y, Kubo S, Takahashi N, et al. A Highly Predictive Risk Model for Pacemaker Implantation After TAVR. JACC Cardiovasc Imaging. avr 2017;

62. De Torres-Alba F, Kaleschke G, Diller GP, Vormbrock J, Orwat S, Radke R, et al. Changes in the Pacemaker Rate After Transition From Edwards SAPIEN XT to SAPIEN 3 Transcatheter Aortic Valve Implantation: The Critical Role of Valve Implantation Height. JACC Cardiovasc Interv. 25 avr 2016;9(8):805-13.

63. Husser O, Pellegrini C, Kessler T, Burgdorf C, Thaller H, Mayr NP, et al. Predictors of Permanent Pacemaker Implantations and New-Onset Conduction Abnormalities With the SAPIEN 3 Balloon-Expandable Transcatheter Heart Valve. JACC Cardiovasc Interv. 8 févr 2016;9(3):244-54.

64. Petronio AS, Sinning J-M, Van Mieghem N, Zucchelli G, Nickenig G, Bekeredjian R, et al. Optimal Implantation Depth and Adherence to Guidelines on Permanent Pacing to Improve the Results of Transcatheter Aortic Valve Replacement With the Medtronic CoreValve System: The CoreValve Prospective, International, Post-Market. JACC Cardiovasc Interv. mai 2015;8(6):837-46.

65. Lange P, Greif M, Vogel A, Thaumann A, Helbig S, Schwarz F, et al. Reduction of pacemaker implantation rates after CoreValve(R) implantation by moderate predilatation. EuroIntervention. févr 2014;9(10):1151-7.

66. Bernardi FL, Ribeiro HB, Carvalho LA, Sarmento-Leite R, Mangione JA, Lemos PA, et al. Direct Transcatheter Heart Valve Implantation Versus Implantation With Balloon Predilatation: Insights From the Brazilian Transcatheter Aortic Valve Replacement Registry. Circ Cardiovasc Interv. août 2016;9(8).

67. Rodes-Cabau J, Urena M, Nombela-Franco L, Amat-Santos I, Kleiman N, Munoz-Garcia A, et al. Arrhythmic Burden as Determined by Ambulatory Continuous Cardiac Monitoring in Patients With New-Onset Persistent Left Bundle Branch Block Following Transcatheter Aortic Valve Replacement: The MARE Study. JACC Cardiovasc Interv. 13 août 2018;11(15):1495-505.

68. Moat NE, Ludman P, de Belder MA, Bridgewater B, Cunningham AD, Young CP, et al. Long-term outcomes after transcatheter aortic valve implantation in high-risk patients with severe aortic stenosis: the U.K. TAVI (United Kingdom Transcatheter Aortic Valve Implantation) Registry. J Am Coll Cardiol. 8 nov 2011;58(20):2130-8.

69. Kodali SK, Williams MR, Smith CR, Svensson LG, Webb JG, Makkar RR, et al. Two-year outcomes after transcatheter or surgical aortic-valve replacement. N Engl J Med. 2012;366(18):1686-95.

70. Tamburino C, Capodanno D, Ramondo A, Petronio AS, Ettori F, Santoro G, et al. Incidence and predictors of early and late mortality after transcatheter aortic valve implantation in 663 patients with severe aortic stenosis. Circulation. 25 janv 2011;123(3):299-308.

71. Dvir D, Waksman R, Barbash IM, Kodali SK, Svensson LG, Tuzcu EM, et al. Outcomes of patients with chronic lung disease and severe aortic stenosis treated with transcatheter versus surgical aortic valve replacement or standard therapy: Insights from the PARTNER trial (placement of AoRTic TraNscathetER valve). J Am Coll Cardiol. 2014;63(3):269-79.

72. Mok M, Nombela-Franco L, Dumont E, Urena M, DeLarochelliere R, Doyle D, et al. Chronic obstructive pulmonary disease in patients undergoing transcatheter aortic valve implantation: insights on clinical outcomes, prognostic markers, and functional status changes. JACC Cardiovasc Interv. oct 2013;6(10):1072-84.

73. Allende R, Webb JG, Munoz-Garcia AJ, de Jaegere P, Tamburino C, Dager AE, et al. Advanced chronic kidney disease in patients undergoing transcatheter aortic valve implantation: insights on clinical outcomes and prognostic markers from a large cohort of patients. Eur Heart J. 2014;35(38):2685-96.

74. Ben-Dor I, Goldstein SA, Pichard AD, Satler LF, Maluenda G, Li Y, et al. Clinical profile, prognostic implication, and response to treatment of pulmonary hypertension in patients with severe aortic stenosis. Am J Cardiol. 1 avr 2011;107(7):1046-51.

75. Lucon A, Oger E, Bedossa M, Boulmier D, Verhoye JP, Eltchaninoff H, et al. Prognostic implications of pulmonary hypertension in patients with severe aortic stenosis undergoing transcatheter aortic valve implantation: study from the FRANCE 2 registry. Circ Cardiovasc Interv. avr 2014;7(2):240-7.

76. Gotzmann M, Pljakic A, Bojara W, Lindstaedt M, Ewers A, Germing A, et al. Transcatheter aortic valve implantation in patients with severe symptomatic aortic valve stenosis-predictors of mortality and poor treatment response. Am Heart J. août 2011;162(2):238-245 e1.

77. Schoenenberger AW, Stortecky S, Neumann S, Moser A, Juni P, Carrel T, et al. Predictors of functional decline in elderly patients undergoing transcatheter aortic valve implantation (TAVI). Eur Heart J. mars 2013;34(9):684-92.

78. Tarantini G, Mojoli M, Urena M, Vahanian A. Atrial fibrillation in patients undergoing transcatheter aortic valve implantation: epidemiology, timing, predictors, and outcome. Eur Heart J. 1 mai 2017;38(17):1285-93.

79. Fan J, Liu X, Yu L, Sun Y, Jaiswal S, Zhu Q, et al. Impact of tricuspid regurgitation and right ventricular dysfunction on outcomes after transcatheter aortic valve replacement: A systematic review and meta-analysis. Clin Cardiol. janv 2019;42(1):206-12.

80. Fukui M, Gupta A, Abdelkarim I, Sharbaugh MS, Althouse AD, Elzomor H, et al. Association of Structural and Functional Cardiac Changes With Transcatheter Aortic Valve Replacement Outcomes in Patients With Aortic Stenosis. JAMA Cardiol. 6 févr 2019;

81. Genereux P, Pibarot P, Redfors B, Mack MJ, Makkar RR, Jaber WA, et al. Staging classification of aortic stenosis based on the extent of cardiac damage. Eur Heart J. 1 déc 2017;38(45):3351-8.

82. Van Belle E, Juthier F, Susen S, Vincentelli A, Iung B, Dallongeville J, et al. Postprocedural aortic regurgitation in balloon-expandable and self-expandable transcatheter aortic valve replacement procedures: analysis of predictors and impact on long-term mortality: insights from the FRANCE2 Registry. Circulation. 1 avr 2014;129(13):1415-27.

83. Jerez-Valero M, Urena M, Webb JG, Tamburino C, Munoz-Garcia AJ, Cheema A, et al. Clinical impact of aortic regurgitation after transcatheter aortic valve replacement: insights into the degree and acuteness of presentation. JACC Cardiovasc Interv. sept 2014;7(9):1022-32.

84. Iung B, Laouénan C, Himbert D, Eltchaninoff H, Chevreul K, Donzeau-Gouge P, et al. Predictive factors of early mortality after transcatheter aortic valve implantation: Individual risk assessment using a simple score. Heart. 2014;100(13):1016-23.

85. Seiffert M, Sinning J-M, Meyer A, Wilde S, Conradi L, Vasa-Nicotera M, et al. Development of a risk score for outcome after transcatheter aortic valve implantation. Clin Res Cardiol Off J Ger Card Soc. août 2014;103(8):631-40.

86. Capodanno D, Barbanti M, Tamburino C, D'Errigo P, Ranucci M, Santoro G, et al. A simple risk tool (the OBSERVANT score) for prediction of 30-day mortality after transcatheter aortic valve replacement. Am J Cardiol. 2014;113(11):1851-8.

87. Debonnaire P, Fusini L, Wolterbeek R, Kamperidis V, van Rosendael P, van der Kley F, et al. Value of the « TAVI2-SCORe » versus surgical risk scores for prediction of one year mortality in 511 patients who underwent transcatheter aortic valve implantation. Am J Cardiol. 15 janv 2015;115(2):234-42.

88. Edwards FH, Cohen DJ, O'Brien SM, Peterson ED, Mack MJ, Shahian DM, et al. Development and Validation of a Risk Prediction Model for In-Hospital Mortality After Transcatheter Aortic Valve Replacement. JAMA Cardiol. 1 avr 2016;1(1):46-52.

89. Afilalo J, Alexander KP, Mack MJ, Maurer MS, Green P, Allen LA, et al. Frailty assessment in the cardiovascular care of older adults. J Am Coll Cardiol. 2014;63(8):747-62.

90. Afilalo J, Lauck S, Kim DH, Lefevre T, Piazza N, Lachapelle K, et al. Frailty in Older Adults Undergoing Aortic Valve Replacement: The FRAILTY-AVR Study. J Am Coll Cardiol. 8 août 2017;70(6):689-700.

91. Schoenenberger AW, Moser A, Bertschi D, Wenaweser P, Windecker S, Carrel T, et al. Improvement of Risk Prediction After Transcatheter Aortic Valve Replacement by Combining Frailty With Conventional Risk Scores. JACC Cardiovasc Interv. 26 févr 2018;11(4):395-403.

92. Arnold SV, O'Brien SM, Vemulapalli S, Cohen DJ, Stebbins A, Brennan JM, et al. Inclusion of Functional Status Measures in the Risk Adjustment of 30-Day Mortality After Transcatheter Aortic Valve Replacement: A Report From the Society of Thoracic Surgeons/American College of Cardiology TVT Registry. JACC Cardiovasc Interv. 26 mars 2018;11(6):581-9.

93. Goldstein BA, Navar AM, Carter RE. Moving beyond regression techniques in cardiovascular risk prediction: applying machine learning to address analytic challenges. Eur Heart J. 14 juin 2017;38(23):1805-14.

94. Anker S, Asselbergs FW, Brobert G, Vardas P, Grobbee DE, Cronin M. Big Data in Cardiovascular Disease. Eur Heart J. 21 juin 2017;38(24):1863-5.

95. Rogers MA, Aikawa E. Cardiovascular calcification: artificial intelligence and big data accelerate mechanistic discovery. Nat Rev Cardiol. 10 déc 2018;

96. Rumsfeld JS, Joynt KE, Maddox TM. Big data analytics to improve cardiovascular care: promise and challenges. Nat Rev Cardiol. juin 2016;13(6):350-9.

97. Berner ES. Clinical decision support systems: State of the Art. AHQR Publ No 09-0069-EF Rockv Md Agency Healthc Res Qual. 2009;

98. Berner ES. Clinical Decision Support Systems: Theory and Practice. Springer, New York, NY; 2007.

99. El-Fakdi A, Gamero F, Meléndez J, Auffret V, Haigron P. eXiTCDSS: A framework for a workflow-based CBR for interventional Clinical Decision Support Systems and its application to TAVI. Expert Syst Appl. 1 févr 2014;41(2):284-94.

100. Choudhury N, Begum SA. A survey on case-based reasoning in medicine. Int J Adv Comput Sci Appl. 2016;7(8):136-44.

101. Bichindaritz I, Montani S. Advances in case-based reasoning in the health sciences. Artif Intell Med. févr 2011;51(2):75-9.

102. Althoff K-D. Case-Based Reasoning. In: Handbook of Software Engineering and Knowledge Engineering [Internet]. World Scientific Publishing Company; 2001 [cité 22 mars 2019]. p. 549-87. Disponible sur: https://doi.org/10.1142/9789812389718_0023

103. Aamodt A, Plaza E. Case-based Reasoning: Foundational Issues, Methodological Variations, and System Approaches. AI Commun. mars 1994;7(1):39–59.

104. Richter M, Weber R. Case-based Reasoning: A Textbook. 1re éd. Springer-Verlag Berlin Heidelberg; 2013.

105. Richter MM. Knowledge containers. Read Case-Based Reason Morgan Kaufmann Publ. 2003;

106. Wilson DR, Martinez TR. Improved heterogeneous distance functions. J Artif Intell Res. 1997;6:1-34.

107. Lesot M, Rifqi M, Benhadda H. Similarity Measures for Binary and Numerical Data: a Survey. Int J Knowl Eng Soft Data Paradigm. déc 2009;1(1):63–84.

108. Choi S-S, Cha S-H, Tappert CC. A survey of binary similarity and distance measures. J Syst Cybern Inform. 2010;8(1):43-8.

109. Wilson DC, Leake DB. Maintaining Case-Based Reasoners: Dimensions and Directions. Comput Intell. 1 mai 2001;17(2):196-213.

110. Reinartz T, Iglezakis I, Roth–Berghofer T. Review and Restore for Case-Base Maintenance. Comput Intell. 1 mai 2001;17(2):214-34.

111. Juarez JM, Craw S, Lopez-Delgado JR, Campos M. Maintenance of Case Bases: Current Algorithms after Fifty Years. In: Proceedings of the Twenty-Seventh International Joint Conference on Artificial Intelligence, IJCAI-18 [Internet]. International Joint Conferences on Artificial Intelligence Organization; 2018. p. 5457–5463. Disponible sur: https://doi.org/10.24963/ijcai.2018/770

112. H. Feuillâtre, V. Auffret, M. Castro, H. Le Breton, M. Garreau, P. Haigron. Study of similarity measures for case-based reasoning in transcatheter aortic valve implantation. In: 2017 Computing in Cardiology (CinC). 2017. p. 1-4.

113. Rocatello G, El Faquir N, De Santis G, Iannaccone F, Bosmans J, De Backer O, et al. Patient-Specific Computer Simulation to Elucidate the Role of Contact Pressure in the Development of New Conduction Abnormalities After Catheter-Based Implantation of a Self-Expanding Aortic Valve. Circ Cardiovasc Interv. févr 2018;11(2):e005344.

114. Wang Q, Kodali S, Primiano C, Sun W. Simulations of transcatheter aortic valve implantation: implications for aortic root rupture. Biomech Model Mechanobiol. janv 2015;14(1):29-38.

115. Schultz C, Rodriguez-Olivares R, Bosmans J, Lefevre T, De Santis G, Bruining N, et al. Patient-specific image-based computer simulation for theprediction of valve morphology and calcium displacement after TAVI with the Medtronic CoreValve and the Edwards SAPIEN valve. EuroIntervention J Eur Collab Work Group Interv Cardiol Eur Soc Cardiol. 22 janv 2016;11(9):1044-52.

116. Morganti S, Conti M, Aiello M, Valentini A, Mazzola A, Reali A, et al. Simulation of transcatheter aortic valve implantation through patient-specific finite element analysis: Two clinical cases. J Biomech. 2014;47(11):2547-55.

117. Morganti S, Brambilla N, Petronio AS, Reali A, Bedogni F, Auricchio F. Prediction of patient-specific post-operative outcomes of TAVI procedure: The impact of the positioning strategy on valve performance. J Biomech. 16 août 2016;49(12):2513-9.

118. Bianchi M, Marom G, Ghosh RP, Rotman OM, Parikh P, Gruberg L, et al. Patient-specific simulation of transcatheter aortic valve replacement: impact of deployment options on paravalvular leakage. Biomech Model Mechanobiol. avr 2019;18(2):435-51.

119. Sahoo P, Soltani S, Wong A, Chen Y. A Survey of Thresholding Techniques, Computer Vision, Graphics, and Image Processing. 1988;

120. Adams R, Bischof L. Seeded region growing. IEEE Trans Pattern Anal Mach Intell. 1994;16(6):641-7.

121. Fan J, Yau DK, Elmagarmid AK, Aref WG. Automatic image segmentation by integrating color-edge extraction and seeded region growing. IEEE Trans Image Process. 2001;10(10):1454-66.

122. Canny J. A computational approach to edge detection. In: Readings in computer vision. Elsevier; 1987. p. 184-203.

123. Yezzi A, Kichenassamy S, Kumar A, Olver P, Tannenbaum A. A geometric snake model for segmentation of medical imagery. IEEE Trans Med Imaging. 1997;16(2):199-209.

124. Osher S, Fedkiw R. Level set methods and dynamic implicit surfaces. Vol. 153. Springer Science & Business Media; 2006.

125. Osher S, Sethian JA. Fronts propagating with curvature-dependent speed: algorithms based on Hamilton-Jacobi formulations. J Comput Phys. 1988;79(1):12-49.

126. Iglesias JE, Sabuncu MR. Multi-atlas segmentation of biomedical images: A survey. Med Image Anal. août 2015;24(1):205-19.

127. Lesage D, Angelini ED, Bloch I, Funka-Lea G. A review of 3D vessel lumen segmentation techniques: models, features and extraction schemes. Med Image Anal. 2009;13(6):819-45.

128. Aylward SR, Bullitt E. Initialization, noise, singularities, and scale in height ridge traversal for tubular object centerline extraction. IEEE Trans Med Imaging. 2002;21(2):61-75.

129. Lee J, Beighley P, Ritman E, Smith N. Automatic segmentation of 3D micro-CT coronary vascular images. Med Image Anal. 2007;11(6):630-47.

130. Szymczak A, Stillman A, Tannenbaum A, Mischaikow K. Coronary vessel trees from 3D imagery: a topological approach. Med Image Anal. 2006;10(4):548-59.

131. Koller TM, Gerig G, Szekely G, Dettwiler D. Multiscale detection of curvilinear structures in 2-D and 3-D image data. In IEEE; 1995. p. 864-9.

132. Frangi AF, Niessen WJ, Vincken KL, Viergever MA. Multiscale vessel enhancement filtering. In Springer; 1998. p. 130-7.

133. Sato Y, Nakajima S, Shiraga N, Atsumi H, Yoshida S, Koller T, et al. Three-dimensional multi-scale line filter for segmentation and visualization of curvilinear structures in medical images. Med Image Anal. 1998;2(2):143-68.

134. Boldak C, Rolland Y, Toumoulin C, Coatrieux J. An improved model-based vessel tracking algorithm with application to computed tomography angiography. Biocybern Biomed Eng. 2003;23(1):41-64.

135. Hoyos MH, Orłowski P, Piątkowska-Janko E, Bogorodzki P, Orkisz M. Vascular centerline extraction in 3D MR angiograms for phase contrast MRI blood flow measurement. Int J Comput Assist Radiol Surg. 2006;1(1):51-61.

136. Larralde A, Boldak C, Garreau M, Toumoulin C, Boulmier D, Rolland Y. Evaluation of a 3D segmentation software for the coronary characterization in multi-slice computed tomography. In Springer; 2003. p. 39-51.

137. Friman O, Hindennach M, Peitgen H-O. Template-based multiple hypotheses tracking of small vessels. In IEEE; 2008. p. 1047-50.

138. Lacoste C, Descombes X, Zerubia J. Point processes for unsupervised line network extraction in remote sensing. IEEE Trans Pattern Anal Mach Intell. 2005;27(10):1568-79.

139. Lacoste C, Finet G, Magnin IE. Coronary tree extraction from X-ray angiograms using marked point processes. In IEEE; 2006. p. 157-60.

140. Wink O, Niessen WJ, Viergever MA. Fast delineation and visualization of vessels in 3-D angiographic images. IEEE Trans Med Imaging. avr 2000;19(4):337-46.

141. Boskamp T, Rinck D, Link F, Kummerlen B, Stamm G, Mildenberger P. New vessel analysis tool for morphometric quantification and visualization of vessels in CT and MR imaging data sets. Radiogr Rev Publ Radiol Soc N Am Inc. févr 2004;24(1):287-97.

142. Wan S-Y, Ritman EL, Higgins WE. Multi-generational analysis and visualization of the vascular tree in 3D micro-CT images. Comput Biol Med. mars 2002;32(2):55-71.

143. Wenli Cai, Frank Dachille, Gordon J. Harris, Hiroyuki Yoshida. Vesselness propagation: a fast interactive vessel segmentation method. In 2006. Disponible sur: https://doi.org/10.1117/12.653637

144. Adalsteinsson D, Sethian JA. A Fast Level Set Method for Propagating Interfaces. J Comput Phys. 1 mai 1995;118(2):269-77.

145. McInerney T, Hamarneh G, Shenton M, Terzopoulos D. Deformable organisms for automatic medical image analysis. Med Image Anal. sept 2002;6(3):251-66.

146. McInerney T, Terzopoulos D. Deformable models in medical image analysis: a survey. Med Image Anal. juin 1996;1(2):91-108.

147. Delingette H, Montagnat J. Shape and Topology Constraints on Parametric Active Contours. Comput Vis Image Underst. 1 août 2001;83(2):140-71.

148. M. Rochery, I. H. Jermyn, J. Zerubia. New higher-order active contour energies for network extraction. In: IEEE International Conference on Image Processing 2005. 2005. p. II-822.

149. Frangi AF, Niessen WJ, Hoogeveen RM, van Walsum T, Viergever MA. Model-based quantitation of 3-D magnetic resonance angiographic images. IEEE Trans Med Imaging. oct 1999;18(10):946-56.

150. Wong WCK, Chung ACS. Augmented vessels for quantitative analysis of vascular abnormalities and endovascular treatment planning. IEEE Trans Med Imaging. juin 2006;25(6):665-84.

151. Fedorov A, Beichel R, Kalpathy-Cramer J, Finet J, Fillion-Robin J-C, Pujol S, et al. 3D Slicer as an image computing platform for the Quantitative Imaging Network. Magn Reson Imaging. nov 2012;30(9):1323-41.

152. Kaladji A, Lucas A, Kervio G, Haigron P, Cardon A. Sizing for endovascular aneurysm repair: clinical evaluation of a new automated three-dimensional software. Ann Vasc Surg. oct 2010;24(7):912-20.

153. Maintz JBA, Viergever MA. A survey of medical image registration. Med Image Anal. 1 mars 1998;2(1):1-36.

154. Łubniewski P, Sarry L, Miguel B, Lohou C. 3D/2D image registration by image transformation descriptors (ITDs) for thoracic aorta imaging. Vol. 8650. 2013.

155. G. Borgefors. Hierarchical chamfer matching: a parametric edge matching algorithm. IEEE Trans Pattern Anal Mach Intell. nov 1988;10(6):849-65.

156. Rohr K, Stiehl HS, Sprengel R, Beil W, Buzug TM, Weese J, et al. Point-based elastic registration of medical image data using approximating thin-plate splines. In: Höhne KH, Kikinis R, éditeurs. Visualization in Biomedical Computing. Springer Berlin Heidelberg; 1996. p. 297-306.

157. P. J. Besl, N. D. McKay. A method for registration of 3-D shapes. IEEE Trans Pattern Anal Mach Intell. févr 1992;14(2):239-56.

158. Xue Z, Shen D, Davatzikos C. Statistical representation of high-dimensional deformation fields with application to statistically constrained 3D warping. Eighth Int Conf Med Imaging Comput Assist Interv – MICCAI 2005. 1 oct 2006;10(5):740-51.

159. H. J. Johnson, G. E. Christensen. Consistent landmark and intensity-based image registration. IEEE Trans Med Imaging. mai 2002;21(5):450-61.

160. P. Hellier, C. Barillot. Coupling dense and landmark-based approaches for nonrigid registration. IEEE Trans Med Imaging. févr 2003;22(2):217-27.

161. Pelizzari C, Chen B, R. Spelbring D, Weichselbaum R, Chen C-T. Accurate Three-Dimensional Registration of CT, PET, and/or MR Images of the Brain. Vol. 13. 1989. 20 p.

162. Rucklidge WJ. Lower bounds for the complexity of the graph of the Hausdorff distance as a function of transformation. Discrete Comput Geom. 1 févr 1996;16(2):135-53.

163. Zollei L. 2D-3D Rigid-Body Registration of X-Ray Fluoroscopy and CT Images. 2004.

164. Bajcsy R, Lieberson R, Reivich M. A Computerized System for the Elastic Matching of Deformed Radiographic Images to Idealized Atlas Images. Vol. 7. 1983. 618 p.

165. G. E. Christensen, P. Yin, M. W. Vannier, K. S. C. Chao, J. F. Dempsey, J. F. Williamson. Large-deformation image registration using fluid landmarks. In: 4th IEEE Southwest Symposium on Image Analysis and Interpretation. 2000. p. 269-73.

166. Horn BKP, Schunck BG. Determining optical flow. Artif Intell. 1 août 1981;17(1):185-203.

167. Thirion J-P. Image matching as a diffusion process: An analogy with Maxwell's demons. Vol. 2. 1998.

168. Dekker R. Applications of maintenance optimization models: a review and analysis. Maint Reliab. 1 mars 1996;51(3):229-40.

169. Markelj P, Tomaževič D, Likar B, Pernuš F. A review of 3D/2D registration methods for image-guided interventions. Comput Assist Interv. 1 avr 2012;16(3):642-61.

170. Goksu C, Haigron P, Acosta O, Lucas A. Endovascular navigation based on real/virtual environments cooperation for computer-assisted TEAM procedures. Vol. 5367. 2004.

171. Dumenil A, Kaladji A, Castro M, Esneault S, Lucas A, Rochette M, et al. Finite-element-based matching of pre- and intraoperative data for image-guided endovascular aneurysm repair. IEEE Trans Biomed Eng. mai 2013;60(5):1353-62.

172. Nguyen DL, Garreau M, Auffret V, Le Breton H, Verhoye JP, Haigron P. Intraoperative tracking of aortic valve plane. Conf Proc Annu Int Conf IEEE Eng Med Biol Soc IEEE Eng Med Biol Soc Annu Conf. 2013;2013:4378-81.

173. Belhaj Soulami R, Verhoye J-P, Nguyen Duc H, Castro M, Auffret V, Anselmi A, et al. Computer-Assisted Transcatheter Heart Valve Implantation in Valve-in-Valve Procedures. Innov Phila Pa. juin 2016;11(3):193-200.

Titre : Aide à la décision pour le remplacement valvulaire aortique percutané.

Mots clés : Sténose aortique; Remplacement valvulaire aortique; Transcatheter Aortic Valve Implantation;

Aide à la décision; Simulation numérique

Résumé : La sténose aortique serrée constitue la valvulopathie acquise de l'adulte la plus fréquente affectant jusqu'à 10% des octogénaires. Sa prise en charge percutanée est en plein essor et confronte les cliniciens à des problématiques nouvelles constituant à ce titre un champ de recherche important. Notre travail s'inscrit dans le cadre des gestes médico-chirurgicaux assistés par ordinateur et vise à proposer des solutions d'aide à la décision basées sur l'assistance informatique. Cette Thèse est ainsi composée de 4 parties.

Une première partie porte sur la problématique médicale dans laquelle s'inscrit le remplacement valvulaire aortique percutané (TAVI) ainsi que le contexte actuel du TAVI en France et s'appuie sur un article évaluant l'évolution des caractéristiques des patients et des procédures à l'échelle nationale entre 2010 et 2015 dans les registres nationaux FRANCE 2 et FRANCE TAVI. Ce premier chapitre identifie des problématiques médicales auxquelles les opérateurs restent confrontés au quotidien notamment la sélection optimale des candidats et la minimisation des complications de la procédure dans le contexte d'une réduction du profil de risque des patients traités.

La seconde partie s'intéresse à l'étude de population, par des méthodes statistiques classiques, pour établir des facteurs prédictifs de résultats du TAVI ou de survenue d'une complication donnée afin d'aider le clinicien dans sa planification de la procédure. Cette partie est articulée autour de 3 articles portant sur les facteurs prédictifs d'accidents vasculaires cérébraux post-TAVI, les troubles conductifs post-TAVI et les facteurs prédictifs de « mauvais résultats » après TAVI. Nous démontrons l'intérêt de ce type d'analyse qui resteront nécessaires à l'avenir mais abordons également leurs limites qui expliquent pourquoi d'autres pistes doivent être explorées pour stocker, trier, restituer les informations pertinentes à l'opérateur voire les augmenter pour faciliter ses décisions notamment en préopératoire.

L'objet de la 3ème partie est d'aborder un système d'aide à la décision par ordinateur de type « case-based reasoning » (CBR) qui pourrait tirer bénéfice de l'identification de ces facteurs pronostiques et à terme les intégrer dans une interface globale et ergonomique d'aide à la décision. Nous avons ainsi travaillé dans le cadre du projet européen H2020 EurValve sur l'élaboration d'un CBR dont la problématique se concentre pour l'instant sur le choix optimal de la voie d'abord, du type et de la taille de prothèse. Notre travail s'est concentré sur une étape analytique de la conception de ce type de système portant sur l'étude et l'amélioration de la mesure de similarité utilisée pour rapprocher le cas à traiter (problème) de ses plus proches voisins (cas déjà traités et leur « solution » thérapeutique).

Enfin, une dernière partie porte sur l'augmentation des informations disponibles pour l'aide à la décision en préopératoire par la simulation numérique spécifique patient. Après un état de l'art des méthodes utilisées dans le domaine du TAVI, nous avons travaillé à l'élaboration et le paramétrage d'un modèle de simulation de l'insertion du guide rigide dans le ventricule gauche (une des premières étapes de la procédure qui peut conditionner le positionnement de la prothèse et donc le résultat final). Afin de réaliser une première validation de cette simulation spécifique patient exploitant l'imagerie tomodensitométrique 3D préopératoire, l'approche proposée repose sur l'extraction de la région d'intérêt dans le volume 3D (segmentation) et sa mise en correspondance avec l'imagerie fluoroscopique 2D peropératoire par le biais d'un recalage 3D/2D. Nos travaux sur ces méthodes de traitement de l'image nécessaires à la mise en œuvre et la validation de notre stratégie de simulation sont également discutés dans cette partie. Enfin nous présentons une application clinique potentielle du modèle de simulation portant sur l'influence de la forme du guide et de ses conditions d'insertion sur sa stabilité et les forces de pression s'exerçant sur le ventricule gauche.

Title : Decision support for transcatheter aortic valve implantation

Keywords : Aortic stenosis; Aortic valve replacement; Transcatheter Aortic Valve Implantation;

Decision support; Numerical simulation.

Abstract: Aortic stenosis represents the most frequent acquired valvular heart disease, affecting up to 10% of octogenarians. Transcatheter aortic valve implantation (TAVI) is booming and confronts clinicians with new issues that constitute a major field of research. Our work falls within the framework of computer-assisted medico-surgical interventions, and aims at proposing computer-assisted decision support systems. The present Thesis is composed of four parts.

The first part focuses on the medical problematic surrounding TAVI, as well as the current French TAVI field on the basis of an article describing temporal trends in patients' and procedural's characteristics from 2010 to 2015 in the FRANCE 2 and FRANCE TAVI nationwide registries. This first part identifies medical issues that operators currently face, especially the optimal selection of TAVI candidates, and the reduction of procedural complications within the current trends towards treatment of patients with lower baseline surgical-risk profile.

The second part deal with population-based studies, through standard statistical methods, to identify predictors of TAVI outcomes or selected procedural complications in order to facilitate procedural planning. Three articles compose this part. The first focuses on predictors of short-term cerebrovascular events post-TAVI, the second deals with conduction disturbances post-TAVI while the third aims at identifying predictors of global poor outcomes. We demonstrate the benefits of these analyses, which will remain necessary in the future, but also address their limitations, which support the use of new methods to store, sort, retrieve, and even augment relevant information to facilitate operators' decision, especially at the pre-procedural step.

The purpose of Part 3 is to address a case-based reasoning (CBR) decision-support system that could benefit from the identification of these prognostic factors and ultimately integrate them into a global and ergonomic interface for decision support. We have worked in the framework of the European project H2020 EurValve on the development of a CBR whose problematic is,for the time being, limited to the optimal choice of the approach, type and size of prosthesis. Our work focused on an analytical step in the design of this type of system dealing with the study and improvement of the similarity measure used to identify nearest neighbours (previously treated cases and their therapeutic "solution") of the current problem (case which clinicians are planning to treat).

Finally, the last part focuses on increasing the information available for preoperative decision support through patient-specific numerical simulation. After a state of the art of the methods used in the field of TAVI, we worked on the elaboration and parameterization of a simulation model of the insertion of the stiff guidewire in the left ventricle (one of the first steps of the procedure that can condition the positioning of the prosthesis and thus the final result). In order to perform a first validation of this patient-specific simulation using preoperative 3D CT imaging, the proposed approach is based on the extraction of the region of interest in the 3D volume (segmentation) and its mapping to intraoperative 2D fluoroscopy through 3D / 2D registration. Our work on these image processing methods needed to implement and validate our simulation strategy is also discussed in this section. Finally, we present a potential clinical application of the simulation model regarding the influence of the shape of the guide and its insertion conditions on its stability and the pressure forces exerted on the left ventricle.